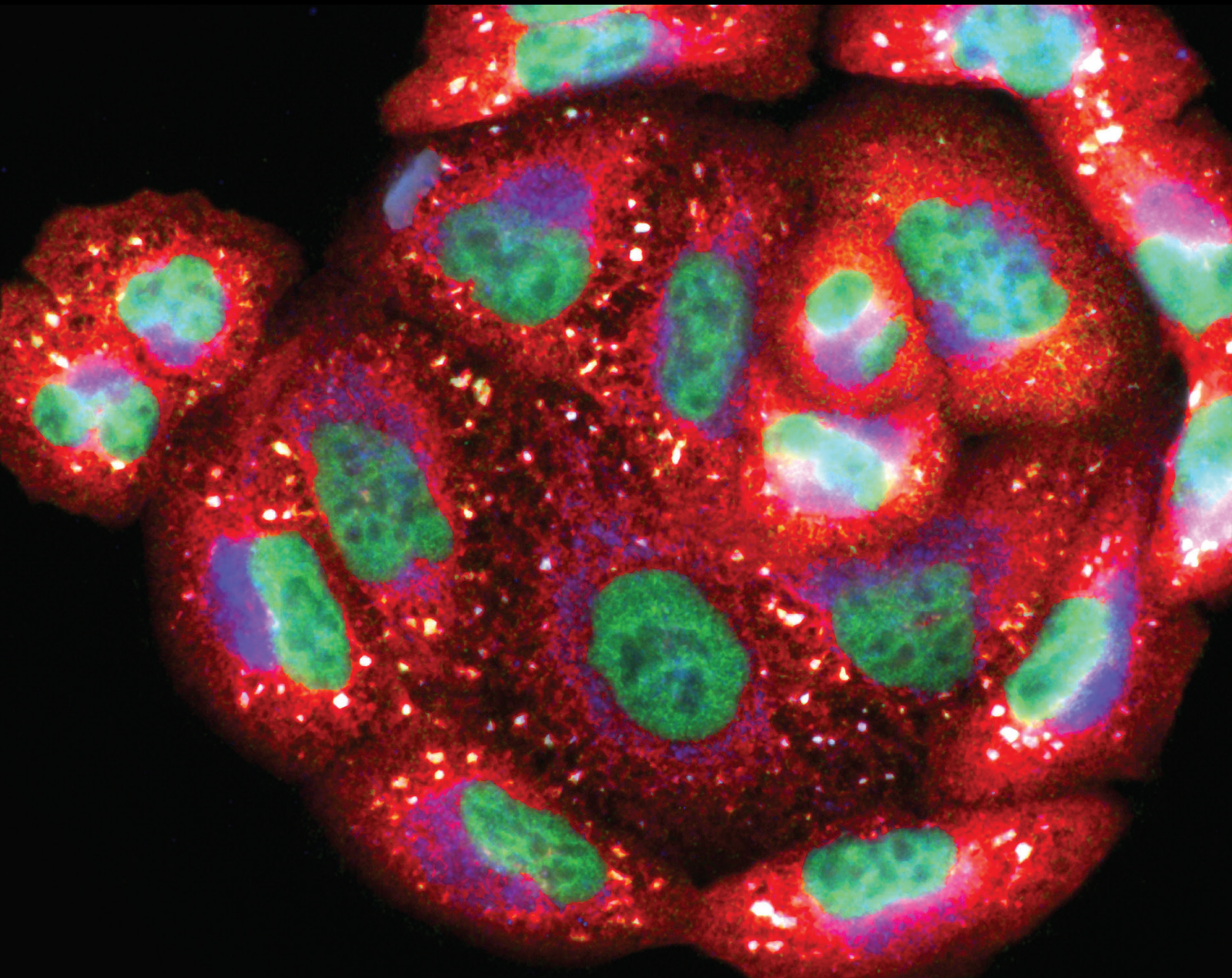


Role of Mitochondria-Endoplasmic Reticulum Contacts in Cardiovascular Disorders

Lead Guest Editor: Yun-dai Chen

Guest Editors: Sang-Bing Ong and Jun Ren





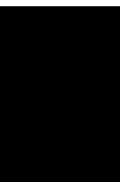
Role of Mitochondria-Endoplasmic Reticulum Contacts in Cardiovascular Disorders

Oxidative Medicine and Cellular Longevity

Role of Mitochondria-Endoplasmic Reticulum Contacts in Cardiovascular Disorders

Lead Guest Editor: Yun-dai Chen

Guest Editors: Sang-Bing Ong and Jun Ren



Copyright © 2022 Hindawi Limited. All rights reserved.

This is a special issue published in "Oxidative Medicine and Cellular Longevity" All articles are open access articles distributed under the Creative Commons Attribution License, which permits unrestricted use, distribution, and reproduction in any medium, provided the original work is properly cited.

Chief Editor

Jeannette Vasquez-Vivar, USA

Associate Editors

Amjad Islam Aqib, Pakistan
Angel Catalá , Argentina
Cinzia Domenicotti , Italy
Janusz Gebicki , Australia
Aldrin V. Gomes , USA
Vladimir Jakovljevic , Serbia
Thomas Kietzmann , Finland
Juan C. Mayo , Spain
Ryuichi Morishita , Japan
Claudia Penna , Italy
Sachchida Nand Rai , India
Paola Rizzo , Italy
Mithun Sinha , USA
Daniele Vergara , Italy
Victor M. Victor , Spain

Academic Editors

Ammar AL-Farga , Saudi Arabia
Mohd Adnan , Saudi Arabia
Ivanov Alexander , Russia
Fabio Altieri , Italy
Daniel Dias Rufino Arcanjo , Brazil
Peter Backx, Canada
Amira Badr , Egypt
Damian Bailey, United Kingdom
Rengasamy Balakrishnan , Republic of Korea
Jiaolin Bao, China
Ji C. Bihl , USA
Hareram Birla, India
Abdelhakim Bouyahya, Morocco
Ralf Braun , Austria
Laura Bravo , Spain
Matt Brody , USA
Amadou Camara , USA
Marcio Carochi , Portugal
Peter Celec , Slovakia
Giselle Cerchiaro , Brazil
Arpita Chatterjee , USA
Shao-Yu Chen , USA
Yujie Chen, China
Deepak Chhangani , USA
Ferdinando Chiaradonna , Italy

Zhao Zhong Chong, USA
Fabio Ciccarone, Italy
Alin Ciobica , Romania
Ana Cipak Gasparovic , Croatia
Giuseppe Cirillo , Italy
Maria R. Ciriolo , Italy
Massimo Collino , Italy
Manuela Corte-Real , Portugal
Manuela Curcio, Italy
Domenico D'Arca , Italy
Francesca Danesi , Italy
Claudio De Lucia , USA
Damião De Sousa , Brazil
Enrico Desideri, Italy
Francesca Diomede , Italy
Raul Dominguez-Perles, Spain
Joël R. Drevet , France
Grégory Durand , France
Alessandra Durazzo , Italy
Javier Egea , Spain
Pablo A. Evelson , Argentina
Mohd Farhan, USA
Ioannis G. Fatouros , Greece
Gianna Ferretti , Italy
Swaran J. S. Flora , India
Maurizio Forte , Italy
Teresa I. Fortoul, Mexico
Anna Fracassi , USA
Rodrigo Franco , USA
Juan Gambini , Spain
Gerardo García-Rivas , Mexico
Husam Ghanim, USA
Jayeeta Ghose , USA
Rajeshwary Ghosh , USA
Lucia Gimeno-Mallench, Spain
Anna M. Giudetti , Italy
Daniela Giustarini , Italy
José Rodrigo Godoy, USA
Saeid Golbidi , Canada
Guohua Gong , China
Tilman Grune, Germany
Solomon Habtemariam , United Kingdom
Eva-Maria Hanschmann , Germany
Md Saquib Hasnain , India
Md Hassan , India

Tim Hofer , Norway
John D. Horowitz, Australia
Silvana Hrelia , Italy
Dragan Hrnčić, Serbia
Zebo Huang , China
Zhao Huang , China
Tarique Hussain , Pakistan
Stephan Immenschuh , Germany
Norsharina Ismail, Malaysia
Franco J. L. , Brazil
Sedat Kacar , USA
Andleeb Khan , Saudi Arabia
Kum Kum Khanna, Australia
Neelam Khaper , Canada
Ramoji Kosuru , USA
Demetrios Kouretas , Greece
Andrey V. Kozlov , Austria
Chan-Yen Kuo, Taiwan
Gaocai Li , China
Guoping Li , USA
Jin-Long Li , China
Qiangqiang Li , China
Xin-Feng Li , China
Jialiang Liang , China
Adam Lightfoot, United Kingdom
Christopher Horst Lillig , Germany
Paloma B. Liton , USA
Ana Lloret , Spain
Lorenzo Loffredo , Italy
Camilo López-Alarcón , Chile
Daniel Lopez-Malo , Spain
Massimo Lucarini , Italy
Hai-Chun Ma, China
Nageswara Madamanchi , USA
Kenneth Maiese , USA
Marco Malaguti , Italy
Steven McAnulty, USA
Antonio Desmond McCarthy , Argentina
Sonia Medina-Escudero , Spain
Pedro Mena , Italy
V́ctor M. Mendoza-Núñez , Mexico
Lidija Milkovic , Croatia
Alexandra Miller, USA
Sara Missaglia , Italy

Premysl Mladenka , Czech Republic
Sandra Moreno , Italy
Trevor A. Mori , Australia
Fabiana Morroni , Italy
Ange Mouithys-Mickalad, Belgium
Iordanis Mourouzis , Greece
Ryoji Nagai , Japan
Amit Kumar Nayak , India
Abderrahim Nemmar , United Arab Emirates
Xing Niu , China
Cristina Nocella, Italy
Susana Novella , Spain
Hassan Obied , Australia
Pál Pacher, USA
Pasquale Pagliaro , Italy
Dilipkumar Pal , India
Valentina Pallottini , Italy
Swapnil Pandey , USA
Mayur Parmar , USA
Vassilis Paschalis , Greece
Keshav Raj Paudel, Australia
Ilaria Peluso , Italy
Tiziana Persichini , Italy
Shazib Pervaiz , Singapore
Abdul Rehman Phull, Republic of Korea
Vincent Pialoux , France
Alessandro Poggi , Italy
Zsolt Radak , Hungary
Dario C. Ramirez , Argentina
Erika Ramos-Tovar , Mexico
Sid D. Ray , USA
Muneeb Rehman , Saudi Arabia
Hamid Reza Rezvani , France
Alessandra Ricelli, Italy
Francisco J. Romero , Spain
Joan Roselló-Catafau, Spain
Subhadeep Roy , India
Josep V. Rubert , The Netherlands
Sumbal Saba , Brazil
Kunihiro Sakuma, Japan
Gabriele Saretzki , United Kingdom
Luciano Saso , Italy
Nadja Schroder , Brazil



Anwen Shao , China
Iman Sherif, Egypt
Salah A Sheweita, Saudi Arabia
Xiaolei Shi, China
Manjari Singh, India
Giulia Sita , Italy
Ramachandran Srinivasan , India
Adrian Sturza , Romania
Kuo-hui Su , United Kingdom
Eisa Tahmasbpour Marzouni , Iran
Hailiang Tang, China
Carla Tatone , Italy
Shane Thomas , Australia
Carlo Gabriele Tocchetti , Italy
Angela Trovato Salinaro, Italy
Rosa Tundis , Italy
Kai Wang , China
Min-qi Wang , China
Natalie Ward , Australia
Grzegorz Wegrzyn, Poland
Philip Wenzel , Germany
Guangzhen Wu , China
Jianbo Xiao , Spain
Qiongming Xu , China
Liang-Jun Yan , USA
Guillermo Zalba , Spain
Jia Zhang , China
Junmin Zhang , China
Junli Zhao , USA
Chen-he Zhou , China
Yong Zhou , China
Mario Zoratti , Italy

Contents

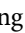





Mitochondria-Endoplasmic Reticulum Contacts: The Promising Regulators in Diabetic Cardiomyopathy

Yan Chen , Yanguo Xin , Yue Cheng , and Xiaojing Liu 
Review Article (13 pages), Article ID 2531458, Volume 2022 (2022)



Beta3-Adrenergic Receptor Activation Alleviates Cardiac Dysfunction in Cardiac Hypertrophy by Regulating Oxidative Stress

Mingming Zhang , Yuerong Xu, Jianghong Chen, Chaoshi Qin, Jing Liu, Dong Guo, Rui Wang, Jianqiang Hu, Qing Zou, Jingxiao Yang, Zikuan Wang, and Xiaolin Niu 
Research Article (13 pages), Article ID 3417242, Volume 2021 (2021)

SIRT5-Related Desuccinylation Modification Contributes to Quercetin-Induced Protection against Heart Failure and High-Glucose-Prompted Cardiomyocytes Injured through Regulation of Mitochondrial Quality Surveillance

Xing Chang , Tian Zhang , Junyan Wang, Yan Liu, Peizheng Yan , Qingyan Meng , Yongtian Yin , and Shiyuan Wang 
Research Article (17 pages), Article ID 5876841, Volume 2021 (2021)



Nicotinamide Riboside Alleviates Cardiac Dysfunction and Remodeling in Pressure Overload Cardiac Hypertrophy

Sai Ma , Jing Feng, Xiuyu Lin, Jing Liu, Yi Tang, Shinan Nie, Jianbin Gong, and Lei Wang 
Research Article (10 pages), Article ID 5546867, Volume 2021 (2021)


Molecular Dysfunctions of Mitochondria-Associated Endoplasmic Reticulum Contacts in Atherosclerosis

Xiaojiao Wang , Dan Luo , and Sisi Wu 
Review Article (8 pages), Article ID 2424509, Volume 2021 (2021)




Protective Effect of Mitochondrial ND2 C5178A Gene Mutation on Cell and Mitochondrial Functions

LiuYang Tian , Chao Zhu, Huanwan Yang, Yang Li, and Yuqi Liu 
Research Article (10 pages), Article ID 4728714, Volume 2021 (2021)


Structure and Function of Mitochondria-Associated Endoplasmic Reticulum Membranes (MAMs) and Their Role in Cardiovascular Diseases

Yi Luan, Ying Luan, Rui-Xia Yuan, Qi Feng, Xing Chen, and Yang Yang 
Review Article (19 pages), Article ID 4578809, Volume 2021 (2021)


Inhibiting miR-205 Alleviates Cardiac Ischemia/Reperfusion Injury by Regulating Oxidative Stress, Mitochondrial Function, and Apoptosis

Yuerong Xu, Wangang Guo, Di Zeng, Yexian Fang, Runze Wang, Dong Guo, Bingchao Qi, Yugang Xue, Feng Xue, Zuolin Jin , Yan Li , and Mingming Zhang 
Research Article (17 pages), Article ID 9986506, Volume 2021 (2021)





The Role of Mitochondrial Quality Control in Cardiac Ischemia/Reperfusion Injury

Jia Huang, Ruibing Li, and Chengbin Wang 
Review Article (13 pages), Article ID 5543452, Volume 2021 (2021)

Protective Effect of Optic Atrophy 1 on Cardiomyocyte Oxidative Stress: Roles of Mitophagy, Mitochondrial Fission, and MAPK/ERK Signaling

Yue Wang, Zhihua Han, Zuojun Xu, and Junfeng Zhang 
Research Article (15 pages), Article ID 3726885, Volume 2021 (2021)

BTK Promotes Atherosclerosis by Regulating Oxidative Stress, Mitochondrial Injury, and ER Stress of Macrophages

Junxiong Qiu , Yuan Fu, Zhiteng Chen, Lisui Zhang, Ling Li, Diefei Liang, Feng Wei, Zhuzhi Wen , Yajing Wang , and Shi Liang 
Research Article (15 pages), Article ID 9972413, Volume 2021 (2021)




The Downregulation of ADAM17 Exerts Protective Effects against Cardiac Fibrosis by Regulating Endoplasmic Reticulum Stress and Mitophagy

Chang Guan, Hai-Feng Zhang , Ya-Jing Wang, Zhi-Teng Chen, Bing-Qing Deng, Qiong Qiu, Si-Xu Chen, Mao-Xiong Wu, Yang-Xin Chen , and Jing-Feng Wang 
Research Article (11 pages), Article ID 5572088, Volume 2021 (2021)







Mitochondrial Dysfunction Contributes to Aging-Related Atrial Fibrillation

Chuanbin Liu, Jing Bai, Qing Dan, Xue Yang, Kun Lin, Zihao Fu, Xu Lu, Xiaoye Xie, Jianwei Liu, Li Fan, and Yang Li 
Research Article (13 pages), Article ID 5530293, Volume 2021 (2021)





Ketogenic Diet Suppressed T-Regulatory Cells and Promoted Cardiac Fibrosis via Reducing Mitochondria-Associated Membranes and Inhibiting Mitochondrial Function

Jun Tao, Hao Chen, Ya-Jing Wang, Jun-Xiong Qiu, Qing-Qi Meng, Rong-Jun Zou, Ling Li, Jun-Gang Huang, Zong-Kai Zhao, Yu-Li Huang , Hai-Feng Zhang , and Jun-Meng Zheng 
Research Article (15 pages), Article ID 5512322, Volume 2021 (2021)

Quercetin Improves Cardiomyocyte Vulnerability to Hypoxia by Regulating SIRT1/TMBIM6-Related Mitophagy and Endoplasmic Reticulum Stress

Xing Chang , Tian Zhang , Qingyan Meng, Shiyuan Wang, Peizheng Yan , Xue Wang, Duosheng Luo , XiuTeng Zhou , and Ruifeng Ji 
Research Article (14 pages), Article ID 5529913, Volume 2021 (2021)

RIPK3 Induces Cardiomyocyte Necroptosis via Inhibition of AMPK-Parkin-Mitophagy in Cardiac Remodelling after Myocardial Infarction


Pingjun Zhu , Kun Wan, Ming Yin, Peng Hu, Yifan Que, Xin Zhou, Lei Zhang, Tianzhi Li, Yingzhen Du , Guogang Xu , and Xiangqun Fang 
Research Article (11 pages), Article ID 6635955, Volume 2021 (2021)

Novel Insight into the Role of Endoplasmic Reticulum Stress in the Pathogenesis of Myocardial Ischemia-Reperfusion Injury

Hang Zhu and Hao Zhou 
Review Article (9 pages), Article ID 5529810, Volume 2021 (2021)

Contents

Bevacizumab-Induced Mitochondrial Dysfunction, Endoplasmic Reticulum Stress, and ERK Inactivation Contribute to Cardiotoxicity

Yue Li, Wei Tian, Dongsheng Yue, Chen Chen, Chenguang Li, Zhenfa Zhang, and Changli Wang 
Research Article (11 pages), Article ID 5548130, Volume 2021 (2021)




ZBTB20 Positively Regulates Oxidative Stress, Mitochondrial Fission, and Inflammatory Responses of ox-LDL-Induced Macrophages in Atherosclerosis

Jun Tao, Junxiong Qiu, Liuyi Lu, Lisui Zhang, Yuan Fu, Meng Wang, Jingjun Han, Maomao Shi, Ling Li, Zongkai Zhao, Feng Wei, Chao Wang, Haifeng Zhang , Shi Liang , and Junmeng Zheng 
Research Article (18 pages), Article ID 5590855, Volume 2021 (2021)


Ndufs1 Deficiency Aggravates the Mitochondrial Membrane Potential Dysfunction in Pressure Overload-Induced Myocardial Hypertrophy

Rongjun Zou , Jun Tao, Junxiong Qiu, Wanting Shi , Minghui Zou , Weidan Chen , Wenlei Li , Na Zhou , Shaoli Wang , Li Ma , and Xinxin Chen 
Research Article (21 pages), Article ID 5545261, Volume 2021 (2021)

Melatonin Attenuates ox-LDL-Induced Endothelial Dysfunction by Reducing ER Stress and Inhibiting JNK/Mff Signaling

Peng Li , Changlian Xie, Jiankai Zhong, Zhongzhou Guo, Kai Guo , and Qiuyun Tu 
Research Article (10 pages), Article ID 5589612, Volume 2021 (2021)

Coronary Endothelium No-Reflow Injury Is Associated with ROS-Modified Mitochondrial Fission through the JNK-Drp1 Signaling Pathway

Yi Chen, Chen Liu, Peng Zhou, Jiannan Li, Xiaoxiao Zhao, Ying Wang, Runzhen Chen, Li Song, Hanjun Zhao, and Hongbing Yan 
Research Article (11 pages), Article ID 6699516, Volume 2021 (2021)

Review Article

Mitochondria-Endoplasmic Reticulum Contacts: The Promising Regulators in Diabetic Cardiomyopathy

Yan Chen ¹, Yanguo Xin ², Yue Cheng ², and Xiaojing Liu ^{1,2}

¹Laboratory of Cardiovascular Diseases, Regenerative Medicine Research Center, West China Hospital, Sichuan University, Chengdu 610041, China

²Department of Cardiology, West China Hospital, Sichuan University, Chengdu 610041, China

Correspondence should be addressed to Xiaojing Liu; liuxq@scu.edu.cn

Received 16 April 2021; Revised 4 August 2021; Accepted 28 March 2022; Published 11 April 2022

Academic Editor: Abdur Rauf

Copyright © 2022 Yan Chen et al. This is an open access article distributed under the Creative Commons Attribution License, which permits unrestricted use, distribution, and reproduction in any medium, provided the original work is properly cited.

Diabetic cardiomyopathy (DCM), as a serious complication of diabetes, causes structural and functional abnormalities of the heart and eventually progresses to heart failure. Currently, there is no specific treatment for DCM. Studies have proved that mitochondrial dysfunction and endoplasmic reticulum (ER) stress are key factors for the development and progression of DCM. The mitochondria-associated ER membranes (MAMs) are a unique domain formed by physical contacts between mitochondria and ER and mediate organelle communication. Under high glucose conditions, changes in the distance and composition of MAMs lead to abnormal intracellular signal transduction, which will affect the physiological function of MAMs, such as alter the Ca^{2+} homeostasis in cardiomyocytes, and lead to mitochondrial dysfunction and abnormal apoptosis. Therefore, the dysfunction of MAMs is closely related to the pathogenesis of DCM. In this review, we summarized the evidence for the role of MAMs in DCM and described that MAMs participated directly or indirectly in the regulation of the pathophysiological process of DCM via the regulation of Ca^{2+} signaling, mitochondrial dynamics, ER stress, autophagy, and inflammation. Finally, we discussed the clinical transformation prospects and technical limitations of MAMs-associated proteins (such as MFN2, FUNDC1, and GSK3 β) as potential therapeutic targets for DCM.

1. Introduction

Diabetes mellitus (DM) is a metabolic disorder characterized by insulin resistance, hyperglycemia, and hyperlipidemia. DM-related complications affect multiple organs. DM causes cardiomyopathy and increases the risk of heart failure, independent of the traditional risk factors, such as hypertension, coronary artery disease, and valvular heart disease, which is clinically known as diabetic cardiomyopathy (DCM) [1]. DCM is a common complication of DM with a poor outcome [2]. The development of DCM is a gradual process. Early-stage DCM is characterized by structural and functional abnormalities, including cardiac hypertrophy, increased myocardial stiffness, myocardial fibrosis, and diastolic dysfunction. As DCM progresses, these abnormalities may lead to heart failure [3]. Effective therapeutic measures for DCM, especially specific therapeutic drugs, are lacking.

The pathophysiology of DCM is multifactorial. Several pathophysiological mechanisms, including hyperglycemia, energy metabolism disturbances, and inflammation, have been proposed. In addition, mitochondrial dysfunction and ER stress are known to be crucial factors in the development and progression of DCM [3] [4]. Both mitochondria and the ER are vital organs in cells, with the functions of mitochondria and the ER highly interconnected. Mitochondria are highly dynamic structures, with their morphologies and compositions constantly changing to meet cellular requirements [5]. They are connected to membranous organelles, including the ER. The contact sites between mitochondria and the ER are known as mitochondria-associated ER membranes (MAMs). MAMs are unique domains that mediate the tight connection between mitochondria and the ER [6]. MAMs serve as the essential hub for intraorganelle communication in cells.

Dysregulation of MAMs contributes to the etiology of many diseases. An increasing amount of data suggests that MAMs play significant roles in pathological conditions, including neurodegenerative disorders [7], metabolic diseases [8], and cardiovascular diseases [9], by regulating intraorganelle lipid exchange, calcium (Ca^{2+}) transfer, mitochondrial dynamics, ER stress, inflammation, autophagy, and apoptosis [10] and that these processes are involved in DCM. As such, MAMs are closely related to the pathophysiological mechanism of DCM.

In DM, destruction of the mitochondria-ER contacts in cardiomyocytes leads to dysfunction of several molecular pathways, thereby inducing cell death and cardiac dysfunction [11]. For example, knockout of MAM components such as Mitofusin 2 (MFN2) [12], inositol 1,4,5-triphosphate receptors (IP3R1), or cyclophilin D (CypD) [13] will interrupt MAM integrity and induce insulin resistance. The latter is closely related to mitochondrial dysfunction, ER stress, and altered Ca^{2+} homeostasis in DCM [11, 14]. Excessive mitochondria-ER coupling also has adverse effects, with recent research showing that enhancement of the MAM formation is involved in metabolic pathologies, such as insulin resistance and diabetes [15]. Therefore, a moderate but not excessive level of MAM formation is necessary for cell function.

We hypothesized that MAMs may be the promising regulator in the physiopathology of DCM. In the present review, we first introduce the structure and components of MAMs. We then we discuss the role of MAMs in DCM and summarize their emerging clinical use as potential biomarkers and therapeutic targets for DCM.

2. Structure of Mitochondria-ER Contacts

In 1990, Vance et al. described the components of membrane coupling between the ER and mitochondria in rat liver [16]. Since then, researchers have used a combination of electron microscopy and cell fluorescence microscopy to reveal the microstructure of MAMs. Using electronic tomography, researchers showed that the ER and mitochondria are connected by tethers and that the distance between the ER and mitochondria is approximately 25 nm for rough ER and approximately 10 nm for smooth ER [17]. Observations using a wide-field digital 3D deconvolution microscope showed that about 20% of the ER is in direct contact with the mitochondrial surface in MAMs [18].

It is important to consider the frequency and spacing between mitochondria and the ER in MAMs because they are dynamic structures, and the contacts and distance between mitochondria and the ER can vary widely under different cellular physiological conditions. The dynamic and flexible characteristics of MAMs results in a highly variable MAM composition. A proteomic study of MAM components showed that as many as 1212 proteins are localized in MAMs [19]. After excluding contaminated samples, approximately 75 proteins, including sorting proteins, chaperone proteins, and protein kinases, were shown to be associated with MAMs [20, 21].

MAMs have a unique structure, with a large number of proteins with various functions (Table 1). Figure 1 shows the key tethering protein complexes between mitochondria and the ER in mammalian cells (Figure 1). (I) The inositol 1,4,5-triphosphate receptor-glucose-regulated protein 75-voltage-dependent anion-selective channel 1 (IP3R-GRP75-VDAC1) complex is composed of IP3Rs in the ER and VDAC1 at the outer mitochondrial membrane (OMM). GRP75 is a chaperone. It bridges the IP3R and VDAC1 to maintain conformational stability and forms an ER-mitochondrial Ca^{2+} tunnel [22]. (II) MFN2 tethers the ER to mitochondria by forming heterotypic or homotypic complexes with MFN1 or MFN2 on the mitochondrial surface. These complexes mediate mitochondrial dynamics and mitochondrial Ca^{2+} uptake [23]. (III) The vesicle-associated membrane protein-associated protein B-protein tyrosine phosphatase interacting protein 51 (VAPB-PTPIP51) complex consists of the OMM protein PTPIP51 and the ER resident protein VAPB, which maintains ER-mitochondrial Ca^{2+} homeostasis [24]. (IV) The B-cell receptor-associated protein 31-mitochondrial fission 1 (BAP31-FIS1) complex is formed via the interaction of ER-localized BAP31 and mitochondrial FIS1, which participates in mitochondrial dynamics and cell apoptosis [25]. (V) Recently, another important protein bridge was reported, with the bridge formed through the interaction of the OMM human protein FUN14 domain-containing 1 (FUNDC1) with the IP3R2, which modulates the Ca^{2+} transport in the ER into mitochondria and maintains mitochondrial dynamics [26]. Various regulators modulate these tether complexes. For example, the IP3Rs-GRP75-VDAC1 complex is regulated by CypD, Sigma-1 receptor (Sig-1R), glycogen synthase kinase-3 β (GSK-3 β) and pyruvate dehydrogenase kinase 4 [27, 28].

Abnormality in MAMs resident proteins and regulators may be associated with the pathology of various diseases. For example, the insulin signaling protein AKT is located in MAMs, interacting with promyelocytic leukemia (PML)-protein phosphatase 2A (PP2A)-IP3R to form a large molecular complex in MAMs and controlled ER Ca^{2+} release [29]. Recently, a few of studies support that the presence of AKT regulate MAMs integrity [29–31]. Under DM condition or insulin resistance, an increased phosphorylation of AKT was found in the mice, which induces disruption of MAMs and may be the critical cause of Ca^{2+} disorder and mitochondrial dysfunction in DCM. Additionally, the key MAM proteins, VDAC1, CypD, and PACS2, decreased significantly in insulin-resistant mice [30], which suggest that MAMs are overtly altered under DCM condition; targeted regulation of these MAMs is expected to alleviate the disease to a certain extent.

In the future, more tethers and regulatory proteins will be identified between the mitochondria and the ER, and studies are required to investigate the alteration of MAMs resident proteins contributing to the pathogenesis of DCM.

3. The Role of MAMs in DCM

In this section, we consider MAM proteins and their regulators that play central roles in ER-mitochondrial crosstalk

TABLE 1: Summary of the functional MAMs proteins.

Functions	MAMs proteins	Relevant functions in MAMs	Reference	
Ca ²⁺ transfer	IP3R1/2/3	Interacts with VDAC via GRP75, a major actor in ER Ca ²⁺ release to mitochondria	[22]	
	VDAC1	Acts as a Ca ²⁺ uptake channel in the OMM	[22]	
	GRP75	Chaperone protein connects IP3R and VDAC to form VDAC1/GRP75/IP3R1 channel complex	[22]	
	PTPIP51	Interacts with VAPB at MAMs and regulates Ca ²⁺ homeostasis	[24]	
	VAPB	Interacts with PTPIP51 at MAMs and regulates Ca ²⁺ homeostasis	[24]	
	SERCA	Acts as an important pump involved in Ca ²⁺ transport into ER	[33]	
	Sig-1R	Generates a chaperone complex with BiP/GRP78 and prolongs Ca ²⁺ signaling stabilizing subunit 3 of IP3R	[105]	
	P53	Regulates SERCA activity and modulates ER-mitochondrial transfer	[106]	
	PML	Regulates Ca ²⁺ transfer and control apoptosis	[29]	
	Calnexin	Interacts with SERCA, regulating Ca ²⁺ transfer between contact sites	[107]	
	Cytc	Interacts with IP3Rs and regulate Ca ²⁺	[108]	
	Bcl-2	Inhibit the opening of IP3Rs and downregulate IP3R-mediated Ca ²⁺ flux	[109]	
	CYPD	A partner of the IP3R1-GRP75-VDAC1 complex and changes the MAM spatial structure	[30]	
	mTORC2	Regulates Ca ²⁺ signaling by Akt regulation	[110]	
	PP2A	Recruited by PML and inactivates AKT, facilitates IP3R-mediated Ca ²⁺ release	[29]	
	PTEN	PTEN regulates ER Ca ²⁺ release through type 3 IP3R in a protein phosphatase-dependent manner	[111]	
	Akt	Akt phosphorylates all IP3R isoforms and inhibits Ca ²⁺ release from the ER	[38]	
	GSK3 β	Regulates organelle Ca ²⁺ exchange	[37]	
	Mitochondrial dynamics	FUNDC1	Binding of FUNDC1 to IP3R2 at the MAMs increases the Ca ²⁺ concentration in both cytosol and mitochondrial matrix	[26]
		MFN2	Forms dimers with either MFN1 or MFN2 located on the mitochondria, controls the mitochondrial fusion	[23]
Bax		Interacts with MFN2 to promote mitochondrial fusion	[112]	
FUNDC1		Interacts with OPA1 to promote mitochondrial fusion; promote mitochondrial fission under hypoxic condition	[46]	
DRP1		Regulates mitochondrial fission	[18]	
INF2		Drives initial mitochondrial constriction	[50]	
MFF		Recruits DRP1 and regulates mitochondrial fission	[113]	
FIS1		Recruits DRP1 and regulates mitochondrial fission	[114]	
MiD49/51		Recruits DRP1 and regulates mitochondrial fission	[55]	
ATG14L		Acts as preautophagosome marker, induces autophagosome formation	[59]	
Autophagy	ATG5	Acts as autophagosome marker	[59]	
	PACS2	Knocking down PACS2 decreases the number of autophagosomes	[115]	
	MFN2	Knocking down MFN2 decreases the number of autophagosomes	[115]	
	VAPB	Regulates autophagy	[24]	
	PTPIP51	Forms a complex with VAPB to regulate autophagy	[24]	
	BECLIN1	Enhances the formation of MAMs and autophagosomes	[60]	
	PINK1	Promote ER-mitochondrial tethering and autophagosome formation	[60]	
Inflammation	NLRP3	NLRP3 inflammasome can be recruited to the MAM sites to sense mitochondrial damage	[70]	
	ASC	The adaptor of NLRP3	[70]	
	TXNIP	TXNIP activates NLRP3 inflammasome activation under mitochondrial oxidative stress conditions	[116]	
	PERK	Induces apoptosis after ROS-based ER stress	[117]	
	ER stress	IRE1 α	Responses to UPR stimulation; IRE1 α ubiquitylation at MAM hinder ER-stress-induced apoptosis	[118]
MFN2		Interacts with PERK and repress its activity	[78]	

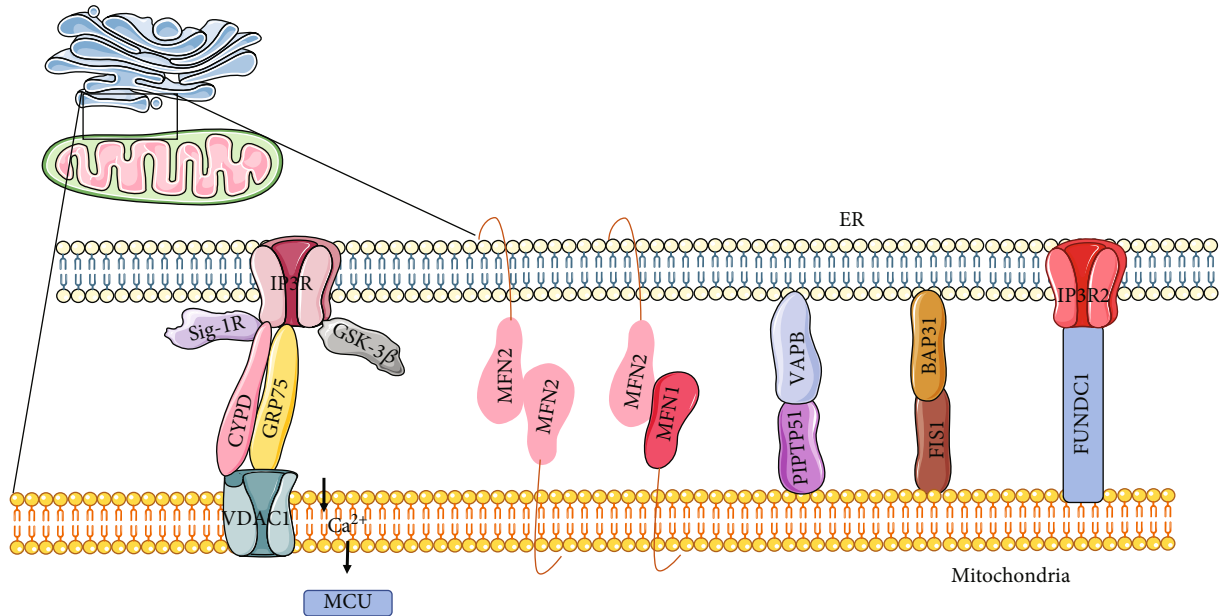


FIGURE 1: A core subset of mitochondria-ER tethering complexes in mammalian cells. IP3R, an ER protein, interacts OMM-localized protein VDAC1 via GRP75. The Sig-1R and GSK3 β interact with IP3Rs-GRP75-VDAC1 complex. MFN2 on the ER tethers the ER to mitochondria by forming complexes with MFN1 or MFN2 on the mitochondrial surface. An ER resident protein, VAPB interacts with the OMM protein PTP51. BAP31, an ER protein, interacts with the mitochondria FIS1. The ER resident IP3R2 interacts the mitochondrial protein FUNDC1. IP3R, inositol 1,4,5-triphosphate receptor; VDAC1, voltage-dependent anion-selective channel; GRP75, glucose-regulated protein 75; MFN2, Mitofusin 2; MFN1, Mitofusin 2; VAPB, vesicle-associated membrane protein-associated protein B; PTP51, protein tyrosine phosphatase interacting protein 51; BAP31, B-cell receptor-associated protein 31; FIS1, mitochondrial fission 1; FUNDC1, FUN14 domain containing 1.

(Table 1). In DM condition, destruction of MAMs integrity in cardiomyocytes directly or indirectly causes imbalances in several biological processes, which may explain the metabolic abnormalities in DCM.

3.1. MAMs Regulate Ca²⁺ Transfer in DCM. Mitochondria and the ER (sarcoplasmic reticulum in muscle cells) are the main organelles that regulate Ca²⁺ homeostasis in cells. Mitochondrial Ca²⁺ uptake is dependent on close binding of MAM-mediated ER to mitochondria [32]. The sarcoplasmic reticulum (SR)/ER Ca²⁺ ATPase (SERCA) is greatly enriched in MAMs, which is an ER membrane influx transporter through which Ca²⁺ from the cytoplasm is transported to the ER [33]. Ca²⁺ from the ER is transferred to mitochondria through MAMs [22] and then enters the mitochondrial matrix through the mitochondrial calcium uniporters (MCUs) [34]. In this process, the distance of the ER and mitochondria is a key parameter for Ca²⁺ transport. At shorter distances, Ca²⁺ transport is more efficient. Conversely, Ca²⁺ transport becomes less efficient as the distance increases [35]. Among MAM tethering protein complexes, IP3R-GRP75-VDAC1 is the most important tethering complex mediating Ca²⁺ efficient transfer in MAMs. The releases of Ca²⁺ from the ER to the OMM through the IP3R-GRP75-VDAC1 channel leads to local inflow of Ca²⁺ in the mitochondrial intermembrane space and the formation of a microdomain of high Ca²⁺ close to MCUs, which facilitates the mitochondrial Ca²⁺ uptake by MCU [36]. As shown in recent studies, the IP3R-GRP75-VDAC1 complex also acts

as a molecular scaffold for several other proteins, such as glycogen synthase kinase-3 β (GSK-3 β) [37], protein kinase B (PKB)/Akt [38], and promyelocytic leukemia (PML) [29]. These proteins are crucial for the fine tuning of Ca²⁺ signaling via IP3R-GRP75-VDAC1 axis (Table 1).

Due to its role in excitation-contraction coupling in muscle tissue, Ca²⁺ signaling is crucial for heart function, and Ca²⁺ disturbance mediated by destruction of the integrity of MAMs is closely associated with cardiac dysfunction in DCM. Interaction between several cellular Ca²⁺ transporter complexes controls the diastolic and systolic functions of the myocardium. During diastole, myocardial relaxation occurs due to reuptake of Ca²⁺ into the SR via SERCA2a [14]. In diabetes, reduced activity and expression of SERCA2a [14]. In diabetes, reduced activity and expression of SERCA2a in cardiomyocytes result in altered Ca²⁺ handling, which leads to impairment of left ventricular diastolic function and the development of DCM [39]. Disordered Ca²⁺ transfer through MAMs is the crucial cause for DCM. In the early stage of DCM, a reduced formation of the IP3R-GRP75-VDAC1 Ca²⁺ channeling complex and decreased IP3R-stimulated Ca²⁺ transfer to mitochondria trigger mitochondrial dysfunction [40]. A decrease in the ER-mitochondrial Ca²⁺ transfer leads to insufficient mitochondrial bioenergetics to match the energy demand for normal heart contraction [40]. However, inconsistent finding on the role of Ca²⁺ transport in DCM has been reported. Hu et al. reported that a high glucose level enhances the connections between the SR and mitochondria and increases the efficiency of Ca²⁺ transfer, which

causes Ca^{2+} overload in mitochondria [41]. Wu's study showed that FUNDC1 is important in mediating MAMs formation in diabetes, with high glucose increasing FUNDC1 levels, IP3R2 levels, and MAMs formation, resulting in increased Ca^{2+} levels, mitochondrial dysfunction, and deterioration of cardiac function [11]. High glucose increases MAMs-associated FUNDC1 levels by downregulating AMP-activated protein kinase (AMPK). And binding of FUNDC1 to the IP3R2 inhibits IP3R2 ubiquitination and proteasome-mediated degradation, which promotes contacts between the ER and mitochondria, resulting in increased Ca^{2+} transport and a decline in the mitochondrial membrane potential [11]. These events trigger long-term mitochondrial permeability transition pore (mPTP) opening and cell apoptosis by promoting mitochondrial Ca^{2+} uptake [42] (Figure 2(a)). We hypothesize that this inconsistent result of Ca^{2+} homeostasis in DCM is due to different severities and stages of the disease.

According to the literature, MFN2 regulates Ca^{2+} transfer in high glucose conditions, with high glucose upregulating the expression of MFN2, decreasing the distance between the ER and mitochondria, and increasing mitochondrial Ca^{2+} uptake in atrial cardiomyocytes [43]. And knocking down MFN2 significantly disrupted ER-mitochondrial tethering and decreased the Ca^{2+} transportation, thereby preventing mitochondrial dysfunction and cell death [43]. However, there is still controversy regarding the role of MFN2. Filadi et al. demonstrated that MFN2 ablation or silencing increased the ER-mitochondrial contacts, enhancing Ca^{2+} transfer between the two organelles, with the function of MFN2 similar to that of a tethered antagonist [44]. The use of different physiological conditions, cell types, and experimental approaches may explain the discord in the literature on the role of MFN2 in DCM. However, the detailed mechanism of how MFN2 participates in the Ca^{2+} transport in DCM is still unclear. In addition to mediating the spatial distance from the ER to mitochondria and affecting the transport efficiency of Ca^{2+} , it is interesting to explore whether it forms a complex with Ca^{2+} channel proteins. The exact mechanism of MFN2 in DCM deserves to be further investigated.

3.2. MAMs Modulate Mitochondrial Dynamics in DCM. Mitochondria are highly dynamic organelles, and balancing mitochondrial dynamics is essential to maintain heart function in response to metabolic or environmental stresses [5]. Various GTPases are involved in the regulation of mitochondrial dynamics, including dynamin-like GTPases optic atrophy 1 (OPA1), which plays a role in inner mitochondrial membrane (IMM) fusion, together with MFN1 [45]. FUNDC1 interacts with OPA1 to coordinate mitochondrial fusion [46]. Under normal physiological conditions, FUNDC1 anchor OPA1 to the inner surface of OMM through its charged lysine residue. Mitochondrial stresses disrupt the connection of FUNDC1 and OPA1 and induce OPA1 cleavage or even degradation, which promotes mitochondrial fission [46]. Extracellular hyperglycemia and metabolic dysregulation create an energy stress in DCM, which reduce the interaction of OPA1 and FUNDC1, increasing mitochondrial fragmentation. MFN1 and MFN2 are crucial for the fusion of

OMM [23], with deletion of MFN1 or MFN2 reduces the mitochondrial fusion rate [47]. In DCM, downregulation of MFN2 contributes to unbalanced mitochondrial dynamics and mitochondrial dysfunction [48]. The downregulation of MFN2 is partly attributed to the decreased expression of the peroxisome proliferator-activated receptor alpha (PPAR α) caused by the lipid metabolism disorder in DCM [49] (Figure 2(b)). Reconstitution of MFN2 improves mitochondrial function by promoting mitochondrial fusion [48]. Accordingly, modulation of mitochondrial dynamics by regulating MFN2 might be a potentially effective target for DCM treatment.

Dynamin-related protein 1 (DRP1) plays a central role in mitochondrial fission [18]. DRP1 is a cytoplasmic protein that can be recruited from the cytosol to the OMM, which is a critical step in the fission process. Friedman et al. showed that MAM is an important platform for mitochondrial fission. In their study, they demonstrated oligomerization and translocation of DRP1 to MAMs, where it induced fission events [18]. Subsequent studies revealed the mechanism that MAMs participate in initial mitochondria contraction. This mechanism involves ER-localized inverted formin 2 (INF2) inducing actin polymerization, which promotes MAMs formation, facilitating Ca^{2+} transfer from ER to mitochondria, followed by IMM contraction and initial mitochondrial constriction. This is followed by DRP1-driven secondary constriction, which completes the fission process [50, 51].

In patients diagnosed with diabetes, myocardial contractile dysfunction is closely associated with mitochondria fission. In diabetes, increased expression of DRP1 initiates mitochondrial fission. Conversely, decreased expression of DRP1 decrease alleviates mitochondrial dysfunction and cardiac dysfunction [52]. Mechanically, lipid overload decreased NAD^+ levels and increased the acetylation of DRP1 at a specific lysine residue (K642). A DRP1 point mutation, K642E, appears to reverse the impact of lipid toxicity. Excessively activation of DRP1 results in DRP1 translocated to mitochondria, induces mPTP and apoptosis, and compromises cardiomyocyte contractile function via VDAC1 [53].

Several proteins have been shown to regulate DRP1 activity at MAMs. Under normal physiological condition, mitochondrial FIS1, mitochondrial fission factor, and mitochondrial dynamics proteins of 49/51 kDa have been reported to recruit DRP1 during mitochondrial fission [54, 55]. Regulating DRP1 activity by handing these molecules at contact site may be an appropriate strategy to prevent the abnormal mitochondrial fission and mitochondrial dysfunction-related DCM.

Despite the high abundance of fusion and fission regulatory proteins in the heart, mitochondria in adult cardiomyocytes exhibit static morphology and infrequent dynamic changes. These fusion and fission proteins may have functions beyond morphology regulation, or they may regulate cardiac function in DCM by regulating the mitochondrial dynamics of other cells in the heart, such as cardiac fibroblasts. As shown by Zhang et al. [56], they pointed to a novel noncanonical function of DRP1, in which DRP1 maintained or positively stimulated mitochondria respiration, biogenetics, and reactive

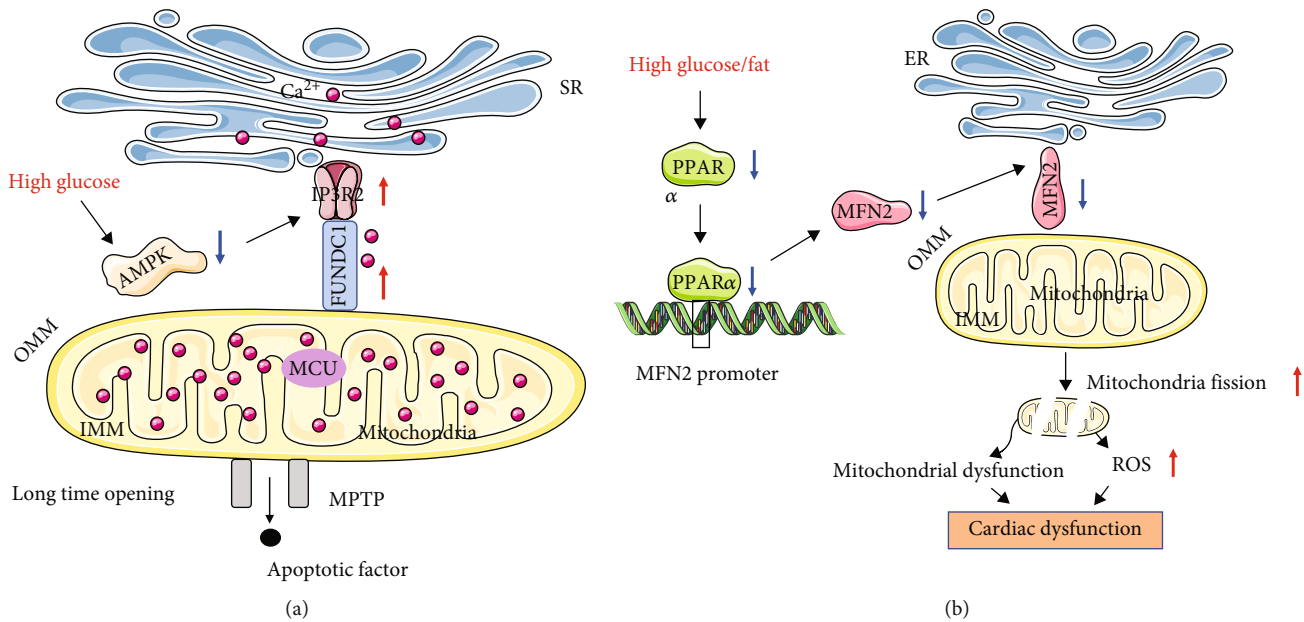


FIGURE 2: (a). The role of FUNDC1 and MFN2 in DCM. Under high glucose condition, FUNDC1 is upregulated by AMPK inactivation. The upregulated FUNDC1 increases MAMs formation by interacts with IP3R2. The increased MAMs contribute to the increased mitochondrial Ca²⁺ uptake, which induce the long-time opening of mPTP and trigger cell apoptosis. (b). High glucose or high fat reduces the PPARα expression. PPARα directly binding to MFN2 promoter and decreases the expression of MFN2. The downregulation of MFN2 induces mitochondrial fission and leads to the ROS production, which cause mitochondrial dysfunction and cardiac dysfunction. MFN2, Mitofusin 2; FUNDC1, FUN14 domain containing 1; AMPK, AMP-activated protein kinase; IP3R2, inositol 1,4,5-triphosphate receptor 2; PPARα, peroxisome proliferator-activated receptor alpha.

oxygen species (ROS) signaling in adult cardiomyocytes, independent of morphological changes. In DCM, whether the fusion and fission proteins function through other mechanisms independent of mitochondrial dynamics remains to be elucidated.

3.3. MAMs Regulate Autophagy in DCM. Autophagy is an evolutionarily conserved lysosome-mediated degradation process that has fundamental roles in cellular homeostasis. Autophagosome and autolysosome formation are key processes in autophagy, which are mediated by autophagy-related genes (ATGs) [57, 58]. Autophagosome formation at MAMs in mammalian cells has been reported, with preautophagosome marker, autophagy-related 14-like, and the omega-gasome marker double FYV1 domain-containing protein1, localized in MAMs initiating autophagosome formation [59]. Another autophagosome formation marker, autophagy-related 2/5 (ATG2/5), also localizes at contact sites until the autophagy process is completed [59]. In addition, Beclin-1, a pro-autophagic protein localized in MAMs, plays a role in autophagosome formation and the autophagy process [60]. Inducing MAM dysfunction by knockout of MFN2 or PACS2 decreases the number of autophagosomes, and MFN2 deficiency impairs autophagosome-lysosome fusion [61]. Hu et al. have also shown that AMPK interacts directly with MFN2 to increase MAM numbers and induce autophagy [62]. Thus, these facts indicated that MAMs play key roles in the induction and execution of autophagy.

Autophagy is a double-edge sword, and basal autophagy is beneficial to the heart, whereas insufficient autophagy or

excessive autophagy may promote pathological cardiomyopathy [63]. Previous studies reported that cardiac autophagy was suppressed in diabetes, accompanied by decrease in ATG5 and Beclin-1 expression levels [64]. However, the role of autophagy in DCM is controversial, as another study pointed to an increase in cardiac autophagy in type 2 diabetes through a Beclin-1-mediated pathway [65]. This discord in the findings is likely related to the unresolved question of whether an accumulation of autophagosomes in cells is the result of upregulation of autophagy or blockade of autophagic flux. As the autophagy process is highly dynamic, quantification of autophagy becomes a challenge [66]. It is important to consider not only the number of intracellular autophagosomes but also the autophagic degradative activity and autophagic flux. As reported previously, increased autophagic flux alleviates diabetes-induced cardiac injury [67]. Thus, autophagic flux insufficiency, resulting in maladaptive cardiac remodeling, should be considered a pivotal pathology in DCM [68].

3.4. MAMs Regulate Inflammasome in DCM. The crucial role of inflammation in the pathogenesis of DCM is widely recognized. Inflammasomes comprise innate immune system receptors and sensors, which are activated in response to cellular stress and trigger the maturation of proinflammatory cytokines and the immune response [69]. To date, NOD-like receptor pyrin domain-containing 3 (NLRP3) is the sole inflammasome reported to be associated with MAMs, and it comprises NLRP3 protein, the adapter apoptosis-associated speck-like protein containing a C-

terminal caspase recruitment domain (ASC) and procaspase-1. Under normal physiological conditions, NLRP3 is localized in the cytosol. When inflammasome is activated, the NLRP3 protein and its adaptor ASC are recruited to MAMs and are activated by MAM-derived effectors [70]. The NLRP3 inflammasome is activated by saturated fatty acids, ceramides, modified low density lipoprotein, and hyperglycemia in obesity and type 2 diabetes [71]. Continuous activation of inflammasomes ultimately leads to cardiac dysfunction [72]. In DCM, an early inflammatory response occurs as a protective mechanism against hyperglycemia. If hyperglycemia continues, a chronic inflammatory response will eventually lead to cardiomyocyte hypertrophy, apoptosis, and myocardial fibrosis [73].

The NLRP3 inflammasome recognizes signs of cellular stress, such as mitochondrial ROS production and Ca^{2+} signaling from damaged cells. Sustained influx of Ca^{2+} into the mitochondria via MAMs triggers mPTP opening, releasing risk-associated molecular patterns, finally leading to the activation of the NLRP3 inflammasome [70]. Yin et al. suggested that ROS could promote NLRP3 inflammasome activation [74]. Zhou et al. showed that mitophagy/autophagy blockade led to the accumulation of ROS, which activated the NLRP3 inflammasome [70]. Therefore, mitochondrial ROS and Ca^{2+} signaling pathways in MAMs are closely bound up with inflammasome activity. Based on the literature, Ca^{2+} communication between mitochondria and the ER may link MAMs to NLRP3 inflammasome activation in DCM. More research is needed to investigate the link of MAMs and inflammasome in DCM.

3.5. MAMs Regulate ER Stress in DCM. The ER plays a vital role in proteins folding. Disruption of ER homeostasis leads to an accumulation of misfolded proteins in the lumen, which triggers unfolded protein response (UPR) and ER stress. The stimulation of the UPR is sensed predominantly by three transmembrane proteins, protein kinase RNA-like endoplasmic reticulum kinase (PERK), inositol-requiring protein 1 (IRE1 α), and activating transcription factor 6 (ATF6), which regulate the protein folding ability of ER [75]. Substantial evidence suggests that ER stress is a key mechanism in the development and progression of DCM. Continuous activation of the UPR mediates upregulation of apoptosis-related gene expression by affecting mitochondrial function, which eventually leads to apoptosis of cardiomyocytes and deterioration of cardiomyopathy.

IRE1 α is expressed mainly in the MAMs, where it binds to the Sigma-1 receptor (Sig1R). Our previous study reported that the IRE1 pathway mediated the stimulatory effect of Sig1R on cardiac fibroblast activation [76]. The PERK signaling pathway plays a key role in ROS-mediated ER stress in DCM [77]. Previous research showed that MFN2 physically interacts with PERK and negatively regulates its activity [78]. Gao et al. indicated that with the aggravation of oxidative stress injury in DM, the cardiac MFN2 mRNA level decreased [79]. A recent study revealed that in high glucose (HG)-induced podocytes, HG activated the PERK pathway by downregulating MFN2 expression and reducing MFN2-PERK interaction [80]. Therefore, we spec-

ulate that the downregulation of MFN2 in cardiomyocytes under high glucose environment may lead to dissociation and continuous activation of PERK, which subsequently initiates UPR and ER stress.

4. MAMs Targeting as a Potential Therapeutic Strategy

4.1. Current Drugs in Treatment of DCM. Metformin is widely used to treat type 2 diabetes. A large-scale prospective study of 1,519 type 2 diabetes mellitus (T2DM) patients with heart failure indicated that treatment with metformin reduces cardiovascular mortality in this patient population [81]. In a preclinical study that examined the effect of metformin treatment for 4 months in type 1 diabetes mice, the authors observed clear improvements in the systolic and diastolic function of the heart [82].

The major mechanism of action of metformin is activation of AMPK [83]. In this review, we focus mainly on metformin's therapeutic effect on DCM through the MAMs proteins-related pathways. The NLRP3 inflammasome is activated in DCM, and AMPK inhibits NLRP3 expression by initiating autophagy. In DCM, metformin exerts cardioprotective and anti-inflammatory effects by activating AMPK autophagy pathway and inhibiting the NLRP3 inflammasome [53]. AKT and GSK3 β are essential MAM components. Yang et al. showed that metformin ameliorates high glucose-induced cardiac damage through the AKT-GSK3 β pathway in high glucose-exposed cardiomyocytes and animal models of diabetes [84]. Combined treatment with metformin and atorvastatin attenuated DCM by inhibiting oxidative stress and the impression of inflammation-related proteins, such as NLRP3, caspase-1, and 1L-1 β . Combination therapy also restrained the apoptosis of cardiomyocytes by decreasing the expression of pro-apoptotic related proteins, including caspase-3 and BAX [85].

Sodium-glucose co-transporter 2 (SGLT2) inhibitors, such as empagliflozin, dapagliflozin, and canagliflozin, also serves as potential antidiabetic agents. In a cardiac magnetic resonance imaging study of changes in cardiac structure and function in 25 patients with T2DM, 6-month treatment with empagliflozin lowered left ventricle end diastolic volume compared to that in a control group [86]. Empagliflozin also suppressed oxidative stress and fibrosis by activating Nrf2/ARE signaling, as well as inactivating the TGF- β /SMAD pathway [87]. In 37 patients (25 males and 12 females) with T2DM, 32% of whom had pre-existing cardiovascular diseases, a 3-month treatment with canagliflozin significantly improved the left ventricular diastolic function [88]. Treatment with dapagliflozin for 6 months in 58 T2DM patients with stable heart failure appeared to have beneficial effects on left ventricle diastolic function [89]. Dapagliflozin reduced NLRP3/ASC inflammasome activation and activated AMPK both *in vivo* and *in vitro*. Attenuation of the NLRP3 inflammasome activation depends on AMPK activation [90]. In addition to activating AMPK, dapagliflozin has been identified activating mTOR [91]. Large-scale clinical trials aiming at investigating the impact of SGLT2 inhibitors on DCM are needed.

The glucagon-like peptide-1 receptor (GLP-1R) agonist is used to treat advanced stage T2DM. Preclinical studies have indicated that GLP-1R agonists, including exendin-4 and liraglutide, induce robust cardio protection [92, 93]. Exendin-4 relieves mitochondrial oxidative stress in diabetic heart. In models of T2DM models, the MFN1/MFN2 ratio was reduced in exendin-4-treated group [94]. Exendin-4 and liraglutide also protected cardiomyocytes under high glucose condition. High glucose incubation of cardiomyocytes significantly upregulated the expression of proapoptotic factor, but exendin and liraglutide abrogated this effect. These two drugs activate autophagy through the classical mTOR/ULK1-dependent pathway [95]. Younce et al. reported that exendin-4 attenuated high glucose-induced cardiomyocyte apoptosis in association with decreased ER stress and enhanced the activity of SERCA2a [96]. In addition, lipid regulation of GLP-1R agonists may improve diastolic function and attenuate diabetic cardiomyopathy. Wu et al. showed that exendin-4 improved the structure and function of diabetic hearts by inhibiting PPAR α -mediated lipid accumulation and toxicity regulated by the PKA/ROCK pathway [97].

Melatonin is widely used to treat insomnia and sleep disorders. Notably, the cardioprotective effects of melatonin have been described [98, 99]. Recent research confirms that melatonin acts as a regulator of MAMs. Application of melatonin inhibits IP3R, stabilizing the physical contacts between mitochondria and ER, and thus improving mitochondrial function and reducing cardiomyocytes damage. Moreover, some other MAM markers, Fis1, BAP31, and MFN2, were also inhibited by melatonin [100]. These data suggest that melatonin-induced cardioprotective effect is mediated via normalization of mitochondria-ER interaction.

4.2. Potential Targets. MFN2 was originally thought to be a mitochondrial protein that mediated OMM fusion. Recent research suggests that MFN2 appears to have a variety of roles in a nonfusion way. For example, MFN2 tether the ER to the mitochondria for Ca²⁺ signaling from the ER to mitochondria. MFN2 ablation or reduction increases the physical distance between mitochondria and the ER and disturb mitochondrial Ca²⁺ uptake [23, 44]. MFN2 is also involved in the cardiac autophagic process. Deficiency of MFN2 impairs autophagosome-lysosome fusion and leads to cardiac vulnerability and dysfunction [61]. Hu demonstrated that MFN2 expression is reduced in diabetic hearts, resulting in excessive mitochondrial fission, leading to mitochondrial dysfunction in DCM [48]. Reconstitution of MFN2 promotes mitochondrial fusion and alleviated mitochondrial dysfunction, consequently inhibiting the development of DCM [48]. Taken together, these findings suggest that regulation of MFN2 might be a potentially effective strategy for DCM treatment.

FUNDC1, an OMM protein, is highly conserved across species from drosophila to humans and highly expressed in cardiac muscle [26]. Diabetes increases FUNDC1 expression and aberrant MAM formation in cardiomyocytes, resulting in an increase in mitochondrial Ca²⁺ levels, mitochondrial dysfunction, and cardiac dysfunction. Cardiac-specific dele-

tion of FUNDC1 improves mitochondrial function and attenuates cardiomyopathy in diabetic mice, confirming the causative role of FUNDC1 in this disorder [11]. However, there is some controversy regarding the role FUNDC1. According to Ren et al., FUNDC1 deficiency accentuated high fat diet-induced cardiac anomalies, including cardiac remodeling and intracellular Ca²⁺ mishandling [101]. The discord in the findings may be due to differences in the expression of FUNDC1 in different stages of DCM disease progression. As mentioned above, the development of DCM is a gradual process. During this process, it is likely that FUNDC1 expression may first increased and then decreased or vice versa. In conditions like DCM, where the disease progresses over time, the findings of these two studies may not necessarily be contradictory. Despite the discord in the findings, both studies prove that FUNDC1 is an extremely important regulator in DCM. FUNDC1 also interacts with OPA1 to coordinate mitochondrial fusion under normal conditions [46]. We speculate that extracellular hyperglycemia and metabolic dysregulation in DCM might reduce the interaction of OPA1 and FUNDC1, thereby increasing mitochondrial fragmentation. These findings collectively support the unique role of FUNDC1 as a powerful therapeutic target in DCM.

GSK3 β is a multifunctional kinase. A fraction of GSK3 β is localized to the MAM in the heart, where it specifically interacts with the IP3R Ca²⁺ channeling complex in MAMs. Apoptosis of cardiomyocytes in DCM involves overexpression of GSK3 β [102]. Pharmacological or genetic inhibition of GSK3 β may decrease the cardiomyocytes apoptosis of T2DM patients.

5. Conclusions

MAMs connect two important organelles (the ER and mitochondria), which have important roles in cellular functions. The importance of the contacts between the ER and mitochondria in the pathogenesis of DCM has been recognized. Several MAM-related proteins participate directly or indirectly in the regulation of the pathophysiological process of DCM via the regulation of lipids synthesis, insulin signaling, Ca²⁺ signaling, mitochondrial dynamics, ER stress, autophagy, and inflammation. Targeting MAMs could lead to the development of more efficient pharmacological approaches and potential biomarkers for the treatment of DCM.

Currently, various existing antidiabetic drugs, such as metformin, SGLT2 inhibitors, and GLP-1 agonists, provide significant cardiovascular protection in both animal models and patients with DCM, and these drugs represent the primary treatment options for patients with DCM. Several MAM proteins, such as MFN2, FUNDC1, and GSK3 β , have been identified that play key roles in DCM. These proteins may have clinical applications as therapeutic targets and intervention strategies in DCM. In addition, several herbal compounds are known to regulate MAM and thus might have potential in DCM treatment. For example, Shengmai injection, a tradition Chinese herbal medicine extracted from Panax ginseng C.A. Mey., *Ophiopogon japonicus* (Thunb.) Ker Gawl., and *Schisandra chinensis* (Turcz.) Baill.,

can activate the AMPK signaling pathway [103]. As AMPK regulates FUNDC1 expression, targeting AMPK may provide a cardioprotective effect. Moreover, obacunone, a natural bioactive compound isolated from the Rutaceae family, downregulates the activity of GSK-3 β , which may target on MAMs to stabilize the mitochondrial membrane potential [104]. Taken together, these findings provide strong evidence that MAMs may be the crucial target of DCM.

There are a number of unanswered questions surrounding the potential of MAMs as therapeutic targets in DCM. First, the pathways or mechanisms of some MAM proteins in DCM have not been clearly explained, even some contradictory views appeared in different researches. Second, the cell types and intervention methods in addition to the carriers, dosages, and targeted treatment sites differ from different researches. Third, current research is limited to *in vitro* cell experiments and animal experiments, and clinical studies are some ways off yet. Uniform research standards and intervention methods are necessary to further explore the functional mechanisms, clinical efficacy, and long-term effects of MAMs in DCM. In the future, more tether proteins will likely be identified between the ER and mitochondria. Further studies are required to shed light on how changes in activity of MAMs resident proteins contribute to the pathogenesis of DCM and how these proteins are expected to be clinically attractive therapeutic strategies.

Conflicts of Interest

The authors declare that they have no conflicts of interest.

Authors' Contributions

Yan Chen drafted and proofread the manuscript. Yanguo Xin edited the manuscript. Xiaojing Liu determined the theme and innovation. Yue Cheng revised the manuscript. All authors have agreed upon the submission and publication of this work. Yan Chen and Yanguo Xin contributed equally to this work.

Acknowledgments

This work was supported by grants from the National Natural Science Foundation of China (No. 12072215) and the Science and Technology Program of Sichuan Province (No. 2021YFS 0120).

References

- [1] T. J. Regan, M. M. Lyons, S. S. Ahmed et al., "Evidence for cardiomyopathy in familial diabetes mellitus," *The Journal of Clinical Investigation*, vol. 60, no. 4, pp. 884–899, 1977.
- [2] B. Bozkurt, D. Aguilar, A. Deswal et al., "Contributory risk and management of comorbidities of hypertension, obesity, diabetes mellitus, hyperlipidemia, and metabolic syndrome in chronic heart failure: a scientific statement from the American Heart Association," *Circulation*, vol. 134, no. 23, pp. e535–e578, 2016.
- [3] G. Jia, M. A. Hill, and J. R. Sowers, "Diabetic cardiomyopathy: an update of mechanisms contributing to this clinical entity," *Circulation Research*, vol. 122, no. 4, pp. 624–638, 2018.
- [4] R. H. Eckel, K. E. Bornfeldt, and I. J. Goldberg, "Cardiovascular disease in diabetes, beyond glucose," *Cell Metabolism*, vol. 33, no. 8, pp. 1519–1545, 2021.
- [5] R. J. Youle and A. M. van der Bliek, "Mitochondrial fission, fusion, and stress," *Science*, vol. 337, no. 6098, pp. 1062–1065, 2012.
- [6] R. Filadi, P. Theurey, and P. Pizzo, "The endoplasmic reticulum-mitochondria coupling in health and disease: molecules, functions and significance," *Cell Calcium*, vol. 62, pp. 1–15, 2017.
- [7] S. Paillusson, R. Stoica, P. Gomez-Suaga et al., "There's something wrong with my MAM; the ER-mitochondria axis and neurodegenerative diseases," *Trends in Neurosciences*, vol. 39, no. 3, pp. 146–157, 2016.
- [8] E. Tubbs and J. Rieusset, "Metabolic signaling functions of ER-mitochondria contact sites: role in metabolic diseases," *Journal of Molecular Endocrinology*, vol. 58, no. 2, pp. R87–r106, 2017.
- [9] P. Gao, Z. Yan, and Z. Zhu, "Mitochondria-associated endoplasmic reticulum membranes in cardiovascular diseases," *Frontiers In Cell And Developmental Biology*, vol. 8, article 604240, 2020.
- [10] G. Csordás, D. Weaver, and G. Hajnóczky, "Endoplasmic reticulum-mitochondrial contactology: structure and signaling functions," *Trends in Cell Biology*, vol. 28, no. 7, pp. 523–540, 2018.
- [11] S. Wu, Q. Lu, Y. Ding et al., "Hyperglycemia-driven inhibition of AMP-activated protein kinase $\alpha 2$ induces diabetic cardiomyopathy by promoting mitochondria-associated endoplasmic reticulum membranes *in vivo*," *Circulation*, vol. 139, no. 16, pp. 1913–1936, 2019.
- [12] D. Sebastián, M. I. Hernández-Alvarez, J. Segalés et al., "Mitofusin 2 (Mfn2) links mitochondrial and endoplasmic reticulum function with insulin signaling and is essential for normal glucose homeostasis," *Proceedings of the National Academy of Sciences of the United States of America*, vol. 109, no. 14, pp. 5523–5528, 2012.
- [13] J. Rieusset, J. Fauconnier, M. Paillard et al., "Disruption of calcium transfer from ER to mitochondria links alterations of mitochondria-associated ER membrane integrity to hepatic insulin resistance," *Diabetologia*, vol. 59, no. 3, pp. 614–623, 2016.
- [14] L. T. Al Kury, "Calcium homeostasis in ventricular myocytes of diabetic cardiomyopathy," *Journal Diabetes Research*, vol. 2020, article 1942086, 12 pages, 2020.
- [15] A. P. Arruda, B. M. Pers, G. Parlakgöl, E. Güney, K. Inouye, and G. S. Hotamisligil, "Chronic enrichment of hepatic endoplasmic reticulum-mitochondria contact leads to mitochondrial dysfunction in obesity," *Nature Medicine*, vol. 20, no. 12, pp. 1427–1435, 2014.
- [16] J. E. Vance, "Phospholipid synthesis in a membrane fraction associated with mitochondria," *The Journal of Biological Chemistry*, vol. 265, no. 13, pp. 7248–7256, 1990.
- [17] G. Csordás, C. Renken, P. Varnai et al., "Structural and functional features and significance of the physical linkage between ER and mitochondria," *The Journal of Cell Biology*, vol. 174, no. 7, pp. 915–921, 2006.
- [18] J. R. Friedman, L. L. Lackner, M. West, J. R. DiBenedetto, J. Nunnari, and G. K. Voeltz, "ER tubules mark sites of

- mitochondrial division,” *Science*, vol. 334, no. 6054, pp. 358–362, 2011.
- [19] C. N. Poston, S. C. Krishnan, and C. R. Bazemore-Walker, “In-depth proteomic analysis of mammalian mitochondria-associated membranes (MAM),” *Journal of Proteomics*, vol. 79, pp. 219–230, 2013.
- [20] A. Raturi and T. Simmen, “Where the endoplasmic reticulum and the mitochondrion tie the knot: the mitochondria-associated membrane (MAM),” *Biochimica et Biophysica Acta*, vol. 1833, no. 1, pp. 213–224, 2013.
- [21] C. Li, L. Li, M. Yang, L. Zeng, and L. Sun, “PACS-2: a key regulator of mitochondria-associated membranes (MAMs),” *Pharmacological Research*, vol. 160, article 105080, 2020.
- [22] G. Szabadkai, K. Bianchi, P. Várnai et al., “Chaperone-mediated coupling of endoplasmic reticulum and mitochondrial Ca²⁺ channels,” *The Journal of Cell Biology*, vol. 175, no. 6, pp. 901–911, 2006.
- [23] O. M. de Brito and L. Scorrano, “Mitofusin 2 tethers endoplasmic reticulum to mitochondria,” *Nature*, vol. 456, no. 7222, pp. 605–610, 2008.
- [24] P. Gomez-Suaga, S. Paillusson, R. Stoica, W. Noble, D. P. Hanger, and C. C. J. Miller, “The ER-mitochondria tethering complex VAPB-PTPIP51 regulates autophagy,” *Current Biology*, vol. 27, no. 3, pp. 371–385, 2017.
- [25] R. Iwasawa, A. L. Mahul-Mellier, C. Datler, E. Pazarentzos, and S. Grimm, “Fis 1 and Bap31 bridge the mitochondria-ER interface to establish a platform for apoptosis induction,” *Embo Journal*, vol. 30, no. 3, pp. 556–568, 2011.
- [26] S. Wu, Q. Lu, Q. Wang et al., “Binding of FUN14 domain containing 1 with inositol 1,4,5-trisphosphate receptor in mitochondria-associated endoplasmic reticulum membranes maintains mitochondrial dynamics and function in hearts in vivo,” *Circulation*, vol. 136, no. 23, pp. 2248–2266, 2017.
- [27] T. Thoudam, C. M. Ha, J. Leem et al., “PDK4 augments ER-mitochondria contact to dampen skeletal muscle insulin signaling during obesity,” *Diabetes*, vol. 68, no. 3, pp. 571–586, 2019.
- [28] P. Gao, W. Yang, and L. Sun, “Mitochondria-associated endoplasmic reticulum membranes (MAMs) and their prospective roles in kidney disease,” *Oxidative Medicine and Cellular Longevity*, vol. 2020, Article ID 3120539, 21 pages, 2020.
- [29] C. Giorgi, K. Ito, H. K. Lin et al., “PML regulates apoptosis at endoplasmic reticulum by modulating calcium release,” *Science*, vol. 330, no. 6008, pp. 1247–1251, 2010.
- [30] E. Tubbs, P. Theurey, G. Vial et al., “Mitochondria-associated endoplasmic reticulum membrane (MAM) integrity is required for insulin signaling and is implicated in hepatic insulin resistance,” *Diabetes*, vol. 63, no. 10, pp. 3279–3294, 2014.
- [31] C. Betz, D. Stracka, C. Prescianotto-Baschong, M. Frieden, N. Demaurex, and M. N. Hall, “Feature article: mTOR complex 2-Akt signaling at mitochondria-associated endoplasmic reticulum membranes (MAM) regulates mitochondrial physiology,” *Proceedings of the National Academy of Sciences of the United States of America*, vol. 110, no. 31, pp. 12526–12534, 2013.
- [32] R. Rizzuto, P. Pinton, W. Carrington et al., “Close contacts with the endoplasmic reticulum as determinants of mitochondrial Ca²⁺ responses,” *Science*, vol. 280, no. 5370, pp. 1763–1766, 1998.
- [33] D. M. Bers, “Cardiac excitation-contraction coupling,” *Nature*, vol. 415, no. 6868, pp. 198–205, 2002.
- [34] J. M. Baughman, F. Perocchi, H. S. Girgis et al., “Integrative genomics identifies MCU as an essential component of the mitochondrial calcium uniporter,” *Nature*, vol. 476, no. 7360, pp. 341–345, 2011.
- [35] G. Csordás, P. Várnai, T. Golenár et al., “Imaging interorganelle contacts and local calcium dynamics at the ER-mitochondrial interface,” *Molecular Cell*, vol. 39, no. 1, pp. 121–132, 2010.
- [36] A. Bononi, S. Missiroli, F. Poletti et al., “Mitochondria-associated membranes (MAMs) as hotspot Ca²⁺ signaling units,” *Advances in Experimental Medicine and Biology*, vol. 740, pp. 411–437, 2012.
- [37] L. Gomez, P. A. Thiebaut, M. Paillard et al., “The SR/ER-mitochondria calcium crosstalk is regulated by GSK3 β during reperfusion injury,” *Cell Death and Differentiation*, vol. 23, no. 2, pp. 313–322, 2016.
- [38] T. Szado, V. Vanderheyden, J. B. Parys et al., “Phosphorylation of inositol 1,4,5-trisphosphate receptors by protein kinase B/Akt inhibits Ca²⁺ release and apoptosis,” *Proceedings of the National Academy of Sciences of the United States of America*, vol. 105, no. 7, pp. 2427–2432, 2008.
- [39] A. Zarain-Herzberg, G. García-Rivas, and R. Estrada-Avilés, “Regulation of SERCA pumps expression in diabetes,” *Cell Calcium*, vol. 56, no. 5, pp. 302–310, 2014.
- [40] M. Dia, L. Gomez, H. Thibault et al., “Reduced reticulum-mitochondria Ca²⁺ transfer is an early and reversible trigger of mitochondrial dysfunctions in diabetic cardiomyopathy,” *Basic Research in Cardiology*, vol. 115, no. 6, p. 74, 2020.
- [41] X. Hu, T. Bai, Z. Xu, Q. Liu, Y. Zheng, and L. Cai, “Pathophysiological fundamentals of diabetic cardiomyopathy,” *Comprehensive Physiology*, vol. 7, no. 2, pp. 693–711, 2017.
- [42] S. Marchi and P. Pinton, “The mitochondrial calcium uniporter complex: molecular components, structure and physiopathological implications,” *The Journal of Physiology*, vol. 592, no. 5, pp. 829–839, 2014.
- [43] M. Yuan, M. Gong, Z. Zhang et al., “Hyperglycemia induces endoplasmic reticulum stress in atrial cardiomyocytes, and mitofusin-2 downregulation prevents mitochondrial dysfunction and subsequent cell death,” *Oxidative Medicine and Cellular Longevity*, vol. 2020, Article ID 6569728, 14 pages, 2020.
- [44] R. Filadi, E. Greotti, G. Turacchio, A. Luini, T. Pozzan, and P. Pizzo, “Mitofusin 2 ablation increases endoplasmic reticulum-mitochondria coupling,” *Proceedings of the National Academy of Sciences of the United States of America*, vol. 112, no. 17, pp. E2174–E2181, 2015.
- [45] S. Cipolat, O. Martins de Brito, B. Dal Zilio, and L. Scorrano, “OPA1 requires mitofusin 1 to promote mitochondrial fusion,” *Proceedings of the National Academy of Sciences of the United States of America*, vol. 101, no. 45, pp. 15927–15932, 2004.
- [46] M. Chen, Z. Chen, Y. Wang et al., “Mitophagy receptor FUNDC1 regulates mitochondrial dynamics and mitophagy,” *Autophagy*, vol. 12, no. 4, pp. 689–702, 2016.
- [47] H. Chen, S. A. Detmer, A. J. Ewald, E. E. Griffin, S. E. Fraser, and D. C. Chan, “Mitofusins Mfn1 and Mfn2 coordinately regulate mitochondrial fusion and are essential for embryonic development,” *The Journal of Cell Biology*, vol. 160, no. 2, pp. 189–200, 2003.

- [48] L. Hu, M. Ding, D. Tang et al., "Targeting mitochondrial dynamics by regulating Mfn2 for therapeutic intervention in diabetic cardiomyopathy," *Theranostics*, vol. 9, no. 13, pp. 3687–3706, 2019.
- [49] T. I. Lee, Y. H. Kao, Y. C. Chen, J. H. Huang, F. C. Hsiao, and Y. J. Chen, "Peroxisome proliferator-activated receptors modulate cardiac dysfunction in diabetic cardiomyopathy," *Diabetes Research and Clinical Practice*, vol. 100, no. 3, pp. 330–339, 2013.
- [50] F. Korobova, V. Ramabhadran, and H. N. Higgs, "An actin-dependent step in mitochondrial fission mediated by the ER-associated formin INF2," *Science*, vol. 339, no. 6118, pp. 464–467, 2013.
- [51] R. Chakrabarti, W. K. Ji, R. V. Stan, S. J. de Juan, T. A. Ryan, and H. N. Higgs, "INF2-mediated actin polymerization at the ER stimulates mitochondrial calcium uptake, inner membrane constriction, and division," *The Journal of Cell Biology*, vol. 217, no. 1, pp. 251–268, 2018.
- [52] M. Ding, N. Feng, D. Tang et al., "Melatonin prevents Drp1-mediated mitochondrial fission in diabetic hearts through SIRT1-PGC1 α pathway," *Journal of Pineal Research*, vol. 65, no. 2, article e12491, 2018.
- [53] Q. Hu, H. Zhang, N. Gutiérrez Cortés et al., "Increased Drp1 acetylation by lipid overload induces cardiomyocyte death and heart dysfunction," *Circulation Research*, vol. 126, no. 4, pp. 456–470, 2020.
- [54] H. Otera, C. Wang, M. M. Cleland et al., "Mff is an essential factor for mitochondrial recruitment of Drp1 during mitochondrial fission in mammalian cells," *The Journal of Cell Biology*, vol. 191, no. 6, pp. 1141–1158, 2010.
- [55] C. S. Palmer, K. D. Elgass, R. G. Parton, L. D. Osellame, D. Stojanovski, and M. T. Ryan, "Adaptor proteins MiD49 and MiD51 can act independently of Mff and Fis1 in Drp1 recruitment and are specific for mitochondrial fission," *The Journal of Biological Chemistry*, vol. 288, no. 38, pp. 27584–27593, 2013.
- [56] H. Zhang, P. Wang, S. Bisetto et al., "A novel fission-independent role of dynamin-related protein 1 in cardiac mitochondrial respiration," *Cardiovascular Research*, vol. 113, no. 2, pp. 160–170, 2017.
- [57] C. A. Lamb, T. Yoshimori, and S. A. Tooze, "The autophagosome: origins unknown, biogenesis complex," *Nature Reviews. Molecular Cell Biology*, vol. 14, no. 12, pp. 759–774, 2013.
- [58] Y. Liao, B. Duan, Y. Zhang, X. Zhang, and B. Xia, "ER-phagy results in ER stress, UPR, and cell death," *The Journal of Biological Chemistry*, vol. 294, no. 52, pp. 20009–20023, 2019.
- [59] M. Hamasaki, N. Furuta, A. Matsuda et al., "Autophagosomes form at ER-mitochondria contact sites," *Nature*, vol. 495, no. 7441, pp. 389–393, 2013.
- [60] V. Gelmetti, P. De Rosa, L. Torosantucci et al., "PINK1 and BECN1 relocalize at mitochondria-associated membranes during mitophagy and promote ER-mitochondria tethering and autophagosome formation," *Autophagy*, vol. 13, no. 4, pp. 654–669, 2017.
- [61] T. Zhao, X. Huang, L. Han et al., "Central role of mitofusin 2 in autophagosome-lysosome fusion in cardiomyocytes," *The Journal of Biological Chemistry*, vol. 287, no. 28, pp. 23615–23625, 2012.
- [62] Y. Hu, H. Chen, L. Zhang et al., "The AMPK-MFN2 axis regulates MAM dynamics and autophagy induced by energy stresses," *Autophagy*, vol. 17, no. 5, pp. 1142–1156, 2021.
- [63] J. M. Bravo-San Pedro, G. Kroemer, and L. Galluzzi, "Autophagy and mitophagy in cardiovascular disease," *Circulation Research*, vol. 120, no. 11, pp. 1812–1824, 2017.
- [64] M. H. Zou and Z. Xie, "Regulation of interplay between autophagy and apoptosis in the diabetic heart: new role of AMPK," *Autophagy*, vol. 9, no. 4, pp. 624–625, 2013.
- [65] P. E. Munasinghe, F. Riu, P. Dixit et al., "Type-2 diabetes increases autophagy in the human heart through promotion of Beclin-1 mediated pathway," *International Journal of Cardiology*, vol. 202, pp. 13–20, 2016.
- [66] K. C. Yang, P. Sathiyaseelan, C. Ho, and S. M. Gorski, "Evolution of tools and methods for monitoring autophagic flux in mammalian cells," *Biochemical Society Transactions*, vol. 46, no. 1, pp. 97–110, 2018.
- [67] B. Wang, Q. Yang, Y. Y. Sun et al., "Resveratrol-enhanced autophagic flux ameliorates myocardial oxidative stress injury in diabetic mice," *Journal of Cellular and Molecular Medicine*, vol. 18, no. 8, pp. 1599–1611, 2014.
- [68] J. Xie, K. Cui, H. Hao et al., "Acute hyperglycemia suppresses left ventricular diastolic function and inhibits autophagic flux in mice under prohypertrophic stimulation," *Cardiovascular Diabetology*, vol. 15, no. 1, p. 136, 2016.
- [69] K. Schroder and J. Tschopp, "The inflammasomes," *Cell*, vol. 140, no. 6, pp. 821–832, 2010.
- [70] R. Zhou, A. S. Yazdi, P. Menu, and J. Tschopp, "A role for mitochondria in NLRP3 inflammasome activation," *Nature*, vol. 469, no. 7329, pp. 221–225, 2011.
- [71] H. Wen, D. Gris, Y. Lei et al., "Fatty acid-induced NLRP3-ASC inflammasome activation interferes with insulin signaling," *Nature Immunology*, vol. 12, no. 5, pp. 408–415, 2011.
- [72] R. Zhou, A. Tardivel, B. Thorens, I. Choi, and J. Tschopp, "Thioredoxin-interacting protein links oxidative stress to inflammasome activation," *Nature Immunology*, vol. 11, no. 2, pp. 136–140, 2010.
- [73] G. Frati, L. Schirone, I. Chimenti et al., "An overview of the inflammatory signalling mechanisms in the myocardium underlying the development of diabetic cardiomyopathy," *Cardiovascular Research*, vol. 113, no. 4, pp. 378–388, 2017.
- [74] Y. Yin, Z. Zhou, W. Liu, Q. Chang, G. Sun, and Y. Dai, "Vascular endothelial cells senescence is associated with NOD-like receptor family pyrin domain-containing 3 (NLRP3) inflammasome activation via reactive oxygen species (ROS)/thioredoxin-interacting protein (TXNIP) pathway," *The International Journal of Biochemistry & Cell Biology*, vol. 84, pp. 22–34, 2017.
- [75] S. Song, J. Tan, Y. Miao, and Q. Zhang, "Crosstalk of ER stress-mediated autophagy and ER-phagy: involvement of UPR and the core autophagy machinery," *Journal of Cellular Physiology*, vol. 233, no. 5, pp. 3867–3874, 2018.
- [76] J. Qu, M. Li, D. Li et al., "Stimulation of sigma-1 receptor protects against cardiac fibrosis by alleviating IRE1 pathway and autophagy impairment," *Oxidative Medicine and Cellular Longevity*, vol. 2021, Article ID 8836818, 25 pages, 2021.
- [77] Z. W. Liu, H. T. Zhu, K. L. Chen et al., "Protein kinase RNA-like endoplasmic reticulum kinase (PERK) signaling pathway plays a major role in reactive oxygen species (ROS)-mediated endoplasmic reticulum stress-induced apoptosis in diabetic cardiomyopathy," *Cardiovascular Diabetology*, vol. 12, no. 1, article 158, 2013.
- [78] J. P. Muñoz, S. Ivanova, J. Sánchez-Wandelmer et al., "Mfn2 modulates the UPR and mitochondrial function via

- repression of PERK,” *The EMBO Journal*, vol. 32, no. 17, pp. 2348–2361, 2013.
- [79] Q. Gao, X. M. Wang, H. W. Ye et al., “Changes in the expression of cardiac mitofusin-2 in different stages of diabetes in rats,” *Molecular Medicine Reports*, vol. 6, no. 4, pp. 811–814, 2012.
- [80] Y. Cao, Z. Chen, J. Hu et al., “Mfn2 regulates high glucose-induced MAMs dysfunction and apoptosis in podocytes via PERK pathway,” *Frontiers In Cell And Developmental Biology*, vol. 9, article 769213, 2021.
- [81] “Effect of intensive blood-glucose control with metformin on complications in overweight patients with type 2 diabetes (UKPDS 34),” *The Lancet*, vol. 352, no. 9131, pp. 854–865, 1998.
- [82] S. P. Romero, J. L. Andrey, A. Garcia-Egido et al., “Metformin therapy and prognosis of patients with heart failure and new-onset diabetes mellitus. A propensity-matched study in the community,” *International Journal of Cardiology*, vol. 166, no. 2, pp. 404–412, 2013.
- [83] Z. Xie, K. Lau, B. Eby et al., “Improvement of cardiac functions by chronic metformin treatment is associated with enhanced cardiac autophagy in diabetic OVE26 mice,” *Diabetes*, vol. 60, no. 6, pp. 1770–1778, 2011.
- [84] Z. Yang, M. Wang, Y. Zhang et al., “Metformin ameliorates diabetic cardiomyopathy by activating the PK2/PKR pathway,” *Frontiers in Physiology*, vol. 11, p. 425, 2020.
- [85] W. Jia, T. Bai, J. Zeng et al., “Combined administration of metformin and atorvastatin attenuates diabetic cardiomyopathy by inhibiting inflammation, apoptosis, and oxidative stress in type 2 diabetic mice,” *Frontiers in Cell and Developmental Biology*, vol. 9, article 634900, 2021.
- [86] N. D. Cohen, S. J. Gutman, E. M. Briganti, and A. J. Taylor, “Effects of empagliflozin treatment on cardiac function and structure in patients with type 2 diabetes: a cardiac magnetic resonance study,” *Internal Medicine Journal*, vol. 49, no. 8, pp. 1006–1010, 2019.
- [87] C. Li, J. Zhang, M. Xue et al., “SGLT2 inhibition with empagliflozin attenuates myocardial oxidative stress and fibrosis in diabetic mice heart,” *Cardiovascular Diabetology*, vol. 18, no. 1, p. 15, 2019.
- [88] D. Matsutani, M. Sakamoto, Y. Kayama, N. Takeda, R. Horiuchi, and K. Utsunomiya, “Effect of canagliflozin on left ventricular diastolic function in patients with type 2 diabetes,” *Cardiovascular Diabetology*, vol. 17, no. 1, p. 73, 2018.
- [89] F. Soga, H. Tanaka, K. Tatsumi et al., “Impact of dapagliflozin on left ventricular diastolic function of patients with type 2 diabetic mellitus with chronic heart failure,” *Cardiovascular Diabetology*, vol. 17, no. 1, p. 132, 2018.
- [90] Y. Ye, M. Bajaj, H. C. Yang, J. R. Perez-Polo, and Y. Birnbaum, “SGLT-2 inhibition with dapagliflozin reduces the activation of the Nlrp3/ASC inflammasome and attenuates the development of diabetic cardiomyopathy in mice with type 2 diabetes. Further augmentation of the effects with saxagliptin, a DPP4 inhibitor,” *Cardiovascular Drugs and Therapy*, vol. 31, no. 2, pp. 119–132, 2017.
- [91] H. Chen, D. Tran, H. C. Yang, S. Nylander, Y. Birnbaum, and Y. Ye, “Dapagliflozin and ticagrelor have additive effects on the attenuation of the activation of the NLRP3 inflammasome and the progression of diabetic cardiomyopathy: an AMPK-mTOR interplay,” *Cardiovascular Drugs and Therapy*, vol. 34, no. 4, pp. 443–461, 2020.
- [92] M. Almutairi, K. Gopal, A. A. Greenwell et al., “The GLP-1 receptor agonist liraglutide increases myocardial glucose oxidation rates via indirect mechanisms and mitigates experimental diabetic cardiomyopathy,” *The Canadian Journal of Cardiology*, vol. 37, no. 1, pp. 140–150, 2021.
- [93] D. J. Drucker, “The cardiovascular biology of glucagon-like peptide-1,” *Cell Metabolism*, vol. 24, no. 1, pp. 15–30, 2016.
- [94] A. Monji, T. Mitsui, Y. K. Bando, M. Aoyama, T. Shigeta, and T. Murohara, “Glucagon-like peptide-1 receptor activation reverses cardiac remodeling via normalizing cardiac steatosis and oxidative stress in type 2 diabetes,” *American Journal of Physiology. Heart and Circulatory Physiology*, vol. 305, no. 3, pp. H295–H304, 2013.
- [95] W. Yu, W. Zha, and J. Ren, “Exendin-4 and liraglutide attenuate glucose toxicity-induced cardiac injury through mTOR/ULK1-dependent autophagy,” *Oxidative Medicine and Cellular Longevity*, vol. 2018, Article ID 5396806, 14 pages, 2018.
- [96] C. W. Younce, M. A. Burmeister, and J. E. Ayala, “Exendin-4 attenuates high glucose-induced cardiomyocyte apoptosis via inhibition of endoplasmic reticulum stress and activation of SERCA2a,” *American Journal of Physiology. Cell Physiology*, vol. 304, no. 6, pp. C508–C518, 2013.
- [97] L. Wu, K. Wang, W. Wang et al., “Glucagon-like peptide-1 ameliorates cardiac lipotoxicity in diabetic cardiomyopathy via the PPAR α pathway,” *Aging Cell*, vol. 17, no. 4, article e12763, 2018.
- [98] H. Zhou, Y. Yue, J. Wang, Q. Ma, and Y. Chen, “Melatonin therapy for diabetic cardiomyopathy: a mechanism involving Syk- mitochondrial complex I-SERCA pathway,” *Cellular Signalling*, vol. 47, pp. 88–100, 2018.
- [99] H. Zhou, Y. Zhang, S. Hu et al., “Melatonin protects cardiac microvasculature against ischemia/reperfusion injury via suppression of mitochondrial fission-VDAC1-HK2-mPTP-mitophagy axis,” *Journal Of Pineal Research*, vol. 63, no. 1, p. e12413, 2017.
- [100] W. Li, B. Liu, L. Wang, J. Liu, X. Yang, and J. Zheng, “Melatonin attenuates cardiac ischemia-reperfusion injury through modulation of IP3R-mediated mitochondria-ER contact,” *Oxidative Medicine And Cellular Longevity*, vol. 2021, Article ID 1370862, 12 pages, 2021.
- [101] J. Ren, M. Sun, H. Zhou et al., “FUNDC1 interacts with FBXL2 to govern mitochondrial integrity and cardiac function through an IP3R3-dependent manner in obesity,” *Science Advances*, vol. 6, no. 38, 2020.
- [102] W. Wu, X. Liu, and L. Han, “Apoptosis of cardiomyocytes in diabetic cardiomyopathy involves overexpression of glycogen synthase kinase-3 β ,” *Bioscience Reports*, vol. 39, no. 1, 2019.
- [103] Y. Li, X. Ruan, X. Xu et al., “Shengmai injection suppresses angiotensin II-induced cardiomyocyte hypertrophy and apoptosis via activation of the AMPK signaling pathway through energy-dependent mechanisms,” *Frontiers in Pharmacology*, vol. 10, p. 1095, 2019.
- [104] J. Zhou, T. Wang, H. Wang, Y. Jiang, and S. Peng, “Obacurone attenuates high glucose-induced oxidative damage in NRK-52E cells by inhibiting the activity of GSK-3 β ,” *Biochemical and Biophysical Research Communications*, vol. 513, no. 1, pp. 226–233, 2019.
- [105] T. Hayashi and T. P. Su, “Sigma-1 receptor chaperones at the ER-mitochondrion interface regulate Ca²⁺ signaling and cell survival,” *Cell*, vol. 131, no. 3, pp. 596–610, 2007.

- [106] C. Giorgi, M. Bonora, G. Sorrentino et al., “p53 at the endoplasmic reticulum regulates apoptosis in a Ca²⁺-dependent manner,” *Proceedings of the National Academy of Sciences of the United States of America.*, vol. 112, no. 6, pp. 1779–1784, 2015.
- [107] E. M. Lynes, M. Bui, M. C. Yap et al., “Palmitoylated TMX and calnexin target to the mitochondria-associated membrane,” *The EMBO Journal*, vol. 31, no. 2, pp. 457–470, 2012.
- [108] D. Boehning, R. L. Patterson, L. Sedaghat, N. O. Glebova, T. Kurosaki, and S. H. Snyder, “Cytochrome *c* binds to inositol (1,4,5) trisphosphate receptors, amplifying calcium-dependent apoptosis,” *Nature Cell Biology*, vol. 5, no. 12, pp. 1051–1061, 2003.
- [109] H. Ivanova, L. E. Wagner 2nd, A. Tanimura et al., “Bcl-2 and IP3 compete for the ligand-binding domain of IP3Rs modulating Ca²⁺ signaling output,” *Cellular and Molecular Life Sciences*, vol. 76, no. 19, pp. 3843–3859, 2019.
- [110] M. S. Yoon, “The role of mammalian target of rapamycin (mTOR) in insulin signaling,” *Nutrients*, vol. 9, no. 11, p. 1176, 2017.
- [111] A. Bononi, M. Bonora, S. Marchi et al., “Identification of PTEN at the ER and MAMs and its regulation of Ca²⁺ signaling and apoptosis in a protein phosphatase-dependent manner,” *Cell Death and Differentiation*, vol. 20, no. 12, pp. 1631–1643, 2013.
- [112] M. Karbowski, K. L. Norris, M. M. Cleland, S. Y. Jeong, and R. J. Youle, “Role of Bax and Bak in mitochondrial morphogenesis,” *Nature*, vol. 443, no. 7112, pp. 658–662, 2006.
- [113] S. Gandre-Babbe and A. M. van der Bliek, “The novel tail-anchored membrane protein Mff controls mitochondrial and peroxisomal fission in mammalian cells,” *Molecular Biology of the Cell*, vol. 19, no. 6, pp. 2402–2412, 2008.
- [114] D. Stojanovski, O. S. Koutsopoulos, K. Okamoto, and M. T. Ryan, “Levels of human Fis1 at the mitochondrial outer membrane regulate mitochondrial morphology,” *Journal of Cell Science*, vol. 117, no. 7, pp. 1201–1210, 2004.
- [115] D. W. Hailey, A. S. Rambold, P. Satpute-Krishnan et al., “Mitochondria supply membranes for autophagosome biogenesis during starvation,” *Cell*, vol. 141, no. 4, pp. 656–667, 2010.
- [116] X. Zhang, J. H. Zhang, X. Y. Chen et al., “Reactive oxygen species-induced TXNIP drives fructose-mediated hepatic inflammation and lipid accumulation through NLRP3 inflammasome activation,” *Antioxidants & Redox Signaling*, vol. 22, no. 10, pp. 848–870, 2015.
- [117] T. Verfaillie, N. Rubio, A. D. Garg et al., “PERK is required at the ER-mitochondrial contact sites to convey apoptosis after ROS-based ER stress,” *Cell Death and Differentiation*, vol. 19, no. 11, pp. 1880–1891, 2012.
- [118] K. Takeda, S. Nagashima, I. Shiiba et al., “MITOL prevents ER stress-induced apoptosis by IRE1 α ubiquitylation at ER-mitochondria contact sites,” *The EMBO Journal*, vol. 38, no. 15, article e100999, 2019.

Research Article

Beta3-Adrenergic Receptor Activation Alleviates Cardiac Dysfunction in Cardiac Hypertrophy by Regulating Oxidative Stress

Mingming Zhang¹, Yuerong Xu², Jianghong Chen¹, Chaoshi Qin¹, Jing Liu¹, Dong Guo¹, Rui Wang¹, Jianqiang Hu¹, Qing Zou¹, Jingxiao Yang¹, Zikuan Wang¹, and Xiaolin Niu¹

¹Department of Cardiology, Tangdu Hospital, The Fourth Military Medical University, Xi'an, China

²Department of Orthodontics, School of Stomatology, The Fourth Military Medical University, Xi'an, China

Correspondence should be addressed to Xiaolin Niu; xiaolinniu@163.com

Received 16 April 2021; Revised 10 August 2021; Accepted 24 August 2021; Published 4 October 2021

Academic Editor: Yun-dai Chen

Copyright © 2021 Mingming Zhang et al. This is an open access article distributed under the Creative Commons Attribution License, which permits unrestricted use, distribution, and reproduction in any medium, provided the original work is properly cited.

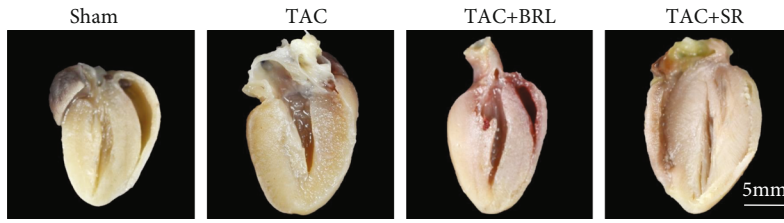
Background. Excessive myocardial oxidative stress could lead to the congestive heart failure. NADPH oxidase is involved in the pathological process of left ventricular (LV) remodeling and dysfunction. β 3-Adrenergic receptor (AR) could regulate cardiac dysfunction proved by recent researches. The molecular mechanism of β 3-AR regulating oxidative stress, especially NADPH oxidase, remains to be determined. **Methods.** Cardiac hypertrophy was constructed by the transverse aortic constriction (TAC) model. ROS and NADPH oxidase subunits expression were assessed after β 3-AR agonist (BRL) or inhibitor (SR) administration in cardiac hypertrophy. Moreover, the cardiac function, fibrosis, heart size, oxidative stress, and cardiomyocytes apoptosis were also detected. **Results.** β 3-AR activation significantly alleviated cardiac hypertrophy and remodeling in pressure-overloaded mice. β 3-AR stimulation also improved heart function and reduced cardiomyocytes apoptosis, oxidative stress, and fibrosis. Meanwhile, β 3-AR stimulation inhibited superoxide anion production and decreased NADPH oxidase activity. Furthermore, BRL treatment increased the neuronal NOS (nNOS) expression in cardiac hypertrophy. **Conclusion.** β 3-AR stimulation alleviated cardiac dysfunction and reduced cardiomyocytes apoptosis, oxidative stress, and fibrosis by inhibiting NADPH oxidases. In addition, the protective effect of β 3-AR is largely attributed to nNOS activation in cardiac hypertrophy.

1. Introduction

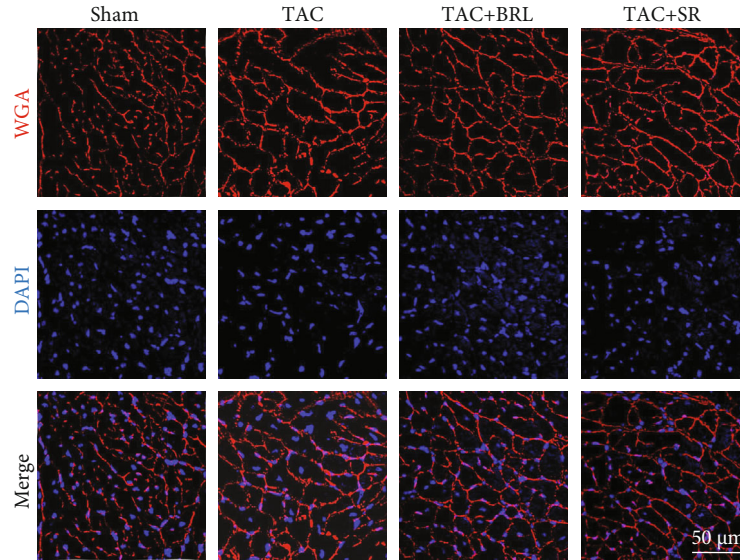
Despite the progress of therapeutic approaches, congestive heart failure (CHF) remains to be a high morbidity and mortality [1, 2]. Considerable evidence suggests that excessive oxidative stress leads to the CHF [3–5]. Experiments found that oxidative stress was activated in animal models with cardiac hypertrophy [6, 7]. Besides, increased ROS could result in not only cardiac hypertrophy and cardiomyocytes apoptosis but also many other diseases such as acute kidney injury [8–12]. Moreover, patients with CHF were also found to have elevated markers of oxidative stress, suggesting that oxidative stress was increased in failing heart [13].

ROS is mainly originated from the NADPH oxidases in cardiovascular system [14]. The typical NADPH oxidases

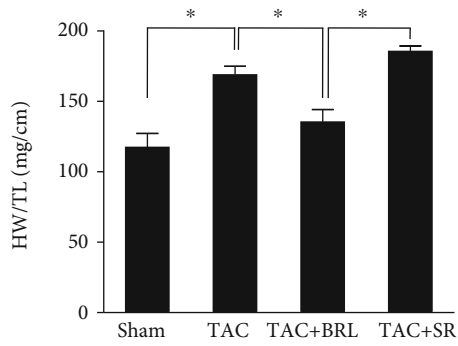
consist NOX, p22phox, p40phox, p47phox, p67phox, and Rac1. When assembled, electron could be transferred from NADPH to molecular oxygen, resulting in the formation of superoxide [15]. The level of NADPH oxidase was increased in an animal model with cardiac hypertrophy and even in CHF patients [5, 16]. Recent studies found that NOX2 deficiency attenuated angiotensin II-induced cardiac hypertrophy [17]. Furthermore, Rac1, an important subunit for NOX2 activation, regulates the occurrence and development of cardiac hypertrophy [18]. Taken together, these results suggested that NADPH oxidases play an essential role in cardiac hypertrophy. However, clinical application of anti-oxidants has yielded disappointing results, indicating that the detailed relationship between oxidative stress and heart failing still needs to be explored [19]. Therefore, our study



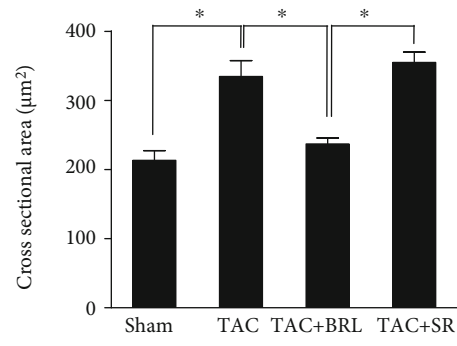
(a)



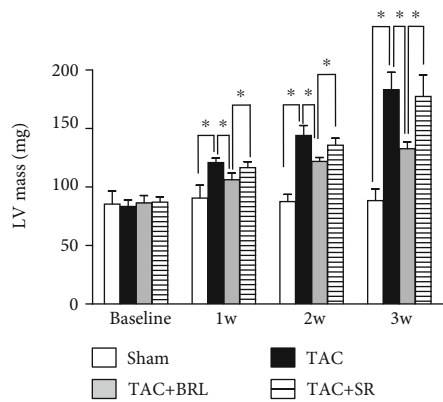
(b)



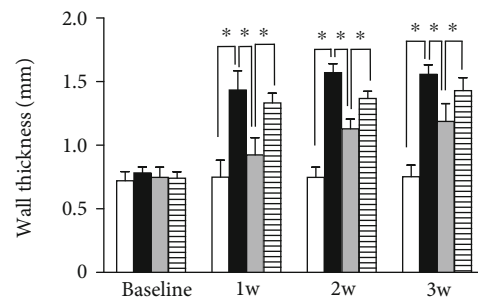
(c)



(d)



(e)



(f)

FIGURE 1: Continued.

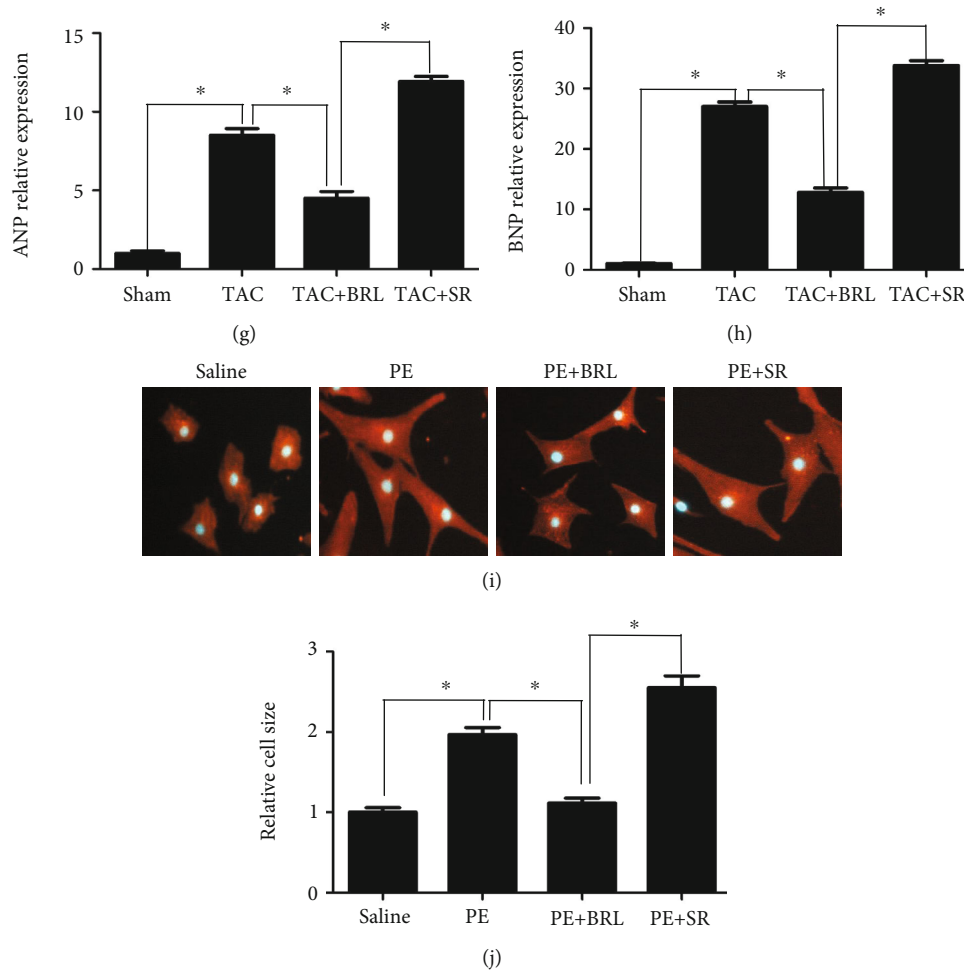


FIGURE 1: β_3 -AR stimulation alleviated cardiac hypertrophy and remodeling in pressure-overloaded mice. (a) Representative images of heart size. (b) Cardiomyocytes size as stained by WGA. (c) HW/TL. (d) Quantitative analysis of cardiomyocytes size. (e, f) LV mass and wall thickness measured by echocardiography. (g, h) The expression level of ANP and BNP. (i, j) Primary cardiomyocytes size as stained by α -actinin. The number of mice ($n = 6$). * $P < 0.05$.

is aimed at exploring the molecular mechanism and finding a novel therapy target to treat heart failure.

Accumulating evidence demonstrated that 3 subtypes of β -ARs regulate the cardiac function when exposed to stress [20, 21]. The biological function of β_1 - and β_2 -AR in mammals is thoroughly studied in the past years [22]. Previous study suggested that β_3 -AR plays a negative inotropic effect, which is the opposite effect of $\beta_1/2$ -ARs [23]. Furthermore, $\beta_3^{-/-}$ mice exacerbated cardiac hypertrophy and heart failure. However, whether the biological function of β_3 -AR is mediated by oxidative stress regulation during heart failure is still uncertain. Therefore, it is necessary to clarify the underline mechanism of β_3 -AR in oxidative stress, especially NADPH oxidase in cardiac hypertrophy.

2. Methods Animals

The 8–10-week-old male C57BL6/J mice were randomly allocated as follows: [1] sham group (Sham); [2] transverse aortic constriction group (TAC); [3] TAC + BRL37344 group (TAC+BRL); and [4] TAC + SR59230A group (TAC

+SR). The experiments were approved by the Fourth Military Medical University Committee on Animal Care.

2.1. Construction of Transverse Aortic Constriction Model. Transverse aortic constriction (TAC) was constructed as previously described. Briefly, mice were anesthetized with 2% isoflurane, endotracheally intubated with a 20G catheter, and ventilated. The transverse aortic arch was surgically accessed. Then, a 25G needle was placed on the transverse aorta, which was secured. Finally, the chest was closed after removing the needle, leaving a stenosis. Mice were administered with BRL37344 (Tocris Bioscience, Ellisville, Missouri) or SR59230A, respectively, at 0.1 mg/kg/hour via osmotic minipumps.

2.2. Primary Cardiomyocytes Culture and Treatments. Primary cardiomyocytes were isolated from the neonatal mouse (1 to 3 days old) hearts as previously described. The cardiomyocytes were treated with hypertrophic agonists, phenylephrine (PE). Then, after 24 hours, the cardiomyocytes

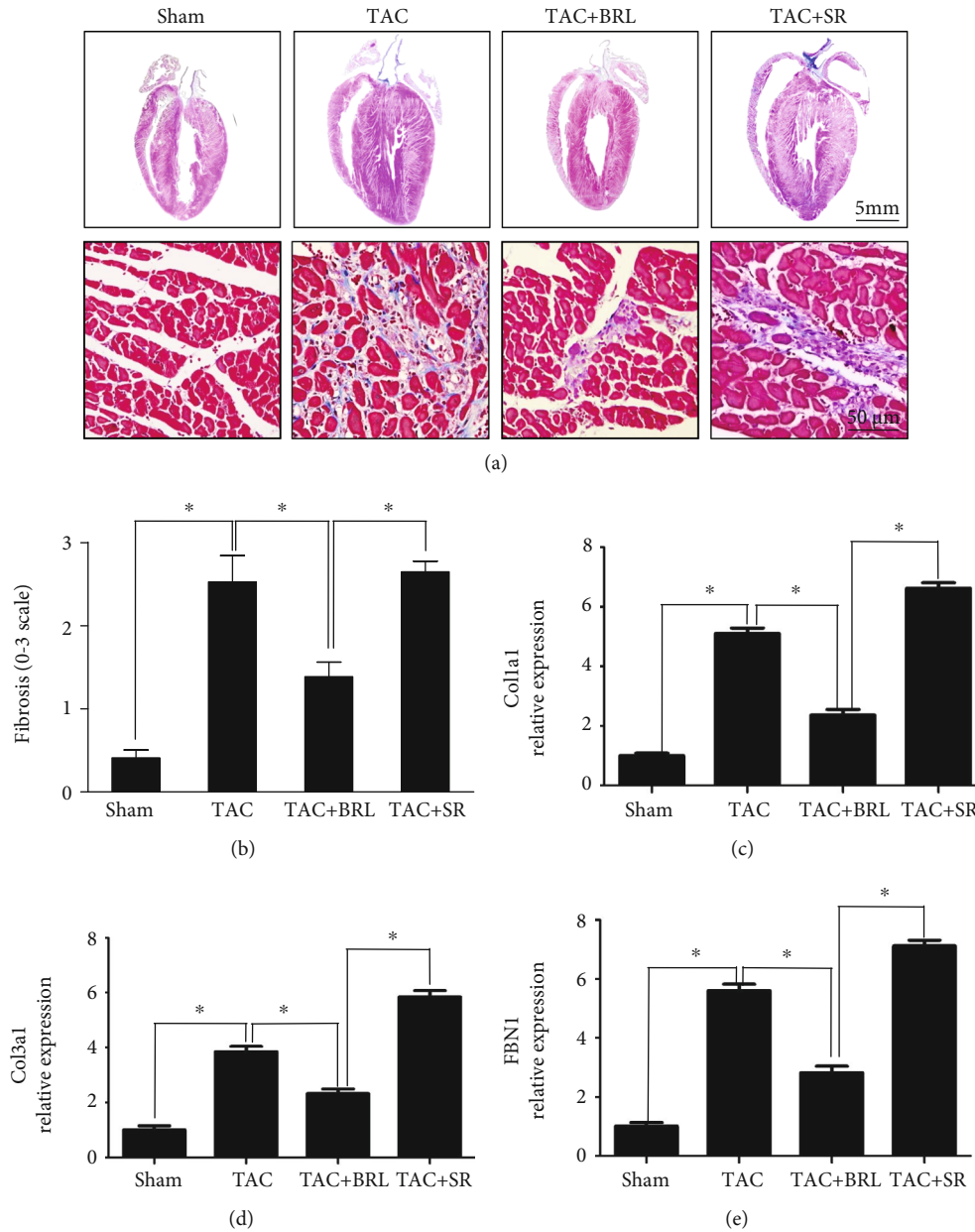


FIGURE 2: β_3 -AR stimulation reduced fibrosis after TAC. (a, b) The level of cardiac fibrosis. (c–e) The expression of fibrotic remodeling marker genes (Colla1, Col3a1, and FBN1). The number of mice ($n = 6$). * $P < 0.05$.

were treated with BRL37344 or SR59230A. The groups are as follows: [1] saline; [2] PE; [3] PE+BRL; and [4] PE+ SR.

2.3. Cell Size. Primary cardiomyocytes were subjected to immunostaining. Antibody sources were as follows: α -actinin (1:200, Abcam); Alexa-594 secondary antibodies (1:500, Invitrogen).

2.4. Histological Analysis and Immunostaining. Three weeks after TAC operation, mice were sacrificed. Tissue sections of hearts were stained with Masson's trichrome (Sigma) for detection of fibrosis. The fibrosis-related genes Colla1, Col3a1, and fibrillin 1 (FBN1) were detected by q-PCR. Meanwhile, wheat germ agglutinin (WGA, Sigma) was used

to outline cardiomyocytes. Mean cardiomyocyte cross-sectional area was determined from digitized images and analyzed using the ImageJ program. ANP and BNP were detected by q-PCR. For analyzing the expressions of myocardial NAD(P)H oxidase subunit, immunohistochemical stainings of NOX2, NOX4, and p22^{phox} were performed as previously described. The primary antibodies are NOX2 (1:200, Abcam), NOX4 (1:200, Abcam), and p22^{phox} (1:200, Abcam).

2.5. Echocardiography. Echocardiography studies were conducted weekly to monitor heart function as previously described [19]. We followed the methods of Xiaolin Liu et al. (2014).

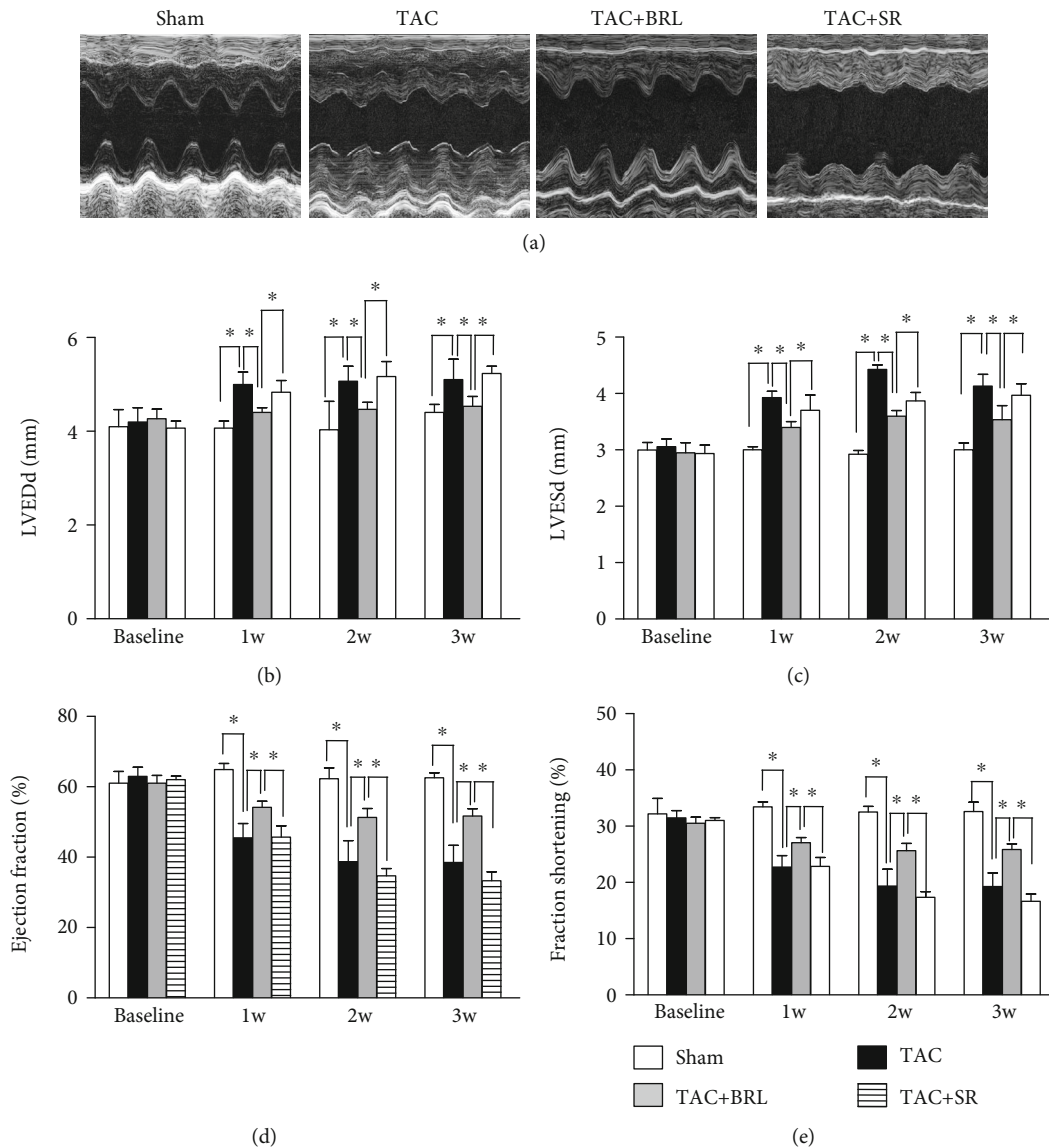


FIGURE 3: β_3 -AR stimulation improved pressure overload-induced cardiac dysfunction. (a) Representative images of echocardiography. (b–e) LVEDd, LVESd, LVEF, and LVFS measured by echocardiography. The number of mice ($n = 6$). * $P < 0.05$.

2.6. Cell Apoptosis Assay. Apoptosis in heart tissue was determined based on TUNEL and caspase-3 activity assay as previously described [19].

2.7. Measurement of Oxidative Stress Level. The production of $O_2^{\bullet-}$ in the LV was measured as previously described. Meanwhile, in situ formation of tissue ROS was detected by staining with DHE and DCF as described recently. Briefly, fresh frozen left ventricular sections were incubated with DHE (2 μ M; Molecular Probes) or DCF (4 μ M; Molecular Probes), respectively. The activities of SOD and GSH were detected according to the Beyotime Kits.

2.8. Protein Preparation and Immunoblotting. Membrane proteins or total cell proteins were extracted from homogenized LV tissue. The primary antibodies included NOX2,

NOX4, p22^{phox}, p47^{phox}, p67^{phox}, Rac-1 (1:500, Abcam); eNOS, p-eNOS^{Ser1177}, p-eNOS^{Thr495}, p-eNOS^{Ser114}, iNOS, nNOS (1:1000, Cell Signaling Technology), β_3 -adrenergic receptor (1:500, Abcam), and β -actin (1:5000, Abcam).

2.9. Statistical Analysis. The results are presented as mean \pm SEM. All experiment data were analyzed by the GraphPad Prism8 software. Statistical comparisons for different group were performed using one-way ANOVA followed by Student's paired, two-tailed t test for two groups' comparison. P values < 0.05 were considered statistically significant.

3. Results

3.1. β_3 -AR Stimulation Alleviated Cardiac Hypertrophy and Remodeling in Pressure-Overloaded Mice. The representative

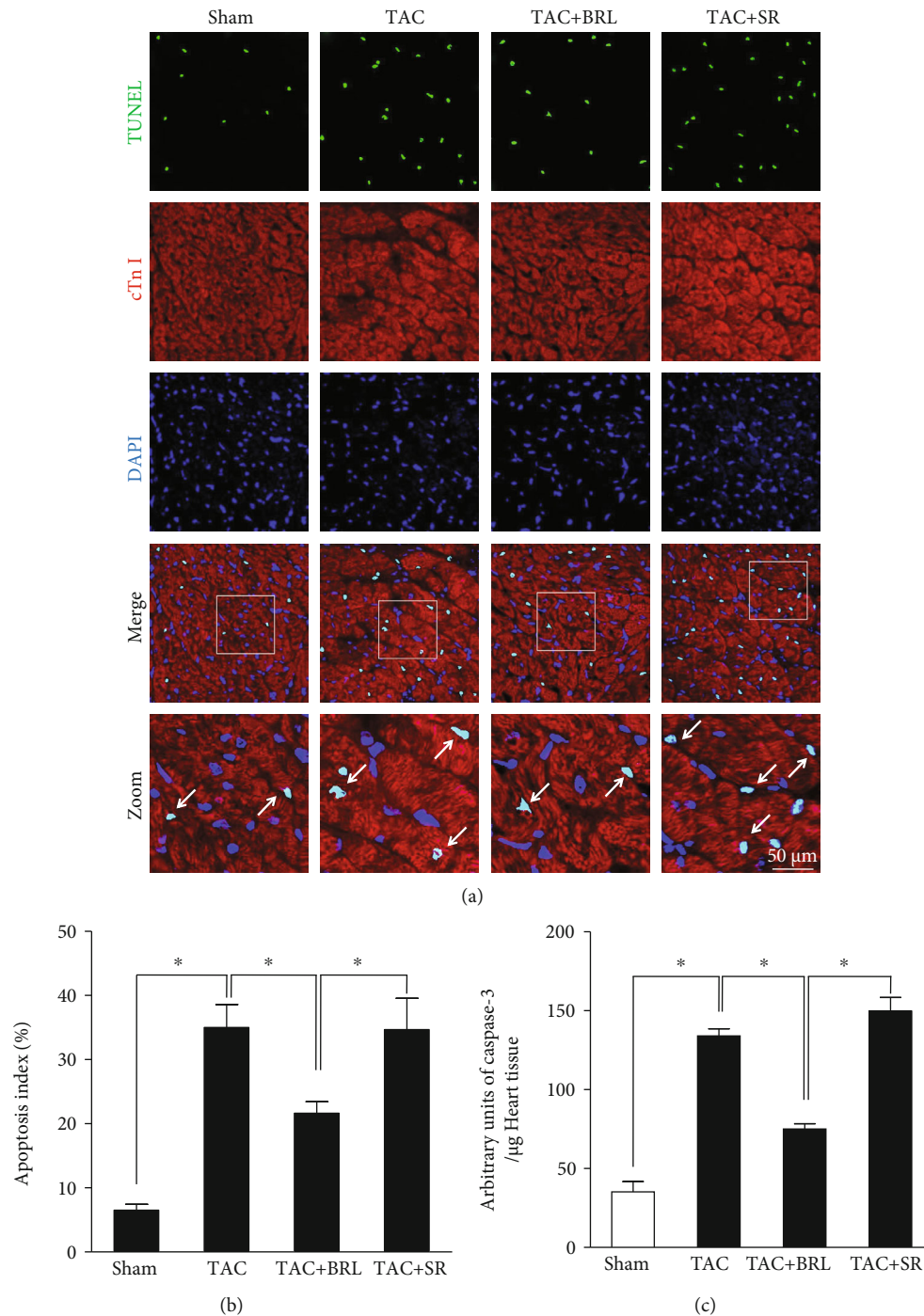


FIGURE 4: Cardiomyocyte apoptosis was inhibited in TAC mice after BRL treatment. (a, b) Representative images of TUNEL staining and the apoptosis index. (c) Caspase-3 activity. The number of mice ($n = 6$). * $P < 0.05$.

figures of hearts demonstrated that pressure overload caused ventricular dilatation (Figure 1(a)). Meanwhile, the heart weight/tibia length ratio (HW/TL ratio) in TAC was significantly increased compared to sham ones (168.9 ± 8.9 mg/cm vs. 117.4 ± 9.8 mg/cm, $P < 0.05$), indicating that pressure overload successfully induced cardiac pathological remodeling. Moreover, cross-sectional area, LV mass, and wall thickness all increased after TAC operation (Figures 1(b) and 1(d)–1(f)). These results suggested that mice developed evi-

dent cardiac hypertrophy induced by TAC. However, 3 weeks of BRL application significantly alleviated LV dilation, cardiac hypertrophy, and cardiac pathological remodeling. ANP and BNP levels significantly decreased after BRL treatment in TAC mice (Figures 1(g) and 1(h)). The size of cardiomyocytes in PE+BRL group was remarkably smaller compared to the PE group (Figures 1(i) and 1(j)). Thus, β_3 -AR stimulation reduced myocardial hypertrophy and remodeling induced by pressure overload.

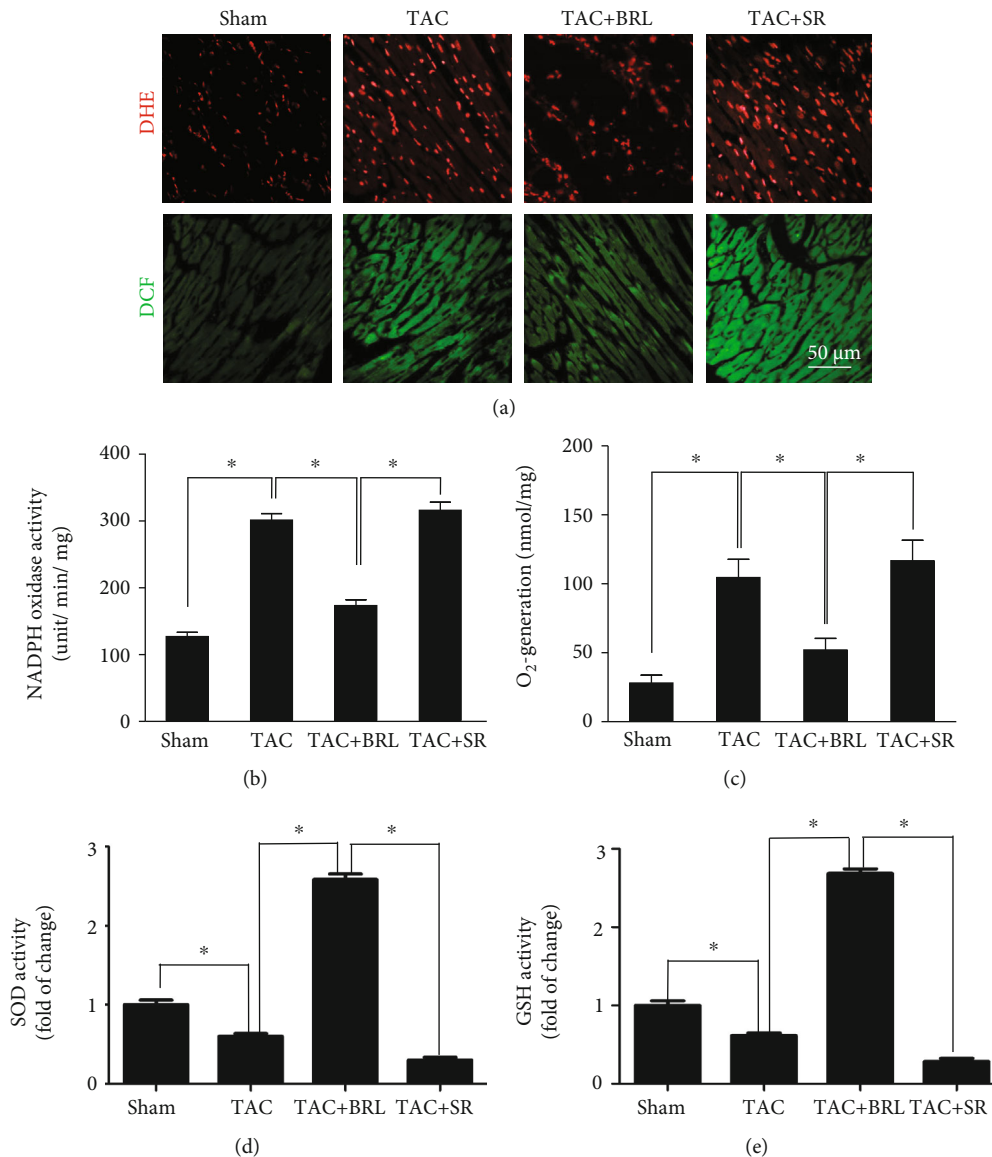


FIGURE 5: β 3-AR stimulation decreased the oxidative stress level in pressure-overloaded mice. (a) Representative images of DHE and DCF staining. (b) NADPH oxidase activity. (c) The production of $O_2^{\bullet-}$ in the heart tissues. (d, e) SOD and GSH activity. The number of mice ($n = 6$). * $P < 0.05$.

3.2. β 3-AR Stimulation Reduced Fibrosis after TAC. BRL treatment significantly reduced fibrosis compared with the TAC group (Figures 2(a) and 2(b)). Moreover, the increasing tendency of interstitial fibrosis was detected in the TAC+SR group, which is a β 3-AR-specific inhibitor, although without significance. Moreover, the levels of Col1a1, Col3a1, and FBN1 were all reduced in the TAC mice after BRL treatment (Figures 2(c)–2(e)).

3.3. β 3-AR Stimulation Improved Cardiac Dysfunction in TAC Mice. As shown in Figure 3(a), systolic dysfunction was revealed in the TAC and TAC+SR groups. Conversely, BRL treatment enhanced LV anterior wall motion after TAC operation, indicating that β 3-AR stimulation could improve cardiac dysfunction induced by pressure overload. Moreover, the LVEDd and LVESd were increased in TAC

mice. In addition, the LVEDd and LVESd were significantly decreased in TAC mice after BRL treatment (Figures 3(b) and 3(c)). Similarly, the enhanced LVEF and FS were observed in the TAC+BRL group, indicating that β 3-AR stimulation improved cardiac dysfunction after TAC (Figures 3(d) and 3(e)).

3.4. Cardiomyocyte Apoptosis Was Inhibited in TAC Mice after BRL Treatment. Figure 4(a) reveals that, compared to the TAC group and TAC+SR group, BRL treatment significantly decreased the cardiomyocyte apoptosis index. The apoptosis index in the TAC+BRL group was $21.67 \pm 1.76\%$, less than that in the TAC group ($35.3 \pm 3.6\%$, $P < 0.05$) and TAC+SR group ($34.7 \pm 4.7\%$, $P < 0.05$) (Figure 4(b)). Meanwhile, caspase-3 enzymatic activity decreased in the TAC+BRL group compared to the TAC group (73.2 ± 3.2

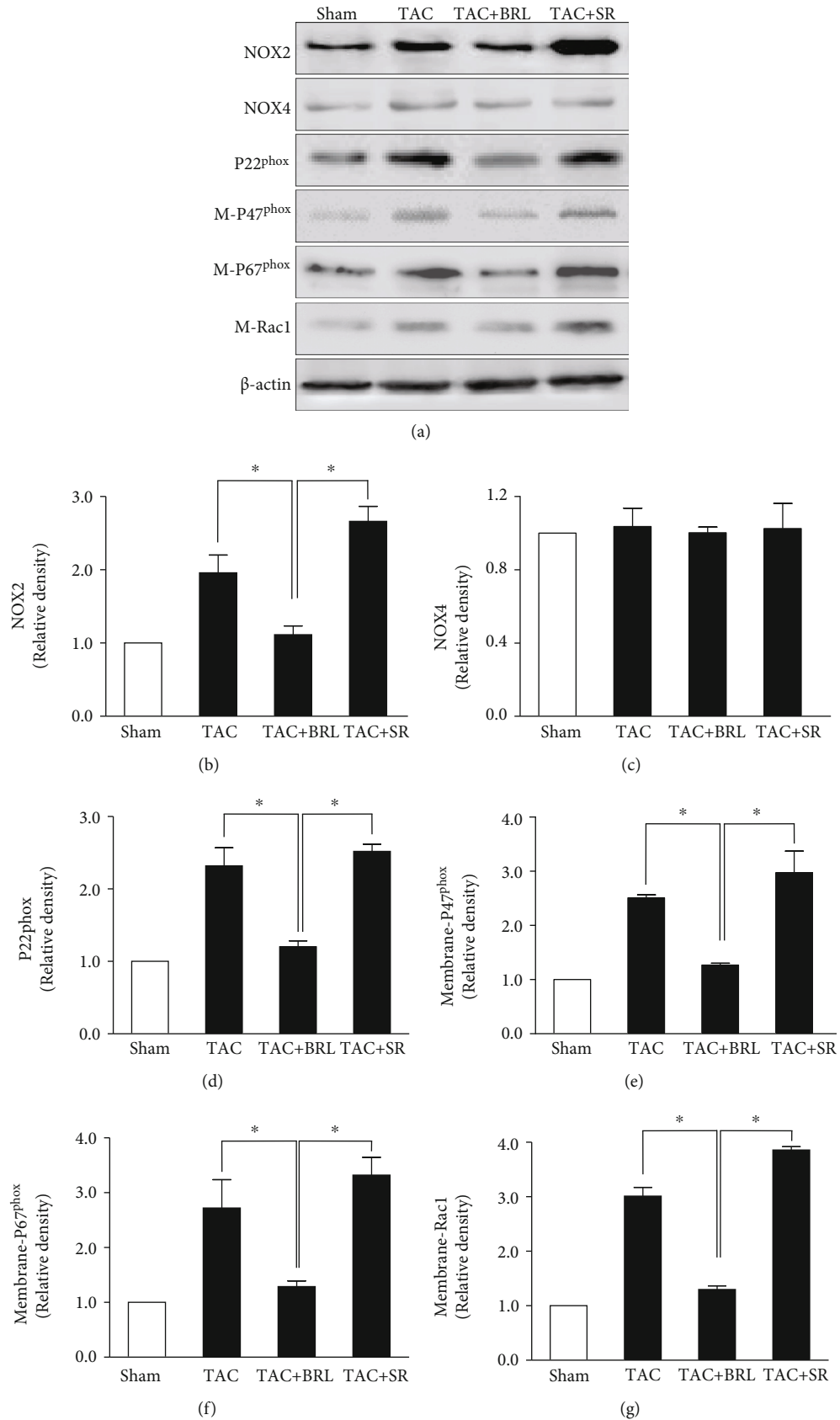


FIGURE 6: BRL treatment regulated the expression and activation of NADPH oxidase subunits. (a–g) Western blot analysis of NOX2, NOX4, p22^{phox}, p47^{phox}, p67^{phox}, and Rac1 expression. * $P < 0.05$.

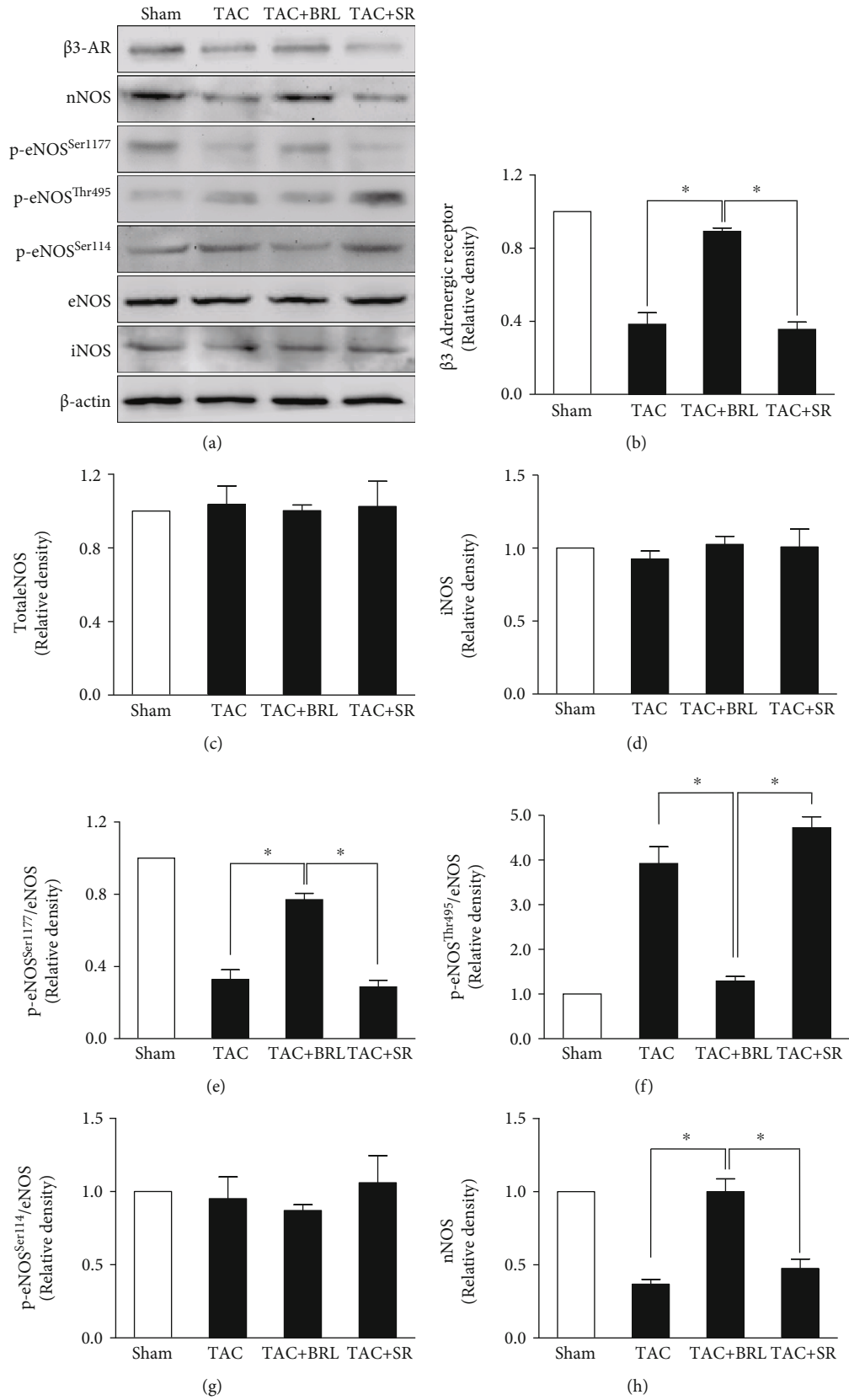


FIGURE 7: β 3-AR stimulation regulates activation and expression of NOS isoforms. (a-h) Western blot analysis of β 3-AR, nNOS, p-eNOS^{Thr495}, p-eNOS^{Ser114}, p-eNOS^{Ser1177}, eNOS, and iNOS. * $P < 0.05$.

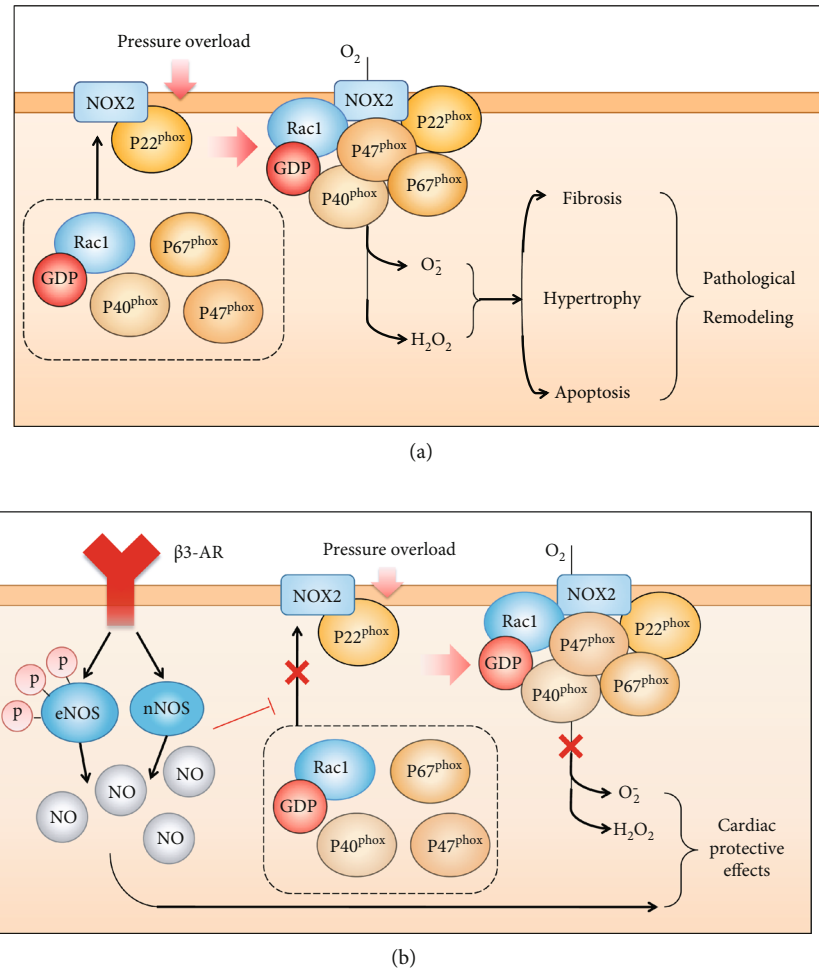


FIGURE 8: Schematic diagram depicting possible mechanisms involved in protective effects of β_3 -AR agonist in cardiac hypertrophy.

vs. 131.5 ± 3.7 , $P < 0.05$) and TAC+SR group (73.2 ± 3.2 vs. 140.2 ± 6.7 , $P < 0.05$) (Figure 4(c)). These data suggested that β_3 -AR stimulation decreased apoptosis in the pressure-overloaded heart.

3.5. β_3 -AR Stimulation Decreased the Oxidative Stress Level in Pressure-Overloaded Mice. The production of ROS, measured by DHE and DCF staining, was significantly increased in the TAC group and TAC+SR group. However, BRL treatment significantly decreased ROS generation in pressure-overloaded mice (Figure 5(a)). Meanwhile, the NADPH oxidase activity increased in the TAC group (301.5 ± 19.1 units/min/mg vs. 127.1 ± 13.1 units/min/mg; $P < 0.05$) and TAC+SR group (316.7 ± 24.5 units/min/mg vs. 127.1 ± 13.1 units/min/mg; $P < 0.05$). NADPH oxidase activity was lower in the TAC+BRL group compared to the TAC group (173.5 ± 17.4 units/min/mg vs. 301.5 ± 19.1 units/min/mg; $P < 0.05$, Figure 5(b)). Similarly, the $O_2^{\bullet-}$ production was lower in the TAC+BRL group compared with that in the TAC group (52.2 ± 8.4 nmol/mg vs. 104.5 ± 13.2 nmol/mg; $P < 0.05$; Figure 5(c)). The level of SOD and GSH was increased in the TAC+BRL group compared to the TAC group (Figures 5(d) and 5(e)). These findings indicated that

β_3 -AR stimulation decreased oxidative stress induced by pressure overload.

3.6. BRL Treatment Regulated the Expression and Activation of NADPH Oxidase Subunits. We assessed the intracellular expressions of NADPH oxidase subunits by Western blot assay. The expression of membrane-bound subunits, p22phox and NOX2, significantly increased in the TAC group, which was abolished by BRL treatment (Figures 6(a)–6(g)). However, the expression of NOX4 was unchanged in all groups. Moreover, the membrane expressions of p47phox, p67phox, and Rac1, which are cytosolic subunits, were significantly upregulated in the TAC group and TAC+SR group. Moreover, BRL treatment resulted in decreased expression of p47phox, p67phox, and Rac1.

3.7. β_3 -AR Stimulation Regulates Activation and Expression of NOS Isoforms. Western blotting assays were performed to evaluate β_3 -AR expression in all groups. The decreased β_3 -AR was observed in the TAC and TAC+SR groups (Figures 7(a) and 7(b)). Conversely, the expression of β_3 -AR increased after BRL treatment. We further evaluated the expression of NOS isoforms in all groups. First, the expression of total eNOS and phosphorylated eNOS^{Ser114}

was unchanged. However, TAC operation significantly decreased the phosphorylation of eNOS^{Thr495} but increased expression of phospho-eNOS^{Ser1177}, which were abolished by the BRL treatment. Furthermore, we examined the expression of iNOS and nNOS. There was no difference in iNOS expression in all groups (Figures 7(a) and 7(d)). In contrary, pressure overload decreased the cardiac expression of nNOS, which was increased by the BRL treatment (Figures 7(a) and 7(h)).

4. Discussion

Cardiac remodeling, a major determinant of CHF, is associated with pathological cardiac hypertrophy [20]. Initially, cardiac hypertrophy occurs as an adaptive response to maintain normal cardiac function and output by ameliorating ventricular wall stress. However, sustained pressure load induces pathological ventricular hypertrophy, resulting in heart failure and malignant arrhythmias [20]. Our study suggested that sustained pressure overload for 3 weeks induced cardiac hypertrophy and increased the oxidative stress and cardiomyocytes apoptosis, which were associated with impaired cardiac function. But these effects of pressure overload could be abolished by β 3-AR stimulation, which was in line with our previous study [24].

Oxidative stress is involved in cardiomyocyte apoptosis, cardiac remodeling, cardiac dysfunction, and heart failure [25–28]. Oxidative stress and related mitochondrial damage are strongly associated with the progression of many diseases [29, 30]. Previous study suggested that increased NADPH oxidase activity was observed in end-stage failing myocardium [16]. And increasing evidence suggested the important role of myocardial NADPH oxidase in cardiovascular diseases [31–33]. NADPH oxidase activity is involved in the pathophysiology of congestive heart failure. In our study, β 3-AR stimulation alleviated the oxidative stress by inhibiting NADPH oxidases. Moreover, the cardiac protective effect of BRL is mediated through NO generating via the nNOS pathway.

The NOX subunit forms a stable heterodimer with the p22phox subunit. Among all NOX subunits, NOX2 and NOX4 are mainly enriched in cardiomyocytes. Previous studies revealed that NOX2 deficiency inhibited cardiac hypertrophy [17]. Interestingly, a recent study demonstrated that cardiac dysfunction was exaggerated in NOX4-null mice. Moreover, NOX4 knockout exaggerated cardiac dysfunction when exposed to chronic overload, indicating NOX4 mediates protection against stress [34]. In current study, TAC treatment increased the NOX2 expression, whereas the expression of NOX4 was unchanged in all groups. Therefore, our results suggested that NOX2 is detrimental during pressure overload-induced remodeling. Furthermore, the expression of cytosolic subunits, including p47phox, p67phox, and Rac1, was significantly upregulated in TAC mice. Taken together, we found that the combination of NOX2 with a series of subunits directly activates the NADPH oxidases and generates superoxide, which subsequently results in the pressure overload-induced cardiac injury.

It has been demonstrated that 3 subtypes of β -ARs may modulate cardiac function. Among them, β 1-AR and β 2-ARs mediate positive chronotropic and inotropic effects [20, 21]. β 3-AR is reported to mediate lipolysis and thermogenesis in adipocytes [35]. However, β 3-AR is also involved in cardiovascular system regulation, which may antagonize the effects of β 1/2-ARs. Moreover, β 3-AR is increased in failing hearts [24]. Meanwhile, β 3-AR overexpression attenuated cardiac hypertrophy [36]. Furthermore, β 3 knockout exacerbated cardiac hypertrophy induced by pressure overload [24]. In current study, β 3-AR stimulation reduced hypertrophy, prevented fibrosis, and preserved cardiac function induced by pressure overload. Furthermore, β 3-AR stimulation reduced the superoxide generation in TAC mice. Meanwhile, NADPH oxidase activity was also decreased after β 3-AR stimulation, indicating that the protective effect of β 3-AR is mediated, at least by part, through inhibiting NADPH oxidases, which contributes to the cardiac oxidative stress induced by pressure overload (Figure 8).

β 3-AR stimulation could increase NO release by NOS activity [36]. Moreover, our previous study has demonstrated that β 3-AR knockout exacerbates NOS uncoupling, suggesting that β 3-AR regulates cardiac oxidative stress by regulating NO generation through NOS activity [24]. Three NOS isoforms are all associated with NO release. However, which NOS isoform regulates cardiac function by β 3-AR signaling still remains unclear. The activity of eNOS is mainly affected by eNOS-PSer1177, eNOS-PThr495, and eNOS-PSer114. Phosphorylation at Ser1177 activates eNOS, whereas phosphorylations at Ser114 and Thr497 inhibit eNOS activity [37]. In the current study, the decreased p-eNOS^{Thr495} and increased p-eNOS^{Ser1177} were observed in chronic pressure overload after BRL treatment. Therefore, β 3-AR stimulation leads to eNOS deactivation rather than activation. In contrary, β 3-AR stimulation increased the expression of nNOS. Moreover, both nNOS expression and nNOS-derived NO production regulate cardiac function [30]. The cardioprotective effects of β 3-AR were actually abolished in nNOS^{-/-} mice [24]. Based on these results, nNOS may be the primary downstream of β 3-AR (Figure 8).

In conclusion, we provide evidence that β 3-AR stimulation regulates the oxidative stress by inhibiting NADPH oxidases, which impaired cardiac function. In addition, these cardioprotective effects of β 3-AR are largely attributed to nNOS activation. These inspiring observations provide novel insight into β 3-AR as a new target for treating cardiac hypertrophy.

Data Availability

The original contributions presented in the study are included in the article; further inquiries can be directed to the corresponding author.

Conflicts of Interest

The authors declare that they have no conflicts of interest.

Authors' Contributions

Mingming Zhang, Yuerong Xu, Jianghong Chen, and Chaoshi Qin contributed equally to this work.

Acknowledgments

This work was supported by the National Natural Science Foundation of China (No. 81570227, No. 81900338), Science and Technology Development Fund (2021XB030), and Shaanxi Province Science and Technology New Star Project (2015KJJK-52).







References

- [1] T. J. Povsic, "Emerging therapies for congestive heart failure," *Clinical Pharmacology and Therapeutics*, vol. 103, no. 1, pp. 77–87, 2018.
- [2] J. Chen, S.-L. T. Normand, Y. Wang, and H. M. Krumholz, "National and regional trends in heart failure hospitalization and mortality rates for Medicare beneficiaries, 1998-2008," *Journal of the American Medical Association*, vol. 306, no. 15, pp. 1669–1678, 2011.
- [3] J. Wang and H. Zhou, "Mitochondrial quality control mechanisms as molecular targets in cardiac ischemia ** – ** reperfusion injury," *Acta Pharmaceutica Sinica B*, vol. 10, no. 10, pp. 1866–1879, 2020.
- [4] B. Zhou and R. Tian, "Mitochondrial dysfunction in pathophysiology of heart failure," *The Journal of Clinical Investigation*, vol. 128, no. 9, pp. 3716–3726, 2018.
- [5] A. G. Nickel, A. von Hardenberg, M. Hohl et al., "Reversal of mitochondrial transhydrogenase causes oxidative stress in heart failure," *Cell Metabolism*, vol. 22, no. 3, pp. 472–484, 2015.
- [6] B. Dong, C. Liu, R. Xue et al., "Fisetin inhibits cardiac hypertrophy by suppressing oxidative stress," *The Journal of Nutritional Biochemistry*, vol. 62, pp. 221–229, 2018.
- [7] C. Wang, Y. Yuan, J. Wu et al., "Plin5 deficiency exacerbates pressure overload-induced cardiac hypertrophy and heart failure by enhancing myocardial fatty acid oxidation and oxidative stress," *Free Radical Biology & Medicine*, vol. 141, pp. 372–382, 2019.
- [8] R. SHENG, Z. L. GU, M. L. XIE, W. X. ZHOU, and C. Y. GUO, "EGCG inhibits cardiomyocyte apoptosis in pressure overload-induced cardiac hypertrophy and protects cardiomyocytes from oxidative stress in rats," *Acta Pharmacologica Sinica*, vol. 28, no. 2, pp. 191–201, 2007.
- [9] Y. Tan, D. Mui, S. Toan, P. Zhu, R. Li, and H. Zhou, "SERCA overexpression improves mitochondrial quality control and attenuates cardiac microvascular ischemia-reperfusion injury," *Mol Ther Nucleic Acids*, vol. 22, pp. 696–707, 2020.
- [10] J. Wang, P. Zhu, R. Li, J. Ren, Y. Zhang, and H. Zhou, "Bax inhibitor 1 preserves mitochondrial homeostasis in acute kidney injury through promoting mitochondrial retention of PHB2," *Theranostics*, vol. 10, no. 1, pp. 384–397, 2020.
- [11] J. Wang, P. Zhu, R. Li, J. Ren, and H. Zhou, "Fundc1-dependent mitophagy is obligatory to ischemic preconditioning-conferred renoprotection in ischemic AKI via suppression of Drp1-mediated mitochondrial fission," *Redox Biology*, vol. 30, p. 101415, 2020.
- [12] H. Zhou, P. Zhu, J. Wang, H. Zhu, J. Ren, and Y. Chen, "Pathogenesis of cardiac ischemia reperfusion injury is associated with CK2 α -disturbed mitochondrial homeostasis via suppression of FUNDC1-related mitophagy," *Cell Death and Differentiation*, vol. 25, no. 6, pp. 1080–1093, 2018.
- [13] B. Kura, B. Szeiffova Bacova, B. Kalocayova, M. Sykora, and J. Slezak, "Oxidative stress-responsive microRNAs in heart injury," *International Journal of Molecular Sciences*, vol. 21, no. 1, p. 358, 2020.
- [14] K. Bedard and K.-H. Krause, "The NOX family of ROS-generating NADPH oxidases: physiology and pathophysiology," *Physiological Reviews*, vol. 87, no. 1, pp. 245–313, 2007.
- [15] Y. Zhang, P. Murugesan, K. Huang, and H. Cai, "NADPH oxidases and oxidase crosstalk in cardiovascular diseases: novel therapeutic targets," *Nature Reviews. Cardiology*, vol. 17, no. 3, pp. 170–194, 2020.
- [16] C. Heymes, J. K. Bendall, P. Ratajczak et al., "Increased myocardial NADPH oxidase activity in human heart failure," *Journal of the American College of Cardiology*, vol. 41, no. 12, pp. 2164–2171, 2003.
- [17] D. J. Grieve, J. A. Byrne, A. Siva et al., "Involvement of the nicotinamide adenosine dinucleotide phosphate oxidase isoform NOX2 in cardiac contractile dysfunction occurring in response to pressure overload," *Journal of the American College of Cardiology*, vol. 47, no. 4, pp. 817–826, 2006.
- [18] L. Lyu, J. Chen, W. Wang et al., "Scoparone alleviates Ang II-induced pathological myocardial hypertrophy in mice by inhibiting oxidative stress," *Journal of Cellular and Molecular Medicine*, vol. 25, no. 6, pp. 3136–3148, 2021.
- [19] A. K. Jain, N. K. Mehra, and N. K. Swarnakar, "Role of antioxidants for the treatment of cardiovascular diseases: challenges and opportunities," *Current Pharmaceutical Design*, vol. 21, no. 30, pp. 4441–4455, 2015.
- [20] R. M. Graff, H. E. Kunz, N. H. Agha et al., " β_2 -Adrenergic receptor signaling mediates the preferential mobilization of differentiated subsets of CD8+ T-cells, NK-cells and non-classical monocytes in response to acute exercise in humans," *Brain, Behavior, and Immunity*, vol. 74, pp. 143–153, 2018.
- [21] M. I. Talan, I. Ahmet, R.-P. Xiao, and E. G. Lakatta, " β_2 AR agonists in treatment of chronic heart failure: long path to translation," *Journal of Molecular and Cellular Cardiology*, vol. 51, no. 4, pp. 529–533, 2011.
- [22] P. B. Molinoff, "Alpha- and beta-adrenergic receptor subtypes properties, distribution and regulation," *Drugs*, vol. 28, Supplement 2, 1984.
- [23] C. Gauthier, D. Langin, and J. L. Balligand, " β_3 -Adrenoceptors in the cardiovascular system," *Trends in Pharmacological Sciences*, vol. 21, no. 11, pp. 426–431, 2000.
- [24] X. Niu, V. L. Watts, O. H. Cingolani et al., "Cardioprotective effect of beta-3 adrenergic receptor agonism: role of neuronal nitric oxide synthase," *Journal of the American College of Cardiology*, vol. 59, no. 22, pp. 1979–1987, 2012.
- [25] H. Takano, Y. Zou, H. Hasegawa, H. Akazawa, T. Nagai, and I. Komuro, "Oxidative stress-induced signal transduction pathways in cardiac myocytes: involvement of ROS in heart diseases," *Antioxidants & Redox Signaling*, vol. 5, no. 6, pp. 789–794, 2003.
- [26] J. Kuroda and J. Sadoshima, "NADPH oxidase and cardiac failure," *Journal of Cardiovascular Translational Research*, vol. 3, no. 4, pp. 314–320, 2010.

- [27] J. Wang, S. Toan, and H. Zhou, "New insights into the role of mitochondria in cardiac microvascular ischemia/reperfusion injury," *Angiogenesis*, vol. 23, no. 3, pp. 299–314, 2020.
- [28] H. Zhou, S. Toan, P. Zhu, J. Wang, J. Ren, and Y. Zhang, "DNA-PKcs promotes cardiac ischemia reperfusion injury through mitigating BI-1-governed mitochondrial homeostasis," *Basic Research in Cardiology*, vol. 115, no. 2, p. 11, 2020.
- [29] R. Li, T. Xin, D. Li, C. Wang, H. Zhu, and H. Zhou, "Therapeutic effect of Sirtuin 3 on ameliorating nonalcoholic fatty liver disease: the role of the ERK-CREB pathway and Bnip3-mediated mitophagy," *Redox Biology*, vol. 18, pp. 229–243, 2018.
- [30] H. Zhou, S. Wang, P. Zhu, S. Hu, Y. Chen, and J. Ren, "Empagliflozin rescues diabetic myocardial microvascular injury via AMPK-mediated inhibition of mitochondrial fission," *Redox Biology*, vol. 15, pp. 335–346, 2018.
- [31] Q. D. Zhao, S. Viswanadhapalli, P. Williams et al., "NADPH oxidase 4 induces cardiac fibrosis and hypertrophy through activating Akt/mTOR and NF κ B signaling pathways," *Circulation*, vol. 131, no. 7, pp. 643–655, 2015.
- [32] L. Yu, G. Yang, X. Zhang et al., "Megakaryocytic leukemia 1 bridges epigenetic activation of NADPH oxidase in macrophages to cardiac ischemia-reperfusion injury," *Circulation*, vol. 138, no. 24, pp. 2820–2836, 2018.
- [33] H. Zhou, J. Wang, P. Zhu et al., "NR4A1 aggravates the cardiac microvascular ischemia reperfusion injury through suppressing FUNDC1-mediated mitophagy and promoting Mff-required mitochondrial fission by CK2 α ," *Basic Research in Cardiology*, vol. 113, no. 4, p. 23, 2018.
- [34] M. Zhang, H. Mongue-Din, D. Martin et al., "Both cardiomyocyte and endothelial cell Nox4 mediate protection against hemodynamic overload-induced remodelling," *Cardiovascular Research*, vol. 114, no. 3, pp. 401–408, 2018.
- [35] J. Gómez-Ambrosi, G. Frühbeck, M. Aguado, F. I. Milagro, J. Margareto, and A. J. Martínez, "Divergent effects of an α 2-adrenergic antagonist on lipolysis and thermogenesis: interactions with a β 3-adrenergic agonist in rats," *International Journal of Molecular Medicine*, vol. 8, no. 1, pp. 103–109, 2001.
- [36] C. Belge, J. Hammond, E. Dubois-Deruy et al., "Enhanced expression of β 3-adrenoceptors in cardiac myocytes attenuates neurohormone-induced hypertrophic remodeling through nitric oxide synthase," *Circulation*, vol. 129, no. 4, pp. 451–462, 2014.
- [37] W. O. Idigo, S. Reilly, M. H. Zhang et al., "Regulation of endothelial nitric-oxide synthase (NOS) S-glutathionylation by neuronal NOS," *The Journal of Biological Chemistry*, vol. 287, no. 52, pp. 43665–43673, 2012.

Research Article

SIRT5-Related Desuccinylation Modification Contributes to Quercetin-Induced Protection against Heart Failure and High-Glucose-Prompted Cardiomyocytes Injured through Regulation of Mitochondrial Quality Surveillance

Xing Chang ^{1,2}, Tian Zhang ¹, Junyan Wang,³ Yan Liu,¹ Peizheng Yan ¹,
Qingyan Meng ¹, Yongtian Yin ¹, and Shiyuan Wang ¹

¹Shandong University of Traditional Chinese Medicine, Jinan, Shandong 250355, China

²Guang'anmen Hospital, Chinese Academy of Traditional Chinese Medicine, Beijing 100053, China

³The First Affiliated Hospital, Guangzhou University of Chinese Medicine, Guangzhou 510405, China

Correspondence should be addressed to Qingyan Meng; mqytc@163.com, Yongtian Yin; yinyongtian2004@163.com, and Shiyuan Wang; wsyuan2009@163.com

Received 14 April 2021; Revised 27 July 2021; Accepted 13 August 2021; Published 24 September 2021

Academic Editor: Yun-dai Chen

Copyright © 2021 Xing Chang et al. This is an open access article distributed under the Creative Commons Attribution License, which permits unrestricted use, distribution, and reproduction in any medium, provided the original work is properly cited.

Myocardial fibrosis represents the primary pathological change associated with diabetic cardiomyopathy and heart failure, and it leads to decreased myocardial compliance with impaired cardiac diastolic and systolic function. Quercetin, an active ingredient in various medicinal plants, exerts therapeutic effects against cardiovascular diseases. Here, we investigate whether SIRT5- and IDH2-related desuccinylation is involved in the underlying mechanism of myocardial fibrosis in heart failure while exploring related therapeutic drugs for mitochondrial quality surveillance. Mouse models of myocardial fibrosis and heart failure, established by transverse aortic constriction (TAC), were administered with quercetin (50 mg/kg) daily for 4 weeks. HL-1 cells were pretreated with quercetin and treated with high glucose (30 mM) *in vitro*. Cardiac function, western blotting, quantitative PCR, enzyme-linked immunosorbent assay, and immunofluorescence analysis were employed to analyze mitochondrial quality surveillance, oxidative stress, and inflammatory response in myocardial cells, whereas IDH2 succinylation levels were detected using immunoprecipitation. Myocardial fibrosis and heart failure incidence increased after TAC, with abnormal cardiac ejection function. Following high-glucose treatment, HL-1 cell activity was inhibited, causing excess production of reactive oxygen species and inhibition of mitochondrial respiratory complex I/III activity and mitochondrial antioxidant enzyme activity, as well as increased oxidative stress and inflammatory response, imbalanced mitochondrial quality surveillance and homeostasis, and increased apoptosis. Quercetin inhibited myocardial fibrosis and improved cardiac function by increasing mitochondrial energy metabolism and regulating mitochondrial fusion/fission and mitochondrial biosynthesis while inhibiting the inflammatory response and oxidative stress injury. Additionally, TAC inhibited SIRT5 expression at the mitochondrial level and increased IDH2 succinylation. However, quercetin promoted the desuccinylation of IDH2 by increasing SIRT5 expression. Moreover, treatment with si-SIRT5 abolished the protective effect of quercetin on cell viability. Hence, quercetin may promote the desuccinylation of IDH2 through SIRT5, maintain mitochondrial homeostasis, protect mouse cardiomyocytes under inflammatory conditions, and improve myocardial fibrosis, thereby reducing the incidence of heart failure.

1. Introduction

Heart failure is a condition that leads to ventricular filling or impaired ejection function due to various organic or functional heart diseases, and it represents the end stage of vari-

ous cardiovascular diseases, particularly those associated with diabetic cardiomyopathy. Thus, heart failure is referred to as “the last battleground of diabetic cardiovascular disease” in clinical practice [1]. In the past few decades, most research has focused on the maintenance of diabetic

myocardial injury, cardiac hemodynamics, and regulation of the islet system. Diabetes in patients with heart failure has been shown to occur significantly earlier than in patients without coronary heart disease, hypertension, or diabetes. Myocardial fibrosis is vulnerable to factors such as oxidative stress, inflammatory response, mitochondrial energy metabolism disorder, and cellular aging [2]. As the main cause of ventricular remodeling [3], myocardial fibrosis can promote decreased myocardial compliance and impaired cardiac systolic and diastolic function. Ultimately, long-term volume or pressure overload can lead to heart failure. Thus, progression from diabetic cardiomyopathy to heart failure is accompanied by severe myocardial fibrosis or cardiac hypertrophy [4, 5]. As such, improving myocardial fibrosis has been shown to delay heart failure and improve heart function and has become a new approach for treating diabetic cardiomyopathy and heart failure [6].

Mitochondria, the energy metabolism centers of cells, produce energy through oxidative phosphorylation to meet the high energy needs of the heart [7, 8]. Many important physiological activities occurring in the heart, such as myocardial contraction and maintenance of intracellular homeostasis, require ATP [9–11]. Mitochondria have their own quality control system to maintain and restore structure and energy metabolism by regulating mitochondrial fission, fusion, biogenesis, and mitophagy [12, 13]. This surveillance system can protect mitochondria and cardiomyocytes from stress stimulation [8, 13]. Moreover, myocardial damage because of diabetic cardiomyopathy may be related to mitochondrial dysfunction caused by an imbalance in mitochondrial quality surveillance.

Therefore, normal cardiac physiological functioning requires intact and fully functioning mitochondria. Indeed, excessive production of mitochondrial reactive oxygen species (ROS) or damage to the myocardial antioxidant system is related to ventricular hypertrophy and wall remodeling, which can lead to myocardial fibrosis and heart failure. Studies have revealed abnormalities in the morphology and structure of myocardial mitochondria in patients with diabetes mellitus complicated with heart failure and diabetic cardiomyopathy. Moreover, mitochondrial membrane damage and structural abnormalities have been reported in canine models of heart failure. Decreased mitochondrial membrane potential, abnormal mitochondrial permeability transition pore (mPTP) opening, decreased ATP synthesis, and excessive ROS production have also been detected [14, 15]. Hence, conducting mitochondrial quality surveillance by targeting mitochondrial mass and homeostasis may be useful for inhibiting oxidative stress and inflammatory responses, thereby improving fibrosis [16]. Oxidative stress and inflammatory responses are important factors that induce myocardial fibrosis and often coexist at the same lesion site in various cardiovascular diseases [16, 17]. When a variety of cardiovascular complications or metabolic cardiomyopathy occur accompanied by acute or chronic myocardial injury, the immune system is activated, releasing numerous inflammatory factors that induce oxidative stress injury, activate myocardial fibroblasts, and cause abnormal collagen metabolism, myocardial cell necrosis, and tissue

degeneration, thus ultimately leading to myocardial fibrosis and heart failure [18, 19].

Sirtuin 5 (SIRT5) is widely distributed in the nucleus, cytoplasm, and mitochondria. Although SIRT5 exhibits deacetylase activity, it can regulate lysine succinylation [20]. Through its N-terminal peroxisome localization signal PTS2, SIRT5 can enter peroxisomes to reduce intracellular H_2O_2 production, thus playing a major role in cell oxidation. Moreover, SIRT5 reportedly promotes desuccinylation as a protective mechanism in acute myocardial infarction [21–23]. Specifically, acute cardiac ischemia and hypoxia may upregulate the expression of SIRT5 through the PGC-1 α /PPAR- γ pathway, leading to subsequent desuccinylation of key proteins involved in cardiomyocyte energy metabolism, thus exerting a protective effect on these cells [24]. Posttranslational modification of SIRT5 occurs primarily in the mitochondria. Also occurring within the mitochondria, NADP⁺-dependent isocitrate dehydrogenase 2 (IDH2) can affect the normal operation of the glutathione- (GSH-) related mitochondrial antioxidant system, including the activities of glutathione peroxidase (GPX) [25]. Moreover, IDH2 provides NADPH to glutathione reductase and thioredoxin reductase, thereby eliciting a regulatory effect to protect mitochondria from oxidative stress [26]. However, few studies have evaluated the regulation of SIRT5 and IDH2 succinylation in heart failure.

Quercetin is a flavonoid that is widely present in nature. Pharmacological studies have reported that quercetin can delay vascular endothelial functional damage and cardiac terminal damage [27]. Quercetin also has a regulatory role in the prevention of myocardial fibrosis [28] and can further regulate islet function. Moreover, we previously found that quercetin can regulate mitophagy and endoplasmic reticulum stress through SIRT1/TMBIM6, improve mitochondrial energy metabolism, and protect human cardiac myocytes [27]. However, the regulatory mechanisms underlying the effect of quercetin on SIRT5 succinylation and its protective effect on myocardial cells remain unclear. Therefore, we hypothesized that succinylation regulated by SIRT5 affects the metabolic growth of cells via mitochondrial quality surveillance and mitochondrial homeostasis. We found that SIRT5 deletion may lead to increased succinylation, which in turn affects cardiomyocyte activity and myocardial fibrosis.

2. Materials and Methods

2.1. Animals and Drug Treatment. All experimental procedures were performed in accordance with the NIH *Guide for the Care and Use of Laboratory Animals* and were approved by the Shandong University of Traditional Chinese Medicine Institutional Animal Care and Use Committee. Briefly, 30 male wild-type C57BL/6J mice (8-week-old) were obtained from the Experimental Animal Center of Shandong University of Traditional Chinese Medicine and randomly divided into three groups: (1) sham operation, (2) transverse aortic constriction (TAC), and (3) TAC+quercetin. The TAC+quercetin group was intraperitoneally administered with 50 mg/kg quercetin daily (Shanghai

Yuanye Biotechnology Company, Shanghai, China) for 15 days. Sham and TAC mice were administered with a corresponding intraperitoneal injection of normal saline.

2.2. Establishment of the Animal Model. A congestive heart failure model was established using TAC [29]. Briefly, the mice were anesthetized by intravenous injection of pentobarbital (50 mg/kg; Sigma-Aldrich, St. Louis, MO, USA), and a ventilator was connected after which thoracotomy was performed. The aorta was ligated with an 8-0 silk thread between the right artery and left common carotid artery and reduced to 25–30% of the original cross-sectional area with a 27 G needle.

2.3. Cell Culture. HL-1 myocytes were provided by the Experimental Center of Shandong University of Traditional Chinese Medicine. The cells were cultured in a Claycomb medium containing 10% fetal bovine serum, 100 U/mL penicillin/streptomycin, 0.1 mM noradrenaline, and 2 mM L-glutamine. The cells were cultured at 37°C and 5% CO₂ [30]. Glucose was purchased from Sigma-Aldrich. Quercetin was obtained from Shanghai Yuanye Biotechnology Company. The cells were randomized into the four experimental groups: (1) control, (2) high glucose (HG), (3) HG+quercetin, and (4) HG+quercetin+si-SIRT5. HL-1 cells were treated with high glucose (30 mmol/L) and quercetin (150 mg/L). For small interfering RNA (siRNA) transfection, Lipofectamine RNAiMAX (Invitrogen, Carlsbad, CA, USA) was used to transfect 50 nM siRNA into the HL-1 cells 24 h before treatment. All siRNAs were obtained from Jikai Biology (Shanghai, China).

2.4. Flow Cytometry. To analyze the apoptosis level, HL-1 cells were resuspended in phosphate-buffered saline (Gibco, Grand Island, NY, USA), fixed with 70% ethanol for 24 h, washed, and then placed in 50 µg/mL propidium iodide solution. After 30 min, the cells were resuspended, and flow cytometry was performed to detect apoptosis as described previously.

2.5. Cell Viability Assay. The viability of HL-1 cells was evaluated using an MTT assay. Cells were seeded into 12-well plates at a density of 50,000 cells/well. After 22 h, the cells were supplemented with fresh growth medium and incubated for 24 h, after which cell viability was determined by MTT assay [31].

2.6. Enzyme-Linked Immunosorbent Assay. An enzyme-linked immunosorbent assay (ELISA) kit was used to quantitatively analyze the activity of antioxidant enzymes and inflammatory factors in mouse myocardial tissue homogenates and HL-1 cells. Briefly, myocardial tissue homogenates and HL-1 cell suspensions were collected.

2.7. Oxygen Consumption Rate. The oxygen consumption rate of HL-1 cells in different groups was measured using a Seahorse XF Cell Mitochondrial Pressure Test kit (Agilent Technologies, Santa Clara, CA, USA), whereas the extracellular acidification rate was measured with a Seahorse XF glycol-

ysis rate assay kit (Agilent Technologies). Both assays were performed according to the manufacturer's instructions.

2.8. Real-Time Quantitative PCR. Total RNA was extracted using TRIzol reagent, and RNA integrity was analyzed by agarose gel electrophoresis. First-strand cDNA was synthesized using an iScript™ cDNA synthesis kit (1 µL of total RNA; Bio-Rad, Hercules, CA, USA) in a total volume of 20 µL. A CFX96 RT-PCR system (Bio-Rad) was used to analyze the level of cDNA twice using 500×10^{-9} nM specific primers. In each experiment, continuously diluted mixed cDNA was used to evaluate the efficiency of the PCR analysis. Gene expression was quantified relative to the geometric mean of housekeeping gene expression amplified in the same sample as the studied gene, and gene expression was determined using the $2^{-\Delta\Delta CT}$ method [32].

2.9. Statistical Analysis. Data are expressed as the mean ± standard deviation of the mean. One-way analysis of variance was used to verify the differences between multiple groups, and Student-Newman-Keuls post hoc test was performed. Two-tailed *t*-tests were used to compare two groups. Statistical analysis was performed using SPSS 22.0 software (SPSS, Inc., Chicago, IL, USA). Statistical significance was set at $P < 0.05$.

3. Results

3.1. Quercetin Alleviates Myocardial Hypertrophy and Cardiac Dysfunction after TAC. C57BL/6J male mice were randomly divided into three groups (control, TAC operation, and TAC operation+quercetin). Quercetin was administered to the TAC+quercetin group (50 mg/kg, every 12 h). Seven weeks after TAC, approximately 20% of the mice in the TAC model group and 10% of in the quercetin treatment group died. Compared with that in the sham operation group, cardiac function in the TAC group deteriorated remarkably after 3 weeks (Figures 1(a)–1(i)). However, cardiac function in mice treated with quercetin was improved compared to mice not treated with quercetin (Figures 1(a)–1(i)).

We then assessed myocardial hypertrophy in TAC mice after TAC+quercetin treatment using hematoxylin and eosin, WGA, and TUNEL staining 8 weeks after TAC (Figures 1(j)–1(m)). Compared with that in the sham operation group, the degree of cardiac hypertrophy and cardiomyocyte hypertrophy or death in TAC mice was significantly increased (Figures 1(j)–1(m)); however, this effect was significantly decreased following quercetin treatment (Figures 1(j)–1(m)).

3.2. Quercetin Attenuates Myocardial Fibrosis and Inflammatory Levels after TAC. We detected collagenase I levels in the myocardium of different groups by immunohistochemistry. The collagenase I/III level in the myocardium of the model group was significantly increased after TAC (Figures 2(h)–2(j)); this effect was reversed by quercetin (Figures 2(h)–2(j)). We also assessed the degree of myocardial fibrosis in different groups by Masson staining. The degree of myocardial fibrosis in the model group was

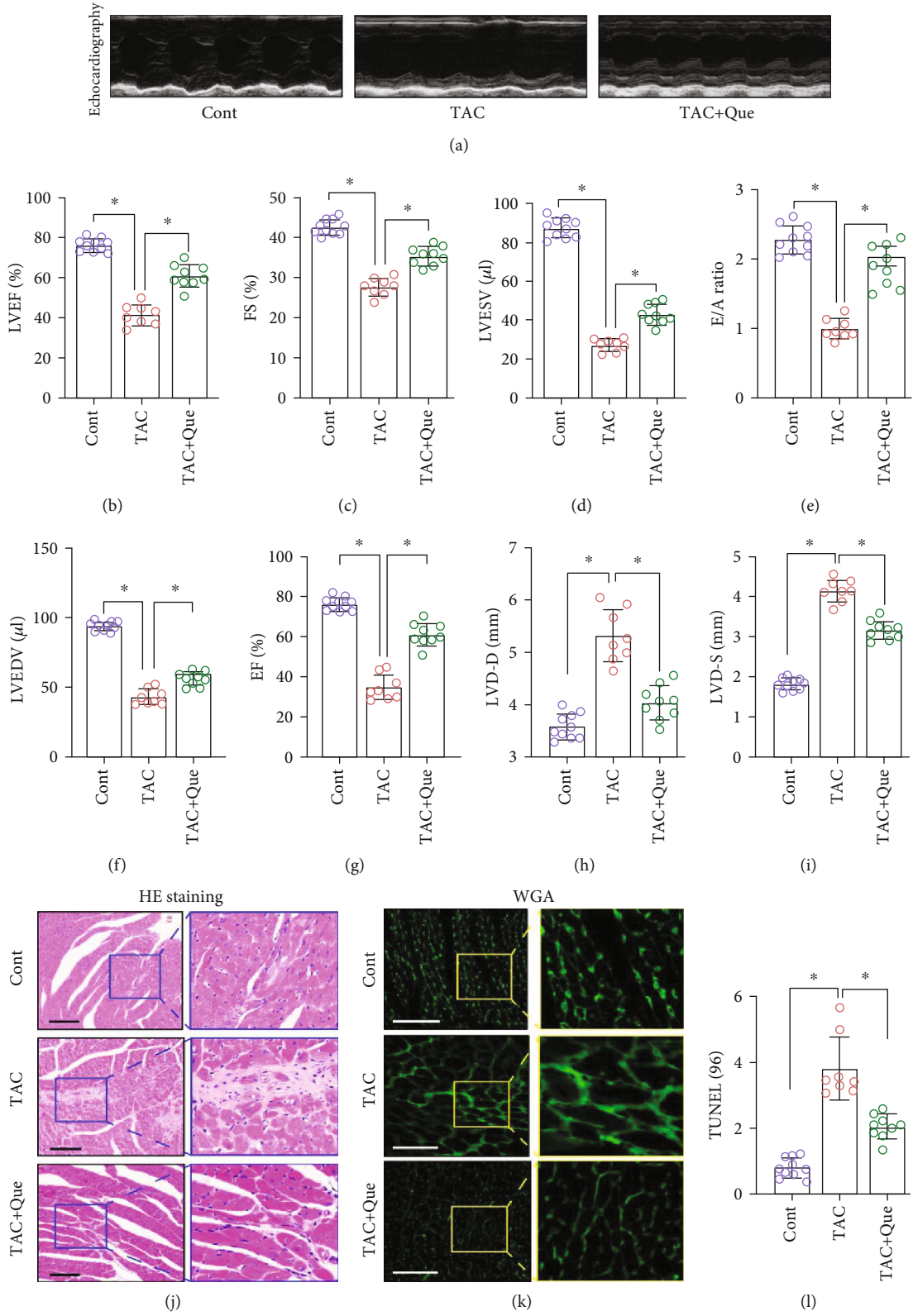


FIGURE 1: Continued.

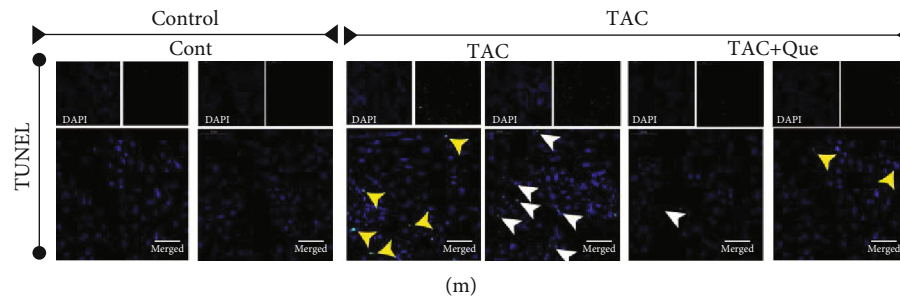


FIGURE 1: Quercetin (Que) alleviates myocardial hypertrophy and cardiac ejection dysfunction after transverse aortic constriction (TAC). (a) Representative M-mode echocardiography recordings. (b) Left ventricular ejection fraction (LVEF)%. (c) Fractional shortening (FS)%. (d) Left ventricular end-systolic volume (LVESV). (e) E/A ratio. (f) Left ventricular end-diastolic volume (LVEDV). (g) EF%. (h) LVD-D (mm). (i) LVD-S (mm). (j) HE staining. (k) WGA fluorescence staining. (l) TUNEL⁺ cells(%). (m) TUNEL staining. Mean \pm SD; * $P < 0.05$.

significantly increased after TAC; treatment with quercetin reversed this phenomenon and protected the myocardial tissue (Figures 2(a) and 2(b)).

Myocardial fibrosis is a complex pathological process primarily caused by long-term pressure overload and inflammatory reactions. Many proinflammatory factors, such as TGF- β , TNF- α , IL-13, IL-18, and MMPs, can participate in myocardial fibrosis. Hence, we detected the abundance of select proinflammatory factors (TNF- α , IL-13, and IL-18) by ELISA, while transcription levels of TGF- β and MMP-9 were detected by RT-PCR. The expression levels of TNF- α , IL-13, and IL-18 and mRNA levels of TGF- β and MMP-9 in the model group were higher than those in the control group (Figures 2(c)–2(g)). Quercetin reversed this phenomenon and inhibited inflammation (Figures 2(c)–2(g)). To verify whether the therapeutic mechanism of quercetin is related to SIRT5 and IDH2, we detected the mRNA and protein expression of SIRT5 and IDH2. The mRNA and protein expression levels were significantly inhibited after TAC (Figures 2(m)–2(p)). Quercetin reversed these effects, indicating that quercetin targets SIRT5 and IDH2 to protect against myocardial fibrosis and heart failure (Figures 2(m)–2(p)).

To further verify the protective mechanism of quercetin on myocardial fibrosis or myocardial injury after TAC, we investigated ROS production in the myocardial tissue and found that it was significantly increased after TAC (Figures 2(k) and 2(l)), whereas quercetin inhibited ROS overproduction (Figures 2(k) and 2(l)). These findings suggest that the protective effect of quercetin on myocardial fibrosis or myocardial injury is related to the regulation of redox homeostasis.

3.3. Quercetin Reduces High-Glucose-Induced HL-1 Inflammation Injury by Regulating Oxidative Stress. The aforementioned experimental results preliminarily showed that quercetin can improve cardiac function and inhibit the level of myocardial fibrosis in mice after TAC. Its protective effect might be related to the regulation of SIRT5 and anti-inflammatory factors; however, whether these events occur through a direct regulatory mechanism remained unclear. To study the regulatory mechanism of quercetin under high-glucose conditions, we induced HL-1 cell injury

by high glucose, treated these cells with quercetin, and knocked down SIRT5 with siRNA. Cell activity was detected using the MTT and CCK-8 assays, apoptosis levels were detected using flow cytometry, and superoxide dismutase (SOD), GSH, TrxR, and malondialdehyde (MDA) activities were detected using ELISA. We used CCK-8 to analyze the viability of HL-1 cells under different glucose concentrations. As shown in Figure 3(j), cell viability decreased significantly at a high-glucose concentration of 30 mM. MTT and flow cytometry revealed that high-glucose conditions inhibited cell activity, increased apoptosis and ROS production, and accelerated cell death (Figures 3(a)–3(e)). Compared with that in the control group, high-glucose stimulation increased MDA activity and inhibited the activity of antioxidant enzymes, such as SOD, GSH, and TrxR (Figures 3(f)–3(i)).

Quercetin inhibited the activity of MDA, increased the activity of SOD, GSH, and TrxR (Figures 3(f)–3(i)), inhibited apoptosis and ROS production (Figures 3(a)–3(e)), and improved cell activity (Figure 3(c)). However, si-SIRT5 + quercetin treatment further enhanced the activity of MDA, increased the level of apoptosis and ROS production, and inhibited cellular activity (Figures 3(a)–3(i)). Collectively, these results demonstrate that quercetin regulates the imbalance in the redox state stimulated by high glucose and protects HL-1 cardiomyocytes. This regulatory effect may be directly related to SIRT5.

3.4. Quercetin Reduces High-Glucose-Induced HL-1 Inflammation Injury by Promoting SIRT5-Related Desuccinylation Modification. Oxidative stress directly affects the structure and function of myocardial cells and can directly activate the signaling molecules associated with myocardial fibrosis, such as MMPs, leading to hypertrophy and apoptosis of myocardial cells, which is related to excessive production of ROS, accompanied by an inflammatory reaction. Excess ROS production can damage mitochondrial macromolecules at or near their formation sites. Mitochondrial structural damage and functional collapse in heart failure are related to increased levels of ROS, primarily manifested as increased mitochondrial lipid peroxide and decreased enzyme activities of mitochondrial respiratory complexes I, III, and IV. However, energy metabolism in

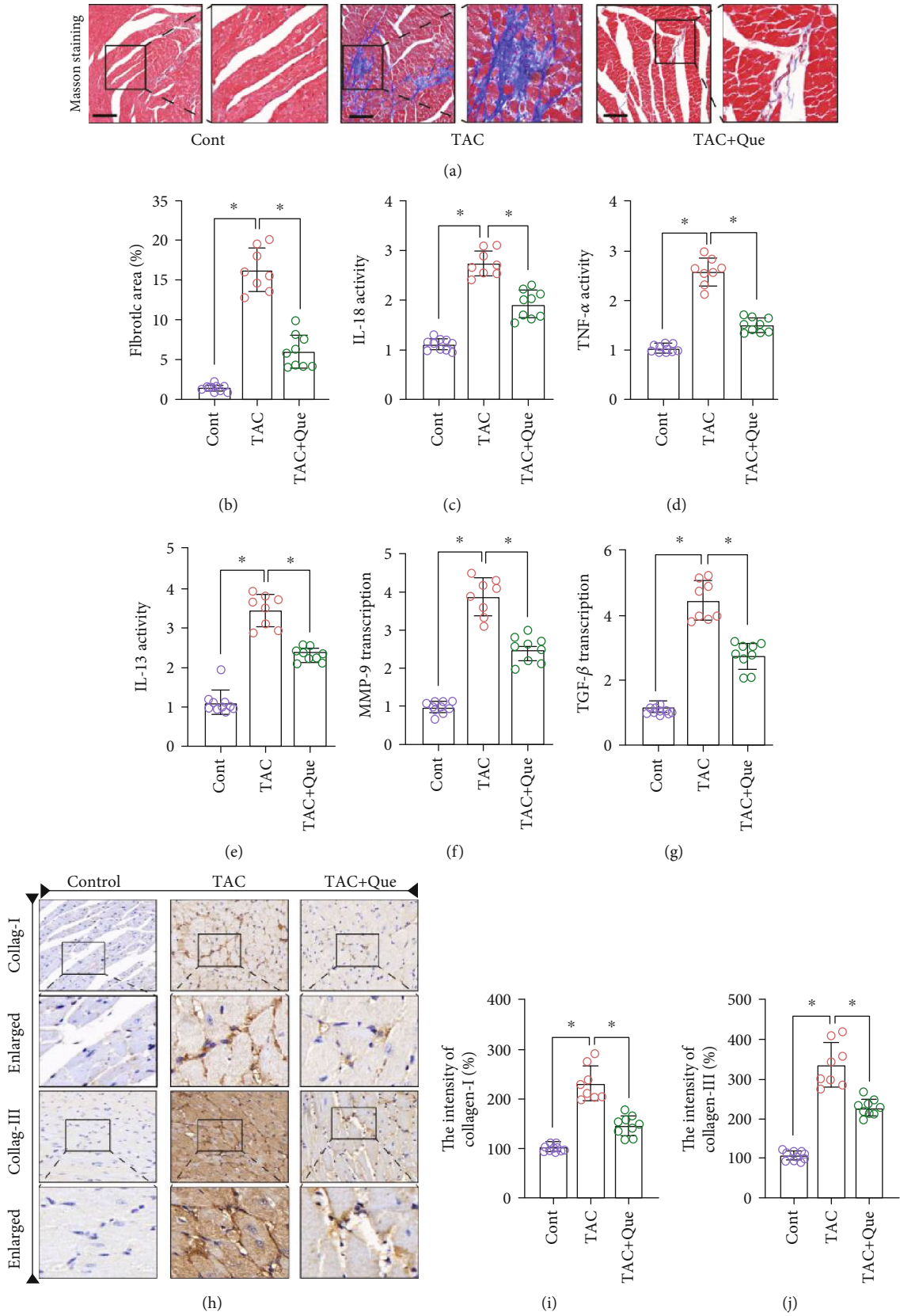


FIGURE 2: Continued.

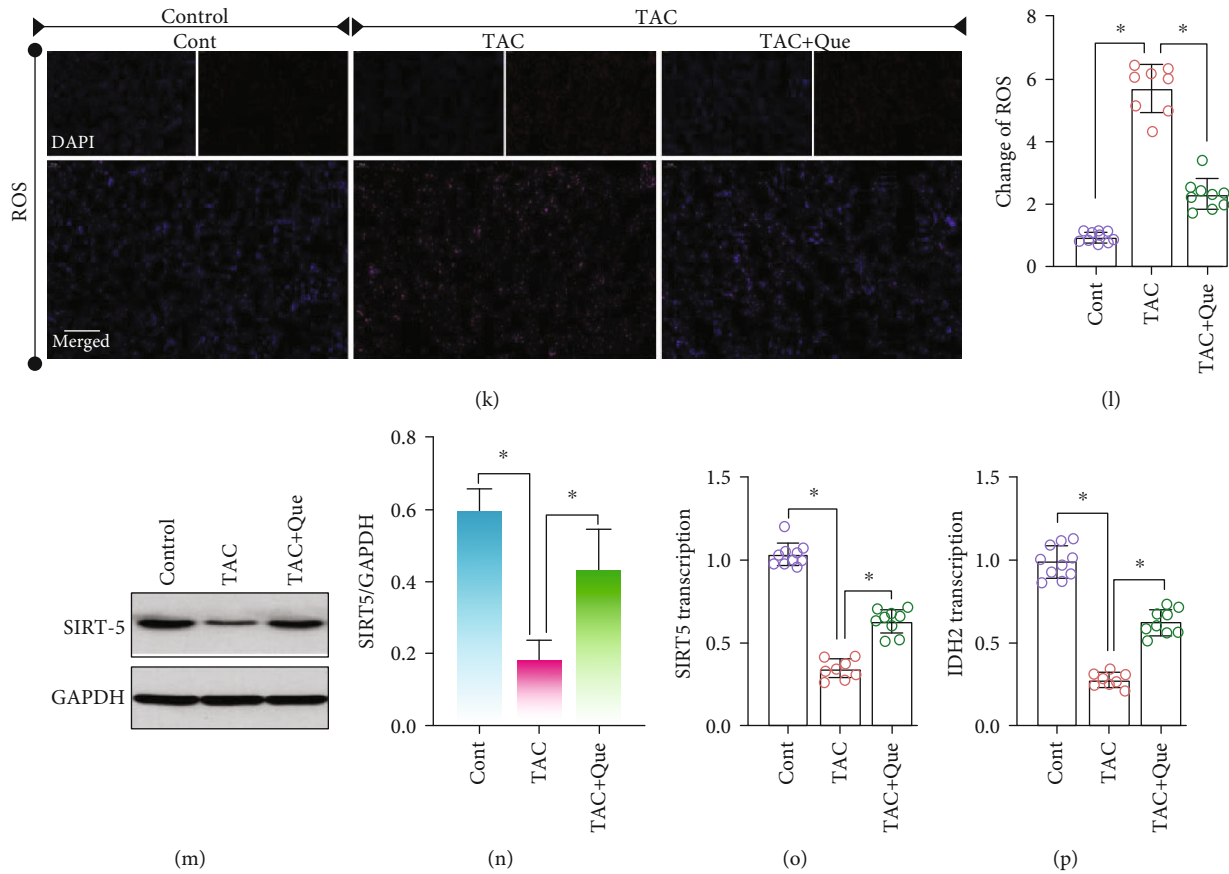


FIGURE 2: Quercetin (Que) attenuates myocardial fibrosis and inflammatory levels after transverse aortic constriction (TAC). (a) Masson staining. (b) Fibrotic area (%). (c–e) Expression levels of IL-18, TNF- α , and IL-13 were detected using ELISA. (f, g) mRNA expression of MMP-9 and TGF- β was detected using RT-PCR. (h–j) Expression of collagenase (collag) I/III was detected using immunohistochemistry. (k, l) Changes of ROS. (m–p) Protein/RNA expression of SIRT5 and IDH2 was detected. Mean \pm SD; * P < 0.05.

mitochondria is regulated by succinylation. Previous experimental results established that the therapeutic effect of quercetin on myocardial fibrosis and heart failure is related to SIRT1.

In the current study, analysis of the mRNA levels of SIRT5 and IDH2 in high-glucose-stimulated HL-1 cells and immunoprecipitation showed that IDH2 expression in HL-1 cells was significantly inhibited following high-glucose stimulation, whereas the succinylation level of IDH2 was significantly increased (Figures 4(a)–4(d)). Moreover, following quercetin intervention, the mRNA expression of SIRT5 and IDH2 and level of IDH2 desuccinylation increased (Figures 4(a)–4(d)). To further verify the effect of SIRT5-mediated succinylation on the mitochondrial respiratory chain, we assessed mitochondrial respiratory complexes I, III, and IV. After high-glucose stimulation, the levels of these complexes were decreased; however, quercetin reversed this phenomenon (Figures 4(e)–4(g)).

The regulatory effect of quercetin on the mitochondrial respiratory complex and IDH2 succinylation were also inhibited following si-SIRT5 treatment (Figures 4(a)–4(g)). Therefore, SIRT5-mediated desuccinylation of IDH2 may be an important regulatory mechanism of myocardial fibrosis and heart failure. Moreover, quercetin may improve the

inflammatory response and oxidative stress injury through SIRT5-mediated desuccinylation of IDH2; however, the regulatory mechanism of mitochondrial homeostasis requires further analysis.

3.5. Quercetin Reduces High-Glucose-Induced HL-1 Inflammation Injury by Regulating Mitochondrial Energy Metabolism and NLRP3. Mitochondrial energy metabolism is regulated by succinylation. However, heart failure or myocardial fibrosis caused by various factors involves an important pathological mechanism of oxidative stress and mitochondrial energy metabolism disorder in the inflammatory state. Therefore, we verified the regulatory effects of quercetin on mitochondrial energy metabolism and homeostasis. Immunofluorescence analysis showed that NLRP3 was highly expressed after high-glucose stimulation, which was reversed by quercetin (Figures 5(f) and 5(g)). Moreover, si-SIRT5 treatment eliminated the regulatory effect of quercetin on NLRP3 (Figures 5(f) and 5(g)).

Regulation of mitochondrial homeostasis is closely related to NLRP3 activation. In fact, NF- κ B can limit activation of NLRP3 by eliminating damaged mitochondria [33, 34]. We found that quercetin affected mitochondrial homeostasis by regulating NLRP3. High-glucose-stimulated HL-1

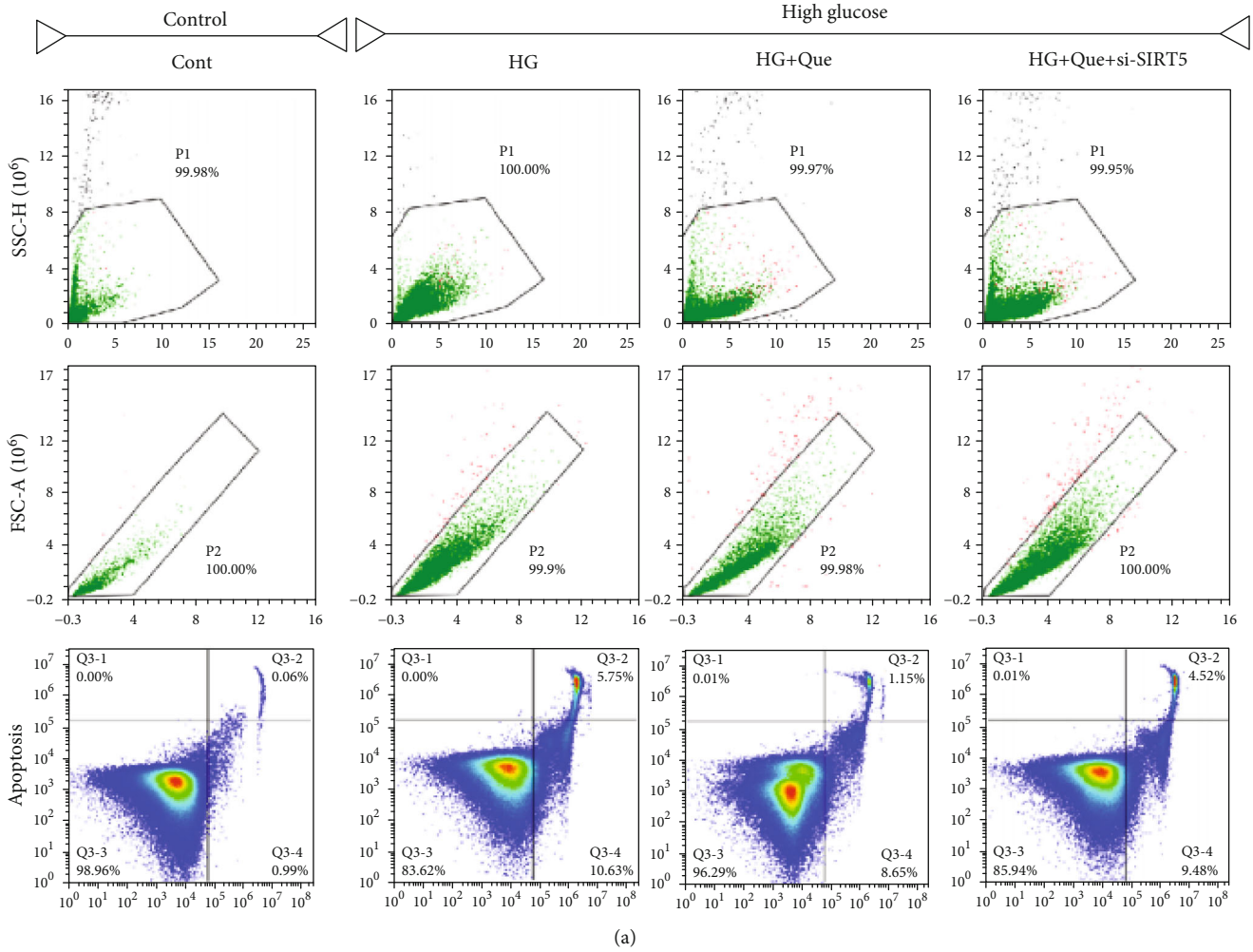


FIGURE 3: Continued.

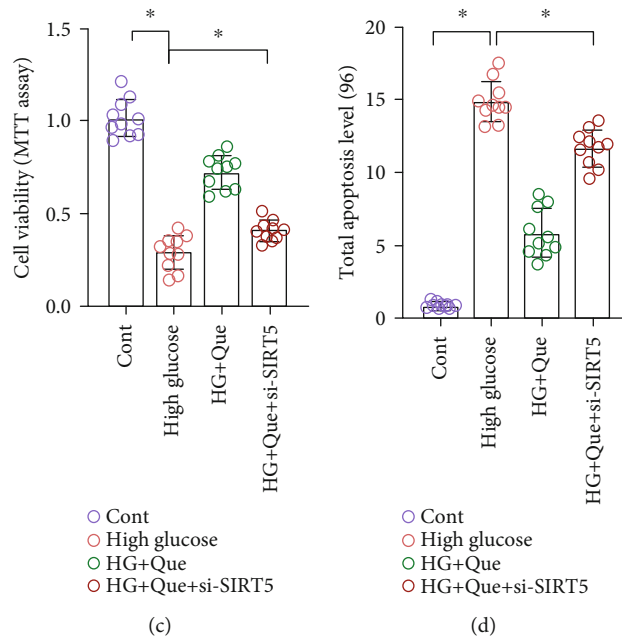
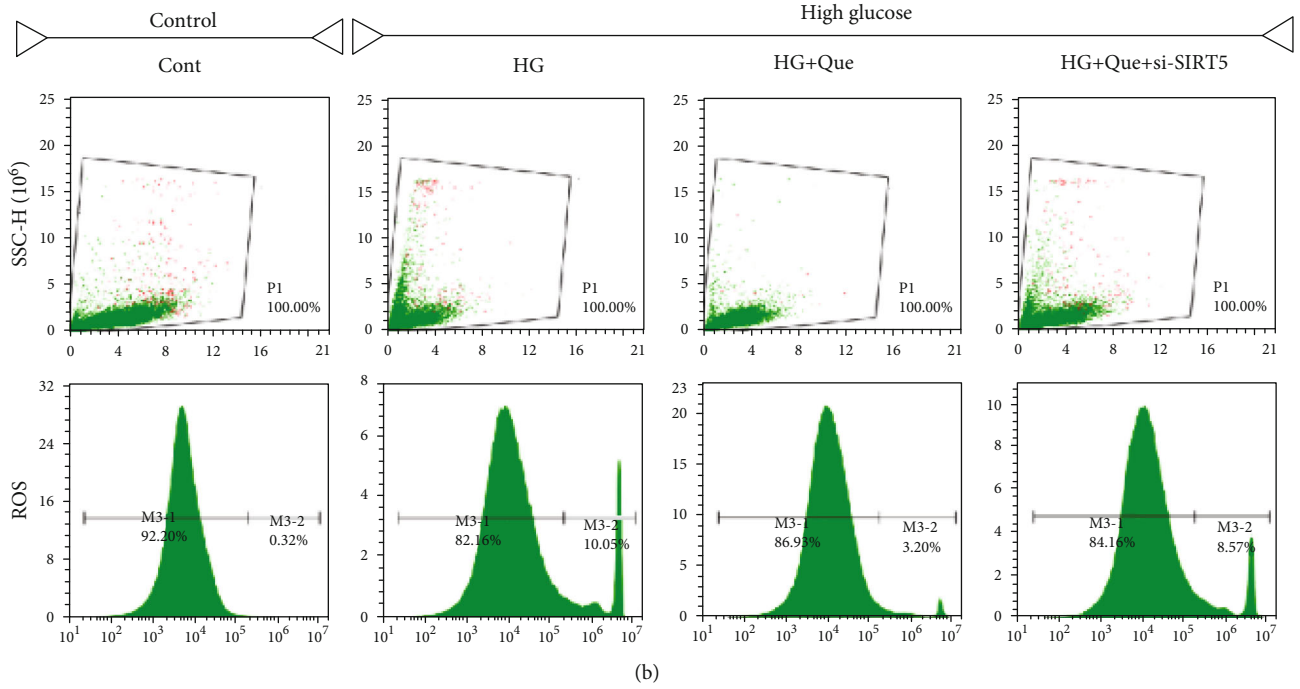


FIGURE 3: Continued.

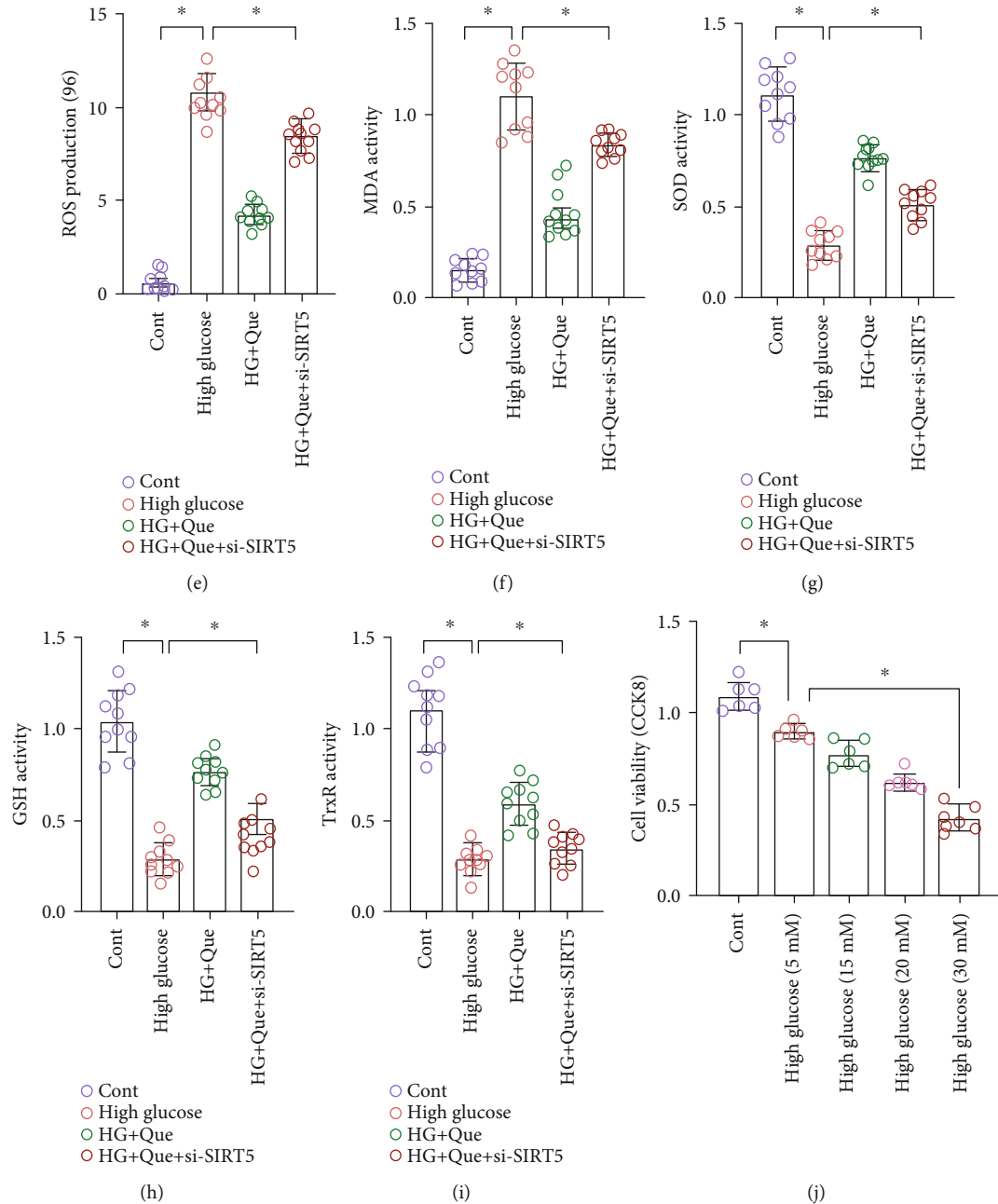


FIGURE 3: Quercetin (Que) reduces high-glucose- (HG-) induced HL-1 inflammation injury by regulating oxidative stress. (a) Apoptosis. (b) ROS levels were detected using flow cytometry. (c) Cell activity was determined using MTT. (d) Total apoptosis level. (e) ROS level. (f–i) MDA, SOD, GSH, and TrxR levels were detected using ELISA. (j) Cell activity was detected using CCK-8 assay. Mean \pm SD; * $P < 0.05$.

cells exhibited serious disorders of mitochondrial energy metabolism. The ATP level, basal respiration, maximal respiration, and respiratory reserve of mitochondria were significantly reduced. Moreover, the mPTP opening was abnormally increased (Figures 5(a)–5(e)). Quercetin reversed these effects and restored mitochondrial energy metabolism and mPTP closure (Figures 5(a)–5(e)). However, si-SIRT5 treatment reversed the regulation induced by quercetin on mitochondrial energy metabolism and mPTP (Figures 5(a)–5(e)). Therefore, excess production of ROS accompanied by inflammation and oxidative stress

can lead to mitochondrial oxidative stress injury, and NLRP3 can interact with mitochondrial energy metabolism. Mitochondria may be the “Trojan horse” of inflammation, which is consistent with the results of a previous study [35].

3.6. Quercetin Reduces High-Glucose-Induced HL-1 Inflammation Injury by Regulating Mitochondrial Quality Surveillance. Mitochondria can alter their shape and size through quality surveillance mechanisms and generate new mitochondria through biosynthesis; thus, the mitochondrial pool is supplemented and the energy metabolism that needs

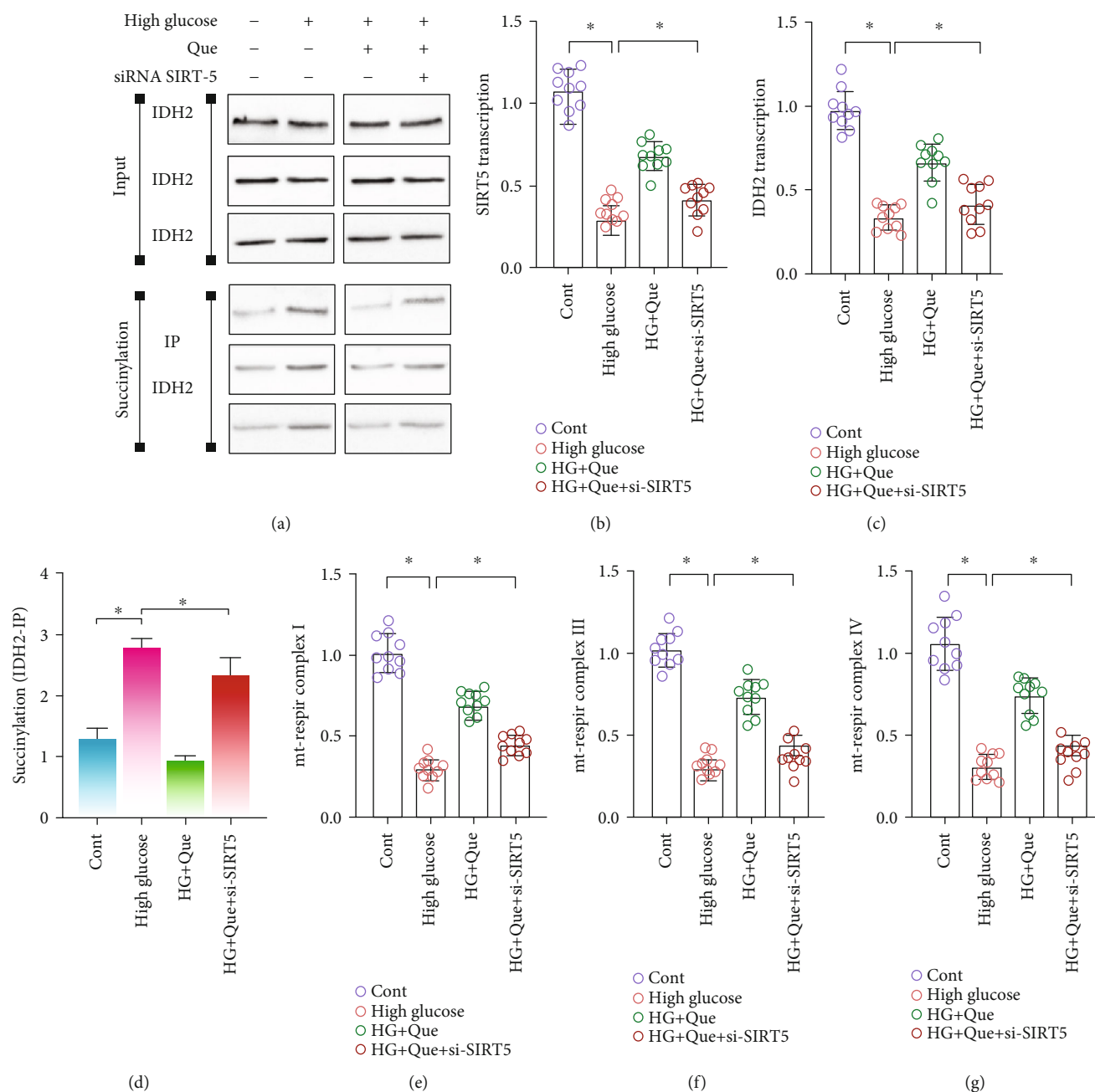


FIGURE 4: Quercetin (Que) reduces high-glucose- (HG-) induced HL-1 inflammation injury by promoting SIRT5-related desuccinylation. (a) Immunoblotting and succinylation of IDH2. RT-PCR was used to detect (b) SIRT5 and (c) IDH2 mRNA expression. (d) IDH2 succinylation. (e–g) Activities of mitochondrial respiratory complexes I/III and IV were detected using ELISA. Mean \pm SD; * $P < 0.05$.

cells under various conditions is met. Mitochondrial quality surveillance is critical for cytoprotective regulation during heart failure and myocardial fibrosis [36]. To explore the regulatory mechanism of quercetin on mitochondrial quality surveillance, we evaluated the mRNA levels of *Drp1/Fis1* and *Mfn1/Mfn2* after 24h of high-glucose stimulation. Gene expression analysis showed high-glucose stimulation upregulated *Drp1* and *Fis1* and downregulated *Mfn1* and *Mfn2* in mitochondria (Figures 6(a)–6(d)); moreover, quercetin reversed these effects (Figures 6(a)–6(d)). We also evaluated mitochondrial biogenesis. qPCR analysis results showed

that, after high-glucose stimulation, the expression of *Tfam* and *PGC1 α* was severely reduced. In turn, quercetin increased the levels of *Tfam* and *PGC1 α* and enhanced mitochondrial biogenesis (Figures 6(e) and 6(f)). It is worth noting that mitochondrial fission was increased significantly following si-SIRT5 treatment, whereas mitochondrial biosynthesis was decreased (Figures 6(e) and 6(f)). Thus, the ability of quercetin to regulate mitochondrial quality surveillance may be closely related to SIRT5.

The results showed that the protective effect of quercetin on HL-1 cells was closely related to its regulation of

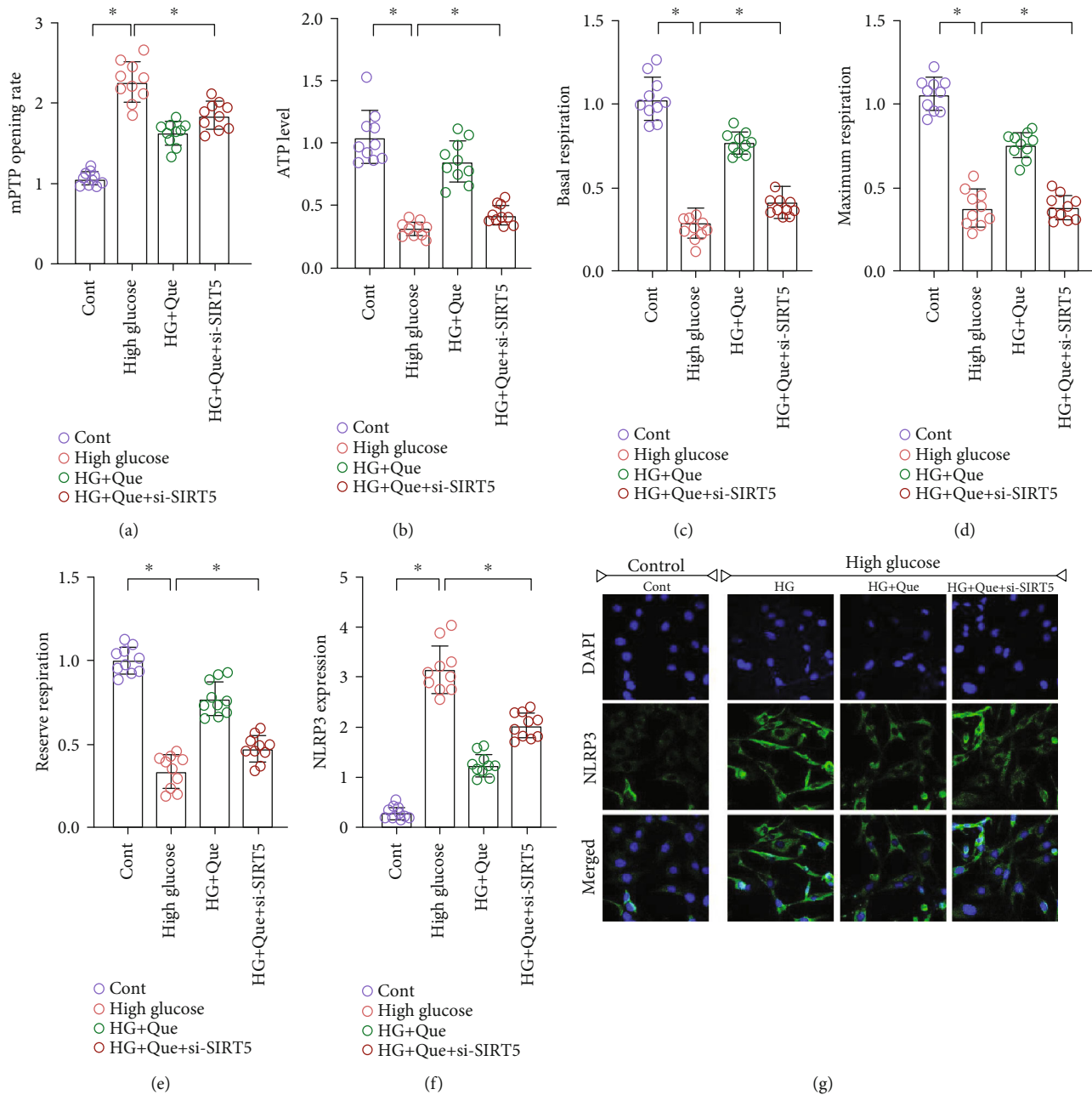


FIGURE 5: Quercetin (Que) reduces high-glucose- (HG-) induced HL-1 inflammation injury by regulating mitochondrial energy metabolism and NLRP3 levels. (a) Detection of mPTP opening rate. (b–e) Mitochondrial energy metabolism detection. (f, g) Immunofluorescence detection of NLRP3 levels. Mean \pm SD; * $P < 0.05$.

mitochondrial quality surveillance. Quercetin may promote the desuccinylation of IDH2 through SIRT5, thereby maintaining mitochondrial respiratory chain function and mitochondrial homeostasis, subsequently improving cell activity.

4. Discussion

Myocardial fibrosis is closely associated with heart failure and is characterized by dysregulated extracellular matrix metabolism and collagen component ratio. It is caused by oxidative stress damage and inflammation induced by heart failure [37]. Oxidative stress and inflammatory cytokines

can cause mitochondrial homeostasis disorders, affect the posttranslational modification of related proteins, cause damage to the contractile function of cardiomyocytes, and induce cardiomyocyte fibrosis, leading to heart failure [38]. Hence, a better understanding regarding the role of mitochondrial function and protein posttranslational modification in myocardial fibrosis injury will provide insights into myocardial remodeling from the perspective of mitochondrial quality surveillance and oxidative stress, while also providing new strategies for improving the prognosis and treatment of heart failure. Specifically, targeted drugs for mitochondrial quality surveillance are urgently needed

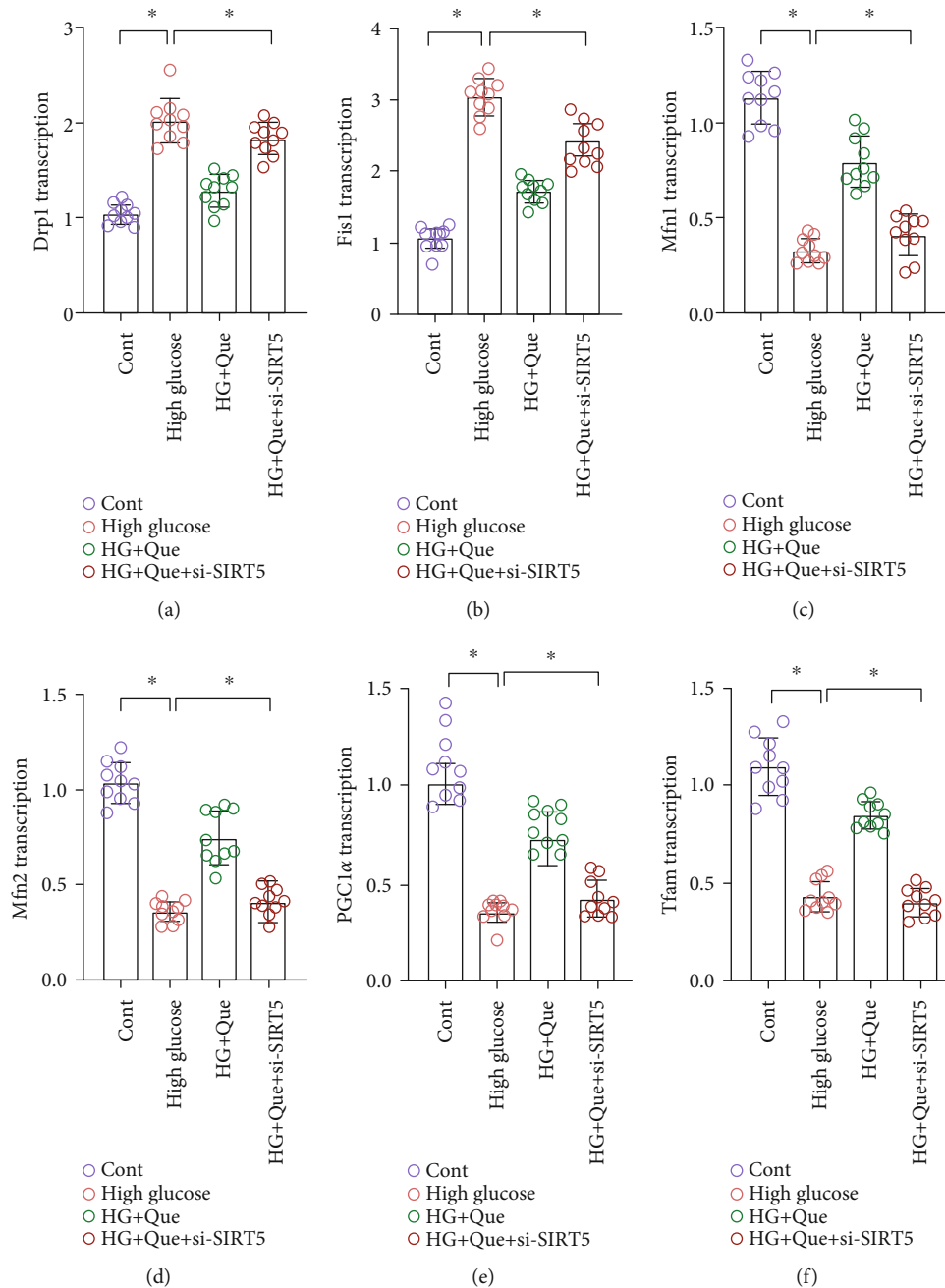


FIGURE 6: Quercetin (Que) reduces high-glucose- (HG-) induced HL-1 inflammation injury by regulating mitochondrial quality surveillance. (a–d) Expression of *Drp1/Fis1* and *Mfn1/Mfn2* as determined using qPCR. (e, f) Transcriptional levels of mitochondrial DNA synthesis markers *PGC1α* and *Tfam* determined using qPCR. Mean \pm SD; * $P < 0.05$.

[39]. In this study, we found that the level of myocardial fibrosis in the mouse myocardium and myocardial cells increased after surgery, whereas the cardiac ejection function decreased. Moreover, quercetin can regulate myocardial cell mitochondrial homeostasis after stress injury, inhibit oxidative stress damage and inflammation, maintain cardiomyocyte activity, and reduce myocardial fibrosis damage in mice with heart failure. Quercetin can also protect myocardial tissue, increase the expression of SIRT5 in cardiomyocytes, and promote IDH2 desuccinylation.

The primary cause of death in diabetic patients is cardiovascular diseases; however, the importance of heart failure in diabetic patients is not yet fully understood. Furthermore, the relationship between these two conditions is not solely at the level of comorbidities, rather an intricate relationship exists resulting in their reciprocal promotion or suppression [40]. Additionally, indicators that are reflective of insulin resistance, including glycosylated hemoglobin (HbA1c), fasting blood glucose, and insulin levels, are related to the risk of heart failure. Additionally, a series of physiological

or metabolic abnormalities, including autonomic neuropathy, microcirculation dysfunction, changes in metabolism or energy, and increased accumulation of advanced glycation end products, may cause insulin resistance or cardiomyopathy in diabetic patients [41].

Moreover, heart failure can increase the risk of insulin resistance, impaired glucose tolerance, and diabetes. Long-term abnormal carbohydrate and lipid metabolism or enhanced fatty acid metabolism and increased oxygen consumption further induce dysfunction of the mitochondrial respiratory chain of cardiomyocytes, resulting in a sharp decline in mitochondrial energy metabolism, which indirectly leads to imbalanced redox homeostasis and the overexpression of inflammatory factors [42]. Specifically, diabetic cardiomyopathy is a type of diabetes complicated by a vascular disease. Utilization of glucose metabolism by myocardial cells in patients with diabetes and heart failure accompanied by myocardial ischemia and hypoxia is reduced [43, 44]. The results of this study also indirectly established that a high-glucose environment can indirectly lead to mitochondrial quality surveillance.

In an oxidative stress environment, the oxygen and blood supply of cardiomyocytes is significantly reduced, resulting in production of a large amount of oxygen free radicals and a variety of intermediate metabolites. It can also cause a metabolic imbalance in the body, damage the myocardial cell membrane, and disrupt the balance between extracellular degradation and synthesis [45, 46]. Proliferation of myocardial fibroblasts leads to myocardial fibrosis, which in turn causes a large amount of intercellular collagen to be deposited and cell structure to become disordered, effectively disrupting the balance between various types of collagen. Hence, severe myocardial fibrosis has been shown to ultimately lead to heart failure. Although most previous studies have focused on the role of quercetin in oxidative stress and inflammatory damage [47], it can also regulate mitochondrial homeostasis, expression of related proteins, and posttranslational modifications [48]. Our results expand on these previous findings that suggest quercetin functions through SIRT5 to promote the desuccinylation of IDH2, thus regulating mitochondrial homeostasis, protecting the activity of myocardial cells, and improving the damage associated with myocardial fibrosis. Hence, quercetin may represent a new therapeutic approach for treating heart failure.

In mice, mitochondrial homeostasis disorders or dysfunctions are primarily caused by overproduction of ROS and insufficient ATP synthesis, which adversely affect the structure and function of the heart, leading to subsequent heart failure [49]. Under conditions of oxidative stress and inflammation, excessive production of ROS can cause oxidative damage to cellular proteins, lipids, and mitochondrial DNA, as well as induce cell damage and apoptosis [50]. This is largely due to the imbalance in mitochondrial homeostasis caused by disruption of redox homeostasis associated with inflammation. Currently, many studies have indicated that the inflammatory response that occurs when heart failure occurs is closely related to oxidative stress [51]. The onset of heart failure is accompanied by severe myocardial hypertrophy and myocardial fibrosis. As far as the pathological

mechanism of heart failure is concerned, when myocardial infarction occurs, factors such as myocardial ischemia, hypoxia, impaired mitochondrial function, and activation of neutrophils and inflammatory factors cause an explosive increase in ROS. This excess production of ROS caused by an imbalance in redox homeostasis is then accompanied by NF- κ B activation and subsequent activation of proinflammatory gene promoters in monocytes. Consequently, inflammatory factor transcription is upregulated, and the NADPH oxidase complex is oxidized on the cell membrane to generate ROS, inhibiting the activity of antioxidant enzymes and further stimulating the occurrence of inflammatory reactions [52]. This vicious circle is an inducing factor for the progressive aggravation of myocardial hypertrophy and fibrosis. ROS can also damage actin and excitatory-contractile coupling proteins, resulting in cardiac muscle systolic/diastolic dysfunction. Moreover, insufficient ATP synthesis leads to a lack of energy supply to cardiomyocytes, which has serious adverse effects on cardiomyocyte survival and cardiac ejection function [53].

In addition, severe diabetic cardiomyopathy with heart failure is accompanied by myocardial hypertrophy, partial myocardial ischemia, and hypoxia [36, 53]. The energy metabolism of myocardial cells is converted from fatty acid oxidation to glycolysis to adapt to hypoxia as a self-protective mechanism. However, this conversion is accompanied by a desuccinylation modification. In this study, we found that high-glucose stimulation can lead to apoptosis or death, which may be caused by the interaction between oxidative stress and the inflammatory reaction. This reaction is also accompanied by an imbalance in mitochondrial energy metabolism and mitochondrial quality surveillance. Similar to hypoxia/ischemia, a high-glucose environment can induce excessive ROS production, resulting in oxidative stress and mitochondrial mass imbalance. Consequently, glucose metabolism disorders further aggravate the primary cardiovascular disease or microcirculation damage, which may represent a key mechanism associated with diabetes mellitus complicated with heart failure.

IDH2 participates in the tricarboxylic acid cycle by catalyzing the conversion of isocitrate to α -ketoglutarate and NADP⁺ to NADPH. Studies have reported that knockout of IDH2 in mice can lead to a decrease in the redox state of NADPH and thioredoxin reductase activity in mitochondria. It can also lead to decreased cell activity and mitochondrial oxygen consumption [54]. Moreover, knockout of IDH2 decreases NADPH levels and mitochondrial GPX activity in mice with hepatic ischemia-reperfusion injury, leading to mitochondrial cristae loss, mitochondrial fragmentation, mitochondrial fissure shift, cytochrome c release, and cell death [55]. A lack of IDH2 can also lead to increased mitochondrial ROS, inhibited histone deacetylase activity, and increased activation of NF- κ B through acetylation, leading to increases in inflammation and apoptosis [56]. Indeed, IDH2-deficient mice exhibit accelerated heart failure, increased apoptosis and hypertrophy, and mitochondrial dysfunction, which is related to an imbalance in redox homeostasis [57]. Our results are consistent with those of previous studies, indicating that mitochondrial homeostasis

and quality control disorders of murine cardiomyocytes are related to the succinylation of IDH2.

Succinylation of lysine is a recently discovered protein posttranslational modification in which a lysine (K) residue in the protein is converted from the succinyl group by succinyl-coenzyme A [58, 59]. Related *in vitro* and *in vivo* studies have shown that quercetin can significantly reduce AngII-induced myocardial contractility, fibrosis, inflammation, and myocardial hypertrophy while inhibiting the expression of fibroblast differentiation markers type I and type III collagen [28]. Quercetin also reverses isoproterenol-induced cardiac hypertrophy by restoring the cellular redox balance and protecting mitochondria [38]. Our results show that quercetin promotes the desuccinylation of IDH2 through SIRT5, regulates the redox balance, maintains mitochondrial homeostasis, inhibits inflammation, protects cardiomyocytes, reduces the level of myocardial fibrosis damage, and restores heart function. These findings are consistent with those of previous studies; that is, high-glucose stimulation causes an imbalance in redox levels, causes inflammation, and activates mitochondrial quality surveillance and homeostasis, as well as the mitochondrial apoptosis pathway. In addition, we show that SIRT5 promotes IDH2 desuccinylation, increases the sensitivity of cells to oxidative stress, and reduces oxidative stress damage to cardiomyocytes, which have also been observed previously [60].

Our study had three main limitations. First, although we conducted *in vivo* studies using animal models of heart failure and myocardial fibrosis to verify the regulatory effect of quercetin, but we did not conduct targeted verification using gene knockout animals. Second, only mitochondrial homeostasis, and not endoplasmic reticulum function, was evaluated. The pathological mechanism of myocardial fibrosis is primarily related to calcium homeostasis. The endoplasmic reticulum is an important intracellular calcium store. Excessive or low calcium levels in the endoplasmic reticulum can cause calcium signaling disorders, leading to abnormal physiological functions in cardiomyocytes and the occurrence of myocardial fibrosis. Third, the interaction between endoplasmic reticulum stress and mitochondrial homeostasis has not been clearly elucidated in the pathogenesis of diabetes mellitus complicated with heart failure; however, myocardial fibrosis was not examined. Despite these limitations, our research shows that quercetin can promote the desuccinylation of IDH2 through SIRT5. Quercetin maintains the regulation of mitochondrial homeostasis and redox balance, inhibits inflammation, and reduces the apoptosis level of cardiomyocytes, as well as the level of muscle fibrosis and recovery of cardiac ejection function.

5. Conclusions

Our results provide insights into the pathological mechanism and clinical treatment of myocardial fibrosis and heart failure. Heart failure is one of the most serious cardiovascular complications in patients with diabetes; however, currently, there are few drugs that can control blood sugar and improve myocardial damage in clinical practice, and the treatment and pathological mechanisms remain unclear.

In this study, it was discovered through *in vivo* experimental studies that quercetin can effectively improve the pathological response of heart failure in mice after TAC, improve cardiac function, inhibit the expression of inflammatory factors and the level of myocardial fibrosis, and protect the myocardium. Furthermore, we showed that quercetin can regulate the redox balance of mouse cardiomyocytes under high-glucose conditions, inhibit the release of NLRP3 inflammasomes, regulate mitochondrial quality surveillance, maintain mitochondrial homeostasis, and inhibit the apoptosis or death of cardiomyocytes in high-glucose environments. In addition, the active ingredient quercetin as a natural medicine affects the SIRT5 regulatory mechanism by promoting desuccinylation. Quercetin can regulate the succinylation of SIRT5, which may improve the tolerance of mitochondria to oxidative stress and inflammation. We infer that quercetin, which has antioxidative stress effects, can regulate mitochondrial quality surveillance through the “inflammation-oxidative stress” pathway. Although there have been great advances in deciphering the pathological mechanism of the “inflammatory-oxidative stress-mitochondrial dysfunction” pathway, the associated crosstalk mechanism has not yet been fully elucidated. The results of this study suggest that quercetin may become a supplementary alternative drug or daily health supplement for patients with diabetes and heart failure; however, large-scale, multicenter clinical studies are needed to further verify its effectiveness and safety.

Data Availability

The data used to support the findings of this study are available from the corresponding authors upon request.

Conflicts of Interest

The authors declare that there is no conflict of interest regarding the publication of this paper.

Authors' Contributions

Xing Chang and Tian Zhang contributed equally to this work.

Acknowledgments

This study was supported by the Natural Science Foundation of Shandong Province (grant number ZR2020MH352) and the National Natural Science Foundation of China (NSFC; grant number 82004233). We would like to thank Editage (<https://www.editage.cn>) for the English language editing.

References

- [1] J. R. Baman and F. S. Ahmad, “Heart failure,” *JAMA*, vol. 324, no. 10, p. 1015, 2020.
- [2] S. F. Mohammed, S. Hussain, S. A. Mirzoyev, W. D. Edwards, J. J. Maleszewski, and M. M. Redfield, “Coronary microvascular rarefaction and myocardial fibrosis in heart failure with preserved ejection fraction,” *Circulation*, vol. 131, no. 6, pp. 550–559, 2015.

- [3] M. Gyöngyösi, J. Winkler, I. Ramos et al., "Myocardial fibrosis: biomedical research from bench to bedside," *European Journal of Heart Failure*, vol. 19, no. 2, pp. 177–191, 2017.
- [4] L. Bacmeister, M. Schwarzl, S. Warnke et al., "Inflammation and fibrosis in murine models of heart failure," *Basic Research in Cardiology*, vol. 114, no. 3, 2019.
- [5] W. J. Paulus and C. Tschöpe, "A novel paradigm for heart failure with preserved ejection fraction: comorbidities drive myocardial dysfunction and remodeling through coronary microvascular endothelial inflammation," *Journal of the American College of Cardiology*, vol. 62, no. 4, pp. 263–271, 2013.
- [6] R. A. de Boer, G. De Keulenaer, J. Bauersachs et al., "Towards better definition, quantification and treatment of fibrosis in heart failure. A scientific roadmap by the Committee of Translational Research of the Heart Failure Association (HFA) of the European Society of Cardiology," *European Journal of Heart Failure*, vol. 21, no. 3, pp. 272–285, 2019.
- [7] C. Li, Q. Ma, S. Toan, J. Wang, H. Zhou, and J. Liang, "SERCA overexpression reduces reperfusion-mediated cardiac microvascular damage through inhibition of the calcium/M-CU/mPTP/necroptosis signaling pathways," *Redox Biology*, vol. 36, p. 101659, 2020.
- [8] H. Zhu, S. Toan, D. Mui, and H. Zhou, "Mitochondrial quality surveillance as a therapeutic target in myocardial infarction," *Acta Physiologica (Oxford, England)*, vol. 231, no. 3, p. e13590, 2021.
- [9] J. Wang, P. Zhu, R. Li, J. Ren, and H. Zhou, "Fundc1-dependent mitophagy is obligatory to ischemic preconditioning-conferred renoprotection in ischemic AKI via suppression of Drp1-mediated mitochondrial fission," *Redox Biology*, vol. 30, p. 101415, 2020.
- [10] J. Wang, P. Zhu, R. Li, J. Ren, Y. Zhang, and H. Zhou, "Bax inhibitor 1 preserves mitochondrial homeostasis in acute kidney injury through promoting mitochondrial retention of PHB2," *Theranostics*, vol. 10, no. 1, pp. 384–397, 2020.
- [11] H. Zhou, P. Zhu, J. Wang, S. Toan, and J. Ren, "DNA-PKcs promotes alcohol-related liver disease by activating Drp 1-related mitochondrial fission and repressing FUNDC1-required mitophagy," *Signal Transduction and Targeted Therapy*, vol. 4, 2019.
- [12] H. M. Cho, J. R. Ryu, Y. Jo et al., "Drp 1-Zip 1 interaction regulates mitochondrial quality surveillance system," *Molecular Cell*, vol. 73, no. 2, 2019.
- [13] H. Zhou, J. Ren, S. Toan, and D. Mui, "Role of mitochondrial quality surveillance in myocardial infarction: from bench to bedside," *Ageing Research Reviews*, vol. 66, p. 101250, 2021.
- [14] J. Wang, S. Toan, and H. Zhou, "Mitochondrial quality control in cardiac microvascular ischemia-reperfusion injury: new insights into the mechanisms and therapeutic potentials," *Pharmacological Research*, vol. 156, p. 104771, 2020.
- [15] Y. Tan, D. Mui, S. Toan, P. Zhu, R. Li, and H. Zhou, "SERCA overexpression improves mitochondrial quality control and attenuates cardiac microvascular ischemia-reperfusion injury," *Molecular Therapy Nucleic Acids*, vol. 22, pp. 696–707, 2020.
- [16] A. A. Gibb, M. P. Lazaropoulos, and J. W. Elrod, "Myofibroblasts and fibrosis: mitochondrial and metabolic control of cellular differentiation," *Circulation Research*, vol. 127, no. 3, pp. 427–447, 2020.
- [17] H. Zhu, Y. Tan, W. Du et al., "Phosphoglycerate mutase 5 exacerbates cardiac ischemia-reperfusion injury through disrupting mitochondrial quality control," *Redox Biology*, vol. 38, p. 101777, 2021.
- [18] H. C. Kenny and E. D. Abel, "Heart failure in type 2 diabetes mellitus," *Circulation Research*, vol. 124, no. 1, pp. 121–141, 2019.
- [19] K. McHugh, A. D. DeVore, J. Wu et al., "Heart Failure With Preserved Ejection Fraction and Diabetes," *Journal of the American College of Cardiology*, vol. 73, no. 5, pp. 602–611, 2019.
- [20] M. J. Lukey, K. S. Greene, and R. A. Cerione, "Lysine succinylation and SIRT5 couple nutritional status to glutamine catabolism," *Molecular & Cellular Oncology*, vol. 7, no. 3, 2020.
- [21] X.-F. Chen, M.-X. Tian, R.-Q. Sun et al., "SIRT5 inhibits peroxisomal ACOX1 to prevent oxidative damage and is downregulated in liver cancer," *EMBO Reports*, vol. 19, no. 5, 2018.
- [22] L. Xu, X. Che, Y. Wu et al., "SIRT5 as a biomarker for response to anthracycline-taxane-based neoadjuvant chemotherapy in triple-negative breast cancer," *Oncology Reports*, vol. 39, no. 5, pp. 2315–2323, 2018.
- [23] J. A. Boylston, J. Sun, Y. Chen, M. Gucek, M. N. Sack, and E. Murphy, "Characterization of the cardiac succinylome and its role in ischemia-reperfusion injury," *Journal of Molecular and Cellular Cardiology*, vol. 88, pp. 73–81, 2015.
- [24] L. Chen, H. Wang, F. Gao et al., "Functional genetic variants in the *_SIRT5_* gene promoter in acute myocardial infarction," *Gene*, vol. 675, pp. 233–239, 2018.
- [25] L. Polletta, E. Vernucci, I. Carnevale et al., "SIRT5 regulation of ammonia-induced autophagy and mitophagy," *Autophagy*, vol. 11, no. 2, pp. 253–270, 2015.
- [26] H. Kim, J. H. Lee, and J. W. Park, "IDH2 deficiency exacerbates acetaminophen hepatotoxicity in mice via mitochondrial dysfunction-induced apoptosis," *Biochimica et Biophysica Acta Molecular Basis of Disease*, vol. 1865, no. 9, pp. 2333–2341, 2019.
- [27] X. Chang, T. Zhang, and Q. Meng, "Quercetin Improves Cardiomyocyte Vulnerability to Hypoxia by Regulating SIRT1/TMBIM6-Related Mitophagy and Endoplasmic Reticulum Stress," *Oxidative Medicine and Cellular Longevity*, vol. 2021, Article ID 5529913, 14 pages, 2021.
- [28] L. Wang, A. Tan, X. An, Y. Xia, and Y. Xie, "Quercetin dihydrate inhibition of cardiac fibrosis induced by angiotensin II in vivo and in vitro," *Biomedicine & Pharmacotherapy*, vol. 127, p. 110205, 2020.
- [29] W. Gao, Z. Zhou, B. Liang et al., "Inhibiting receptor of advanced glycation end products attenuates pressure overload-induced cardiac dysfunction by preventing excessive autophagy," *Frontiers in Physiology*, vol. 9, 2018.
- [30] V. Samokhvalov, K. L. Jamieson, J. Vriend, S. Quan, and J. M. Seubert, "CYP epoxygenase metabolites of docosahexaenoic acid protect HL-1 cardiac cells against LPS-induced cytotoxicity through SIRT1," *Cell Death Discovery*, vol. 1, no. 1, 2015.
- [31] F. Trindade, R. Vitorino, A. Leite-Moreira, and I. Falcão-Pires, "Pericardial fluid: an underrated molecular library of heart conditions and a potential vehicle for cardiac therapy," *Basic Research in Cardiology*, vol. 114, no. 2, 2019.
- [32] T. Xin, W. Lv, D. Liu, Y. Jing, and F. Hu, "Opa 1 reduces hypoxia-induced cardiomyocyte death by improving mitochondrial quality control," *Frontiers in Cell and Development Biology*, vol. 8, 2020.

- [33] Z. Zhong, S. Liang, E. Sanchez-Lopez et al., "New mitochondrial DNA synthesis enables NLRP3 inflammasome activation," *Nature*, vol. 560, no. 7717, pp. 198–203, 2018.
- [34] Z. Zhong, A. Umemura, E. Sanchez-Lopez et al., "NF- κ B restricts inflammasome activation via elimination of damaged mitochondria," *Cell*, vol. 164, no. 5, pp. 896–910, 2016.
- [35] A. A. Manfredi and P. Rovere-Querini, "The Mitochondrion-A Trojan horse that kicks off inflammation?," *The New England Journal of Medicine*, vol. 362, no. 22, pp. 2132–2134, 2010.
- [36] X. Chang, Z. Zhao, W. Zhang et al., "Natural antioxidants improve the vulnerability of cardiomyocytes and vascular endothelial cells under stress conditions: a focus on mitochondrial quality control," *Oxidative Medicine and Cellular Longevity*, vol. 2021, Article ID 6620677, 27 pages, 2021.
- [37] J. Yang, K. Savvatis, J. S. Kang et al., "Targeting LOXL2 for cardiac interstitial fibrosis and heart failure treatment," *Nature Communications*, vol. 7, no. 1, 2016.
- [38] G. R. Xu, C. Zhang, H. X. Yang et al., "Modified citrus pectin ameliorates myocardial fibrosis and inflammation via suppressing galectin-3 and TLR4/MyD88/NF- κ B signaling pathway," *Biomedicine & Pharmacotherapy*, vol. 126, p. 110071, 2020.
- [39] J. Wang, S. Toan, and H. Zhou, "New insights into the role of mitochondria in cardiac microvascular ischemia/reperfusion injury," *Angiogenesis*, vol. 23, no. 3, pp. 299–314, 2020.
- [40] P. Balakumar, U. K. Maung, and G. Jagadeesh, "Prevalence and prevention of cardiovascular disease and diabetes mellitus," *Pharmacological Research*, vol. 113, no. Part A, pp. 600–609, 2016.
- [41] G. Jia, M. A. Hill, and J. R. Sowers, "Diabetic cardiomyopathy: an update of mechanisms contributing to this clinical entity," *Circulation Research*, vol. 122, no. 4, pp. 624–638, 2018.
- [42] L. Hu, M. Ding, D. Tang et al., "Targeting mitochondrial dynamics by regulating Mfn 2 for therapeutic intervention in diabetic cardiomyopathy," *Theranostics*, vol. 9, no. 13, pp. 3687–3706, 2019.
- [43] J. C. Kovacic, J. M. Castellano, M. E. Farkouh, and V. Fuster, "The relationships between cardiovascular disease and diabetes: focus on pathogenesis," *Endocrinology and Metabolism Clinics of North America*, vol. 43, no. 1, pp. 41–57, 2014.
- [44] A. Norhammar and K. Schenck-Gustafsson, "Type 2 diabetes and cardiovascular disease in women," *Diabetologia*, vol. 56, no. 1, pp. 1–9, 2013.
- [45] A. C. Maritim, R. A. Sanders, and J. B. Watkins 3rd, "Diabetes, oxidative stress, and antioxidants: a review," *Journal of Biochemical and Molecular Toxicology*, vol. 17, no. 1, pp. 24–38, 2003.
- [46] S. Svegliati, T. Spadoni, G. Moroncini, and A. Gabrielli, "NADPH oxidase, oxidative stress and fibrosis in systemic sclerosis," *Free Radical Biology & Medicine*, vol. 125, pp. 90–97, 2018.
- [47] X. Chang, T. Zhang, W. Zhang, Z. Zhao, and J. Sun, "Natural drugs as a treatment strategy for cardiovascular disease through the regulation of oxidative stress," *Oxidative Medicine and Cellular Longevity*, vol. 2020, 20 pages, 2020.
- [48] R. T. Magar and J. K. Sohng, "A review on structure, modifications and structure-activity relation of quercetin and its derivatives," *Journal of Microbiology and Biotechnology*, vol. 30, no. 1, pp. 11–20, 2020.
- [49] G. M. Latypova, M. A. Bychenkova, V. A. Katayev et al., "Composition and cardioprotective effects of *Primula veris* L. solid herbal extract in experimental chronic heart failure," *Phytomedicine: International Journal of Phytotherapy and Phytopharmacology*, vol. 54, pp. 17–26, 2019.
- [50] T. Hussain, B. Tan, Y. Yin, F. Blachier, M. C. Tossou, and N. Rahu, "Oxidative stress and inflammation: what polyphenols can do for us?," *Oxidative Medicine and Cellular Longevity*, vol. 2016, 9 pages, 2016.
- [51] T. J. Guzik and R. M. Touyz, "Oxidative stress, inflammation, and vascular aging in hypertension," *Hypertension (Dallas, Tex: 1979)*, vol. 70, no. 4, pp. 660–667, 2017.
- [52] P. K. Bagul, N. Deepthi, R. Sultana, and S. K. Banerjee, "Resveratrol ameliorates cardiac oxidative stress in diabetes through deacetylation of NF κ B-p65 and histone 3," *The Journal of Nutritional Biochemistry*, vol. 26, no. 11, pp. 1298–1307, 2015.
- [53] X. Chang, W. Zhang, Z. Zhao et al., "Regulation of mitochondrial quality control by natural drugs in the treatment of cardiovascular diseases: potential and advantages," *Frontiers in Cell and Development Biology*, vol. 8, 2020.
- [54] Y.-R. Kim, J.-I. Baek, S. H. Kim et al., "Therapeutic potential of the mitochondria-targeted antioxidant MitoQ in mitochondrial-ROS induced sensorineural hearing loss caused by *Idh2* deficiency," *Redox Biology*, vol. 20, pp. 544–555, 2019.
- [55] S. J. Han, H. S. Choi, J. I. Kim, J. W. Park, and K. M. Park, "IDH2 deficiency increases the liver susceptibility to ischemia-reperfusion injury via increased mitochondrial oxidative injury," *Redox Biology*, vol. 14, pp. 142–153, 2018.
- [56] H. Cha, S. Lee, S. Hwan Kim et al., "Increased susceptibility of IDH2-deficient mice to dextran sodium sulfate- induced colitis," *Redox Biology*, vol. 13, pp. 32–38, 2017.
- [57] H. J. Ku, Y. Ahn, J. H. Lee, K. M. Park, and J. W. Park, "IDH2 deficiency promotes mitochondrial dysfunction and cardiac hypertrophy in mice," *Free Radical Biology & Medicine*, vol. 80, pp. 84–92, 2015.
- [58] W. You, W. Zheng, S. Weiss, K. F. Chua, and C. Steegborn, "Structural basis for the activation and inhibition of sirtuin 6 by quercetin and its derivatives," *Scientific Reports*, vol. 9, no. 1, p. 19176, 2019.
- [59] V. Heger, J. Tyni, A. Hunyadi, L. Horáková, M. Lahtela-Kakkonen, and M. Rahnasto-Rilla, "Quercetin based derivatives as sirtuin inhibitors," *Biomedicine & Pharmacotherapy*, vol. 111, pp. 1326–1333, 2019.
- [60] L. Zhou, F. Wang, R. Sun et al., "SIRT5 promotes IDH2 desuccinylation and G6PD deglutarylation to enhance cellular antioxidant defense," *EMBO Reports*, vol. 17, no. 6, pp. 811–822, 2016.

Research Article

Nicotinamide Riboside Alleviates Cardiac Dysfunction and Remodeling in Pressure Overload Cardiac Hypertrophy

Sai Ma ¹, Jing Feng,² Xiuyu Lin,³ Jing Liu,¹ Yi Tang,¹ Shinan Nie,² Jianbin Gong,¹ and Lei Wang ¹

¹Department of Cardiology, Jinling Hospital, Medical School of Nanjing University, Nanjing, China 210002

²Department of Emergency Medicine, Jinling Hospital, Medical School of Nanjing University, Nanjing, China 210002

³Department of Ultrasound Diagnostic, Jinling Hospital, Medical School of Nanjing University, Nanjing, China 210002

Correspondence should be addressed to Lei Wang; wangleiyes@sina.com

Received 31 March 2021; Accepted 26 August 2021; Published 17 September 2021

Academic Editor: Jan Gebicki

Copyright © 2021 Sai Ma et al. This is an open access article distributed under the Creative Commons Attribution License, which permits unrestricted use, distribution, and reproduction in any medium, provided the original work is properly cited.

Background. Cardiac hypertrophy is a compensatory response to pressure overload, which eventually leads to heart failure. The current study explored the protective effect of nicotinamide riboside (NR), a NAD⁺ booster that may be administered through the diet, on the occurrence of myocardial hypertrophy and revealed details of its underlying mechanism. **Methods.** Transverse aortic constriction (TAC) surgery was performed to establish a murine model of myocardial hypertrophy. Mice were randomly divided into four groups: sham, TAC, sham+NR, and TAC+NR. NR treatment was given daily by oral gavage. Cardiac structure and function were assessed using small animal echocardiography. Mitochondrial oxidative stress was evaluated by dihydroethidium (DHE) staining, malondialdehyde (MDA) content, and superoxide dismutase (SOD) activity. Levels of expression of atrial natriuretic peptide (ANP), brain natriuretic peptide (BNP), IL-1 β , TNF- α , and Sirtuin3 were measured by real-time PCR and ELISA. Expression levels of Caspase-1, Caspase-1 pro, cleaved Gasdermin D (GSDMD), NLRP3, ASC, Sirtuin3, ac-MnSOD, and total MnSOD were measured by Western blot. **Results.** Reductions in the heart/body mass ratio (HW/BW) and lung/body mass ratio (LW/BW) and in ANP, BNP, and LDH levels were observed in the TAC group on the administration of NR ($P < 0.05$). Moreover, echocardiography data showed that cardiac dysfunction and structural changes caused by TAC were improved by NR treatment ($P < 0.05$). NR treatment also reduced levels of the inflammatory cytokines, IL-1 β and TNF- α , and attenuated activation of NLRP3 inflammasomes induced by TAC. Furthermore, changes in DHE staining, MDA content, and SOD activity indicated that NR treatment alleviated the oxidative stress caused by TAC. Data from ELISA and Western blots revealed elevated myocardial NAD⁺ content and Sirtuin3 activity and decreased acetylation of MnSOD after NR treatment, exposing aspects of the underlying signaling pathway. **Conclusion.** NR treatment alleviated TAC-induced pathological cardiac hypertrophy and dysfunction. Mechanically, these beneficial effects were attributed to the inhibition of NLRP3 inflammasome activation and myocardial inflammatory response by regulating the NAD⁺-Sirtuin3-MnSOD signaling pathway.

1. Introduction

Cardiac hypertrophy is a feature common to many cardiovascular diseases [1]. Hypertrophy develops as a benign, adaptive response to physiological and pathological stimuli and results in increased heart contractility. However, with continued stimulation, hypertrophy progresses to cardiac remodeling and dysfunction and becomes pathological hypertrophy, a complex process which eventually leads to heart failure [2]. Recent research has identified a number of mechanisms that

contribute to pathological hypertrophy, including cellular metabolism, the immune response, abnormal expression of lncRNAs, and epigenetic changes [3, 4]. However, there still remains a need to conduct further exploration in order to identify molecular targets for treatment.

Inflammation is considered a critical hallmark of hypertrophy [5]. However, the pathogenic role of inflammation during hypertrophy is incompletely understood. The cytosolic inflammasome is a multiprotein complex, comprising key regulators of the inflammatory response to numerous

stimuli. The resulting activation of Caspase-1 induces maturation of proinflammatory cytokines [6]. There is increasing evidence that links the nucleotide-binding and leucine-rich repeat pyrin domains protein 3 (NLRP3) inflammasome and its stimulation of cytokine secretion with the pathogenesis of various cardiovascular diseases, including atherosclerosis, acute myocardial infarction (AMI), acute myocarditis, and progression to heart failure (HF). Such findings expose the possibility of oral administration of NLRP3 inflammasome inhibitors to treat cardiovascular disorders [7]. Hence, there is increasing scrutiny of inflammasome-based approaches to cardiovascular treatment.

Nicotinamide adenine dinucleotide (NAD⁺) is a coenzyme involved in diverse biological processes [8]. Decreased NAD⁺ levels and subsequent mitochondrial protein hyperacetylation have been reported to be associated with the development of HF. Thus, there is the potential for elevating NAD⁺ levels during therapy for cardiovascular diseases [9]. Notably, the potential benefits of dietary administration of NAD⁺ boosters have attracted much attention [10]. However, the salubrious effects of such agents in the hypertrophic heart have not been explored.

In the present study, we have used a transverse aortic constriction (TAC) mouse model to demonstrate that NLRP3 inflammasome activation is associated with the progression of heart hypertrophy. Furthermore, we have identified a cardioprotective role for nicotinamide riboside (NR), an NAD⁺ booster available through the diet and which inhibits the NLRP3 inflammasome and inflammatory responses via regulation of the Sirtuin3-MnSOD signaling pathway.

2. Materials and Methods

2.1. Materials

2.1.1. Animals. Male C57BL/6J mice (8 weeks, 180–200 g weight) were purchased from the Animal Center of Jinling Hospital. Animals were maintained under standard conditions of temperature (21 ± 2°C) and humidity (55 ± 2%) with an alternating 12 h light/12 h dark cycle. The animals had free access to tap water and were fed adequate food. The procedures of *in vivo* study were approved by the Jinling Hospital Committee on Animal Care. All animal study procedures were carried out in accordance with the Chinese National Institutes of Health Guidelines on the Use of Laboratory Animals.

2.1.2. Reagents. NR was purchased from China Thompson Biological Co., Ltd. DHE probe was purchased from Biolab company (Frozen Section ROS Detection Kit, Biolab, Beijing, China). Antibodies raised against Caspase-1, Caspase-1 pro, NLRP3, ASC, Sirtuin3, and β -actin for Western blotting were purchased from Cell Signaling Technology (Cell Signaling Technology, USA), and antibodies raised against cleaved GSDMD, MnSOD (total), and ac-MnSOD (MnSOD-acetyl K68) were purchased from Abcam (Abcam, USA).

2.2. Methods

2.2.1. Experimental Grouping and Surgical Treatments. A mouse model of cardiac hypertrophy was established using

TAC surgery. A total of 40 experimental mice were randomly assigned to one of four groups: sham, TAC, sham +NR and TAC+NR with 10 mice in each group. The TAC procedure is as follows. Mice were anesthetized with 2% isoflurane. Under aseptic conditions, with the mouse supine, the second rib on the left side of the thoracic cavity was cut off with surgical scissors and the thymus lightly plucked to fully expose the aortic arch. A 27G pillow was placed along the direction of the aortic arch, followed by ligation with a 7-0 thin thread to constrict the aortic arch to about 0.4 mm in diameter when the pillow was removed. Mice in the sham group were subjected to skin incisions and blunt separation without constriction of the aorta. The chest cavity was closed and the skin disinfected with iodophor. Postsurgery, penicillin was injected intraperitoneally to prevent infection. Echocardiography was performed one week after TAC surgery to confirm the position of the ligation thread. Mice in the sham+NR and TAC+NR groups were given NR by daily oral gavage at a dose of 400 mg/kg/d for 8 weeks.

2.2.2. Tissue Collection and Measurement. Eight weeks postsurgery, mice were fasted for 12 hours, weighed, and anesthetized by intraperitoneal injection of 2% sodium pentobarbital. Blood was taken from the carotid artery, and the heart and lungs were removed and weighed. The heart/body mass ratio (HW/BW): heart mass (mg)/body mass (g) and lung/body mass ratio (LW/BW): lung mass (mg)/body mass (g) were calculated. After standing for 15 minutes, carotid blood was centrifuged at 2,000g for 10 min to harvest serum. The activity of the myocardial injury marker, lactate dehydrogenase (LDH), was measured spectrophotometrically using a commercially available kit (Jiancheng Bioengineering Institute, Nanjing, China). Levels of IL-1 β and TNF- α in myocardial tissue were measured using ELISA kits according to the manufacturer's instructions.

2.2.3. Evaluation of Heart Function by Echocardiography. A Vevo 2100 ultrasound echocardiography system (VisualSonics, Toronto, Canada) was used to evaluate cardiac function. In brief, mice were anesthetized with isoflurane throughout. The heart was imaged in the two-dimensional parasternal short-axis view and an M-mode echocardiogram of the midventricle produced. Detailed procedures are as reported previously [11].

2.2.4. Measurement of Myocardial Oxidative Stress. Dihydroethidium (DHE) staining was used to evaluate the production of myocardial reactive oxygen species (ROS) in response to TAC. Briefly, frozen tissue sections were incubated with DHE solution for 30 min in the dark at 37°C. Cell nuclei were counterstained by DAPI (1 mg/mL) for 5 min. After washing, the slides were visualized under a laser scanning confocal microscope (Olympus FV1200, Olympus, Tokyo, Japan). Three replicate sections were analyzed to calculate the mean data.

Levels of malondialdehyde (MDA) and activities of superoxide dismutase (SOD) in myocardial tissue were measured with commercial assay kits (Beyotime, Shanghai, China), according to the manufacturer's instructions.

2.2.5. ELISA Assay. Levels of inflammatory cytokines, IL-1 β and TNF- α , were measured in myocardial tissue using commercial ELISA kits (IL-1 β and TNF- α ELISA kit: abs520001, Abison Shanghai Biotechnology Co., Ltd., China), according to the manufacturer's instructions. Each sample was tested in triplicate.

2.2.6. Sirtuin3 Activity. The Sirtuin3 activity was analyzed using a commercial kit (Sirtuin3 Activity Assay Kit, Abcam, Cambridge, MA, USA), according to the manufacturer's instructions. Fluorescence at Ex/Em = 340 – 360/440 – 460 nm was measured using a microplate reader. Sirtuin3 activities are presented relative to the sham group.

2.2.7. Quantitative Real-Time PCR. Quantitative real-time PCR was performed as described previously [11]. Briefly, total RNA was isolated from myocardial tissue, and cDNA was synthesized using a QuantiTect reverse transcription kit (Qiagen, Hilden, Germany). A real-time PCR procedure was performed using the KAPA SYBR FAST qPCR Kit (KAPA Biosystems, Woburn, MA, USA). Primer sequences are listed in Table 1. Forty cycles of amplification for genes encoding ANP and BNP were carried out (94°C for 30 s, 60°C for 60 s, and 72°C for 1 min). Relative mRNA expressions were calculated by the $\Delta\Delta$ CT method using the 7500 System SDS Software Version 1.2.1.22 (Applied Biosystems). GAPDH (housekeeping gene) was included as an internal standard.

2.2.8. Western Blotting. In brief, heart tissue was collected into Eppendorf tubes. Proteins were extracted by homogenizing tissue in RIPA buffer (Thermo RIPA buffer, Thermo Fisher Scientific, Waltham, MA) containing 1% Thermo Scientific Halt Protease Inhibitor Cocktail. Protein quantification was performed using the Thermo Scientific Pierce BCA Protein Assay Kit (Thermo Fisher Scientific, Waltham, MA). For the Western blot assay, the tissue homogenate was loaded onto SDS-PAGE gels; bands were transferred to the NC membrane (Millipore, Billerica, MA) and blocked with 5% adipoprotein, followed by incubation with the primary antibody at 4°C overnight (Caspase-1, Caspase-1 pro, NLRP3, ASC, GSDMD, Sirtuin3, MnSOD, MnSOD-acetyl K68, and β -actin (1:2000)). Membranes were washed with TBST solution and incubated with corresponding secondary antibody for 1 h at room temperature. Bands were visualized by a chemiluminescence detection kit (Thermo Electron Corp, Rockford, IL) and analyzed with ImageJ software (NIH ImageJ System, Bethesda, MD).

2.2.9. Statistics. All data were statistically analyzed with Prism 6.0 software. The experimental data are expressed as the mean \pm standard deviation (mean \pm SD). Data comparison was performed by one-way ANOVA analysis, followed by Tukey's analysis. $P < 0.05$ is considered to be the threshold for statistical significance.

3. Results

3.1. NR Attenuated the Myocardial Hypertrophy Markers in TAC Mice. The results of ultrasound echocardiography, performed one week after TAC, are shown in Figure 1(a).

The aorta was narrowed in the TAC group compared with the sham group. The effects of NR treatment on markers of myocardial hypertrophy, including cardiac mass index, ANP and BNP level, and LDH activity, were evaluated 8 weeks after TAC surgery. As shown in Figures 1(b) and 1(c), the HW/BW and LW/BW ratios in the TAC group (HW/BW: 5.342 ± 0.323 and LW/BW: 8.397 ± 0.320) were significantly higher than that in the sham group (4.771 ± 0.122 ; $P < 0.05$ and 6.426 ± 0.253 ; $P < 0.05$). NR treatment significantly reduced the ratios. The TAC+NR group had HW/BW: 5.011 ± 0.109 and LW/BW: 7.544 ± 0.332 compared with 5.342 ± 0.323 and 8.397 ± 0.320 , respectively, for the TAC group ($P < 0.05$). Levels of ANP and BNP were lower in the NR+TAC group compared with the TAC group (ANP: 1.32 ± 0.08 vs. 1.76 ± 0.06 ; $P < 0.05$; BNP: 1.74 ± 0.05 vs. 2.31 ± 0.06 ; $P < 0.05$), indicating that NR treatment significantly improved the myocardial hypertrophy induced by TAC (Figure 1(d)). TAC caused an increase in activities of the cardiac injury marker, LDH, compared with the sham group (TAC: 2978 ± 332 U/L vs. sham: 1268 ± 219 U/L; $P < 0.05$), and activities were reduced on treatment with NR (TAC+NR: 2300 ± 221 U/L; $P < 0.05$) (Figure 1(e)).

3.2. NR Alleviated the Cardiac Dysfunction Caused by TAC. Heart structure and function were evaluated by ultrasound echocardiography. Figure 2(a) shows the M-mode echocardiograms of the midventricle at the level of the papillary muscles. There was no significant difference in the mouse heart rate (HR) among groups with the HR ranging from 400 to 450 bpm (Figure 2(b)). The ejection fraction (EF) and fractional shortening (FS) were markedly decreased in the TAC group (EF: TAC: 59.2 ± 4.2 vs. sham: 75.8 ± 2.3 ; FS: TAC: 32.3 ± 2.2 vs. sham: 50.1 ± 1.6 ; $P < 0.05$), suggesting impaired myocardial function induced by TAC. NR treatment restored the left ventricular systolic function of TAC mice (EF: TAC+NR: 64.3 ± 2.1 vs. TAC: 59.2 ± 4.2 ; FS: TAC+NR: 43.2 ± 2.3 vs. TAC: 32.3 ± 2.2 ; $P < 0.05$) (Figures 2(c) and 2(d)). As is shown in Figures 2(e)–2(g), TAC caused changes in the structure of the mouse heart, manifested as left ventricular end-diastolic dimension (LV EDD), left ventricular end-systolic dimension (LV ESD), and left ventricular wall thickness (LV wall thickness) increases (LV EDD: TAC: 4.096 ± 0.122 vs. sham: 3.379 ± 0.092 ; LV ESD: TAC: 2.071 ± 0.096 vs. sham: 1.400 ± 0.115 ; LV wall thickness: TAC: 1.428 ± 0.040 vs. sham: 1.156 ± 0.066 ; $P < 0.05$). NR treatment significantly improved TAC-induced changes in cardiac structure (LV EDD: TAC+NR: 3.644 ± 0.154 vs. TAC: 4.096 ± 0.122 ; LV ESD: TAC+NR: 1.676 ± 0.087 vs. TAC: 2.071 ± 0.096 ; LV wall thickness: TAC+NR: 1.288 ± 0.023 vs. TAC: 1.428 ± 0.040 ; $P < 0.05$).

3.3. NR Inhibits the NLRP3 Inflammasome Activation and Inflammatory Cytokine Expression Induced by TAC. The results of ELISA and Western blot measurements of inflammatory cytokines are shown in Figure 3. Levels of inflammatory factors, IL-1 β and TNF- α , were increased in the myocardial tissue of the TAC group (IL-1 β : TAC: 267.58 ± 10.23 vs. sham: 195.32 ± 6.23 ; $P < 0.05$; TNF- α : TAC: 472.9 ± 17.30 vs. sham: 312.2 ± 18.11 ; $P < 0.05$), and NR

TABLE 1: Primer sequences for real-time PCR.

	Forward primer	Reverse primer
ANP	GCTTCCAGGCCATATGGAGCA	TCTCTCAGAGGTGGGTTGACCT
BNP	ATGGATCTCCTGAAGGTGCTGT	GCAGCTTGAGATATGTGTCACC
GAPDH	GGCACAGTCAAGGCTGAGAATG	ATGGTGGTGAAGACGCCAGTA

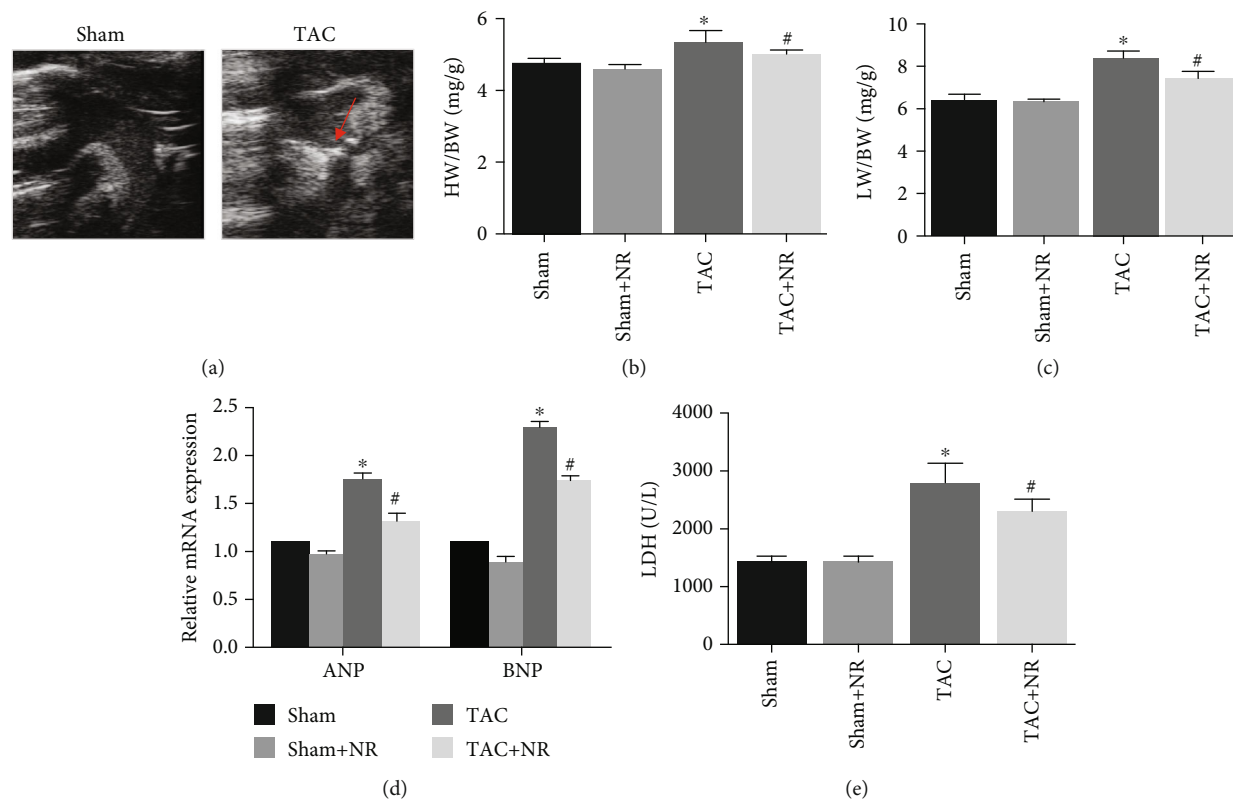


FIGURE 1: NR attenuates the myocardial hypertrophy markers in TAC mice. (a) Narrowed aorta (red arrow) in the TAC group. (b) The HW/BW ratio in the TAC+NR group was significantly reduced compared with the TAC group (5.011 ± 0.109 vs. 5.342 ± 0.323 , $P < 0.05$). (c) NR reduced TAC-induced LW/BW ratio augmentation (7.544 ± 0.332 vs. 8.397 ± 0.320 , $P < 0.05$). (d) NR significantly reduced ANP and BNP in TAC mice (ANP: 1.32 ± 0.08 vs. 1.76 ± 0.06 , $P < 0.05$; BNP: 1.74 ± 0.05 vs. 2.31 ± 0.06 , $P < 0.05$). (e) NR treatment reduced LDH level in hypertrophied mice (2300 ± 221 vs. 2978 ± 332 U/L, $P < 0.05$). TAC: transverse aortic constriction; HW/BW: heart/body mass ratio; LW/BW: lung/body mass ratio. * $P < 0.05$ vs. sham group; # $P < 0.05$ vs. TAC group.

treatment significantly reduced these levels (IL-1 β : TAC+NR: 233.17 ± 7.12 vs. TAC: 267.58 ± 10.23 ; $P < 0.05$; TNF- α : TAC+NR: 366.9 ± 13.40 vs. TAC: 472.9 ± 17.30 ; $P < 0.05$). Western blot results (Figure 3(c)) showed that the ratio of Caspase-1/Caspase-1 pro in the myocardium of the TAC group increased ($P < 0.05$), along with the expression of cleaved GSDMD and NLRP3 protein. NR treatment reduced the expression of NLRP3 and cleaved GSDMD, along with Caspase-1 activation in the TAC+NR group ($P < 0.05$). These results demonstrate the inhibitory effects of NR on the inflammasome activation induced by TAC.

3.4. NR Alleviated TAC-Induced Oxidative Stress. Mitochondrial ROS production was measured via DHE staining of myocardial tissue. Figures 4(a) and 4(b) show that the DHE fluorescence intensity was increased in the TAC myo-

cardial tissue ($P < 0.05$), an effect which was reduced by NR treatment ($P < 0.05$). In addition, the myocardial MDA level was elevated in the TAC group compared with the sham, suggesting severe oxidative stress ($P < 0.05$). NR treatment reduced MDA levels ($P < 0.05$, Figure 4(c)). Furthermore, TAC also impaired the activity of the myocardial antioxidant enzyme, SOD, the activity of which was restored by NR treatment ($P < 0.05$, Figure 4(d)).

3.5. NR Regulates NLRP3 Inflammasome Activation through the NAD⁺-Sirtuin3-MnSOD Axis. The therapeutic effectiveness of NR is dependent on the NAD⁺ pool. Figure 5(a) shows that NAD⁺ content was reduced in the myocardial tissue of the TAC group ($P < 0.05$), an effect which was ameliorated by NR treatment ($P < 0.05$). Moreover, the TAC-induced reduction of Sirtuin3 protein was also ameliorated

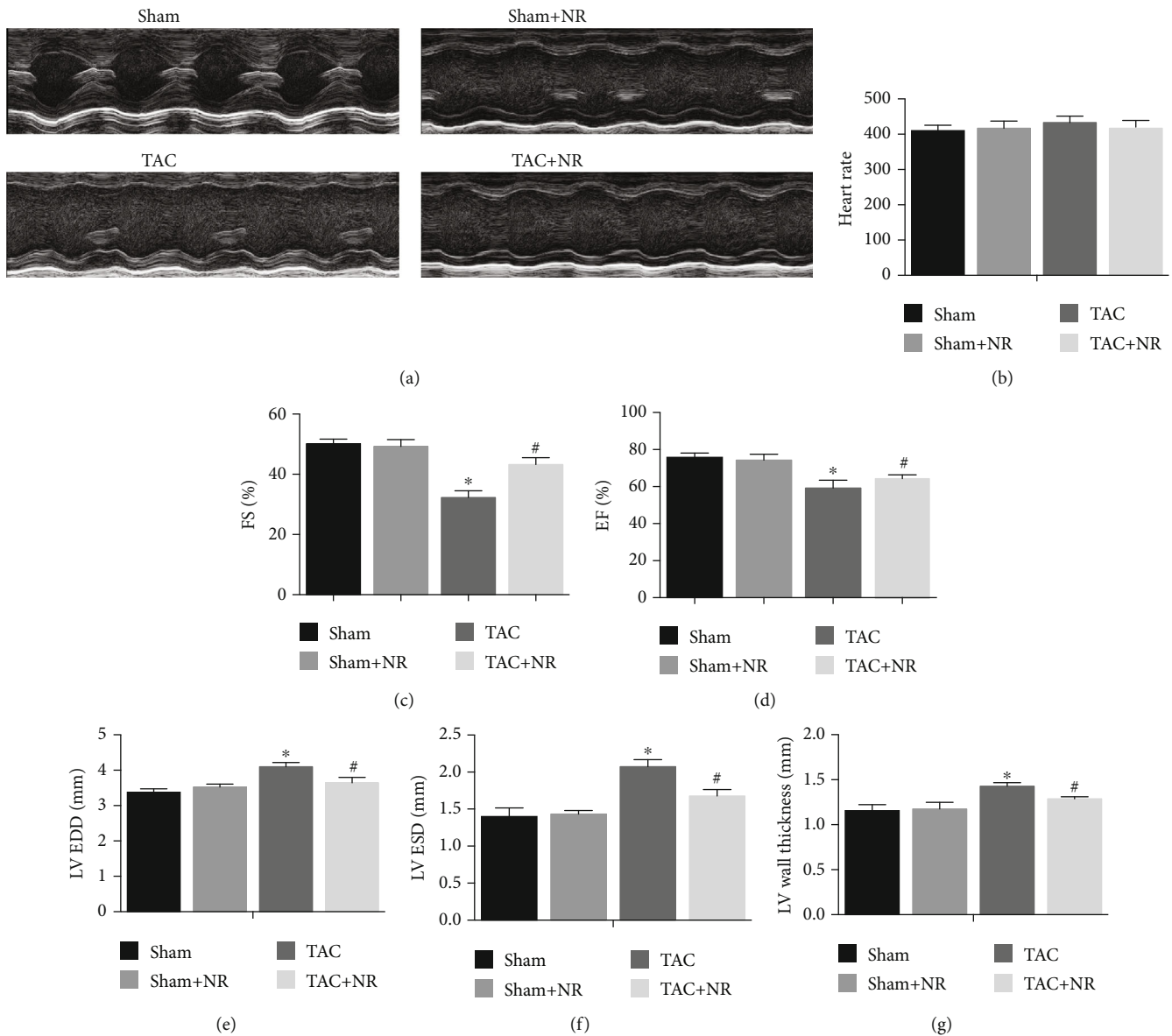


FIGURE 2: NR significantly alleviates the cardiac dysfunction caused by TAC. (a) The M-mode echocardiograms of the midventricle at the level of the papillary muscles. (b) There was no significant difference in mouse heart rate (HR) among groups ($P > 0.05$). (c, d) NR treatment significantly improved the left ventricular systolic function of TAC mice (EF: 64.3 ± 2.1 vs. 59.2 ± 4.2 ; FS: 43.2 ± 2.3 vs. 32.3 ± 2.2 , $P < 0.05$). (e–g) NR treatment significantly improved TAC-induced changes in cardiac structure (LV EDD: 3.644 ± 0.154 vs. 4.096 ± 0.122 ; LV ESD: 1.676 ± 0.087 vs. 2.071 ± 0.096 ; LV wall thickness: 1.288 ± 0.023 vs. 1.428 ± 0.040 , $P < 0.05$). HR: heart rate; EF: ejection fraction; FS: fractional shortening; LV EDD: left ventricular end-diastolic dimension; LV ESD: left ventricular end-systolic dimension. * $P < 0.05$ vs. sham group; # $P < 0.05$ vs. TAC group.

by NR treatment ($P < 0.05$, Figure 5(b)). MnSOD is the regulatory substrate of Sirtuin3 and a key protein in the regulation of cellular oxidative stress. Figure 5(c) shows that levels of ac-MnSOD protein increased after TAC treatment, an effect which was partially reversed by NR treatment ($P < 0.05$). These changes are consistent with the altered levels of Sirtuin3 activity.

4. Discussion

In the present study, we have demonstrated that NLRP3 inflammasome activation, along with accompanying secre-

tion of cytokines, contributed to the progression of cardiac hypertrophy in a TAC mouse model. Furthermore, our data established the therapeutic potential of NR, an NAD⁺ booster which can be administered orally through the diet. The underlying mechanism was revealed to involve the Sirtuin3-MnSOD signaling pathway and its inhibition of the NLRP3 inflammasome.

Individuals with cardiac hypertrophy are vulnerable to heart failure and arrhythmia as a result of pathological cardiac remodeling [12]. Hence, there is an urgent need to investigate the mechanistic causes of hypertrophic progression. Previous studies have implicated inflammatory

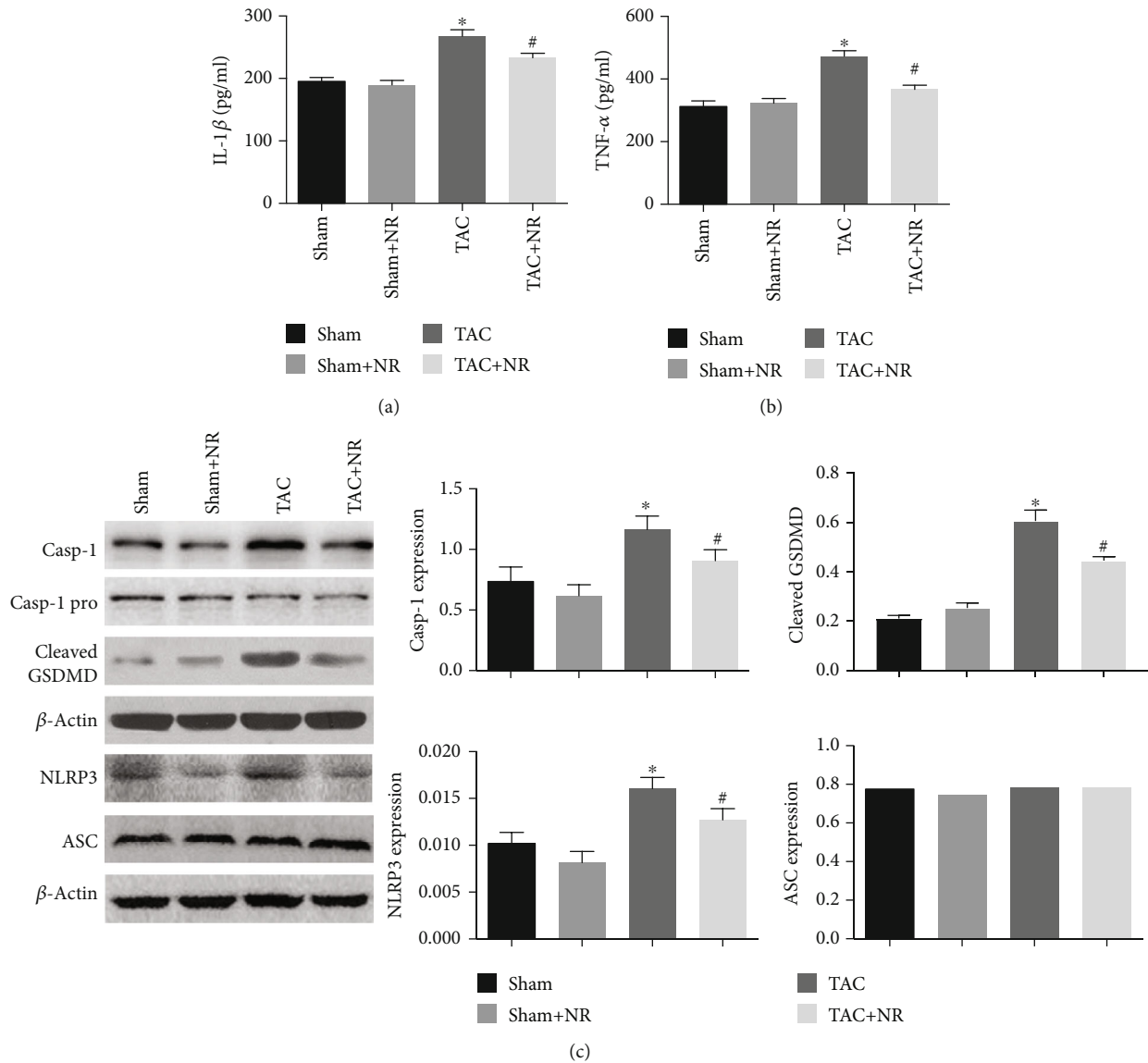


FIGURE 3: NR inhibits NLRP3 inflammasome activation induced by TAC. (a, b) NR significantly reduced the levels of high inflammatory factors caused by myocardial hypertrophy (IL-1 β : 233.17 ± 7.12 vs. 267.58 ± 10.23 ; TNF- α : 366.9 ± 13.40 vs. 472.9 ± 17.30 , $P < 0.05$). (c) Western blot results showed that NR treatment significantly reduced the Caspase-1/Caspase-1 pro and cleaved GSDMD expression in TAC mice ($P < 0.05$). Furthermore, NR markedly reduced the NLRP3 expression in the TAC+NR group ($P < 0.05$). There was no significant difference in ASC expression ($P > 0.05$). NR: nicotinamide riboside. * $P < 0.05$ vs. sham group; # $P < 0.05$ vs. TAC group.

processes in the pathophysiology of cardiac hypertrophy, and the identification of such mechanisms exposes potential targets for pharmacological modulation [13, 14]. NLRP3 is a pattern recognition receptor (PRR) which allows the cell to respond to danger signals. Activated NLRP3 interacts with adapter apoptosis-associated speck-like protein containing a C-terminal caspase recruitment domain (ASC) to form the NLRP3 inflammasome which activates Caspase-1 and results in the production of proinflammatory cytokines [15]. The current study establishes the presence of excessive NLRP3 inflammasome activation in TAC-induced cardiac hypertrophy and dysfunction. Inhibition of the NLRP3 inflammatory response had a beneficial impact on the hypertrophic heart. The findings of previous work have also suggested that selective NLRP3 inflammasome inhibition

has a cardioprotective effect, reducing the risk of heart failure or other cardiovascular diseases [16, 17]. However, there is a certain degree of controversy surrounding these conclusions. Li et al. reported opposing findings that NLRP3 expression was downregulated during the hypertrophic process and the deficiency of NLRP3 exacerbated pressure overload-induced cardiac remodeling [18]. However, the apparent discrepancy between these results and the conclusions of the current study may be explained by the effect of NLRP3 protein on downregulating Toll-like receptor (TLR) 4 and does not take into account the more wide-ranging role of the complete NLRP3 inflammasome. The balance of opinion is predominantly in favor of the detrimental effect that the NLRP3 inflammasome contributes to the pathological process of cardiovascular disease and acknowledges that

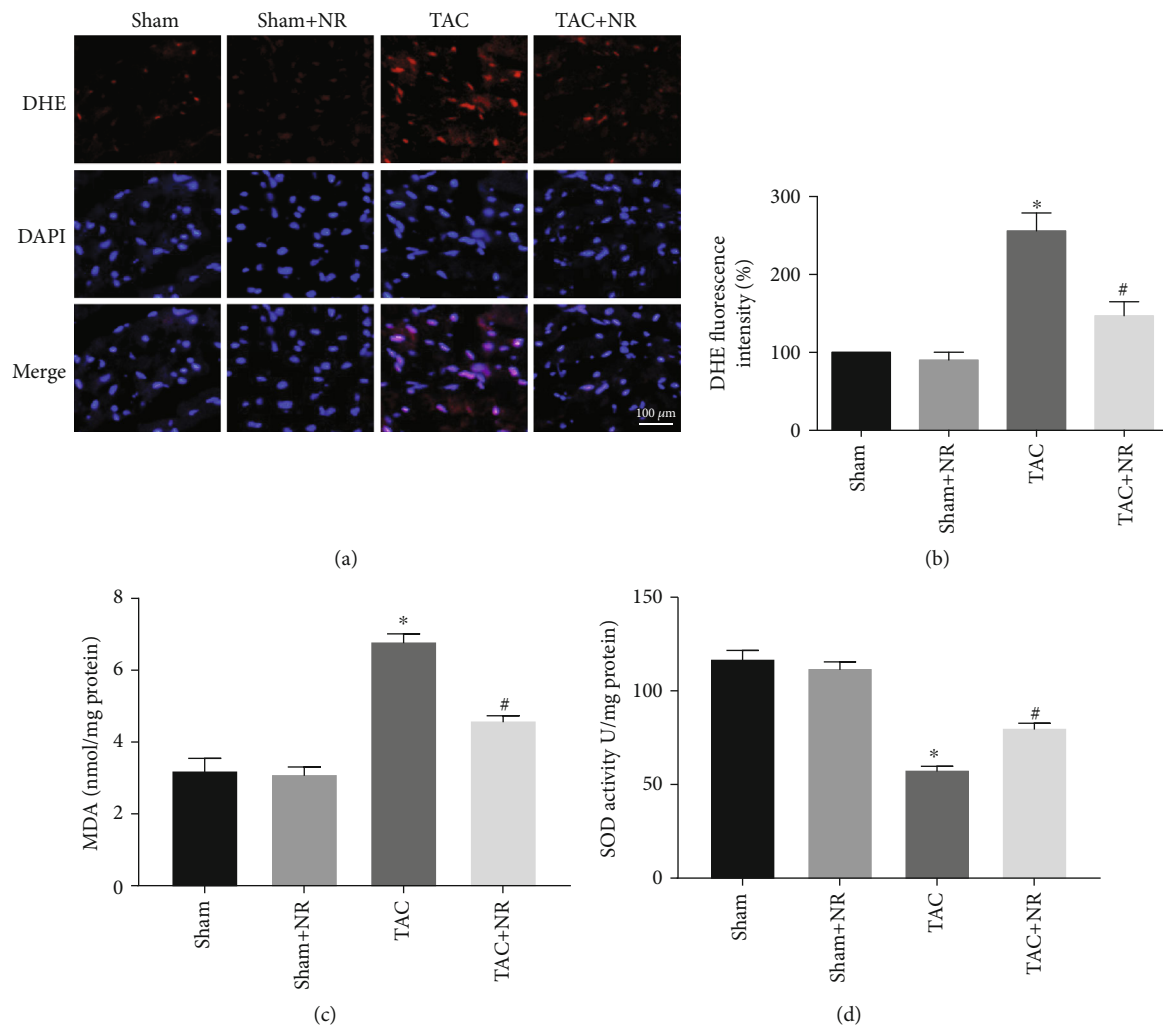


FIGURE 4: NR alleviates TAC-induced oxidative stress. (a) Myocardial DHE staining images. Scale bar: 100 μm . (b) DHE fluorescence intensity revealed that NR treatment markedly reduced the augmentation of superoxide generation in the TAC+NR group ($P < 0.05$). (c) NR treatment markedly attenuated the increased MDA content level in TAC mice ($P < 0.05$). (d) NR restored the impaired SOD activity in TAC mice ($P < 0.05$). * $P < 0.05$ vs. sham group; # $P < 0.05$ vs. TAC group.

the NLRP3 inflammasome is a promising therapeutic target [19, 20].

NAD⁺ is an abundant molecule which is ubiquitous in its participation in biological processes [21]. In the last decade, there has been renewed interest in NAD⁺ as a result of its association with the Sirtuins (Sirtuin1–7), a family of NAD-dependent protein deacylases [22]. Levels of NAD⁺ are considered to decrease with age, and pathological condition and NAD⁺ supplementation have been suggested as a therapy for cardiovascular diseases [23]. The findings of the current study indicate that levels of NAD⁺ were reduced in the TAC mouse model. Supplementation with NR, a pharmacological NAD⁺ precursor, contributed to the restoration of heart function and remodeling. A previous clinical study has reported that a single oral dose of 1000 mg NR raised the blood NAD⁺ level by 2.7-fold, demonstrating the feasibility of NAD⁺ supplementation for the human patient [23]. More recently, Zhou et al. have reported attenuated proinflammatory activation of heart failure in patients given oral NR to augment NAD levels [24]. Collectively, these studies indicate great potential

for clinical NAD⁺ repletion in the treatment of cardiovascular disorders. Further research is necessary to clarify the therapeutic potential of NAD⁺ booster treatment to ameliorate cardiac hypertrophy in patients.

The current study also explored the relationship between NAD⁺ supplementation and NLRP3 inflammasome activation in hypertrophic hearts. Generation of mitochondrial ROS is considered a key to NLRP3 inflammasome activation [25, 26]. Thus, we considered the possibility that regulation of oxidative stress might favorably orchestrate NLRP3 inflammatory responses. We found that NR supplementation attenuated TAC-induced myocardial oxidative stress, and this showed a consistent relationship with NLRP3 inflammasome activation. These findings strongly suggest that the inhibitory effect of NR on the NLRP3 inflammasome could be attributed to mitochondrial ROS production.

Previous studies have revealed reduced Sirtuin3 expression and elevated lysine acetylation of mitochondrial proteins in models of hypertensive heart failure, indicating an association of impaired Sirtuin3 activity with pathological

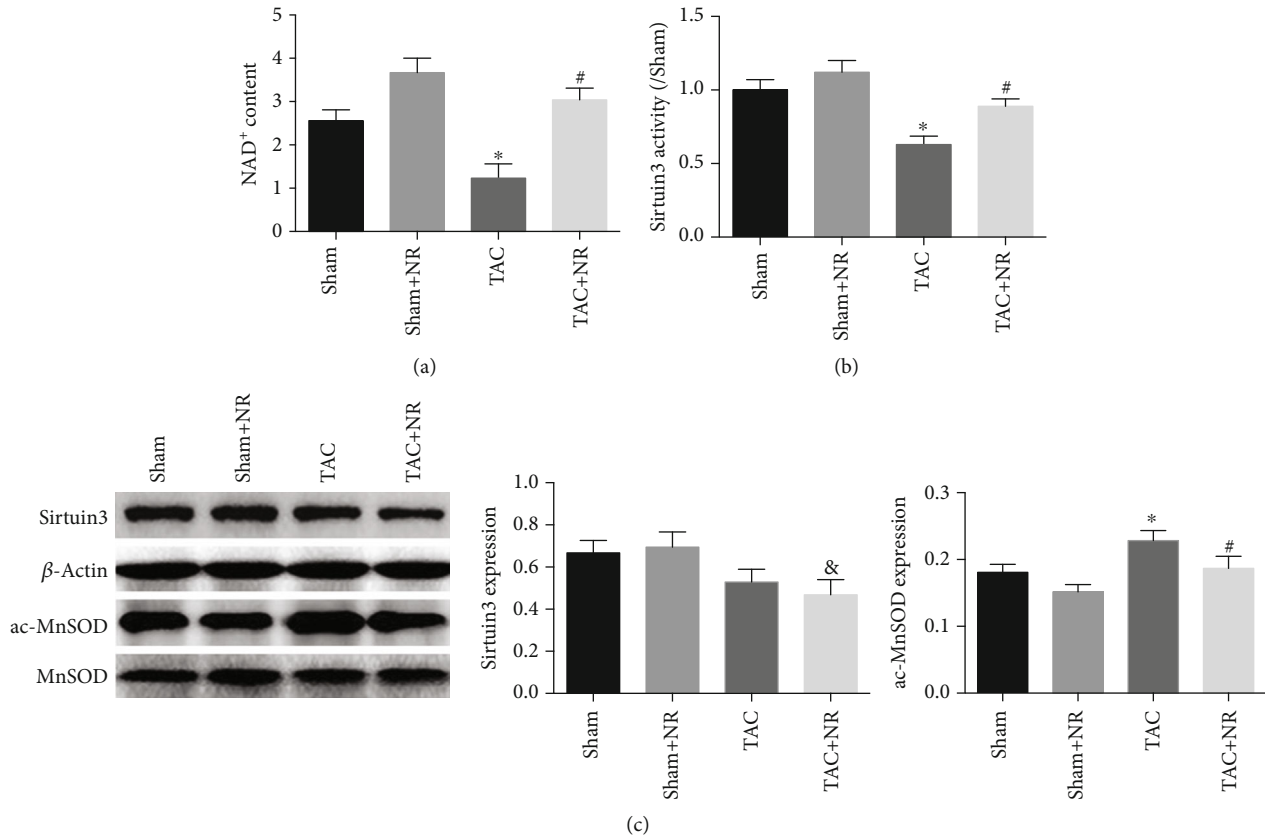


FIGURE 5: NR regulates the NAD⁺-Sirtuin-MnSOD axis. (a) The NAD⁺ content was reduced in TAC grouped myocardium, while NR significantly elevated the NAD⁺ content in the TAC+NR group ($P < 0.05$). (b) NR treatment can significantly increase the activity of Sirtuin3 protein in the TAC+NR group ($P < 0.05$). (c) Western blot results show decreased Sirtuin3 expression in the TAC and TAC+NR groups ($P < 0.05$). The acMOD protein level in the myocardial tissue of mice was significantly increased in the TAC group, while NR treatment can significantly reduce the acMOD protein level ($P < 0.05$). * $P < 0.05$ vs. sham group; # $P < 0.05$ vs. TAC group; & $P < 0.05$ vs. sham+NR group.

cardiac remodeling [27]. Our findings demonstrated that boosting NAD⁺ levels through NR supplementation caused elevated Sirtuin3 activity and deacetylation of MnSOD and alleviated TAC-induced myocardial oxidative stress. These findings from the current study are in agreement with preclinical data reported by Lee et al. who found that normalization of the NADH/NAD⁺ imbalance attenuated mitochondrial protein hyperacetylation in heart failure models [9]. The current study identified that the beneficial effect of Sirtuin3 was mediated by Mn superoxide dismutase (MnSOD), a superoxide scavenger, with reduced superoxide production resulting in attenuation of oxidative stress. However, a previous study by Diguët et al. observed that dietary NR supplementation attenuates the development of HF in mice without an impact on global cardiac protein deacetylation, and they observed robustly increased acetylation levels of FOXO1 and p53 transcription factors. By contrast, we have presented evidence that NR causes elevated myocardial Sirtuin3 activity and decreased acetylation level of MnSOD [28]. There are a number of acetylases and deacetylases, some of which are NAD⁺-dependent while others are NAD⁺-independent. Further preclinical and clinical investigations of the impact of augmented NAD⁺ on protein acetylation are warranted.

The present study confined the analysis to the activity of Sirtuin3, a member of the larger family of Sirtuin proteins. Sirtuins1-7 are major downstream mediators of the NAD⁺ regulation of biological processes [22]. There have been several studies which have reported the NAD⁺-dependent activation of Sirtuin1 and Sirtuin6 following supplementation with NR [29–31]. It is conceivable that other members of the Sirtuin family are also targets for NR supplementation in the context of the TAC model. Further investigations are required to better understand the effects and underlying mechanisms involved in NAD⁺ booster treatment.

5. Conclusions

Taken all together, the findings of the present study demonstrate the utility of NR as a booster for NAD⁺ levels in attenuating cardiac hypertrophy induced by pressure overload. We have revealed a mechanism associated with reduced oxidative stress and inhibition of NLRP3 inflammasome activation via the Sirtuin3-MnSOD signaling pathway. We conclude that NR, an NAD⁺ booster that can be given through the diet, has great promise as a novel therapeutic intervention for cardiac hypertrophy.

Data Availability

Data are available on request.

Conflicts of Interest

All authors declare that no competing financial interests exist.

Authors' Contributions

Sai Ma and Jing Feng contributed equally to this work.

Acknowledgments

This work was supported by the National Natural Science Foundation of China (81900409 and 81773963) and PLA Youth Training Project for Medical Science (19QNP037).

References

- [1] M. J. Zeitz and J. W. Smyth, "Translating translation to mechanisms of cardiac hypertrophy," *Journal of Cardiovascular Development and Disease*, vol. 7, no. 1, p. 9, 2020.
- [2] M. Nakamura and J. Sadoshima, "Mechanisms of physiological and pathological cardiac hypertrophy," *Nature Reviews Cardiology*, vol. 15, no. 7, pp. 387–407, 2018.
- [3] C. J. Oldfield, T. A. Duhamel, and N. S. Dhalla, "Mechanisms for the transition from physiological to pathological cardiac hypertrophy," *Canadian Journal of Physiology and Pharmacology*, vol. 98, no. 2, pp. 74–84, 2020.
- [4] I. Shimizu and T. Minamino, "Physiological and pathological cardiac hypertrophy," *Journal of Molecular and Cellular Cardiology*, vol. 97, pp. 245–262, 2016.
- [5] M. Samak, J. Fatullayev, A. Sabashnikov et al., "Cardiac hypertrophy: an introduction to molecular and cellular basis," *Medical Science Monitor Basic Research*, vol. 22, pp. 75–79, 2016.
- [6] D. Liu, X. Zeng, X. Li, J. L. Mehta, and X. Wang, "Role of NLRP3 inflammasome in the pathogenesis of cardiovascular diseases," *Basic Research in Cardiology*, vol. 113, no. 1, p. 5, 2018.
- [7] A. Abbate, S. Toldo, C. Marchetti, J. Kron, B. W. Van Tassel, and C. A. Dinarello, "Interleukin-1 and the inflammasome as therapeutic targets in cardiovascular disease," *Circulation Research*, vol. 126, no. 9, pp. 1260–1280, 2020.
- [8] W. Hong, F. Mo, Z. Zhang, M. Huang, and X. Wei, "Nicotinamide mononucleotide: a promising molecule for therapy of diverse diseases by targeting NAD⁺ metabolism," *Frontiers in Cell and Development Biology*, vol. 8, p. 246, 2020.
- [9] C. F. Lee, J. D. Chavez, L. Garcia-Menendez et al., "Normalization of NAD⁺ redox balance as a therapy for heart failure," *Circulation*, vol. 134, no. 12, pp. 883–894, 2016.
- [10] B. E. Kang, J. Y. Choi, S. Stein, and D. Ryu, "Implications of NAD⁺ boosters in translational medicine," *European Journal of Clinical Investigation*, vol. 50, no. 10, article e13334, 2020.
- [11] S. Ma, J. Feng, R. Zhang et al., "SIRT1 activation by resveratrol alleviates cardiac dysfunction via mitochondrial regulation in diabetic cardiomyopathy mice," *Oxidative Medicine and Cellular Longevity*, vol. 2017, Article ID 4602715, 15 pages, 2017.
- [12] M. Tian, X. Jiang, X. Li, J. Yang, C. Zhang, and W. Zhang, "LKB1IP promotes pathological cardiac hypertrophy by targeting PTEN/Akt signalling pathway," *Journal of Cellular and Molecular Medicine*, vol. 25, no. 5, pp. 2517–2529, 2021.
- [13] T. P. Mikolajczyk, P. Szczepaniak, F. Vidler, P. Maffia, G. J. Graham, and T. J. Guzik, "Role of inflammatory chemokines in hypertension," *Pharmacology & Therapeutics*, vol. 223, article 107799, 2021.
- [14] F. J. Carrillo-Salinas, N. Ngwenyama, M. Anastasiou, K. Kaur, and P. Alcaide, "Heart inflammation: immune cell roles and roads to the heart," *The American Journal of Pathology*, vol. 189, no. 8, pp. 1482–1494, 2019.
- [15] W. Zhou, C. Chen, Z. Chen et al., "NLRP3: a novel mediator in cardiovascular disease," *Journal of Immunology Research*, vol. 2018, Article ID 5702103, 8 pages, 2018.
- [16] C. Yao, T. Veleva, L. Scott Jr. et al., "Enhanced cardiomyocyte NLRP3 inflammasome signaling promotes atrial fibrillation," *Circulation*, vol. 138, no. 20, pp. 2227–2242, 2018.
- [17] S. Sano, K. Oshima, Y. Wang et al., "Tet2-mediated clonal hematopoiesis accelerates heart failure through a mechanism involving the IL-1 β /NLRP3 inflammasome," *Journal of the American College of Cardiology*, vol. 71, no. 8, pp. 875–886, 2018.
- [18] F. Li, H. Zhang, L. Yang et al., "NLRP3 deficiency accelerates pressure overload-induced cardiac remodeling via increased TLR4 expression," *Journal of Molecular Medicine*, vol. 96, no. 11, pp. 1189–1202, 2018.
- [19] A. I. Suceveanu, L. Mazilu, N. Katsiki et al., "NLRP3 inflammasome biomarker-could be the new tool for improved cardiometabolic syndrome outcome," *Metabolites*, vol. 10, no. 11, p. 448, 2020.
- [20] N. An, Y. Gao, Z. Si et al., "Regulatory mechanisms of the NLRP3 inflammasome, a novel immune-inflammatory marker in cardiovascular diseases," *Frontiers in Immunology*, vol. 10, p. 1592, 2019.
- [21] H. R. Ansari and G. P. Raghava, "Identification of NAD interacting residues in proteins," *BMC Bioinformatics*, vol. 11, no. 1, p. 160, 2010.
- [22] L. Rajman, K. Chwalek, and D. A. Sinclair, "Therapeutic Potential of NAD-Boosting Molecules: The *In Vivo* Evidence," *Cell Metabolism*, vol. 27, no. 3, pp. 529–547, 2018.
- [23] S. A. Trammell, M. S. Schmidt, B. J. Weidemann et al., "Nicotinamide riboside is uniquely and orally bioavailable in mice and humans," *Nature Communications*, vol. 7, no. 1, article 12948, 2016.
- [24] B. Zhou, D. D. Wang, Y. Qiu et al., "Boosting NAD level suppresses inflammatory activation of PBMCs in heart failure," *The Journal of Clinical Investigation*, vol. 130, no. 11, pp. 6054–6063, 2020.
- [25] H. S. Jin, H. W. Suh, S. J. Kim, and E. K. Jo, "Mitochondrial control of innate immunity and inflammation," *Immune Network*, vol. 17, no. 2, pp. 77–88, 2017.
- [26] P. Gurung, J. R. Lukens, and T. D. Kanneganti, "Mitochondria: diversity in the regulation of the NLRP3 inflammasome," *Trends in Molecular Medicine*, vol. 21, no. 3, pp. 193–201, 2015.
- [27] J. M. Grillon, K. R. Johnson, K. Kotlo, and R. S. Danziger, "Non-histone lysine acetylated proteins in heart failure," *Biochimica et Biophysica Acta*, vol. 1822, no. 4, pp. 607–614, 2012.
- [28] N. Diguët, S. Trammell, C. Tannous et al., "Nicotinamide riboside preserves cardiac function in a mouse model of dilated cardiomyopathy," *Circulation*, vol. 137, no. 21, pp. 2256–2273, 2018.

- [29] C. Cantó, R. H. Houtkooper, E. Pirinen et al., “The NAD⁺ Precursor Nicotinamide Riboside Enhances Oxidative Metabolism and Protects against High-Fat Diet-Induced Obesity,” *Cell Metabolism*, vol. 15, no. 6, pp. 838–847, 2012.
- [30] B. A. Harlan, M. Pehar, K. M. Killoy, and M. R. Vargas, “Enhanced SIRT6 activity abrogates the neurotoxic phenotype of astrocytes expressing ALS-linked mutant SOD1,” *The FASEB Journal*, vol. 33, no. 6, pp. 7084–7091, 2019.
- [31] C. A. Stoyas, D. D. Bushart, P. M. Switonski et al., “Nicotinamide pathway-dependent Sirt1 activation restores calcium homeostasis to achieve neuroprotection in spinocerebellar ataxia type 7,” *Neuron*, vol. 105, no. 4, pp. 630–644.e9, 2020.

Review Article

Molecular Dysfunctions of Mitochondria-Associated Endoplasmic Reticulum Contacts in Atherosclerosis

Xiaojiao Wang , Dan Luo , and Sisi Wu 

Core Facilities of West China Hospital, Sichuan University, Chengdu 610041, China

Correspondence should be addressed to Sisi Wu; wusisi@wchscu.cn

Received 17 April 2021; Accepted 11 July 2021; Published 22 July 2021

Academic Editor: Sang-Bing Ong

Copyright © 2021 Xiaojiao Wang et al. This is an open access article distributed under the Creative Commons Attribution License, which permits unrestricted use, distribution, and reproduction in any medium, provided the original work is properly cited.

Atherosclerosis is a chronic lipid-driven inflammatory disease that results in the formation of lipid-rich and immune cell-rich plaques in the arterial wall, which has high morbidity and mortality in the world. The mechanism of atherosclerosis is still unclear now. Potential hypotheses involved in atherosclerosis are chronic inflammation theory, lipid percolation theory, mononuclear-macrophage theory, endothelial cell (EC) injury theory, and smooth muscle cell (SMC) mutation theory. Changes of phospholipids, glucose, critical proteins, etc. on mitochondria-associated endoplasmic reticulum membrane (MAM) can cause the progress of atherosclerosis. This review describes the structural and functional interaction between mitochondria and endoplasmic reticulum (ER) and explains the role of critical molecules in the structure of MAM during atherosclerosis.

1. Introduction

Atherosclerosis remains a leading cause of cardiovascular disease worldwide [1]. In the early stage of atherosclerosis, a large number of foam cells derived from macrophages and SMCs gather in the arterial intima lesions, forming dots or stripes of yellow fatty streaks [2]. As the disease progresses, fatty streaks will develop into fibrous plaques containing a large number of collagen fibers, foam cells, SMCs, extracellular matrix, and inflammatory cells [3]. In the end-stage of atherosclerosis, the deep cells of the fibrous plaque become necrotic and develop into atheromatous plaque (also named atheroma), with granulation tissue, a small number of lymphocytes, and foam cells [4]. Secondary changes such as plaque hemorrhage, rupture, thrombosis, calcification, aneurysm, and vascular lumen stenosis will occur during atherosclerosis [5]. The exact cause of atherosclerosis remains unclear. Hyperlipidemia, hypertension, smoking, diabetes, hyperinsulinemia, hypothyroidism, genetic factors, age, gender, obesity, and other factors are all considered risk factors for atherosclerosis [1]. The mechanism of atherosclerosis has not been well clarified. Cumulative low-density lipoprotein (LDL) arterial burden is a central determinant for the initiation and progression of atherosclerosis [6]. In the arte-

rial intima, where plaque is easy to form, it is easy to retain and accumulate cholesterol-rich apolipoprotein B- (apoB-) containing lipoproteins (including LDL, their remnants, intermediate-density lipoprotein (IDL), and lipoprotein (a)) [1]. LDL could penetrate into the arterial intima exhibiting a strong atherosclerotic effect. With a weak antioxidant effect, LDL could further aggravate atherosclerosis after entering the lipid-rich atheromatous plaque. Various cardiovascular risk factors such as hyperlipidemia, diabetes, and vascular inflammation can induce endothelial cells damage and apoptosis during atherosclerosis [7]. Chronic inflammation driven by lipid is intimately involved in all stages of atherosclerosis progression. The infiltration and modification of the inner membrane of plasma-derived lipoproteins and their uptake are mainly from macrophages, which then form lipid-filled foam cells, triggering the formation of atherosclerotic lesions, while apoptotic cells and foam cells lack effective removal leading to the progression of the disease [8]. B cells, T cells, and some inflammatory factors also play a critical role in atherosclerosis [9–11]. Pan et al. combined SMC fate mapping and single-cell RNA sequencing of both mouse and human atherosclerotic plaques a novel cell state during SMC phenotypic switching and potential therapeutic targets for atherosclerosis [12]. Researches based on proteomics

proves atherosclerotic samples had significant reductions in mitochondrial protein abundance [13]. Prolonged ER stress is an important cause of macrophage and possibly EC apoptosis in advanced lesions [14]. Additional ER stress-mediated proinflammatory effects in these cells may also affect early atherogenesis [14].

As the site of oxidative phosphorylation, the double-membrane organelle, mitochondria provide a highly efficient route for eukaryotic cells to generate ATP from energy-rich molecules [15]. Mitochondria are not only the hub of biosynthesis, they can also balance redox equivalents and can also manage wastes such as ammonia, reactive oxygen species (ROS), and hydrogen sulfide [16]. The ER is a central intracellular organelle responsible for various key functions, including protein synthesis, folding, posttranslational modification and transportation; lipid and steroid synthesis; membrane synthesis and transportation; the metabolism of drugs and xenobiotics; the storage and release of intracellular Ca^{2+} ; the regulation of gene expression and energy metabolism; and the signaling to the nucleus, cytoplasm, mitochondria, and plasma membrane [17]. ER has a broad localization throughout the cell and forms direct physical contact with all other classes of membranous organelles, including the mitochondrial membrane [18]. ER and the mitochondrial membrane are closely connected in structure (called MAM, which has the properties of a lipid raft) and are highly related in function, regulating lipid metabolism, signaling transduction, the regulation of Ca^{2+} signaling, and the control of mitochondrial and ER biogenesis and intracellular transport [19]. The communication imbalance between ER and mitochondria will affect the function of MAM (Figure 1), which will lead to the occurrence of diseases.

Atherosclerosis has been associated with mitochondria dysfunction and damage, as well as ER stress [13, 20–22]. Studies have shown that the occurrence and development of atherosclerosis are closely related to the molecular changes on MAM [23]. This review is aimed at discussing the role of MAM structure and function in the pathophysiological process of atherosclerosis; it also clarifies how atherosclerosis-related proteins affect the structure and function of MAM.

2. Structural and Functional Proteins of MAMs Involved in Atherosclerosis

2.1. Calcium Signaling

2.1.1. IP3R-Grp75-VDAC1. The voltage-dependent anion channel 1 (VDAC1) located in the outer mitochondrial membrane interacts with the inositol 1,4,5-triphosphate receptor (IP3R) on the ER through the glucose regulatory protein 75 (Grp75) (molecular chaperone), allowing Ca^{2+} from the ER is transferred to the mitochondria [24]. During the development of atherosclerosis, apoE may open the mitochondrial permeability transition pore (MPTP) through the interaction of apoE and VDAC1, thereby playing an important role in mitochondrial dysfunction induced by negatively charged LDL [25]. The secretion of apoE by macrophages occurs through protein kinase A (PKA) and Ca^{2+} -dependent

pathways along the microtubule network, and its specific expression can prevent atherosclerosis [26].

2.1.2. SERCA- Ca^{2+} . Sarco ER Ca^{2+} -ATPase (SERCA), located in ER, is recognized as the main pump system that controls the cytoplasmic Ca^{2+} of muscle cells. This system could induce relaxation of Ca^{2+} from the cytosol. For each ATP hydrolyzed, SERCA pumps in two Ca^{2+} and releases less than four H^+ into the cytoplasm, which indicates that the transport reaction is partially electrically induced [27]. Mitochondria can store large amounts of Ca^{2+} in its matrix. This feature only has a temporary effect, because if the mitochondria are forced to continuously accumulate Ca^{2+} , they will not synthesize ATP, and ultimately deprive the Ca^{2+} pump of the energy necessary to remove Ca^{2+} from the cytosol, thus, triggering a vicious circle and aggravating Ca^{2+} production [27, 28]. Adenosine 5'-monophosphate- (AMP-) activated protein kinase (AMPK) acts as a physiological inhibitor of ER stress by maintaining SERCA activity and intracellular Ca^{2+} homeostasis, thereby alleviating the progression of atherosclerosis [29].

2.2. Mitochondria and ER Dynamics

2.2.1. MFNs. Mitofusin (MFN), a membrane-bound dynamin-like protein named after its mitochondrial fusion activity, locating on the outer mitochondrial membrane (OMM) and mediates the merging of opposing OMMs in a GTP-dependent manner [30]. There are two types of MFNs in mammals, namely, MFN1 and MFN2, which have different roles in mediating OMM fusion. Both localize to OMM, while a small proportion of MFN2 is located at ER membranes. They form a complex in vitro in terms of structure and function, which has a greater fusion effect on isolated mitochondria [31]. MFN-mediated anchoring of mitochondria to transport proteins may contribute to mitochondrial motility [32]. MFN2 is a major (but not the only) protein tether linking mitochondria to ER/sarcoplasmic reticulum (SR) is substantial, perhaps incontrovertible [33, 34]. Mitochondrial-localized AIBP is related to MFN1 and MFN2 through its N-terminal domain and regulates their ubiquitination, thereby enhancing mitochondrial autophagy and participating in mitochondrial quality control, protecting macrophages from cell death in atherosclerosis [35]. Flavonoid binding protein 4 (FBP4) inhibits the expression of MFN1 in human aortic endothelial cells, but enhances the expression of dynamin-related protein1 (Drp1) and mitochondrial fission protein 1 (Fis1), suggesting mitochondrial fusion and fission dynamics are impaired, which induces oxidative damage of blood vessels and promotes the development of atherosclerosis [36].

2.2.2. BAP31-Fis1-Drp1. There is an interaction between the resident ER protein B cell receptor-associated protein 31 (BAP31), which is involved in the initiation of mitochondrial fission process and the OMM mitochondrial fission 1 (Fis1) protein [37]. In the fission cycle, Drp1 first binds to the mitochondrial fission factor (Mff) on the mitochondrial surface and then enters the complex containing Fis1 and BAP31 at the ER-mitochondrial interface, thereby inducing

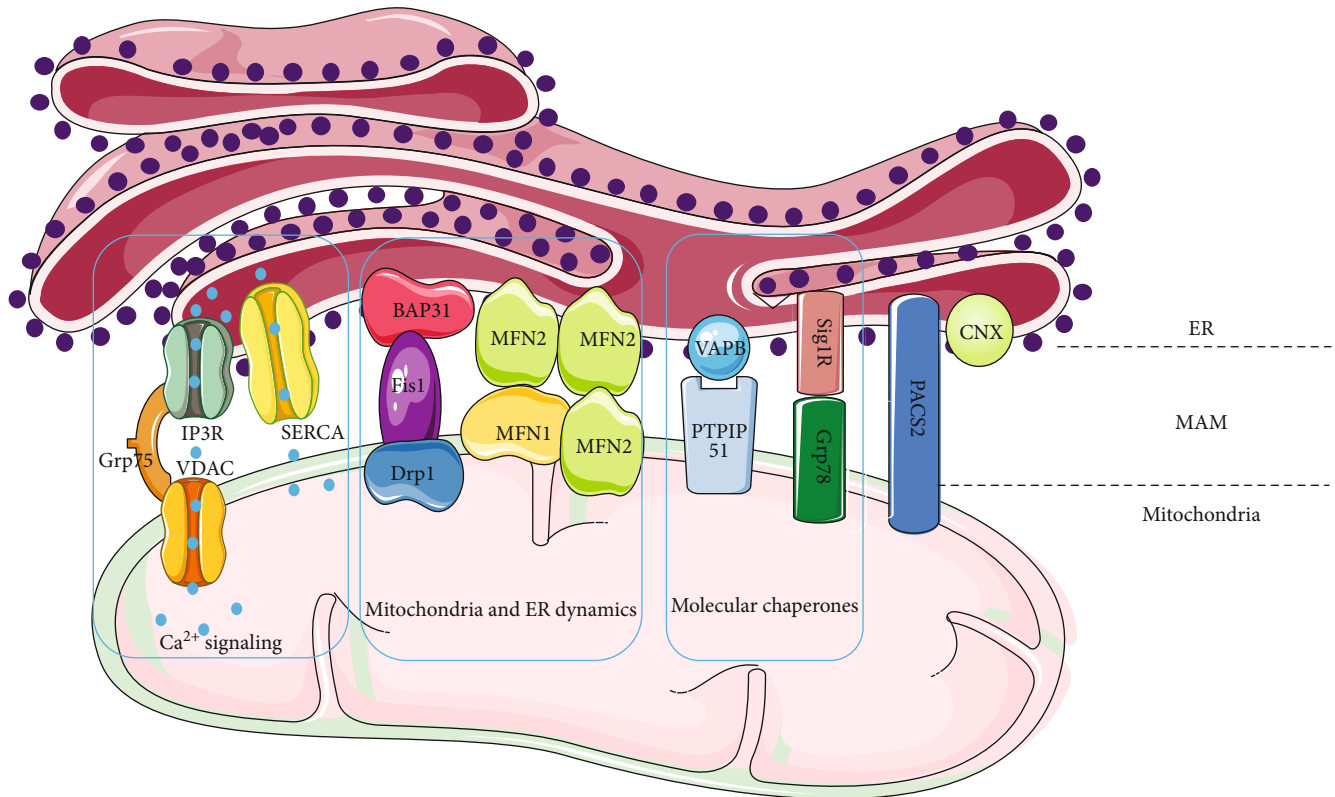


FIGURE 1: Convergence of signal transduction and metabolism at the MAM. The signal pathways that play the main biological functions on MAM including (1) calcium signaling (IP3R-Grp75-VDAC1 and SERCA- Ca^{2+}) maintain the homeostasis of intracellular Ca^{2+} and regulate the mitochondria and ER functions; (2) mitochondria and ER dynamics (MFNs and BAP31-Fis1-Drp1) regulate the fission and fusion of mitochondria thus regulating their functions; (3) MAM is the main place for the synthesis and transport of a variety of lipids; (4) molecular chaperones (VAPB-PTPIP51 and Sig1R-GRP78) participate in the secretion, folding, transport, and activation of proteins; (5) signal pathways such as PACS2-PSS1 can play other roles such as sorting and translocation.

mitochondrial fission and downstream degradation [38]. Studies have confirmed that in the receptor for advanced glycation end products (RAGE) mice, increased mitochondrial fragmentation and increased expression of mitochondrial fission proteins Drp1 and Fis1 may promote the clearance of damaged mitochondria, thereby attenuating vascular oxidative stress and atherosclerosis caused by high-fat diet [39]. In human aortic endothelial cells induced by high glucose, mitochondrial fragmentation increased, Fis1 and Drp1 expression increased, indicating that increased mitochondrial fission may impair endothelial function by increasing reactive oxygen species, causing the process of atherosclerosis [40].

2.3. Lipid Metabolism. ER is the main site of lipid biosynthesis, but the synthesis and transportation of many kinds of lipids need to be completed at this specific site—MAM. For example, the unique pathway of intracellular phospholipid transmembrane transport occurs on MAM; MAM may serve as a site for the synthesis of cholesterol and neutral lipids; steroid production basically depends on the shuttle between sterols and mitochondria; MAM can also be used as a transport route for ceramide from ER into mitochondria [41]. MAM strictly regulates lipid transport between the ER and mitochondria. Long-chain acyl-CoA synthase (ACSL4 or

FACLA) is a commonly used MAM marker. ACSL4 is located in MAM and plays an essential role in the regulation of mitochondrial fusion during cell steroid production [42]. Several enzymes related to cholesterol metabolism and transport have been found in MAM, including acetyl coenzyme A acetyltransferase 1 (ACAT1 or SOAT1) and acute regulatory proteins for steroid production (StAR) [43]. Caveolin-1 (Cav1) is an important regulator of cholesterol intracellular transport and membrane organization and is also identified as a key component of MAM. Loss of Cav1 gene in mice reduces the stability of ER mitochondrial contact sites and the accumulation of free cholesterol in MAM [44]. Macrophage cholesterol efflux capacity is dramatically reduced by inhibition of mitochondrial ATP synthase [45]. But how macrophage-derived foam cells control their energy metabolism is still unknown. The overexpression of StAR affects the lipid and inflammatory phenotypes of macrophages through cytochrome P450 27A1 (CYP27A1), liver X receptor β (LXR β) activation pathway and ATP-binding cassette transporter A1 (ABCA1/ABCG1) mRNA and protein induction pathway and promotes the efflux of cholesterol to apoA-I and/or high-density lipoprotein (HDL) [46, 47]. In addition, the injection of a viral vector expressing StAR into the tail vein of apoE (-/-) mice can reduce aortic lipids and atherosclerosis [48].

2.4. Molecular Chaperones

2.4.1. VAPB-PTPIP51. Vesicle-associated membrane protein-associated protein B (VAPB) is an ER protein enriched in MAM, and protein tyrosine phosphatase interacting protein 51 (PTPIP51) is known as an OMM protein [49, 50]. VAPB was shown to bind to PTPIP51 to form at least some of the MAM tethers [51]. Regulating the expression of VAPB or PTPIP51 affects the Ca^{2+} exchange between the ER and mitochondria [50, 51]. Knockdown of VAPB or PTPIP51 by small interfering RNA (siRNA) decreases, while overexpression significantly increases ER-mitochondrial contact [51, 52]. A study showed that loosening ER-mitochondria contacts via loss of VAPB or PTPIP51 induces whereas tightening contacts by overexpression of VAPB or PTPIP51 impairs basal autophagy [53]. Existing studies have not found that VAPB or PTPIP51 are directly related to the progression of atherosclerosis. Oxidative stress, ER stress, and autophagy in macrophages are important causes of macrophage apoptosis in late atherosclerotic lesions, which can promote plaque necrosis, thereby exacerbating acute atherosclerotic cardiovascular events [54, 55]. It can be expected that future studies may find that autophagy caused by VAPB or PTPIP51 may be related to atherosclerosis caused by macrophage autophagy.

2.4.2. Sig1R-Grp78. Sigma-1 receptor (Sig1R) is an ER molecular chaperone protein composed of 223 amino acids, which is highly expressed on MAM [56]. When the cell is stimulated by the outside, Sig1R can transfer from the ER to other parts of the cell. Sig1R is known to play an important role in many cellular activities such as ion channel activation, protein kinase A activation, neurotransmitter release, and inositol triphosphate receptor-mediated calcium transport from the ER to mitochondria [57]. The ER lumen and glucose regulatory protein 78/binding protein (Grp78 or BiP) is a member of the heat shock protein 70 family, a molecular chaperone and an ER stress sensor in MAM that aids in protein folding and secretion [58]. It folds the StAR transporting cholesterol for delivery to the OMM [59]. Under physiological conditions, Sig-1R forms a complex with Grp78 in MAM [60]. During ER stress, unfolded or misfolded proteins aggregate to dissociate and activate protein kinase R-like endoplasmic reticulum kinase (PERK), inositol-requiring enzyme 1 (IRE1), activating Transcription Factor 6 (ATF 6) and GRP78, which in turn triggers downstream signal transduction pathways [61, 62]. Unfold protein response (UPR) produces adaptive or proapoptotic responses based on the duration and/or intensity of stress [63]. The initial study showed that ER stress caused by increased Grp78 is related to the development of atherosclerotic lesions in apoE^{-/-} mice [64]. Anti-GRP78 autoantibodies induce endothelial cell activation and accelerate the development of atherosclerotic lesions by activating the NF- κ B pathway, thereby inducing the expression of intercellular cell adhesion molecule-1 (ICAM-1) and vascular cell adhesion molecule-1 (VCAM-1) [65]. Recently, ER stress has been introduced into clinical applications: circulating GRP78/BiP is used as a sign of metabolic diseases and atherosclerosis [66].

2.5. Other Functions

2.5.1. PACS2-PSS1. Phosphofurin acid cluster classification protein 2 (PACS2) is a multifunctional sorting protein which can interact with several cargo proteins and regulate their position in MAM [67]. PACS2 can transport Bim (Bcl-2-like protein 11) to lysosomes, participate in Ca^{2+} transfer from ER to mitochondria through IP3R positioning, and can also transport Bid (BH3 interaction domain) to mitochondria to control the induction of apoptosis [68, 69]. In mammalian cells, two different enzymes, phosphatidylserine synthase 1 (PSS1) and -2 (PSS2) in the MAM and the ER, perform de novo synthesis of phosphatidylserine (PS) [70]. Overexpression of PACS2 increased the level of PSS1 in MAM, indicating that PACS2 and PSS1 are functionally related [69]. A study found an increase in ER and mitochondria contacts as in PACS-2-associated MAMs upon stimulation with atherogenic lipids, while the disruption of MAM contacts by PACS-2 knockdown impaired mitophagosome formation and mitophagy, thus, potentiating VSMC apoptosis [23].

3. The MAM Hypothesis in the Pathophysiological Process of Atherosclerosis

3.1. The Role of MAM in the Development of Atherosclerosis Caused by Lipid Infiltration. On the one hand, LDL can penetrate the arterial intima and exhibit a strong atherosclerotic effect. On the other hand, LDL has a weak antioxidant effect. After entering the lipid-rich atherosclerotic plaque, it may further aggravate atherosclerosis. Researchers found that EC apoptosis induced by oxidized LDL (ox-LDL) is the initial step of atherosclerosis and is related to calcium overload [71]. The accumulation of Ox-LDL can increase cell apoptosis, accompanied by the increase of mitochondrial Ca^{2+} , the loss of mitochondrial membrane potential (MMP), the production of ROS, and the release of cytochrome c [71]. PACS2 plays an important role in ox-LDL-induced EC apoptosis by regulating the formation of MAM and the increase of mitochondrial Ca^{2+} , suggesting that PACS2 may be a promising target for atherosclerosis [71]. Recently, oxidized-LDL-mediated foamy macrophages were shown to exhibit an alternative mitochondrial metabolic switch from oxidative phosphorylation (OxPHOS) to superoxide production [72]. The content of MAM increases in atherosclerosis [23]. PACS2 has also been shown to be upregulated after atherosclerotic lipid load in VSMC [23].

3.2. The Role of MAM in the Development of Atherosclerosis Caused by Changes in VSMCs. The proliferation and migration of vascular SMCs (VSMCs) are one of the causes of atherosclerosis. VSMCs are the main cell type in all stages of atherosclerotic plaque. According to the “response to injury” and “vulnerable plaque” hypotheses, contractile VSMCs recruited from the media undergo phenotypic conversion to proliferative synthetic cells that generate extracellular matrix to form the fibrous cap and hence stabilize plaques [73]. The first important components that contribute to arterial stiffening are VSMCs, which not only regulate

actomyosin interactions for contraction but mediate also mechanotransduction in cell-extracellular matrix (ECM) homeostasis [74]. Excessive saturated fatty acids have a damaging effect on VSMCs. A study proved that saturated fatty acids synthesized by the reaction of glycerol-3-phosphate acyltransferase 4 (GPAT4) at the contact site of ω and MAM can significantly inhibit the autophagic flux in VSMCs, thereby contributing to vascular calcification and apoptosis [75]. VSMC apoptosis accelerates atherogenesis and the progression of advanced lesions, leading to atherosclerotic plaque vulnerability and medial degeneration, suggesting MAM may be a new target to modulate VSMC fate and favor atherosclerotic plaque stability [23]. In addition, knocking out NgBR can cause MAM destruction and increase the phosphorylation of IPR3 through pAkt, is accompanied by mitochondrial dysfunction, including decreased Ca^{2+} respiration and mitochondrial superoxide, and increased mitochondrial membrane potential and HIF-1 α nuclear localization, indicating that the dysregulation of NgBR promotes VSMC proliferation through the destruction of MAM and the increase of IPR3 phosphorylation, thereby contributing to reduce Ca^{2+} and mitochondrial damage [76].

3.3. The Role of MAM in the Development of Atherosclerosis Caused by Inflammation. Atherosclerosis is a chronic inflammation of the blood vessel wall. Inflammation is not only involved in the process of atherosclerosis but also causes complications such as thrombus and plaque rupture. Constituents of ox-LDL particles may induce inflammation and furnish neo-epitopes that stimulate humoral and adaptive immunity [77]. Many risk factors for atherosclerosis are involved in the activation of inflammatory pathways. In turn, inflammation can also change the function of arterial wall cells by driving atherosclerosis. These extravascular sites of inflammation can affect distant artery walls, as they release soluble inflammatory mediators such as cytokines that can activate cells in the intima [78, 79]. In macrophages from patients with atherosclerosis, mitochondria consumed more oxygen, generated more ATP, and built tight interorganelle connections with the ER, forming MAM [80]. The transfer of calcium through the MAM site continues to cause mitochondria to be overactive and depends on the inactivation of glycogen synthase kinase 3b (GSK3b), which controls the inflow of mitochondrial fuel, and therefore, represents a potential therapeutic target for anti-inflammatory therapy [80]. MAMs play a critical role in initiating inflammation by acting as an inflammatory platform [81]. The destruction of MAM in ECs attenuates mitochondrial damage, apoptosis, and inflammation and increases the release of NO [82]. Endothelial Drp1 silencing can prevent leukocyte adhesion and proinflammatory proteome induction, indicating that there may be cross-communication between typical inflammatory pathways and mitochondrial fission [83].

3.4. The Role of MAM in the Development of Atherosclerosis Caused by EC Injury. In a healthy state, when the lining of vascular endothelial cells is intact, SMCs can protect arteries from atherosclerosis and reduce endothelial inflammation; but when the lining of endothelial cells is damaged, changes

in shear stress may directly affect the function of SMCs [84]. Under multiple overstimulations such as vascular shear stress, blood pressure, and cell mechanics, vascular endothelial cells induce endothelial cell proliferation or death by generating the degree of cytoskeleton deformation and reorganization allowed by the geometric shape of its environment [85, 86]. The injured endothelial cells secrete growth factors such as monocyte chemoattractant protein 1 (MCP1), platelet-derived growth factor (PDGF), and transforming growth factor β (TGF- β) and continuously ingest the lipids that enter the inner membrane and undergo oxidation to form foam cells. Downregulation of adipocyte PPAR γ can activate ER stress through the TLR4 pathway to upregulate the expression and secretion of the MCP1 gene, leading to enhanced chemotaxis of macrophages [87]. In atherosclerosis, pretreatment with tunicamycin (Tm), an ER stress inducer, significantly inhibited platelet-derived growth factor- (PDGF-) BB-induced VSMC proliferation and migration in a dose-dependent manner without causing significant apoptosis [88].

4. Conclusions

A large number of existing studies have described the structure and function of MAMs. MAM dysfunction has also received increasing attention from researchers on the occurrence and development of atherosclerosis. Any disturbance of calcium signaling, mitochondrial and ER dynamics, lipid metabolism, and molecular chaperones are all involved in the process of atherosclerosis. Atherosclerosis causes many morbidities and deaths worldwide, including most myocardial infarctions and many strokes, as well as disabling peripheral artery disease. This review describes the structural and functional interaction between mitochondria and ER and explains the role of critical molecules in the structure of MAM during atherosclerosis. It is expected that researchers can use MAM as one of the effective targets for the treatment of atherosclerosis in the future.

Data Availability

All data included in this study are available upon request by contact with the corresponding author.

Conflicts of Interest

The authors declare that there are no commercial or financial conflicts of interest.

Acknowledgments

This work was supported by the National Natural Science Foundation of China (grant nos. 81870221 and 81670249).

References

- [1] P. Libby, J. E. Buring, L. Badimon et al., "Atherosclerosis," *Nature Reviews Disease Primers*, vol. 5, no. 1, 2019.
- [2] G. Franck, G. Even, A. Gautier et al., "Haemodynamic stress-induced breaches of the arterial intima trigger inflammation

- and drive atherogenesis,” *European Heart Journal*, vol. 40, no. 11, pp. 928–937, 2019.
- [3] G. L. Basatemur, H. F. Jørgensen, M. C. H. Clarke, M. R. Bennett, and Z. Mallat, “Vascular smooth muscle cells in atherosclerosis,” *Nature Reviews Cardiology*, vol. 16, no. 12, pp. 727–744, 2019.
 - [4] B. G. Childs, D. J. Baker, and E. Al, “Senescent intimal foam cells are deleterious at all stages of atherosclerosis.[J],” *Science*, vol. 354, no. 6311, pp. 468–472, 2016.
 - [5] J. F. Toussaint, G. M. LaMuraglia, J. F. Southern, V. Fuster, and H. L. Kantor, “Magnetic resonance images lipid, fibrous, calcified, hemorrhagic, and thrombotic components of human atherosclerosis in vivo,” *Circulation*, vol. 94, no. 5, pp. 932–938, 1996.
 - [6] B. A. Ference, H. N. Ginsberg, I. Graham et al., “Low-density lipoproteins cause atherosclerotic cardiovascular disease. 1. Evidence from genetic, epidemiologic, and clinical studies. A consensus statement from the European Atherosclerosis Society Consensus Panel,” *European Heart Journal*, vol. 38, no. 32, pp. 2459–2472, 2017.
 - [7] J. S. Pober, W. Min, and J. R. Bradley, “Mechanisms of endothelial dysfunction, injury, and death,” *Annual Review of Pathology*, vol. 4, no. 1, pp. 71–95, 2009.
 - [8] M. Bäck, A. Yurdagul Jr., I. Tabas, K. Öörni, and P. T. Kovanen, “Inflammation and its resolution in atherosclerosis: mediators and therapeutic opportunities,” *Nature Reviews Cardiology*, vol. 16, no. 7, pp. 389–406, 2019.
 - [9] A. P. Sage, D. Tsiantoulas, C. J. Binder, and Z. Mallat, “The role of B cells in atherosclerosis,” *Nature Reviews Cardiology*, vol. 16, no. 3, pp. 180–196, 2019.
 - [10] R. Saigusa, H. Winkels, and K. Ley, “T cell subsets and functions in atherosclerosis,” *Nature Reviews Cardiology*, vol. 17, no. 7, pp. 387–401, 2020.
 - [11] D. Tousoulis, E. Oikonomou, E. K. Economou, F. Crea, and J. C. Kaski, “Inflammatory cytokines in atherosclerosis: current therapeutic approaches,” *European Heart Journal*, vol. 37, no. 22, pp. 1723–1732, 2016.
 - [12] H. Pan, C. Xue, B. J. Auerbach et al., “Single-cell genomics reveals a novel cell state during smooth muscle cell phenotypic switching and potential therapeutic targets for atherosclerosis in mouse and human,” *Circulation*, vol. 142, no. 21, pp. 2060–2075, 2020.
 - [13] D. M. Herrington, C. Mao, S. J. Parker et al., “Proteomic architecture of human coronary and aortic atherosclerosis,” *Circulation*, vol. 137, no. 25, pp. 2741–2756, 2018.
 - [14] I. Tabas, “The role of endoplasmic reticulum stress in the progression of atherosclerosis,” *Circulation Research*, vol. 107, no. 7, pp. 839–850, 2010.
 - [15] D. C. Chan, “Mitochondria: dynamic organelles in disease, aging, and development [J],” *Cell*, vol. 125, no. 7, pp. 1241–1252, 2006.
 - [16] J. B. Spinelli and M. C. Haigis, “The multifaceted contributions of mitochondria to cellular metabolism,” *Nature Cell Biology*, vol. 20, no. 7, pp. 745–754, 2018.
 - [17] J. Groenendyk, L. B. Agellon, and M. Michalak, “Coping with endoplasmic reticulum stress in the cardiovascular system,” *Annual Review of Physiology*, vol. 75, no. 1, pp. 49–67, 2013.
 - [18] Y. Saheki and P. De Camilli, “Endoplasmic reticulum-plasma membrane contact sites,” *Annual Review of Biochemistry*, vol. 86, no. 1, pp. 659–684, 2017.
 - [19] A. A. Rowland and G. K. Voeltz, “Endoplasmic reticulum-mitochondria contacts: function of the junction,” *Nature Reviews Molecular Cell Biology*, vol. 13, no. 10, pp. 607–615, 2012.
 - [20] G. G. Dorighello, B. A. Paim, S. F. Kiihl et al., “Correlation between mitochondrial reactive oxygen and severity of atherosclerosis,” *Oxidative Medicine and Cellular Longevity*, vol. 2016, Article ID 7843685, 10 pages, 2016.
 - [21] S. M. Davidson and D. M. Yellon, “Mitochondrial DNA damage, oxidative stress, and atherosclerosis,” *Circulation*, vol. 128, no. 7, pp. 681–683, 2013.
 - [22] J. Ren, Y. Bi, J. R. Sowers, C. Hetz, and Y. Zhang, “Endoplasmic reticulum stress and unfolded protein response in cardiovascular diseases,” *Nature Reviews Cardiology*, vol. 18, no. 7, pp. 499–521, 2021.
 - [23] M. Moulis, E. Grousset, J. Faccini, K. Richetin, G. Thomas, and C. Vindis, “The multifunctional sorting protein PACS-2 controls mitophagosome formation in human vascular smooth muscle cells through mitochondria-ER contact sites,” *Cells*, vol. 8, no. 6, p. 638, 2019.
 - [24] G. Szabadkai, K. Bianchi, P. Várnai et al., “Chaperone-mediated coupling of endoplasmic reticulum and mitochondrial Ca²⁺ channels,” *The Journal of Cell Biology*, vol. 175, no. 6, pp. 901–911, 2006.
 - [25] W. Y. Chen, Y. F. Chen, H. C. Chan et al., “Role of apolipoprotein E in electronegative low-density lipoprotein-induced mitochondrial dysfunction in cardiomyocytes,” *Metabolism*, vol. 107, p. 154227, 2020.
 - [26] M. Kockx, D. L. Guo, T. Huby et al., “Secretion of apolipoprotein E from macrophages occurs via a protein kinase A- and calcium-dependent pathway along the microtubule network,” *Circulation Research*, vol. 101, no. 6, pp. 607–616, 2007.
 - [27] M. Brini and E. Carafoli, “Calcium pumps in health and disease,” *Physiological Reviews*, vol. 89, no. 4, pp. 1341–1378, 2009.
 - [28] E. Carafoli, “Calcium-mediated cellular signals: a story of failures,” *Trends in Biochemical Sciences*, vol. 29, no. 7, pp. 371–379, 2004.
 - [29] Y. Dong, M. Zhang, B. Liang et al., “Reduction of AMP-activated protein kinase $\alpha 2$ increases endoplasmic reticulum stress and atherosclerosis in vivo,” *Circulation*, vol. 121, no. 6, pp. 792–803, 2010.
 - [30] S. Gao and J. Hu, “Mitochondrial fusion: the machineries in and out,” *Trends in Cell Biology*, vol. 31, no. 1, pp. 62–74, 2021.
 - [31] N. Ishihara, Y. Eura, and K. Mihara, “Mitofusin 1 and 2 play distinct roles in mitochondrial fusion reactions via GTPase activity,” *Journal of Cell Science*, vol. 117, no. 26, pp. 6535–6546, 2004.
 - [32] G. W. Dorn, “Mitofusins as mitochondrial anchors and tethers,” *Journal of Molecular and Cellular Cardiology*, vol. 142, pp. 146–153, 2020.
 - [33] G. Csordas, D. Weaver, and G. Hajnoczky, “Endoplasmic reticulum-mitochondrial contactology: structure and signaling functions,” *Trends in Cell Biology*, vol. 28, no. 7, pp. 523–540, 2018.
 - [34] I. Gordaliza-Alaguero, C. Canto, and A. Zorzano, “Metabolic implications of organelle-mitochondria communication,” *EMBO Reports*, vol. 20, no. 9, article e47928, 2019.
 - [35] S. H. Choi, C. Agatista-Boyle, A. Gonen et al., “Intracellular AIBP (Apolipoprotein A-I Binding Protein) Regulates Oxidized LDL (Low-Density Lipoprotein)-Induced Mitophagy in

- Macrophages,” *Arteriosclerosis, Thrombosis, and Vascular Biology*, vol. 41, no. 2, pp. e82–e96, 2021.
- [36] J. Wang, H. Chen, Y. Liu, W. Zhou, R. Sun, and M. Xia, “Retinol binding protein 4 induces mitochondrial dysfunction and vascular oxidative damage,” *Atherosclerosis*, vol. 240, no. 2, pp. 335–344, 2015.
- [37] A. Pagliuso, P. Cossart, and F. Stavru, “The ever-growing complexity of the mitochondrial fission machinery,” *Cellular and Molecular Life Sciences*, vol. 75, no. 3, pp. 355–374, 2018.
- [38] Q. Shen, K. Yamano, B. P. Head et al., “Mutations in Fis1 disrupt orderly disposal of defective mitochondria,” *Molecular Biology of the Cell*, vol. 25, no. 1, pp. 145–159, 2014.
- [39] Y. Yu, L. Wang, F. Delguste et al., “Advanced glycation end products receptor RAGE controls myocardial dysfunction and oxidative stress in high-fat fed mice by sustaining mitochondrial dynamics and autophagy-lysosome pathway,” *Free Radical Biology & Medicine*, vol. 112, pp. 397–410, 2017.
- [40] S. M. Shenouda, M. E. Widlansky, K. Chen et al., “Altered mitochondrial dynamics contributes to endothelial dysfunction in diabetes mellitus,” *Circulation*, vol. 124, no. 4, pp. 444–453, 2011.
- [41] T. Hayashi, R. Rizzuto, G. Hajnoczky, and T. P. Su, “MAM: more than just a housekeeper,” *Trends in Cell Biology*, vol. 19, no. 2, pp. 81–88, 2009.
- [42] C. Poderoso, A. Duarte, M. Cooke et al., “The spatial and temporal regulation of the hormonal signal. Role of mitochondria in the formation of a protein complex required for the activation of cholesterol transport and steroids synthesis,” *Molecular and Cellular Endocrinology*, vol. 371, no. 1–2, pp. 26–33, 2013.
- [43] M. Prasad, J. Kaur, K. J. Pawlak, M. Bose, R. M. Whittal, and H. S. Bose, “Mitochondria-associated endoplasmic reticulum membrane (MAM) regulates steroidogenic activity via steroidogenic acute regulatory protein (StAR)-voltage-dependent anion channel 2 (VDAC2) interaction*,” *The Journal of Biological Chemistry*, vol. 290, no. 5, pp. 2604–2616, 2015.
- [44] A. Sala-Vila, I. Navarro-Lérida, M. Sánchez-Alvarez et al., “Interplay between hepatic mitochondria-associated membranes, lipid metabolism and caveolin-1 in mice,” *Scientific Reports*, vol. 6, no. 1, 2016.
- [45] D. Castano, C. Rattanasopa, V. F. Monteiro-Cardoso et al., “Lipid efflux mechanisms, relation to disease and potential therapeutic aspects,” *Advanced Drug Delivery Reviews*, vol. 159, pp. 54–93, 2020.
- [46] J. M. Taylor, F. Borthwick, C. Bartholomew, and A. Graham, “Overexpression of steroidogenic acute regulatory protein increases macrophage cholesterol efflux to apolipoprotein AI,” *Cardiovascular Research*, vol. 86, no. 3, pp. 526–534, 2010.
- [47] Q. Bai, X. Li, Y. Ning, F. Zhao, and L. Yin, “Mitochondrial cholesterol transporter, StAR, inhibits human THP-1 monocyte-derived macrophage apoptosis,” *Lipids*, vol. 45, no. 1, pp. 29–36, 2010.
- [48] Y. Ning, L. Xu, S. Ren, W. M. Pandak, S. Chen, and L. Yin, “StAR overexpression decreases serum and tissue lipids in apolipoprotein E-deficient mice,” *Lipids*, vol. 44, no. 6, pp. 511–519, 2009.
- [49] S. Paillusson, R. Stoica, P. Gomez-Suaga et al., “There’s something wrong with my MAM; the ER-mitochondria axis and neurodegenerative diseases,” *Trends in Neurosciences*, vol. 39, no. 3, pp. 146–157, 2016.
- [50] K. J. de Vos, G. M. Mórotz, R. Stoica et al., “VAPB interacts with the mitochondrial protein PTPIP51 to regulate calcium homeostasis,” *Human Molecular Genetics*, vol. 21, no. 6, pp. 1299–1311, 2012.
- [51] R. Stoica, K. J. de Vos, S. Paillusson et al., “ER-mitochondria associations are regulated by the VAPB-PTPIP51 interaction and are disrupted by ALS/FTD-associated TDP-43,” *Nature Communications*, vol. 5, no. 1, 2014.
- [52] R. Galmes, A. Houcine, A. R. Vliet, P. Agostinis, C. L. Jackson, and F. Giordano, “ORP5/ORP8 localize to endoplasmic reticulum-mitochondria contacts and are involved in mitochondrial function,” *EMBO Reports*, vol. 17, no. 6, pp. 800–810, 2016.
- [53] P. Gomez-Suaga, S. Paillusson, R. Stoica, W. Noble, D. P. Hanger, and C. C. J. Miller, “The ER-mitochondria tethering complex VAPB-PTPIP51 regulates autophagy,” *Current Biology*, vol. 27, no. 3, pp. 371–385, 2017.
- [54] X. Liao, J. C. Sluimer, Y. Wang et al., “Macrophage autophagy plays a protective role in advanced atherosclerosis,” *Cell Metabolism*, vol. 15, no. 4, pp. 545–553, 2012.
- [55] K. J. Moore and I. Tabas, “Macrophages in the pathogenesis of atherosclerosis,” *Cell*, vol. 145, no. 3, pp. 341–355, 2011.
- [56] B. S. Hellewell, A. Bruce, G. Feinstein, J. Orringer, W. Williams, and W. D. Bowen, “Rat liver and kidney contain high densities of σ_1 and σ_2 receptors: characterization by ligand binding and photoaffinity labeling,” *European Journal of Pharmacology: Molecular Pharmacology*, vol. 268, no. 1, pp. 9–18, 1994.
- [57] H. R. Schmidt and A. C. Kruse, “The molecular function of σ receptors: past, present, and future,” *Trends in Pharmacological Sciences*, vol. 40, no. 9, pp. 636–654, 2019.
- [58] M. S. Gorbatyuk and O. S. Gorbatyuk, “The molecular chaperone GRP78/BiP as a therapeutic target for neurodegenerative disorders: a mini review,” *Journal of Genetic Syndromes & Gene Therapy*, vol. 4, no. 2, 2013.
- [59] M. Prasad, K. J. Pawlak, W. E. Burak et al., “Mitochondrial metabolic regulation by GRP78,” *Science Advances*, vol. 3, no. 2, p. e1602038, 2017.
- [60] T. Hayashi and T. P. Su, “Sigma-1 receptor chaperones at the ER-mitochondrion interface regulate Ca^{2+} signaling and cell survival,” *Cell*, vol. 131, no. 3, pp. 596–610, 2007.
- [61] A. K. Mishra, T. Mavlyutov, D. R. Singh et al., “The sigma-1 receptors are present in monomeric and oligomeric forms in living cells in the presence and absence of ligands,” *The Biochemical Journal*, vol. 466, no. 2, pp. 263–271, 2015.
- [62] H. Tagashira, M. S. Bhuiyan, and K. Fukunaga, “Diverse regulation of IP3 and ryanodine receptors by pentazocine through σ_1 -receptor in cardiomyocytes,” *American Journal of Physiology. Heart and Circulatory Physiology*, vol. 305, no. 8, pp. H1201–H1212, 2013.
- [63] C. Hetz and F. R. Papa, “The unfolded protein response and cell fate control,” *Molecular Cell*, vol. 69, no. 2, pp. 169–181, 2018.
- [64] J. Zhou, G. H. Werstuck, S. Lhoták et al., “Association of multiple cellular stress pathways with accelerated atherosclerosis in hyperhomocysteinemic apolipoprotein E-deficient mice,” *Circulation*, vol. 110, no. 2, pp. 207–213, 2004.
- [65] E. D. Crane, A. A. al-Hashimi, J. Chen et al., “Anti-GRP78 autoantibodies induce endothelial cell activation and accelerate the development of atherosclerotic lesions,” *JCI Insight*, vol. 3, no. 24, 2018.
- [66] J. Girona, C. Rodríguez-Borjabad, D. Ibarretxe et al., “The circulating GRP78/BiP is a marker of metabolic diseases and

- atherosclerosis: bringing endoplasmic reticulum stress into the clinical scenario," *Journal of Clinical Medicine*, vol. 8, no. 11, p. 1793, 2019.
- [67] C. Li, L. Li, M. Yang, L. Zeng, and L. Sun, "PACS-2: a key regulator of mitochondria-associated membranes (MAMs)," *Pharmacological Research*, vol. 160, p. 105080, 2020.
- [68] N. W. Werneburg, S. F. Bronk, M. E. Guicciardi et al., "Tumor necrosis factor-related apoptosis-inducing ligand (TRAIL) protein-induced lysosomal translocation of proapoptotic effectors is mediated by phosphofurin acidic cluster sorting protein-2 (PACS-2)*," *The Journal of Biological Chemistry*, vol. 287, no. 29, pp. 24427–24437, 2012.
- [69] T. Simmen, J. E. Aslan, A. D. Blagoveshchenskaya et al., "PACS-2 controls endoplasmic reticulum-mitochondria communication and bid-mediated apoptosis," *The EMBO Journal*, vol. 24, no. 4, pp. 717–729, 2005.
- [70] A. K. Kimura and T. Kimura, "Phosphatidylserine biosynthesis pathways in lipid homeostasis: toward resolution of the pending central issue for decades," *The FASEB Journal*, vol. 35, no. 1, article e21177, 2021.
- [71] S. Yu, L. Zhang, C. Liu, J. Yang, J. Zhang, and L. Huang, "PACS2 is required for ox-LDL-induced endothelial cell apoptosis by regulating mitochondria-associated ER membrane formation and mitochondrial Ca²⁺ elevation," *Experimental Cell Research*, vol. 379, no. 2, pp. 191–202, 2019.
- [72] Y. Chen, M. Yang, W. Huang et al., "Mitochondrial metabolic reprogramming by CD36 signaling drives macrophage inflammatory responses," *Circulation Research*, vol. 125, no. 12, pp. 1087–1102, 2019.
- [73] M. R. Bennett, S. Sinha, and G. K. Owens, "Vascular smooth muscle cells in atherosclerosis," *Circulation Research*, vol. 118, no. 4, pp. 692–702, 2016.
- [74] P. Lacolley, V. Regnault, P. Segers, and S. Laurent, "Vascular smooth muscle cells and arterial stiffening: relevance in development, aging, and disease," *Physiological Reviews*, vol. 97, no. 4, pp. 1555–1617, 2017.
- [75] Y. Shiozaki, S. Miyazaki-Anzai, K. Okamura, A. L. Keenan, M. Masuda, and M. Miyazaki, "GPAT4-generated saturated LPAs induce lipotoxicity through inhibition of autophagy by abnormal formation of omegasomes," *iScience*, vol. 23, no. 5, p. 101105, 2020.
- [76] Y. D. Yang, M. M. Li, G. Xu et al., "Nogo-B receptor directs mitochondria-associated membranes to regulate vascular smooth muscle cell proliferation," *International Journal of Molecular Sciences*, vol. 20, no. 9, p. 2319, 2019.
- [77] A. Gistera and G. K. Hansson, "The immunology of atherosclerosis," *Nature Reviews. Nephrology*, vol. 13, no. 6, pp. 368–380, 2017.
- [78] P. Libby, M. Nahrendorf, and F. K. Swirski, "Leukocytes link local and systemic inflammation in ischemic cardiovascular disease: an expanded "cardiovascular continuum"," *Journal of the American College of Cardiology*, vol. 67, no. 9, pp. 1091–1103, 2016.
- [79] P. Libby, J. Loscalzo, P. M. Ridker et al., "Inflammation, immunity, and infection in atherothrombosis," *Journal of the American College of Cardiology*, vol. 72, no. 17, pp. 2071–2081, 2018.
- [80] M. Zeisbrich, R. E. Yanes, H. Zhang et al., "Hypermetabolic macrophages in rheumatoid arthritis and coronary artery disease due to glycogen synthase kinase 3b inactivation," *Annals of the Rheumatic Diseases*, vol. 77, no. 7, pp. 1053–1062, 2018.
- [81] P. Gao, Z. Yan, and Z. Zhu, "Mitochondria-associated endoplasmic reticulum membranes in cardiovascular diseases," *Frontiers in Cell and Development Biology*, vol. 8, p. 604240, 2020.
- [82] Y. D. Yang, M. M. Li, G. Xu et al., "Targeting mitochondria-associated membranes as a potential therapy against endothelial injury induced by hypoxia," *Journal of Cellular Biochemistry*, vol. 120, no. 11, pp. 18967–18978, 2019.
- [83] S. J. Forrester, K. J. Preston, H. A. Cooper et al., "Mitochondrial fission mediates endothelial inflammation," *Hypertension*, vol. 76, no. 1, pp. 267–276, 2020.
- [84] Z. Ding, N. V. K. Pothineni, A. Goel, T. F. Luscher, and J. L. Mehta, "PCSK9 and inflammation: role of shear stress, pro-inflammatory cytokines, and LOX-1," *Cardiovascular Research*, vol. 116, no. 5, pp. 908–915, 2020.
- [85] G. Garoffolo and M. Pesce, "Mechanotransduction in the cardiovascular system: from developmental origins to homeostasis and pathology," *Cell*, vol. 8, no. 12, p. 1607, 2019.
- [86] C. S. Chen, M. Mrksich, S. Huang, G. M. Whitesides, and D. E. Ingber, "Geometric control of cell life and death," *Science*, vol. 276, no. 5317, pp. 1425–1428, 1997.
- [87] M. T. Nguyen, A. Chen, W. J. Lu et al., "Regulation of chemokine and chemokine receptor expression by PPAR γ in adipocytes and macrophages," *PLoS One*, vol. 7, no. 4, article e34976, 2012.
- [88] N. Yi, S. Y. Chen, A. Ma et al., "Tunicamycin inhibits PDGF-BB-induced proliferation and migration of vascular smooth muscle cells through induction of HO-1," *Anat Rec (Hoboken)*, vol. 295, no. 9, pp. 1462–1472, 2012.

Research Article

Protective Effect of Mitochondrial ND2 C5178A Gene Mutation on Cell and Mitochondrial Functions

Liuyang Tian ^{1,2} Chao Zhu,^{2,3} Huanwan Yang,² Yang Li,² and Yuqi Liu ^{2,4,5,6}

¹School of Medicine, Nankai University, Tianjin 300071, China

²Cardiac Department, The Institute of Geriatric Cardiology PLA General Hospital, Beijing 100853, China

³Department of Cardiology, Beijing Friendship Hospital, Capital Medical University, Beijing 100050, China

⁴Department of Cardiology & National Clinical Research Center of Geriatrics Disease, Chinese PLA General Hospital, Beijing 100853, China

⁵Beijing Key Laboratory of Chronic Heart Failure Precision Medicine, Chinese PLA General Hospital, Beijing 100853, China

⁶National Key Laboratory of Kidney Diseases, Chinese PLA General Hospital, Beijing 100853, China

Correspondence should be addressed to Yuqi Liu; ametuof980869@163.com

Received 8 April 2021; Revised 15 June 2021; Accepted 26 June 2021; Published 20 July 2021

Academic Editor: Ana Lloret

Copyright © 2021 Liuyang Tian et al. This is an open access article distributed under the Creative Commons Attribution License, which permits unrestricted use, distribution, and reproduction in any medium, provided the original work is properly cited.

Background. Mitochondrial NADH dehydrogenase subunit 2 (MT-ND2) m. 5178C>A gene mutation has protective effects against various diseases, but the molecular mechanism is still unclear. In previous study, we found a heteroplasmy level of MT-ND2 m. 5178C>A mutation in normotensive controls. Peripheral blood samples were obtained from essential hypertension individuals carrying the mutation and healthy controls without gene mutation to establish immortalized lymphocyte lines. To investigate the effect of the MT-ND2 m. 5178C>A gene mutation, comparative analyses of the two group cell lines were performed, including measurements of cell proliferation, viability, ATP synthesis, mitochondrial oxidative stress, and oxidative phosphorylation. **Results.** The cell proliferation rate and viability of the MT-ND2 m. 5178C>A mutant lymphocyte line were higher than those of the control group. Mitochondrial functions of the MT-ND2 m. 5178C>A mutant lymphocyte were increased, including increased ATP synthesis, decreased ROS production, increased mitochondrial membrane potential and Bcl-2 gene transcription and protein translation, decreased Caspase 3/7 activity, and decreased early apoptosis and late apoptosis. The oxygen consumption rate (OCR) of the mutant lymphocyte line was higher than that of the control group, including basal OCR, ATP-linked OCR, maximal OCR, proton leak OCR, and reserve OCR, and there was no significant difference in nonmitochondrial OCR. The activity of Mitochondrial Complex I of the mutant group was increased than that of the control group. **Conclusions.** The MT-ND2 m. 5178C>A mutation is a protective mutation that may be related to improvement of mitochondrial functions and decrease in apoptosis.

1. Background

Mitochondrial DNA (mtDNA) mutations have been reported in many diseases such as Leber hereditary optic neuropathy [1], maternally inherited deafness, aminoglycoside-induced Deafness [2], mitochondrial encephalomyopathy, lactic acidosis, and stroke-like episodes [3]. Mitochondria are the main site of oxidative phosphorylation (OXPHOS) in eukaryotic cells. Each cell contains 100 to 1000 mitochondria, each containing an independently encoded double-stranded circular

DNA. Human (mammalian) mtDNA has 16 569 base pairs with 37 coding genes, including 22 mitochondrial transport RNA (tRNA) genes, two ribosomal RNA (12r RNA and 16r RNA) genes, and 13 peptides associated with the OXPHOS respiratory chain complex [4]. Mitochondrial dysfunction has been proved to be associated with many common human diseases, including diabetes, coronary heart disease, and cancer; neurodegenerative changes; and aging [5] OXPHOS contains approximately 90 proteins, and there is a close association between genes that transcribe and translate

OXPPOS-related proteins, including nuclear and mitochondrial genes, to maintain and regulate the metabolic processes [6]. Further research found that the gene defect encoding OXPPOS protein directly leads to impaired OXPPOS function, further leading to a series of problems such as metabolic disorders, and is one of the important causes of various diseases [7]. In our previous study, we found that there is a heteroplasmy level of m. 5178C>A mutation between essential hypertension (EH) and normotensive controls. The heteroplasmy level of MT-ND2 m. 5178C>A in EH patients is much lower than that in control subjects. The MT-ND2 m. 5178C>A polymorphism of NADH dehydrogenase subunit 2 (ND2) 237Leu/Met was first reported to be associated with longevity [8]. Recently, the MT-ND2 m. 5178C>A mutation has been found to have protective effects in a variety of diseases such as myocardial infarction [9], cerebrovascular disease [10], type 2 diabetes [11], and atherosclerosis [12]. However, the mechanism of how MT-ND2 m. 5178C>A mutation associated with lots of diseases has not been elucidated. Therefore, we enrolled five cases from the EH group without MT-ND2 m. 5178C>A gene mutation and control groups with m. 5178C>A gene mutation. The gender, age, body mass index, and laboratory indexes were matched in two groups. Lymphoblastoid cell lines were immortalized by transformation with Epstein-Barr virus from the peripheral whole blood of each participant. Then, we investigated the mechanisms of the MT-ND2 m. 5178C>A gene mutation in cell and mitochondrial functions of lymphocyte lines to explain the protective effect of MT-ND2 m. 5178C>A gene mutation in the mechanism against EH.

2. Results

2.1. Clinical Characteristics. Basic clinical characteristics were compared between mutant and control groups. Triglyceride, SBP, and DBP were lower in the mutant group than in the control group (Table 1).

2.2. Lymphocyte Line Viability and Proliferation. Mitochondrial gene sequence analyses revealed that the mutation group carried the MT-ND2 m. 5178C>A gene mutation (Figure 1(a)). A previous study showed that this site mutation leads to amino acid substitution in the ND2-encoding gene from leucine (Leu) to methionine (Met) [8].

To further investigate whether ND2 gene mutations affect cell proliferation, we used the Epstein-Barr virus to infect lymphocytes. Figure 1(b) shows the proliferation of the two groups after infection. The nucleuses of the mutant lymphocytes were more obvious under high magnification, and the cell membrane boundaries were blurry (Figure 1(b)). Proliferation of the mutant group was significantly higher than that of the control group (34.67 ± 4.16 vs. 20.67 ± 3.06 , $P = 0.009$, Figure 1(c)).

2.3. Lymphocyte Line Proliferation. CCK-8 was used to compare the cell viability of mutant and nonmutated lymphocyte lines. Luciferin, the nonluminescent peptide, was transferred to luminescent luciferase and ATP under the action of Caspase 3/7, and the value of Caspase 3/7 is recorded by a Centro LB90 microplate luminometer. The activities of the mutant

TABLE 1: The clinical characteristics compared between the mutant and control groups.

Variables	mt5178C (n = 5)	mt5178A (n = 5)	P value
Age (years)	55.3 ± 3.2	54.6 ± 3.1	0.734
Male, n (%)	4 (80.0)	4 (80.0)	1
BMI (kg/m ²)	26.2 ± 3.5	24.1 ± 2.5	0.306
Smoking, n (%)	3 (60.0)	3 (60.0)	1
Drinking, n (%)	2 (40.0)	3 (60.0)	0.655
TC (mmol/L)	4.73 ± 0.63	4.27 ± 0.42	0.214
Triglyceride (mmol/L)	1.79 ± 0.14	1.18 ± 0.43	0.016*
LDL (mmol/L)	2.75 ± 0.36	2.51 ± 0.17	0.214
HDL (mmol/L)	1.17 ± 0.36	1.28 ± 0.23	0.581
Creatinine (μmol/L)	82.91 ± 8.92	76.19 ± 9.42	0.280
BUN (μmol/L)	5.29 ± 0.14	4.42 ± 0.16	0.051
SBP (mmHg)	148.00 ± 14.00	115.00 ± 7.00	0.015*
DBP (mmHg)	87.00 ± 7.00	76.00 ± 4.00	0.015*

BMI: body mass index; TC: total cholesterol; LDL: low-density lipoprotein; HDL: high-density lipoprotein; BUN: blood urea nitrogen; SBP: systolic blood pressure; DBP: diastolic blood pressure. * indicates $P < 0.05$.

cells and control group were linearly related to the number of cells. At the same cell number, the activity of the mutant group was higher than that of the control group ($P < 0.05$, Figure 1(d)).

2.4. Lymphocyte Line ATP Synthesis. Mitochondria are a cell's powerpacks. To determine whether mitochondrial gene mutation affects the ability of oxidative phosphorylation (OXPPOS) to synthesize ATP, we measured ATP production by a luciferin/luciferase luminescence assay. There was a linear correlation between ATP production and the cell number in both mutant and control cell lines. ATP production of the mutant cells was significantly higher than that of the control group ($P < 0.05$, Figure 2(a)).

2.5. Lymphocyte Line ROS Synthesis. Mitochondrial oxidative stress damage is the most important mechanisms of which mitochondria regulate cell apoptosis. In our study, we measure the intracellular ROS production through fluorescent probe DCFH-DA. The ROS production in the mutant cell line was significantly lower than that in the control cell line (39 ± 13.79 vs. 112.66 ± 23.13 , $P = 0.001$, Figure 2(b)).

2.6. Mitochondrial Membrane Potential. Mitochondrial membrane potential ($\Delta\Psi_m$) means the proton electrochemical gradient of mitochondrial membrane, which is reflective of the functional metabolic status of mitochondria [13]. This assay uses the ratio of red/green fluorescence of JC-10 Ex/Em = 540/590 and 490/525 nm (FL590/FL525) to reflect $\Delta\Psi_m$. The $\Delta\Psi_m$ value of the mutant cell line was significantly higher than that of the control group (0.0587 ± 0.0187 vs. 0.0469 ± 0.0165 , $P = 0.001$, Figure 2(c)).

2.7. Apoptosis Protein Caspase 3/7 Activity. Another important function of mitochondria is to regulate cell apoptosis

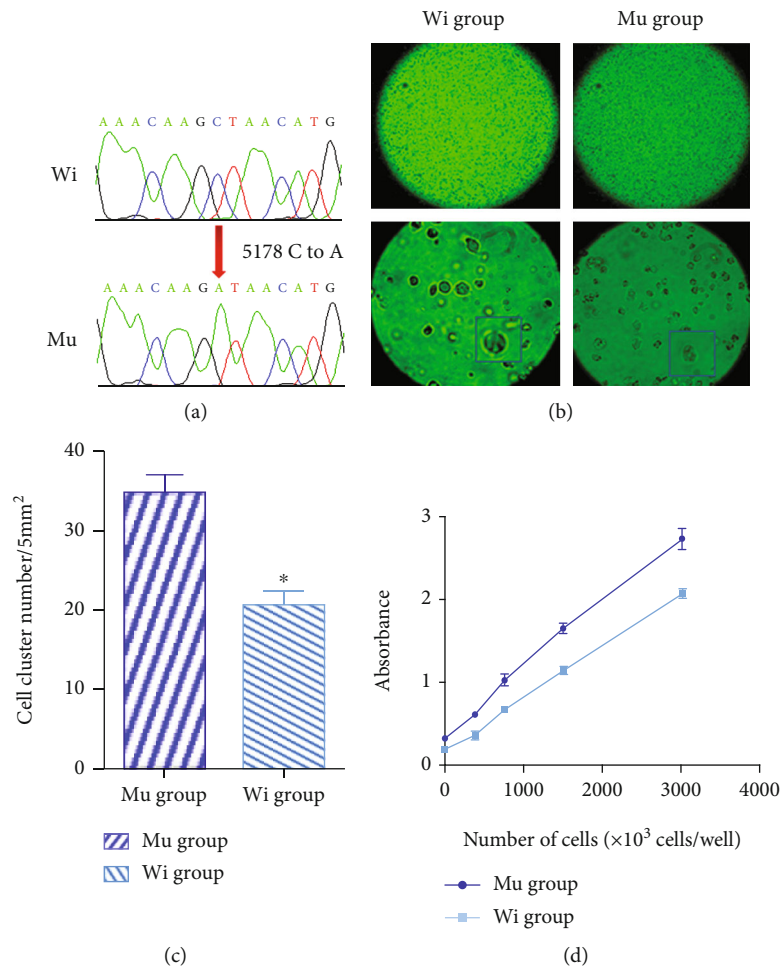


FIGURE 1: Cell activity and proliferation. (a) Partial sequence chromatograms with mutation at the ND2 5718 site. (b) The proliferation of the two groups of immortalized lymphocyte lines. (c) Comparison of cell proliferation in mutant and control cell lines. Proliferation of the mutant group was significantly higher than that of the control group. (d) Comparison of cell activity in mutant and control cell lines. CCK-8 was used to compare the cell viability of mutant and nonmutated lymphocyte lines. At the same cell number, the activity of the mutant group was higher than that of the control group. (* $P < 0.05$).

[14]. Caspase 3/7 is a specific molecular marker of apoptosis [15]. There was a linear correlation between Caspase 3/7 expression and the cell number in both mutant and control cells. At the same cell number, the expression level of Caspase 3/7 in the mutant group was significantly lower than that in the control group ($P < 0.05$, Figure 3(a)).

2.8. The Expression of Proliferation and Apoptosis Genes and Proteins. To evaluate the mechanism implicated in the MT-ND2 m. 5178C>A gene mutation decreased apoptosis, we measured the genes of apoptotic signal pathway through transcription and the protein expression. The mutant group showed increased Bcl-2 gene transcription compared with control group (1.58 ± 0.063 vs. $1.00 \pm 0.036\%$, $P = 0.0014$) (Figure 3(b)). And mutant cells also showed increased Bcl-2 protein level than the control group (Figure 3(c)).

2.9. Apoptosis Assay. The apoptosis rate was detected by the FITC Annexin V Apoptosis Detection Kit. Cells that are in early apoptosis are FITC Annexin V positive and PI negative, and cells that are in late apoptosis are both Annexin V and PI

positive. The living cell ratio of the mutant group was higher than that of the control group ($94.9 \pm 4.9\%$ vs. $74 \pm 3.20\%$, $P = 0.0229$, Figure 3(d)) when the total cell number was almost the same. The early apoptosis and late apoptosis in the mutant group are significant decreased than those in the control group ($3.6 \pm 0.75\%$ vs. $22.9 \pm 3.00\%$, $P = 0.0229$; $0.76 \pm 0.27\%$ vs. $2.89 \pm 0.42\%$, $P = 0.0125$, Figure 3(d)).

2.10. Mitochondrial OCR Assay. To assess whether the MT-ND2 m. 5178C>A gene mutation affects mitochondrial respiratory functions, we calculated OCR curves of mutants and control cell lines after administration of various inhibitors. Basal OCR refers to the difference in OCR after treatment with rotenone and antimycin A before oligomycin treatment, reflecting the basic OCR of mitochondria. The basal OCR of the mutant group was increased by 42.3% compared with that of the control group (104.39 ± 8.7 vs. 60.6 ± 8.14 , $P < 0.01$, Figure 4).

ATP-linked OCR refers to the difference in OCR between oligomycin treatment and posttreatment, reflecting the OCR of mitochondrial OXPHOS coupling. The

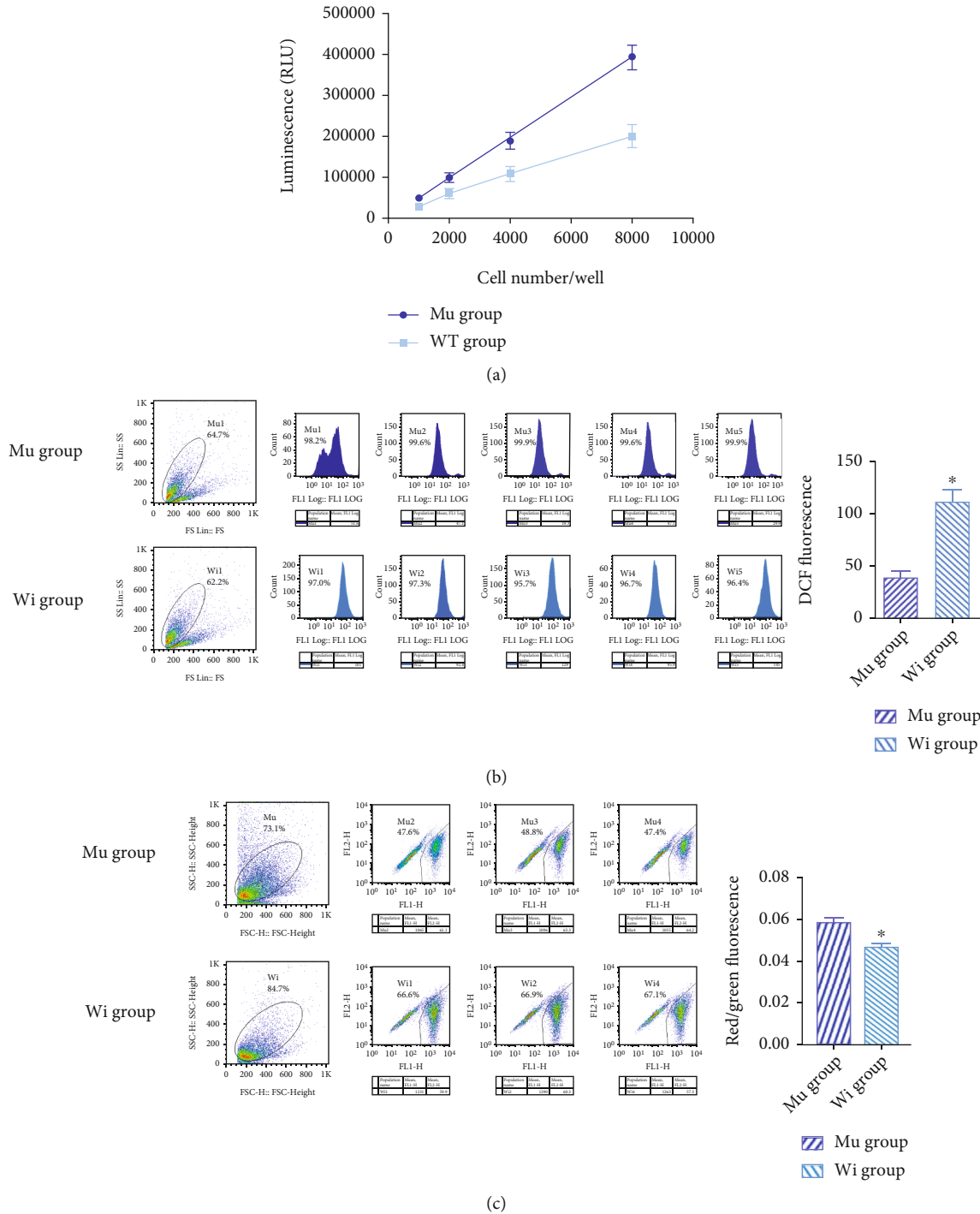


FIGURE 2: Mitochondrial functions of mutant and control cell lines. (a) ATP synthesis: ATP production was measured by a luciferin/luciferase luminescence assay. The ATP production of the mutant cells was significantly higher than the control group. (b) ROS synthesis: ROS production was detected through fluorescent probe DCFH-DA by flow cytometry. ROS produced by the mutant cell line was significantly lower than that in the control group. (c) Mitochondrial membrane potential: mitochondrial membrane potential reflects the functional metabolic status of mitochondria which is calculated by the ratio of red/green fluorescence. The value of the mutant cell line was significantly higher than control group. (* $P < 0.05$).

ATP-linked OCR of the mutant group was increased by 37.7% compared with the control group (50.1 ± 5.65 vs. 35.6 ± 5.03 , $P < 0.01$, Figure 4).

The maximum OCR value refers to the difference between the OCR when treated with FCCP and the nonmito-

chondrial OCR when treated with rotenone and antimycin A, reflecting the buffering capacity of mitochondrial oxygen utilization. The maximal OCR of the mutation group was increased by 50.38% compared with the control group (233.68 ± 35.5 vs. 115.94 ± 16.18 , $P < 0.01$, Figure 4).

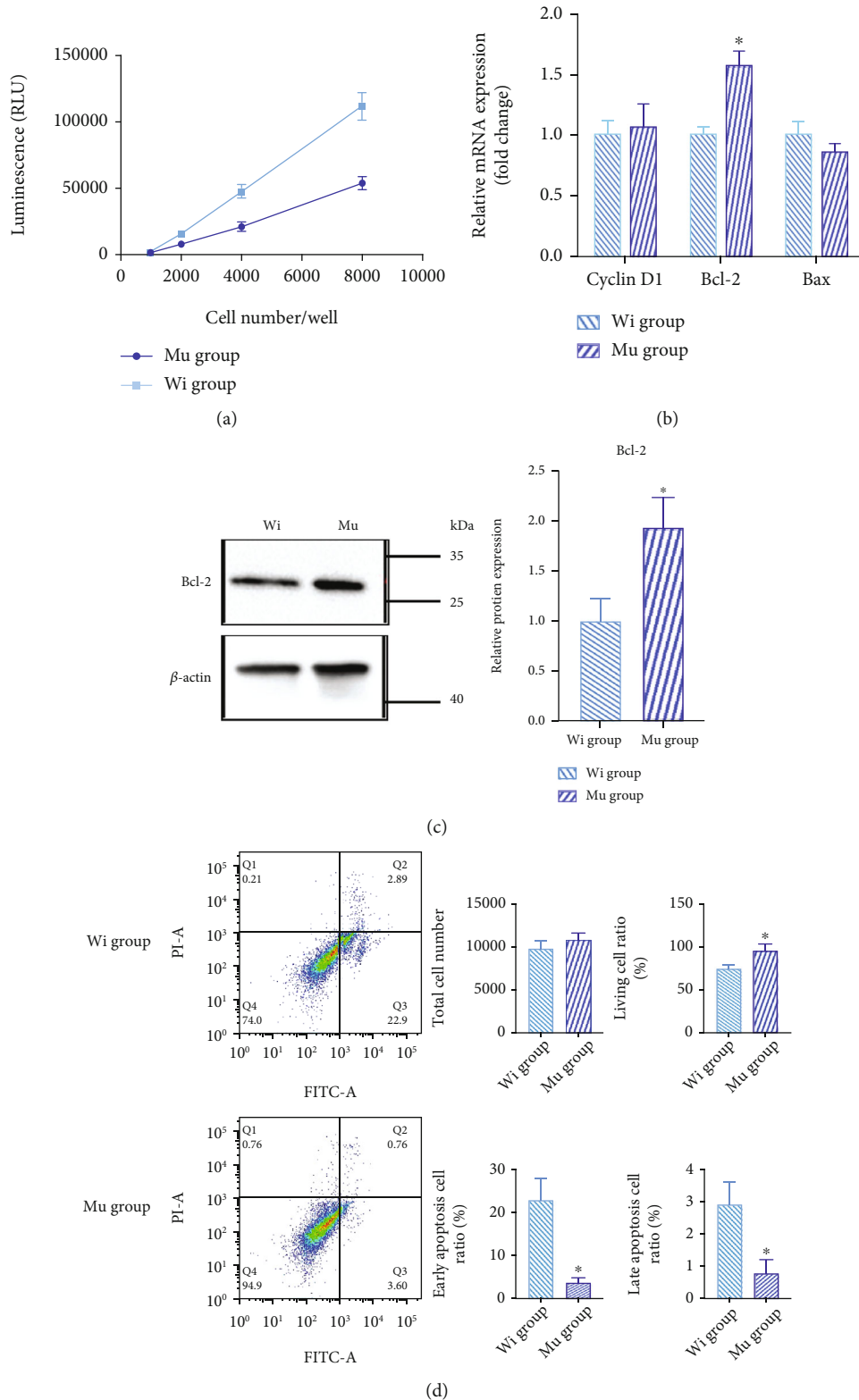


FIGURE 3: Proliferation and apoptosis of mutant and control cell lines. (a) Caspase 3/7 activity: Caspase 3/7 is a specific molecular marker of apoptosis. The expression level of Caspase 3/7 in the mutant group was significantly lower than that in the control group. (b) The transcription of proliferation and apoptosis genes: the mutant group showed increased Bcl-2 gene transcription compared with the control group. But there was no significant difference between Bax and Cyclin D1 gene transcription. (c) The protein expression of proliferation and apoptosis genes: the mutant cells showed increased Bcl-2 protein level. (d) Apoptosis assay: the apoptosis rate was detected by the FITC Annexin V Apoptosis Detection Kit. The living cell ratio of the mutant group was higher than that of the control group. The early apoptosis and late apoptosis in the mutant group are significantly decreased than those in the control group. (* $P < 0.05$).

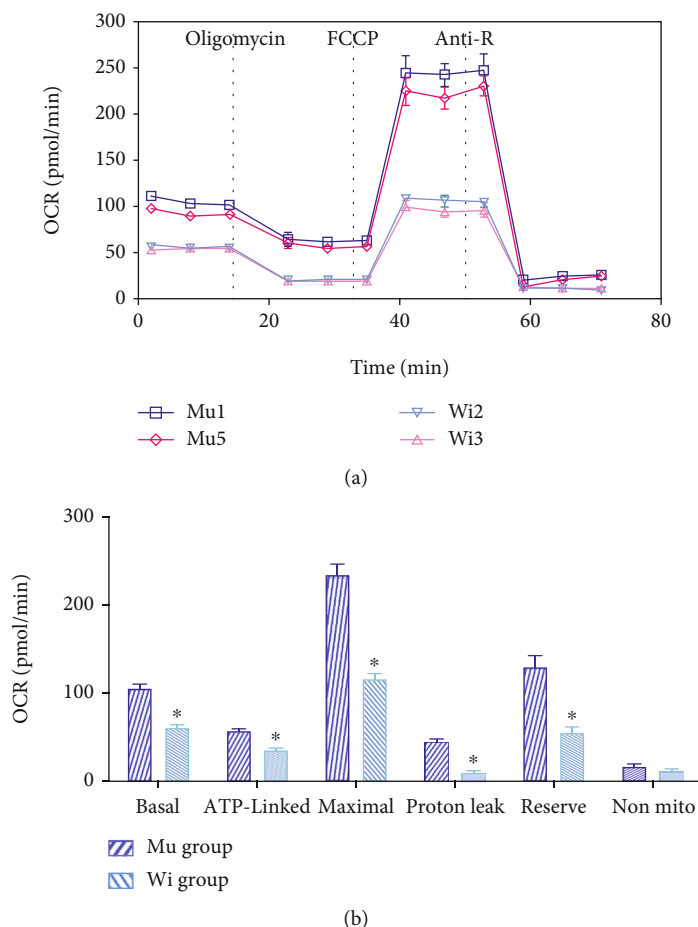


FIGURE 4: Detection of mitochondrial OCR in mutant and control cell lines. (a) OCR curves of mutant and control cell lines after treatment with various inhibitors. The compounds (oligomycin, FCCP, and a mix of rotenone and antimycin A) are serially injected to measure ATP production, maximal respiration, and nonmitochondrial respiration, respectively. Proton leak and spare respiratory capacity are then calculated using these parameters and basal respiration. (b) Statistical analysis of the basic OCR, ATP-coupled OCR, maximum OCR, proton leak OCR, buffered OCR, and nonmitochondrial OCR of mutant and control cell lines (* $P < 0.05$).

Proton leak OCR refers to the remaining OCR after treatment with rotenone and antimycin A, reflecting the rate of oxygen consumption not used by mitochondria. The proton leak OCR of the mutant group was increased by 78% compared with that of the control group (45.16 ± 5.65 vs. 9.9 ± 6.27 , $P < 0.01$, Figure 4).

Reserve OCR is the difference between maximum and base OCRs, reflecting the buffering capacity of mitochondrial oxygen utilization. The reserve capacity of the mutation group was increased by 57.2% compared with that of the control group (129.41 ± 32.33 vs. 55.33 ± 16.47 , $P < 0.01$, Figure 4).

Nonmitochondrial OCR refers to the remaining OCR after treatment with rotenone and antimycin A, reflecting the consumption rate of oxygen that is not used by mitochondria. The nonmitochondrial OCR of the mutant group was increased by 28.2% compared with that of the control group (17.17 ± 7.65 vs. 12.33 ± 4.68 , $P = 0.149$, Figure 4).

2.11. Mitochondrial Complex I Activity. To investigate whether C5178A gene mutation influences Mitochondrial Complex I function, we calculate the activity of Mitochondrial Complex I through measuring the oxidation rate of

NADH. The activity of Mitochondrial Complex I of the mutant group was increased than that of the control group ($2.312e - 005 \pm 1.775e - 006$ vs. $1.361e - 005 \pm 6.19e - 007$, $P = 0.0369$, Figure 5).

3. Discussion

Mitochondria are important organelles of eukaryotic cells, which provide more than 90% energy to cells through the electron transport chain, the main source of energy [16]. The OXPHOS complex consists of five multisubunit complexes (I–V) located on the inner mitochondrial membrane. Complex I contains seven mtDNA-encoded polypeptides, and complexes III–V contain 1, 3, and 2 mtDNA-encoded polypeptides, respectively. In the previous study, we found a MT-ND2 m. 5178C>A gene mutation in the genetic screening of 817 EH cases and 821 controls in a Chinese general population [17]. ND2 is a subunit of complex I [18]. The MT-ND2 m. 5178C>A mutation leads to replacement of leucine (Leu) with methionine (Met). In 1998, Tanaka et al. [8] first reported that MT-ND2 m. 5178C>A gene mutation was more frequent in healthy controls and centenarians,

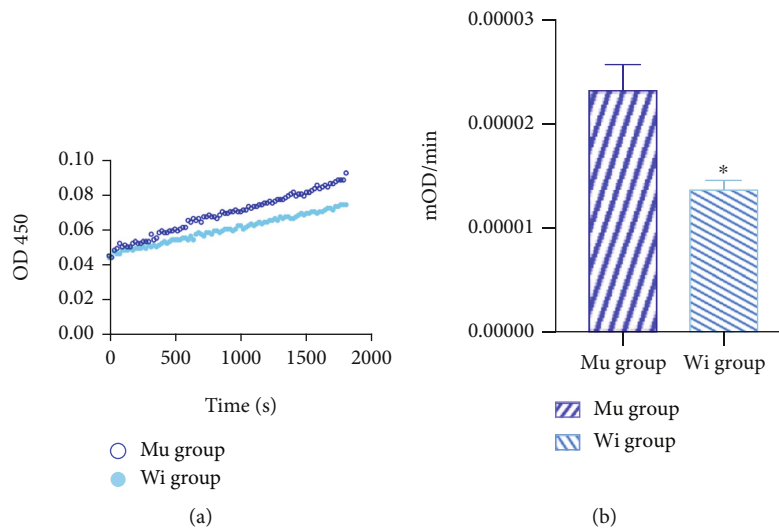


FIGURE 5: Mitochondrial Complex I activity. (a) The activity of Mitochondrial Complex I was calculated through measuring the oxidation rate of NADH. The oxidation rate of NADH was detected on OD450nm. (b) The linear growth rate represents the activity of Mitochondrial Complex I ($*P < 0.05$).

suggesting that MT-ND2 m. 5178C>A gene mutation was associated with longevity. And this conclusion was further verified in a larger sample population. Later, Raule et al. [19] carried out whole mitochondrial sequencing analysis on 2200 ultranagenarians and controls and proved that the mutations of mtDNA can lead to the synthesis obstacle of OXPHOS complex. They found that mutations in subunits of the OXPHOS complex I had a beneficial effect on longevity. A study has shown that the substitution of methionine plays an endogenous antioxidant role in protecting mitochondria [20]. However, the specific effect of MT-ND2 m. 5178C>A mutation on OXPHOS and apoptosis is not clear.

MT-ND2 m. 5178C>A has also been reported to be associated with protective effects against various diseases. In alloxan-resistant mice, the MT-ND2 m. 4738C>A mutation is a homologous site with the human MT-ND2 m. 5178C>A mutation, which also results in replacement of Leu by Met [21], indicating that the MT-ND2 m. 5178C>A mutation is a protective factor for type 1 diabetes. In our previous study, the mutation rate of MT-ND2 m. 5178C>A in hypertensive patients was significantly lower than that in the normal control group. This study showed that ATP production of the MT-ND2 m. 5178C>A mutant group was significantly higher than that of the control group. It has been speculated that this mutation contributes to the stability of complexes of the electron transport system, less susceptibility to attack by internal and external factors, and improvement of OXPHOS and ATP synthesis. ROS produced by the mutant cell line was significantly lower than that in the control group. The improvement of mitochondrial complex I activity may be associated with prevention of the damage induced by ROS in mitochondria and other organelles. ND2 is a subunit of mitochondrial respiratory chain complex I. The complex I is the initiation of the mitochondrial respiratory chain. The action of the respiratory chain complex forms a certain proton electron gradient (mitochondrial membrane poten-

tial) between the mitochondrial inner and outer membranes. It is this gradient that drives the F₀F₁ ATP synthase, which promotes the synthesis of ATP [22]. This increase of ATP synthesis can further promote cell activity.

OCR is another basic indicator for mitochondrial function [23]. In this study, the mitochondrial pressure test was performed using the Seahorse XF Energy Analyzer to measure the mitochondrial OCR. Increased basal OCR, ATP-linked OCR, maximal OCR, and reserve capacity OCR reflect that the mitochondrial OCR of the mutant cells is higher than that of the control group, which was associated with improved OXPHOS. Mitochondrial membrane potential plays an important role in the maintenance of mitochondrial function and structure and participates in various diseases [24, 25]. Mitochondrial dysfunction often first shows a decrease in mitochondrial membrane potential [26]. Our previous studies have found that, in the absence of ATP or calcium overload, mitochondrial swelling leads to mitochondrial permeability transition pore (mPTP) opening, causing cytochrome C and apoptotic factor to be released from mitochondria into the cytoplasm, which activates apoptosis cascade reactions such as activation of Caspase 3/7 [27, 28]. This study showed that Caspase 3/7 produced by mutant cell lines was significantly lower than that in the control group. The early apoptosis and late apoptosis in the mutant group are significantly decreased than those in the control group. The mitochondrial membrane potential is a guarantee for ATP synthesis by complex V [22, 29]. This study showed that the MT-ND2 m. 5178C>A gene mutation maintained cell stability by maintaining stability of the intracellular mitochondrial membrane potential, reducing apoptosis, and synthesizing more ATP.

4. Conclusions

In conclusion, MT-ND2 m. 5178C>A gene mutation improves the function of mitochondrial respiratory chain

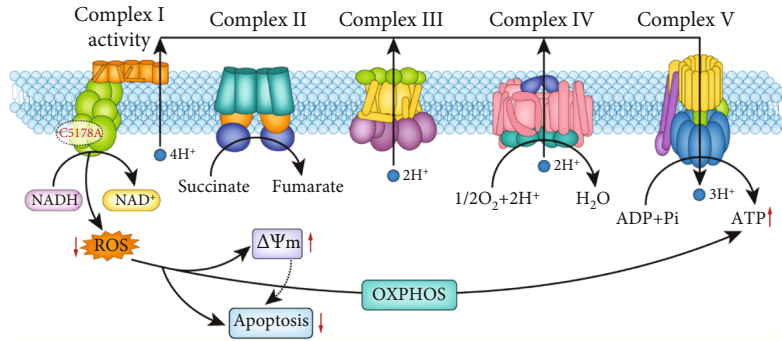


FIGURE 6: The mechanism of mitochondrial ND2 5178C>A on mitochondrial effect.

complex I, reduces ROS production, inhibits the damage induced by ROS in mitochondria and other organelles, and maintains the intracellular steady state of the mitochondrial membrane potential. It also increases OCR during OXPHOS, produces more ATP, increases the cell proliferation rate, and reduces apoptosis (Figure 6). These reveal that a possible mechanism of MT-ND2 m. 5178C>A gene mutation decreased the incidence of EH and provide a new target to explore the pathogenesis of EH.

5. Materials and Methods

5.1. Study Population and Cell Lines. This study clarified the effect of MT-ND2 m. 5178C>A gene mutation on cell and mitochondrial functions. In the Chinese mitochondrial genetic screening research program [30], informed consent, blood samples, and clinical evaluations were obtained from all participating family members under protocols approved by the Ethics Committee of the Chinese PLA General Hospital Institutional Review Board. Written informed consent and consent for publication were obtained from all participants. According to the sequencing results, five individuals with the MT-ND2 m. 5178C>A gene mutation and controls were selected to establish immortalized lymphocyte lines (for more details, see reference [4]).

5.2. Cell Proliferation and Activity Measurements. Cell suspensions (100 μ L/well) were seeded in a 96-well plate at 2000, 4000, 6000, and 8000 cells/well. CCK-8 solution (CCK8 test kit, Japan) was added to each well according to the manufacturer's instructions. Plates were incubated in a cell culture incubator for 4 h and then analyzed at 450 nm using a microplate reader (BioTek, U.S.).

5.3. The Expression of Proliferation and Apoptosis Genes and Proteins. Cells were seeded at 2000, 4000, 6000, and 8000 cells/well, and then, 100 μ L Caspase-Glo[®] 3/7 Reagent (Caspase-Glo[®] 3/7 Assays, Promega corporation, U.S.) was added to each well. The samples were mixed gently and incubated for 3 h at room temperature. The amount of luminescence was measured in a Centro LB960 XS3 luminometer (Berthold, Germany).

Total RNA was collected by TRIzol reagent (TaKaRa, Japan) following the manufacturer's instruction. Then, RNA was reverse transcribed to cDNA by using reverse tran-

scriptase (Promega GoTaq qPCR Master Mix, China). The sequences of Cyclin D1 primers were forward: 5'-CCCA CTCCTACGATACGC-3'; reverse: 5'-AGCCTC CCAAAC ACCC-3'. The sequences of BCL-2 primers were forward: 5'-GATTGT GGCCTTCTTTGAGTT-3'; reverse: 5'-AGTTCACAAAGGCATCCCA-3'. The sequences of BAX primers were forward: 5'-GGGTTGTCGCCCTTTTC TACTT-3'; reverse: 5'-TGTCAGCCCATGATGGTTCT-3'. qRT-PCR analysis was actualized by Bio-Rad CFX96 Real-Time PCR Detection System (Bio-Rad, U.S.).

Cells were resuspended in lysis buffer (20 mM Tris pH 7.5, 2 mM EDTA, 3 mM EGTA, 2 mM dithiothreitol, 250 mM sucrose, 0.1 mM phenylmethylsulfonyl fluoride, and 1% Triton X-100) with a protease inhibitor cocktail at 4°C for 1 h. Then, the cells were centrifuged at 13,000 rpm at 4°C for 30 min. Supernatants were boiled and separated on SDS-polyacrylamide gel, then transferred to nitrocellulose membranes. The membranes were coincubated with anti Bcl-2 antibody (Santa Cruz Biotechnology, U.S.) at 4°C overnight. After washing 4 times, the membranes were incubated with secondary antibodies conjugated with horseradish peroxidase (HRP). Antigen-antibody complexes were visualized by enhanced chemiluminescence. The densitometric measurements were analyzed by using ImageJ software.

5.4. Apoptosis Rate Assay. The apoptosis rate was calculated through the FITC Annexin V Apoptosis Detection Kit I (BD Pharmingen, U.S.) according to the instruction from the manufacturer. The numbers of 5×10^5 cells were collected and washed with PBS and resuspended with 100 μ L 1* Annexin V Binding Buffer. Then, 5 μ L FITC Annexin V and 5 μ L propidium iodide were added and incubated for 15 minutes in the dark environment. Then, another 400 μ L 1* Annexin V Binding Buffer was added before being analyzed by flow cytometry (Becton Dickinson, U.S.).

5.5. ATP Synthesis Detection. Cells were seeded at 2000, 4000, 6000, and 8000 cells/well and incubated for 30 min at room temperature. The same amount of reagents (CellTiter-Glo Cell ATP Detection Kit, Promega Corporation, U.S.) was added to the medium per well. Cells were shaken on a shaker for 2 min to induce lysis. The cells were incubated for 10 min

at room temperature to stabilize the fluorescence signals, and luminescence was recorded.

5.6. ROS Synthesis Assay. Fluorescent probe DCFH-DA was diluted at 1 : 1000 in RPMI 1640 medium to 10 μ M. Logarithmically growing cells were collected and adjusted to 1×10^6 /mL. The cell lines were incubated for 30 min at 37°C with 5% CO₂ and then mixed for 3 min. The cells were washed three times with serum-free medium to remove DCFH-DA. The cell lines were harvested and analyzed for ROS by flow cytometry (Becton Dickinson, U.S.) at 488 nm excitation and 525 nm emission.

5.7. Mitochondrial Membrane Potential ($\Delta\Psi_m$) Detection. To prepare the JC-10 dye loading solution, 50 μ L of 100 \times JC-10 was added to 5 mL Assay Buffer A. The negative control group was medium only, and the positive control group was 2 mM FCCP or CCCP. The cell lines were resuspended in 50 μ L/well JC-10 dye loading solution and incubated at 37°C with 5% CO₂ while protected from light for 30 min. The fluorescence intensity was then detected in cell lines.

5.8. Mitochondrial OCR Assay. Cell suspensions (80 μ L) were added to a Cell-Tak well plate. Then, 25 μ L of different reagents was added to A–D while facing the sensor cartridge: A well: oligomycin (2 μ M); B well: FCCP (1 μ M); and C well: rotenone/antimycin A (0.5 μ M) at a final concentration of 1 μ M. Cellular oxygen consumption was detected by an XF96 cell energy metabolism real-time analyzer (Seahorse, U.S.) [31].

5.9. Mitochondrial Complex I Activity. Mitochondrial Complex I also known as NADH dehydrogenase is the largest protein complex in the inner mitochondrial membrane. Complex I can catalyze the dehydrogenation of NADH to generate NAD⁺. The oxidation rate of NADH is measured at 340 nm using a microplate reader (BioTek, U.S.) to calculate the size of the enzyme activity. Mitochondrial Complex I activity detection kit (mitochondrial respiratory chain complex I activity detection kit, Abcam, U.S.) was added to each well according to the manufacturer's instructions.

5.10. Statistical Analysis. Continuous variables are expressed as mean \pm standard deviation. Nonparametric test was used for the comparison between the two groups. Statistical analyses were performed using the Statistical Package for Social Sciences software (SPSS, version 18.0). The test criteria were statistically significant at $P < 0.05$.

Abbreviations

ND2:	NADH dehydrogenase subunit 2
OCR:	Oxygen consumption rate
mtDNA:	Mitochondrial DNA
OXPPOS:	Oxidative phosphorylation
rRNA:	Ribosomal RNA
Leu:	Leucine
Met:	Methionine
$\Delta\Psi_m$:	Mitochondrial membrane potential
BAX:	Bcl-2-associated X protein
Bcl-2:	B cell lymphoma 2 protein.

Data Availability

The data material used and analyzed during this study is available from the corresponding author on reasonable request.

Ethical Approval

This study has been approved by the Ethics Committee of the Chinese PLA General Hospital Institutional Review Board.

Consent

Written informed consent and written consent for publication were obtained from all participants.

Conflicts of Interest

The authors declare that they have no conflicts of interests.

Authors' Contributions

Tian L carried out the analyses of the mitochondrial genomics, ROS, and ATP synthesis. Zhu C carried out the data collection. Yang H did the statistical analysis. Li Y participated in the study design. Liu Y participated in the design of the study, the interpretation of the results, and the draft of the manuscript. All authors read and approved the final manuscript. Liuyang Tian and Yang Li contributed equally to this work. Liuyang Tian and Yang Li are co-first authors.

Acknowledgments

This work was supported by National Science Foundation of China Grants 82070434/H0214 and 81470542/H0214 and Beijing Nova Program of science and technology cross cooperation project Z191100001119020 (to Y. Q. Liu).

References

- [1] A. Majander, K. Huoponen, M. L. Savontaus, E. Nikoskelainen, and M. Wikström, "Electron transfer properties of NADH:ubiquinone reductase in the ND1/3460 and the ND4/11778 mutations of the Leber hereditary optic neuropathy (LHON)," *FEBS Letters*, vol. 292, no. 1-2, pp. 289–292, 1991.
- [2] M. Nakagawa, Y. Kaminishi, Y. Isashiki et al., "Familial mitochondrial encephalomyopathy with deaf-mutism, ophthalmoplegia and leukodystrophy," *Acta Neurologica Scandinavica*, vol. 92, no. 1, pp. 102–108, 1995.
- [3] M. Kuriyama and A. Igata, "Mitochondrial encephalopathy, lactic acidosis, and stroke-like syndrome (MELAS)," *Annals of Neurology*, vol. 18, no. 5, pp. 625–626, 1985.
- [4] T. Suzuki, A. Nagao, and T. Suzuki, "Human mitochondrial tRNAs: biogenesis, function, structural aspects, and diseases," *Annual Review of Genetics*, vol. 45, no. 1, pp. 299–329, 2011.
- [5] D. C. Wallace, "A mitochondrial paradigm of metabolic and degenerative diseases, aging, and cancer: a dawn for evolutionary medicine," *Annual Review of Genetics*, vol. 39, no. 1, pp. 359–407, 2005.

- [6] B. Wagner, T. Kitami, T. J. Gilbert et al., "Large-scale chemical dissection of mitochondrial function," *Nature Biotechnology*, vol. 26, no. 3, pp. 343–351, 2008.
- [7] J. Smeitink, M. Zeviani, D. M. Turnbull, and H. T. Jacobs, "Mitochondrial medicine: a metabolic perspective on the pathology of oxidative phosphorylation disorders," *Cell Metabolism*, vol. 3, no. 1, pp. 9–13, 2006.
- [8] M. Tanaka, J. S. Gong, J. Zhang, M. Yoneda, and K. Yagi, "Mitochondrial genotype associated with longevity," *The Lancet*, vol. 351, no. 9097, pp. 185–186, 1998.
- [9] K. Takagi, Y. Yamada, J. S. Gong, T. Sone, M. Yokota, and M. Tanaka, "Association of a 5178C->A (Leu237Met) polymorphism in the mitochondrial DNA with a low prevalence of myocardial infarction in Japanese individuals," *Atherosclerosis*, vol. 175, no. 2, pp. 281–286, 2004.
- [10] R. Ohkubo, M. Nakagawa, K. I. Ikeda et al., "Cerebrovascular disorders and genetic polymorphisms: mitochondrial DNA5178C is predominant in cerebrovascular disorders," *Journal of the Neurological Sciences*, vol. 198, no. 1-2, pp. 31–35, 2002.
- [11] W. Liao, Y. Pang, C. A. Yu, J. Y. Wen, Y. G. Zhang, and X. H. Li, "Novel mutations of mitochondrial DNA associated with type 2 diabetes in Chinese Han population," *The Tohoku Journal of Experimental Medicine*, vol. 215, no. 4, pp. 377–384, 2008.
- [12] T. Ito, A. Kokaze, M. Ishikawa et al., "Joint effects of mitochondrial DNA 5178 C/a polymorphism and coffee consumption or alcohol consumption on clustering of cardiovascular risk factors in middle-aged Japanese men: a cross-sectional study," *Journal of Diabetes and Metabolic Disorders*, vol. 13, no. 1, 2014.
- [13] J. S. Teodoro, C. M. Palmeira, and A. P. Rolo, "Mitochondrial membrane potential ($\Delta\Psi$) fluctuations associated with the metabolic states of mitochondria," *Methods in Molecular Biology*, vol. 1782, pp. 109–119, 2018.
- [14] F. J. Bock and S. W. G. Tait, "Mitochondria as multifaceted regulators of cell death," *Nature Reviews. Molecular Cell Biology*, vol. 21, no. 2, pp. 85–100, 2020.
- [15] M. K. Shim, H. Y. Yoon, S. Lee et al., "Caspase-3/-7-specific metabolic precursor for bioorthogonal tracking of tumor apoptosis," *Scientific Reports*, vol. 7, no. 1, p. 16635, 2017.
- [16] M. Paz, D. H. González Maglio, F. S. Weill, J. Bustamante, and J. Leoni, "Mitochondrial dysfunction and cellular stress progression after ultraviolet B irradiation in human keratinocytes," *Photodermatology, Photoimmunology & Photomedicine*, vol. 24, no. 3, pp. 115–122, 2008.
- [17] X. Chen, X. Y. He, C. Zhu et al., "Interaction between mitochondrial NADH dehydrogenase subunit-2 5178 C > A and clinical risk factors on the susceptibility of essential hypertension in Chinese population," *BMC Medical Genetics*, vol. 20, no. 1, p. 121, 2019.
- [18] J. Leonard and A. Schapira, "Mitochondrial respiratory chain disorders I: mitochondrial DNA defects," *The Lancet*, vol. 355, no. 9200, pp. 299–304, 2000.
- [19] N. Raule, F. Sevini, S. Li et al., "The co-occurrence of mtDNA mutations on different oxidative phosphorylation subunits, not detected by haplogroup analysis, affects human longevity and is population specific," *Aging Cell*, vol. 13, no. 3, pp. 401–407, 2014.
- [20] R. Levine, L. Mosoni, B. S. Berlett, and E. R. Stadtman, "Methionine residues as endogenous antioxidants in proteins," *Proceedings of the National Academy of Sciences of the United States of America*, vol. 93, no. 26, pp. 15036–15040, 1996.
- [21] C. Mathews, E. H. Leiter, O. Spirina et al., "mt-Nd2 allele of the ALR/Lt mouse confers resistance against both chemically induced and autoimmune diabetes," *Diabetologia*, vol. 48, no. 2, pp. 261–267, 2005.
- [22] G. Lenaz, C. Bovina, M. D'aurelio et al., "Role of mitochondria in oxidative stress and aging," *Annals of the New York Academy of Sciences*, vol. 959, no. 1, pp. 199–213, 2002.
- [23] J. Hu, N. C. de Souza-Pinto, K. Haraguchi et al., "Repair of formamidopyrimidines in DNA involves different glycosylases," *The Journal of Biological Chemistry*, vol. 280, no. 49, pp. 40544–40551, 2005.
- [24] L. Skárka and B. Ostádal, "Mitochondrial membrane potential in cardiac myocytes," *Physiological Research*, vol. 51, no. 5, pp. 425–434, 2002.
- [25] B. Kadenbach, R. Ramzan, R. Moosdorf, and S. Vogt, "The role of mitochondrial membrane potential in ischemic heart failure," *Mitochondrion*, vol. 11, no. 5, pp. 700–706, 2011.
- [26] B. Zhang, D. G. Wang, F. F. Guo, and C. Xuan, "Mitochondrial membrane potential and reactive oxygen species in cancer stem cells," *Familial Cancer*, vol. 14, no. 1, pp. 19–23, 2015.
- [27] L. Yuqi, G. Lei, L. Yang et al., "Voltage-dependent anion channel (VDAC) is involved in apoptosis of cell lines carrying the mitochondrial DNA mutation," *BMC Medical Genetics*, vol. 10, no. 1, 2009.
- [28] D. Green and G. Kroemer, "The pathophysiology of mitochondrial cell death," *Science*, vol. 305, no. 5684, pp. 626–629, 2004.
- [29] A. Tulah and M. Birch-Machin, "Stressed out mitochondria: the role of mitochondria in ageing and cancer focussing on strategies and opportunities in human skin," *Mitochondrion*, vol. 13, no. 5, pp. 444–453, 2013.
- [30] S. Wang, R. Li, A. Fettermann et al., "Maternally inherited essential hypertension is associated with the novel 4263A>G mutation in the mitochondrial tRNA^{Ile} gene in a large Han Chinese family," *Circulation Research*, vol. 108, no. 7, pp. 862–870, 2011.
- [31] P. Mullen, A. Zahno, P. Lindinger et al., "Susceptibility to simvastatin-induced toxicity is partly determined by mitochondrial respiration and phosphorylation state of Akt," *Biochimica et Biophysica Acta*, vol. 1813, no. 12, pp. 2079–2087, 2011.

Review Article

Structure and Function of Mitochondria-Associated Endoplasmic Reticulum Membranes (MAMs) and Their Role in Cardiovascular Diseases

Yi Luan,¹ Ying Luan,² Rui-Xia Yuan,¹ Qi Feng,³ Xing Chen,¹ and Yang Yang¹ 

¹Department of Translational Medicine Center, The First Affiliated Hospital of Zhengzhou University, Zhengzhou 450052, China

²Department of Physiology and Neurobiology, School of Basic Medical Sciences, Zhengzhou University, Zhengzhou 450001, China

³Research Institute of Nephrology, Zhengzhou University, Zhengzhou 450052, China

Correspondence should be addressed to Yang Yang; yangyangbio@163.com

Received 16 April 2021; Accepted 30 June 2021; Published 12 July 2021

Academic Editor: Sang-Bing Ong

Copyright © 2021 Yi Luan et al. This is an open access article distributed under the Creative Commons Attribution License, which permits unrestricted use, distribution, and reproduction in any medium, provided the original work is properly cited.

Abnormal function of suborganelles such as mitochondria and endoplasmic reticulum often leads to abnormal function of cardiomyocytes or vascular endothelial cells and cardiovascular disease (CVD). Mitochondria-associated membrane (MAM) is involved in several important cellular functions. Increasing evidence shows that MAM is involved in the pathogenesis of CVD. MAM mediates multiple cellular processes, including calcium homeostasis regulation, lipid metabolism, unfolded protein response, ROS, mitochondrial dynamics, autophagy, apoptosis, and inflammation, which are key risk factors for CVD. In this review, we discuss the structure of MAM and MAM-associated proteins, their role in CVD progression, and the potential use of MAM as the therapeutic targets for CVD treatment.

1. Introduction

Cardiovascular disease (CVD) is the leading cause of mortality in humans. Globally, there were nearly 523.2 million new cases and 18.6 million deaths from CVD in 2019. Its incidence has increased by 17.1% over the past decade [1, 2]. In China, CVD is the leading cause of overall death (40% of all disease mortality) [3].

CVD is caused by multiple risk factors and pathological mechanisms [4, 5]. At the cellular level, various aberrations, including metabolic abnormalities, energy deficit, autophagy defect, endoplasmic reticulum (ER) stress, reactive oxygen species (ROS) production, and apoptosis activation, may lead to CVD [6]. A substantial amount of energy, which is mainly produced by mitochondria, is essential for normal physiological function of the heart. Thus, the abnormality (dysfunction or malfunction) of mitochondria is the main cause of these cellular perturbations [7]. Being extremely sensitive to oxidative stress, vascular endothelial cells are easily adapted to changing environments, such as altered oxygen levels, pathogens, and endogenous damaging stimuli [8]. In addition, the

circulating immune cells might also affect adjacent vascular endothelial cells (ECs) by the initiation of immune reactions, leading to the earliest stages of atherosclerosis and preceding atherosclerotic plaque formation. Mitochondria are closely involved in these processes, which makes them attractive candidates for therapeutic intervention [9]. Meanwhile, a failing heart is accompanied by defected oxidative phosphorylation (OXPHOS) and decreased ATP levels, contributing to defective cardiac performance [10].

The endoplasmic reticulum (ER), as a multifunctional organelle, provides a distinct subcellular compartment with multiple functions, including lipid biosynthesis, calcium storage, and protein folding and processing [11]. Disturbance in proper ER function may cause ER stress, which in turn causes severe impairment in protein folding and therefore poses the risk of proteotoxicity. ER stress has been highlighted as an important regulator of cardiovascular diseases [12]. For example, CHOP is the most widely studied ER stress biomarker involved in ER stress-associated apoptotic signaling in cardiovascular disease [13]. In atherosclerosis, CHOP is elevated by the unfolded protein response (UPR) in

the ER, accompanied with a progression of atherosclerosis in the aorta [14]. Another important protein is the PAK2, a stress-responsive kinase localized in close proximity to the ER membrane. Its depletion in cardiomyocyte leads to defect in ER response, cardiac function, and cardiac cell death after being induced with tunicamycin, thus indicating a protective ER stress response against heart failure through modulation of PAK2 levels [15].

Mitochondria and ER have different living cells' roles. Accumulating evidence suggested an interaction between the two [16]. Mitochondria-associated membranes (MAM), also known as mitochondria-ER contact sites (MERCs), are specialized regions, in which this interaction occurs [17]. Growing evidence shows that MAM has a variety of cellular functions that are vital in the regulation of cardiovascular diseases and can also be potential targets for CVD therapy. In this review, we discussed the structure of MAM and MAM-associated proteins, their role in CVD progression, and the potential use of MAM as the therapeutic targets for CVD treatment.

2. The Structural Composition of the Mitochondria-Associated Membranes (MAMs)

The existence of MAMs was first reported in the late 1950s. MAM was then isolated, and its biochemical functions were examined in the 1990s [18]. The first identification related to the composition of MAMs was performed by Gao et al., using limited proteolysis [19], while the first comprehensive analysis of MAM proteome was performed by Zhang et al. [19, 20]. Approximately 991 proteins in the MAM fraction were identified. Later on, Poston et al. identified 1212 candidates, including weak soluble proteins at the MAM [21]. Until now, various proteins (approximately 1000) localized within the MAMs were identified in the brain and liver with the aid of in-depth mass spectrometry analysis [22]. Above all, the components within MAMs were highly conserved among species and tissues. The above proteomic analyses were also conducted under pathological conditions, such as diabetes [23].

Perrone et al. have suggested that MAM is mainly involved in calcium homeostasis, lipid metabolism, and protein transfer between mitochondria and ER [24]. Furthermore, Gao et al. found that MAM is also involved in inflammasome formation, autophagy, ER stress, and mitochondria morphology [25]. The proteins located on MAMs either take part in MAM physical interaction or modulation of the tethering complex in MAMs [26]. Tethering proteins, ranging from Ca^{2+} channels to apoptotic proteins, constitute the molecular bridges combining the ER and mitochondrial membrane together [27]. From a physical point of view, the distance between membranes in MAMs ranges from 10 to 25 nm for smooth ER, and 50 to 80 nm for rough ER. Besides, the coverage of MAMs takes about 4 to 20% of the total mitochondrial surface, depending on its cellular stress and metabolic state [20].

The well-established MAM proteins include (1) the pro-tethering complexes: (i) mitofusin 2 (MFN2), (ii) the com-

plex formed by vesicle-associated membrane protein-associated protein B (VAPB) and protein tyrosine phosphatase interacting protein 51 (PTPIP51), (iii) PTPIP51 and motile sperm domain-containing protein 2 (MOSPD2), (iv) glucose-regulated protein 75 (GRP75) bridging inositol triphosphate receptor (IP3R) to voltage-dependent anion channel 1 (VDAC1), (v) the mitochondrial fission 1 protein- (Fis1-) B cell receptor-associated protein 31 (BAP31) complex, (vi) the FUN14 domain-containing 1- (FUNDC1-) IP3R2 complex, (vii) the phosphor acidic cluster sorting protein 2 (PACS2), (viii) PDZD8, (ix) Beclin1 (BECN1), and (x) MITOL, Parkin, and AMPK α , which regulate MAM formation by directly interacting with MFN2 on the outer mitochondrial membrane (OMM) side; (2) proteins that regulate IP3R/GRP75/VDAC complexes: mitochondrial translocase of the outer membrane 70 (TOM70), Sigma-1 receptor (Sig-1R), cyclophilin D (CypD), pyruvate dehydrogenase kinases 4 (PDK4), thymocyte-expressed, positive selection-associated gene 1 (Tespa1), reticulon 1C (RTN-1C), glycogen synthase kinase-3 β (GSK3 β), disrupted-in-schizophrenia 1 (DISC1), transglutaminase type 2 (TGM2), Wolfram syndrome 1 (WFS1), and etoposide-induced protein 2.4 (EI24); (3) antitethering factors: (i) trichoplein/mitostatin (TpMs) that negatively regulates MAMs tethering via MFN2, (ii) FATE1 uncoupling MAMs by interacting with ER chaperones and emerin (EMD) and the mitofilin, (iii) Caveolin-1; and (4) upstream regulators of MAM formation: (i) glycogen synthase kinase-3 β (GSK3 β), (ii) p38 MAPK, (iii) cGMP-dependent protein kinase (PKG), (iv) FOXO1, (v) cAMP-dependent protein kinase (PKA), and (vi) AMPK α (Figure 1) [28].

According to the localization of these MAMs, these proteins can be classified into the following three groups: (1) MAM-localized proteins that are only located at the MAM, (2) MAM-enriched proteins that can also be detected in other regions of the cell, and (3) MAM-associated proteins that are transiently found in MAM in a condition-dependent manner [29]. Because of the high dynamics of MAM, the detailed feature of its components has remained elusive.

The IP3R1-GRP75-VDAC1 complex was the first identified tethering complex. It consists of ER-residing IP3R1s and VDAC1 at the OMM [30]. The OMM-localized FUNDC1 directly binds to IP3R2 to form a bridge between the ER and the mitochondria, favoring Ca^{2+} flux to the mitochondria by enhancing the mitochondria-ER connection in cardiomyocytes [31]. The loss of FUNDC1 promotes IP3R2 ubiquitination and degradation and decreases the levels of the MAM-maintenance protein PACS2 [32]. Additionally, the interaction between IP3Rs and VDAC1 is monitored by GRP75, which maintains the conformational stability of IP3Rs that participate in Ca^{2+} transport from the ER to the mitochondria [30]. The increased IP3R expression level has been found in cardiac hypertrophy, failing myocardium, atrial fibrillation, ischemic dilated cardiomyopathy, and hypertension (Table 1) [33]. Through the IP3R-VDAC complex, Sig-1R participates in cardiac function regulation by interacting with other endoplasmic reticulum chaperones, as the Binding Ig Protein (BiP) forming Ca^{2+} -sensitive

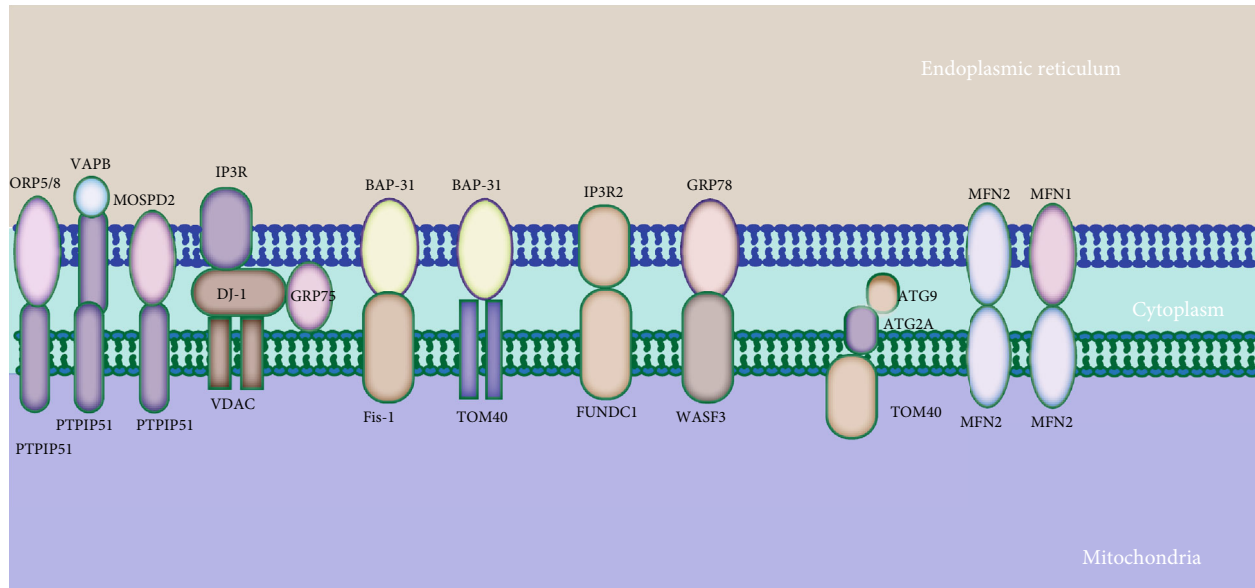


FIGURE 1: Major mitochondria-ER tethering complexes. Mitochondria are connected to the ER by several protein complexes. The ER protein ORP5/8, VAPB, or MOSPD2 interacts with the mitochondrial PTPIP51. ER-resident IP3R is anchored to OMM-localized protein VDAC via GRP75. The ER-localized BAP31 interacts with the mitochondrial Fis1 and TOM40. The IP3R2 located on the ER partners with the mitochondrial protein FUNDC1. The ER chaperone GRP78 interacts with WASF3. Mitochondrial TOM40 directs ATG2A to MAMs. The ER-localized MFN2 interacts with either MFN1 or MFN2 in the mitochondria.

complexes that extend ionic signaling from ER to mitochondria [34]. The interaction of Sig-1R with lipids is important for their localization and enrichment in MAMs. In skeletal muscle, PDK4 induces the formation of MAMs by interacting with the GRP75-IP3R-VDAC complex at MAMs [35].

MFN2 is known for its role in mitochondrial fusion. It is localized at ER and mitochondrial membranes and forms a hetero- or homodimer with mitofusin-1 (MFN1) or another MFN2 in the outer mitochondrial membrane (OMM) [36, 37]. MFN2 knockdown increases MAM and Ca^{2+} transfer, implying the notion that MFN2 is not a physical tether [38]. Recently, researchers found that loss of MFN2 causes a decrease in the distance between ER and mitochondria membranes, impairing Ca^{2+} uptake into the mitochondria (Figure 2(a)) [39]. Overall, MFN2 is recognized as a key component of MAMs and is crucial for the proper functioning of MAMs. Downregulation of MFN2 has been observed in rat models of cardiac hypertrophy, including spontaneously hypertensive rats, transverse aortic banding, and myocardial infarction, which contribute to cardiomyocyte remodeling. Contrary, its upregulation ameliorates the cardiac hypertrophy induced by angiotensin II [40]. Furthermore, MFN2 is crucial for cardiac differentiation in embryonic stem cells [41].

The BAP31-Fis1 complex consists of ER-localized BAP31 and OMM-localized Fis1 [42]. The BAP31-Fis1 complex is responsible for the recruitment and activation of procaspase 8 and transmission of proapoptotic signals from the mitochondria to the ER. BAP31 is cleaved to form proapoptotic p20BAP31, which transmits calcium from ER to mitochondria and the apoptotic signal via the IP3 receptor complex at ER-mitochondria juxtapositions [43]. Besides, through interaction with TOM40, mitochondrial respiratory chain

complexes, and NADH ubiquinone oxidoreductase (mitochondrial complex 1) core subunit 4 (NDUFS4) located on MAMs, BAP31 modulates mitochondrial oxygen consumption and autophagy and maintains mitochondrial homeostasis [43]. These data imply that BAP31 is a required platform for the transmittance of apoptotic signals between ER and mitochondria. BAP31 is also involved in the attenuated sepsis-mediated myocardial depression by melatonin [42]. Recent data have suggested that synaptojanin-2-binding protein (SYNJ2BP) localized on the OMM interacts with ribosome-binding protein 1 (RRBP1), and once SYNJ2BP is overexpressed, the mitochondria-ER contacts dramatically increase [44].

The VAPB-PTPIP51 complex is composed of ER-residing protein VAPB, which is responsible for vesicle trafficking and the unfolded protein response, and PTPIP51, a protein in OMM modulating cellular development and tumorigenesis [45]. The aberrant interactions between VAPB and PTPIP51 may directly result in a decrease in MAMs and disturbance of Ca^{2+} handling, further leading to a delay in mitochondria Ca^{2+} uptake [46]. PTPIP51 or VAPB alterations are also concomitant with the coverage changes of MAMs on mitochondrial surface. Furthermore, the mutant VAPB also leads to the accumulation of the mitochondria and decreases Ca^{2+} handling [46]. Other proteins can modulate the interaction between PTPIP51 and VAPB complex. A mutation in α -synuclein disrupts the VAPB-PTPIP51 complex, contributing to the uncoupling of ER-mitochondria contacts, aberrant Ca^{2+} transfer, and reduced mitochondrial ATP production in the process of Parkinson's disease [45]. TAR DNA-binding domain protein 43 (TDP-43), as a highly conserved and widely expressed nuclear protein, is also responsible for the regulation of the VAPB-PTPIP51

TABLE 1: Components of MAMs involved in cardiovascular disease.

Proteins	Relevant function(s) in MAMs	Functions in CVD	Expression in cardiovascular system
Protethering proteins			
GRP75	Increased MAM formation and mitochondria Ca^{2+} uptake	Mitochondrial calcium overload and hypoxia/reoxygenation injury in cardiomyocytes	High
IP3Rs	Interacts with GRP75 and VDACs, modulates calcium in MAMs	Upregulation in cardiac hypertrophy. Modulates excitation-contraction coupling in ventricular and atrial cardiomyocytes	Low
VDACs	Interacts with GRP75 and IP3Rs, regulates intracellular Ca^{2+} level	Marked elevation of VDAC1 in myocardial infarction. VDAC1 inhibition alleviates excessive fibrosis in the atrial myocardium	Medium
MFN2	Modulator of ER-mitochondria tethering and mitochondrial fusion	Downregulation in cardiac hypertrophy. MFN2 upregulation ameliorated the cardiac hypertrophy.	Medium
MFN1	Tethering mitochondria to MAMs via interaction with ER-resident MFN2	Represses cardiac hypertrophy and ischemia/reperfusion injury	Not detected
Fis1	Modulates ER-mitochondria tethering and induces apoptosis. Induces mitophagy	Inhibition of the CREB/Fis1 pathway leads to heart disease	High
BECN1	Enhances MAM formation and autophagosomes	Deregulation leads to heart diseases, through altered myocardial autophagy and apoptosis	Low
FUNDC1	Promotes mitochondrial fission and mitophagy. Increases Ca^{2+}	Required for cardiac ischemia/reperfusion injury-activated mitophagy	Medium
Parkin	Mediates mitophagy. Increases the ER-mitochondria contacts and induces Ca^{2+} transfer and ATP synthesis	Upregulated during I/R injury	Low
IP3Rs/GRP75/VDAC complex-modulated proteins			
Sig-1R	Prolongs Ca^{2+} signaling; Sig-1R increase represses ER stress response, whereas Sig-1R decrease induces apoptosis	Sig-1R activation represses hypertrophy and cardiomyocyte injury. Sig-1R KO displays cardiac remodeling	High
CypD	Regulates Ca^{2+} transfer from the ER to mitochondria through IP3R1	The CypD/GRP75/IP3R/VDAC complex inhibition improved hypoxia/reoxygenation injury in cardiomyocytes	NA
GSK3 β	Inhibition of GSK3 β results in decreased ER Ca^{2+} release as well as sensitivity to apoptosis	GSK3 β inhibition reduced infarct size in reperfused hearts	Not detected
Antitethering proteins			
CAV1	Negatively regulates the formation of MAMs and impairs Ca^{2+} transfer	CAV1 ablation aggravates cardiac dysfunction and decreases survival in myocardial ischemia	Medium
Upstream regulators of the formation of MAMs			
p38 MAPK	Phosphorylation of Gp78 at S538 by p38 MAPK inhibits MAM formation and mitochondrial fusion by promoting degradation of MFN1/2	p38 MAPK has been implicated in cardiomyocyte dysfunction and apoptosis	Medium
FOXO1	Augments MAM formation by inducing PDK4 and promotes mitochondrial Ca^{2+} accumulation, mitochondrial dysfunction, and ER stress	FOXO1 protein is associated with ischemic heart disease (IHD)	Not detected

complex [47]. TDP-43 accumulation reduces binding in the VAPB-PTPIP51 complex and disrupts Ca^{2+} homeostasis by promoting the phosphorylation and activation of glycogen synthase kinase-3 β (GSK3 β) [47, 48]. Besides, OMM-residing PTPIP51 connection with oxysterol-binding

protein-related protein 5/8 (ORP5/8) at the ER membrane facing the cytosol promotes the transportation of the phosphatidylserine (PS) to the mitochondria. Thus, we suppose that MAMs greatly influence the normal physiological function of mitochondria, which can be modulated by the VAPB-

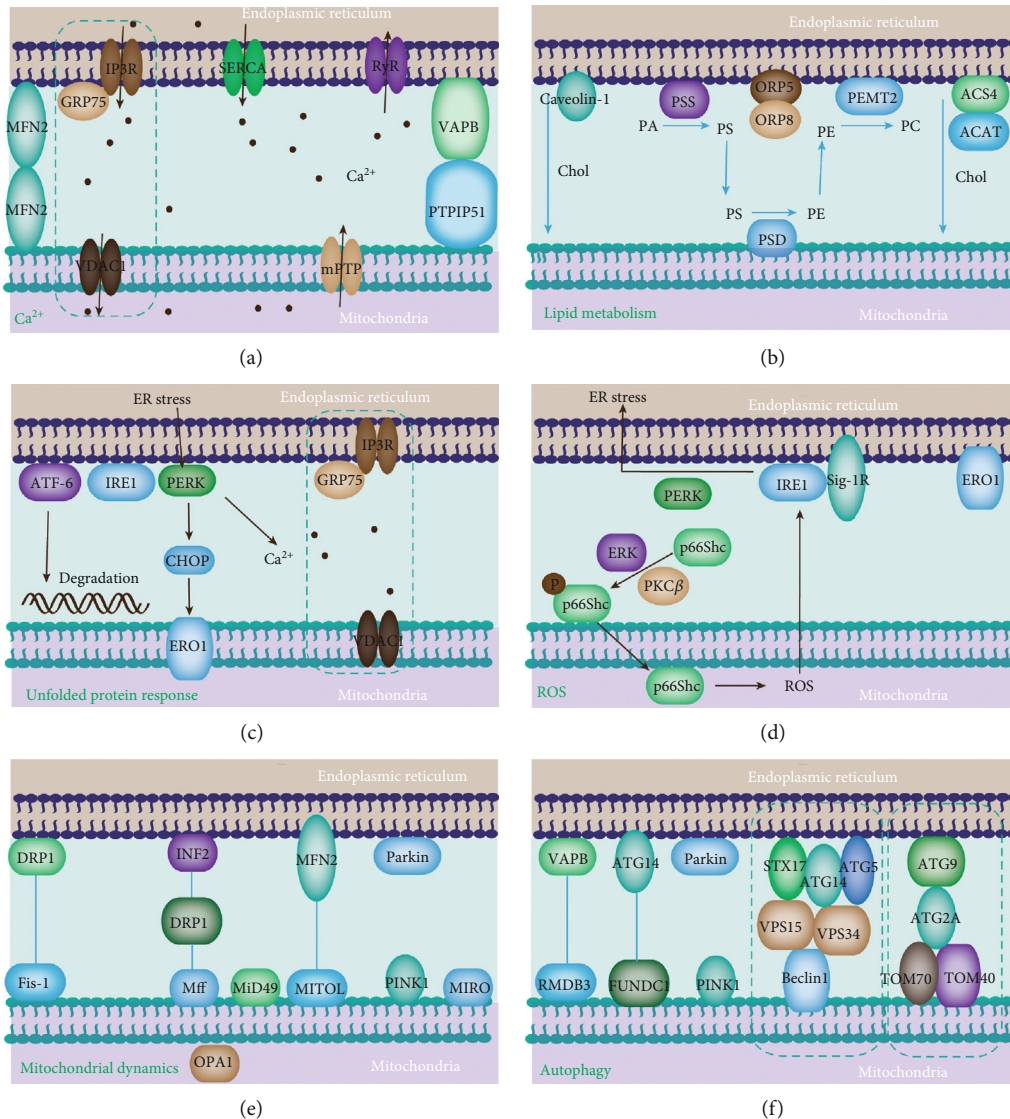


FIGURE 2: Key cellular functions handled at mitochondria-ER contact sites. Key proteins are involved in related cellular processes and their regulatory mechanisms. (a) Calcium homeostasis regulation. (b) Lipid metabolism. (c) Unfolded protein response. (d) ROS regulation. (e) Mitochondrial dynamics. (f) Autophagy.

PTPIP51 tethering complex [46]. More recently, the ER-anchored MOSPD2 has been proposed as a tethering protein that interacts with PTPIP51 and functions in both intracellular exchange and communication [49].

The GRP78-WASF-ATAD3A complex consists of cytoplasm-localized protein WASF3, the inner mitochondrial membrane (IMM) protein ATPase family AAA domain-containing 3A (ATAD3A), and the ER protein GRP78, by penetrating the OMM and binding to ATAD3A at its N-terminal region [50]. This newly constituted mitochondria-ER tethering complex induces cell invasion in breast and colon cancer [50, 51]. ATAD3A also interacts with OMM and ER-resident proteins, including MFN2, dynamin-related protein 1 (Drp1), and BiP via the cytosolic protein WASF3 [52]. Instead of the above-discussed protein tethers, MAMs harbor a wide variety of regulatory proteins. TG2 modulates Ca^{2+} flux and protein composition through interaction with GRP75 [53].

For obtaining a more comprehensive knowledge of proteins in maintaining ER-mitochondria contacts, identification of additional tethers or spacers is essential. Further studies related to single-protein ablation should evaluate whether the activity or the localization of MAMs is the proper method for identification of cooperating protein complexes.

3. The MAM-Mediated Regulation of Cellular Homeostasis in the Cardiovascular System

MAMs participate in various cellular processes, such as calcium homeostasis, lipid metabolism, mitochondrial physiology, mitophagy, ER stress, and inflammation [54]. The proteins enriched in the cardiomyocyte MAMs and their role in MAM-regulated processes are shown in Figure 3. The BAP31-Fis1 complex, PTPIP51-VAPB complex, MFN1/2 complex, IP3R-GRP75-VDAC1 complex, and SERCA-

TMX1 were involved in the cardiovascular system. The detailed functions of these complexes were discussed in the following sections.

4. Calcium Transfer

Ca²⁺ transfer between organelles seems to affect both the heart and the vascular system [25, 55]. During ischemia and reperfusion, mitochondria calcium increases accompanied with mitochondrial permeability transition pore (mPTP) activation. Sarcoplasmic reticulum (SR), formed by ER, is a membrane-bound structure existing in muscle cells (myocardium and skeletal muscle), similar to ER in other cells [28]. The main function of SR is to store Ca²⁺. SR releases Ca²⁺ in response to electrical stimulation or pharmacological activation of RyR and increases mitochondrial Ca²⁺ level [56]. Ca²⁺ is free to enter the outer mitochondrial membrane with the aid of VDAC1. However, the inner mitochondrial membrane is not permeable, and calcium can enter the inner mitochondrial membrane only through a mitochondrial calcium uniporter (MCU) channel [30]. Therefore, MCU may have a marked impact on cardiac myocyte metabolism and function.

Ca²⁺ transmission from the ER to mitochondria is involved in mitochondrial apoptosis and energy generation with the aid of MAMs (Figure 2(a)). IP3R3-GRP75-VDAC1 complex is the main channel responsible for Ca²⁺ release from the ER to mitochondria [30]. IP3R1 forms a high concentration of Ca²⁺ in the vicinity of ER. The VDAC1 functions as a Ca²⁺ uptake channel in the OMM. GRP75 connects two channels through their cytosolic domains to form VDAC1/GRP75/IP3R1 channel complex [25]. The IP3R3-GRP75-VDAC1 complex also acts as a molecular scaffold for other calcium-handling players (Sig-1R, BiP, Bcl-2, and IRBIT), which are essential for the precise regulation of the calcium signaling through the IP3R3-GRP75-VDAC1 axis at the MAM (Figure 2(a)) [57, 58]. The increased level of IP3R expression has been observed in cardiac hypertrophy, failing myocardium, atrial fibrillation, ischemic dilated cardiomyopathy, and hypertension, suggesting its contribution to the development of cardiac hypertrophy [31, 32]. Additionally, IP3Rs could modulate excitation-contraction coupling both in ventricular and atrial cardiomyocytes [33]. Sig-1R maintains the stability of IP3R to ensure appropriate Ca²⁺ signaling between the ER and mitochondria [34]. Interaction of VAPB with PTPIP51 facilitates ER-mitochondria Ca²⁺ exchange (Figure 2(a)).

RNA-dependent protein kinase- (PKR-) like ER kinase (PERK) as a key ER stress protein is involved in calcium regulation, the maintenance of ER morphology, and MAM construction [59]. In addition, calnexin (CNX), which is involved in protein folding, interacts with ER calcium pumps. Deficiencies in these proteins cause obvious reduced mitochondrial Ca²⁺ import and impairment in Ca²⁺ dynamics [60]. The homeostasis of mitochondria Ca²⁺ is closely related with mitochondrial ATP production [61]. Excess transfer of calcium from ER to mitochondria induces mitochondrial Ca²⁺ overload and oxidative stress [62]. On the contrary, when the ER-mitochondria interaction is weak-

ened, excess calcium will release to the cytosol, leading to cytosolic Ca²⁺ wave. Recently, transient receptor potential cation channel (TRPM8) was identified as a compartment in the maintenance of cellular and mitochondrial Ca²⁺ in the vascular smooth muscle (VSMC) cells [63]. Activation of TRPM8 relieved mitochondrial respiratory dysfunction and excess ROS generation induced by angiotensin II by preserving mitochondrial Ca²⁺-dependent PDH activity, thus lowering blood pressure in cold or in angiotensin II-induced hypertensive mice [63]. However, the exploration of other TRP channels in MAM responsible for calcium transportation from ER to mitochondria remains to be further illustrated.

5. Lipid Synthesis and Exchange

Lipid molecules are involved in multiple cellular processes, such as cell membrane formation, cell signaling transduction, and synaptic transmission [64, 65]. While ER has a paramount role in lipid synthesis, other organelles' assistance is essential since several of the key enzymes are located on the membrane of organelles, such as mitochondria [66]. MAMs tethering proteins involved in phospholipid synthesis and transport include diacylglycerol O-acyltransferase 2 (DGAT2), fatty acid CoA ligase 4 (FACL4), phosphatidylethanolamine N-methyltransferase 2 (PEMT2), cholesterol acyltransferase/sterol O-acyltransferase 1 (ACAT1/SOAT1), and PSS1 and PSS2 with an ascribed function as a platform for lipid biosynthesis and exchange (Figure 2(b)) [65]. FACL4 is considered one of the most reliable MAM markers and is responsible for synthesizing triacylglycerol [67]. ACAT1, as another mitochondrial enzyme related to lipid metabolism, catalyzes the cholesteryl ester formation from free cholesterol, maintaining the dynamic balance between membrane-bound and cytoplasmic lipid droplet stored cholesterol [68]. MAMs are identified as cholesterol-rich membranes characterized by the sterol-interacting protein caveolin. MAM-associated caveolin-1 (CAV1) is involved in cholesterol efflux through its interaction with VDAC2, and silencing CAV1 in liver MAM leads to aberrant intracellular free cholesterol accumulation, as well as the reduced physical extension and integrity of MAM (Figure 2(b)) [69]. Ablation of the CAV1 gene aggravates cardiac dysfunction and decreases survival in mice exposed to myocardial ischemia [70]. Moreover, inhibition of CAV1 and *ApoE* in mice increased protection against atherosclerotic lesions compared to *ApoE*^{-/-} mice [71].

Additionally, MAM-enriched proteins induce the formation of the main structural component of biological membranes, phosphatidylcholine, PE, and phosphatidylserine. Phosphatidylserine is first synthesized by PSS1 and PSS2 in the MAM, after which it is transferred to the tightly connected mitochondria via the MAMs' lipid transfer tethering ORP5/8-PTPIP51 [72]. It is converted into phosphatidylethanolamine (PE) in the inner mitochondrial membrane by a decarboxylase. The newly generated PE is then transferred from the mitochondria, where it is methylated by the MAM-enriched PEMT2 to generate phosphatidylcholine (PC), a major component of the cell membrane. PC must

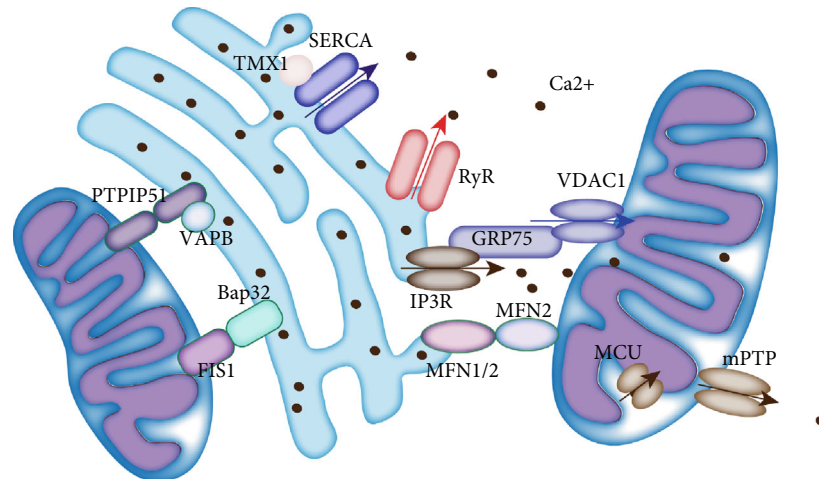


FIGURE 3: Components of MAMs in the cardiovascular system. Graphic representation of the proteins that are part of the MAMs in the cardiovascular system.

be transferred back to mitochondria once again since it is a component of the mitochondrial membrane. The phospholipid acids are synthesized in ER and transferred to mitochondria to modify cardioprotective mitochondrial cardiolipin, which is necessary for stability and activity of mitochondrial Ca^{2+} uniporter (Figure 2(b)) [73]. The level of cholesterol esters, PEs, and triacylglycerols are closely related to cardiovascular diseases. MAMs are also involved in the production of ceramide, a bioactive sphingolipid that is important for regulating cell growth arrest, differentiation, apoptosis, and inflammation.

The changes in MAM-maintaining proteins affect lipid anabolism. The HDL cholesterol and phospholipids have shown to be significantly elevated in ORP8-depleted mice [74]. Additionally, primary hepatocytes with ORP8 deficiency produce nascent HDL particles, suggesting changed HDL biosynthesis [74]. *ATAD3* gene cluster deletions in human fibroblasts perturbed cholesterol and lipid metabolism [53]. Human MFN2 exerts antiatherogenic properties in a rabbit model of atherosclerosis, while MFN2 overproduction leads to reduced VSMC proliferation/hyperplasia and diminished plaque progression [75]. PACS2 depletion diminishes the levels of the fatty acid metabolism enzymes PSS1 and FAACL4 in human skin melanoma cells [76]. Thus, PACS2 might be a promising therapeutic target for atherosclerosis by having an important role in oxidized low-density lipoprotein- (OxLDL-) induced EC apoptosis, perturbing MAM formation and mitochondrial Ca^{2+} elevation.

6. MAM Modulates ER Stress

ER stress occurs when the misfolded proteins aggregate in the lumen and the homeostasis of ER is disrupted [77]. ER stress is mediated by the ER-localized sensor protein kinase PERK, ATF6, and IRE1 α , which are maintained in an inactive form by GRP78 [78]. GRP78 is upregulated in the heart under multiple cardiac pathological conditions, such as dilated or ischemic cardiomyopathy. The activation of these proteins triggers an ER-specific UPR, which is strongly induced by

myocardial ischemia. ER stress signaling is modulated by MAM-tethering proteins since the activity of PERK is repressed by MFN2 by binding (Figure 2(c)) [79]. PERK is involved in the maintenance of the mitochondria-ER contacts and enhancement of the ROS-induced mitochondrial apoptosis. Once MFN2 is depleted, PERK is activated, and the PERK-EiF2 α -ATF4-CHOP pathway is enhanced (Figure 2(c)) [80]. Studies have suggested that ATF6 interacts with the tethering protein VAPB to suppress the UPR directly. ATF6 transcription is attenuated by VAPB overexpression in HEK293 and NSC34 cells [78]. IRE1 α accumulation in MAMs either leads to cell survival by splicing the *Xbp1* mRNA or cell death induction by promoting mitochondrial Ca^{2+} overload (Figure 2(c)) [78]. Ubiquitylation of IRE1 α at MAM could hinder ER stress-induced apoptosis [81]. Cardiac-specific *Xbp1* knockout mice (cKO) exhibited a significant increase in myocyte death and more profound pathological remodeling in cKO mice, thus suggesting that induction of *Xbp1* is necessary to protect the heart from ischemia/reperfusion (I/R) injury *in vivo*. In addition, depletion of other MAMs, such as PACS2, Sig-1R, MFN2, or CypD triggers ER stress by disrupting the ER-mitochondria communication. In contrast, mitochondria-ER contacts could also be modulated by the ER stress proteins. The ER-mitochondria contacts mediated by an initial ER stress enhance mitochondrial ATP production and Ca^{2+} uptake, thus leading to cellular adaptation to ER stress.

6.1. Regulation of Oxidative Stress. Under normal conditions, ROS is produced at physical levels, which is necessary for the maintenance of cellular homeostasis [82]. The production of excessive ROS, especially mitochondrial ROS (mtROS), can lead to oxidative damage to proteins, lipids, and DNA, which eventually leads to CVD [83]. MAM-mediated excessive Ca^{2+} transfer is reported to promote mtROS generation. For instance, diabetes promotes the formation of MAMs in podocytes, resulting in elevation of Ca^{2+} transfer from the ER to mitochondria, finally leading to mtROS overgeneration. However, MAM formation suppression induced by

FUNDC1 depletion alleviated mtROS production. These studies confirmed the relationship between MAM alterations and mtROS excess (Figure 2(d)) [31]. Also, several Ca^{2+} channel regulators in MAMs were found to regulate Ca^{2+} and MAM-dependent mtROS generation. For instance, MAMs highly enriched ER representative oxidoreductases, oxidoreductin-1 α (Ero1 α), and endoplasmic reticulum resident protein 44 (ERp44) can trigger the excess production of mtROS [84]. Mechanically, Ero1 α induces IP3R1 oxidation, leading to the dissociation of ERp44 from IP3R1, thereby enhancing the transfer of Ca^{2+} from the ER to mitochondria, contributing to excess mtROS production [85]. Selenoprotein N (SEPN1), a type II transmembrane protein of the ER, is enriched in MAMs and senses luminal calcium with its EF-hand domain [86]. When ER calcium is consumed, SEPN1 regulates ER calcium supplements mediated by the SERCA, protecting cells from ER stress. SEPN1 also resists oxidation elicited by Ero1 α , leading to the inactivation of SERCA. SEPN1 depletion triggers decreased ER-mitochondria contacts, reduced organelle Ca^{2+} content, and damaged OXPHOS [86].

Glutathione peroxidase 8 (GPX8), another type II transmembrane protein, also localized at MAMs, has a role in the modulation of Ca^{2+} dynamics [87]. In particular, GPX8 overexpression causes a decreased ER calcium coupled with a reduction of the ER-mitochondria calcium flux [88]. ER chaperones and folding assistants modulate cell metabolism and survival by controlling ER-mitochondria calcium flux. MAMs could also regulate the production of mtROS via DsbA-L and p66Shc [89]. DsbA-L, a multifunctional protein, is localized in the mitochondrial matrix, ER, and the MAM fraction, which is also closely related to the production of mtROS. The positive regulation of p66Shc in mtROS production and mitochondrial fission was well established and largely dependent on Ser36 phosphorylation. Notably, p66Shc phosphorylation also initially translocates p66Shc to the MAM fraction, therefore participating in mtROS production [90]. Further analysis revealed that the transfer of p66Shc to the MAMs correlates well with the production of mtROS (Figure 2(d)).

In summary, these findings imply that MAMs have a key role in the maintenance of the mitochondrial redox state and, consequently, in the homeostasis of cellular redox. However, the detailed function of MAMs in ROS excess production and its function in the occurrence and progression of CVD are not fully understood and need to be further investigated.

7. MAM Regulates Mitochondrial Physiology

In addition to the modulation of mitochondrial Ca^{2+} transport, MAM also affects mitochondrial physiology, including mitochondrial bioenergetics, dynamics, and mitophagy (Figure 2(e)). Since the heart is an energy-hungry organ and heart muscle cells are rich in mitochondria, the intact mitochondrial homeostasis is essential for the heart functions such as contractile function and cardiomyocyte metabolism, and the dysfunction of mitochondrial dynamics ultimately results in various CVDs. Mitochondrial dynamics include mitochondrial fission, fusion, and motility.

7.1. Mitochondrial Fission. During fission, Drp1 forms a helix around mitochondria that constricts and divides the mitochondrion into two parts after it is recruited to the OMM. The recruitment of Drp1 is dependent on its receptors, such as Fis1, mitochondrial fission factor (Mff), and mitochondrial dynamics proteins of 49 and 51 kDa (MiD49/MiD51), which are localized at the ER-mitochondria interface before mitochondrial fission (Figure 2(e)) [91]. The binding of Drp1 to F-actin *in vitro* stimulates the oligomerization and GTPase activity of Drp1, subsequently enabling Drp1 to spiral around the precontracted mitochondria, thus mediating their fission [92]. As a new mitochondrial receptor for Drp1, FUNDC1 promotes mitochondrial fission by interacting with the ER-resident protein calnexin in response to hypoxia [32]. However, even in the absence of Drp1, mitochondrial constriction can also form in the vicinity of mitochondria-ER contacts, implying that ER tubules may precede mitochondrial fission and define the position of mitochondrial division sites. Mice with a Drp1 mutation develop cardiomyopathy along with spotty calcifications in heart tissue [93]. Other proteins involved in mitochondrial fission regulation, such as inverted formin 2 (INF2), syntaxin 17 (STX17), and Rab32, were also detected at the MAM. For instance, INF2 launches mitochondrial constriction and division through binding, actin-nucleating protein Spire, Spire1C (Figure 2(e)) [94]. STX17 1 induces mitochondrial fission by determining Drp1 localization and activity. [93]. Mechanistically, decreasing MAM formation reduces the Ca^{2+} concentrations in both mitochondria and cytosol. Decreasing intracellular Ca^{2+} levels can repress the binding activity of cAMP response element-binding protein (CREB) to the *Fis1* promoter, thus inhibiting *Fis1* expression and mitochondrial fission. Upregulation of dynamin-related protein 1 (Dnp1), a fission protein, leads to fragmentation of mitochondria and heart ischemia. The formation of proapoptotic complex with MFN2 and Bax on the OMM is accompanied by the mPTP opening, cytochrome c (Cyto C) release, mitochondrial fragmentation, and cardiomyocyte apoptosis induction [95]. Inhibition of Dnp1 may protect cardiac mitochondria from fragmentation and prevent apoptosis.

7.2. Mitochondrial Fusion. Mitochondrial fusion is mainly modulated by outer mitochondrial membrane protein MFN and the IMM protein optic atrophy 1 (OPA1). MFN2 promotes mitochondrial tethering and mitochondrial fusion [96]. *MFN2* null hearts in adult mice showed better recovery from ischemia/reperfusion injury compared to *MFN2*-floxed controls [97]. Besides, MFN2 tethering with the mitochondrial ubiquitin ligase MITOL regulates mitochondrial dynamics (Figure 2(e)) [98]. Mitochondrial fusion facilitates the content exchange between mitochondria and restores impaired mitochondria. A recent study proposed that the fission and fusion processes initiate at the same ER-mitochondria contact site for the maintenance of mitochondrial morphology in response to external insults and metabolic cues, such as the nutrient availability, while MFNs also accumulate at the MAMs where fusion occurs [99]. However, it remains unclear how the positions of

mitochondrial fusion sites are determined. Both membrane fission and fusion are considered to be promoted by the specialized lipid environment of the MAM [100]. In addition, the high Ca^{2+} condition favors the initiation of fission and fusion. Moreover, it is still unclear whether interrupted ER-mitochondria contacts cause mitochondrial elongation or mitochondrial fragmentation. A previous study mentioned reduced mitochondrial and cytosolic Ca^{2+} levels in response to decreased MAM formation; decreased intracellular Ca^{2+} concentration repressed Fis1 expression and mitochondrial fission, leading to mitochondrial elongation [101]. In contrast, Tian et al. observed increased cytosolic Ca^{2+} levels in response to defective ER-mitochondria contact, indirectly activating Drp1 by means of activating calcineurin phosphatase and subsequently leading to mitochondrial fragmentation [93]. Although the mechanism for this contradiction remains unclear, we suppose the integrity degree of MAMs may be a relevant factor. Consequently, further investigations should focus on the distance between the ER and mitochondria for a better understanding of the relationship between alterations in mitochondrial morphology and ER-mitochondria contact.

7.3. Mitochondrial Motility. The mitochondria are transferred to satisfy local energy demands and Ca^{2+} buffering demands. The transportation along microtubules is associated with mitochondrial Rho GTPase 1 (MIRO1) and MIRO2 [102]. The relation of MIRO1/2 in the involvement of mitochondria motility is supported by previous studies [103]. However, due to the low calcium affinity of MIRO1/2, the binding requires a high Ca^{2+} concentration, making MAMs an ideal site for mitochondria redistribution [104]. Also, excess ER-mitochondria contact and Ca^{2+} transfer may result in defects in axonal mitochondrial transport. Microproteins, Ca^{2+} -sensitive GTPases localized on the OMM, interact with the TRAK adaptors and dynein/kinesin motors for the regulation of microtubule-dependent transport of the mitochondria [105]. The motor protein KIF5B was found to actively deliver mitochondrial DNA (mtDNA) nucleoids promoted by ER-mitochondria contacts via mitochondrial dynamic tubulation [106]. Mic60 on the mitochondrial inner membrane seems to link mitochondrial nucleoids to the mitochondrial outer membrane protein Miro1 and KIF5B at MAMs [107]. Such active transportation is an essential mechanism for the proper distribution of nucleoids in the cell's peripheral zone.

8. MAMs and Autophagy

MAMs are a crucial compartment for the induction and execution of autophagy. Many autophagy-related gene (ATG) proteins are enriched at MAMs, including ATG14 (autophagosome marker), ATG2/5 (autophagosome-formation marker), double FYVE domain-containing protein 1 (DFCPI, a platform for autophagosome formation), Beclin1, and VPS15/34. Moreover, TOM40/70 directs ATG2A to MAMs to mediate phagophore expansion (Figure 2(f)) [108]. On the MAMs, ATG2A directs the delivery of ATG9-vesicle to stimulate phagophore expansion and effi-

cient autophagic flux (Figure 2(f)) [109]. Impaired ER-mitochondria connection induced by PACS2 and MFN2 knockdown efficiently inhibits the formation of ATG14 puncta. Also, the formation of autophagosomes could be modulated by promyelocytic leukemia protein (PML), a tumor suppressor, localized at the MAMs by regulating the activity of the AMPK/mTOR/ULK1 pathway via affecting the transport of calcium ions from the ER to mitochondria [110]. Mitophagy removes impaired and dysfunctional mitochondria. Mitophagy occurs at the MAM site among species [111]. The mitophagy process is composed of the following six steps: autophagy induction, the isolation membrane nucleation (also known as the phagophore), the isolation membrane expansion, the autophagosome formation, the autophagosome fusion with a lysosome to form an autolysosome. Two major pathways were reported to be involved in mitophagy induction: (1) Parkin-dependent pathways, composed of Parkin and PTEN-induced putative kinase1 (PINK1) (Figure 2(f)), and (2) adaptor-dependent mitophagy, mediated directly by Bcl2 interacting protein 3 (BNIP3), Bcl2 interacting protein 3 like (BNIP3L/NIX), and FUNDC1, which possess an LC3 interacting region (LIR) and interact with light chain 3 (LC3) to mediate mitophagy (Figure 2(f)) [112–114]. Both mitophagy pathways were accordant with MAMs. Mitophagy protects myocardial cells from I/R injury. I/R reduces mitophagy and stimulates apoptosis in cardiomyocytes. An appropriate increase in mitophagy potentially alleviates I/R-induced cardiomyocyte apoptosis. Simultaneously, mitophagy may also have a negative role in I/R injury [114]. Inhibition of mitophagy potentially protects the myocardium against I/R injury, reduces cardiomyocyte apoptosis, improves cardiac function, and protects mitochondrial integrity.

8.1. PINK/Parkin-Mediated Mitophagy. The PINK1 and Parkin pathway, one of the best known and most well-studied pathways of mitophagy, is implicated in the progression of Parkinson's disease [113]. Under physiological conditions, PINK is continuously delivered to the mitochondria and degraded by matrix processing peptidases (MPPs). The degraded product is then incised by presenilin-associated rhomboid-like (PARL). Then, cleaved PINK is transferred to the cytoplasm for eventual degradation in lysosomes [115]. Under pathological conditions, the cleavage of PINK is blocked due to defective mitochondrial function. The non-cleaved PINK accumulates on the mitochondria's outer membrane through a process of translocation of the OMM protein to the outer membrane (TOM). In addition, the aggregation of PINK on the OMM can also be affected by the level of mitochondrial pyruvate by facilitating the direct interaction between PINK1 and TOM [114]. The accumulation of PINK on the OMM leads to the phosphorylation of ubiquitin, thereby recruiting Parkin. Subsequently, PINK phosphorylates and activates Parkin on the OMM and then activates Parkin polyubiquitinate proteins, such as VDAC1 and p62/SQSTM1. The binding of ubiquitinated substrates and autophagic membrane proteins, LC3 via LIR motif, promotes recruitment of the autophagosomal membrane around the mitochondria. The normal signaling pathway of

PINK/Parkin-mediated mitophagy is a fundamental process for the homeostasis of intracellular mitochondria, and defects in this process may lead to many diseases, such as CVD [116]. A previous study reported that PINK1 and Parkin were upregulated and enhanced Parkin transfer and activation during I/R injury accompanied with BNIP3 upregulation and FUNDC1 downregulation [112]. *PINK1* knockout mice were more susceptible to overload-induced heart stress and consequent heart failure compared to wildtype mice.

BECN1, a key component of the class III phosphatidylinositol 3-kinase (PtdIns3K) complex, is present in MAMs, where it enhances the ER and mitochondria contacts and initiates the formation of autophagosome precursors [113]. Thus, PINK/Parkin-dependent mitophagy initiates at the site of MAMs. Loss of PINK inhibits the accumulation of BECN1 at MAMs, which is PARK independent, thus suggesting a novel function of PINK in regulating mitophagy. BECN1 is aberrantly expressed or posttranslationally modified in many heart diseases, including ischemia/reperfusion, myocardial infarction, cardiac hypertrophy, and heart failure [117]. BECN1 deregulation leads to heart disease development through altered myocardial autophagy and apoptosis [110]. Furthermore, Glycoprotein 78 (Gp78), a MAM-located ubiquitin ligase (E3), has been reported to be involved in mitophagy. The existing evidence implies that the core proteins related to PINK/Parkin-mediated mitophagy are enriched in MAMs and are responsible for the regulation of MAMs' integrity and function. As a driver of Parkin-mediated mitophagy, AMPK has a protective role in cardiac functions [110]. The hypoxic injury and myocardial infarction (MI) are associated with increased RIPK3 expression, leading to inactivation of AMPK.

8.2. FUNDC1-Mediated Mitophagy. In mammalian cells, FUNDC1, a highly conserved protein, is involved in the receptor-mediated mitophagy pathway [118]. During hypoxia, the LC3-binding regions (LIR) domain of FUNDC1 located in the mitochondrial outer membrane recruits LC3 to induce mitophagy. FUNDC1-related mitophagy is modulated by a variety of stress factors and cellular proteins [119]. Under normoxic conditions, FUNDC1 can be phosphorylated by Src and casein kinase 2 (CK2), respectively, inhibiting the binding with LC3 to initiate autophagy [120]. During hypoxic conditions, FUNDC1 is dephosphorylated by the mitochondrial protein phosphatase PGAM5, resulting in the binding of FUNDC1 to LC3 to induce the formation of autophagosomes [121]. ULK1, a Ser/Thr kinase, mediates the formation of early autophagosomes and is closely associated with FUNDC1-dependent mitophagy [122]. ULK1 expression level is increased and recruited to the fragmented mitochondria under hypoxia or treatment with FCCP. In addition, transferred ULK1 interacts with FUNDC1 to promote the phosphorylation FUNDC1, thereby initiating autophagy [123]. MARCH5, a mitochondrial E3 ligase, is involved in the regulation of mitophagy; MARCH5 can directly interact and degrade FUNDC1 by inducing its ubiquitination [124].

FUNDC1-mediated mitophagy is confirmed as directly related to MAMs via binding to IP3R2 to mediate IP3R-

dependent Ca^{2+} signaling from ER to mitochondria and cytoplasm [125]. When FUNDC1 expression level is decreased, the intracellular Ca^{2+} decreases, and Fis1 expression level is inhibited through Ca^{2+} -sensitive CREB, leading to mitochondrial dysfunction [126]. In addition, the reduced expression level of FUNDC1 impaired the interaction between the ER and mitochondria and reduced the protein abundance in MAMs. Under normoxic conditions, the accumulation of FUNDC1 in MAMs remains low in content, while under hypoxia conditions, FUNDC1 substantially aggregates in MAMs.

CNX may be indispensable during this process. The N terminus of CNX directly binds to the hydrophilic domain of FUNDC1. However, due to the localization of the N terminus of CNX in the lumen of the ER, there must exist an unknown protein that mediates the interaction between CNX and FUNDC1 [127]. Under hypoxic conditions, CNX depletion represses FUNDC1 translocation to the MAMs, further confirming the vital importance of CNX in the translocation of FUNDC1. Despite the requirement of further study on the function of MAMs in FUNDC1-mediated mitophagy, existing evidence suggests that MAM offers a platform for FUNDC1 to exert its biological functions. FUNDC1 is required for cardiac ischemia/reperfusion injury-activated mitophagy. Hypoxic pretreatment induces FUNDC1-dependent mitophagy in platelets and reduces I/R-induced heart injury [128]. Another research also mentioned that MAM-localized STX17 could bind to ATG14, an autophagosome marker, and transfer it to the MAM until the completion of autophagosome formation. This supports the idea that the autophagosome forms at MAMs.

9. Other Functions of MAMs

9.1. Apoptosis. Apoptosis is a tightly regulated, cellular deletion process found in various cardiovascular diseases, such as myocardial infarction, reperfusion injury, and heart failure [42]. Excess transfer of calcium leading to calcium overload can induce cell apoptosis. Specifically, mitochondrial calcium overload induces mPTP opening, IMM permeabilization, mitochondrial depolarization, and finally cell apoptosis. The binding between Fis1 to BAP31 contributes to ER-mitochondria tethering in the process of apoptosis [129]. Also, the formation of the Fis1-BAP31-tethering complex can be induced by exogenous inducers of apoptosis [43]. Consistent with the previous data, cell apoptosis-related to Fis1 overexpression is associated with the excessive ER-mitochondria Ca^{2+} transfer [130].

The relationship between cell apoptosis and mitochondrial dynamics is not fully understood. After the induction of the cell apoptosis process, massive Drp1 is recruited to the OMM, leading to an increase of mitochondrial network fragmentation [93]. In line with this data, a dominant-negative mutation in Drp1 inhibits cell apoptosis. Contrary, Drp1 overexpression protects against Ca^{2+} -mediated apoptosis. Therefore, the function of Drp1 in Ca^{2+} -induced apoptosis is still controversial. In addition, Drp1 induces cell apoptosis by facilitating oligomerization of Bax under apoptotic conditions [101]. The mechanism of Bax in apoptosis

is similar to Drp1 [92]. The speculation that MAMs are involved in this programmed cell death is confirmed by the fact that Bax oligomerization on the OMM is conducted by key lipid effectors of Bax between ER and mitochondria [131].

Knowing that Bax and MFN2 are colocalized in foci during apoptosis, it is speculated that MFN2 functions in OMM permeabilization and in response to apoptotic stimuli [52]. A recent study suggested an induction of Drp1 SUMOylation in response to the activation of apoptosis, during which cytochrome c release is a requisite for the process [91]. The MAM contact sites stabilized by SUMOylated Drp1 act as a place for mitochondrial constriction, calcium flux, cristae remodeling, and cytochrome c release. SUMOylated Drp1 can lead to mitochondrial dysfunction contributing to cardiac hypertrophy. Taken together, these data suggested a complicated network for apoptosis, mitochondrial dynamics, and MAMs, which deserves further studies.

9.2. Inflammation. Inflammation has been implicated to be involved in one of the MAM-related pathways [132]. As a cytosolic multiprotein complex, the inflammasome is responsible for the activation of inflammatory responses. The NLRP3 complex is currently the only known MAM-related inflammasome complex [133]. A wide variety of stimuli can be used to activate NLRP3. However, the exact activation mechanism remains unclear.

NLRP3 activation is implicated in mitochondrial dysfunction, the release of mtROS and mtDNA into the cytosol. In addition, enhanced NLRP3 activation is accompanied by increased damaged and dysfunctional mitochondria induced by the inhibitors of mitophagy [134]. NLRP3 activation is consistent with the shift of thioredoxin-interacting protein (TXNIP) from cytosolic thioredoxin 1 to the NLRP3 inflammasome on the MAM. Interestingly, MAM-enriched VDAC is indispensable for inflammation since the elimination of VDAC1/2 abrogates the formation of the inflammatory body. Rats with myocardial infarction exhibited a marked increase of VDAC1 in both ventricular and atrial tissues. VDAC1 inhibition can alleviate excessive fibrosis in the atrial myocardium, which may have important therapeutic implications [112].

Besides the functions in NLRP3 activation, mitochondria may also participate in inflammasome assembly, because of the contact of activated inflammasome with both mitochondria and MAMs. Furthermore, the contact between NLRP3 and mitochondria is mediated by at least three mitochondrial factors: mitochondrial antiviral-signaling protein (MAVS), MFN2, and cardiolipin. The physical interaction between MAVS and NLRP3 is required for NLRP3 inflammasome activation during viral infection [135]. Also, MFN2 directly binds to NLRP3 during viral infection. Cardiolipin is a mitochondrial inner membrane lipid, and has been shown to externalize and directly bind NLRP3; disruption of its expression is harmful for NLRP3 activation [136]. Overall, MAMs are closely associated with inflammation, and further studies are required to understand the mechanisms.

9.3. Antiviral Response. The relationship between MAMs and immune response has also been identified during RNA virus

infection. Viral infection induces host innate immune responses by activating transcription factors NF- κ B and IRF3 that modulate type-I interferons' expression level to inhibit viral replication. RIG-I is one of the retinoic acid-inducible gene- (RIG-) like receptors (RLRs) that detect virus intracellular dsRNA. Once the virus dsRNA is recognized, the cytoplasmic RIG-I translocates to MAMs and interacts with MAVS, activating NF- κ B and IRF3 pathways [137]. In addition, MAVS from the MAM can be targeted and cleaved by the viral NS3/4A protease to ablate innate immune signaling during HCV infection, implying that the RIG-I pathway function against HCV is likely coordinated by MAM-resident MAVS [138].

The stimulator of interferon genes (STING) was identified as a positive regulator of RIG-I-associated IFN- β signaling [137]. The complex of STING and RIG-I recruits MAVS-induced IRF3 phosphorylation and IFN production in response to RNA and DNA viruses. In addition, STING is a target for HCV-NS4B to block RIG-I-mediated activation of IFN- β production by blocking its interaction with MAVS. NS4B and STING are localized on ER and MAM [139]. MAM-resident factor Gp78 was also found to be involved in innate antiviral signaling by targeting MAVS during vesicular stomatitis virus (VSV) infection [140]. Still, the association between MAMs and antiviral response should be further studied to advance the understanding of the potential therapeutics in viral infections.

10. MAM Is Widely Involved in the Homeostasis Regulation of the Cardiovascular System

Once the mitochondrial membrane potential is inhibited or partially inhibited, the calcium kinetics during contraction is altered, accompanied by the enhanced reduction of shortening degree of cardiomyocytes. This result suggested the involvement of calcium transportation from SR to mitochondria in cardiac contraction. The dysregulation between the ER and mitochondria in the pathogenesis of CVD is gradually recognized. The effect of MAMs' dysfunction on CVD is probably due to the involvement of multiple pathways, including lipid metabolism disorders, aberrant calcium levels, activation of ROS and ER stress, mitochondria dysfunction and mitophagy, activation of inflammation response, apoptosis, and autophagy disorders (Figure 4).

Several key MAM-associated proteins affect the progression of CVD. Cardiac-specific *MFN2* knockout mice displayed cardiac hypertrophy and moderate diastolic dysfunction [141]. Under β -adrenergic stress conditions, the same mice showed obvious systolic dysfunction. Moreover, *MFN2* knockout mice displayed abnormal large and elongated mitochondria morphology and reduced SR and mitochondria contacts. In addition, deficiency in *MFN2* in cardiomyocytes resulted in the abnormal spatial distribution of mitochondria, low mitochondrial membrane potential, and reduced Ca^{2+} uptake [142].

The *FUNDC1* deficiency reduces the contact in ER and mitochondria [143]. *FUNDC1* knockout mice displayed diastolic and systolic dysfunction. Besides, these mice exhibited

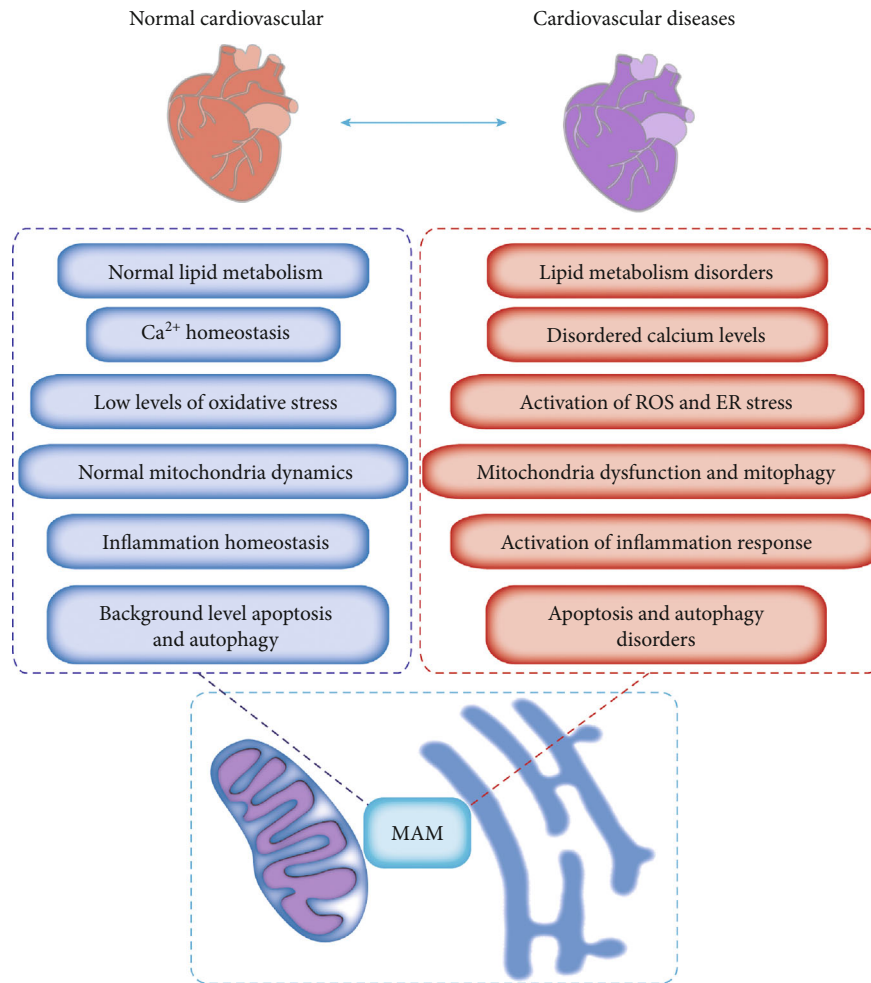


FIGURE 4: The alteration of MAM-mediated cellular functions in cardiovascular diseases. Major MAM-mediated abnormalities leading to CVD include lipid metabolism disorders, abnormal calcium levels, the activation of ROS and ER stress, the dysfunction of mitochondria and mitophagy, the activation of inflammation response, and the disorders of apoptosis and autophagy.

obviously lower early and late ventricular filling velocity ratio and decreased ejection fraction [126, 144].

The mitochondrial dynamics in myocardial tissue are an important aspect of cardiac function. *Drp1* knockout mice exhibited a lower beating rate in isolated cardiomyocytes [145]. The potential mechanism may be mitochondrial respiration defects, suppressed autophagy, and increased mitochondrial ROS production [143, 146]. Above all, the normal mitochondrial fission for a myocardial cell can be vital for energy supply. Therefore, cardiac-specific *Drp1* ablation mice led to decreased life span, diminished survival, cardiac hypertrophy, fibrosis, and reduced systolic function [93].

Mitochondrial damage, mPTP, and ER stress are considered as the main factors related to the reperfusion damage in I/R. Since MAMs modulate the calcium dynamics, it has a vital role in mediating the opening of mPTP and the damage in I/R. The CypD-GRP75-IP3R-VDAC complex inhibition improved hypoxia/reoxygenation injury in cardiomyocytes [147]. The hypoxia/reoxygenation process induced the increased interaction of CypD-GRP75-IP3R-VDAC complex and GSK3 β , leading to cell death. Moreover, GSK3 β inhibition induces cytosolic and mitochondrial calcium overload,

accompanied by reduced cell death and infarct size in reperfused hearts [148]. Due to the negative involvement of SERCA activity in cytosolic Ca²⁺, mitochondrial ROS overproduction, and activation of mitochondrial fission pathway in the myocardium, proteins that could modulate SERCA activity are associated with the susceptibility of the heart to I/R, such as TMX-1 and FUNDC1 [57]. Inhibition of SERCA2b activity in normal conditions by TMX1, a redox-sensitive oxidoreductase localized at MAMs, triggers enhanced ER-mitochondria contacts, thus preventing calnexin during homeostatic conditions.

Diabetic cardiomyopathy (DCM) is characterized by lipid accumulation in the cardiomyocytes and hypertrophy in the left ventricle. DCM is triggered by apoptosis and excessive ROS production, accompanied by the compensatory signaling pathway activation. Cardiac-specific PERK ablation prevents apoptosis in response to high glucose concentrations, which indicates the potential beneficial role of MAM in the prevention of DCM [59]. FUNDC1 contributes to mitochondrial dysfunction after Ca²⁺ increase in diabetes [32]. Additionally, AMPK aberration results in DCM, along with a deregulated number of FUNDC1-related MAMs in

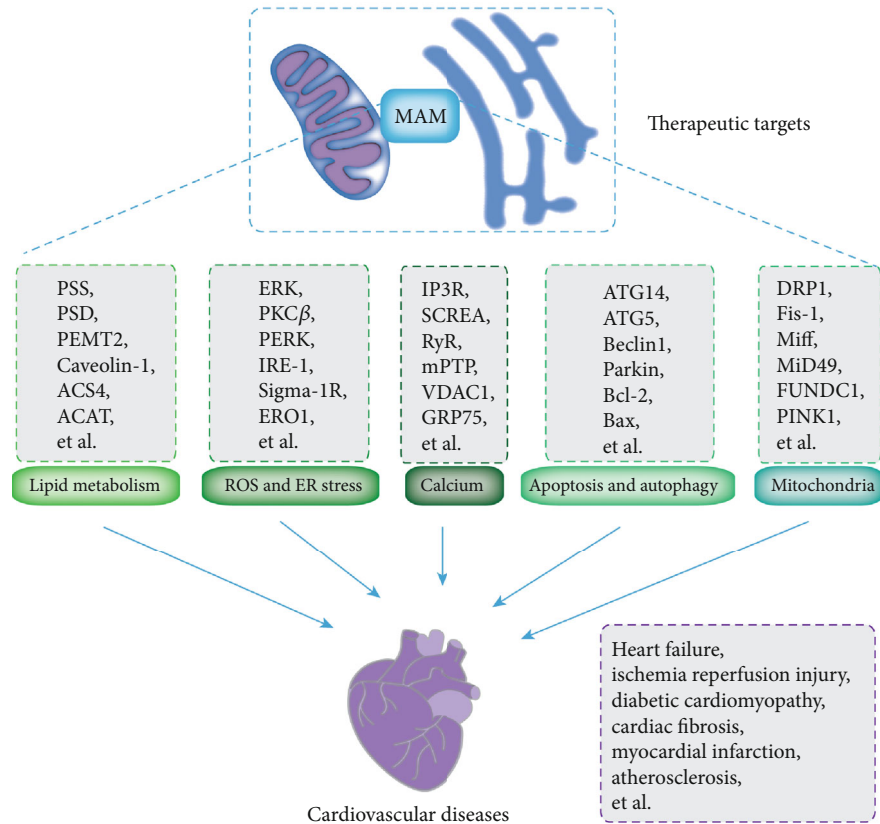


FIGURE 5: MAM-enriched proteins as potential new therapeutic targets for treatment of CVD-associated pathologies. MAM regulates some major cellular processes, including lipid metabolism, ROS, endoplasmic reticulum pressure, calcium homeostasis, apoptosis and autophagy, and mitochondrial function. The abnormality of these processes often leads to CVD. Notably, the key regulatory proteins of these processes can serve as potential therapeutic targets for CVD.

diabetic hearts due to the interaction between AMPK and MAMs in cardiomyocytes. Therefore, FUNDC1-related MAM modulation provides new insights into the treatment of DCM.

Heart failure (HF) is a progressive disorder of myocardial remodeling. The increased distance between the SR and mitochondria and diminished mitochondrial Ca^{2+} reuptake are the main characteristics of prohypertrophy induced by norepinephrine in cardiomyocytes [149]. The reduction of Ero1 activity sensitizes hearts to adrenalin, and prevents HF progression in response to hemodynamic overload *in vivo* [149]. Patients diagnosed with HF exhibit a reduced expression of FUNDC1 accompanied by a lower number of SR-mitochondria contacts [127]. FUNDC1 reduction in MAMs induces heart disease. Sig-1R is one of the fundamental proteins of MAMs in HF. Sig-1R inhibition promotes autophagy in cardiomyocytes under oxidative stress conditions [34]. Highly specific agonists of Sig-1R could modulate cardiomyocytes' contractility. In addition, Sig-1R activation represses hypertrophy and cardiomyocyte injury induced by angiotensin II. Sig-1R KO mouse displayed dysfunction and abnormal morphology of mitochondria as well as cardiac remodeling, resulting in contractile dysfunction. Recently, the interaction of desmin, VDAC, Mic-60 (a central component in mitochondrial contact sites of the cristae organizing system, MICOS), and ATP synthase were identified in

heart failure mice, implying the potential beneficial function of such complex in cardiac function.

11. Conclusion

In this study, we discussed the molecular structure of MAM and summarized its cellular functions. As a bridge between the endoplasmic reticulum and mitochondria, MAM is mainly involved in calcium homeostasis, lipid metabolism, mitochondrial dynamics, autophagy, apoptosis, and inflammation. Dysregulation of this process has been associated with the pathogenesis of CVD. These data further confirmed the potential use of MAM and related proteins as targets for CVD treatment.

It is important to understand the regulatory mechanisms and targeting proteins involved in the maintenance of MAMs' integrity to explore novel therapeutic targets for the prevention or treatment of heart-associated pathologies. For instance, as fluvoxamine has a high affinity towards Sig-1R, it has been used and tested for the treatment of heart failure and cardiac dysfunction in transverse aortic constriction models in both mice and rats [150]. Additionally, as an antioxidant, N-acetylcysteine was used to treat mitochondrial damage and muscle dysfunction, suggesting the involvement of ROS [151]. Chemical chaperones like 4-phenylbutyrate (PBA) and tauroursodeoxycholic acid can prevent and

reverse the established pulmonary arterial hypertension in two rodent disease models by inhibiting the disruption of the ER-mitochondria unit and reducing SR stress [151].

New and more effective therapies are urgently needed for CVD. MAM-related proteins and their inhibitors can directly affect the pathogenesis of CVD, which is of great significance for improving the survival of patients. Future studies should focus on screening new MAM-related protein inhibitors and exploring the possibility and potential of these inhibitors in the treatment of CVD from the molecular mechanism.

Data Availability

All data generated or analyzed in this study are available from the corresponding author on reasonable request.

Conflicts of Interest

The authors declare that they have no competing interests.

Authors' Contributions

Yang Yang and Yi Luan conceptualized and wrote the manuscript and created Figures 1–5. Ying Luan contributed to the writing of the manuscript. Qi Feng, Rui-Xia Yuan, and Xing Chen reviewed and modified the manuscript. All authors approved the final version of the manuscript.

Acknowledgments

This work was supported by the National Natural Science Foundation of China (No. 31900502), the Henan Medical Science and Technology Joint Building Program (Nos. LHGJ20190236, LHGJ20190223, LHGJ20190265, and LHGJ20190229), and the Science and Technology Research Project of Henan Province (No. 212102310194).

References

- [1] M. Amini, F. Zayeri, and M. Salehi, "Trend analysis of cardiovascular disease mortality, incidence, and mortality-to-incidence ratio: results from global burden of disease study 2017," *BMC Public Health*, vol. 21, no. 1, p. 401, 2021.
- [2] D. J. A. Jenkins, M. Dehghan, A. Mente et al., "Glycemic index, glycemic load, and cardiovascular disease and mortality," *The New England Journal of Medicine*, vol. 384, no. 14, pp. 1312–1322, 2021.
- [3] J. Hu, H. Xu, J. Zhu et al., "Association between body mass index and risk of cardiovascular disease-specific mortality among adults with hypertension in Shanghai, China," *Aging (Albany NY)*, vol. 13, no. 5, pp. 6866–6877, 2021.
- [4] M. Pecoraro, A. Pinto, and A. Popolo, "Mitochondria and cardiovascular disease: a brief account," *Critical Reviews in Eukaryotic Gene Expression*, vol. 29, no. 4, pp. 295–304, 2019.
- [5] H. E. Verdejo, A. del Campo, R. Troncoso et al., "Mitochondria, myocardial remodeling, and cardiovascular disease," *Current Hypertension Reports*, vol. 14, no. 6, pp. 532–539, 2012.
- [6] Y. Yang, H. Gao, H. Zhou et al., "The role of mitochondria-derived peptides in cardiovascular disease: recent updates," *Biomedicine & Pharmacotherapy*, vol. 117, p. 109075, 2019.
- [7] J. R. Koenitzer and B. A. Freeman, "Redox signaling in inflammation: interactions of endogenous electrophiles and mitochondria in cardiovascular disease," *Annals of the New York Academy of Sciences*, vol. 1203, no. 1, pp. 45–52, 2010.
- [8] E. Murphy, D. Bers, and R. Rizzuto, "Mitochondria: from basic biology to cardiovascular disease," *Journal of Molecular and Cellular Cardiology*, vol. 46, no. 6, pp. 765–766, 2009.
- [9] F. Forini, P. Canale, G. Nicolini, and G. Iervasi, "Mitochondria-targeted drug delivery in cardiovascular disease: a long road to nano-cardio medicine," *Pharmaceutics*, vol. 12, no. 11, p. 1122, 2020.
- [10] M. Rocha, N. Apostolova, A. Hernandez-Mijares, R. Herance, and M. V. Victor, "Oxidative stress and endothelial dysfunction in cardiovascular disease: mitochondria-targeted therapeutics," *Current Medicinal Chemistry*, vol. 17, no. 32, pp. 3827–3841, 2010.
- [11] T. Minamino, I. Komuro, and M. Kitakaze, "Endoplasmic reticulum stress as a therapeutic target in cardiovascular disease," *Circulation Research*, vol. 107, no. 9, pp. 1071–1082, 2010.
- [12] J. Hong, K. Kim, J. H. Kim, and Y. Park, "The role of endoplasmic reticulum stress in cardiovascular disease and exercise," *International Journal of Vascular Medicine*, vol. 2017, Article ID 2049217, 9 pages, 2017.
- [13] B. Ning, Q. Zhang, N. Wang, M. Deng, and Y. Fang, "β-Asarone regulates ER stress and autophagy via inhibition of the PERK/CHOP/Bcl-2/Beclin-1 pathway in 6-OHDA-induced Parkinsonian rats," *Neurochemical Research*, vol. 44, no. 5, pp. 1159–1166, 2019.
- [14] J. H. Joo, E. Ueda, C. D. Bortner, X. P. Yang, G. Liao, and A. M. Jetten, "Farnesol activates the intrinsic pathway of apoptosis and the ATF4-ATF3-CHOP cascade of ER stress in human T lymphoblastic leukemia Molt4 cells," *Biochemical Pharmacology*, vol. 97, no. 3, pp. 256–268, 2015.
- [15] X. Peng, Q. He, G. Li, J. Ma, and T. P. Zhong, "Rac1-PAK2 pathway is essential for zebrafish heart regeneration," *Biochemical and Biophysical Research Communications*, vol. 472, no. 4, pp. 637–642, 2016.
- [16] M. Yang, C. Li, S. Yang et al., "Mitochondria-associated ER membranes—the origin site of autophagy," *Frontiers in Cell and Development Biology*, vol. 8, p. 595, 2020.
- [17] A. M. English, M. H. Schuler, T. Xiao, B. Kornmann, J. M. Shaw, and A. L. Hughes, "ER-mitochondria contacts promote mitochondrial-derived compartment biogenesis," *The Journal of Cell Biology*, vol. 219, no. 12, 2020.
- [18] J. E. Vance, S. J. Stone, and J. R. Faust, "Abnormalities in mitochondria-associated membranes and phospholipid biosynthetic enzymes in the *mnd/mnd* mouse model of neuronal ceroid lipofuscinosis," *Biochimica et Biophysica Acta*, vol. 1344, no. 3, pp. 286–299, 1997.
- [19] P. Gao, W. Yang, and L. Sun, "Mitochondria-associated endoplasmic reticulum membranes (MAMs) and their prospective roles in kidney disease," *Oxidative Medicine and Cellular Longevity*, vol. 2020, Article ID 3120539, 21 pages, 2020.
- [20] K. Zhang, Q. Zhou, Y. Guo, L. Chen, and L. Li, "Mitochondria-associated endoplasmic reticulum membranes (MAMs) involve in the regulation of mitochondrial dysfunction and heart failure," *Acta Biochimica et Biophysica Sinica*, vol. 50, no. 6, pp. 618–619, 2018.
- [21] C. N. Poston, S. C. Krishnan, and C. R. Bazemore-Walker, "In-depth proteomic analysis of mammalian mitochondria-

- associated membranes (MAM),” *Journal of Proteomics*, vol. 79, pp. 219–230, 2013.
- [22] W. Yu, H. Jin, and Y. Huang, “Mitochondria-associated membranes (MAMs): a potential therapeutic target for treating Alzheimer’s disease,” *Clinical Science (London, England)*, vol. 135, no. 1, pp. 109–126, 2021.
- [23] S. Yang, R. Zhou, C. Zhang, S. He, and Z. Su, “Mitochondria-associated endoplasmic reticulum membranes in the pathogenesis of type 2 diabetes mellitus,” *Frontiers in Cell and Development Biology*, vol. 8, p. 571554, 2020.
- [24] M. Perrone, N. Carocchia, I. Genovese et al., “The role of mitochondria-associated membranes in cellular homeostasis and diseases,” *International Review of Cell and Molecular Biology*, vol. 350, pp. 119–196, 2020.
- [25] P. Gao, Z. Yan, and Z. Zhu, “Mitochondria-associated endoplasmic reticulum membranes in cardiovascular diseases,” *Frontiers in Cell and Development Biology*, vol. 8, p. 604240, 2020.
- [26] B. Lan, Y. He, H. Sun, X. Zheng, Y. Gao, and N. Li, “The roles of mitochondria-associated membranes in mitochondrial quality control under endoplasmic reticulum stress,” *Life Sciences*, vol. 231, article 116587, 2019.
- [27] A. Bassot, M.-A. Chauvin, N. Bendridi et al., “Regulation of mitochondria-associated membranes (MAMs) by NO/sGC/PKG participates in the control of hepatic insulin response,” *Cell*, vol. 8, no. 11, p. 1319, 2019.
- [28] L. Barazzuol, F. Giamogante, and T. Cali, “Mitochondria associated membranes (MAMs): architecture and physiopathological role,” *Cell Calcium*, vol. 94, article 102343, 2021.
- [29] H. Cheng, X. Gang, G. He et al., “The molecular mechanisms underlying mitochondria-associated endoplasmic reticulum membrane-induced insulin resistance,” *Frontiers in Endocrinology*, vol. 11, article 592129, 2020.
- [30] V. Basso, E. Marchesan, and E. Ziviani, “A trio has turned into a quartet: DJ-1 interacts with the IP3R-Grp75-VDAC complex to control ER-mitochondria interaction,” *Cell Calcium*, vol. 87, p. 102186, 2020.
- [31] S. Wu, Q. Lu, Q. Wang et al., “Binding of FUN14 domain containing 1 with inositol 1,4,5-trisphosphate receptor in mitochondria-associated endoplasmic reticulum membranes maintains mitochondrial dynamics and function in hearts in vivo,” *Circulation*, vol. 136, no. 23, pp. 2248–2266, 2017.
- [32] S. Wu, Q. Lu, Y. Ding et al., “Hyperglycemia-driven inhibition of AMP-activated protein kinase $\alpha 2$ induces diabetic cardiomyopathy by promoting mitochondria-associated endoplasmic reticulum membranes in vivo,” *Circulation*, vol. 139, no. 16, pp. 1913–1936, 2019.
- [33] G. Mo, X. Liu, Y. Zhong et al., “IP3R1 regulates Ca^{2+} transport and pyroptosis through the NLRP3/Caspase-1 pathway in myocardial ischemia/reperfusion injury,” *Cell Death Discovery*, vol. 7, no. 1, p. 31, 2021.
- [34] M. Ortiz-Rentería, R. Juárez-Contreras, R. González-Ramírez et al., “TRPV1 channels and the progesterone receptor Sig-1R interact to regulate pain,” *Proceedings of the National Academy of Sciences of the United States of America*, vol. 115, no. 7, pp. E1657–E1666, 2018.
- [35] T. Thoudam, C. M. Ha, J. Leem et al., “PDK4 augments ER-mitochondria contact to dampen skeletal muscle insulin signaling during obesity,” *Diabetes*, vol. 68, no. 3, pp. 571–586, 2019.
- [36] Y. Eura, N. Ishihara, T. Oka, and K. Mihara, “Identification of a novel protein that regulates mitochondrial fusion by modulating mitofusin (Mfn) protein function,” *Journal of Cell Science*, vol. 119, no. 23, pp. 4913–4925, 2006.
- [37] S. Y. Choi, P. Huang, G. M. Jenkins, D. C. Chan, J. Schiller, and M. A. Frohman, “A common lipid links Mfn-mediated mitochondrial fusion and SNARE-regulated exocytosis,” *Nature Cell Biology*, vol. 8, no. 11, pp. 1255–1262, 2006.
- [38] G. Mu, Y. Deng, Z. Lu, X. Li, and Y. Chen, “miR-20b suppresses mitochondrial dysfunction-mediated apoptosis to alleviate hyperoxia-induced acute lung injury by directly targeting MFN1 and MFN2,” *Acta Biochimica et Biophysica Sinica*, vol. 53, no. 2, pp. 220–228, 2021.
- [39] S. Han, P. Nandy, Q. Austria et al., “Mfn2 Ablation in the Adult Mouse Hippocampus and Cortex Causes Neuronal Death,” *Cell*, vol. 9, no. 1, 2020.
- [40] D. Sun, C. Li, J. Liu et al., “Expression profile of microRNAs in hypertrophic cardiomyopathy and effects of microRNA-20 in inducing cardiomyocyte hypertrophy through regulating GeneMFN2,” *DNA and Cell Biology*, vol. 38, no. 8, pp. 796–807, 2019.
- [41] H. Y. Yu, Y. H. Guo, and W. Gao, “Mitochondrial fusion protein Mfn2 and cardiovascular diseases,” *Sheng Li Ke Xue Jin Zhan*, vol. 41, no. 1, pp. 11–16, 2010.
- [42] B. Wang, M. Nguyen, N. C. Chang, and G. C. Shore, “Fis1, Bap31 and the kiss of death between mitochondria and endoplasmic reticulum,” *The EMBO Journal*, vol. 30, no. 3, pp. 451–452, 2011.
- [43] R. Iwasawa, A. L. Mahul-Mellier, C. Datler, E. Pazarentzos, and S. Grimm, “Fis1 and Bap31 bridge the mitochondria-ER interface to establish a platform for apoptosis induction,” *The EMBO Journal*, vol. 30, no. 3, pp. 556–568, 2011.
- [44] C. Hartmann, Y. A. Schwietzer, D. Kummer et al., “The mitochondrial outer membrane protein SYNJ2BP interacts with the cell adhesion molecule TMIGD1 and can recruit it to mitochondria,” *BMC Molecular and Cell Biology*, vol. 21, no. 1, p. 30, 2020.
- [45] P. Gómez-Suaga, B. G. Pérez-Nievas, E. B. Glennon et al., “The VAPB-PTPIP51 endoplasmic reticulum-mitochondria tethering proteins are present in neuronal synapses and regulate synaptic activity,” *Acta Neuropathologica Communications*, vol. 7, no. 1, p. 35, 2019.
- [46] K. J. de Vos, G. M. Mórotz, R. Stoica et al., “VAPB interacts with the mitochondrial protein PTPIP51 to regulate calcium homeostasis,” *Human Molecular Genetics*, vol. 21, no. 6, pp. 1299–1311, 2012.
- [47] R. Stoica, K. J. de Vos, S. Paillusson et al., “ER-mitochondria associations are regulated by the VAPB-PTPIP51 interaction and are disrupted by ALS/FTD-associated TDP-43,” *Nature Communications*, vol. 5, no. 1, p. 3996, 2014.
- [48] R. Stoica, S. Paillusson, P. Gomez-Suaga et al., “ALS/FTD-associated FUS activates GSK-3 β to disrupt the VAPB-PTPIP51 interaction and ER-mitochondria associations,” *EMBO Reports*, vol. 17, no. 9, pp. 1326–1342, 2016.
- [49] T. di Mattia, L. P. Wilhelm, S. Ikhlef et al., “Identification of MOSPD2, a novel scaffold for endoplasmic reticulum membrane contact sites,” *EMBO Reports*, vol. 19, no. 7, 2018.
- [50] K. C. Huang, S. F. Chiang, P. C. Yang et al., “ATAD3A stabilizes GRP78 to suppress ER stress for acquired chemoresistance in colorectal cancer,” *Journal of Cellular Physiology*, vol. 236, no. 9, pp. 6481–6495, 2021.
- [51] Y. Teng, X. Ren, H. Li, A. Shull, J. Kim, and J. K. Cowell, “Mitochondrial ATAD3A combines with GRP78 to regulate

- the WASF3 metastasis-promoting protein,” *Oncogene*, vol. 35, no. 3, pp. 333–343, 2016.
- [52] M. Karbowski, Y. J. Lee, B. Gaume et al., “Spatial and temporal association of Bax with mitochondrial fission sites, Drp1, and Mfn2 during apoptosis,” *The Journal of Cell Biology*, vol. 159, no. 6, pp. 931–938, 2002.
- [53] B. Gilquin, E. Taillebourg, N. Cherradi et al., “The AAA+ ATPase ATAD3A controls mitochondrial dynamics at the interface of the inner and outer membranes,” *Molecular and Cellular Biology*, vol. 30, no. 8, pp. 1984–1996, 2010.
- [54] A. R. van Vliet, T. Verfaillie, and P. Agostinis, “New functions of mitochondria associated membranes in cellular signaling,” *Biochimica et Biophysica Acta*, vol. 1843, no. 10, pp. 2253–2262, 2014.
- [55] S. De la Fuente and S. S. Sheu, “SR-mitochondria communication in adult cardiomyocytes: a close relationship where the Ca^{2+} has a lot to say,” *Archives of Biochemistry and Biophysics*, vol. 663, pp. 259–268, 2019.
- [56] L. K. Townsend, H. S. Brunetta, and M. A. S. Mori, “Mitochondria-associated ER membranes in glucose homeostasis and insulin resistance,” *American Journal of Physiology. Endocrinology and Metabolism*, vol. 319, no. 6, pp. E1053–E1060, 2020.
- [57] J. Chai, Q. Xiong, P. Zhang, R. Zheng, J. Peng, and S. Jiang, “Induction of Ca^{2+} signal mediated apoptosis and alteration of IP3R1 and SERCA1 expression levels by stress hormone in differentiating C2C12 myoblasts,” *General and Comparative Endocrinology*, vol. 166, no. 2, pp. 241–249, 2010.
- [58] V. R. Yadav, T. Song, L. Mei, L. Joseph, Y. M. Zheng, and Y. X. Wang, “PLC γ 1-PKC ϵ -IP3R1 signaling plays an important role in hypoxia-induced calcium response in pulmonary artery smooth muscle cells,” *American Journal of Physiology. Lung Cellular and Molecular Physiology*, vol. 314, no. 5, pp. L724–L735, 2018.
- [59] Z. Liu, H. Cai, H. Zhu et al., “Protein kinase RNA-like endoplasmic reticulum kinase (PERK)/calcineurin signaling is a novel pathway regulating intracellular calcium accumulation which might be involved in ventricular arrhythmias in diabetic cardiomyopathy,” *Cellular Signalling*, vol. 26, no. 12, pp. 2591–2600, 2014.
- [60] Y. Wang, Y. Kuramitsu, B. Baron et al., “PERK/CHOP contributes to the CGK733-induced vesicular calcium sequestration which is accompanied by non-apoptotic cell death,” *Oncotarget*, vol. 6, no. 28, pp. 25252–25265, 2015.
- [61] T. Wakai and R. A. Fissore, “Constitutive IP3R1-mediated Ca^{2+} release reduces Ca^{2+} store content and stimulates mitochondrial metabolism in mouse GV oocytes,” *Journal of Cell Science*, vol. 132, no. 3, 2019.
- [62] H. Matsuzaki, T. Fujimoto, M. Tanaka, and S. Shirasawa, “Tesp1 is a novel component of mitochondria-associated endoplasmic reticulum membranes and affects mitochondrial calcium flux,” *Biochemical and Biophysical Research Communications*, vol. 433, no. 3, pp. 322–326, 2013.
- [63] F. Huang, M. Ni, J. M. Zhang, D. J. Li, and F. M. Shen, “TRPM8 downregulation by angiotensin II in vascular smooth muscle cells is involved in hypertension,” *Molecular Medicine Reports*, vol. 15, no. 4, pp. 1900–1908, 2017.
- [64] J. Li, X. Liu, H. Wang, W. Zhang, D. C. Chan, and Y. Shi, “Lysocardiolipin acyltransferase 1 (ALCAT1) controls mitochondrial DNA fidelity and biogenesis through modulation of MFN2 expression,” *Proceedings of the National Academy of Sciences of the United States of America*, vol. 109, no. 18, pp. 6975–6980, 2012.
- [65] I. Anastasia, N. Ilacqua, A. Raimondi et al., “Mitochondria-rough-ER contacts in the liver regulate systemic lipid homeostasis,” *Cell Reports*, vol. 34, no. 11, p. 108873, 2021.
- [66] C. Petrunaro and B. Kornmann, “Lipid exchange at ER-mitochondria contact sites: a puzzle falling into place with quite a few pieces missing,” *Current Opinion in Cell Biology*, vol. 57, pp. 71–76, 2019.
- [67] Y. Cao, E. Traer, G. A. Zimmerman, T. M. McIntyre, and S. M. Prescott, “Cloning, expression, and chromosomal localization of human long-chain fatty acid-CoA ligase 4 (FACL4),” *Genomics*, vol. 49, no. 2, pp. 327–330, 1998.
- [68] D. E. Dove, Y. R. Su, L. L. Swift, M. R. F. Linton, and S. Fazio, “ACAT1 deficiency increases cholesterol synthesis in mouse peritoneal macrophages,” *Atherosclerosis*, vol. 186, no. 2, pp. 267–274, 2006.
- [69] Y. Fu, A. Hoang, G. Escher, R. G. Parton, Z. Krozowski, and D. Sviridov, “Expression of caveolin-1 enhances cholesterol efflux in hepatic cells,” *The Journal of Biological Chemistry*, vol. 279, no. 14, pp. 14140–14146, 2004.
- [70] T. Meshulam, J. R. Simard, J. Wharton, J. A. Hamilton, and P. F. Pilch, “Role of caveolin-1 and cholesterol in transmembrane fatty acid movement,” *Biochemistry*, vol. 45, no. 9, pp. 2882–2893, 2006.
- [71] Q. Hu, X.-J. Zhang, C.-X. Liu, X.-P. Wang, and Y. Zhang, “PPAR γ 1-induced caveolin-1 enhances cholesterol efflux and attenuates atherosclerosis in apolipoprotein E-deficient mice,” *Journal of Vascular Research*, vol. 47, no. 1, pp. 69–79, 2010.
- [72] M. Sohn, M. Korzeniowski, J. P. Zewe et al., “PI(4,5)P2 controls plasma membrane PI4P and PS levels via ORP5/8 recruitment to ER-PM contact sites,” *The Journal of Cell Biology*, vol. 217, no. 5, pp. 1797–1813, 2018.
- [73] H. Zhao and T. Wang, “PE homeostasis rebalanced through mitochondria-ER lipid exchange prevents retinal degeneration in *Drosophila*,” *PLoS Genetics*, vol. 16, no. 10, article e1009070, 2020.
- [74] D. Yan, M. I. Mäyränpää, J. Wong et al., “OSBP-related protein 8 (ORP8) suppresses ABCA1 expression and cholesterol efflux from macrophages,” *The Journal of Biological Chemistry*, vol. 283, no. 1, pp. 332–340, 2008.
- [75] M. Liu, X. Li, and D. Huang, “Mfn2 overexpression attenuates cardio-cerebrovascular ischemia-reperfusion injury through mitochondrial fusion and activation of the AMPK/Sirt3 signaling,” *Frontiers in Cell and Development Biology*, vol. 8, p. 598078, 2020.
- [76] C. Li, L. Li, M. Yang, L. Zeng, and L. Sun, “PACS-2: a key regulator of mitochondria-associated membranes (MAMs),” *Pharmacological Research*, vol. 160, article 105080, 2020.
- [77] T. Matsuda, Y. Kido, S. I. Asahara et al., “Ablation of C/EBP β alleviates ER stress and pancreatic beta cell failure through the GRP78 chaperone in mice,” *The Journal of Clinical Investigation*, vol. 120, no. 1, pp. 115–126, 2010.
- [78] M. Shuda, N. Kondoh, N. Imazeki et al., “Activation of the ATF6, XBP1 and grp78 genes in human hepatocellular carcinoma: a possible involvement of the ER stress pathway in hepatocarcinogenesis,” *Journal of Hepatology*, vol. 38, no. 5, pp. 605–614, 2003.
- [79] J. P. Muñoz, S. Ivanova, J. Sánchez-Wandelmer et al., “Mfn2 modulates the UPR and mitochondrial function via

- repression of PERK,” *The EMBO Journal*, vol. 32, no. 17, pp. 2348–2361, 2013.
- [80] X. Liu, R. Huang, Y. Gao, M. Gao, J. Ruan, and J. Gao, “Calcium mitigates fluoride-induced kallikrein 4 inhibition via PERK/eIF2 α /ATF4/CHOP endoplasmic reticulum stress pathway in ameloblast-lineage cells,” *Archives of Oral Biology*, vol. 125, p. 105093, 2021.
- [81] Y. J. Chern, J. C. T. Wong, G. S. W. Cheng et al., “The interaction between SPARC and GRP78 interferes with ER stress signaling and potentiates apoptosis via PERK/eIF2 α and IRE1 α /XBP-1 in colorectal cancer,” *Cell Death & Disease*, vol. 10, no. 7, p. 504, 2019.
- [82] K. Shimoke, M. Kudo, and T. Ikeuchi, “MPTP-induced reactive oxygen species promote cell death through a gradual activation of caspase-3 without expression of GRP78/Bip as a preventive measure against ER stress in PC12 cells,” *Life Sciences*, vol. 73, no. 5, pp. 581–593, 2003.
- [83] M. K. Gupta, F. G. Tahrir, T. Knezevic et al., “GRP78 interacting partner Bag5 responds to ER stress and protects cardiomyocytes from ER stress-induced apoptosis,” *Journal of Cellular Biochemistry*, vol. 117, no. 8, pp. 1813–1821, 2016.
- [84] A. M. Benham, A. Cabibbo, A. Fassio, N. Bulleid, R. Sitia, and I. Braakman, “The CXXCXXC motif determines the folding, structure and stability of human Ero1-L α ,” *The EMBO Journal*, vol. 19, no. 17, pp. 4493–4502, 2000.
- [85] G. Li, M. Mongillo, K. T. Chin et al., “Role of ERO1- α -mediated stimulation of inositol 1,4,5-triphosphate receptor activity in endoplasmic reticulum stress-induced apoptosis,” *The Journal of Cell Biology*, vol. 186, no. 6, pp. 783–792, 2009.
- [86] C. Rocca, T. Pasqua, L. Boukhzar, Y. Anouar, and T. Angelone, “Progress in the emerging role of selenoproteins in cardiovascular disease: focus on endoplasmic reticulum-resident selenoproteins,” *Cellular and Molecular Life Sciences*, vol. 76, no. 20, pp. 3969–3985, 2019.
- [87] E. D. Yoboue, A. Rimessi, T. Anelli, P. Pinton, and R. Sitia, “Regulation of calcium fluxes by GPX8, a type-II transmembrane peroxidase enriched at the mitochondria-associated endoplasmic reticulum membrane,” *Antioxidants & Redox Signaling*, vol. 27, no. 9, pp. 583–595, 2017.
- [88] J. Zhang, Y. Liu, Y. Guo, and Q. Zhao, “GPX8 promotes migration and invasion by regulating epithelial characteristics in non-small cell lung cancer,” *Thoracic Cancer*, vol. 11, no. 11, pp. 3299–3308, 2020.
- [89] K. Oniki, H. Nohara, R. Nakashima et al., “The *Dsba-L* gene is associated with respiratory function of the elderly via its adiponectin multimeric or antioxidant properties,” *Scientific Reports*, vol. 10, no. 1, p. 5973, 2020.
- [90] J. Bai, C. Cervantes, J. Liu et al., “DsbA-L prevents obesity-induced inflammation and insulin resistance by suppressing the mtDNA release-activated cGAS-cGAMP-STING pathway,” *Proceedings of the National Academy of Sciences of the United States of America*, vol. 114, no. 46, pp. 12196–12201, 2017.
- [91] Z. Zhang, L. Liu, S. Wu, and D. Xing, “Drp1, Mff, Fis1, and MiD51 are coordinated to mediate mitochondrial fission during UV irradiation-induced apoptosis,” *The FASEB Journal*, vol. 30, no. 1, pp. 466–476, 2016.
- [92] O. C. Losón, Z. Song, H. Chen, and D. C. Chan, “Fis1, Mff, MiD49, and MiD51 mediate Drp1 recruitment in mitochondrial fission,” *Molecular Biology of the Cell*, vol. 24, no. 5, pp. 659–667, 2013.
- [93] L. Tian, M. Neuber-Hess, J. Mewburn et al., “Ischemia-induced Drp1 and Fis1-mediated mitochondrial fission and right ventricular dysfunction in pulmonary hypertension,” *Journal of Molecular Medicine (Berlin, Germany)*, vol. 95, no. 4, pp. 381–393, 2017.
- [94] Y. Xi, D. Feng, K. Tao et al., “MitoQ protects dopaminergic neurons in a 6-OHDA induced PD model by enhancing Mfn2-dependent mitochondrial fusion via activation of PGC-1 α ,” *Biochimica et Biophysica Acta (BBA) - Molecular Basis of Disease*, vol. 1864, no. 9, Part B, pp. 2859–2870, 2018.
- [95] A. H. Pham, S. Meng, Q. N. Chu, and D. C. Chan, “Loss of Mfn2 results in progressive, retrograde degeneration of dopaminergic neurons in the nigrostriatal circuit,” *Human Molecular Genetics*, vol. 21, no. 22, pp. 4817–4826, 2012.
- [96] H. Chen, S. A. Detmer, A. J. Ewald, E. E. Griffin, S. E. Fraser, and D. C. Chan, “Mitofusins Mfn1 and Mfn2 coordinately regulate mitochondrial fusion and are essential for embryonic development,” *The Journal of Cell Biology*, vol. 160, no. 2, pp. 189–200, 2003.
- [97] C. Rouzier, S. Bannwarth, A. Chaussonnet et al., “The MFN2 gene is responsible for mitochondrial DNA instability and optic atrophy ‘plus’ phenotype,” *Brain*, vol. 135, no. 1, pp. 23–34, 2012.
- [98] D. Sebastian, M. I. Hernandez-Alvarez, J. Segales et al., “Mitofusin 2 (Mfn2) links mitochondrial and endoplasmic reticulum function with insulin signaling and is essential for normal glucose homeostasis,” *Proceedings of the National Academy of Sciences of the United States of America*, vol. 109, no. 14, pp. 5523–5528, 2012.
- [99] A. Martorell-Riera, M. Segarra-Mondejar, J. P. Muñoz et al., “Mfn2 downregulation in excitotoxicity causes mitochondrial dysfunction and delayed neuronal death,” *The EMBO Journal*, vol. 33, no. 20, pp. 2388–2407, 2014.
- [100] A. R. Hall, N. Burke, R. K. Dongworth et al., “Hearts deficient in both Mfn1 and Mfn2 are protected against acute myocardial infarction,” *Cell Death & Disease*, vol. 7, no. 5, article e2238, 2016.
- [101] C. S. Palmer, K. D. Elgass, R. G. Parton, L. D. Osellame, D. Stojanovski, and M. T. Ryan, “Adaptor proteins MiD49 and MiD51 can act independently of Mff and Fis1 in Drp1 recruitment and are specific for mitochondrial fission,” *The Journal of Biological Chemistry*, vol. 288, no. 38, pp. 27584–27593, 2013.
- [102] I. G. Castro, D. M. Richards, J. Metz et al., “A role for mitochondrial rho GTPase 1 (MIRO1) in motility and membrane dynamics of peroxisomes,” *Traffic*, vol. 19, no. 3, pp. 229–242, 2018.
- [103] E. Shlevkov, T. Kramer, J. Schapansky, M. J. LaVoie, and T. L. Schwarz, “Miro phosphorylation sites regulate Parkin recruitment and mitochondrial motility,” *Proceedings of the National Academy of Sciences of the United States of America*, vol. 113, no. 41, pp. E6097–E6106, 2016.
- [104] X. Wang, D. Winter, G. Ashrafi et al., “PINK1 and Parkin target Miro for phosphorylation and degradation to arrest mitochondrial motility,” *Cell*, vol. 147, no. 4, pp. 893–906, 2011.
- [105] S. Modi, G. López-Doménech, E. F. Halff et al., “Miro clusters regulate ER-mitochondria contact sites and link cristae organization to the mitochondrial transport machinery,” *Nature Communications*, vol. 10, no. 1, p. 4399, 2019.
- [106] K. I. Cho, Y. Cai, H. Yi, A. Yeh, A. Aslanukov, and P. A. Ferreira, “Association of the kinesin-binding domain of RanBP2

- to KIF5B and KIF5C determines mitochondria localization and function," *Traffic*, vol. 8, no. 12, pp. 1722–1735, 2007.
- [107] Y. Tanaka, Y. Kanai, Y. Okada et al., "Targeted Disruption of Mouse Conventional Kinesin Heavy Chain *kif5B*, Results in Abnormal Perinuclear Clustering of Mitochondria," *Cell*, vol. 93, no. 7, pp. 1147–1158, 1998.
- [108] S. Patergnani, S. Missiroli, S. Marchi, and C. Giorgi, "Mitochondria-associated endoplasmic reticulum membranes microenvironment: targeting autophagic and apoptotic pathways in cancer therapy," *Frontiers in Oncology*, vol. 5, p. 173, 2015.
- [109] Z. Tang, Y. Takahashi, and H. G. Wang, "ATG2 regulation of phagophore expansion at mitochondria-associated ER membranes," *Autophagy*, vol. 15, no. 12, pp. 2165–2166, 2019.
- [110] Y. Hu, Y. Zhang, T. Deng et al., "PDPK1 regulates autophagosome biogenesis by binding to PIK3C3," *Autophagy*, vol. 9, pp. 1–18, 2020.
- [111] G. Jin, C. Xu, X. Zhang et al., "Atad3a suppresses Pink1-dependent mitophagy to maintain homeostasis of hematopoietic progenitor cells," *Nature Immunology*, vol. 19, no. 1, pp. 29–40, 2018.
- [112] G. L. McLelland, T. Goiran, W. Yi et al., "Mfn2 ubiquitination by PINK1/parkin gates the p97-dependent release of ER from mitochondria to drive mitophagy," *eLife*, vol. 7, 2018.
- [113] V. Gelmetti, P. de Rosa, L. Torosantucci et al., "PINK1 and BECN1 relocalize at mitochondria-associated membranes during mitophagy and promote ER-mitochondria tethering and autophagosome formation," *Autophagy*, vol. 13, no. 4, pp. 654–669, 2017.
- [114] P. Li, J. Wang, X. Zhao et al., "PTEN inhibition attenuates endothelial cell apoptosis in coronary heart disease via modulating the AMPK-CREB-Mfn2-mitophagy signaling pathway," *Journal of Cellular Physiology*, vol. 235, no. 5, pp. 4878–4889, 2020.
- [115] J. Gu, T. Zhang, J. Guo, K. Chen, H. Li, and J. Wang, "PINK1 activation and translocation to mitochondria-associated membranes mediates mitophagy and protects against hepatic ischemia/reperfusion injury," *Shock*, vol. 54, no. 6, pp. 783–793, 2020.
- [116] Z. Zhang and J. Yu, "NR4A1 promotes cerebral ischemia reperfusion injury by repressing Mfn2-mediated mitophagy and inactivating the MAPK-ERK-CREB signaling pathway," *Neurochemical Research*, vol. 43, no. 10, pp. 1963–1977, 2018.
- [117] Y. Sun, Y. Cai, S. Qian, H. Chiou, and Q. S. Zang, "Beclin-1 improves mitochondria-associated membranes in the heart during endotoxemia," *FASEB BioAdvances*, vol. 3, no. 3, pp. 123–135, 2021.
- [118] M. A. Lampert, A. M. Orogo, R. H. Najor et al., "BNIP3L/NIX and FUNDC1-mediated mitophagy is required for mitochondrial network remodeling during cardiac progenitor cell differentiation," *Autophagy*, vol. 15, no. 7, pp. 1182–1198, 2019.
- [119] L. Liu, D. Feng, G. Chen et al., "Mitochondrial outer-membrane protein FUNDC1 mediates hypoxia-induced mitophagy in mammalian cells," *Nature Cell Biology*, vol. 14, no. 2, pp. 177–185, 2012.
- [120] H. Zhou, P. Zhu, J. Wang, H. Zhu, J. Ren, and Y. Chen, "Pathogenesis of cardiac ischemia reperfusion injury is associated with CK2 α -disturbed mitochondrial homeostasis via suppression of FUNDC1-related mitophagy," *Cell Death and Differentiation*, vol. 25, no. 6, pp. 1080–1093, 2018.
- [121] H. Zhou, J. Wang, P. Zhu et al., "NR4A1 aggravates the cardiac microvascular ischemia reperfusion injury through suppressing FUNDC1-mediated mitophagy and promoting Mff-required mitochondrial fission by CK2 α ," *Basic Research in Cardiology*, vol. 113, no. 4, p. 23, 2018.
- [122] W. Wu, W. Tian, Z. Hu et al., "ULK1 translocates to mitochondria and phosphorylates FUNDC1 to regulate mitophagy," *EMBO Reports*, vol. 15, no. 5, pp. 566–575, 2014.
- [123] L. Wang, P. Wang, H. Dong et al., "ULK1/FUNDC1 prevents nerve cells from hypoxia-induced apoptosis by promoting cell autophagy," *Neurochemical Research*, vol. 43, no. 8, pp. 1539–1548, 2018.
- [124] Z. Chen, L. Liu, Q. Cheng et al., "Mitochondrial E3 ligase MARCH5 regulates FUNDC1 to fine-tune hypoxic mitophagy," *EMBO Reports*, vol. 18, no. 3, pp. 495–509, 2017.
- [125] J. Ren, M. Sun, H. Zhou et al., "FUNDC1 interacts with FBXL2 to govern mitochondrial integrity and cardiac function through an IP3R3-dependent manner in obesity," *Science Advances*, vol. 6, no. 38, article eabc8561, 2020.
- [126] W. Yu, M. Xu, T. Zhang, Q. Zhang, and C. Zou, "Mst1 promotes cardiac ischemia-reperfusion injury by inhibiting the ERK-CREB pathway and repressing FUNDC1-mediated mitophagy," *The Journal of Physiological Sciences*, vol. 69, no. 1, pp. 113–127, 2019.
- [127] H. Zhou, P. Zhu, J. Wang, S. Toan, and J. Ren, "DNA-PKcs promotes alcohol-related liver disease by activating Drp1-related mitochondrial fission and repressing FUNDC1-required mitophagy," *Signal Transduction and Targeted Therapy*, vol. 4, no. 1, p. 56, 2019.
- [128] Y. Xiao, W. Chen, Z. Zhong et al., "Electroacupuncture preconditioning attenuates myocardial ischemia-reperfusion injury by inhibiting mitophagy mediated by the mTORC1-ULK1-FUNDC1 pathway," *Biomedicine & Pharmacotherapy*, vol. 127, article 110148, 2020.
- [129] T. Namba, F. Tian, K. Chu et al., "CDIPI-BAP31 complex transduces apoptotic signals from endoplasmic reticulum to mitochondria under endoplasmic reticulum stress," *Cell Reports*, vol. 5, no. 2, pp. 331–339, 2013.
- [130] J. Chen, H. Guo, H. Jiang et al., "A BAP31 intrabody induces gastric cancer cell death by inhibiting p27(kip1) proteasome degradation," *International Journal of Cancer*, vol. 144, no. 8, pp. 2051–2062, 2019.
- [131] Y. J. Lee, S. Y. Jeong, M. Karbowski, C. L. Smith, and R. J. Youle, "Roles of the mammalian mitochondrial fission and fusion mediators Fis1, Drp1, and Opa1 in apoptosis," *Molecular Biology of the Cell*, vol. 15, no. 11, pp. 5001–5011, 2004.
- [132] S. Missiroli, S. Patergnani, N. Caroccia et al., "Mitochondria-associated membranes (MAMs) and inflammation," *Cell Death & Disease*, vol. 9, no. 3, p. 329, 2018.
- [133] Y. Chen, M. Zeng, Y. Zhang, H. Guo, W. Ding, and T. Sun, "Nlrp3 deficiency alleviates angiotensin II-induced cardiomyopathy by inhibiting mitochondrial dysfunction," *Oxidative Medicine and Cellular Longevity*, vol. 2021, Article ID 6679100, 10 pages, 2021.
- [134] Q. Liu, X. Ci, Z. Wen, and L. Peng, "Diosmetin alleviates lipopolysaccharide-induced acute lung injury through activating the Nrf2 pathway and inhibiting the NLRP3 Inflammasome," *Biomolecules & Therapeutics*, vol. 26, no. 2, pp. 157–166, 2018.
- [135] J. Kai, X. Yang, Z. Wang et al., "Oroxilin a promotes PGC-1 α /Mfn2 signaling to attenuate hepatocyte pyroptosis via

- blocking mitochondrial ROS in alcoholic liver disease,” *Free Radical Biology & Medicine*, vol. 153, pp. 89–102, 2020.
- [136] F. Xu, H. Qi, J. Li et al., “*Mycobacterium tuberculosis* infection up-regulates MFN2 expression to promote NLRP3 inflammasome formation,” *The Journal of Biological Chemistry*, vol. 295, no. 51, pp. 17684–17697, 2020.
- [137] A. Rajput, A. Kovalenko, K. Bogdanov et al., “RIG-I RNA helicase activation of IRF3 transcription factor is negatively regulated by caspase-8-mediated cleavage of the RIP1 protein,” *Immunity*, vol. 34, no. 3, pp. 340–351, 2011.
- [138] A. Sen, A. J. Pruijssers, T. S. Dermody, A. Garcia-Sastre, and H. B. Greenberg, “The early interferon response to rotavirus is regulated by PKR and depends on MAVS/IPS-1, RIG-I, MDA-5, and IRF3,” *Journal of Virology*, vol. 85, no. 8, pp. 3717–3732, 2011.
- [139] S. Hardy, B. Jackson, S. Goodbourn, and J. Seago, “Classical swine fever virus NproAntagonizes IRF3 to prevent Interferon-Independent TLR3- and RIG-I-mediated apoptosis,” *Journal of Virology*, vol. 95, no. 5, 2021.
- [140] N. A. Dalrymple, V. Cimica, and E. R. Mackow, “Dengue virus NS proteins inhibit RIG-I/MAVS signaling by blocking TBK1/IRF3 phosphorylation: dengue virus serotype 1 NS4A is a unique interferon-regulating virulence determinant,” *mBio*, vol. 6, no. 3, article e00553-15, 2015.
- [141] L. Wang, D. Qin, H. Shi, Y. Zhang, H. Li, and Q. Han, “MiR-195-5p promotes cardiomyocyte hypertrophy by targeting MFN2 and FBXW7,” *BioMed Research International*, vol. 2019, Article ID 1580982, 10 pages, 2019.
- [142] K. Mahdavian, I. Y. Benador, S. Su et al., “Mfn2 deletion in brown adipose tissue protects from insulin resistance and impairs thermogenesis,” *EMBO Reports*, vol. 18, no. 7, pp. 1123–1138, 2017.
- [143] M. Chen, Z. Chen, Y. Wang et al., “Mitophagy receptor FUNDC1 regulates mitochondrial dynamics and mitophagy,” *Autophagy*, vol. 12, no. 4, pp. 689–702, 2016.
- [144] J. Wang, P. Zhu, R. Li, J. Ren, and H. Zhou, “Fundc1-dependent mitophagy is obligatory to ischemic preconditioning-conferred renoprotection in ischemic AKI via suppression of Drp1-mediated mitochondrial fission,” *Redox Biology*, vol. 30, p. 101415, 2020.
- [145] C. Y. Huang, C. H. Lai, C. H. Kuo et al., “Inhibition of ERK-Drp1 signaling and mitochondria fragmentation alleviates IGF-IIR-induced mitochondria dysfunction during heart failure,” *Journal of Molecular and Cellular Cardiology*, vol. 122, pp. 58–68, 2018.
- [146] W. Wu, W. Li, H. Chen, L. Jiang, R. Zhu, and D. Feng, “FUNDC1 is a novel mitochondrial-associated-membrane (MAM) protein required for hypoxia-induced mitochondrial fission and mitophagy,” *Autophagy*, vol. 12, no. 9, pp. 1675–1676, 2016.
- [147] C. Angebault, M. Panel, M. Lacôte, J. Rieusset, A. Lacampagne, and J. Fauconnier, “Metformin reverses the enhanced myocardial SR/ER-mitochondria interaction and impaired complex I-driven respiration in dystrophin-deficient mice,” *Frontiers in Cell and Development Biology*, vol. 8, article 609493, 2020.
- [148] G. P. Meares, A. A. Zmijewska, and R. S. Jope, “HSP105 interacts with GRP78 and GSK3 and promotes ER stress-induced caspase-3 activation,” *Cellular Signalling*, vol. 20, no. 2, pp. 347–358, 2008.
- [149] K. T. Chin, G. Kang, J. Qu et al., “The sarcoplasmic reticulum luminal thiol oxidase ERO1 regulates cardiomyocyte excitation-coupled calcium release and response to hemodynamic load,” *The FASEB Journal*, vol. 25, no. 8, pp. 2583–2591, 2011.
- [150] R. Orlando, S. de Martin, L. Andrighetto, M. Floreani, and P. Palatini, “Fluvoxamine pharmacokinetics in healthy elderly subjects and elderly patients with chronic heart failure,” *British Journal of Clinical Pharmacology*, vol. 69, no. 3, pp. 279–286, 2010.
- [151] C. Wang, K. Chen, Y. Xia et al., “N-Acetylcysteine attenuates ischemia-reperfusion-induced apoptosis and autophagy in mouse liver via regulation of the ROS/JNK/Bcl-2 pathway,” *PLoS One*, vol. 9, no. 9, article e108855, 2014.

Research Article

Inhibiting miR-205 Alleviates Cardiac Ischemia/Reperfusion Injury by Regulating Oxidative Stress, Mitochondrial Function, and Apoptosis

Yuerong Xu,^{1,2} Wangang Guo,¹ Di Zeng,¹ Yexian Fang,¹ Runze Wang,¹ Dong Guo,¹ Bingchao Qi,¹ Yugang Xue,¹ Feng Xue,¹ Zuolin Jin ², Yan Li ¹, and Mingming Zhang ¹

¹Department of Cardiology, Tangdu Hospital, The Fourth Military Medical University, Xi'an, China

²Department of Orthodontics, School of Stomatology, The Fourth Military Medical University, Xi'an, China

Correspondence should be addressed to Zuolin Jin; zuolinj@fmmu.edu.cn, Yan Li; profleeyan@163.com, and Mingming Zhang; winterzhang3@163.com

Received 7 April 2021; Revised 18 May 2021; Accepted 2 June 2021; Published 30 June 2021

Academic Editor: Yun-dai Chen

Copyright © 2021 Yuerong Xu et al. This is an open access article distributed under the Creative Commons Attribution License, which permits unrestricted use, distribution, and reproduction in any medium, provided the original work is properly cited.

Background. miR-205 is important for oxidative stress, mitochondrial dysfunction, and apoptosis. The roles of miR-205 in cardiac ischemia/reperfusion (I/R) injury remain unknown. The aim of this research is to reveal whether miR-205 could regulate cardiac I/R injury by focusing upon the oxidative stress, mitochondrial function, and apoptosis. **Methods.** Levels of miR-205 and Rnd3 were examined in the hearts with I/R injury. Myocardial infarct size, cardiac function, oxidative stress, mitochondria function, and cardiomyocyte apoptosis were detected in mice with myocardial ischemia/reperfusion (MI/R) injury. The primary neonatal cardiomyocytes underwent hypoxia/reoxygenation (H/R) to simulate MI/R injury. **Results.** miR-205 levels were significantly elevated in cardiac tissues from I/R in comparison with those from Sham. In comparison with controls, levels of Rnd3 were significantly decreased in the hearts from mice with MI/R injury. Furthermore, inhibiting miR-205 alleviated MI/R-induced apoptosis, reduced infarct size, prevented oxidative stress increase and mitochondrial fragmentation, and improved mitochondrial functional capacity and cardiac function. Consistently, overexpression of miR-205 increased infarct size and promoted apoptosis, oxidative stress, and mitochondrial dysfunction in mice with MI/R injury. In cultured mouse neonatal cardiomyocytes, downregulation of miR-205 reduced oxidative stress in H/R-treated cardiomyocytes. Finally, inhibiting Rnd3 ablated the cardioprotective effects of miR-205 inhibitor in MI/R injury. **Conclusions.** We conclude that inhibiting miR-205 reduces infarct size, improves cardiac function, and suppresses oxidative stress, mitochondrial dysfunction, and apoptosis by promoting Rnd3 in MI/R injury. miR-205 inhibitor-induced Rnd3 activation is a valid target to treat MI/R injury.

1. Introduction

Despite remarkable progress in disease prevention, diagnosis, and better control of risk factors, heart disease remains the most major contributor to mortality and morbidity worldwide [1, 2]. The myocardium that suffered from acute myocardial infarction (AMI) becomes ischemic and is consequently replaced by fibrosis [3]. Although ischemic myocardium can be treated by drugs or surgery, reperfusion causes damage to the heart, known as reperfusion injury [4]. Though coronary heart disease (CHD) mortality declined about 1%-1.8% annually in the past 20 years, thanks to percu-

taneous coronary intervention, estimated years of life lost because of MI are still very high [5]. Such circumstance indicates that great effort is still needed in research into alleviating cardiac I/R injury.

MicroRNAs (miRs) are small noncoding RNAs with sizes around 18–24 nucleotides, which could promote the translation or degradation of mRNAs and then regulate gene expression [6]. Based on this character, miRs involve in various biological process such as development, cancer, metabolic diseases, inflammation, and cardiovascular diseases [7–10]. Moreover, miRs also have the potential to be novel biomarkers and therapeutic agents [11, 12]. Specific to

cardiac I/R injury, miRs often play its role through regulating genes expression in key signaling pathways. For example, miR-19a suppresses myocardial apoptosis in I/R injury [13]. Besides, miR-20b-5p could downregulate Smad7, activate TGF- β /Smad pathway, and thus accelerate ventricular remodeling in I/R injury [14]. Therefore, our research decides to put emphasis on the miRs. miR-205-5p is one of the highly conserved miRNAs, located in the region of chromosome 1q32.2 of human genome. However, the role of miR-205-5p in MI/R injury still remains unclear.

Mitochondria suffer a deficiency to supply the cardiomyocyte with energy in MI/R injury [15]. Mitochondria dysfunction induced by MI/R injury leads to systolic dysfunction of heart because of insufficient energy [16]. The primary function of mitochondria is to produce abundant ATP, which is of critical importance for the normal work of heart. While in diseases, abnormalities of mitochondria are often discovered in form of mitochondrial enlargement, matrix derangement, and cristae loss, which all indicates abnormality of mitochondrial quality control [17]. Besides, oxidative stress is also an indicator of mitochondrial abnormality. Mitochondrial quality control includes mitochondrial biogenesis, mitochondrial dynamics, and mitophagy [18]. Kubli et al. generated parkin-deficient mice, which displayed impaired mitophagy and were more sensitive to myocardial infarction [19]. Mitochondrial quality surveillance may be a therapeutic target in myocardial infarction [20]. Taken together, this evidence demonstrate that cardiac restoration post injury is greatly related to mitochondrial function.

Oxidative stress originated from the overwhelmed ROS and the insufficient antioxidant defense systems [21]. The generation of ROS is promoted during I/R injury [22]. Oxidative stress resulted in alterations in protein function and oxidation of mitochondrial DNA. At the same time, mitochondrial damage induced the generation of ROS [23]. Ultimately, oxidative stress activates caspases and promotes cell apoptosis [24].

Small guanosine triphosphatases (GTPases) are enzymes which can hydrolyze guanosine triphosphate (GTP), and the most well-known GTPase family is Ras GTPases [25]. RND3, also called as RhoE, belongs to Ras homologous (Rho) family 31. Different from other GTPases, RND3 is lack of GTPase activity, but it is actively involved in actin cytoskeletal dynamics, apoptosis, differentiation, and other physiological process [26, 27]. Based on the discovered downregulation of RND3 in human falling heart, Yue et al. generated Rnd3^{+/-} haploinsufficient mice. Compared to wild-type ones, Rnd3^{+/-} mice displayed apoptotic cardiomyopathy when exposed to pressure overload. Researchers also found that total deletion of RND3 would result in embryonic death because of fetal arrhythmias [28, 29]. While mice with RND3 knockdown could survive to adulthood, knockdown of RND3 would disturb the ubiquitination of β 2-adrenergic receptor and finally lead to irregular spontaneous Ca²⁺ release [30]. In addition to above, under stress, RND3 could stabilize HIF1 α and promote VEGF expression [31]. This cardioprotective effect of RND3 is evidenced by reserved cardiac function of Rnd3 transgenic mice exposed to pressure overload. All these data illustrate that RND3 exert multiple

effects in various cardiovascular diseases. Based on TargetScan, the RND3 is the target of miR-205-5p. However, no efforts have been made to explore the effects of miR-205/Rnd3 in MI/R injury.

2. Research Design and Methods

2.1. Ethics and Subjects. The experiments were performed in adherence with the National Institutes of Health Guidelines on the Use of Laboratory Animals and were approved by the Fourth Military Medical University Ethic Committee on Animal Care.

2.2. Experiment Protocols. Male C57BL/6 mice of 6-8 weeks were randomly divided into the following groups with $n = 6$ each: (1) Sham; (2) MI/R+NC; (3) MI/R+miR-205 inhibitor; (4) MI/R+Control mimic; and (5) MI/R+miR-205 mimic. To illustrate whether miR-205 regulates cardiac I/R injury through Rnd3, mice were randomized to receive one of the following treatments with $n = 6$ each: (1) MI/R; (2) MI/R+AAV9-sh-Rnd3; (3) MI/R+miR-205 inhibitor; and (4) MI/R+miR-205 inhibitor+AAV9-sh-Rnd3. MI/R model construction was performed as previously described [32]. A 6-0 silk suture slipknot was placed at the proximal one-third of the left anterior descending artery. After 30 minutes of ischemia, the slipknot was released, and the myocardium was reperfused for 3 h.

2.3. Intracardiac Injection of miRNA Mimics and AAV9-sh-Rnd3. Mice were randomly subjected to intracardiac injection of miR-205 mimics or inhibitors (10 μ g per mouse heart), respectively, before MI/R. miR-205 mimics or inhibitors (10 μ g per heart) in a total volume of 50 μ l were injected immediately before the ligation of LAD coronary artery. The miRNA mimics, miRNA inhibitors, and AAV9-sh-Rnd3 (2×10^{11} viral genome particles per mouse heart) were evenly injected into three sites around the infarcted area (anterior wall, lateral wall, and apex area).

2.4. Primary Cardiomyocytes Culture and In Vitro Simulated Ischemia/Reperfusion Model Construction. Primary cardiomyocytes were isolated and cultured as previously described. The hearts of 1- to 3-day-old mice were isolated. The ventricular tissue was cut into pieces and digested with 5 ml collagenase type II at a concentration of 1 mg/ml for 7 min. The supernatant was fed into a 15 ml centrifuge tube, and the digestion was terminated with the same amount of DMEM and 10% fetal bovine serum (FBS). The above steps were repeated until the heart tissue is completely digested. The isolated cells were cultured in a 37°C culture flask for 2 hours to enrich the culture with cardiomyocytes. The nonadherent cardiomyocytes were collected and then plated onto gelatin-coated plated. For induction of simulated I/R injury, cells were cultured in D-Hanks solution in a modular incubator chamber (Biospherix) with 1% O₂, 5% CO₂, and 94% N₂ for 4 h (simulated ischemia for 4 h), then exposed to atmosphere of 21% O₂, 5% CO₂, and 74% N₂, and cultured for 4 h (simulate reperfusion for 4 h). Primary cardiomyocytes were randomly divided into the following groups: (1) Con; (2) H/R+NC; (3) H/R+miR-205 inhibitor; (4) H/R+Control

mimic; and (5) H/R+miR-205 mimic. To illustrate whether miR-205 regulates H/R injury in cardiomyocytes through Rnd3, cardiomyocytes were randomized to receive one of the following treatments: (1) H/R; (2) H/R+Ad-sh-Rnd3; (3) H/R+miR-205 inhibitor; and (4) H/R+miR-205 inhibitor+Ad-sh-Rnd3.

2.5. Measurement of Myocardial Infarct Size. Myocardial Infarct Size was evaluated by Evans Blue/TTC staining as previously described [32].

2.6. Determination of Myocardial Apoptosis. Myocardial apoptosis was determined by terminal deoxynucleotidyl transferase-mediated dUTP-biotin nick end labeling (TUNEL) staining as previously described [32].

2.7. Determination of Cardiac Function. Echocardiography was performed at 24 h after reperfusion as previously described [32].

2.8. Calcium Retention Capacity (mCRC). The mitochondrial calcium retention capacity (mCRC) was detected as previously described [29].

2.9. ROS Production and MnSOD Activity. The production of ROS was measured as previously described [33]. MnSOD was assayed as previously described [33].

2.10. Western Blot Evaluation. Total proteins from cardiomyocytes were separated by SDS-PAGE, blotted and probed with anti- β -actin antibody (Santa Cruz, CA, USA), anti-Rnd3 (Cell Signaling, Danvers, MA, USA), anti-Cleaved Caspase-3, and anti-Cleaved Caspase-9 (Sigma, St. Louis, MO, USA). The signals were quantified by densitometry and normalized to β -actin.

2.11. Citrate Synthase (CS), ATP Content, Mitochondria Isolation, Immunostaining Assay, and Transmission Electron Microscopy (TEM). Citrate synthase and the ATP content of the myocardium were measured as previously described [29]. Mitochondria isolation, immunostaining assay, and transmission electron microscopy (TEM) were performed as previously described [30].

2.12. Mitochondrial Membrane Potential ($\Delta\Psi$) Detection. The $\Delta\Psi$ of cardiomyocytes was assessed by the JC-1 assay kit (Beyotime, CHINA) [34].

2.13. Statistical Analysis. Continuous variables that approximated the normal distribution were expressed as means \pm SD. Comparison between groups was subjected to ANOVA followed by the Bonferroni correction for post hoc *t*-test. Data expressed as proportions were assessed with a Chi-square test. Two-sided tests have been used throughout, and *p* values < 0.05 were considered statistically significant. The SP4SS software package version 17.0 (SPSS, Chicago, IL) was used for data analysis.

3. Results

3.1. miR-205 Inhibitor Alleviates, while miR-205 Mimic Administration Aggravates Cardiac MI/R Injury in Mice. miR-205 was significantly increased in the MI/R group (Figure 1(a)). Compared with the MI/R group, LDH and CK-MB were significantly decreased in the miRNA-205 inhibitor group, while increased in the miRNA-205 mimic group (Figures 1(b) and 1(c)). Echocardiography showed that the significant increase of cardiac function markers LVEF and LVFS and the significant decrease of LVESD and LVEDD were observed in the MI/R+miR-205 inhibitor group (Figures 1(d)–1(g)). Furthermore, miR-205 mimic significantly decreased LVEF and LVFS and increased LVESD and LVEDD compared with the MI/R group (Figures 1(d)–1(g)). Representative images of infarct size are shown in Figure 1(h). miR-205 inhibitor significantly decreased infarct size after MI/R injury compared with the MI/R group (Figure 1(i)). Meanwhile, miR-205 mimic administration significantly increased infarct size after MI/R injury compared with the MI/R group (Figure 1(i)). Figure 1(j) reveals that there was no significant difference in the ratio of area at risk (AAR) to left ventricle (LV) area among groups.

3.2. miR-205 Inhibitor Improves, while miR-205 Mimic Administration Aggravates Mitochondrial Dysfunction and Oxidative Stress in Mice that Underwent MI/R Injury. TEM revealed that miRNA-205 inhibitor treatment alleviated mitochondrial structural damage after MI/R injury (Figure 2(a)). Compared to the MI/R group, mitochondrial ATP content (Figure 2(b)) and CS activity (Figure 2(c)) were significantly elevated in the MI/R+miRNA-205 inhibitor group and decreased in the MI/R+miRNA-205 mimic group. Compared to the MI/R group, the mCRC in the MI/R+miRNA-205 inhibitor group was significantly enhanced (Figure 2(d)). ROS levels (Figure 2(e)) and mitochondrial MnSOD activity (Figure 2(f)) were significantly decreased in the miR-205 inhibitor-injected hearts, while increased in the miRNA-205 mimic-injected hearts. Moreover, miRNA-205 inhibitor increased, while miRNA-205 overexpression administration decreased the expression of Rnd3 (Figures 2(g) and 2(h)).

3.3. Inhibiting miR-205 Improves, while miR-205 Overexpression Administration Aggravates Apoptosis in Mice that Underwent Cardiac MI/R Injury. TUNEL-positive cardiomyocytes in the MI/R+miRNA-205 inhibitor group were less frequently observed compared with the MI/R group (Figures 3(a) and 3(b)). miRNA-205 mimic increased the apoptosis rate after MI/R injury (Figures 3(a) and 3(b)). Concomitantly, miRNA-205 inhibitor administration decreased cleaved caspase-3 and cleaved caspase-9 after MI/R injury (Figures 3(c)–3(e)). miRNA-205 mimic administration increased cleaved caspase-3 and cleaved caspase-9 after MI/R injury (Figures 3(c)–3(e)).

3.4. Inhibiting RND3 Ablated the Cardioprotective Effects of miRNA-205 Inhibitor. To elucidate the mechanism of miR-205 on MI/R injury in mice, we checked the TargetScan and find Rnd3. AAV9-sh-Rnd3 was injected to the mice with

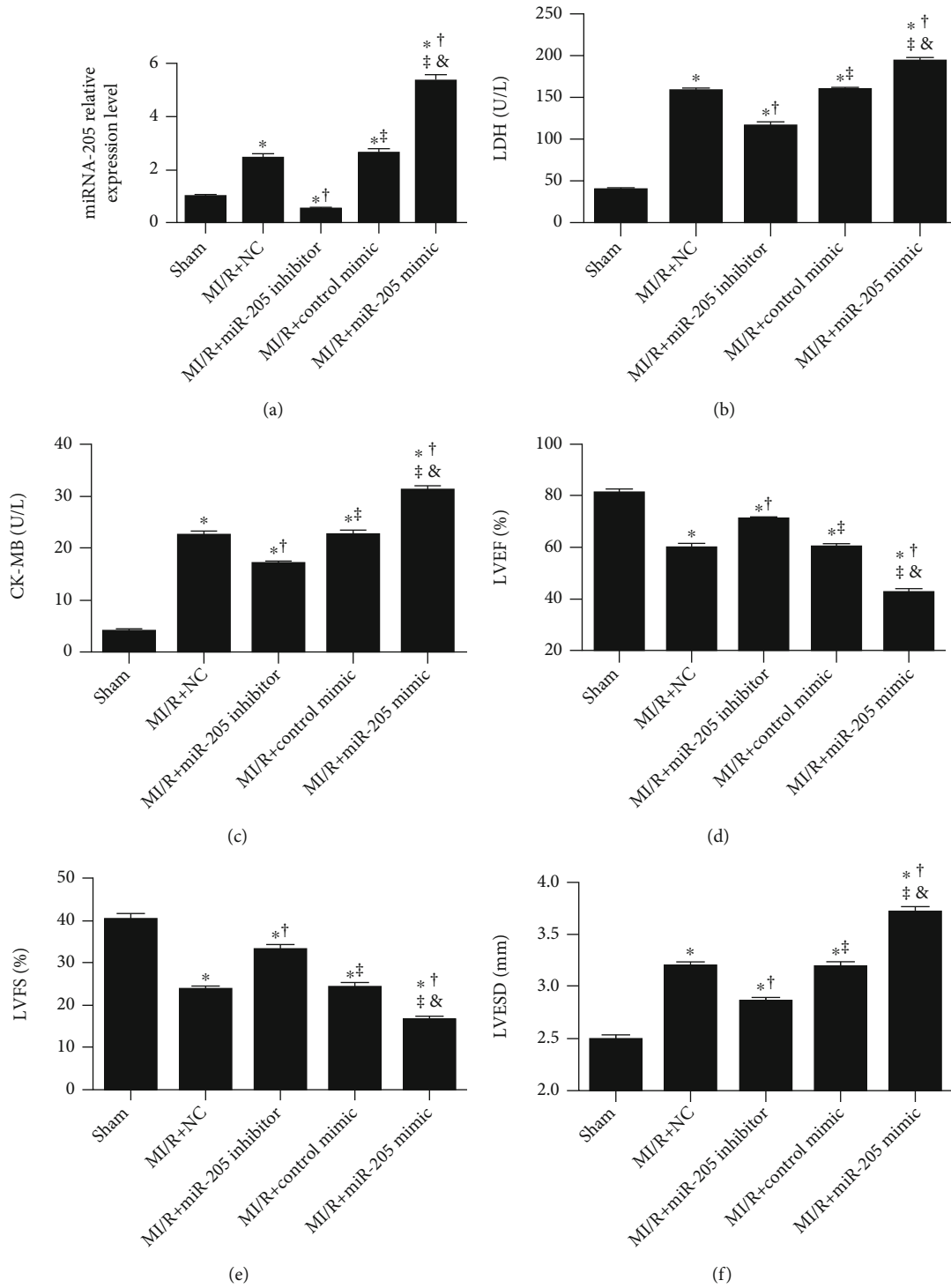


FIGURE 1: Continued.

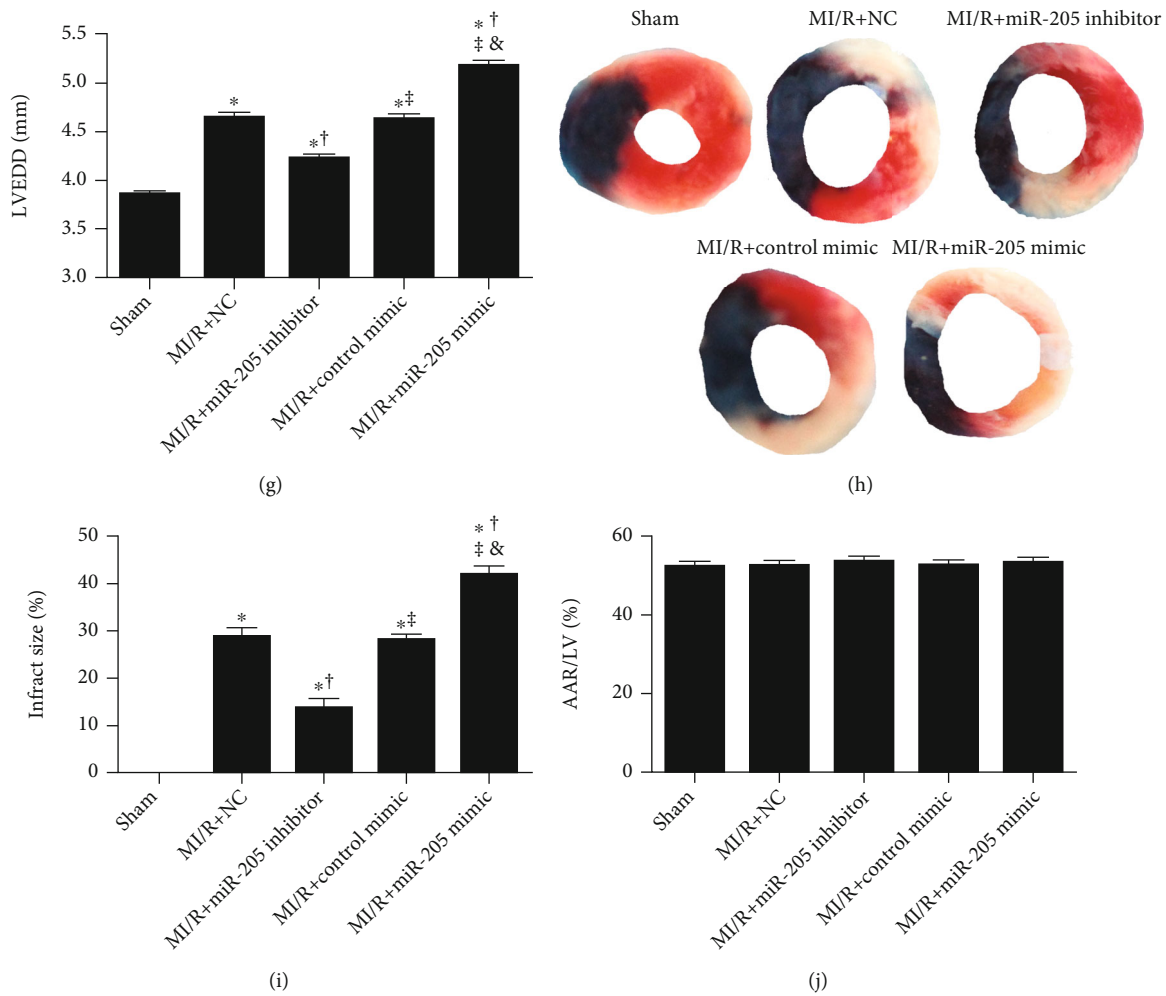


FIGURE 1: miR-205 inhibitor alleviates, while miR-205 mimic administration aggravates cardiac MI/R injury in mice. (a) Relative expression of miRNA-205. (b, c) Lactate dehydrogenase (LDH) and creatine kinase-MB (CK-MB) release after myocardial I/R injury in mice. (d–g) Left ventricular ejection fraction (LVEF), left ventricular fraction shortening (LVFS), left ventricular end systolic diameter (LVESD), and left ventricular end diastolic diameter (LVEDD) measured by echocardiography. (h) Representative images of infarct size as stained by Evans Blue and TTC. (i, j) Quantitative analysis of infarct size and AAR/LV at 3 h after I/R injury in mice. $n = 6$ in each group. The columns and errors bars represent means and SD. * $p < 0.05$ vs. Sham, † $p < 0.05$ vs. MI/R+NC, ‡ $p < 0.05$ vs. MI/R+miR-205 inhibitor, & $p < 0.05$ vs. MI/R+Control mimic.

MI/R injury. As is shown in Figures 4(a) and 4(b), a significant increase of cardiac injury markers LDH and CK-MB was observed in AAV9-sh-Rnd3-injected mice after MI/R injury. The infarct size was significantly larger in the AAV9-sh-Rnd3-injected mice compared with the MI/R mice (Figures 4(g)–4(i)). Additionally, we observed injured cardiac function, as indicated by decreased LVEF and LVFS and increased LVESD and LVEDD in MI/R+AAV9-sh-Rnd3 mice (Figures 4(c)–4(f)). Interestingly, miR-205 inhibitor did not exhibit protective effects in AAV9-sh-Rnd3-injected mice with MI/R injury, as evidenced by infarct size and cardiac function (Figure 4). The result of mitochondrial function, oxidative stress, and apoptosis was consistent with the above results (Figures 5 and 6). miR-205 inhibitor alleviated the mitochondria ultrastructure disorder in MI/R hearts but not in MI/R+miR-205 inhibitor+AAV9-sh-Rnd3 hearts (Figure 5(a)). AAV9-sh-Rnd3 significantly further decreased

ATP content and CS activity in the MI/R+AAV9-sh-Rnd3 group, while miR-205 inhibitor insignificantly increased ATP content and CS activity in the MI/R+miR-205 inhibitor+AAV9-sh-Rnd3 group (Figures 5(b) and 5(c)). The result of mCRC, ROS levels, and mitochondrial MnSOD activity was consistent with above results. Consistently, AAV9-sh-Rnd3 treatment decreased mCRC and increased ROS levels, and mitochondrial MnSOD activity underwent MI/R injury. AAV9-sh-Rnd3 treatment decreased the expression of Rnd3 in the MI/R+miR-205 inhibitor+AAV9-sh-Rnd3 hearts (Figures 5(g) and 5(h)). Coincidentally, AAV9-sh-Rnd3 injection increased the TUNEL-positive cardiomyocytes and the expression of cleaved caspase-3 and cleaved caspase-9 (Figures 6(a)–6(e)). However, the miR-205 inhibitor did not decrease cardiomyocyte apoptosis in the presence of AAV9-sh-Rnd3 after MI/R injury. The miR-205 inhibitor had no effect on the cleaved caspase-3

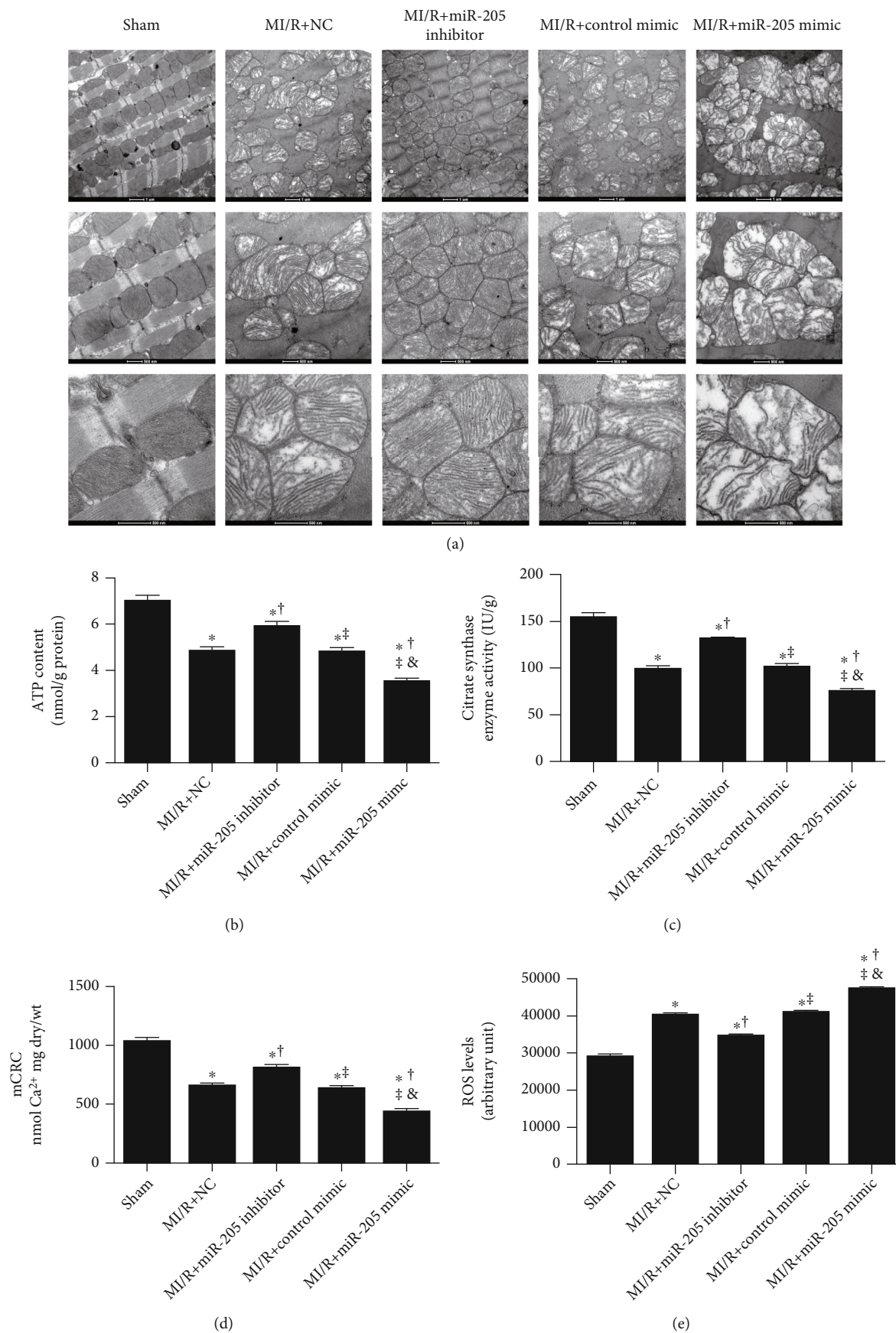


FIGURE 2: Continued.

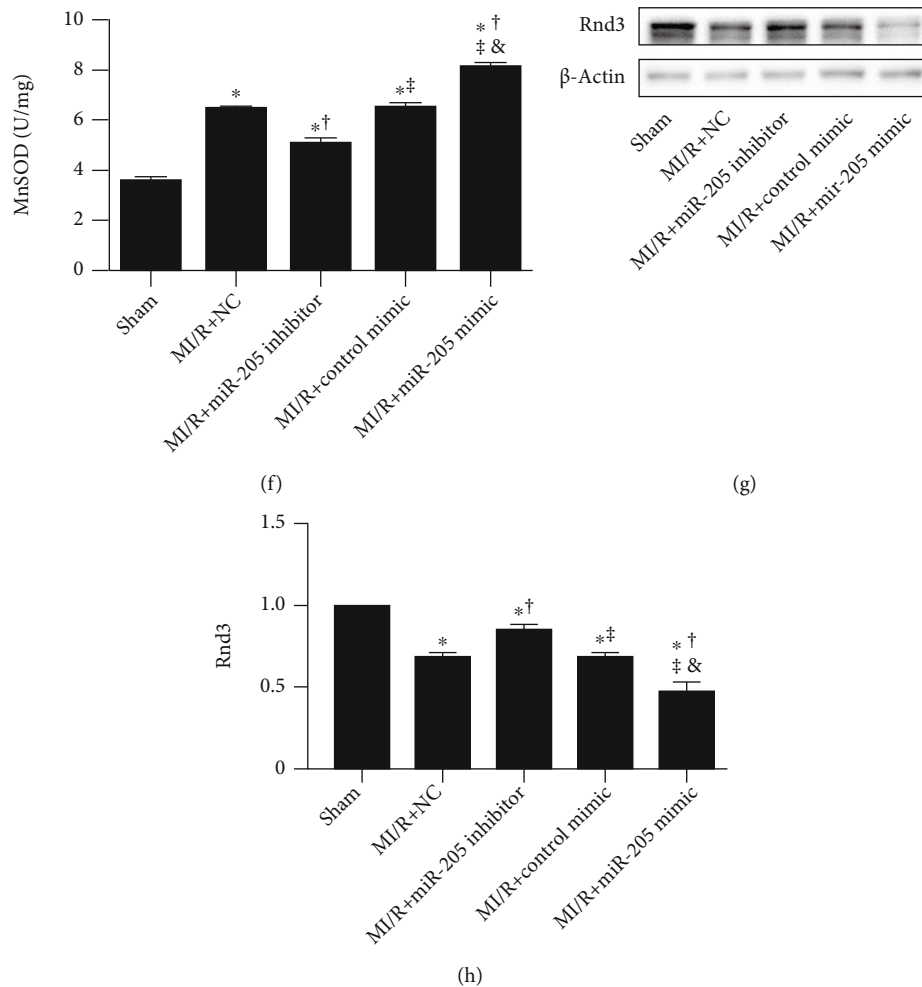


FIGURE 2: miR-205 inhibitor improves, while miR-205 mimic administration aggravates mitochondrial dysfunction and oxidative stress in mice that underwent MI/R injury. (a) Mitochondria morphological defects (magnification: upper panel $\times 9900$; middle panel $\times 20500$; lower panel $\times 43000$). (b, c) ATP content and citrate synthase (CS) activity in the ischemic myocardium in mice subjected to MI/R injury. (d) Sensitivity of the mitochondrial permeability transition pore (mPTP) opening to calcium as evidenced by mCRC measurement. (e) ROS levels assessed by EPR spectroscopy. (f) Mitochondrial MnSOD activity. (g, h) Western blot analysis of Rnd3 expression. $n = 6$ in each group. * $p < 0.05$ vs. Sham, † $p < 0.05$ vs. MI/R+NC, ‡ $p < 0.05$ vs. MI/R+miR-205 inhibitor, & $p < 0.05$ vs. MI/R+Control mimic.

and cleaved caspase-9 in the MI/R mice subjected to AAV9-sh-Rnd3 injection (Figures 6(a)–6(e)). All these results indicate that miR-205 inhibitor alleviates MI/R injury by promoting Rnd3 expression.

3.5. Inhibiting miR-205 Improves H/R-Induced Oxidative Stress, while Inhibiting Rnd3 Ablated the Cardioprotective Effects of miR-205 Inhibitor in Primary Cardiomyocytes. Consistent with these observations, miR-205 inhibitor significantly decreased, while miR-205 mimic increased the level of mitochondrial ROS, which was measured by a MitoSOX kit, in cardiomyocytes compared with the H/R group (Figures 7(a) and 7(b)). JC-1 fluorescence images revealed that miR-205 inhibitor increased the $\Delta\Psi$, while miR-205 mimic reduced the $\Delta\Psi$ in cardiomyocytes that underwent H/R injury (Figures 7(c) and 7(d)). Moreover, Ad-sh-Rnd3 increased the level of mitochondrial ROS in cardiomyocytes that underwent H/R injury. However, miR-205 inhibitor

reduced oxidative stress in cardiomyocyte after H/R, which almost disappeared after downregulation of Rnd3 (Figures 7(e) and 7(f)). JC-1 fluorescence images reveal that Ad-sh-Rnd3 reduced the $\Delta\Psi$ in cardiomyocytes that underwent H/R injury, and it could block the effect of miR-205 inhibitor on the increase of $\Delta\Psi$ that underwent H/R injury (Figures 7(g) and 7(h)).

4. Discussion

The morbidity and mortality of patients with AMI are high worldwide [35]. In patients with MI, the myocardial reperfusion treatment for salvaging viable myocardium, limiting MI size, and decreasing mortality is timely and effective [36]. However, reperfusion itself induces cardiac injury, named as reperfusion injury, and there is still lack of effective therapy for MI/R injury. It has always been a great threat to human's health and life. Numerous studies and clinical

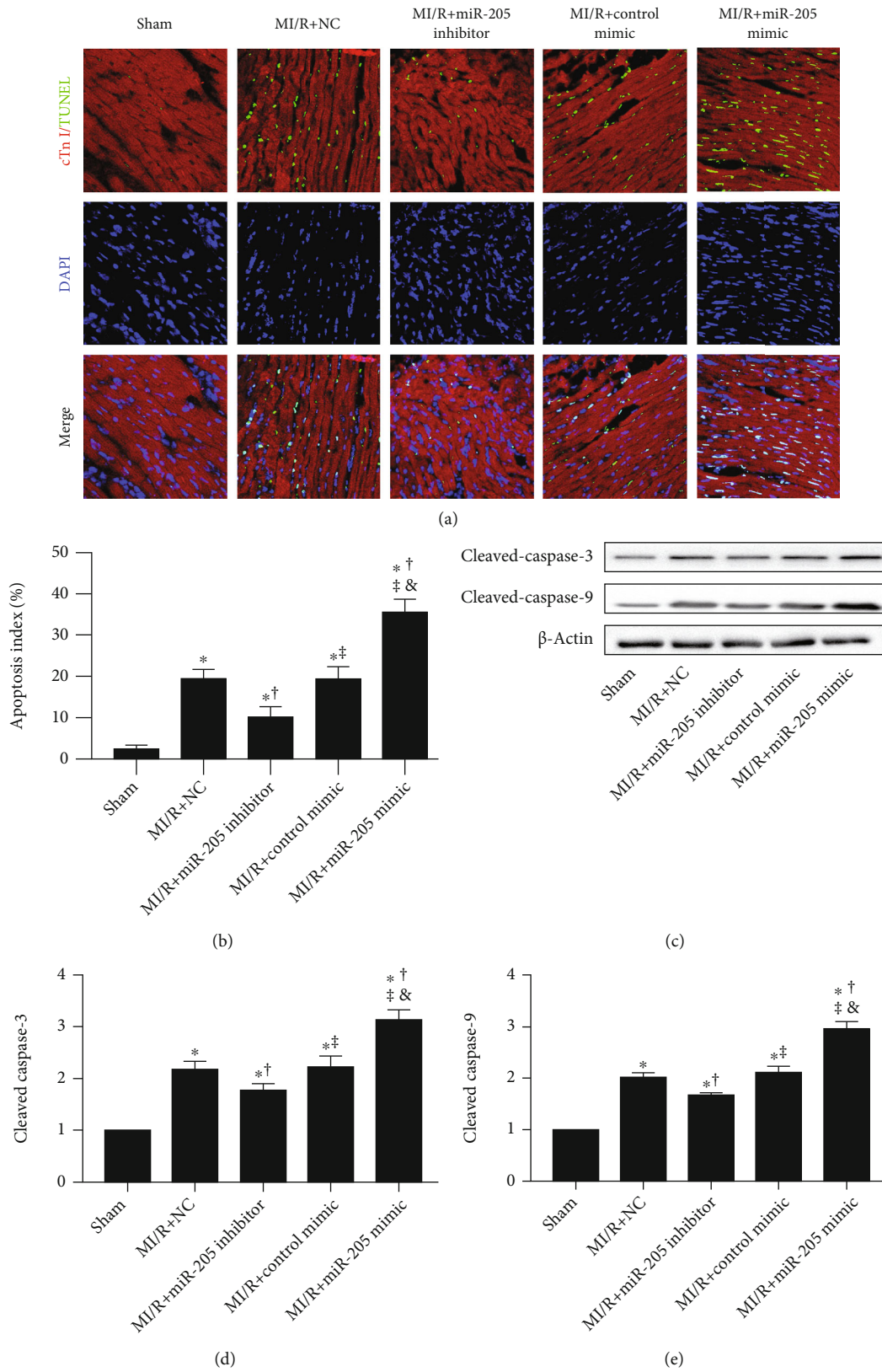


FIGURE 3: Inhibiting miR-205 improves, while miR-205 overexpression administration aggravates apoptosis in mice that underwent cardiac MI/R injury. (a, b) Representative images of TUNEL staining and percentage of TUNEL-positive nuclei, scale bars = 50 μ m. (c–e) Western blot analysis of cleaved caspase-3 and cleaved caspase-9 expression. $n = 6$ in each group. * $p < 0.05$ vs. Sham, † $p < 0.05$ vs. MI/R+NC, ‡ $p < 0.05$ vs. MI/R+miR-205 inhibitor, & $p < 0.05$ vs. MI/R+Control mimic.

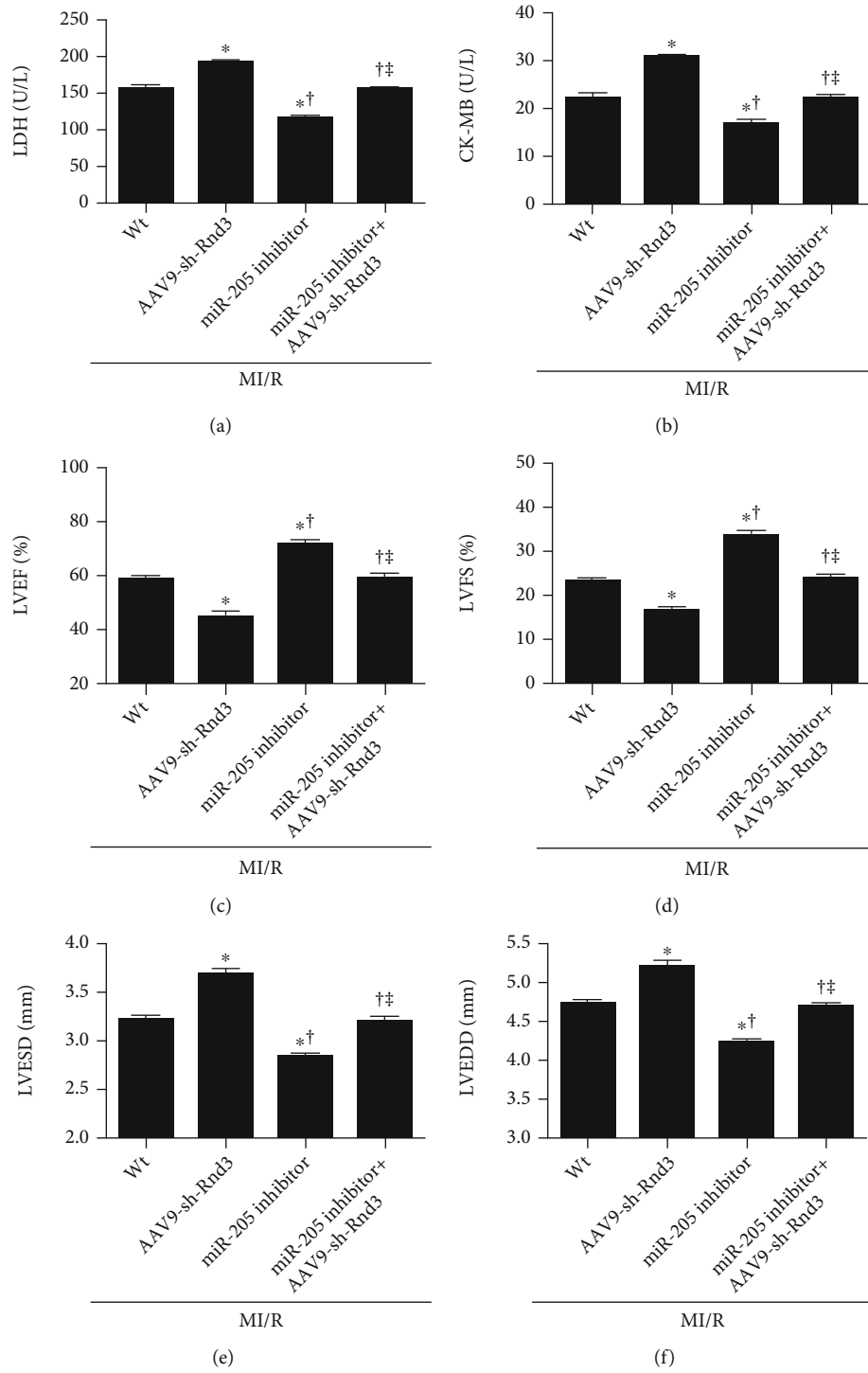


FIGURE 4: Continued.

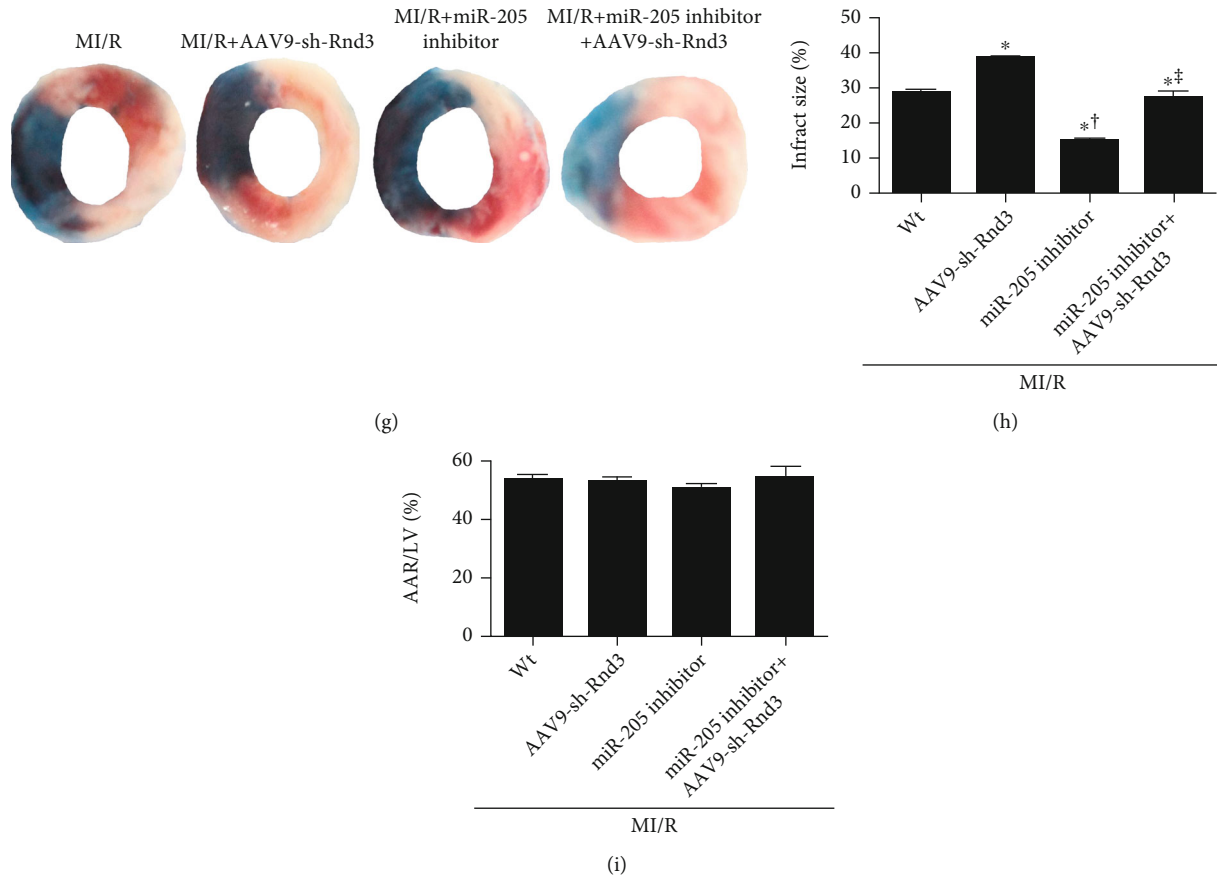
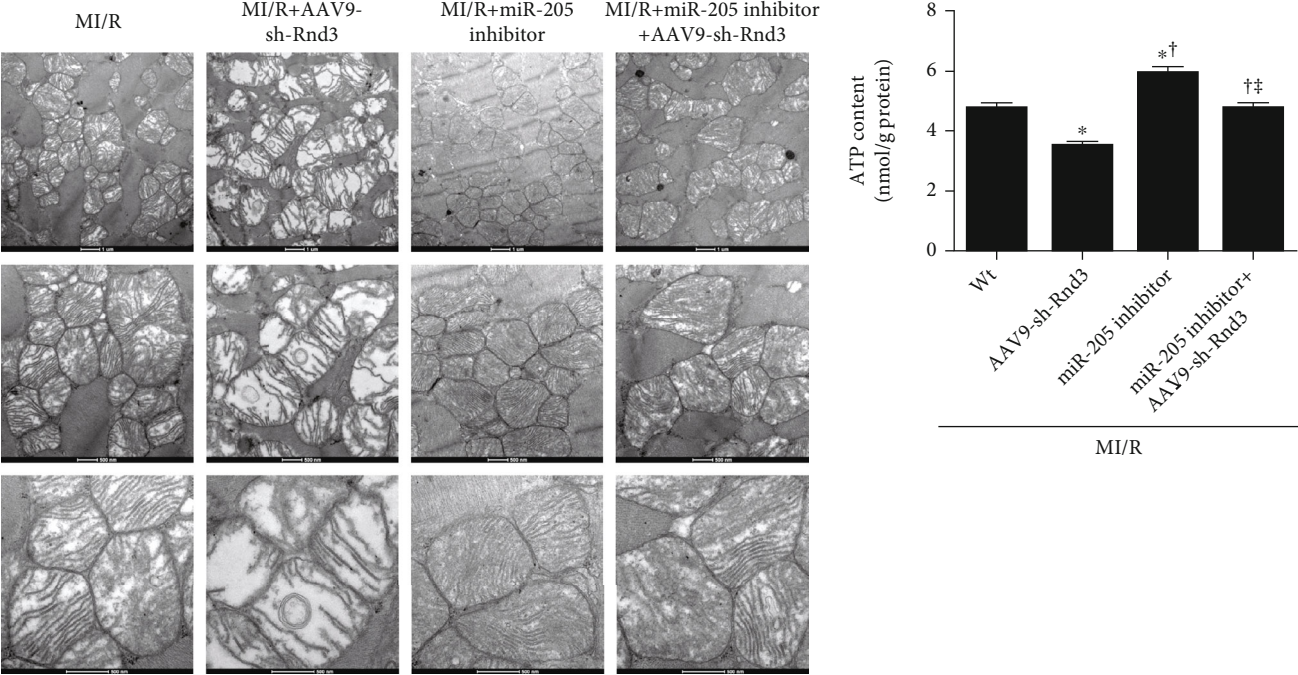


FIGURE 4: Inhibiting RND3 ablated the cardioprotective effects of miRNA-205 inhibitor. (a, b) Lactate dehydrogenase (LDH) and creatine kinase-MB (CK-MB) release. (c–f) Left ventricular ejection fraction (LVEF), left ventricular fraction shortening (LVFS), left ventricular end systolic diameter (LVESD), and left ventricular end diastolic diameter (LVEDD). (g) Representative images of infarct size as stained by Evans Blue and TTC. (h, i) Infarct size. AAR/LV had no statistical difference between groups 3 h after I/R injury. $n = 6$ in each group. The columns and errors bars represent means and SD. * $p < 0.05$ vs. MI/R, † $p < 0.05$ vs. MI/R+AAV9-sh-Rnd3, ‡ $p < 0.05$ vs. MI/R+miR-205 inhibitor.

evidence support the notion that miRNAs play essential roles in cardiovascular diseases, such as myocardial infarction, cardiac hypertrophy, cardiomyopathy, and arrhythmias, and could be used for the diagnosis and prevention of cardiovascular diseases. miR-205 is discovered to be a suppressor factor in breast cancer, which can target E2F transcription factor 1, angiotensin, and other genes, and then to reduce cell proliferation, inhibit invasion, and increase apoptosis. Ling et al. found that miR-205 was markedly inhibited in air pollution that induced myocardial inflammation, and the inhibition of miR-205 activated the IRAK2/TRAF6/NF- κ B signaling pathway [37]. Except these, miR-205 is also found to be increased in animals treated with imatinib mesylate and doxorubicin and animals with chronic heart failure [38, 39]. We found that inhibiting miR-205 improved cardiac dysfunction and mitochondrial dysfunction and reduced infarct size, oxidative stress, and apoptosis by promoting Rnd3 in MI/R injury. The results suggested that miR-205 is detrimental in MI/R injury. Moreover, the cardiac protective effects of miR-205 inhibitor are abolished through inhibiting Rnd3.

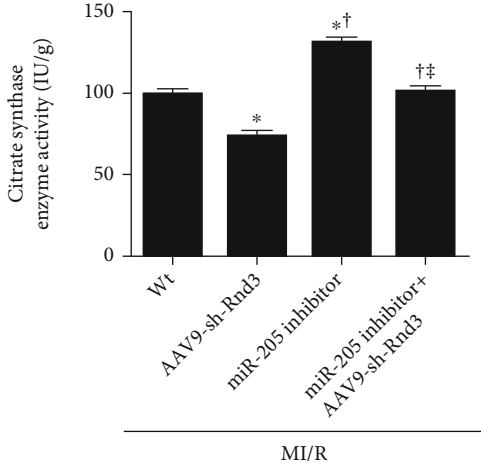
Mitochondrial dysfunction leads to contractile dysfunction and pathological ventricular remodeling, which is associated with heart failure and mortality of patients. In the current study, we found that miR-205 inhibitor improved mitochondrial dysfunction, which was associated with impaired cardiac function. Meanwhile, miR-205 mimic exaggerated contractile dysfunction and mitochondrial dysfunction. The alterations in the mitochondrial function suggested that miR-205 inhibitor may play a protective role in pathological process of MI/R injury. Moreover, these protective effects of miR-205 inhibitor were abolished by knocking down Rnd3, which was in line with our previous study.

Oxidative stress has been identified as a major cause of cardiac injury in cardiovascular system. Under pathological conditions, excessive production of ROS impairs the balance between ROS and antioxidant substance, which is called oxidative stress. Oxidative stress results in negative effects on normal cardiac structure and cardiometabolic homeostasis [40]. Increased oxidative stress is implicated in MI/R injury, contractile dysfunction, mitochondrial dysfunction, myocyte

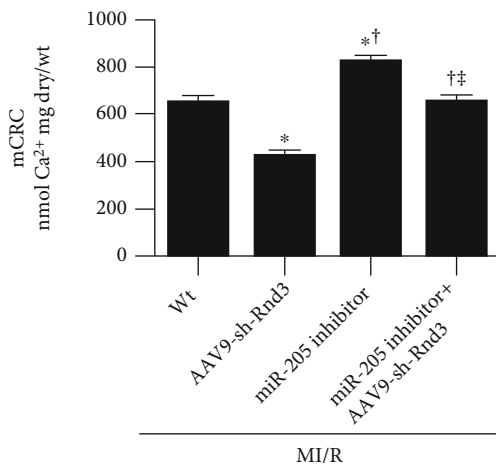


(a)

(b)



(c)



(d)

FIGURE 5: Continued.

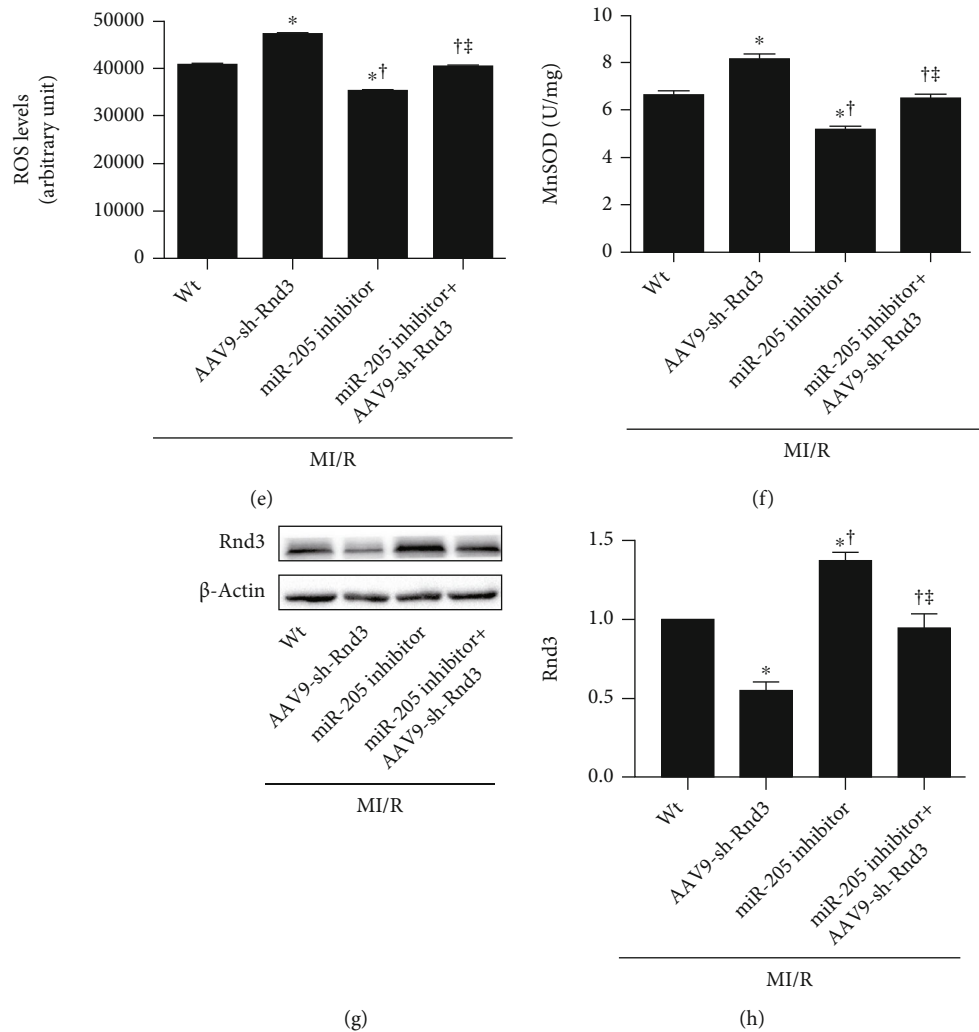


FIGURE 5: Inhibiting RND3 ablated the cardioprotective effects of miRNA-205 inhibitor in mitochondrial dysfunction and oxidative stress in mice that underwent MI/R injury. (a) Mitochondria morphological defects (magnification: upper panel $\times 9900$; middle panel $\times 20500$; lower panel $\times 43000$). (b, c) ATP content and citrate synthase (CS) activity in the ischemic myocardium in the isolated mitochondrial in mice subjected to cardiac I/R injury. (d) Sensitivity of the mitochondrial permeability transition pore (mPTP) opening to calcium as evidenced by mCRC measurement. (e) ROS levels assessed by EPR spectroscopy. (f) Mitochondrial MnSOD activity. (g, h) Western blot analysis of Rnd3 expression. $n = 6$ in each group. * $p < 0.05$ vs. MI/R, † $p < 0.05$ vs. MI/R+AAV9-sh-Rnd3, ‡ $p < 0.05$ vs. MI/R+miR-205 inhibitor.

apoptosis, and the progressive downward spiral of heart failure [41–44]. Cytoplasm, mitochondria, and peroxisomes are main sources of ROS. NADPH oxidase (NOX) family and mitochondrial complexes I-III are the most well-known contributors of production of cytoplasmic ROS and mitochondrial ROS, respectively. Overall, detrimental effects of excessive ROS in heart are attributed to dysfunction in electrophysiology, contractibility, energy metabolism, and fibrosis [45]. Excessive ROS could directly modify proteins involved in potassium channels, sodium-calcium exchanger, and other important ion channel and thus influence electrophysiology in heart [46]. Oxidative stress was increased in cardiac hypertrophy, and ROS-mediated activation of MAPKs and NF- κ B was discovered [47]. Our study has demonstrated that the miR-205 mimic exacerbates ROS level and subsequent increased superoxide generation. Furthermore,

the current study demonstrated a substantial reduction of MI/R-induced ROS after miR-205 inhibitor treatment. Oxidative stress was significantly upregulated in MI/R mice with Rnd3 knockdown. Taken together, these results indicate that miR-205 inhibitor inhibited, while miR-205 mimic promoted the oxidative stress during exposure to MI/R injury.

The cardiomyocyte apoptosis is the chief player in MI/R injury [48]. Previous studies have revealed that downregulating miR-205 reduces myocardial apoptosis in rats with chronic heart failure [39]. In the current study, miR-205 inhibitor inhibited, while miR-205 mimic promoted cardiomyocyte apoptosis.

Rnd3, a member of the Rnd family, has been proved as a key factor in the pathophysiology process of cardiomyopathy, heart failure, and cancer [27]. Rnd3 can reduce

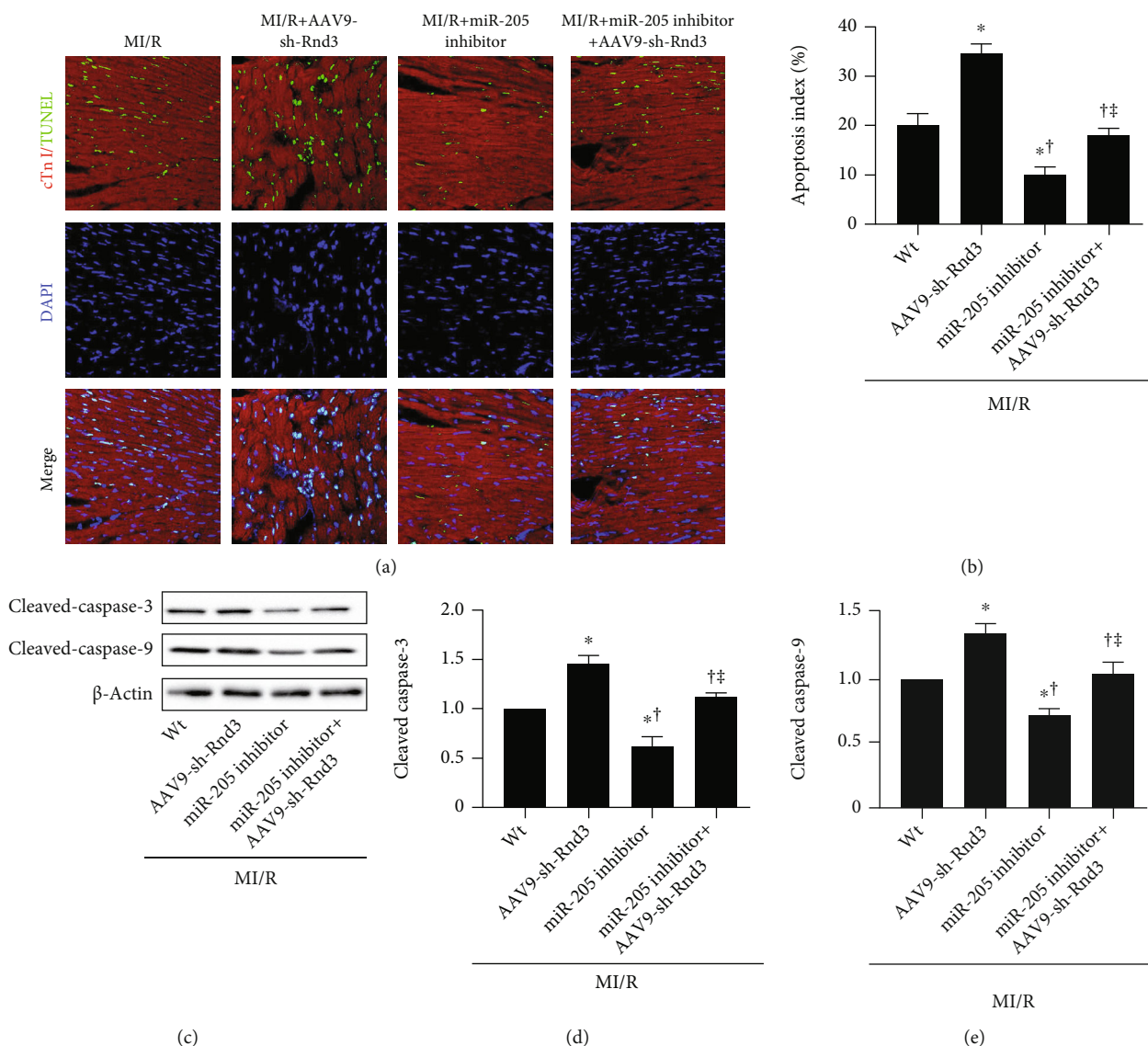
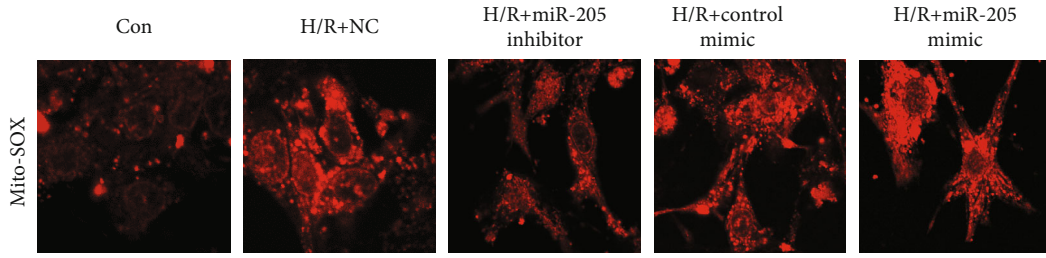


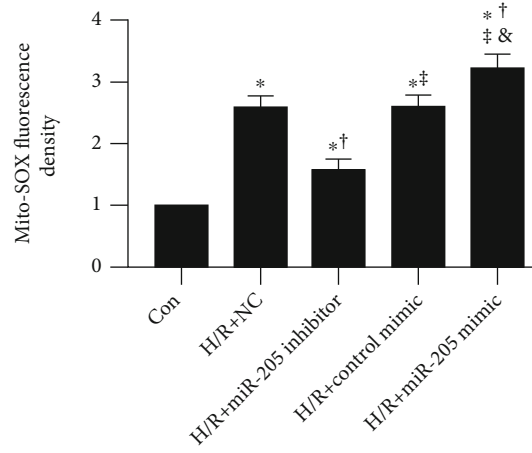
FIGURE 6: Inhibiting RND3 ablated the cardioprotective effects of miRNA-205 inhibitor in apoptosis in mice that underwent cardiac MI/R injury (a, b) Representative images of TUNEL staining and percentage of TUNEL-positive nuclei, scale bars = 50 μ m. (c-e) Western blot analysis of cleaved caspase-3 and cleaved caspase-9 expression. $n = 6$ in each group. * $p < 0.05$ vs. MI/R, † $p < 0.05$ vs. MI/R+AAV9-sh-Rnd3, ‡ $p < 0.05$ vs. MI/R+miR-205 inhibitor.

microvascular leakage after injury [49]. Recent research suggested that coronary microvascular may be a new frontier in cardioprotection after MI/R injury [50]. Further evidence has revealed that insufficient Rnd3 results in apoptotic cardiomyopathy with heart failure. In cardiac I/R injury, RND3 deficiency promotes some proinflammatory gene expressions including tumor necrosis factor (TNF) superfamily and interferons. While cardiac RND3 overexpression inhibits inflammation post-MI and improves cardiac function [51]. Increased evidence suggested an essential role for myocardial Rnd3 in modulating cardiac function. Although the precise roles remain uncertain, previous studies have revealed that Rnd3 also mediates obesity and insulin resistance [52]. miR-205 was significantly increased in mice with I/R injury,

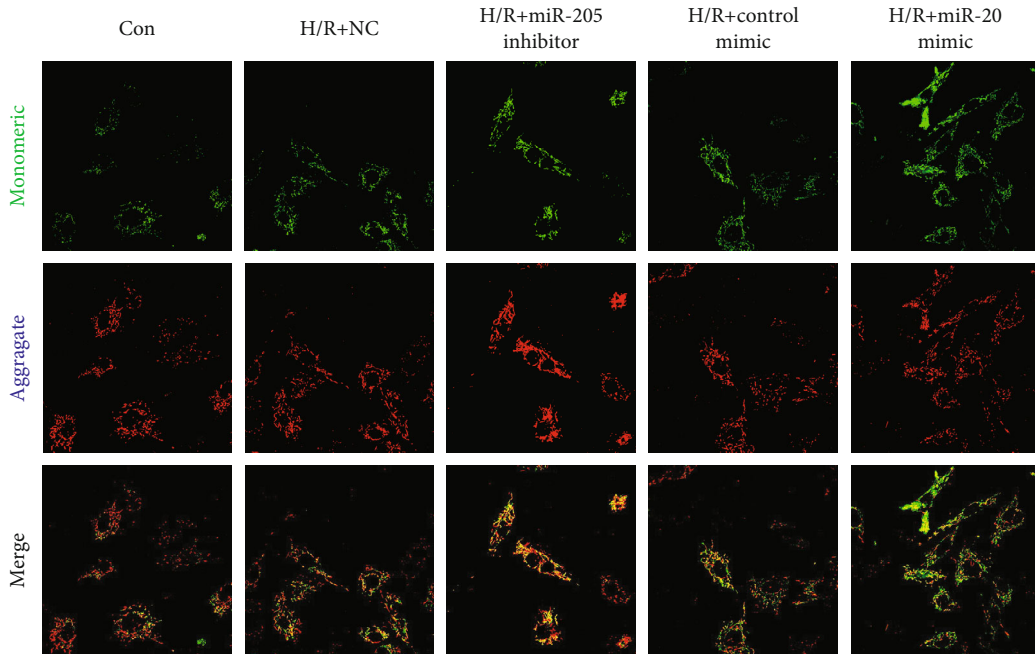
whereas the expression of Rnd3 was decreased. Meanwhile, Rnd3 knockdown abolished the cardioprotective effect in MI/R injury after miR-205 inhibitor treatment, suggesting that miR-205 inhibitor alleviates the MI/R injury by promoting Rnd3. Furthermore, our study demonstrated that Rnd3 knockdown exhibited exacerbated cardiac systolic dysfunction and mitochondrial dysfunction and increased oxidative stress and apoptosis. We observed that miR-205 inhibitor decreased the infarct size, oxidative stress, and cardiomyocyte apoptosis and improved the mitochondrial function, which was abolished by downregulating Rnd3. Taken together, these results support Rnd3 as the primary downstream of miR-205 which maintains cardiac function in the MI/R.



(a)



(b)



(c)

FIGURE 7: Continued.

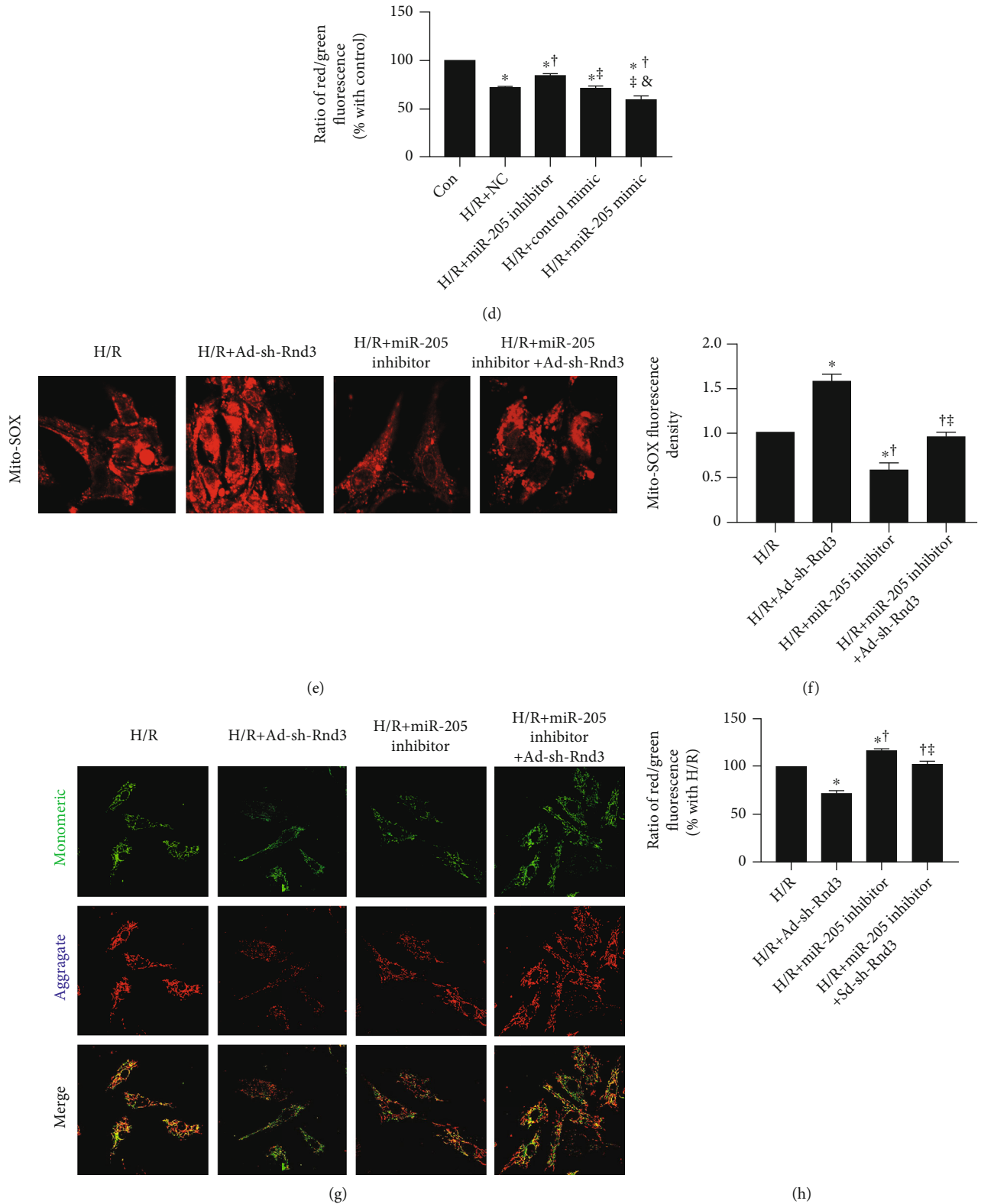


FIGURE 7: Inhibiting miR-205 improves H/R-induced oxidative stress, while inhibiting RND3 ablated the cardioprotective effects of miR-205 inhibitor in primary cardiomyocytes. (a, b) Representative images of mitochondrial ROS in primary cardiomyocytes, scale bars = 50 μ m. (c, d) Representative images of JC-1 and the ratio of aggregated (red) and monomeric (green) in neonatal mice cardiomyocytes, scale bars = 20 μ m. * $p < 0.05$ vs. Con, † $p < 0.05$ vs. H/R+NC, ‡ $p < 0.05$ vs. H/R+miR-205 inhibitor, & $p < 0.05$ vs. H/R+Control mimic. (e, f) Representative images of mitochondrial ROS in neonatal mice cardiomyocytes, scale bars = 50 μ m. (g, h) Representative images of JC-1 and the ratio of aggregated (red) and monomeric (green) in neonatal mice cardiomyocytes, scale bars = 20 μ m. The number of cardiomyocytes was counted ($n = 50$ in each group). * $p < 0.05$ vs. H/R, † $p < 0.05$ vs. H/R+AAV9-sh-Rnd3, ‡ $p < 0.05$ vs. H/R+miR-205 inhibitor.

In conclusion, we provided evidence that miR-205 inhibitor alleviated the cardiac I/R injury. In addition, these cardiac protective effects of miR-205 inhibitor are largely attributable to the Rnd3 activation. Although these data collectively indicate that miR-205 Inhibitor as a therapeutic target for MI/R injury, further studies are needed to test the clinical implications of miR-205 inhibitor in protecting against cardiac I/R injury.

Data Availability

The data used to support the findings of this study are available from the corresponding authors upon request.

Conflicts of Interest

The authors declare that they have no conflicts of interest.

Authors' Contributions

Yuerong Xu, Wangang Guo, Di Zeng, and Yexian Fang contributed equally to this work.

Acknowledgments

This work was supported by the National Natural Science Foundation of China (No. 81900338), Shaanxi Natural Science Basic Research Program (No. 2020JQ455), and Eagle Program from The Fourth Military Medical University (No. 015210).


References

- [1] S. S. Virani, A. Alonso, E. J. Benjamin et al., "Heart Disease and Stroke Statistics-2020 update: a report from the American Heart Association," *Circulation*, vol. 141, no. 9, pp. e139–e596, 2020.
- [2] D. P. Leong, P. G. Joseph, M. McKee et al., "Reducing the global burden of cardiovascular disease, part 2: prevention and treatment of cardiovascular disease," *Circulation Research*, vol. 121, no. 6, pp. 695–710, 2017.
- [3] F. J. P. Bernink, L. Timmers, A. M. Beek et al., "Progression in attenuating myocardial reperfusion injury: an overview," *International Journal of Cardiology*, vol. 170, no. 3, pp. 261–269, 2014.
- [4] B. Ibáñez, G. Heusch, M. Ovize, and F. Van de Werf, "Evolving therapies for myocardial ischemia/reperfusion injury," *Journal of the American College of Cardiology*, vol. 65, no. 14, pp. 1454–1471, 2015.
- [5] T. Sugiyama, K. Hasegawa, Y. Kobayashi, O. Takahashi, T. Fukui, and Y. Tsugawa, "Differential time trends of outcomes and costs of care for acute myocardial infarction hospitalizations by ST elevation and type of intervention in the United States, 2001–2011," *Journal of the American Heart Association*, vol. 4, no. 3, article e001445, 2015.
- [6] M. Correia de Sousa, M. Gjorgjieva, D. Dolicka, C. Sobolewski, and M. Foti, "Deciphering miRNAs' action through miRNA editing," *International Journal of Molecular Sciences*, vol. 20, no. 24, p. 6249, 2019.
- [7] Y. Ekdahl, H. S. Farahani, M. Behm, J. Lagergren, and M. Öhman, "A-to-I editing of microRNAs in the mammalian brain increases during development," *Genome Research*, vol. 22, no. 8, pp. 1477–1487, 2012.
- [8] Z. Sun, K. Shi, S. Yang et al., "Effect of exosomal miRNA on cancer biology and clinical applications," *Molecular Cancer*, vol. 17, no. 1, p. 147, 2018.
- [9] M. Li, W. Ding, M. A. Tariq et al., "A circular transcript of ncx1 gene mediates ischemic myocardial injury by targeting miR-133a-3p," *Theranostics*, vol. 8, no. 21, pp. 5855–5869, 2018.
- [10] A. Jusic and Y. Devaux, "Mitochondrial noncoding RNA-regulatory network in cardiovascular disease," *Basic Research in Cardiology*, vol. 115, no. 3, p. 23, 2020.
- [11] S. Mishra, T. Yadav, and V. Rani, "Exploring miRNA based approaches in cancer diagnostics and therapeutics," *Critical Reviews in Oncology/Hematology*, vol. 98, pp. 12–23, 2016.
- [12] N. Abbas, F. Perbellini, and T. Thum, "Non-coding RNAs: emerging players in cardiomyocyte proliferation and cardiac regeneration," *Basic Research in Cardiology*, vol. 115, no. 5, p. 52, 2020.
- [13] Z. Ma, Y. H. Lan, Z. W. Liu, M. X. Yang, H. Zhang, and J. Y. Ren, "miR-19a suppress apoptosis of myocardial cells in rats with myocardial ischemia/reperfusion through PTEN/Akt/P-Akt signaling pathway," *European Review for Medical and Pharmacological Sciences*, vol. 24, no. 6, pp. 3322–3330, 2020.
- [14] Z. G. Liang, H. Yao, R. S. Xie, C. L. Gong, and Y. Tian, "Micro-RNA-20b-5p promotes ventricular remodeling by targeting the TGF- β /Smad signaling pathway in a rat model of ischemia-reperfusion injury," *International Journal of Molecular Medicine*, vol. 42, no. 2, pp. 975–987, 2018.
- [15] A. E. Consolini, M. I. Ragone, P. Bonazzola, and G. A. Colarada, "Mitochondrial bioenergetics during ischemia and reperfusion," *Advances in Experimental Medicine and Biology*, vol. 982, pp. 141–167, 2017.
- [16] E. J. Lesnefsky, Q. Chen, B. Tandler, and C. L. Hoppel, "Mitochondrial dysfunction and myocardial ischemia-reperfusion: implications for novel therapies," *Annual Review of Pharmacology and Toxicology*, vol. 57, no. 1, pp. 535–565, 2017.
- [17] D. Dutta, R. Calvani, R. Bernabei, C. Leeuwenburgh, and E. Marzetti, "Contribution of impaired mitochondrial autophagy to cardiac aging: mechanisms and therapeutic opportunities," *Circulation Research*, vol. 110, no. 8, pp. 1125–1138, 2012.
- [18] A. Picca, R. T. Mankowski, J. L. Burman et al., "Mitochondrial quality control mechanisms as molecular targets in cardiac ageing," *Nature Reviews. Cardiology*, vol. 15, no. 9, pp. 543–554, 2018.
- [19] D. A. Kubli, X. Zhang, Y. Lee et al., "Parkin protein deficiency exacerbates cardiac injury and reduces survival following myocardial infarction," *J Biol Chem.*, vol. 288, no. 2, pp. 915–926, 2013.
- [20] H. Zhu, S. Toan, D. Mui, and H. Zhou, "Mitochondrial quality surveillance as a therapeutic target in myocardial infarction," *Acta Physiologica*, vol. 231, no. 3, p. e13590, 2021.
- [21] H. Tsutsui, S. Kinugawa, and S. Matsushima, "Oxidative stress and heart failure," *American Journal of Physiology. Heart and Circulatory Physiology*, vol. 301, no. 6, pp. H2181–H2190, 2011.
- [22] S. J. Forrester, D. S. Kikuchi, M. S. Hernandez, Q. Xu, and K. K. Griending, "Reactive oxygen species in metabolic and inflammatory signaling," *Circulation Research*, vol. 122, no. 6, pp. 877–902, 2018.

- [23] I. Plantamura, A. Cataldo, G. Cosentino, and M. V. Iorio, "miR-205 in breast cancer: state of the Art," *International Journal of Molecular Sciences*, vol. 22, no. 1, p. 27, 2021.
- [24] C. Piovani, D. Palmieri, G. Di Leva et al., "Oncosuppressive role of p53-induced miR-205 in triple negative breast cancer," *Molecular Oncology*, vol. 6, no. 4, pp. 458–472, 2012.
- [25] P. Madaule and R. Axel, "A novel ras-related gene family," *Cell*, vol. 41, no. 1, pp. 31–40, 1985.
- [26] A. J. Ridley, "Rho GTPases and actin dynamics in membrane protrusions and vesicle trafficking," *Trends in Cell Biology*, vol. 16, no. 10, pp. 522–529, 2006.
- [27] W. Jie, K. C. Andrade, X. Lin, X. Yang, X. Yue, and J. Chang, "Pathophysiological functions of Rnd3/RhoE," *Comprehensive Physiology*, vol. 6, no. 1, pp. 169–186, 2015.
- [28] R. Foster, K. Q. Hu, Y. Lu, K. M. Nolan, J. Thissen, and J. Settleman, "Identification of a novel human Rho protein with unusual properties: GTPase deficiency and in vivo farnesylation," *Molecular and Cellular Biology*, vol. 16, no. 6, pp. 2689–2699, 1996.
- [29] X. Yue, X. Yang, X. Lin et al., "Rnd3 haploinsufficient mice are predisposed to hemodynamic stress and develop apoptotic cardiomyopathy with heart failure," *Cell Death & Disease*, vol. 5, no. 6, article e1284, 2014.
- [30] X. Yang, T. Wang, X. Lin et al., "Genetic deletion of Rnd3/RhoE results in mouse heart calcium leakage through upregulation of protein kinase a signaling," *Circulation Research*, vol. 116, no. 1, pp. e1–e10, 2015.
- [31] X. Yue, X. Lin, T. Yang et al., "Rnd3/RhoE modulates hypoxia-inducible factor 1 α /vascular endothelial growth factor signaling by stabilizing hypoxia-inducible factor 1 α and regulates responsive cardiac angiogenesis," *Hypertension*, vol. 67, no. 3, pp. 597–605, 2016.
- [32] M. Zhang, C. Wang, J. Hu et al., "Notch3/Akt signaling contributes to OSM-induced protection against cardiac ischemia/reperfusion injury," *Apoptosis*, vol. 20, no. 9, pp. 1150–1163, 2015.
- [33] M. Zhang, J. Lin, S. Wang et al., "Melatonin protects against diabetic cardiomyopathy through Mst1/Sirt3 signaling," *Journal of Pineal Research*, vol. 63, no. 2, 2017.
- [34] X. Shi, Y. Liu, D. Zhang, and D. Xiao, "Valproic acid attenuates sepsis-induced myocardial dysfunction in rats by accelerating autophagy through the PTEN/AKT/mTOR pathway," *Life Sciences*, vol. 232, p. 116613, 2019.
- [35] G. W. Reed, J. E. Rossi, and C. P. Cannon, "Acute myocardial infarction," *Lancet*, vol. 389, no. 10065, pp. 197–210, 2017.
- [36] B. Vogel, B. E. Claessen, S. V. Arnold et al., "ST-segment elevation myocardial infarction," *Nature Reviews. Disease Primers*, vol. 5, no. 1, p. 39, 2019.
- [37] L. Feng, J. Wei, S. Liang, Z. Sun, and J. Duan, "miR-205/IRAK2 signaling pathway is associated with urban airborne PM2.5-induced myocardial toxicity," *Nanotoxicology*, vol. 14, no. 9, pp. 1198–1212, 2020.
- [38] B. Hanousková, M. Skála, V. Brynychová et al., "Imatinib-induced changes in the expression profile of microRNA in the plasma and heart of mice—a comparison with doxorubicin," *Biomed Pharmacother.*, vol. 115, p. 108883, 2019.
- [39] Y. Xuan, S. Liu, Y. Li et al., "Short-term vagus nerve stimulation reduces myocardial apoptosis by downregulating microRNA-205 in rats with chronic heart failure," *Molecular Medicine Reports*, vol. 16, no. 5, pp. 5847–5854, 2017.
- [40] D. Zhao, J. Yang, and L. Yang, "Insights for oxidative stress and mTOR signaling in myocardial ischemia/reperfusion injury under diabetes," *Oxidative Medicine and Cellular Longevity*, vol. 2017, Article ID 6437467, 12 pages, 2017.
- [41] J. González-Montero, R. Brito, A. I. J. Gajardo, and R. Rodrigo, "Myocardial reperfusion injury and oxidative stress: therapeutic opportunities," *World Journal of Cardiology*, vol. 10, no. 9, pp. 74–86, 2018.
- [42] H. Bugger and K. Pfeil, "Mitochondrial ROS in myocardial ischemia reperfusion and remodeling," *Biochimica et Biophysica Acta - Molecular Basis of Disease*, vol. 1866, no. 7, p. 165768, 2020.
- [43] S. Cadenas, "ROS and redox signaling in myocardial ischemia-reperfusion injury and cardioprotection," *Free Radical Biology & Medicine*, vol. 117, pp. 76–89, 2018.
- [44] J. Wang, S. Toan, and H. Zhou, "New insights into the role of mitochondria in cardiac microvascular ischemia/reperfusion injury," *Angiogenesis*, vol. 23, no. 3, pp. 299–314, 2020.
- [45] A. van der Pol, W. H. van Gilst, A. A. Voors, and P. van der Meer, "Treating oxidative stress in heart failure: past, present and future," *European Journal of Heart Failure*, vol. 21, no. 4, pp. 425–435, 2019.
- [46] E. Takimoto and D. A. Kass, "Role of oxidative stress in cardiac hypertrophy and remodeling," *Hypertension*, vol. 49, no. 2, pp. 241–248, 2007.
- [47] M. Seddon, Y. H. Looi, and A. M. Shah, "Oxidative stress and redox signalling in cardiac hypertrophy and heart failure," *Heart*, vol. 93, no. 8, pp. 903–907, 2007.
- [48] X. Xiao, Z. Lu, V. Lin et al., "MicroRNA miR-24-3p reduces apoptosis and regulates Keap1-Nrf2 pathway in mouse cardiomyocytes responding to ischemia/reperfusion injury," *Oxidative Medicine and Cellular Longevity*, vol. 2018, Article ID 7042105, 9 pages, 2018.
- [49] J. W. Breslin, D. A. Daines, T. M. Doggett et al., "Rnd3 as a novel target to ameliorate microvascular leakage," *Journal of the American Heart Association*, vol. 5, no. 4, article e003336, 2016.
- [50] G. Heusch, "Coronary microvascular obstruction: the new frontier in cardioprotection," *Basic Research in Cardiology*, vol. 114, no. 6, p. 45, 2019.
- [51] Y. Dai, J. Song, W. Li et al., "RhoE fine-tunes inflammatory response in myocardial infarction," *Circulation*, vol. 139, no. 9, pp. 1185–1198, 2019.
- [52] S. N. Dankel, T. H. Røst, A. Kulyté et al., "The Rho GTPase RND3 regulates adipocyte lipolysis," *Metabolism*, vol. 101, p. 153999, 2019.

Review Article

The Role of Mitochondrial Quality Control in Cardiac Ischemia/Reperfusion Injury

Jia Huang,^{1,2} Ruibing Li,¹ and Chengbin Wang¹ 

¹Department of Clinical Laboratory Medicine, the First Medical Centre, Chinese PLA General Hospital, China

²Medical School of Chinese PLA, Beijing, China

Correspondence should be addressed to Chengbin Wang; wangcb301@163.com

Received 26 February 2021; Revised 18 April 2021; Accepted 19 May 2021; Published 10 June 2021

Academic Editor: Daniele Vergara

Copyright © 2021 Jia Huang et al. This is an open access article distributed under the Creative Commons Attribution License, which permits unrestricted use, distribution, and reproduction in any medium, provided the original work is properly cited.

A healthy mitochondrial network produces a large amount of ATP and biosynthetic intermediates to provide sufficient energy for myocardium and maintain normal cell metabolism. Mitochondria form a dynamic and interconnected network involved in various cellular metabolic signaling pathways. As mitochondria are damaged, controlling mitochondrial quantity and quality is activated by changing their morphology and tube network structure, mitophagy, and biogenesis to replenish a healthy mitochondrial network to preserve cell function. There is no doubt that mitochondrial dysfunction has become a key factor in many diseases. Ischemia/reperfusion (IR) injury is a pathological manifestation of various heart diseases. Cardiac ischemia causes temporary tissue and organelle damage. Although reperfusion is essential to compensate for nutrient deficiency, blood flow restoration inconsequently further kills the previously ischemic cardiomyocytes. To date, dysfunctional mitochondria and disturbed mitochondrial quality control have been identified as critical IR injury mechanisms. Many researchers have detected abnormal mitochondrial morphology and mitophagy, as well as aberrant levels and activity of mitochondrial biogenesis factors in the IR injury model. Although mitochondrial damage is well-known in myocardial IR injury, the causal relationship between abnormal mitochondrial quality control and IR injury has not been established. This review briefly describes the molecular mechanisms of mitochondrial quality control, summarizes our current understanding of the complex role of mitochondrial quality control in IR injury, and finally speculates on the possibility of targeted control of mitochondria and the methods available to mitigate IR injury.

1. Introduction

Mitochondria are the primary sites where eukaryotic cells conduct aerobic respiration. The myocardium highly relies on aerobic metabolism to maintain its cellular viability and systolic function. Mitochondria account for over 30% of the total volume of cardiomyocytes in the myocardium to produce sufficient ATP and are closely related to cardiomyocyte metabolism [1]. Therefore, the self-regulation mechanism to maintain the normal function of mitochondria is fundamental. Mitochondria undergo specific physiological processes related to quantity, shape, and quality in response to physiological environment changes to ensure cardiomyocyte activity. These physiological processes are prerequisites for mitochondrial quality control, including mitochondrial biogenesis, protein homeostasis maintenance, mitochondrial fission/fusion, and removal of damaged mitochondria or protein by fusing

with lysosomes [2, 3]. The mitochondrial fission and fusion processes segregate damaged mitochondria and promote the balance of mitochondrial components such as DNA and proteins. Dysfunctional mitochondria are cleared and recycled by lysosomes under oxidative stress and nutrient deprivation in a mitophagic fashion to form mitochondrial spheroids or mitochondrial-derived vesicles (MDVs). Mitochondrial biogenesis is responsible for a healthy mitochondrial network via mitochondrial turnover in cardiomyocytes [3–5].

Meanwhile, mitochondria are also closely linked to cell death in both necrotic and apoptotic forms. Under ischemia/reperfusion (IR) injury, mitochondria are vulnerable to cell stress such as hypoxia and oxidative stress built-up by ischemia and reperfusion, leading to overproduction of reactive oxygen species (ROS), Ca²⁺ overload, and apoptotic proteins activity. This will open the mitochondrial permeability transition pore (mPTP) and form a channel to release

cytochrome c into the cytoplasm, inducing a cascade of apoptosis [6]. When exposed to mitochondrial injury, cells first respond to active antioxidation, repair DNA, and regulate protein folding to maintain original structure and composition. If the first line of defense fails, the quality control system will be activated. Changing the mitochondrial function and structure is not only an adaptive response to ischemia and reperfusion but also a key process of apoptosis or necrosis of myocardial cells. Therefore, targeted intervention in mitochondrial quality control may slow down the degree of IR damage to some extent.

2. Mitochondrial-Centric Damage in Ischemia/Reperfusion Injury

Ischemia-induced tissue damage is a major cause of fatal disease. IR injury is a leading cause of chronic heart failure and the main pathological manifestation of coronary artery disease (CAD) [7]. Acute myocardial infarction (AMI) is induced by coronary artery occlusion, causing a cessation of blood flow (ischemia) and reperfusion damage [8]. Myocardial ischemia injury is mainly caused by myocardial hypoxia and nutrient deprivation resulting in necrosis or temporary functional impairment of myocardial cells. The free radicals produced by reoxygenation after long-term ischemia are the real factors that cause tissue damage. ROS were previously believed to kill cells directly through oxidative stress. However, the current view gradually favors that ROS triggers physiological or procedural pathways of cell death [9], for example, by inducing prolonged mPTP opening, which ultimately destroys mitochondria, cells, and tissues. Among various mechanisms speculated for cardiac IR injury, such as oxidative stress, mitochondrial Ca^{2+} overload, endothelial dysfunction, inflammation, autophagy failure, and apoptosis, mitochondria play a central role in mediating these pathophysiological processes with impaired mitochondrial function [10, 11]. The prolonged mPTP opening is the key link to tissue damage caused by mitochondria. Due to the existence of voltage-dependent anion channels (VDAC), the outer mitochondrial membrane (OMM) is much more permeable than the inner mitochondrial membrane (IMM), allowing metabolites and certain small molecules to exchange between cytoplasm and mitochondria. The permeability of IMM is determined by mPTP [12]. Transient mPTP opening has a critical physiologic role in regulating ROS signaling, cardiomyocyte development, and mitochondrial Ca^{2+} outflow. Prolonged mPTP opening results in depolarization of mitochondrial membrane potential, ATP synthesis cessation, and mitochondrial swelling and death [13]. Unregulated opening of mPTP is a key factor in inducing ischemia-reperfusion injury and heart failure [14]. Therefore, stringent mitochondrial quality control is critical during all IR injury stages.

After ischemia and reperfusion, microcirculation disturbance and tissue damage gradually develop, including ischemia, acute, subacute, and chronic reperfusion stages [15]. At the ischemia stage, hypoxia and nutritional deficiencies block subunits of mitochondrial respiratory chain expression, decreasing ATP synthesis [16]. Coupled with ATP consumption by surrounding tissues, ATP amount is hard to meet the

energy demands for actin polymerization to form contractile devices in heart muscle cells [17]. Additionally, ATP deprivation can also lead to endothelial junction protein phosphorylation and increased vascular permeability [18]. Reperfusion is undoubtedly crucial for restoring blood supply and myocardial salvage. The current clinical practice believes that early rapid patency, a short time to reperfusion, and complete restoration of normal flow can effectively reduce overall mortality [19]. However, this process will also cause further damage, such as continuous ATP decline and excessive peroxide generation from mitochondria, even excess insult during initial ischemia. Injury and downregulation of complex I and II in mitochondria block ATP production. Moreover, electron transfer during reperfusion also causes complex I to form large amounts of peroxides and ROS release [20]. Elevated mitochondrial ROS levels not only drive mitochondrial oxidative damage and disturbing respiratory mechanism and ATP production but also attack cellular components and promote releasing inflammatory cytokines through activating several intracellular signaling pathways [21]. In intact cardiomyocytes, mitochondrial ROS and calcium dysregulation result in prolonged mPTP opening, providing a channel for releasing cytochrome c, activating classical mitochondrial-death pathway by acting with caspase-9 and caspase-3 in cytoplasm [22, 23]. In addition, mPTP not only opens to change mitochondrial membrane potential and induces mitochondrial-dependent apoptosis under long-term ischemia and reoxygenation but also further disrupts the respiratory chain and simultaneously produces more ROS, leading to IR-induced apoptosis and necrotic cell death, which is called ROS-induced ROS release (RIRR) [12]. The RIRR then spreads and amplifies damage to other tissues [24], while ATP absence and oxidative stress during reperfusion will further stimulate mPTP to aggravate the damage.

Furthermore, mPTP opening was also closely correlated with increasing mitochondrial matrix Ca^{2+} ($[\text{Ca}^{2+}]_m$). Intracellular Ca^{2+} ($[\text{Ca}^{2+}]_i$) enters the mitochondrial matrix through a group of highly selective Ca^{2+} channels in IMM called mitochondrial calcium uniporters (MCUs) and stimulates ATP production under physiological conditions [25]. However, excessive Ca^{2+} entering mitochondria increases $[\text{Ca}^{2+}]_m$ levels that may activate mPTP and harm mitochondrial function. The current view supports that $[\text{Ca}^{2+}]_i$ and $[\text{Ca}^{2+}]_m$ are involved in mitochondrial quality control and regulate appropriate mitochondrial function, through which specific proteins are produced and eliminated during normal physiological functions and mitochondrial and endoplasmic reticulum stress [26]. In some genetic studies, MCU deficiency seems to alleviate cardiac IR injury, suggesting that there may be less Ca^{2+} entering mitochondria via MCU in these models, but this hypothesis has not been quantitatively tested [27, 28].

The central role of mitochondria in cardiac IR injury has been well proven, but the causal relationship and potential mechanism during cardiac IR injury of mitochondrial quality control remain unexplored. This article reviews the mechanism of mitochondrial quality control and its role in ischemia-reperfusion injury (Figure 1).

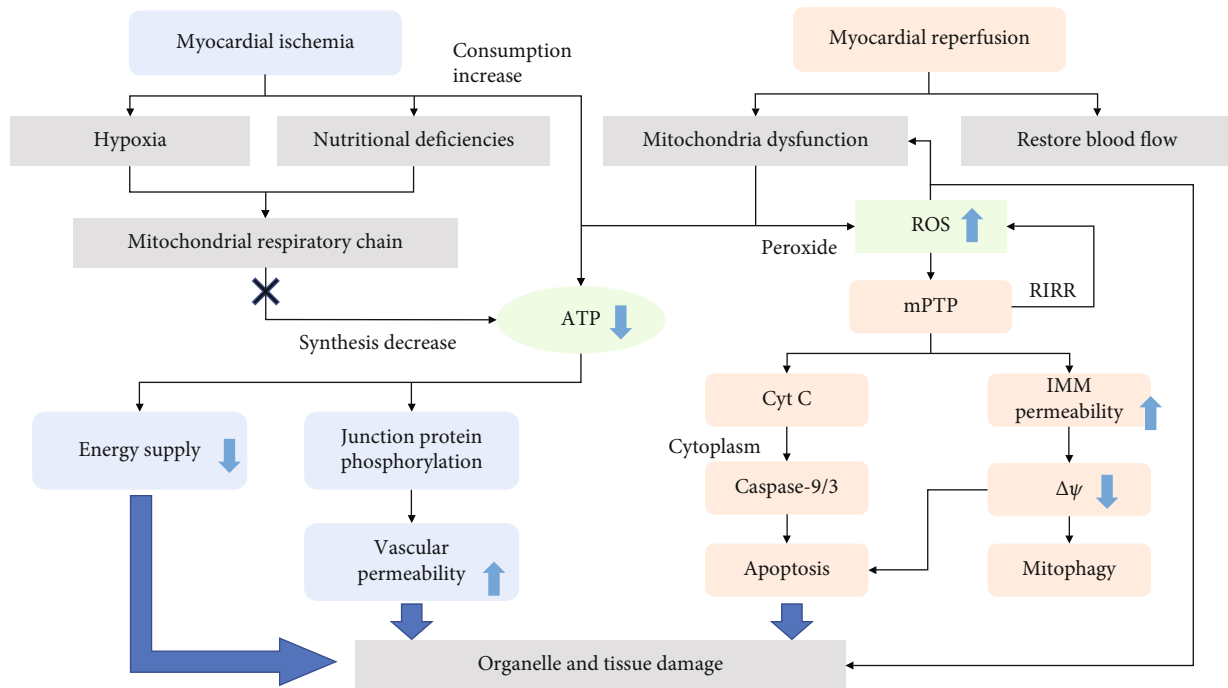


FIGURE 1: Injury mechanism involved in mitochondria at different stages of myocardial ischemia-reperfusion. Ischemia/reperfusion (IR) injury is divided into two stages, ischemia and reperfusion. Both involve a decline in ATP synthesis. In the phase of ischemia, the damaged mitochondrial respiratory chain will reduce ATP synthesis, coupled with continuous energy consumption of other tissues and organelles, resulting in a significant decrease in ATP content. Due to a lack of energy supply and increased vascular permeability, myocardial ischemia can cause temporary tissue damage. In the reperfusion phase, in addition to the continuous decline of ATP synthesis, the mitochondrial respiratory chain will also excessively produce ROS. ROS mediates prolonged mPTP opening that forms a channel to release cytochrome c and then activate the apoptotic cascade of cardiomyocytes, which further aggravates tissue damage.

3. Mitochondrial Dynamics

3.1. Mitochondrial Fission. Mitochondria are highly dynamic in the cardiovascular system and are spatially and functionally organized in a filamentous network undergoing fusion and fission, through which mitochondria constantly change between elongated and fragmented morphology responding to various environmental stimuli and cellular requirements [29, 30]. In mammalian cells, mitochondrial fission is mediated by dynamin-related peptide 1 (Drp1), mitochondrial fission protein 1 (Fis1), mitochondrial fission factor (Mff), and 49kd and 51kd mitochondrial dynamics proteins (Mid49/51), while mitochondrial fusion is primarily regulated by dynamin-related GTPases mitofusins (Mfn1 and Mfn2) and optic atrophy protein 1 (Opa1) [31]. Drp1 distributed widely in cytosol and translocates to OMM when activated by phosphorylation/dephosphorylation via actin and microtubule mechanisms [32]. After that, Drp1 interacts with Fis1, Mff, and Mid49/51 and then constricts and cleaves mitochondria by GTP hydrolysis [33]. As a key factor in mediating fission, regulating Drp1 at multiple levels, including transcriptional control, alternative splicing, and posttranslational modification is important [34]. In immune cells, Drp1-X01 subtype, unique to microtubules and phosphorylated for fission, is derived from alternative splicing of Drp1. This splicing variant stabilized microtubules and resulted in reduced apoptosis [35]. However, major regulatory mechanisms in most cardiovascular diseases are

posttranslational modification processes, including phosphorylation, dephosphorylation, ubiquitination, sumoylation, nitrosylation, and acylation [34, 36]. Protein kinase A (PKA) phosphorylates and inactivates Drp1 while Ca^{2+} -calmodulin-dependent phosphatase calcineurin dephosphorylates Drp1 and promotes mitochondrial fission [37, 38]. Drp1 phosphorylation at Ser616 promotes its oligomerization around OMM and induces division loop formation at the mitochondrial potential fission site [39]. In contrast, phosphorylation at Ser637 inhibits Drp1 oligomerization and prevents mitochondrial division [40].

Many studies focus on distinct functions of Drp1-mediated fission involved in diverse biological processes. On the one hand, mitochondrial fission is regarded as a prerequisite for mitophagy through which dysfunctional mitochondria containing damaged proteins, destabilized membranes, and mutated or damaged mitochondrial DNA (mtDNA) are segregated [41]. Additionally, Drp1-serine 616 phosphorylation allows the mitochondria to be evenly distributed in daughter cells during mitosis [40]. However, in response to IR injury, on the other hand, Brady et al. [42] first discovered extensively fragmented mitochondria when Bax translocates from cytosol to mitochondria during ischemia, which could be disturbed by mPTP CsA and p38 MAPK SB203580 inhibitors. Moreover, Karbowski et al. [43] inhibited apoptotic fragmentation of mitochondria with Drp1K38A, a dominant-negative mutant of Drp1, and found that Bax translocation to potential mitochondrial scission

sites cannot be affected, improving that Bax initiates apoptotic fragmentation through Drp1 mediation. Moreover, Mff-mediated fission, a receptor of Drp1, was also reported to hold essential function in fatal mitochondrial fission during IR injury [44, 45]. Acute cardiac IR injury upregulates NR4A1 expression, nuclear receptor subfamily 4 group A member 1, to activate serine/threonine kinase casein kinase2 α (CK2 α), which phosphorylates and activates Mff, enhancing Drp1 translocation and producing detrimental fragmented mitochondria [44]. Mff binds to Drp1 to induce mitochondrial division, leading to excessive ROS production and oxidizing cardiolipin. It also triggers hexokinase 2 (HK2) dissociation, opens mPTP, releases mitochondrial cytochrome c into cytoplasm, and initiates caspase-dependent apoptosis [46]. DUSP1, dual-specificity protein phosphatase1, is downregulated in cardiac IR injury to promote the phosphorylation level of Mff via JNK pathway activation. DUSP1 restoration could alleviate the lethal mitochondrial division and promote cell survival in myocardial tissue [45].

3.2. Mitochondrial Fusion. Compared to mitochondrial fission, mitochondrial fusion is usually crucial for the health and physiological functions of mitochondria, including replenishing damaged mitochondrial DNAs and maintaining membrane potential [47]. Mfns were first discovered in 2001 embedded in OMM fusing adjacent mitochondria through concerted oligomerization and GTP hydrolysis, while Opa1 is situated in IMM and mediates its fusion [48]. Ablation of Mfn1 and Mfn2 genes in adult mice (8 weeks of age) hearts resulted in mitochondrial rupture, impaired mitochondrial respiratory function, and severe fatal cardiomyopathy after 7-8 weeks, suggesting that mitochondrial fusion proteins are essential for normal myocardial mitochondrial morphology and respiratory function [49]. Studies indicate that Mfn1 plays different roles from Mfn2. Mfn1 is primarily responsible for the fusion of two mitochondria, whereas Mfn2 acts as a protein stabilizing the interaction because of lower GTPase activity [50]. In cardiac IR injury, overexpression of Mfns and Drp1 inhibition prevents mPTP opening, which is a critical mediator of IR injury and reduces cell death [51, 52]. Ablation of Mfns or Opa1 induces mitochondrial fragmentation that can activate mitochondrial apoptosis in IR injury [53]. The activity of Mfns is inhibited by ubiquitination and blocking the process of removing damaged mitochondria by mitophagy [54]. In mice, myocardial IR, and myocardial cell hypoxia/reoxygenation models, MCU upregulation responsible for calcium overload, which underlies mPTP opening during the IR phase, increases calpain expression, which is proved to blunt Opa1 expression and activate calcineurin to phosphorylate Drp1 leading to excessive fission [55].

In conclusion, restoration or stimulation of fusion may be an effective means to reduce myocardial IR injury. A study found that melatonin can upregulate OPA1 expression transcriptionally through the AMPK pathway, thereby increasing the ability of mitochondria and cardiomyocytes to survive under IR injury [56]. Pharmacological mitochondrial fusion promoter-M1 could increase Mfn2 expression to regulate the dynamics and reduce mitochondrial dysfunction. Administration of M1 before ischemia can significantly

improve reducing mitochondrial fusion protein observed in cardiac IR injury, reduce arrhythmia incidence, and reduce the infarct area and cardiac apoptosis, thus, preserving cardiac function and reducing mortality. M1 given during ischemia and at the beginning of reperfusion also has a cardioprotective effect but is less effective than M1 given before ischemia [57]. Another study reported that M1 also improves brain mitochondrial dysfunction and blood-brain breakdown induced by cardiac IR injury [58]. These findings suggest that these may be promising interventions that offer cardioprotective effects in the clinical setting of myocardial IR injury.

4. Mitophagy

Mitophagy is an evolutionarily conserved self-degradation process in which mitochondria are delivered to lysosomes for degradation in a selective macrophage form. Typically, basic mitophagy performs as a life-sustaining mechanism through the circulation of proteins and metabolites, especially under nutrient deprivation. In the heart, the mitophagy level needs to adapt to environmental changes and respond to various heart diseases, such as cardiomyopathy due to ischemia/reperfusion, cardiac hypertrophy, and heart failure [59]. However, how individual mitochondria are identified and whether mitophagy plays a protective or harmful role in heart disease has not yet been determined. In most cases, mitochondria can clear mitochondrial defects in IR injury and are considered a protective or adaptive mechanism. However, uncontrolled or excessive (maladaptive) mitochondria may lead to a shortage of functional or healthy mitochondria produced by ATP, resulting in impaired cell survival.

The current view is that initiating mammalian autophagy is activated by phosphorylation of the ULK1 complex (ATG13, ULK1, and FIP200), a downstream target of AMPK-mTOR and that ATG9 vesicles fuse with lipid membranes derived from the endoplasmic reticulum to form a phagophore [60, 61]. Using Atg12-Atg5-Atg16 and LC3/Atg8 systems, damaged mitochondria are recognized and encapsulated by LC3 on endoplasmic reticulum-derived bilayer structure and eventually degraded by fusing with lysosomes. It is currently known that phagophore mitochondria recognition can be mediated by several pathways and play primary roles under distinct tissues and situations. However, mitochondrial identification pathways are coordinated with each other in the mitophagy process rather than being independent [62]. Nevertheless, specific connections and mechanisms between these independent pathways require further research.

4.1. PINK1/Parkin-Mediated Mitophagy. PINK1/Parkin-mediated mitophagy is a ubiquitin-dependent pathway that mainly plays a role in the nervous system. Under normal circumstances, PINK1 is located in IMM and is rapidly degraded by PARL [63]. When mitochondrial membrane potential stability decreases, PINK1 is transferred to OMM, phosphorylating, and recruiting Parkin, or phosphorylated PINK1 directly ubiquitinates other outer membrane proteins [64]. The ubiquitinated outer membrane protein acts as a signal to promote phosphorylation of cargo receptors by kinase

TBK1. Cargo receptors contain LC3/GABARAP-interacting region (LIR) motifs, which can recruit LC3 to mitochondria and mediate phagocytosis. Other cargo receptors such as p62, NBR1, and TAX1BP1 have been shown to play an essential role in other selective autophagy, but their role in mitophagy is weak [65]. Due to its unique relationship with Parkinson's disease, PINK1/Parkin-mediated mitophagy pathway has been extensively studied, mainly in brain tissues. However, many recent studies have demonstrated the protective role of the PINK1/Parkin-mediated mitophagy pathway in cardiac IR injury [56]. Yu et al. [66] found that patients with diabetic cardiomyopathy (DCM) have an increased susceptibility to myocardial IR injury. In the DCM model of IR injury, Drp1-mediated mitochondrial fission was enhanced (mean mitochondrial size was significantly reduced, the number of fragmented mitochondria was significantly increased), oxidative phosphorylation complex was damaged, and FUNDC1 and Parkin expressions involved in mitophagy were also significantly decreased. Melatonin reversed this adverse effect through SRIT6 and AMPK-PGC-1 α -Akt signaling and protects the myocardium from IR injury. It also suggests an inseparable relationship between mitochondrial biogenesis, division, and mitophagy. In contrast, Zhou et al. [67] proposed that IR injury opens mPTP and promotes Parkin-mediated mitophagy and ultimately leads to cell death. This phenomenon has a negligible effect on the signal pathway involved in mitophagy, but due to homeostasis disorder caused by excessive mitophagy, which leads to declining ATP production capacity, causing mitochondria to be unable to meet the basic requirements of cells for energy and reduces the resistance of cells to IR injury.

4.2. BNIP3/NIX-Mediated Mitophagy. The second is a receptor-mediated mitophagy pathway, which BNIP3/NIX mediates. BNIP3 (Bcl2 and adenovirus E1B19KDa interacting protein 3) and NIX (BNIP3-like) are proteins homologous to Bcl-2 in BH3 domain and embedded in mitochondria and endoplasmic reticulum. NIX and BNIP3 have putative and classical LIR, respectively. Phosphorylation of serine residues 17 and 24 on both LIR sides of BNIP3 promotes its binding to LC3 [68]. The protein structure determines the dual function of BNIP3/NIX, which induces cell death and participates in mitophagy [69]. Physiologically, the BNIP3 expression level was very low in organs, and NIX is involved in mitophagy promoting degradation of mitochondria in reticulocytes and plays an indispensable role in the maturation process of red blood cells [70]. In cardiomyocytes, the pathological mechanism involved in NIX is mainly related to cardiomyocyte hypertrophy and regulated by G α q-dependent signaling, while BNIP3 is significantly induced by hypoxia in addition to a combination of hypoxia and acidosis under prolonged myocardial ischemia [71, 72]. Studies have confirmed that BNIP3 is a downstream target of hypoxia-inducing factor-1 α (HIF-1 α). The expression level of BNIP3 is regulated by HIF-1 α transcription to determine cardiac cell death and mitophagy in the case of hypoxia built-up by IR injury or cancer. In addition to HIF-1, BNIP3 is also the target of other transcription factors, such as PLAGL2, E2F1, and FoxO3, which eventually induce apoptosis and mitophagy [73].

BNIP3 causes cell death in three ways, including activating mitochondrial-dependent apoptosis pathway, inducing cell necrosis, and triggering pyroptosis [74]. Hypoxia-induced cardiomyocyte death demonstrates apoptotic characteristics, although it is unclear whether caspase is involved in this process [72, 75]. BNIP3/NIX interacts with BCL-2 and BCL-XL and induces apoptosis through the C-terminal transmembrane domain, and both have similar promoting activities [76]. Mice with gene ablation or dominant inhibition of BNIP3 can reduce apoptosis of cardiomyocytes in hypoxia and significantly improve ventricular remodeling after IR injury [77]. Hypoxia also upregulates EIF4A3- (eukaryotic translation initiation factor 4A3-) induced Circ-BNIP3 and promotes BNIP3 expression through performing as a miRNA-27a-3p sponge to aggravate hypoxia-induced injury with increased caspase-3 activity and Bax level [78]. Apart from inducing apoptosis, BNIP3 also causes mitochondrial depolarization via mPTP opening and mediates the BNIP3-caspase-3-GSDME pyroptosis pathway in cardiac injury [79]. However, mitophagy function mediated by BNIP3/NIX remains controversial.

When mitochondria are exposed to external stimulation, BNIP3 dimerizes and binds to LC3 to activate mitophagy [80]. In IR injury, hypoxia and ROS activate BNIP3-mediated mitophagy by inducing HIF-1 expression and play a protective role in myocardial ischemia reperfusion [81]. In diabetic ischemia-reperfusion model, a combination of deferoxamine (DFO) and sevoflurane posttreatment (SPostC) can protect the myocardium through HIF-1/BNIP3-mediated mitophagy [82]. Another study showed that berberine (BBR) could induce cardiomyocyte proliferation, inhibit cardiomyocyte apoptosis, and enhance HIF-1 α and BNIP3 promoter binding to mediate BNIP3 expression, thereby activating the HIF-1 α /BNIP3-mediated mitophagy pathway and protecting myocardial IR injury [83]. However, according to another experiment, Bnip3 expression was upregulated in cells treated with hypoxia and reoxygenation to mimic IR condition in vitro. DUSP1 was downregulated after acute cardiac IR injury and amplified BNIP3 phosphorylation and activation through the JNK pathway, leading to mitophagy which eventually caused myocardial injury [45]. Therefore, BNIP3/NIX exhibited dual properties during myocardial ischemia/reperfusion injury, inducing cell death and participating in mitophagy process. In some cases, BNIP3/NIX-induced mitophagy is defensive, while in others, it leads to cell death. Mitophagy-related cell death is unclear whether it is due to overmitophagy or the process of mitophagy itself is fatal.

4.3. FUNDC1-Mediated Mitophagy. Another mitophagy receptor, FUNDC1 (FUN14 domain containing 1), a mitochondrial protein on OMM, has also been confirmed to activate hypoxia-induced mitophagy [84]. FUNDC1 contains three transmembrane (TM) domains. The N-terminal region is exposed to the cytoplasm with a typical LIR, Y (18) XXL. Conservative Y18 and L21 are essential to mediate the interaction between FUNDC1 and LC3 [85]. It is regulated by LIR motif autophosphorylation instead of transcription [86]. Currently, FUNDC1 dephosphorylation is believed to be an

activated state, which can promote mitophagy and protect cardiomyocytes and endothelial cells. In contrast, FUNDC1 phosphorylation by upstream factors will inactivate it, hinder mitophagy, and have a damaging effect on the heart [85]. CK2 α is upregulated after acute myocardial ischemia-reperfusion injury. CK2 α effectively inhibits mitophagy by phosphorylating and blunting FUNDC1 function through upregulating NR4A1 expression, finally leading to the failure to clear mitochondrial damage and mitochondrial apoptosis [44, 87]. Regarding depolarization of mitochondrial membrane potential or hypoxia, mitochondrial phosphoglycerate mutase PGAM5 dephosphorylates and activates FUNDC1 at ser-13, promoting mitophagy occurrence, which can be reversed by CK2 α [88]. FUNDC1 as a substrate of Src kinase can be phosphorylated and inactivated at Tyr-18, which will prevent mitophagy. Src kinase inactivation during hypoxia dephosphorylates FUNDC1, and LC3 will preferentially bind to dephosphorylated FUNDC1 and promote mitophagy under hypoxic conditions [85]. Interestingly, ULK expression increases under hypoxia or mitochondrial uncoupling agent (FCCP) and translocates to mitochondria that need to be cleared. FUNDC1, as a substrate of ULK, binds with ULK and is phosphorylated at ser-17, promoting the interaction between FUNDC1 and LC3, which is essential for phagocytic vesicles to recognize damaged mitochondria [86]. The mTORC1-ULK1-FUNDC1 pathway mediates mitophagy, effectively regulates mitochondrial quality and cell survival, and inhibits the occurrence of myocardial ischemia-reperfusion injury [89].

FUNDC1 in cardiomyocytes also binds to ER-resided inositol 1,4,5-trisphosphate type 2 receptor (IP3R2), modulating calcium ions release from ER into mitochondria and cytosol. FUNDC1 ablation accumulates calcium ions in ER and reduces the level of calcium ions in cytoplasm, which suppresses the expression of mitochondrial fission 1 protein (Fis1) to raise elongated mitochondria and mitochondrial dysfunction [90]. ATFS-1 is a transcription factor that plays a central role in the mitochondrial unfolded protein response (UPR^{mt}). In hypoxia-reoxygenation, the protective effect of FUNDC1 on cardiomyocytes also needs to be coordinated with ATFS-1. In the absence of FUNDC1, ATFS-1-dependent stress response and metabolic remodeling will occur [91].

In conclusion, FUNDC1-mediated mitophagy plays a prosurvival role in reperfusion heart tissue. Mammalian STE20-like kinase 1 (Mst1) is significantly increased in reperfusion heart, which decreases FUNDC1 expression through MAPK/ERK-CREB pathway. The protective mitophagy loss increases tissue damage in cardiomyocytes [92]. FUNDC1-induced mitophagy was proved to protect the myocardium by inhibiting platelet activation. Physiologically, mitophagy maintains good mitochondrial quality and platelet activation by clearing “toxic” platelet mitochondria. In IR injury, vascular obstruction caused by platelet adhesion constitutes a hypoxic environment that increases FUNDC1-mediated mitophagy level in platelets and subsequently reduces platelet activation to prevent I/R injury deterioration [93]. Therefore, it seems that we can further explore the FUNDC1 domain and explore more sites that can be regulated by phosphorylation or dephosphorylation after transcription or translation,

as well as factors or proteins that target these sites. The IR injury degree could be regulated by intervening in the mitophagy pathway involved in FUNDC1.

5. Mitochondrial Biogenesis and Proteostasis

Given the role of mitochondria in energy production, they are usually exposed to peroxide like ROS leading to mitochondrial DNA (mtDNA) mutations and protein misfolding. Mitophagy clears damaged ones, and mitochondrial biogenesis generates new mitochondrial ingredients, including protein and lipids, which cooperate to ensure reticular mitochondria replenishment. Mitochondrial biogenesis can be regarded as the growth and division of the original mitochondria. Three parts, including mitochondrial genome, proteins, and lipids on IMM and OMM, ensure the complete biological function of mitochondria and spatial structure of biochemical reaction [94]. Human mtDNA is a double-stranded loop molecule that can copy independently, approximately 16.5 KB in length, containing 37 genes that encode for 13 polypeptides involved in the electron transport chain (complexes I, III, IV, and V) responsible for oxidative phosphorylation, 22 tRNAs, and 2 rRNAs [95]. About 99% of mitochondrial proteins are synthesized on cytosolic ribosomes and then are introduced into mitochondria with specific proteins. Precursor protein translated by nuclear genes' mRNAs, without folding conformation, choose different mitochondrial membrane protein transfer enzyme complexes based on sequence information through the inside and outside mitochondria membrane. After entering the mitochondria, unfolded precursor proteins are folded by a molecular chaperone in the mitochondrial matrix [96]. Cells adopt various means to protect the mitochondrial proteome, including preventing the import of aberrant peptides, regulating protein turnover in mitochondria, and detecting protein homeostasis [97]. As an essential part of mitochondria, lipids' synthesis is similar to that of proteins: a small portion is made in mitochondria, and the rest is made in the endoplasmic reticulum before entering mitochondria [98].

5.1. Mitochondrial Biogenesis. The mtDNA is vulnerable to oxidative stress because of its proximity to the respiratory chain and lack of protective histone-like proteins and introns. Once mtDNA is damaged, encoding of critical proteins for the respiratory chain becomes deficient, aggravating ROS production and mitochondrial dysfunction. Moreover, mtDNA depletion alone could cause cardiomyocyte death. PGC-1, PPAR- (peroxisome proliferator-activated receptor) γ coactivator-1, is a main factor regulating both mitophagy and mitochondrial biogenesis. The ectopic expression of PGC-1 in white adipose tissue upregulates transcription of UCP-1 and key enzymes of the mitochondrial respiratory chain and increases the cellular content of mtDNA. PGC-1 has two types: PGC-1 α and PGC-1 β . PGC-1 α mainly regulates mitochondrial biogenesis by activating different transcription factors. PGC-1 α activates nuclear respiratory factors 1 (NRF-1) and nuclear factor erythroid 2-related factor 2 (NRF2) to bind to NRF-related sites on the promoter of mitochondrial transcription factor A (Tfam) to

increase its expression. NRFs regulate complexes' expression in the electron transport chain (ETC), while Tfam encoded by nuclear genes is responsible for transcription and replicating mtDNA [99]. Besides, PGC-1 α interacts with and activates other transcription factors like PPARs and ERRs. ERR targets several genes linked to many biological metabolism processes and mitochondrial biogenesis [100]. Studies proved that AMPK, NO, SIRT1, and TORC1 control mitochondrial biogenesis by interacting with PGC-1 α [101–104]. Yue et al. [105] found that IR injury decreased Tfam protein level and exposed mtDNA to oxidative damage, destroying the respiratory chain and overproducing ROS that could be reversed by antioxidant-like lycopene. S100A8/A9, the most significantly upregulated gene in the early reperfusion stage analyzed by dynamic transcriptome, downregulates NDUF gene expression through Toll-like receptor 4/ERK-mediated PPAR γ coactivator 1 α /NRF 1 signaling, followed by mitochondrial complex I inhibition. This caused mitochondrial respiratory dysfunction in cardiomyocytes that can be reversed by S100a9 neutralizing antibody [106].

5.2. Mitochondrial Proteostasis. About 1,500 kinds of human mitochondrial proteins play a central role in cell energy metabolism and improve cell viability [107]. In addition to respiratory chain complexes involved in basic respiration, mitochondrial enzymes catalyze the biosynthesis of lipids and amino acids, central reactions of the urea cycle, and formation of heme and iron-sulfur clusters. Meanwhile, mitochondrial proteins could control cristae formation and maintenance, establish membrane contact sites with ER for lipid exchange, and regulate mitochondrial dynamics and signal transduction (such as calcium signaling) [108, 109]. The mitochondrial proteome shows high plasticity to allow the mitochondrial function to adapt to cellular requirements. Defects in mitochondrial protein homeostasis lead to toxic protein damage and ultimately cell death [110]. Thus, cell evolves several ways to maintain proteostasis.

Cytosolic protein quality control mechanism ensures that correctly synthesized polypeptide is imported and remains unfolded protein before being imported into mitochondria. The cytosolic ubiquitin-proteasome system (UPS) controls transmembrane transport of polypeptides and removes damaged and mislocalized protein. Chaperones in mitochondrial matrix help fold nuclear-encoded and mitochondrial-encoded protein properly. A selective autophagy approach independent of mitophagy can remove a portion or entire mitochondria via generating MDVs. Under mitochondrial oxidative stress conditions, ROS production triggers small vesicles that contain a subset group of oxidized proteins to bud off of damaged mitochondria to form MDVs. MDVs are fused with endosomes and multivesicular bodies and subsequently delivered to lysosomes to selectively degrade damaged mitochondrial contents [111]. In heart tissue, constant MDVs act as the first line of defense against stress in healthy conditions, and the number of MDVs is rapidly upregulated in response to stress [112]. A study has shown that MDVs inhibit the apoptosis of myocardial cells induced by hypoxia/ischemia through transferring Bcl-2 and play an

endogenous protective role in early hypoxia [113]. However, the molecular mechanism controlling MDV formation remains unclear. ROS production also activates another mitochondrial remodeling and quality control mechanism, which is named mitochondrial spheroids. Mitochondrial spheroids have a ring or cup-like morphology with squeezed mitochondrial matrix and contain cytosol contents such as endoplasmic reticulum or other mitochondria. Forming mitochondrial spheroids is regulated by Mfn1 and Mfn2 and further acquires lysosomal markers to fusion with lysosomes [114]. Mitochondrial spheroids have been detected in mice's livers on acute alcohol or high-fat diets [115]. This suggests that mitochondrial spheroids may act as a general mitochondrial structural remodeling in response to various physiological and pathological stresses and may serve as a mechanism to regulate IR injury that needs to be further explored.

Besides, during stress events associated with abnormal mitochondrial protein accumulation, such as heat or oxidative stress, cells also launch UPR^{mt} through upregulating chaperones, proteases, and antioxidants to mitigate potential toxic protein damage [97, 116]. UPR^{mt} is regulated by transcription factor ATFS-1 in *Caenorhabditis elegans* and by transcription factor ATF5 in mammals. Under normal circumstances, ATF5 is imported to mitochondria and degraded by AAA⁺ proteases LON. When the cell is exposed to oxidative stress, the damaged protein homeostasis impedes importing ATF5 into mitochondria, resulting in ATF5 retention in the cytoplasm and subsequent translocation to the nucleus to enhance transcription of mitochondrial chaperones and proteases [117]. Interestingly, there are conflicting claims about the role of UPR^{mt} in heart disease. Most studies have shown that UPR^{mt} has a protective effect against heart injury, but a few studies have found that UPR^{mt} can promote heart disease development. Preinduction of UPR^{mt} with nicotinamide ribose is sufficient to prevent cardiac dysfunction caused by chronic hemodynamic overloading in rodents [118]. Increased and activation of UPR^{mt} was also found in the hearts of aging mice and cardiac tissue from patients with aortic stenosis [118, 119]. Under IR injury, pharmacological UPR^{mt} induction with oligomycin or doxycycline was cardioprotective in an ATF5-dependent manner *in vivo*. However, this approach did not reduce the severity of myocardial infarction in ATF5-deficient mice [120]. In addition, mammalian cells require ATF5 to maintain mitochondrial activity and promote organelle recovery during mitochondrial stress. These findings open a new avenue for cardiovascular disease treatment strategies targeting mitochondrial protein disorder under stress (Figure 2).

6. Interventions Based on Mitochondrial Quality Control

So far, among IR injury studies, the most likely mechanisms are overfission and abnormal mitophagy. However, the interaction between fission and mitophagy remains unclear. Mitochondrial fission is often a signal of cell damage. Overdivision induces mitochondrial fragmentation, aggravates oxidative stress, activates mitochondrial apoptosis, and reduces cell viability. In contrast, mitophagy is generally a

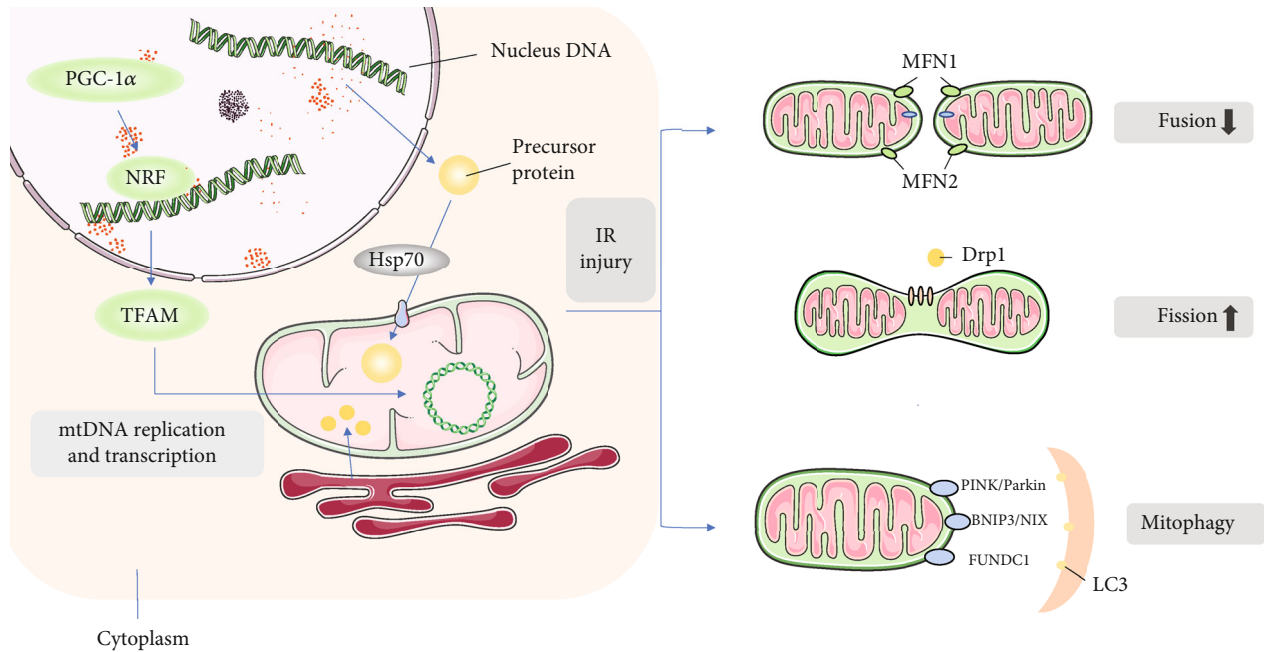


FIGURE 2: Quality control mechanism of mitochondria in IR injury. In normal mitochondrial biogenesis, mtDNA synthesis is mainly regulated by PGC-1, and PGC-1 interacts with nuclear receptors (including NRF-1 and NRF-2) to participate in the expression of various nuclear coding genes and Tfam, and transcription factors Tfam and NRFs are jointly responsible for regulating mtDNA replication and transcription. Nuclear DNA synthesizes precursor proteins in the cytoplasm and is transported in an unfolded form into the mitochondria, where precursor proteins fold into functional proteins with molecular chaperones. A small portion of lipids are synthesized in mitochondria, and the rest are transported into mitochondria after synthesis in the endoplasmic reticulum to form the inner and outer membrane structure. Mitochondrial fission is a signal of injury. After activation by phosphorylation, Drp1 translocates from the cytoplasm to the mitochondrial membrane and binds to Drp1 receptors (Mff, Fis1, and Mid49/51), which are the sites of enclosing mitochondria to be separated and mediate the mitochondrial division into fragments. Excessive mitochondrial fragmentation during IR eventually leads to cell death. Mitochondrial fusion inhibits mitochondrial fragmentation, reticular structure destruction, and mitochondrial cristae remodeling. Mfn1 and Mfn2 mediate OMM fusion, and Opa1 mediates IMM fusion. Mitochondrial fusion decreased significantly during IR injury. The function of mitophagy in myocardial IR remains unclear. Three main pathways are found to mediate mitophagy: PINK1/Parkin pathway may induce excessive mitophagy in myocardial IR, thereby promoting cell death; BNIP3/NIX is a protein located in OMM, which directly binds to LC3 on autophagosomes and mediates mitophagy. But its function in myocardial IR remains controversial; FUNDC1 is also an LC3 receptor located in mitochondria, and its LIR binds to LC3 to mediate mitophagy, which mainly plays a protective role in myocardial IR injury.

protective signal. Normal mitophagy clears mitochondrial debris, protects oxidative stress, inhibits mitochondrial apoptosis, and maintains cell viability. However, abnormal fission and mitophagy will occur in IR injury, resulting in cell damage [121]. Given that myocardial cell is the status of terminal differentiation of cells after mitotic division, they cannot be further divided and subsequent cell replacement, therefore, removed by mitochondrial dysfunction of mitochondria balance between mitochondrial biology and health, mitochondria maintain steady is crucial to maintain a healthy heart and prevent cardiac injury [6]. We could consider mitochondrial quality control and intervene in any part of the overall quality control process to alleviate IR injury.

Several studies have currently improved IR damage by intervening in the quality control of mitochondria. Dapagliflozin administration before ischemia improves left ventricular function during cardiac IR injury by reducing myocardial apoptosis, improving myocardial mitochondrial function, biogenesis, and dynamics, thereby maximizing myocardial protection [122]. Various antioxidants such as melatonin can act as a protective factor against myocardial IR injury

by regulating mitochondrial fission and mitophagy. Platelet activation is an important pathophysiological mechanism of IR injury. Melatonin can improve downregulation of PPAR γ expression after reperfusion, inhibiting platelet activation from attenuating myocardial IR injury by blocking FUNDC1-mediated mitophagy [123]. Underlying the microvascular IR injury, $[Ca^{2+}]_i$ cannot be rapidly and timely recirculated into ER. $[Ca^{2+}]_i$ accumulation not only leads to endothelial cell stiffness but also catalyzes XO to produce excessive ROS, which is the consequence of mitochondria damage. Sarcoplasmic/endoplasmic reticulum Ca^{2+} -ATPase (SERCA) is a channel responsible for transporting $[Ca^{2+}]_i$ back to ER. It can reduce IR injury by inhibiting calcium overload, inactivating xanthine oxidase (XO), and reducing intracellular/mitochondrial ROS to regulate mitochondrial motility, bioenergy, biogenesis, and mitochondrial autophagy [124]. Istaroxime, as a nonglycoside inhibitor of sodium-potassium-ATPase, has an additional stimulatory effect on SERCA. Nitro donors have been developed and shown effective vasodilators in early animal studies [125]. Gene therapy by regulating circular RNAs is a promising

TABLE 1: Therapeutic application targeting MQC to attenuate IR injury.

Therapies	Mechanisms	References
Dapagliflozin	Improve left ventricular function	Lahnwong et al., 2020 [122]
Melatonin	Improve PPAR γ expression	Zhou et al., 2017 [123]
Istaroxime	Stimulate SERCA to dilate blood vessels and decrease ROS production	Hasenfuss et al., 2011 [125]
SS31-Mito	Enhance LVEF and energy integrity with higher PGC-1 α and Cyt c	Lee et al., 2018 [127]

means to improve heart contractile performance [126]. Combined SS31-mitochondria (Mito) therapy (rather than either therapy alone) increased SIRT1/SIRT3 expression and ATP levels, by which it suppressed oxidative stress and protected mitochondrial integrity. IR rats treated with SS31-Mito exhibited higher left ventricular ejection fraction (LVEF) and energy integrity (PGC-1 α /mitochondrial cytochrome c) markers, demonstrating that combined SS31-Mito therapy is an efficient means to protect myocardium from IR injury [127]. Moreover, trimetazidine, electroacupuncture (EA) preconditioning also prevents IR injury by regulating mitochondrial quality and function [89]. Therefore, exploring the quality control mechanism that can regulate macroscopic mitochondria is highly demanding. However, when the number or overall state of mitochondria is not good, regulating the biogenesis of mitochondria itself or controlling unfolded proteins within mitochondria are also very worthy to be explored (Table 1).

7. Conclusion

Mitochondrial quality control has been well demonstrated as a central link in the IR injury mechanism mediated by Ca²⁺ overload and mPTP opening. Abnormal mitochondrial quality control, such as excessive fission and mitophagy, in addition to decreased mitochondrial fusion and proteostasis disorder, is a factor that further aggravates tissue damage. However, the extent to which mitochondrial clearance and production can damage tissue and save cell homeostasis remains unclear. The exact mechanism of the upstream regulatory pathway of mitochondrial quality control and factors that can affect mitochondrial function should be further investigated. The role of mitochondrial outer membrane proteins in IR injury is widely studied, but the proteins in mitochondria and interactions between mitochondria and other organelles such as ER perhaps play a similar important role in IR injury. Therefore, ensuring balance and interaction of portion of mitochondrial quality control seems critical to reducing damage under disease.

In addition, familiarity with physiological and pathological characteristics of mitochondrial quality control helps basic and clinical studies. Many studies have shown that genetic or pharmaceutical interventions in mitochondrial quality control can improve tissue damage and cardiovascular function caused by IR. But the limitation lies in that few studies have been clinically verified, most of which proved the efficacy of the drug in animal models. In conclusion, understanding the mechanism of mitochondrial action in IR damage can provide targeted therapeutic means for clinical use and develop new drug research. Furthermore, timely

and effective intervention for the long-term pathological process of IR injury will significantly alleviate the degree of damage to the body to a certain extent.

Conflicts of Interest

The authors declare that they have no conflicts of interest.

References

- [1] F. Tullio, C. Angotti, M. G. Perrelli, C. Penna, and P. Pagliaro, "Redox balance and cardioprotection," *Basic Research in Cardiology*, vol. 108, no. 6, p. 392, 2013.
- [2] J. A. Nicolás-Ávila, A. V. Lechuga-Vieco, L. Esteban-Martínez et al., "A network of macrophages supports mitochondrial homeostasis in the heart," *Cell*, vol. 183, no. 1, pp. 94–109.e23, 2020.
- [3] H. M. Ni, J. A. Williams, and W. X. Ding, "Mitochondrial dynamics and mitochondrial quality control," *Redox Biology*, vol. 4, pp. 6–13, 2015.
- [4] A. T. Moehlman and R. J. Youle, "Mitochondrial quality control and restraining innate immunity," *Annual Review of Cell and Developmental Biology*, vol. 36, no. 1, pp. 265–289, 2020.
- [5] A. R. Kulek, A. Anzell, J. M. Wider, T. H. Sanderson, and K. Przyklenk, "Mitochondrial quality control: role in cardiac models of lethal ischemia-reperfusion injury," *Cell*, vol. 9, no. 1, p. 214, 2020.
- [6] F. G. Tahrir, D. Langford, S. Amini, T. Mohseni Ahooyi, and K. Khalili, "Mitochondrial quality control in cardiac cells: mechanisms and role in cardiac cell injury and disease," *Journal of Cellular Physiology*, vol. 234, no. 6, pp. 8122–8133, 2019.
- [7] A. Mokhtari-Zaer, N. Marefati, S. L. Atkin, A. E. Butler, and A. Sahebkar, "The protective role of curcumin in myocardial ischemia-reperfusion injury," *Journal of Cellular Physiology*, vol. 234, no. 1, pp. 214–222, 2018.
- [8] A. R. Anzell, R. Maizy, K. Przyklenk, and T. H. Sanderson, "Mitochondrial quality control and disease: insights into ischemia-reperfusion injury," *Molecular Neurobiology*, vol. 55, no. 3, pp. 2547–2564, 2018.
- [9] R. Mittler, "ROS are good," *Trends in Plant Science*, vol. 22, no. 1, pp. 11–19, 2017.
- [10] M. Yang, B. S. Linn, Y. Zhang, and J. Ren, "Mitophagy and mitochondrial integrity in cardiac ischemia-reperfusion injury," *Biochimica et Biophysica Acta - Molecular Basis of Disease*, vol. 1865, no. 9, pp. 2293–2302, 2019.
- [11] J. Ren and Y. Zhang, "Editorial: new therapeutic approaches in the management of ischemia reperfusion injury and cardiometabolic diseases: opportunities and challenges," *Current Drug Targets*, vol. 18, no. 15, pp. 1687–1688, 2017.
- [12] D. B. Zorov, M. Juhaszova, Y. Yaniv, H. B. Nuss, S. Wang, and S. J. Sollott, "Regulation and pharmacology of the

- mitochondrial permeability transition pore,” *Cardiovascular Research*, vol. 83, no. 2, pp. 213–225, 2009.
- [13] J. Q. Kwong and J. D. Molkentin, “Physiological and pathological roles of the mitochondrial permeability transition pore in the heart,” *Cell Metabolism*, vol. 21, no. 2, pp. 206–214, 2015.
- [14] M. Crompton and A. Costi, “A heart mitochondrial Ca²⁺(+)-dependent pore of possible relevance to re-perfusion-induced injury. Evidence that ADP facilitates pore interconversion between the closed and open states,” *The Biochemical Journal*, vol. 266, no. 1, pp. 33–39, 1990.
- [15] J. Y. Han, Q. Li, Z. Z. Ma, and J. Y. Fan, “Effects and mechanisms of compound Chinese medicine and major ingredients on microcirculatory dysfunction and organ injury induced by ischemia/reperfusion,” *Pharmacology & Therapeutics*, vol. 177, pp. 146–173, 2017.
- [16] K. He, L. Yan, C. S. Pan et al., “ROCK-dependent ATP5D modulation contributes to the protection of notoginsenoside NR1 against ischemia-reperfusion-induced myocardial injury,” *American Journal of Physiology. Heart and Circulatory Physiology*, vol. 307, no. 12, pp. H1764–H1776, 2014.
- [17] T. D. Pollard and G. G. Borisy, “Cellular motility driven by assembly and disassembly of actin filaments,” *Cell*, vol. 112, no. 4, pp. 453–465, 2003.
- [18] N. S. Harhaj and D. A. Antonetti, “Regulation of tight junctions and loss of barrier function in pathophysiology,” *The International Journal of Biochemistry & Cell Biology*, vol. 36, no. 7, pp. 1206–1237, 2004.
- [19] B. Ibanez, S. James, S. Agewall et al., “2017 ESC guidelines for the management of acute myocardial infarction in patients presenting with ST-segment elevation: the task force for the management of acute myocardial infarction in patients presenting with ST-segment elevation of the European Society of Cardiology (ESC),” *European Heart Journal*, vol. 39, no. 2, pp. 119–177, 2018.
- [20] V. R. Pell, E. T. Chouchani, M. P. Murphy, P. S. Brookes, and T. Krieg, “Moving forwards by blocking back-flow,” *Circulation Research*, vol. 118, no. 5, pp. 898–906, 2016.
- [21] A. M. Lefer and D. J. Lefer, “The role of nitric oxide and cell adhesion molecules on the microcirculation in ischaemia-reperfusion,” *Cardiovascular Research*, vol. 32, no. 4, pp. 743–751, 1996.
- [22] F. Bagheri, V. Khori, A. M. Alizadeh, S. Khalighfar, S. Khodayari, and H. Khodayari, “Reactive oxygen species-mediated cardiac-reperfusion injury: mechanisms and therapies,” *Life Sciences*, vol. 165, pp. 43–55, 2016.
- [23] H. Zhou, J. Yang, T. Xin et al., “Exendin-4 protects adipose-derived mesenchymal stem cells from apoptosis induced by hydrogen peroxide through the PI3K/Akt-Sfrp2 pathways,” *Free Radical Biology & Medicine*, vol. 77, pp. 363–375, 2014.
- [24] D. B. Zorov, C. R. Filburn, L. O. Klotz, J. L. Zweier, and S. J. Sollott, “Reactive oxygen species (Ros-induced) ROS release,” *The Journal of Experimental Medicine*, vol. 192, no. 7, pp. 1001–1014, 2000.
- [25] Y. Kirichok, G. Krapivinsky, and D. E. Clapham, “The mitochondrial calcium uniporter is a highly selective ion channel,” *Nature*, vol. 427, no. 6972, pp. 360–364, 2004.
- [26] L. Boyman, M. Karbowski, and W. J. Lederer, “Regulation of mitochondrial ATP production: Ca²⁺ signaling and quality control,” *Trends in Molecular Medicine*, vol. 26, no. 1, pp. 21–39, 2020.
- [27] J. Q. Kwong, X. Lu, R. N. Correll et al., “The mitochondrial calcium uniporter selectively matches metabolic output to acute contractile stress in the heart,” *Cell Reports*, vol. 12, no. 1, pp. 15–22, 2015.
- [28] T. S. Luongo, J. P. Lambert, A. Yuan et al., “The mitochondrial calcium uniporter matches energetic supply with cardiac workload during stress and modulates permeability transition,” *Cell Reports*, vol. 12, no. 1, pp. 23–34, 2015.
- [29] D. C. Chan, “Dissecting mitochondrial fusion,” *Developmental Cell*, vol. 11, no. 5, pp. 592–594, 2006.
- [30] H. Chen, S. A. Detmer, A. J. Ewald, E. E. Griffin, S. E. Fraser, and D. C. Chan, “Mitofusins Mfn1 and Mfn2 coordinately regulate mitochondrial fusion and are essential for embryonic development,” *The Journal of Cell Biology*, vol. 160, no. 2, pp. 189–200, 2003.
- [31] C. Vásquez-Trincado, I. García-Carvajal, C. Pennanen et al., “Mitochondrial dynamics, mitophagy and cardiovascular disease,” *The Journal of Physiology*, vol. 594, no. 3, pp. 509–525, 2016.
- [32] K. J. de Vos, V. J. Allan, A. J. Grierson, and M. P. Sheetz, “Mitochondrial function and actin regulate dynamin-related protein 1-dependent mitochondrial fission,” *Current Biology*, vol. 15, no. 7, pp. 678–683, 2005.
- [33] E. Ingerman, E. M. Perkins, M. Marino et al., “Dnm1 forms spirals that are structurally tailored to fit mitochondria,” *The Journal of Cell Biology*, vol. 170, no. 7, pp. 1021–1027, 2005.
- [34] W. W. Sharp and S. L. Archer, “Mitochondrial dynamics in cardiovascular disease: fission and fusion foretell form and function,” *Journal of Molecular Medicine (Berlin, Germany)*, vol. 93, no. 3, pp. 225–228, 2015.
- [35] S. Strack, T. J. Wilson, and J. T. Cribbs, “Cyclin-dependent kinases regulate splice-specific targeting of dynamin-related protein 1 to microtubules,” *The Journal of Cell Biology*, vol. 201, no. 7, pp. 1037–1051, 2013.
- [36] S. Wasiak, R. Zunino, and H. M. McBride, “Bax/Bak promote sumoylation of DRP1 and its stable association with mitochondria during apoptotic cell death,” *The Journal of Cell Biology*, vol. 177, no. 3, pp. 439–450, 2007.
- [37] C. R. Chang and C. Blackstone, “Cyclic AMP-dependent Protein Kinase Phosphorylation of Drp1 Regulates Its GTPase Activity and Mitochondrial Morphology,” *The Journal of Biological Chemistry*, vol. 282, no. 30, pp. 21583–21587, 2007.
- [38] G. M. Cereghetti, A. Stangherlin, O. M. de Brito et al., “Dephosphorylation by calcineurin regulates translocation of Drp1 to mitochondria,” *Proceedings of the National Academy of Sciences of the United States of America*, vol. 105, no. 41, pp. 15803–15808, 2008.
- [39] S. Xu, P. Wang, H. Zhang et al., “CaMKII induces permeability transition through Drp1 phosphorylation during chronic β -AR stimulation,” *Nature Communications*, vol. 7, no. 1, p. 13189, 2016.
- [40] W. W. Sharp, Y. H. Fang, M. Han et al., “Dynamin-related protein 1 (Drp1)-mediated diastolic dysfunction in myocardial ischemia-reperfusion injury: therapeutic benefits of Drp1 inhibition to reduce mitochondrial fission,” *The FASEB Journal*, vol. 28, no. 1, pp. 316–326, 2014.
- [41] D. F. Suen, D. P. Narendra, A. Tanaka, G. Manfredi, and R. J. Youle, “Parkin overexpression selects against a deleterious mtDNA mutation in heteroplasmic cybrid cells,” *Proceedings of the National Academy of Sciences of the United States of America*, vol. 107, no. 26, pp. 11835–11840, 2010.

- [42] N. R. Brady, A. Hamacher-Brady, and R. A. Gottlieb, "Proapoptotic BCL-2 family members and mitochondrial dysfunction during ischemia/reperfusion injury, a study employing cardiac HL-1 cells and GFP biosensors," *Biochimica et Biophysica Acta*, vol. 1757, no. 5-6, pp. 667-678, 2006.
- [43] M. Karbowski, Y. J. Lee, B. Gaume et al., "Spatial and temporal association of Bax with mitochondrial fission sites, Drp1, and Mfn2 during apoptosis," *The Journal of Cell Biology*, vol. 159, no. 6, pp. 931-938, 2002.
- [44] H. Zhou, J. Wang, P. Zhu et al., "NR4A1 aggravates the cardiac microvascular ischemia reperfusion injury through suppressing FUNDC1-mediated mitophagy and promoting Mff-required mitochondrial fission by CK2 α ," *Basic Research in Cardiology*, vol. 113, no. 4, p. 23, 2018.
- [45] Q. Jin, R. Li, N. Hu et al., "DUSP1 alleviates cardiac ischemia/reperfusion injury by suppressing the Mff- required mitochondrial fission and Bnip3-related mitophagy via the JNK pathways," *Redox Biology*, vol. 14, pp. 576-587, 2018.
- [46] H. Zhou, S. Hu, Q. Jin et al., "Mff-dependent mitochondrial fission contributes to the pathogenesis of cardiac microvasculature ischemia/reperfusion injury via induction of mROS-mediated cardiolipin oxidation and HK2/VDAC1 disassociation-involved mPTP opening," *Journal of the American Heart Association*, vol. 6, no. 3, 2017.
- [47] T. Ono, K. Isobe, K. Nakada, and J. I. Hayashi, "Human cells are protected from mitochondrial dysfunction by complementation of DNA products in fused mitochondria," *Nature Genetics*, vol. 28, no. 3, pp. 272-275, 2001.
- [48] S. B. Ong and D. J. Hausenloy, "Mitochondrial morphology and cardiovascular disease," *Cardiovascular Research*, vol. 88, no. 1, pp. 16-29, 2010.
- [49] K. N. Papanicolaou, R. Kikuchi, G. A. Ngoh et al., "Mitofusins 1 and 2 are essential for postnatal metabolic remodeling in heart," *Circulation Research*, vol. 111, no. 8, pp. 1012-1026, 2012.
- [50] N. Ishihara, Y. Eura, and K. Mihara, "Mitofusin 1 and 2 play distinct roles in mitochondrial fusion reactions via GTPase activity," *Journal of Cell Science*, vol. 117, Part 26, pp. 6535-6546, 2004.
- [51] D. J. Hausenloy and D. M. Yellon, "The mitochondrial permeability transition pore: its fundamental role in mediating cell death during ischaemia and reperfusion," *Journal of Molecular and Cellular Cardiology*, vol. 35, no. 4, pp. 339-341, 2003.
- [52] S. B. Ong, S. Subrayan, S. Y. Lim, D. M. Yellon, S. M. Davidson, and D. J. Hausenloy, "Inhibiting mitochondrial fission protects the heart against ischemia/reperfusion injury," *Circulation*, vol. 121, no. 18, pp. 2012-2022, 2010.
- [53] L. Griparic, N. N. van der Wel, I. J. Orozco, P. J. Peters, and A. M. van der Blik, "Loss of the Intermembrane Space Protein Mgm1/OPA1 Induces Swelling and Localized Constrictions along the Lengths of Mitochondria," *The Journal of Biological Chemistry*, vol. 279, no. 18, pp. 18792-18798, 2004.
- [54] M. E. Gegg, J. M. Cooper, K. Y. Chau, M. Rojo, A. H. V. Schapira, and J. W. Taanman, "Mitofusin 1 and mitofusin 2 are ubiquitinated in a PINK1/parkin-dependent manner upon induction of mitophagy," *Human Molecular Genetics*, vol. 19, no. 24, pp. 4861-4870, 2010.
- [55] L. Guan, Z. Che, X. Meng et al., "MCU up-regulation contributes to myocardial ischemia-reperfusion injury through calpain/OPA-1-mediated mitochondrial fusion/mitophagy inhibition," *Journal of Cellular and Molecular Medicine*, vol. 23, no. 11, pp. 7830-7843, 2019.
- [56] Y. Zhang, Y. Wang, J. Xu et al., "Melatonin attenuates myocardial ischemia-reperfusion injury via improving mitochondrial fusion/mitophagy and activating the AMPK-OPA1 signaling pathways," *Journal of Pineal Research*, vol. 66, no. 2, article e12542, 2019.
- [57] C. Maneechote, S. Palee, S. Kerdphoo, T. Jaiwongkam, S. C. Chattapakorn, and N. Chattapakorn, "Balancing mitochondrial dynamics via increasing mitochondrial fusion attenuates infarct size and left ventricular dysfunction in rats with cardiac ischemia/reperfusion injury," *Clinical Science (London, England)*, vol. 133, no. 3, pp. 497-513, 2019.
- [58] P. Surinkaew, N. Apaijai, P. Sawaddiruk et al., "Mitochondrial fusion promoter alleviates brain damage in rats with cardiac ischemia/reperfusion injury," *Journal of Alzheimer's Disease*, vol. 77, no. 3, pp. 993-1003, 2020.
- [59] D. Glick, S. Barth, and K. F. Macleod, "Autophagy: cellular and molecular mechanisms," *The Journal of Pathology*, vol. 221, no. 1, pp. 3-12, 2010.
- [60] H. Yamamoto, S. Kakuta, T. M. Watanabe et al., "Atg9 vesicles are an important membrane source during early steps of autophagosome formation," *The Journal of Cell Biology*, vol. 198, no. 2, pp. 219-233, 2012.
- [61] J. Kim, M. Kundu, B. Viollet, and K. L. Guan, "AMPK and mTOR regulate autophagy through direct phosphorylation of Ulk1," *Nature Cell Biology*, vol. 13, no. 2, pp. 132-141, 2011.
- [62] W. Lu, S. S. Karuppagounder, D. A. Springer et al., "Genetic deficiency of the mitochondrial protein PGAM5 causes a Parkinson's-like movement disorder," *Nature Communications*, vol. 5, no. 1, p. 4930, 2014.
- [63] C. Meissner, H. Lorenz, A. Weihofen, D. J. Selkoe, and M. K. Lemberg, "The mitochondrial intramembrane protease PARL cleaves human Pink1 to regulate Pink1 trafficking," *Journal of Neurochemistry*, vol. 117, no. 5, pp. 856-867, 2011.
- [64] F. Koyano, K. Okatsu, H. Kosako et al., "Ubiquitin is phosphorylated by PINK1 to activate parkin," *Nature*, vol. 510, no. 7503, pp. 162-166, 2014.
- [65] S. A. Killackey, D. J. Philpott, and S. E. Girardin, "Mitophagy pathways in health and disease," *The Journal of Cell Biology*, vol. 219, no. 11, 2020.
- [66] L. M. Yu, X. Dong, X. D. Xue et al., "Melatonin attenuates diabetic cardiomyopathy and reduces myocardial vulnerability to ischemia-reperfusion injury by improving mitochondrial quality control: role of SIRT6," *Journal of Pineal Research*, vol. 70, no. 1, article e12698, 2021.
- [67] H. Zhou, Y. Zhang, S. Hu et al., "Melatonin protects cardiac microvasculature against ischemia/reperfusion injury via suppression of mitochondrial fission-VDAC1-HK2-mPTP-mitophagy axis," *Journal of Pineal Research*, vol. 63, no. 1, p. e12413, 2017.
- [68] Y. Zhu, S. Massen, M. Terenzio et al., "Modulation of Serines 17 and 24 in the LC3-interacting Region of Bnip3 Determines Pro-survival Mitophagy versus Apoptosis," *The Journal of Biological Chemistry*, vol. 288, no. 2, pp. 1099-1113, 2013.
- [69] E. Y. Wang, H. Gang, Y. Aviv, R. Dhingra, V. Margulets, and L. A. Kirshenbaum, "p53 mediates autophagy and cell death by a mechanism contingent on Bnip3," *Hypertension*, vol. 62, no. 1, pp. 70-77, 2013.

- [70] H. Sandoval, P. Thiagarajan, S. K. Dasgupta et al., "Essential role for Nix in autophagic maturation of erythroid cells," *Nature*, vol. 454, no. 7201, pp. 232–235, 2008.
- [71] J. Zhang and P. A. Ney, "Role of BNIP3 and NIX in cell death, autophagy, and mitophagy," *Cell Death and Differentiation*, vol. 16, no. 7, pp. 939–946, 2009.
- [72] L. A. Kubasiak, O. M. Hernandez, N. H. Bishopric, and K. A. Webster, "Hypoxia and acidosis activate cardiac myocyte death through the Bcl-2 family protein BNIP3," *Proceedings of the National Academy of Sciences of the United States of America*, vol. 99, no. 20, pp. 12825–12830, 2002.
- [73] G. Chinnadurai, S. Vijayalingam, and S. B. Gibson, "BNIP3 subfamily BH3-only proteins: mitochondrial stress sensors in normal and pathological functions," *Oncogene*, vol. 27, Supplement 1, pp. S114–S127, 2008.
- [74] S. Rikka, M. N. Quinsay, R. L. Thomas et al., "Bnip3 impairs mitochondrial bioenergetics and stimulates mitochondrial turnover," *Cell Death and Differentiation*, vol. 18, no. 4, pp. 721–731, 2011.
- [75] K. M. Regula, K. Ens, and L. A. Kirshenbaum, "Inducible expression of BNIP3 provokes mitochondrial defects and hypoxia-mediated cell death of ventricular myocytes," *Circulation Research*, vol. 91, no. 3, pp. 226–231, 2002.
- [76] G. Chen, J. Cizeau, C. Vande Velde et al., "Nix and Nip3 form a subfamily of pro-apoptotic mitochondrial proteins," *The Journal of Biological Chemistry*, vol. 274, no. 1, pp. 7–10, 1999.
- [77] A. Diwan, M. Krenz, F. M. Syed et al., "Inhibition of ischemic cardiomyocyte apoptosis through targeted ablation of Bnip3 restrains postinfarction remodeling in mice," *The Journal of Clinical Investigation*, vol. 117, no. 10, pp. 2825–2833, 2007.
- [78] Y. Li, S. Ren, J. Xia, Y. Wei, and Y. Xi, "EIF4A3-induced circ-BNIP3 aggravated hypoxia-induced injury of H9c2 cells by targeting miR-27a-3p/BNIP3," *Mol Ther Nucleic Acids*, vol. 19, pp. 533–545, 2020.
- [79] X. Zheng, T. Zhong, Y. Ma et al., "Bnip3 mediates doxorubicin-induced cardiomyocyte pyroptosis via caspase-3/GSDME," *Life Sciences*, vol. 242, p. 117186, 2020.
- [80] R. A. Hanna, M. N. Quinsay, A. M. Orogo, K. Giang, S. Rikka, and Å. B. Gustafsson, "Microtubule-associated protein 1 light chain 3 (LC3) interacts with Bnip3 protein to selectively remove endoplasmic reticulum and mitochondria via autophagy," *The Journal of Biological Chemistry*, vol. 287, no. 23, pp. 19094–19104, 2012.
- [81] Y. Zhang, D. Liu, H. Hu, P. Zhang, R. Xie, and W. Cui, "HIF-1 α /BNIP3 signaling pathway-induced-autophagy plays protective role during myocardial ischemia-reperfusion injury," *Biomedicine & Pharmacotherapy*, vol. 120, p. 109464, 2019.
- [82] L. Yang, P. Xie, J. Wu et al., "Deferoxamine treatment combined with sevoflurane postconditioning attenuates myocardial ischemia-reperfusion injury by restoring HIF-1/BNIP3-mediated mitochondrial autophagy in GK rats," *Frontiers in Pharmacology*, vol. 11, p. 6, 2020.
- [83] N. Zhu, J. Li, Y. Li et al., "Berberine protects against simulated ischemia/reperfusion injury-induced H9C2 cardiomyocytes apoptosis in vitro and myocardial ischemia/reperfusion-induced apoptosis in vivo by regulating the mitophagy-mediated HIF-1 α /BNIP3 pathway," *Frontiers in Pharmacology*, vol. 11, p. 367, 2020.
- [84] W. Zhang, H. Ren, C. Xu et al., "Hypoxic mitophagy regulates mitochondrial quality and platelet activation and determines severity of I/R heart injury," *eLife*, vol. 5, 2016.
- [85] L. Liu, D. Feng, G. Chen et al., "Mitochondrial outer-membrane protein FUNDC1 mediates hypoxia-induced mitophagy in mammalian cells," *Nature Cell Biology*, vol. 14, no. 2, pp. 177–185, 2012.
- [86] W. Wu, W. Tian, Z. Hu et al., "ULK1 translocates to mitochondria and phosphorylates FUNDC1 to regulate mitophagy," *EMBO Reports*, vol. 15, no. 5, pp. 566–575, 2014.
- [87] H. Zhou, P. Zhu, J. Wang, H. Zhu, J. Ren, and Y. Chen, "Pathogenesis of cardiac ischemia reperfusion injury is associated with CK2 α -disturbed mitochondrial homeostasis via suppression of FUNDC1-related mitophagy," *Cell Death and Differentiation*, vol. 25, no. 6, pp. 1080–1093, 2018.
- [88] G. Chen, Z. Han, D. Feng et al., "A regulatory signaling loop comprising the PGAM5 phosphatase and CK2 controls receptor-mediated mitophagy," *Molecular Cell*, vol. 54, no. 3, pp. 362–377, 2014.
- [89] Y. Xiao, W. Chen, Z. Zhong et al., "Electroacupuncture preconditioning attenuates myocardial ischemia-reperfusion injury by inhibiting mitophagy mediated by the mTORC1-ULK1-FUNDC1 pathway," *Biomedicine & Pharmacotherapy*, vol. 127, p. 110148, 2020.
- [90] S. Wu, Q. Lu, Q. Wang et al., "Binding of FUN14 domain containing 1 with inositol 1,4,5-trisphosphate receptor in mitochondria-associated endoplasmic reticulum membranes maintains mitochondrial dynamics and function in hearts in vivo," *Circulation*, vol. 136, no. 23, pp. 2248–2266, 2017.
- [91] Y. Lim, B. Berry, S. Viteri et al., "FNDC-1-mediated mitophagy and ATFS-1 coordinate to protect against hypoxia-reoxygenation," *Autophagy*, pp. 1–13, 2021.
- [92] W. Yu, M. Xu, T. Zhang, Q. Zhang, and C. Zou, "Mst1 promotes cardiac ischemia-reperfusion injury by inhibiting the ERK-CREB pathway and repressing FUNDC1-mediated mitophagy," *The Journal of Physiological Sciences*, vol. 69, no. 1, pp. 113–127, 2019.
- [93] W. Zhang, S. Siraj, R. Zhang, and Q. Chen, "Mitophagy receptor FUNDC1 regulates mitochondrial homeostasis and protects the heart from I/R injury," *Autophagy*, vol. 13, no. 6, pp. 1080–1081, 2017.
- [94] M. J. Baker, T. Tatsuta, and T. Langer, "Quality control of mitochondrial proteostasis," *Cold Spring Harbor Perspectives in Biology*, vol. 3, no. 7, 2011.
- [95] F. R. Jornayvaz and G. I. Shulman, "Regulation of mitochondrial biogenesis," *Essays in Biochemistry*, vol. 47, pp. 69–84, 2010.
- [96] M. J. Baker, A. E. Frazier, J. M. Gulbis, and M. T. Ryan, "Mitochondrial protein-import machinery: correlating structure with function," *Trends in Cell Biology*, vol. 17, no. 9, pp. 456–464, 2007.
- [97] J. Song, J. M. Herrmann, and T. Becker, "Quality control of the mitochondrial proteome," *Nature Reviews. Molecular Cell Biology*, vol. 22, no. 1, pp. 54–70, 2021.
- [98] T. Tatsuta, M. Scharwey, and T. Langer, "Mitochondrial lipid trafficking," *Trends in Cell Biology*, vol. 24, no. 1, pp. 44–52, 2014.
- [99] J. V. Virbasius and R. C. Scarpulla, "Activation of the human mitochondrial transcription factor A gene by nuclear respiratory factors: a potential regulatory link between nuclear and mitochondrial gene expression in organelle biogenesis," *Proceedings of the National Academy of Sciences of the United States of America*, vol. 91, no. 4, pp. 1309–1313, 1994.

- [100] V. Giguère, “Transcriptional control of energy homeostasis by the estrogen-related receptors,” *Endocrine Reviews*, vol. 29, no. 6, pp. 677–696, 2008.
- [101] H. Zong, J. M. Ren, L. H. Young et al., “AMP kinase is required for mitochondrial biogenesis in skeletal muscle in response to chronic energy deprivation,” *Proceedings of the National Academy of Sciences of the United States of America*, vol. 99, no. 25, pp. 15983–15987, 2002.
- [102] E. Nisoli, E. Clementi, C. Paolucci et al., “Mitochondrial biogenesis in mammals: the role of endogenous nitric oxide,” *Science*, vol. 299, no. 5608, pp. 896–899, 2003.
- [103] J. T. Rodgers, C. Lerin, W. Haas, S. P. Gygi, B. M. Spiegelman, and P. Puigserver, “Nutrient control of glucose homeostasis through a complex of PGC-1 α and SIRT1,” *Nature*, vol. 434, no. 7029, pp. 113–118, 2005.
- [104] Z. Wu, X. Huang, Y. Feng et al., “Transducer of regulated CREB-binding proteins (TORCs) induce PGC-1 α transcription and mitochondrial biogenesis in muscle cells,” *Proceedings of the National Academy of Sciences of the United States of America*, vol. 103, no. 39, pp. 14379–14384, 2006.
- [105] R. Yue, X. Xia, J. Jiang et al., “Mitochondrial DNA oxidative damage contributes to cardiomyocyte ischemia/reperfusion-injury in rats: cardioprotective role of lycopene,” *Journal of Cellular Physiology*, vol. 230, no. 9, pp. 2128–2141, 2015.
- [106] Y. Li, B. Chen, X. Yang et al., “S100a8/a9 signaling causes mitochondrial dysfunction and cardiomyocyte death in response to ischemic/reperfusion injury,” *Circulation*, vol. 140, no. 9, pp. 751–764, 2019.
- [107] M. Morgenstern, S. B. Stiller, P. Lübbert et al., “Definition of a high-confidence mitochondrial proteome at quantitative scale,” *Cell Reports*, vol. 19, no. 13, pp. 2836–2852, 2017.
- [108] N. Pfanner, B. Warscheid, and N. Wiedemann, “Mitochondrial proteins: from biogenesis to functional networks,” *Nature Reviews Molecular Cell Biology*, vol. 20, no. 5, pp. 267–284, 2019.
- [109] M. Giacomello, A. Pyakurel, C. Glytsou, and L. Scorrano, “The cell biology of mitochondrial membrane dynamics,” *Nature Reviews Molecular Cell Biology*, vol. 21, no. 4, pp. 204–224, 2020.
- [110] S. Pickles, P. Vigié, and R. J. Youle, “Mitophagy and quality control mechanisms in mitochondrial maintenance,” *Current Biology*, vol. 28, no. 4, pp. R170–r185, 2018.
- [111] G. McLelland, V. Soubannier, C. X. Chen, H. McBride, and E. A. Fon, “Parkin and PINK1 function in a vesicular trafficking pathway regulating mitochondrial quality control,” *The EMBO Journal*, vol. 33, no. 4, pp. 282–295, 2014.
- [112] V. J. Cadete, S. Deschênes, A. Cuillerier et al., “Formation of mitochondrial-derived vesicles is an active and physiologically relevant mitochondrial quality control process in the cardiac system,” *The Journal of Physiology*, vol. 594, no. 18, pp. 5343–5362, 2016.
- [113] B. Li, H. Zhao, Y. Wu et al., “Mitochondrial-derived vesicles protect cardiomyocytes against hypoxic damage,” *Frontiers in Cell and Development Biology*, vol. 8, p. 214, 2020.
- [114] W. X. Ding, F. Guo, H. M. Ni et al., “Parkin and mitofusins reciprocally regulate mitophagy and mitochondrial spheroid formation,” *The Journal of Biological Chemistry*, vol. 287, no. 50, pp. 42379–42388, 2012.
- [115] H. M. Ni, J. A. Williams, H. Jaeschke, and W. X. Ding, “Zonated induction of autophagy and mitochondrial spheroids limits acetaminophen-induced necrosis in the liver,” *Redox Biology*, vol. 1, no. 1, pp. 427–432, 2013.
- [116] J. Wang and H. Zhou, “Mitochondrial quality control mechanisms as molecular targets in cardiac ischemia - reperfusion injury,” *Acta Pharmaceutica Sinica B*, vol. 10, no. 10, pp. 1866–1879, 2020.
- [117] P. Deng and C. M. Haynes, “Mitochondrial dysfunction in cancer: potential roles of ATF5 and the mitochondrial UPR,” *Seminars in Cancer Biology*, vol. 47, pp. 43–49, 2017.
- [118] I. Smyrniak, S. P. Gray, D. O. Okonko et al., “Cardioprotective effect of the mitochondrial unfolded protein response during chronic pressure overload,” *Journal of the American College of Cardiology*, vol. 73, no. 14, pp. 1795–1806, 2019.
- [119] L. H. M. Bozi, J. C. Campos, E. R. Gross, and J. C. B. Ferreira, “Mitochondrial Unfolded Protein Response (UPR^{mt}) Activation in Cardiac Diseases: Opportunities and Challenges,” *Journal of the American College of Cardiology*, vol. 74, no. 7, pp. 1011–1012, 2019.
- [120] Y. T. Wang, Y. Lim, M. N. McCall et al., “Cardioprotection by the mitochondrial unfolded protein response requires ATF5,” *American Journal of Physiology-Heart and Circulatory Physiology*, vol. 317, no. 2, pp. H472–h478, 2019.
- [121] Y. C. Wong, D. Ysselstein, and D. Krainc, “Mitochondria-lysosome contacts regulate mitochondrial fission via RAB7 GTP hydrolysis,” *Nature*, vol. 554, no. 7692, pp. 382–386, 2018.
- [122] S. Lahnwong, S. Palee, N. Apaijai et al., “Acute dapagliflozin administration exerts cardioprotective effects in rats with cardiac ischemia/reperfusion injury,” *Cardiovascular Diabetology*, vol. 19, no. 1, p. 91, 2020.
- [123] H. Zhou, D. Li, P. Zhu et al., “Melatonin suppresses platelet activation and function against cardiac ischemia/reperfusion injury via PPAR γ /FUNDC1/mitophagy pathways,” *Journal of Pineal Research*, vol. 63, no. 4, 2017.
- [124] Y. Tan, D. Mui, S. Toan, P. Zhu, R. Li, and H. Zhou, “SERCA overexpression improves mitochondrial quality control and attenuates cardiac microvascular ischemia-reperfusion injury,” *Molecular Therapy - Nucleic Acids*, vol. 22, pp. 696–707, 2020.
- [125] G. Hasenfuss and J. R. Teerlink, “Cardiac inotropes: current agents and future directions,” *European Heart Journal*, vol. 32, no. 15, pp. 1838–1845, 2011.
- [126] S. Zhang, W. Wang, X. Wu, and X. Zhou, “Regulatory roles of circular rnas in coronary artery disease,” *Molecular Therapy - Nucleic Acids*, vol. 21, pp. 172–179, 2020.
- [127] F. Y. Lee, P. L. Shao, C. G. Wallace et al., “Combined therapy with SS31 and mitochondria mitigates myocardial ischemia-reperfusion injury in rats,” *International Journal of Molecular Sciences*, vol. 19, no. 9, p. 2782, 2018.

Research Article

Protective Effect of Optic Atrophy 1 on Cardiomyocyte Oxidative Stress: Roles of Mitophagy, Mitochondrial Fission, and MAPK/ERK Signaling

Yue Wang, Zhihua Han, Zuojun Xu, and Junfeng Zhang 

Department of Cardiology, Shanghai Ninth People's Hospital, Shanghai Jiaotong University School of Medicine, Shanghai 200011, China

Correspondence should be addressed to Junfeng Zhang; 611121@sh9hospital.org.cn

Received 9 April 2021; Revised 8 May 2021; Accepted 21 May 2021; Published 8 June 2021

Academic Editor: Yun-dai Chen

Copyright © 2021 Yue Wang et al. This is an open access article distributed under the Creative Commons Attribution License, which permits unrestricted use, distribution, and reproduction in any medium, provided the original work is properly cited.

Myocardial infarction is associated with oxidative stress and mitochondrial damage. However, the regulatory mechanisms underlying cardiomyocyte oxidative stress during myocardial infarction are not fully understood. In the present study, we explored the cardioprotective action of optic atrophy 1- (Opa1-) mediated mitochondrial autophagy (mitophagy) in oxidative stress-challenged cardiomyocytes, with a focus on mitochondrial homeostasis and the MAPK/ERK pathway. Our results demonstrated that overexpression of Opa1 in cultured rat H9C2 cardiomyocytes, a procedure that stimulates mitophagy, attenuates oxidative stress and increases cellular antioxidant capacity. Activation of Opa1-mediated mitophagy suppressed cardiomyocyte apoptosis by downregulating Bax, caspase-9, and caspase-12 and upregulating Bcl-2 and c-IAP. Using mitochondrial tracker staining and a reactive oxygen species indicator, our assays showed that Opa1-mediated mitophagy attenuated mitochondrial fission and reduced ROS production in cardiomyocytes. In addition, we found that inhibition of the MAPK/ERK pathway abolished the antioxidant action of Opa1-mediated mitophagy in these cells. Taken together, our data demonstrate that Opa1-mediated mitophagy protects cardiomyocytes against oxidative stress damage through inhibition of mitochondrial fission and activation of MAPK/ERK signaling. These findings reveal a critical role for Opa1 in the modulation of cardiomyocyte redox balance and suggest a potential target for the treatment of myocardial infarction.

1. Introduction

Oxidative stress in cardiomyocytes has been regarded as the primary pathological factor in many cardiovascular disorders including, but not limited to, diabetic cardiomyopathy, heart failure, myocardial hypertrophy, cardiac fibrosis, and dilated cardiomyopathy [1–3]. Particularly, recent studies have highlighted the important role of oxidative stress in the induction of myocardial infarction [2, 4, 5]. At the molecular level, oxidative stress induces the peroxidation of cellular membranes, including the mitochondrial membrane, the endoplasmic reticulum membrane, and the plasma membrane. Damage to the cellular membrane system disrupts cellular metabolism, accelerates cellular senescence, and promotes cell death [6, 7]. Although several antioxidative therapies have been developed to promote the recovery of

cardiomyocyte function in cardiovascular disease, several questions remain regarding the upstream regulatory mechanisms controlling antioxidant responses in these cells [8–11].

Oxidative stress is primarily caused by excessive production and intracellular accumulation of reactive oxygen species (ROS) [12]. Since most cellular ROS are produced in the mitochondrion during oxidative phosphorylation [13], this organelle is widely recognized as a crucial target in the treatment of cardiovascular conditions [14–16]. Whereas physiological (low) ROS levels serve signaling functions and contribute to adaptive responses to hypoxia, excess ROS overwhelms the cells' antioxidant defenses and exacerbates mitochondrial ROS production to ultimately promote cell death [17]. Therefore, strategies aiming at protecting mitochondria and attenuating ROS production have great therapeutic potential in the management of cardiovascular

disease [18]. Our previous study has reported a mitochondrial self-protection program involving mitochondrial autophagy (mitophagy) regulated by optic atrophy 1 (Opa1), a protein located at the inner mitochondrial membrane [19]. Moderate mitochondrial mitophagy promotes mitochondrial turnover, accelerates the recycling of damaged mitochondrial population, and blocks mitochondria-mediated cell death signaling [20–23]. However, the role of Opa1-related mitophagy in modulating cellular oxidative stress is not fully understood, especially in the setting of myocardial infarction.

Mitochondrial ROS production seems to be mainly affected by mitochondrial fission, a process necessary to control mitochondrial metabolism and oxidative phosphorylation [24, 25]. An increased mitochondrial population, as a result of mitochondrial fission, will accelerate glucose metabolism and therefore promote ATP production, an effect that is accompanied by enhanced ROS generation. Accordingly, inhibition of mitochondrial fission has been found to attenuate ROS levels in cardiomyocytes [26]. Although mitophagy serves as a mechanism to remove excess/fragmented organelles resulting from mitochondrial fission, it is unclear whether Opa1-mediated mitochondrial mitophagy exerts antioxidative effects through inhibition of mitochondrial fission.

The MAPK/ERK pathway has been reported as a main upstream regulator of mitochondrial fission [27]. Interestingly, there is also a close association between MAPK/ERK signaling and the activity of the cellular antioxidant system [28]. However, the relationship between Opa1-related mitochondrial mitophagy, the MAPK/ERK pathway, and mitochondrial fission remains unclear. Thus, in the present study, the hypothesis that Opa1-related mitophagy inhibits mitochondrial fission and oxidative stress through a mechanism involving the activation of the MAPK/ERK pathway was tested using control and Opa1-overexpressing H9C2 cardiomyocytes challenged with H₂O₂ to model myocardial infarction *in vitro*.

2. Materials and Methods

2.1. Cell Culture and Adenoviral Transduction. H9C2 cells were obtained from ATCC and cultured in DMEM/F12 supplemented with 10% FBS (Abcam, USA) at 37°C and 5% CO₂ [29, 30]. Cells (2×10^5) were seeded in six-well plates and transduced with an Opa1-encoding adenovirus (Ad-Opa1; VENDOR) at 37°C for 48 h using Lipofectamine® 2000 (Invitrogen, USA) [31]. To induce oxidative stress damage, H₂O₂ (0.3 mM) was added into the medium of H9C2 cardiomyocytes for 12 h [32].

2.2. CCK-8 Assay. Control and Ad-Opa1-transduced H9C2 cells were seeded onto 96-well plates and incubated with H₂O₂ (0.3 mM) for 12 h. A CCK-8 reagent was then added to each well and incubated for 4 h. Absorbance was detected at 490 nm [33].

2.3. Evaluation of Mitochondrial Morphology. H9C2 cells were seeded at a density of 6×10^5 cells/well into 6-well

plates, cultured for 24 h at 37°C in 5% CO₂, and infected at an MOI of 50 with Ad-Opa1 for 48 h. Noninfected H9C2 cells were used as negative controls. After exposure to H₂O₂ (0.3 mM) or vehicle for 12 h, the cells were incubated in the dark for 30 min at 37°C in the presence of 4 μM of MitoTracker™ Red [34]. Fluorescence microscopy (Olympus, Tokyo, Japan) was used to analyze mitochondrial morphology.

2.4. Assessment of Mitochondrial Membrane Potential. H9C2 cells were plated and transduced with Ad-Opa1 as described above, treated with vehicle or H₂O₂ (0.3 mM) for 12 h, and incubated in the dark for 20 min at 37°C in the presence of 1 μL JC-1 in 1 mL of DMEM [35]. Fluorescence microscopy was then used to determine mitochondrial membrane potential [36].

2.5. ROS Assay. A cellular ROS red fluorescence assay kit (Cat. no. GMS10111.1; GENMED Scientifics, Inc., USA) was used to detect intracellular ROS. H9C2 cells (1×10^4) were plated in 96-well plates and two days later exposed to H₂O₂ for 12 h. In some experiments, the cells were pretreated with FCCP, an activator of mitochondrial fission, or PD98059, a MAPK/ERK inhibitor, before being exposed to H₂O₂. The culture medium was aspirated, and 100 μL of staining working solution was added according to the manufacturer's instructions [37]. The mixture was incubated at 37°C for 20 min in the dark and then washed with PBS three times. ROS fluorescence ($E_x/E_m = 540/590$ nm) was measured on a microplate reader controlled by SkanIt software (Cat. no. N16699; Thermo Scientific, Inc., USA) [38, 39]. The results were presented as percentage fluorescence relative to the control group. Fluorescence microscopy was also performed in cells seeded on 6-well plates after exposure to H₂O₂ for 12 h. Following DAPI staining, an EVOS® FL Cell Imaging System (Life Technologies, USA) was used to conduct fluorescence imaging [40].

2.6. Evaluation of Cellular Antioxidant Activities. The activity of cellular antioxidant enzymes was measured through ELISA as previously described [41]. Colorimetric determinations of cellular antioxidant enzyme activities were performed using a Glutathione Reductase Assay Kit (Beyotime, China, Cat. No: S0055), a Total Superoxide Dismutase Assay Kit (Beyotime, Cat. No: S0101), and a Cellular Glutathione Peroxidase Assay Kit (Beyotime, Cat. No: S0056) [42].

2.7. TUNEL Staining. Cardiomyocyte apoptosis was determined using a One Step TUNEL apoptosis Assay Kit (Beyotime) according to the manufacturer's instructions [43]. After TUNEL labeling and DAPI counterstain, images were captured by fluorescence microscopy. Apoptosis was expressed as a percentage relative to the control group [44, 45].

2.8. Western Blot Analysis. Cells were harvested and lysed in RIPA buffer containing 1% protease inhibitor and 1% phosphatase inhibitor (Wako, USA). The lysates were mixed with 3x SDS sample buffer with 2-mercaptoethanol and boiled at 95°C for 5 min prior to SDS-PAGE [46]. Proteins were transferred to a PVDF membrane (Millipore, USA) and

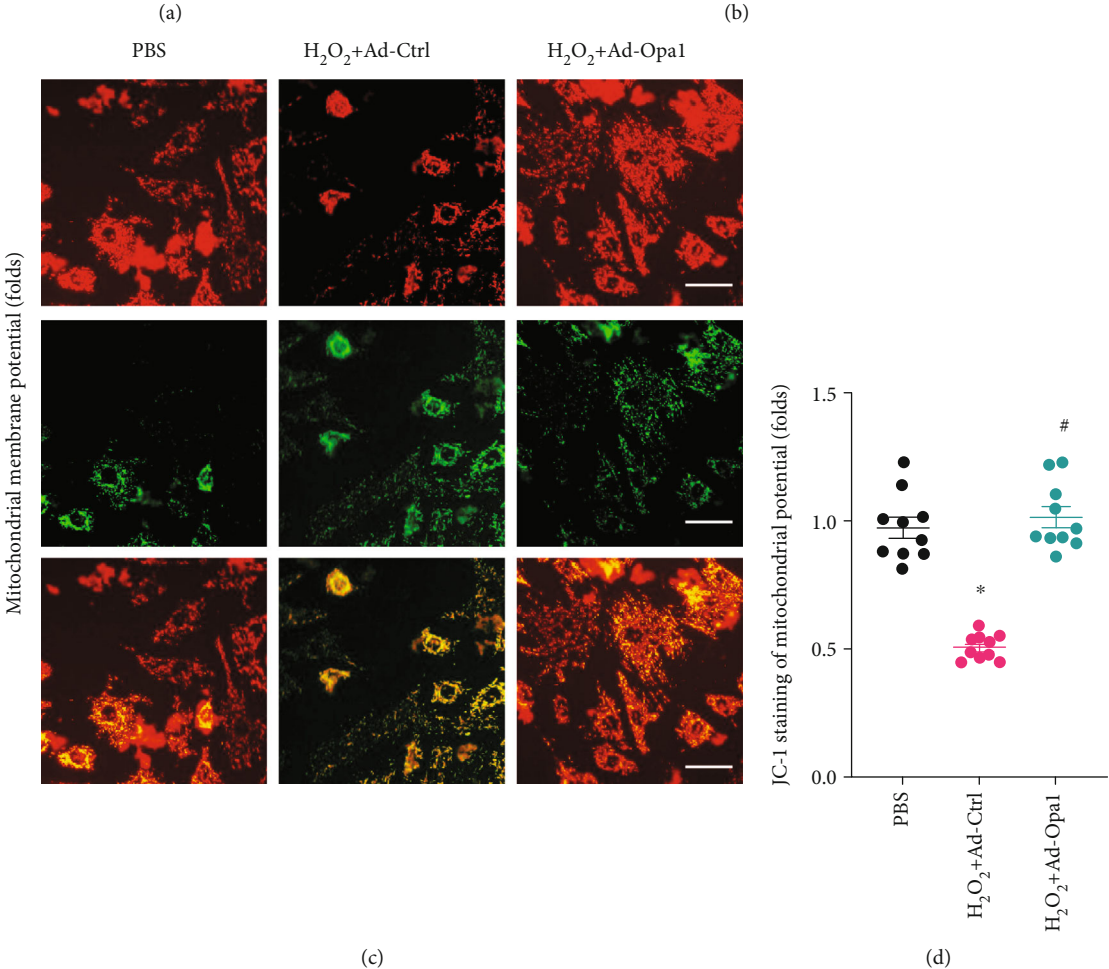
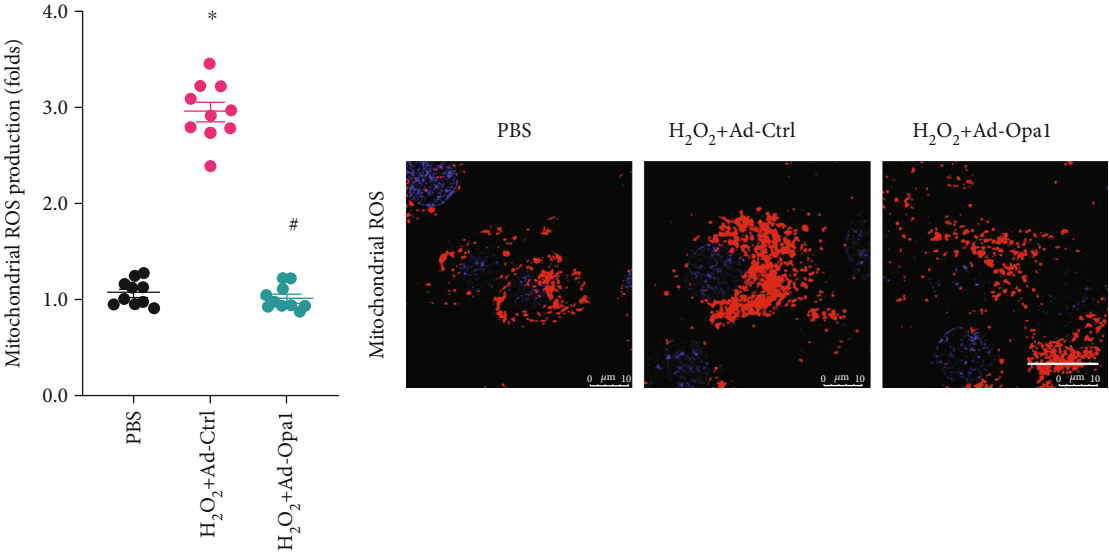


FIGURE 1: Continued.

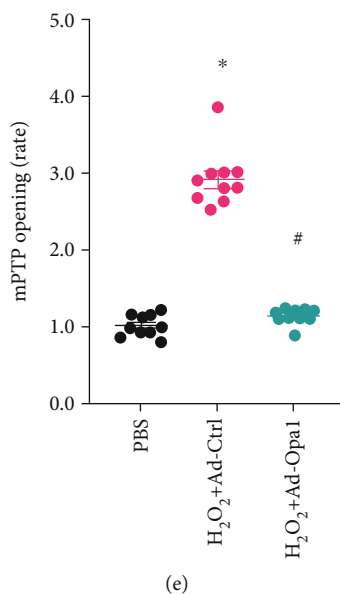


FIGURE 1: Opa1-mediated mitophagy attenuates mitochondrial ROS production and reduces mitochondrial dysfunction. Control (nontransduced) and Ad-Opa1-transduced H9C2 cardiomyocytes were treated with 0.3 mM H₂O₂ for 12 h. (a, b) Fluorescent detection of ROS production. Bar: 15 μ m. (c, d) Assessment of mitochondrial membrane potential via JC-1 staining. Bar: 40 μ m. (e) Results of the mPTP opening assay. * $p < 0.05$ vs. control group, # $p < 0.05$ vs. H₂O₂+Ad-Ctrl group.

immunoblotted with the primary antibodies. The membranes were then incubated with anti-mouse or anti-rabbit HRP-conjugated secondary antibodies (1:1000, Bio-Rad, USA) and visualized using a chemiluminescence kit (Santa Cruz Biotechnology, USA) or SuperSignal West Femto Maximum Sensitivity Substrate (Thermo Fisher Scientific) [47].

2.9. RT-PCR. Total RNA was extracted with a TRIzol reagent (Invitrogen) and treated with DNase I to remove genomic DNA. Then, 500 ng of RNA was reversely transcribed into cDNA with the SuperScript IV First-Strand Synthesis System (Invitrogen) [48, 49] and quantitative real-time RT-PCR was performed using a Fast SYBR Green Master Mix (Fisher Scientific) according to the manufacturer's instructions and as described previously [50]. The PCR protocol consisted of 40 cycles of denaturation at 94°C for 15 s, annealing at 60°C for 15 s, and extension at 72°C for 1 minute, followed by a single, 7 min extension period at 72°C [51]. Expression levels of target genes were normalized to those of the endogenous glyceraldehyde phosphate dehydrogenase (GAPDH) [52].

2.10. Statistics. Data are presented as mean \pm SEM. Each *in vitro* experiment was performed at least three times. Significance ($p < 0.05$) was determined via Student's *t*-test for comparisons between two groups and via two-way ANOVA for comparisons between three or more groups.

3. Results

3.1. Opa1-Mediated Mitophagy Attenuates ROS Production and Mitochondrial Dysfunction. To investigate the role of Opa1-related mitophagy on ROS production and mitochondrial dysfunction, cultured H9C2 cardiomyocytes were transduced with an adenoviral vector encoding Opa1 (Ad-Opa1)

before being exposed to H₂O₂ (0.3 mM) to induce an oxidative stress microenvironment. Nontransduced cells were used as the control. As shown in Figures 1(a) and 1(b), the production of mitochondrial ROS was significantly increased in nontransduced cardiomyocytes and significantly inhibited in cells overexpressing Opa1. Since mitochondrial ROS overproduction is associated with oxidative stress and mitochondrial and cellular dysfunction, we next evaluated the functionality of mitochondria in both control and Opa1-transduced cardiomyocytes. As shown in Figures 1(c) and 1(d), mitochondrial membrane potential was reduced by H₂O₂ exposure in control cells but remained largely unaffected after Opa1 overexpression. Excessive mitochondrial damage is associated with mitochondria-dependent cardiomyocyte death. Using ELISA, we found that the rate of mitochondrial permeability transition pore (mPTP) opening, an early marker of cardiomyocyte death following ischemia-reperfusion injury, was significantly elevated in control cardiomyocytes treated with H₂O₂. However, overexpression of Opa1 was able to block mPTP opening (Figure 1(e)). These data demonstrate that Opa1-mediated mitophagy suppresses mitochondrial ROS production and maintains mitochondrial function under an oxidative stress microenvironment.

3.2. Opa1-Induced Mitophagy Increases the Activity of Cellular Antioxidant Enzymes. Since mitochondrial oxidative stress can also result from decreased antioxidant capacity, we asked whether Opa1-induced mitophagy would also regulate the activity of antioxidant enzymes. We found that the levels of GSH, SOD, and GPX were significantly reduced in H₂O₂-treated cardiomyocytes. Interestingly, these changes were reversed by Opa1 overexpression (Figures 2(a)–2(c)). Since the activity of cellular antioxidant enzymes is primarily

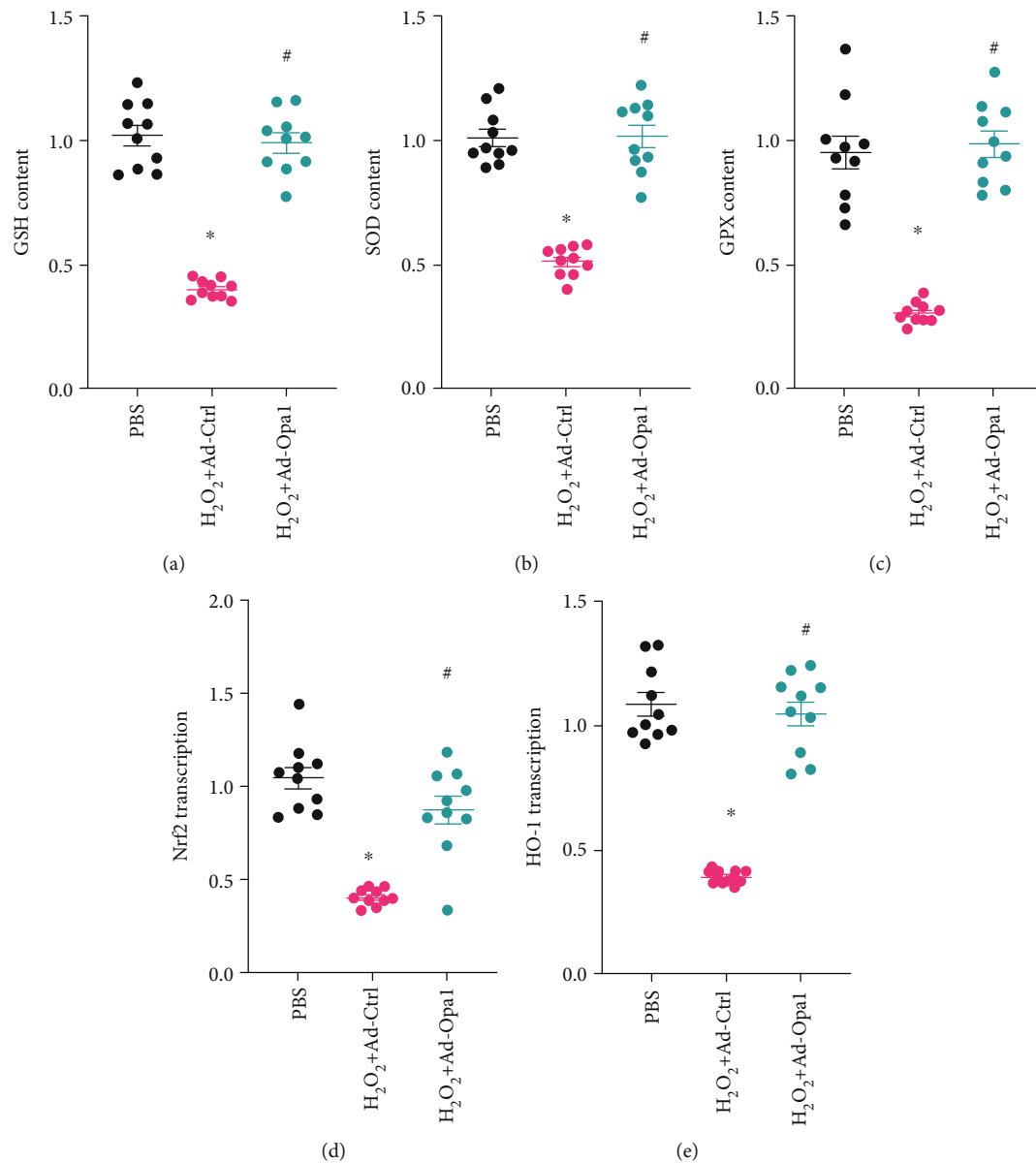


FIGURE 2: Opa1-mediated mitophagy increases the activity of cellular antioxidant enzymes. Control (nontransduced) and Ad-Opa1-transduced H9C2 cardiomyocytes were treated with 0.3 mM H₂O₂ for 12 h. (a–c) Colorimetric determination of GSH, SOD, and GPX activities. (d, e) Results of qPCR assays to analyze the transcriptional profiles of Nrf2 and HO-1. * $p < 0.05$ vs. control group, # $p < 0.05$ vs. H₂O₂+Ad-Ctrl group.

regulated at the transcriptional level, we assessed the impact of Opa1 overexpression on the expression of two key transcription factors, namely, Nrf2 and HO-1, governing the expression of antioxidant enzymes. Results of qPCR analysis demonstrated that Nrf2 and HO-1 mRNA levels were markedly downregulated in cardiomyocytes treated with H₂O₂ but upregulated instead after Opa1 overexpression (Figures 2(d) and 2(e)). These data indicate that Opa1-mediated mitophagy enhances the antioxidant potential of cardiomyocytes through upregulation of the transcription of HO-1 and Nrf2.

3.3. Opa1-Mediated Mitophagy Sustains Cardiomyocyte Viability under Oxidative Stress Conditions.

Under oxidative

stress conditions, impaired mitochondrial function and limited antioxidant capacity reduce the viability of cardiomyocytes by activating cell death pathways. Results of CCK-8 assays demonstrated that the viability of H9C2 cells was significantly reduced in response to H₂O₂ treatment. In contrast, cell viability was significantly rescued by Opa1 overexpression (Figure 3(a)). This finding was further analyzed using TUNEL staining. As shown in Figures 3(b) and 3(c), apoptosis was significantly promoted after exposure to H₂O₂. In turn, induction of mitophagy via Opa1 overexpression markedly decreased the number of apoptotic cardiomyocytes. To investigate the molecular basis underlying Opa1-mediated antiapoptotic action, western blots were used

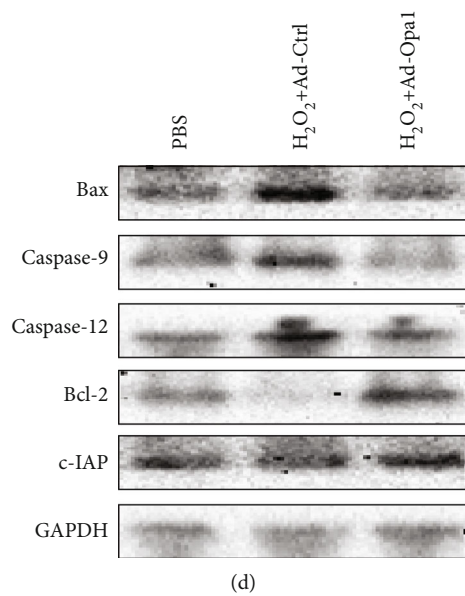
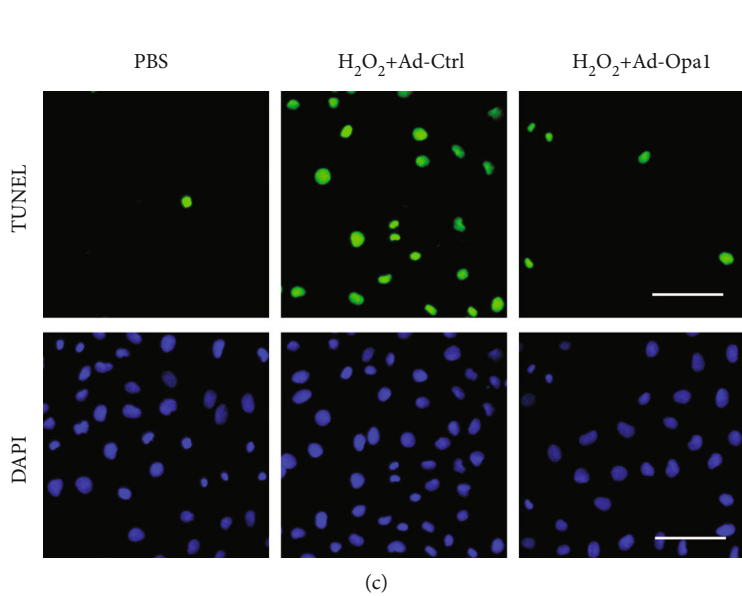
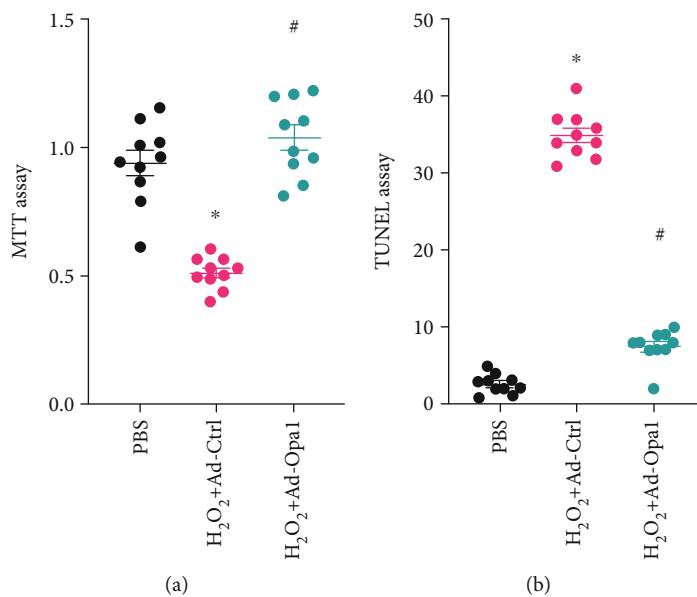


FIGURE 3: Continued.

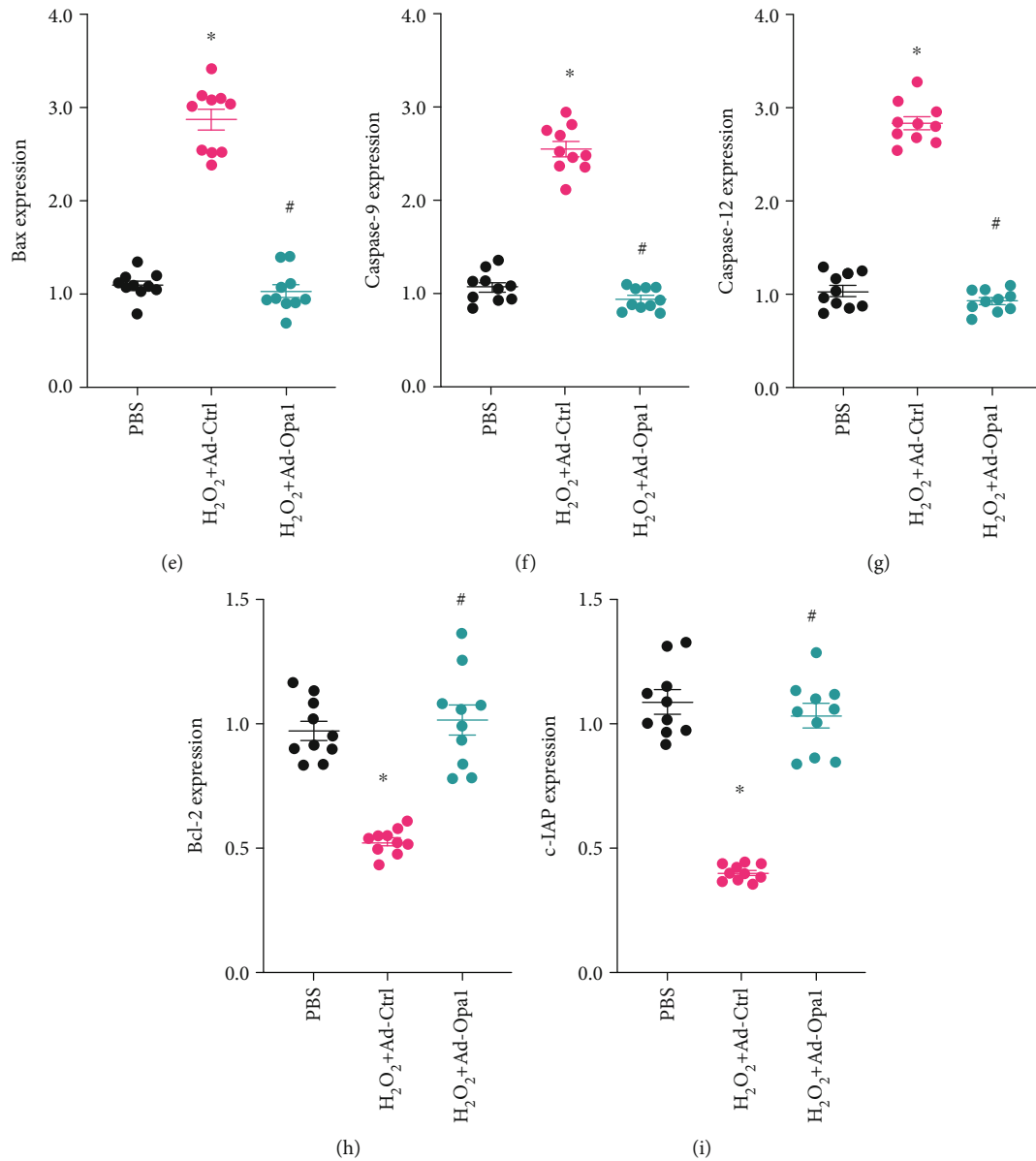


FIGURE 3: Opa1-mediated mitophagy sustains cardiomyocyte viability under oxidative stress. Control (nontransduced) and Ad-Opa1-transduced H9C2 cardiomyocytes were exposed to 0.3 mM H₂O₂ for 12 h. (a) Analysis of cardiomyocyte viability using the CCK-8 assay. (b, c) Assessment of apoptosis by TUNEL assay. Bar: 90 μ m. (d–i) Western blotting analysis of Bax, caspase-9, caspase-12, Bcl-2, and c-IAP expression. * p < 0.05 vs. control group, # p < 0.05 vs. H₂O₂+Ad-Ctrl group.

to analyze changes in cell death-related protein expression. As shown in Figures 3(d)–3(i), a significant increase in Bax, caspase-9, and caspase-12 expression, paralleled by down-regulation of Bcl-2 and c-IAP expression, was observed in cardiomyocytes treated with H₂O₂. Interestingly, after overexpression of Opa1, the expression of proapoptotic proteins was reduced, while the levels of antiapoptotic proteins were restored to near normal levels. These data indicate that the reduction in cardiomyocyte viability mediated by H₂O₂ exposure can be reversed by Opa1-induced mitophagy.

3.4. Opa1-Mediated Mitophagy Inhibits Mitochondrial Fission. Recent studies have reported that mitochondrial fis-

sion is the primary trigger of mitochondrial ROS overproduction through accelerated glucose metabolism. To evaluate whether Opa1-mediated mitophagy can attenuate abnormal mitochondrial fission under oxidative stress conditions, mitochondrial morphology was first examined in cultured H9C2 cardiomyocytes using MitoTracker staining. As shown in Figures 4(a)–4(c), H₂O₂ treatment elicited substantial mitochondrial fragmentation, evidenced by an increase in the organelles' average length and number. In contrast, both these variables were significantly normalized in Ad-Opa1-transduced cardiomyocytes. To provide more evidence to support the regulatory role played by Opa1-related mitophagy on mitochondrial fission, qPCR was performed to analyze transcriptional levels of fission-related proteins. As

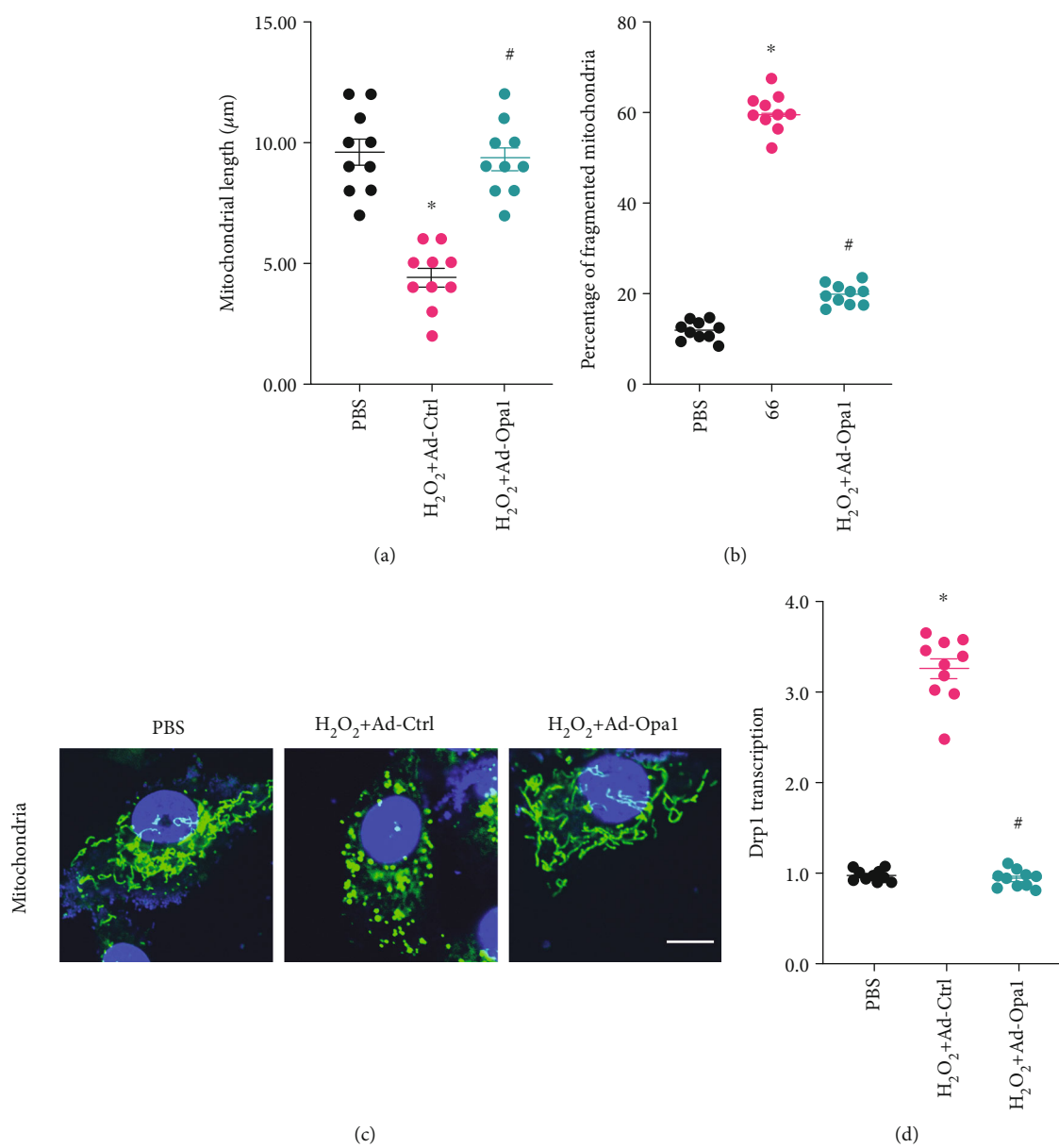


FIGURE 4: Continued.

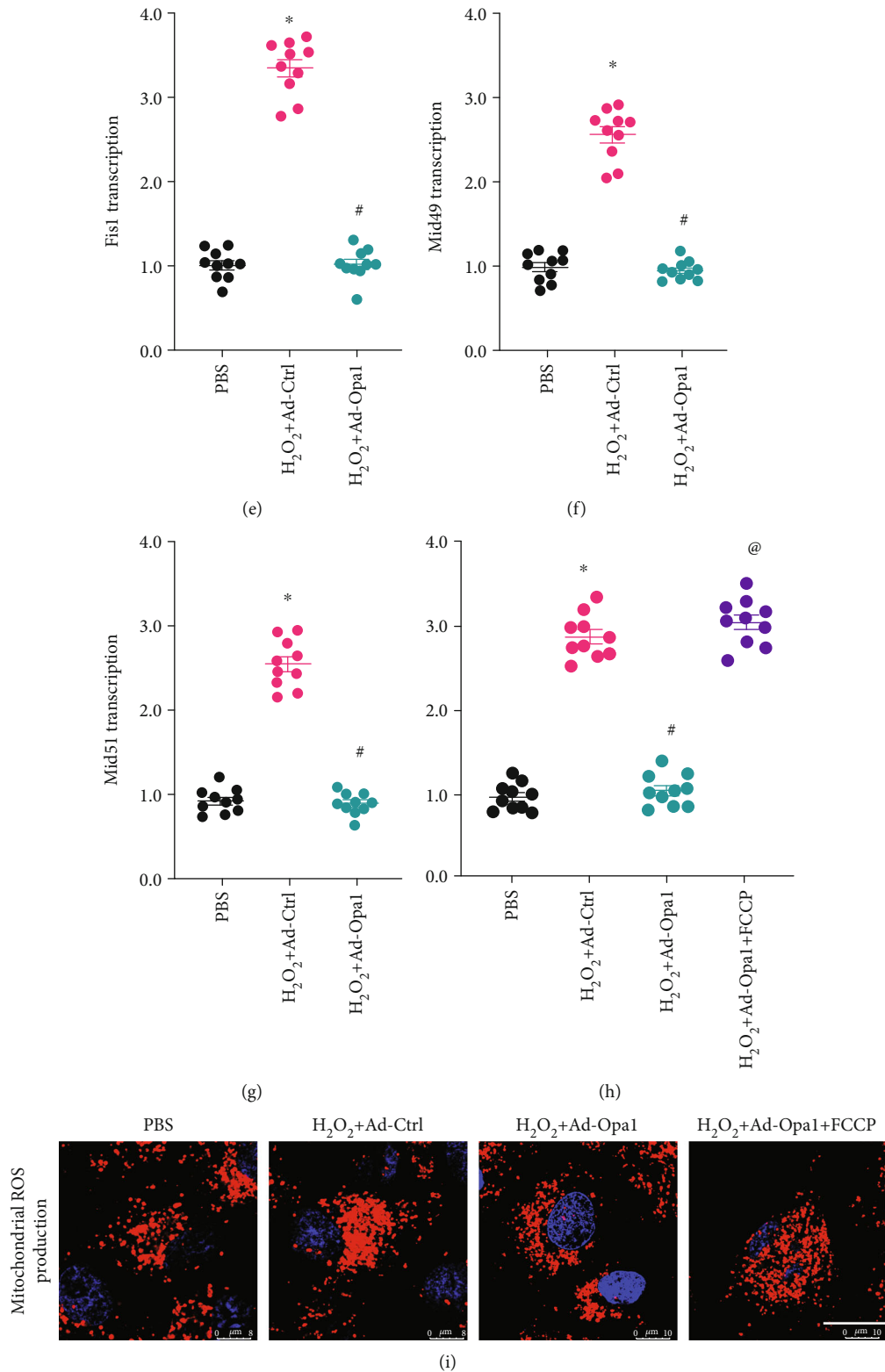


FIGURE 4: Opal-mediated mitophagy inhibits mitochondrial fission. Control (nontransduced) and Ad-Opal1-transduced H9C2 cardiomyocytes were exposed to 0.3 mM H₂O₂ for 12 h. (a–c) Evaluation of mitochondrial morphology by MitoTracker Red staining. Bar: 20 μm. (d–g) Results of qPCR assays to analyze the transcriptional profiles of Drp1, Fis1, Mid49, and Mid51. (h, i) Fluorescent detection of ROS production in H9C2 cells pretreated with or without the mitochondrial fission activator FCCP. Bar: 25 μm. **p* < 0.05 vs. control group, #*p* < 0.05 vs. H₂O₂+Ad-Ctrl group, @*p* < 0.05 vs. H₂O₂+Ad-Opal1 group.

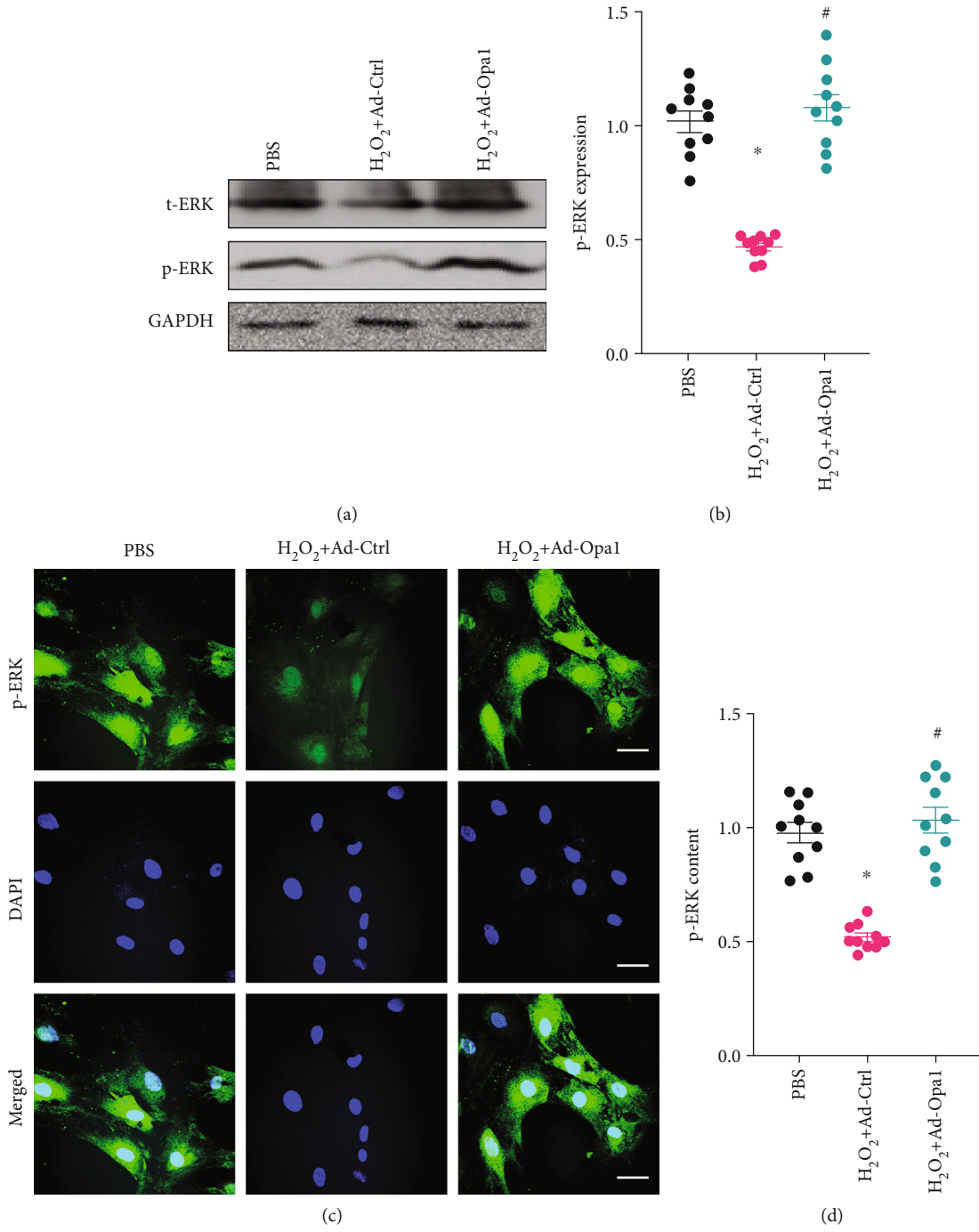


FIGURE 5: Continued.

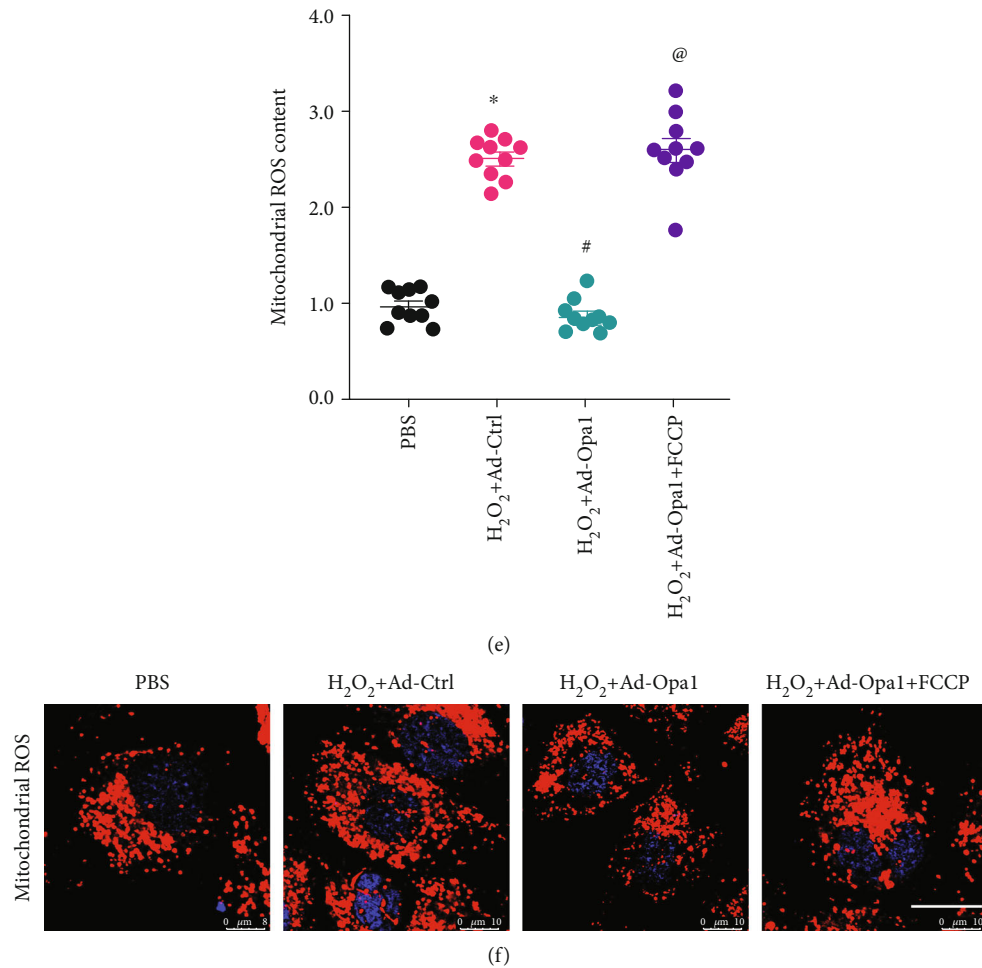


FIGURE 5: Opa1-mediated mitophagy activates the MAPK/ERK signaling pathway. Control (nontransduced) and Ad-Opa1-transduced H9C2 cardiomyocytes were treated with 0.3 mM H₂O₂ for 12 h. (a, b) Western blotting analysis of ERK and p-ERK expression. (c, d) Analysis of ERK and p-ERK expression through immunofluorescence. Bar: 75 μm. (e, f) Fluorescent detection of ROS production in cells pretreated with the MAPK/ERK inhibitor PD98059. Bar: 25 μm. **p* < 0.05 vs. control group, #*p* < 0.05 vs. H₂O₂+Ad-Ctrl group, @*p* < 0.05 vs. H₂O₂+Ad-Opa1 group.

shown in Figures 4(d)–4(g), compared to the control group, the expression of Drp1, Fis1, Mid49, and Mid51 was significantly increased in cardiomyocytes treated with H₂O₂. However, after transduction with Opa1 to stimulate mitophagy, Drp1, Fis1, Mid49, and Mid51 mRNA levels were markedly upregulated. Taken together, these results demonstrated that Opa1-related mitophagy inhibits mitochondrial fission in H₂O₂-treated cardiomyocytes.

To evaluate whether Opa1 represses mitochondrial ROS through inactivation of mitochondrial fission, before being exposed to H₂O₂, Opa1-overexpressing cardiomyocytes were pretreated with FCCP, an activator of mitochondrial fission. As shown in Figures 4(h) and 4(i), FCCP abolished the inhibition of ROS production elicited by Opa1 overexpression. Overall, our data illustrated that Opa1-mediated mitochondrial ROS suppression is attributable to decreased mitochondrial fission.

3.5. Opa1-Mediated Mitophagy Activates the MAPK/ERK Signaling Pathway. Since the MAPK/ERK pathway has been

reported to be a regulator of mitochondrial ROS production, we wanted to know whether Opa1-mediated mitophagy restricts ROS production in cardiomyocytes by activating MAPK/ERK signaling. Western blot results demonstrated that the expression of p-ERK was significantly downregulated in cardiomyocytes treated with H₂O₂, and this effect was inhibited upon Ad-Opa1 transduction (Figures 5(a) and 5(b)). As shown in Figures 5(c) and 5(d), similar results were observed after p-ERK immunofluorescence. Based on the above data suggesting that Opa1-mediated mitophagy is an upstream activator of the MAPK/ERK pathway, the involvement of MAPK/ERK activation in Opa1-mediated mitochondrial ROS suppression was evaluated using PD98059, a MAPK/ERK signaling inhibitor. As shown in Figures 5(e) and 5(f), the inhibition exerted by Opa1 overexpression on H₂O₂-induced mitochondrial ROS production was significantly suppressed after PD98059 incubation. Overall, these data suggest that Opa1-mediated mitophagy attenuates mitochondrial ROS production by activating the MAPK/ERK signaling pathway.

4. Discussion

Although timely reperfusion therapies have been introduced for clinical treatment of myocardial infarction, organ recovery is hampered by cardiomyocyte death resulting from these treatments. Oxidative stress has been identified as a primary pathological factor mediating cardiomyocyte dysfunction and death during myocardial infarction and after reperfusion therapy. Although several antioxidant therapies have been developed for the management of patients with myocardial infarction, the mechanisms that regulate antioxidant responses in the postinfarcted heart remain unclear. In the present study, we identified Opa1-mediated mitophagy as a negative regulator of cardiomyocyte oxidative stress by preventing mitochondrial fission and activating the MAPK/ERK pathway. To our knowledge, this is the first evidence supporting the relationship between Opa1-mediated mitophagy and cardiomyocyte oxidative stress in an *in vitro* model of myocardial infarction. Therefore, our findings suggest a promising new target for the treatment of this condition and the pathological manifestations of ischemia-reperfusion.

Cardiomyocytes contain numerous mitochondria, which metabolize glucose to produce the large amounts of ATP required to sustain cardiac function. Accordingly, mitochondrial damage induces adverse metabolic reprogramming, resulting in cardiomyocyte dysfunction and death [53]. Since mitochondria also play a fundamental role in transmitting and amplifying proapoptotic signals during ischemic insults, these organelles represent a primary target for the treatment of myocardial infarction [54, 55]. Indeed, intensive research has revealed potential therapeutic avenues targeting mitochondrial dysfunction in cardiac cells. For example, thioredoxin has been found to sustain mitochondrial morphology and thus attenuate myocardial infarction through redox-dependent activation of CREB signaling [56]. Improvement in mitochondrial function during myocardial infarction through stabilization of the expression of Mzb1 was reported to attenuate the inflammatory response and delay cardiac fibrosis [57]. Inhibition of mitochondrial ROS production and thus attenuation of oxidative stress has been found to enhance cardiomyocyte ATP supply and sustain contractile function during hypoxia/reoxygenation stress [58–60]. Blockade of mitochondria-mediated cell death through deletion of PGAM5 was shown to improve mitochondrial quality control and reduce myocardial infarction size [61]. In turn, reduction in mitochondrial calcium overload through overexpression of SERCA was reported to improve myocardial perfusion and metabolism [62].

In the present study, mitochondrial damage induced by oxidative stress is featured by decreased mitochondrial membrane potential, increased mitochondrial ROS production, and elevated expression of mitochondria-related proapoptotic proteins. Importantly, we further show that enhanced mitophagy mediated by Opa1 overexpression is able to attenuate mitochondrial damage in oxidative stress-challenged cardiomyocytes. The protective mechanism afforded by Opa1-mediated mitophagy involves inhibition of mitochondrial fission and activation of the MAPK/ERK pathway. The protective role of mitophagy on mitochondrial homeostasis and

cardiomyocyte viability has been widely reported [63–65]. For example, irisin treatment significantly activates Opa1-mediated mitophagy and thus inhibits cardiomyocyte mitochondrial apoptosis following myocardial infarction [66–68]. In turn, activation of Fundc1 leading to mitophagy sustains mitochondrial metabolism and promotes mitochondrial biogenesis in the ischemic myocardium [69, 70]. These findings are thus consistent with our results. Interestingly, our data further illustrate the regulatory role of Opa1-mediated mitophagy in the suppression of mitochondrial fission, by removing fragmented mitochondria via lysosomal degradation.

Finally, we also report that Opa1-mediated mitophagy is an upstream trigger of the MAPK/ERK pathway in cardiomyocytes. This is in line with previous studies, conducted in aged parkinsonian mice [71–73], in a murine model of sleep apnea [74], and in a model of doxorubicin-induced cardiotoxicity [75] that highlighted the relationship between mitophagy and the ERK signaling pathway. Considering the necessary role played by ERK in regulating cardiomyocyte metabolism and ATP generation, mitophagy-induced ERK activation appears as a critical mechanism to support mitochondrial metabolism and oxidative phosphorylation under hypoxic conditions.

Taken together, our results demonstrated that Opa1-mediated mitophagy functions as a protective program against oxidative stress in cardiomyocytes through two different mechanisms: one involved in the inhibition of mitochondrial fission and the other driven by activation of the MAPK/ERK pathway. However, our study has many limitations that need to be addressed. First, we employed only *in vitro* experiments to elucidate the protective effects of Opa1-mediated mitophagy in oxidative stress-challenged cardiomyocytes. Thus, animal experiments are necessary to validate our findings *in vivo* [76]. Also, although our study stresses the functional importance of Opa1-mediated mitophagy in cardiomyocyte survival and function, further research on its protective mechanisms are limited by the lack of drugs to specifically activate Opa1 in cardiomyocytes [77].

Data Availability

The analyzed data sets generated during the present study are available from the corresponding author on reasonable request.

Conflicts of Interest

The authors declare that they have no conflicts of interests.

Authors' Contributions

Conceptualization and methodology were handled by Yue Wang and Zhihua Han; formal analysis and data curation were handled by Yue Wang and Zuojun Xu; validation and investigation were handled by Yue Wang; and original draft preparation, review, and editing were handled by Junfeng Zhang and Yue Wang. All authors read and approved the final manuscript before submission.

Acknowledgments

This study is supported by the NSFC (No. 81970289) and Shanghai Natural Science Foundation General Project (No. 12ZR141740).

References

- [1] A. Daiber, I. Andreadou, M. Oelze, S. M. Davidson, and D. J. Hausenloy, "Discovery of new therapeutic redox targets for cardioprotection against ischemia/reperfusion injury and heart failure," *Free Radical Biology & Medicine*, vol. 163, pp. 325–343, 2021.
- [2] J. Wang, Z. Xue, C. Hua et al., "Metabolomic analysis of the ameliorative effect of enhanced proline metabolism on hypoxia-induced injury in cardiomyocytes," *Oxidative Medicine and Cellular Longevity*, vol. 2020, Article ID 8866946, 15 pages, 2020.
- [3] L. Hauck, K. Dadson, S. Chauhan, D. Grothe, and F. Billia, "Inhibiting the Pkm2/b-catenin axis drives in vivo replication of adult cardiomyocytes following experimental MI," *Cell Death and Differentiation*, vol. 28, no. 4, pp. 1398–1417, 2021.
- [4] J. Wang and H. Zhou, "Mitochondrial quality control mechanisms as molecular targets in cardiac ischemia-reperfusion injury," *Acta Pharmaceutica Sinica B*, vol. 10, no. 10, pp. 1866–1879, 2020.
- [5] H. Zhou and S. Toan, "Pathological roles of mitochondrial oxidative stress and mitochondrial dynamics in cardiac microvascular ischemia/reperfusion injury," *Biomolecules*, vol. 10, no. 1, p. 85, 2020.
- [6] J. Wang, S. Toan, and H. Zhou, "Mitochondrial quality control in cardiac microvascular ischemia-reperfusion injury: new insights into the mechanisms and therapeutic potentials," *Pharmacological Research*, vol. 156, article 104771, 2020.
- [7] G. Heusch, "Coronary microvascular obstruction: the new frontier in cardioprotection," *Basic Research in Cardiology*, vol. 114, no. 6, p. 45, 2019.
- [8] H. Zhou, Y. Zhang, S. Hu et al., "Melatonin protects cardiac microvasculature against ischemia/reperfusion injury via suppression of mitochondrial fission-VDAC1-HK2-mPTP-mitophagy axis," *Journal of Pineal Research*, vol. 63, no. 1, article e12413, 2017.
- [9] H. Zhou, S. Wang, P. Zhu, S. Hu, Y. Chen, and J. Ren, "Empagliflozin rescues diabetic myocardial microvascular injury via AMPK-mediated inhibition of mitochondrial fission," *Redox Biology*, vol. 15, pp. 335–346, 2018.
- [10] E. Dubois-Deruy, V. Peugnet, A. Turkieh, and F. Pinet, "Oxidative stress in cardiovascular diseases," *Antioxidants (Basel)*, vol. 9, no. 9, p. 864, 2020.
- [11] T. L. Capasso, B. Li, H. J. Volek et al., "BMP10-mediated ALK1 signaling is continuously required for vascular development and maintenance," *Angiogenesis*, vol. 23, no. 2, pp. 203–220, 2020.
- [12] B. Kalyanaraman, "Teaching the basics of repurposing mitochondria-targeted drugs: from Parkinson's disease to cancer and back to Parkinson's disease," *Redox Biology*, vol. 36, article 101665, 2020.
- [13] P. Rojas-Morales, J. Pedraza-Chaverri, and E. Tapia, "Ketone bodies, stress response, and redox homeostasis," *Redox Biology*, vol. 29, article 101395, 2020.
- [14] A. Rout, U. S. Tantry, M. Novakovic, A. Sukhi, and P. A. Gurbel, "Targeted pharmacotherapy for ischemia reperfusion injury in acute myocardial infarction," *Expert Opinion on Pharmacotherapy*, vol. 21, no. 15, pp. 1851–1865, 2020.
- [15] C. J. A. Ramachandra, S. Hernandez-Resendiz, G. E. Crespo-Avilan, Y. H. Lin, and D. J. Hausenloy, "Mitochondria in acute myocardial infarction and cardioprotection," *eBioMedicine*, vol. 57, article 102884, 2020.
- [16] J. Chen, F. L. Lin, J. Y. K. Leung et al., "A drug-tunable Flt23k gene therapy for controlled intervention in retinal neovascularization," *Angiogenesis*, vol. 24, no. 1, article 9745, pp. 97–110, 2021.
- [17] M. J. Boyer and S. Eguchi, "A cytoskeletal anchor connects ischemic mitochondrial fission to myocardial senescence," *Science Signaling*, vol. 11, no. 556, p. eaav3267, 2018.
- [18] I. Cuijpers, S. J. Simmonds, M. van Bilsen et al., "Microvascular and lymphatic dysfunction in HFpEF and its associated comorbidities," *Basic Research in Cardiology*, vol. 115, no. 4, p. 39, 2020.
- [19] Y. Zhang, Y. Wang, J. Xu et al., "Melatonin attenuates myocardial ischemia-reperfusion injury via improving mitochondrial fusion/mitophagy and activating the AMPK-OPA1 signaling pathways," *Journal of pineal research*, vol. 66, no. 2, article e12542, 2019.
- [20] J. Wang, P. Zhu, R. Li, J. Ren, and H. Zhou, "Fundc1-dependent mitophagy is obligatory to ischemic preconditioning-conferred renoprotection in ischemic AKI via suppression of Drp1-mediated mitochondrial fission," *Redox Biology*, vol. 30, article 101415, 2020.
- [21] H. Zhou, S. Toan, P. Zhu, J. Wang, J. Ren, and Y. Zhang, "DNA-PKcs promotes cardiac ischemia reperfusion injury through mitigating BI-1-governed mitochondrial homeostasis," *Basic Research in Cardiology*, vol. 115, no. 2, p. 11, 2020.
- [22] D. V. C. de Jel, F. J. M. Disch, S. Kroon, J. J. Mager, and F. J. Verdam, "Intranasal Efundix reduces epistaxis in hereditary hemorrhagic telangiectasia," *Angiogenesis*, vol. 23, no. 3, pp. 271–274, 2020.
- [23] M. M. Vaeyens, A. Jorge-Peñas, J. Barrasa-Fano et al., "Matrix deformations around angiogenic sprouts correlate to sprout dynamics and suggest pulling activity," *Angiogenesis*, vol. 23, no. 3, pp. 315–324, 2020.
- [24] H. Zhou, J. Wang, S. Hu, H. Zhu, S. Toan, and J. Ren, "BI1 alleviates cardiac microvascular ischemia-reperfusion injury via modifying mitochondrial fission and inhibiting XO/ROS/F-actin pathways," *Journal of Cellular Physiology*, vol. 234, no. 4, pp. 5056–5069, 2019.
- [25] J. Wang, S. Toan, and H. Zhou, "New insights into the role of mitochondria in cardiac microvascular ischemia/reperfusion injury," *Angiogenesis*, vol. 23, no. 3, pp. 299–314, 2020.
- [26] H. Zhou, S. Hu, Q. Jin et al., "Mff-dependent mitochondrial fission contributes to the pathogenesis of cardiac microvasculature ischemia/reperfusion injury via induction of mROS-mediated cardiolipin oxidation and HK2/VDAC1 disassociation-involved mPTP opening," *Journal of the American Heart Association*, vol. 6, no. 3, 2017.
- [27] X. Liang, S. Wang, L. Wang, A. Ceylan, J. Ren, and Y. Zhang, "Mitophagy inhibitor liensinine suppresses doxorubicin-induced cardiotoxicity through inhibition of Drp1-mediated maladaptive mitochondrial fission," *Pharmacological Research*, vol. 157, article 104846, 2020.

- [28] J. Zhang, X. Wang, V. Vikash et al., "ROS and ROS-mediated cellular signaling," *Oxidative medicine and cellular longevity*, vol. 2016, Article ID 4350965, 18 pages, 2016.
- [29] L. Du, J. Wang, Y. Chen et al., "Novel biphenyl diester derivative AB-38b inhibits NLRP3 inflammasome through Nrf2 activation in diabetic nephropathy," *Cell Biology and Toxicology*, vol. 36, no. 3, pp. 243–260, 2020.
- [30] S. A. Watson, A. Dendorfer, T. Thum, and F. Perbellini, "A practical guide for investigating cardiac physiology using living myocardial slices," *Basic Research in Cardiology*, vol. 115, no. 6, p. 61, 2020.
- [31] F. Cao, M. L. Maguire, D. J. McAndrew et al., "Overexpression of mitochondrial creatine kinase preserves cardiac energetics without ameliorating murine chronic heart failure," *Basic Research in Cardiology*, vol. 115, no. 2, p. 12, 2020.
- [32] R. K. Adapala, A. K. Kanugula, S. Paruchuri, W. M. Chilian, and C. K. Thodeti, "TRPV4 deletion protects heart from myocardial infarction-induced adverse remodeling via modulation of cardiac fibroblast differentiation," *Basic Research in Cardiology*, vol. 115, no. 2, p. 14, 2020.
- [33] J. Bai, M. Khajavi, L. Sui et al., "Angiogenic responses in a 3D micro-engineered environment of primary endothelial cells and pericytes," *Angiogenesis*, vol. 24, no. 1, pp. 111–127, 2021.
- [34] D. Bausch, S. Fritz, L. Bolm et al., "Hedgehog signaling promotes angiogenesis directly and indirectly in pancreatic cancer," *Angiogenesis*, vol. 23, no. 3, pp. 479–492, 2020.
- [35] Z. Wang, Y. L. Lu, W. T. Zhao et al., "Distinct origins and functions of cardiac orthotopic macrophages," *Basic Research in Cardiology*, vol. 115, no. 2, p. 8, 2020.
- [36] J. Wang, S. Toan, R. Li, and H. Zhou, "Melatonin fine-tunes intracellular calcium signals and eliminates myocardial damage through the IP3R/MCU pathways in cardiorenal syndrome type 3," *Biochemical Pharmacology*, vol. 174, article 113832, 2020.
- [37] M. M. Bekhite, A. González Delgado, F. Menz et al., "Longitudinal metabolic profiling of cardiomyocytes derived from human-induced pluripotent stem cells," *Basic Research in Cardiology*, vol. 115, no. 4, p. 37, 2020.
- [38] A. L. Bayliss, A. Sundararaman, C. Granet, and H. Mellor, "Raftlin is recruited by neuropilin-1 to the activated VEGFR2 complex to control proangiogenic signaling," *Angiogenesis*, vol. 23, no. 3, pp. 371–383, 2020.
- [39] J. Wang, Z. Chen, Q. Dai et al., "Intravenously delivered mesenchymal stem cells prevent microvascular obstruction formation after myocardial ischemia/reperfusion injury," *Basic Research in Cardiology*, vol. 115, no. 4, p. 40, 2020.
- [40] J. Wang, P. Zhu, S. Toan, R. Li, J. Ren, and H. Zhou, "Pum2-Mff axis fine-tunes mitochondrial quality control in acute ischemic kidney injury," *Cell Biology and Toxicology*, vol. 36, no. 4, pp. 365–378, 2020.
- [41] M. R. Detter, R. Shenkar, C. R. Benavides et al., "Novel murine models of cerebral cavernous malformations," *Angiogenesis*, vol. 23, no. 4, article 9736, pp. 651–666, 2020.
- [42] F. Dei Zotti, R. Verdoy, D. Brusa, I. I. Lobysheva, and J. L. Balligand, "Redox regulation of nitrosyl-hemoglobin in human erythrocytes," *Redox biology*, vol. 34, article 101399, 2020.
- [43] B. Behrouzi, J. J. Weyers, X. Qi et al., "Action of iron chelator on intramyocardial hemorrhage and cardiac remodeling following acute myocardial infarction," *Basic Research in Cardiology*, vol. 115, no. 3, p. 24, 2020.
- [44] E. Bridges, H. Sheldon, E. Kleibeuker et al., "RHOQ is induced by DLL4 and regulates angiogenesis by determining the intracellular route of the notch intracellular domain," *Angiogenesis*, vol. 23, no. 3, pp. 493–513, 2020.
- [45] M. Wagner, E. Bertero, A. Nickel et al., "Selective NADH communication from α -ketoglutarate dehydrogenase to mitochondrial transhydrogenase prevents reactive oxygen species formation under reducing conditions in the heart," *Basic Research in Cardiology*, vol. 115, no. 5, p. 53, 2020.
- [46] Q. Guo, T. Wang, Y. Yang et al., "Transcriptional factor Yin Yang 1 promotes the stemness of breast cancer cells by suppressing miR-873-5p transcriptional activity," *Molecular Therapy-Nucleic Acids*, vol. 21, pp. 527–541, 2020.
- [47] D. Lee, D. W. Kim, and J. Y. Cho, "Role of growth factors in hematopoietic stem cell niche," *Cell Biology and Toxicology*, vol. 36, no. 2, pp. 131–144, 2020.
- [48] M. Burtscher, "A breath of fresh air for mitochondria in exercise physiology," *Acta Physiologica*, vol. 229, no. 3, article e13490, 2020.
- [49] M. Heimerl, I. Sieve, M. Ricke-Hoch et al., "Neuraminidase-1 promotes heart failure after ischemia/reperfusion injury by affecting cardiomyocytes and invading monocytes/macrophages," *Basic Research in Cardiology*, vol. 115, no. 6, p. 62, 2020.
- [50] P. Fournier, C. Viillard, A. Dejda, P. Sapiéha, B. Larrivée, and I. Royal, "The protein tyrosine phosphatase PTPRJ/DEP-1 contributes to the regulation of the notch-signaling pathway and sprouting angiogenesis," *Angiogenesis*, vol. 23, no. 2, pp. 145–157, 2020.
- [51] D. B. Buglak, E. J. Kushner, A. P. Marvin, K. L. Davis, and V. L. Bautch, "Excess centrosomes disrupt vascular lumenization and endothelial cell adherens junctions," *Angiogenesis*, vol. 23, no. 4, article 9737, pp. 567–575, 2020.
- [52] O. Bakhta, A. Pascaud, X. Dieu et al., "Tryptophane-kynurenine pathway in the remote ischemic conditioning mechanism," *Basic research in cardiology*, vol. 115, no. 2, p. 13, 2020.
- [53] E. D. Luczak, Y. Wu, J. M. Granger et al., "Mitochondrial CaMKII causes adverse metabolic reprogramming and dilated cardiomyopathy," *Nature Communications*, vol. 11, no. 1, p. 4416, 2020.
- [54] H. Zhu, S. Toan, D. Mui, and H. Zhou, "Mitochondrial quality surveillance as a therapeutic target in myocardial infarction," *Acta Physiologica*, vol. 231, no. 3, article e13590, 2021.
- [55] H. Zhou, J. Ren, S. Toan, and D. Mui, "Role of mitochondrial quality surveillance in myocardial infarction: from bench to bedside," *Ageing Research Reviews*, vol. 66, article 101250, 2021.
- [56] J. Subramani, V. Kundumani-Sridharan, and K. C. Das, "Thioredoxin protects mitochondrial structure, function and biogenesis in myocardial ischemia-reperfusion via redox-dependent activation of AKT-CREB-PGC1 α pathway in aged mice," *Ageing (Albany NY)*, vol. 12, no. 19, article 104071, pp. 19809–19827, 2020.
- [57] L. Zhang, Y. N. Wang, J. M. Ju et al., "Mzb1 protects against myocardial infarction injury in mice via modulating mitochondrial function and alleviating inflammation," *Acta Pharmacologica Sinica*, vol. 42, no. 5, pp. 691–700, 2021.
- [58] Q. Jin, Y. Jiang, L. Fu, Y. Zheng, Y. Ding, and Q. Liu, "Wenxin granule ameliorates hypoxia/reoxygenation-induced oxidative stress in mitochondria via the PKC- δ /NOX2/ROS pathway in H9c2 cells," *Oxidative Medicine and Cellular Longevity*, vol. 2020, Article ID 3245483, 16 pages, 2020.

- [59] A. Wincewicz and P. Woltanowski, "Leopold Auerbach's achievements in the field of vascular system," Tech. Rep. 4, Article ID 3245483, *Angiogenesis*, 2020.
- [60] A. K. Vlacil, J. Schuett, V. Ruppert et al., "Deficiency of nucleotide-binding oligomerization domain-containing proteins (NOD) 1 and 2 reduces atherosclerosis," *Basic Research in Cardiology*, vol. 115, no. 4, p. 47, 2020.
- [61] H. Zhu, Y. Tan, W. Du et al., "Phosphoglycerate mutase 5 exacerbates cardiac ischemia-reperfusion injury through disrupting mitochondrial quality control," *Redox Biology*, vol. 38, article 101777, 2021.
- [62] Y. Tan, D. Mui, S. Toan, P. Zhu, R. Li, and H. Zhou, "SERCA overexpression improves mitochondrial quality control and attenuates cardiac microvascular ischemia-reperfusion injury," *Molecular Therapy-Nucleic Acids*, vol. 22, pp. 696–707, 2020.
- [63] F. Cecconi, "Autophagy, replication stress and DNA synthesis, an intricate relationship," *Cell Death and Differentiation*, vol. 27, no. 2, pp. 829–830, 2020.
- [64] E. M. Mills, V. L. Barlow, L. Y. P. Luk, and Y. H. Tsai, "Applying switchable Cas9 variants to in vivo gene editing for therapeutic applications," *Cell Biology and Toxicology*, vol. 36, no. 1, pp. 17–29, 2020.
- [65] M. Ding, C. Liu, R. Shi et al., "Mitochondrial fusion promoter restores mitochondrial dynamics balance and ameliorates diabetic cardiomyopathy in an optic atrophy 1-dependent way," *Acta Physiologica*, vol. 229, no. 1, article e13428, 2020.
- [66] T. Xin and C. Lu, "Irisin activates Opa1-induced mitophagy to protect cardiomyocytes against apoptosis following myocardial infarction," *Aging (Albany NY)*, vol. 12, no. 5, article 102899, pp. 4474–4488, 2020.
- [67] P. Villacampa, S. E. Liyanage, I. P. Klaska et al., "Stabilization of myeloid-derived HIFs promotes vascular regeneration in retinal ischemia," *Angiogenesis*, vol. 23, no. 2, pp. 83–90, 2020.
- [68] D. E. Vatner, M. Oydanich, J. Zhang, D. Babici, and S. F. Vatner, "Secreted frizzled-related protein 2, a novel mechanism to induce myocardial ischemic protection through angiogenesis," *Basic Research in Cardiology*, vol. 115, no. 4, p. 48, 2020.
- [69] H. Zhou, P. Zhu, J. Wang, H. Zhu, J. Ren, and Y. Chen, "Pathogenesis of cardiac ischemia reperfusion injury is associated with CK2 α -disturbed mitochondrial homeostasis via suppression of FUNDC1-related mitophagy," *Cell Death and Differentiation*, vol. 25, no. 6, pp. 1080–1093, 2018.
- [70] E. A. Allen and E. H. Baehrecke, "Autophagy in animal development," *Cell Death and Differentiation*, vol. 27, no. 3, pp. 903–918, 2020.
- [71] H. Liu, P. W. Ho, C. T. Leung et al., "Aberrant mitochondrial morphology and function associated with impaired mitophagy and DNMI1L-MAPK/ERK signaling are found in aged mutant Parkinsonian LRRK2R1441Gmice," *Autophagy*, vol. 18, pp. 1–25, 2020.
- [72] J. Cao, X. Liu, Y. Yang et al., "Decylubiquinone suppresses breast cancer growth and metastasis by inhibiting angiogenesis via the ROS/p53/ BAI1 signaling pathway," *Angiogenesis*, vol. 23, no. 3, pp. 325–338, 2020.
- [73] C. Veith, D. Neghabian, H. Luitel et al., "FHL-1 is not involved in pressure overload-induced maladaptive right ventricular remodeling and dysfunction," *Basic Research in Cardiology*, vol. 115, no. 2, p. 17, 2020.
- [74] L. J. Gong, X. Y. Wang, W. Y. Gu, and X. Wu, "Pinocembrin ameliorates intermittent hypoxia-induced neuroinflammation through BNIP3-dependent mitophagy in a murine model of sleep apnea," *Journal of Neuroinflammation*, vol. 17, no. 1, p. 337, 2020.
- [75] P. Kleinbongard, "Cardioprotection by early metoprolol-attenuation of ischemic vs. reperfusion injury," *Basic Research in Cardiology*, vol. 115, no. 5, p. 54, 2020.
- [76] M. V. Panajatovic, F. Singh, N. J. Roos et al., "PGC-1 α plays a pivotal role in simvastatin-induced exercise impairment in mice," *Acta Physiologica*, vol. 228, no. 4, article e13402, 2020.
- [77] B. Portal, S. Delcourte, R. Rovera et al., "Genetic and pharmacological inactivation of astroglial connexin 43 differentially influences the acute response of antidepressant and anxiolytic drugs," *Acta Physiologica*, vol. 229, no. 1, article e13440, 2020.

Research Article

BTK Promotes Atherosclerosis by Regulating Oxidative Stress, Mitochondrial Injury, and ER Stress of Macrophages

Junxiong Qiu ¹, Yuan Fu,¹ Zhiteng Chen,² Lisui Zhang,¹ Ling Li,¹ Diefei Liang,³ Feng Wei,¹ Zhuzhi Wen ², Yajing Wang ⁴, and Shi Liang ¹

¹Department of Cardiovascular Surgery, Sun Yat-sen Memorial Hospital, Sun Yat-sen University, Guangzhou, China 510120

²Department of Cardiology, Sun Yat-sen Memorial Hospital, Sun Yat-sen University, Guangzhou, China 510120

³Department of Endocrinology, Sun Yat-sen Memorial Hospital, Sun Yat-sen University, Guangzhou, China 510120

⁴Department of Otorhinolaryngology-Head and Neck Surgery, Sun Yat-sen Memorial Hospital, Sun Yat-sen University, Guangzhou, China 510120

Correspondence should be addressed to Zhuzhi Wen; wenzhzh5@mail.sysu.edu.cn, Yajing Wang; wangyj95@mail.sysu.edu.cn, and Shi Liang; md02ls@mail2.sysu.edu.cn

Received 27 March 2021; Revised 15 April 2021; Accepted 3 May 2021; Published 27 May 2021

Academic Editor: Yun-dai Chen

Copyright © 2021 Junxiong Qiu et al. This is an open access article distributed under the Creative Commons Attribution License, which permits unrestricted use, distribution, and reproduction in any medium, provided the original work is properly cited.

Atherosclerosis (AS) is a chronic metabolic disease in arterial walls, characterized by lipid deposition and persistent aseptic inflammation. AS is regarded as the basis of a variety of cardiovascular and cerebrovascular diseases. It is widely acknowledged that macrophages would become foam cells after internalizing lipoprotein particles, which is an initial factor in atherogenesis. Here, we showed the influences of Bruton's tyrosine kinase (BTK) in macrophage-mediated AS and how BTK regulates the inflammatory responses of macrophages in AS. Our bioinformatic results suggested that BTK was a potential hub gene, which is closely related to oxidative stress, ER stress, and inflammation in macrophage-induced AS. Moreover, we found that BTK knockdown could restrain ox-LDL-induced NK- κ B signaling activation in macrophages and repressed M1 polarization. The mechanistic studies revealed that oxidative stress, mitochondrial injury, and ER stress in macrophages were also suppressed by BTK knockdown. Furthermore, we found that sh-BTK adenovirus injection could alleviate the severity of AS in ApoE^{-/-} mice induced by a high-fat diet in vivo. Our study suggested that BTK promoted ox-LDL-induced ER stress, oxidative stress, and inflammatory responses in macrophages, and it may be a potential therapeutic target in AS.

1. Introduction

AS, which underlies myocardial infarction, vascular occlusive disease, and stroke, is a chronic metabolic disease in arterial walls, characterized by lipid deposition and persistent aseptic inflammation [1]. AS is an important component in the pathobiology of many cardiovascular diseases, involving vascular endothelial activation, monocyte recruitment, and cholesterol accumulation in macrophages [2]. It is widely recognized that macrophages, which would become foam cells after internalizing lipoprotein particles, play an important role in atherogenesis [3–5]. Oxidative low-density lipoprotein (ox-LDL) is contributing to atherogenesis, foam cell formation, and AS progression [6]. M1 macrophages, with the low ability to clear cholesterol and high susceptibility to

become foam cells, are involved in the initial progression of AS by producing a variety of proinflammatory factors, as well as associated with endoplasmic reticulum stress (ER stress) and mitochondrial stress [7–9]. Excessive reactive oxygen species (ROS), produced by ER, mitochondria, and other organelles, participated not only in the initial development of atherogenesis but also in many cardiovascular diseases [10]. Mitochondria-associated membranes (MAMs) are a molecule dynamic platform that is tightly associated with ER and mitochondria, and MAMs regulated multiple signaling pathways, especially inflammatory pathways, which may have an impact on the responses of macrophages [11]. In the meantime, M2 macrophages, with anti-inflammatory factor secretion and high phagocytic ability, would subsequently shift to the M1 type at the advanced stage of AS [12, 13].

BTK is a member of the Tec family in nonreceptor tyrosine kinases that regulate innumerable processes, such as cell development, proliferation, differentiation, innate immunity, and adaptive immunity [14]. Given its established roles in immune B cell inflammation, some studies reported that BTK is a drug target for B cell malignancies and autoimmune disorders [15, 16]. Functionally, BTK is considered to activate the NF- κ B signaling pathway by phosphorylating I κ B α protein, a main repressor of NF- κ B, as well as promoting the nuclear translocation of p65, and some researchers found that suppressing BTK would block the B cell receptor-dependent NF- κ B signaling pathway [17, 18]. NF- κ B signaling is regarded as a significant pathway related to inflammation in atherosclerotic plaque formation, and the genes that target the NF- κ B signaling pathway may provide an antiatherogenic profile [19]. Accumulating evidence revealed that BTK inhibition could make sense on tumor metastasis and infection by regulating macrophage polarization, phagocytosis, and proinflammatory factor secretion, which suggested a viable therapeutic opportunity in inflammatory diseases, such as AS [20–23]. Importantly, it is reported that BTK inhibitors, such as acalabrutinib and ONO/GS-4059, made a difference in AS treatment as antiplatelet drugs to inhibit platelet aggregation in atherosclerotic plaques [24]. However, the role of BTK in macrophages on the progression of AS has not been elucidated, and further elucidation of the correlation between BTK and macrophages in atherogenesis is expected.

Here, we elucidated that BTK knockdown restrained ox-LDL-induced NF- κ B signaling in macrophages and repressed the M1 polarization but promoted the M2 polarization of macrophages. Moreover, we discovered that oxidative stress, mitochondrial injury, and ER stress in ox-LDL-stimulated macrophages were also regulated after inhibiting BTK. A well-established diet-induced mouse model that mimics human atherogenesis is recognized as a critical methodology to understand the function and mechanism of potential targets in human AS [25]. Therefore, we elucidated that the severity of AS in ApoE^{-/-} mice induced by a high-fat diet was alleviated by the sh-BTK adenovirus injection, suggesting that BTK may represent a potential therapeutic target to combat AS.

2. Materials and Methods

2.1. Clinical Samples. We collected the clinical specimens from 8 females and 7 males, with an average age of 54.6 ± 9.7 years, who accepted coronary bypass surgery from 2018 to 2020. The coronary arteries with AS plaques and the internal mammary arteries were gathered. The study was approved by the Ethical Committee of Sun Yat-sen University, Sun Yat-sen Memorial Hospital (SYSEC-KY-KS2020-090).

2.2. Cell Line. RAW264.7 macrophages (CL-0190, Procell), which were maintained at 37°C in a humidified 5% CO₂ incubator, grew in high-glucose DMEM, with 10% fetal bovine serum and penicillin (100 U/ml)-streptomycin (0.1 mg/ml). Twenty-four hours before further experiments, the cells would be seeded in culture dishes or 6-well plates [26, 27].

2.3. Small Interfering RNA (siRNA) and Treatment. The siRNA was designed and synthesized by RiboBio, China. Macrophages were seeded at a concentration of 5×10^5 cells per well in 6-well plates. After 24 hours, macrophages were added with BTK-siRNA with the RNAiMAX reagent (13778075, Thermo Fisher Scientific). The transfected macrophages were collected after 48 hours. The ox-LDL (Cat. No. YB-002, Yiyuan Biotech) was used at a concentration of 50 μ g/ml as previously described [28, 29].

2.4. PPI Network Establishment and Hub Gene Identification. The raw CEL data of the GSE70126 dataset was downloaded from the GEO database of NCBI. And the bioinformatic analysis was performed essentially as described by Qiu et al. [30]. Briefly, STRING and Cytoscape software programs were used to construct the protein-protein interaction (PPI) network and screen differentially expressed genes. MCODE and cytoHubba applications of Cytoscape, as well as the Metascape online tool, were applied (<https://metascape.org>) [31, 32].

2.5. qRT-PCR. Total RNA was isolated from RAW264.7 macrophages using RNAiso Plus (TaKaRa) [33, 34]. RNA was converted into cDNA using PrimeScript RT Mix (TaKaRa). Afterward, qRT-PCR experiments were conducted in a LightCycler PCR system (Roche) with UNICONTM SYBR Green (11198ES08, Yeasen). The sequences of all the primers used are shown in Table 1.

2.6. Western Blot and ELISA. The experiments of Western blot and ELISA were performed essentially as described in Li et al. [35]. Shortly, RAW264.7 macrophages were lysed with the RIPA buffer to obtain total protein, additionally with a nuclear and cytoplasmic extraction kit (CWbiotech) according to the manufacturer's protocol. Proteins were quantified with a bicinchoninic acid (BCA) assay kit (Thermo Fisher Scientific) and analyzed by SDS-PAGE with 10% polyacrylamide gel. The primary antibodies of NRF2, histone H3, p-PERK, p-IRE1, BTK, p-p65, p-IRF3, DRP1, FIS1, and β -actin (Cell Signaling Technology) were used. An enhanced chemiluminescence (ECL) reagent detection kit (Thermo Fisher Scientific) was used, and an imaging machine (2200 Pro, Kodak) was employed to detect the protein bands. For ELISA, the supernatants of RAW264.7 macrophages were collected to detect the concentration of TNF- α and IL-6 (Neobioscience, China) [36, 37].

2.7. Flow Cytometry and ROS Detection. M1 and M2 macrophage polarization was detected by their makers, iNOS and COX-2, respectively. In brief, the macrophages with different treatments were incubated with the iNOS antibody or COX-2 antibody for 20 min. Then, the cells were trypsinized, washed with PBS, and resuspended in PBS. A DHE-DA staining kit (KGAF019, KeyGen Biotech) was used for analyzing the production of ROS as described before [38, 39]. Flow cytometry (BD FACSVerser) was applied to detect M1 polarization, M2 polarization, and ROS production [40, 41].

2.8. MitoTracker Staining. The macrophages were stained with MitoTracker Red (Beyotime) for the analysis of change

TABLE 1: Primers.

BTK	Forward	GAGGAGAGGTGAGGAGTCTAGT
	Reverse	AGCTCTTCAGTTGGGGAGAAAA
iNOS	Forward	GGAGTGACGGCAAACATGACT
	Reverse	TCGATGCACAACTGGGTGAAC
COX-2	Forward	TGCACTATGGTTACAAAAGCTGG
	Reverse	TCAGGAAGCTCCTTATTTCCCTT
GAPDH	Forward	TGTGTCCGTCGTGGATCTGA
	Reverse	TTGCTGTTGAAGTCGCAGGAG

in mitochondrial injury. Macrophages were cultured in 96-well plates and incubated for 30 minutes with MitoTracker Red. Then, the macrophages were counterstained with DAPI for 10 min and visualized by fluorescence microscopy (LSM 710, Carl Zeiss) [42, 43].

2.9. Immunofluorescent Staining and Confocal Microscopy. The experiments of immunofluorescent staining and confocal microscopy were performed essentially as described in Fang et al. [44]. Shortly, macrophages were seeded in confocal dishes fixed with 4% paraformaldehyde after different treatments. After being blocked by goat serum, RAW264.7 macrophages were incubated with different primary antibodies (p65, ATF6, TNF- α , and IL-6; Cell Signaling Technology) overnight at 4°C. A secondary antibody (goat anti-rabbit, Abcam) and a DAPI-containing Anti-Fade Fluorescence Mounting Medium (HelixGen Co., Ltd.) were used for visualization with confocal microscopy (Carl Zeiss) [45].

2.10. Immunohistochemistry Assay. The sections of the mouse hearts with aortic roots were heated for 2 h, then dewaxed with xylene and dehydrated with ethanol. An H&E staining kit (AR1180, Boster Biological Technology Co., Ltd.) was used, as described by Qiu et al. [30]. For the observation of the sections of mouse aortic roots, a Leica biomicroscope was employed [46].

2.11. Mouse Atherosclerosis Model Establishment. The mouse AS model was established as described in our previous study [28]. Briefly, ApoE^{-/-} mice (males, 8 weeks old, and 20 g body weight) with C57BL/6J background were purchased from GemPharmatech Co., Ltd. All mice were reared in a specific pathogen-free environment with a 12 h light/12 h dark cycle at the temperature of 22 ± 2°C and the relative humidity of 40–55%. ApoE^{-/-} mice were fed a diet containing 21% wt/wt saturated fat and 0.2% wt/wt cholesterol (Western diet) for 12 weeks for the establishment of the AS model. Recombinant adenovirus for the mouse *Btk* interference (sh-BTK adenovirus), alone with sh-NC adenovirus as the control, was synthesized by GeneChem Co., Ltd. The Western diet-fed mice have been applied with a tail vein injection of adenovirus. All the animal procedures were approved by the Laboratory Animal Welfare and Ethics Committee of Sun Yat-sen University.

2.12. Atherosclerotic Lesion Analysis. Mice were anesthetized, and the mouse hearts with aortic roots as well as whole aortas

were harvested. For inner face plaque analyses, the whole aortas without adipose tissue, fixed in 4% paraformaldehyde overnight, were stained with Oil Red O solution for 15 min and washed with 70% ethanol. For aortic root cross-section analysis, the mouse hearts with aortic roots were embedded and sliced into several sections, followed by staining with Oil Red O solution as described in our previous study [28]. Images were viewed by a biomicroscope (DM200, Leica) [47, 48]. The percentage of Oil Red O-positive areas, presumed to be atherosclerotic lesions, was quantified by ImageJ software.

2.13. Statistical Analysis. Three independent experiments were carried out. Data were analyzed to verify data normality using Kolmogorov-Smirnov tests and are expressed as mean ± standard deviation (SD). A two-sided Student's *t*-test was performed between two groups. And one-way analysis of variance (ANOVA) and Fisher's least significant difference (LSD) test were utilized among three or more than three groups. The threshold of statistical significance was a *P* value of <0.05.

3. Results

3.1. Oxidative Stress, Mitochondrial Injury, and ER Stress Were Triggered by ox-LDL in Macrophages. To investigate the underlying mechanism by which ox-LDL accelerates AS, we stimulated macrophages with ox-LDL for different periods. We then found that the number of ROS-positive macrophages significantly increased after ox-LDL treatment for 24 h (Figures 1(a) and 1(b)). Furthermore, the nucleus protein level of NRF2 in macrophages increased after 4 h and 8 h of stimulation for ox-LDL (Figure 1(c)). Concurrently, the mitochondria-specific fluorescence probe (MitoTracker Red) was used, and the result showed that ox-LDL induced the structural disorder of mitochondria in macrophages, suggesting an obvious mitochondrial injury (Figure 1(d)). As for ER stress, we found that ox-LDL could induce the phosphorylation of PERK and IRE1 (Figure 1(e)). Moreover, our fluorescent staining results showed that ATF6 protein (green) translocated into the nucleus after ox-LDL treatment in macrophages (Figure 1(f)). The activation of these 3 unfolded protein response (UPR) activator proteins indicated that ox-LDL triggered ER stress in macrophages.

3.2. BTK Was the Hub Gene Related to Oxidative Stress, ER Stress, and Inflammation in Macrophage-Induced AS. To assess the potential hub genes in atherosclerosis induced by macrophages, the differentially expressed genes (DEGs) from the GSE70126 dataset were obtained. We found 1125 differentially expressed genes in foam cell macrophages, as compared with nonfoamy macrophages: 592 were upregulated, and 533 were downregulated. The volcano plot (Figure 2(a)) and the heat map (Figure 2(b)) were shown, respectively. STRING and Cytoscape software programs were used to construct the PPI network, and we obtained 19 hub genes through the MCODE application, of which BTK had a high score (Figure 2(c)). Besides, by using the cytoHubba application, we built the hub gene network following core gene scores (Figure 2(d)). Furthermore, the functional clustering network

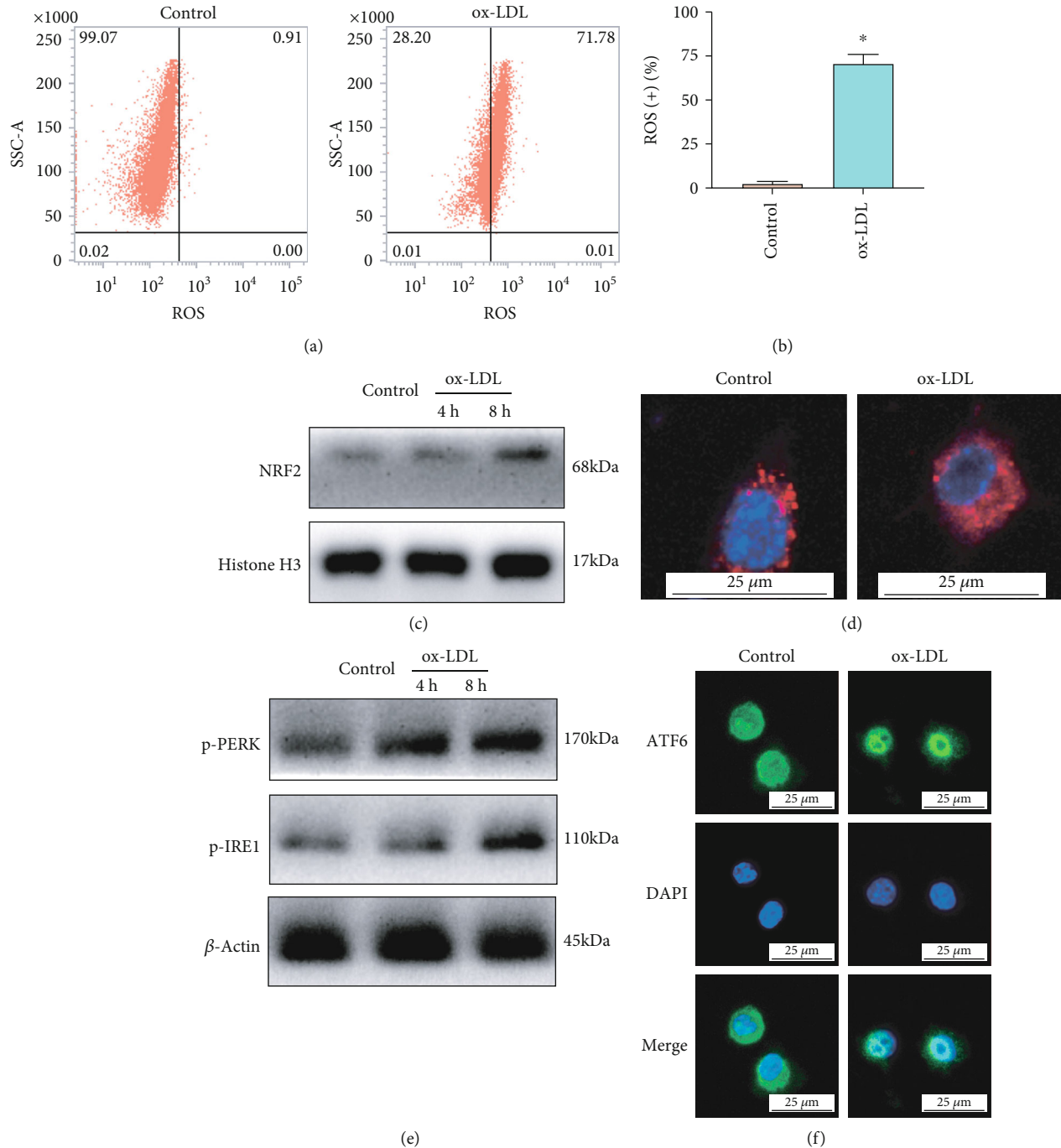


FIGURE 1: ox-LDL triggers oxidative stress, mitochondrial injury, and ER stress in macrophages. (a, b) The number of ROS-positive macrophages increased after ox-LDL treatment for 24 h. (c) The expression levels of nuclear NRF2 by Western blot in macrophages after ox-LDL stimulation for 4 h and 8 h. (d) Mitochondria-specific fluorescence probes (MitoTracker Red) in macrophages captured by confocal microscopy. (e) The phosphorylation levels of PERK and IRE1 in macrophages after ox-LDL stimulation for 4 h and 8 h. (f) ATF6 protein (green) translocated into the nucleus after ox-LDL treatment in macrophages. The threshold of statistical significance was set at $*P < 0.05$.

from the Metascape database indicated that BTK was closely related to oxidative stress, ER stress, and inflammation (Figure 2(e)).

3.3. BTK Knockdown Suppressed the Inflammatory Responses of ox-LDL-Induced Macrophages. To explore the relationship

between the BTK gene and AS, immunohistochemical staining was performed. A high cytoplasm protein level of BTK was found in the lesion area of the aortas from the AS patients (Figures 3(a) and 3(b)). Besides, we stimulated macrophages with ox-LDL for different periods (6, 12, and 24 h for BTK qRT-PCR; 24 and 48 h for BTK Western blot; 48 h

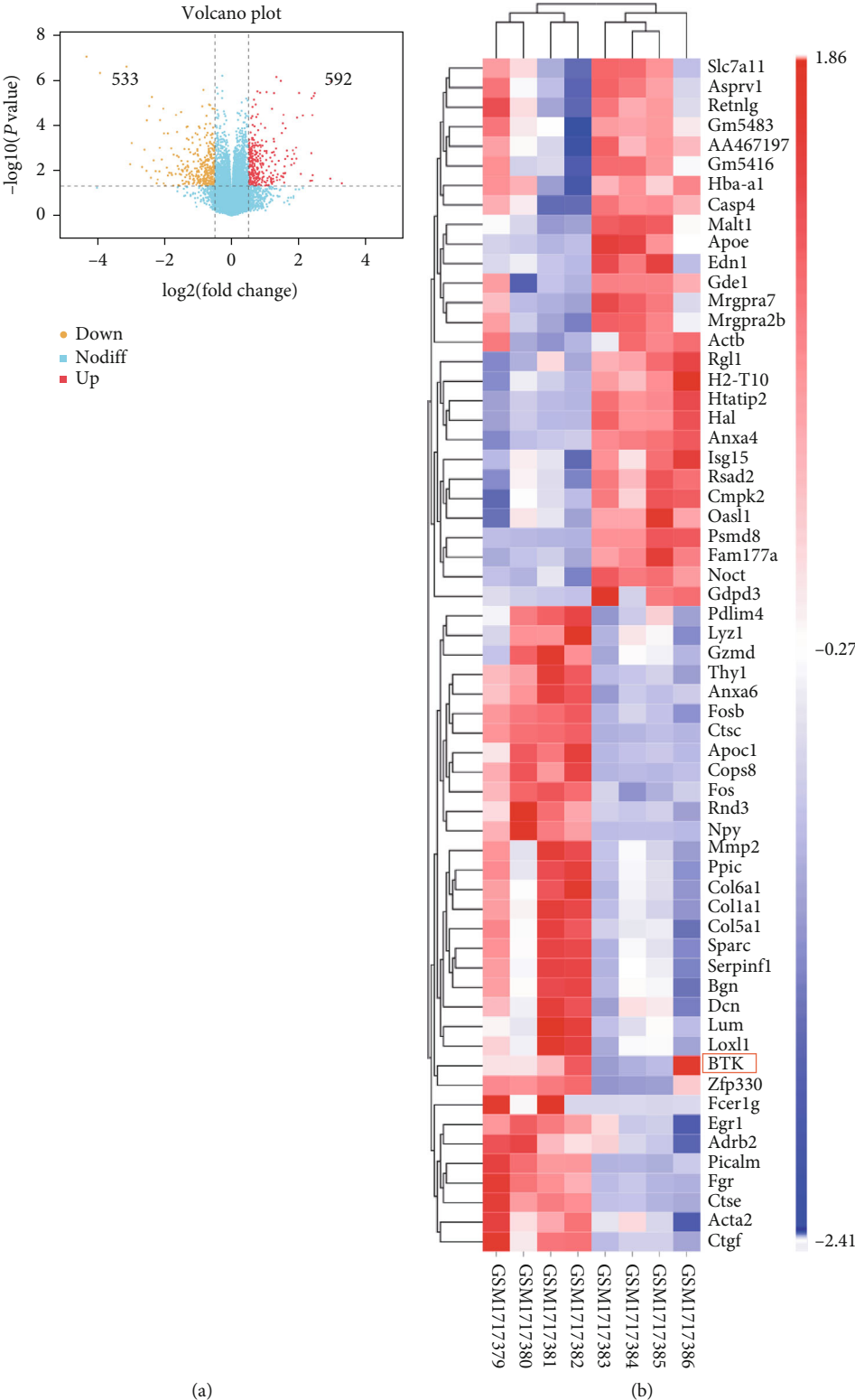
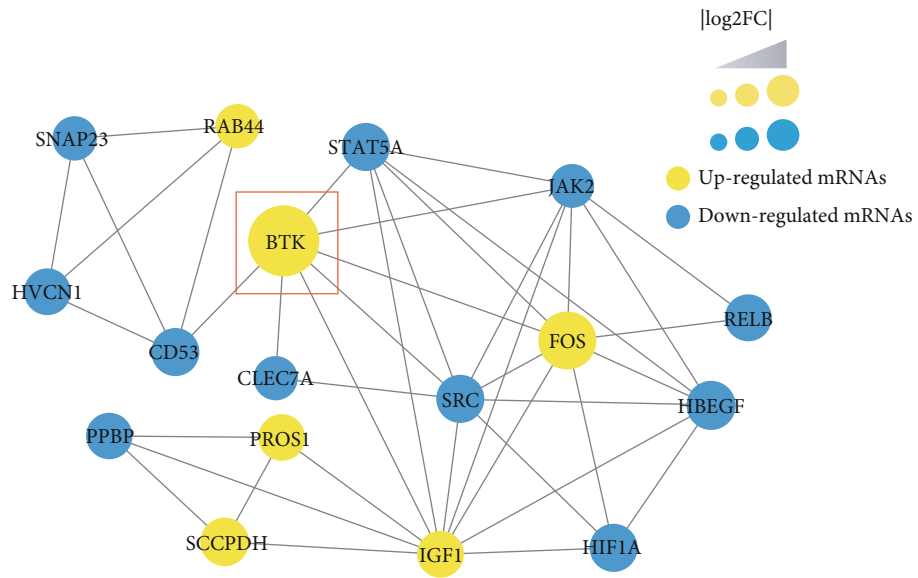
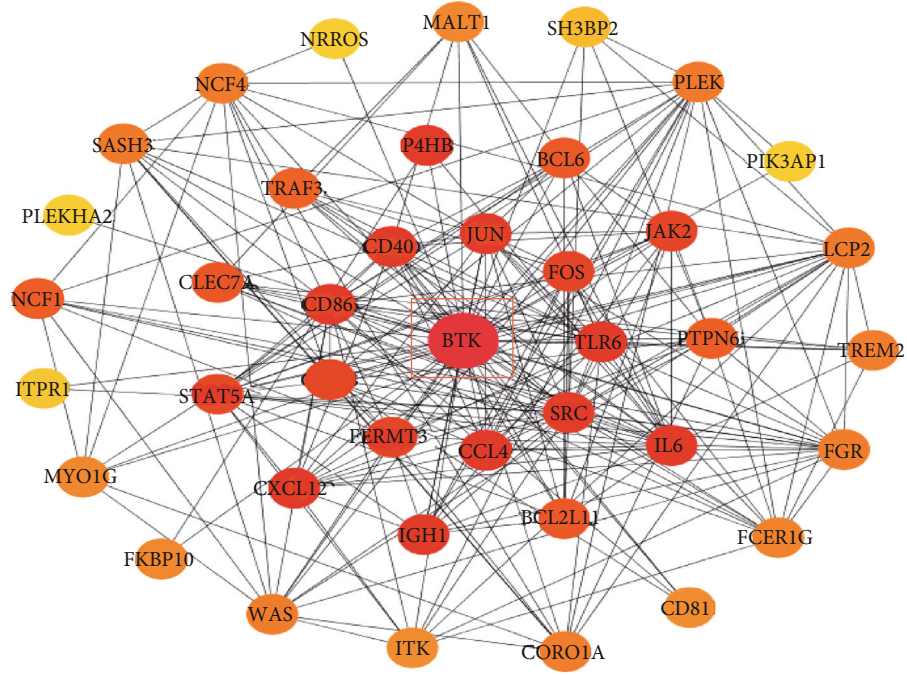


FIGURE 2: Continued.



(c)



(d)

FIGURE 2: Continued.

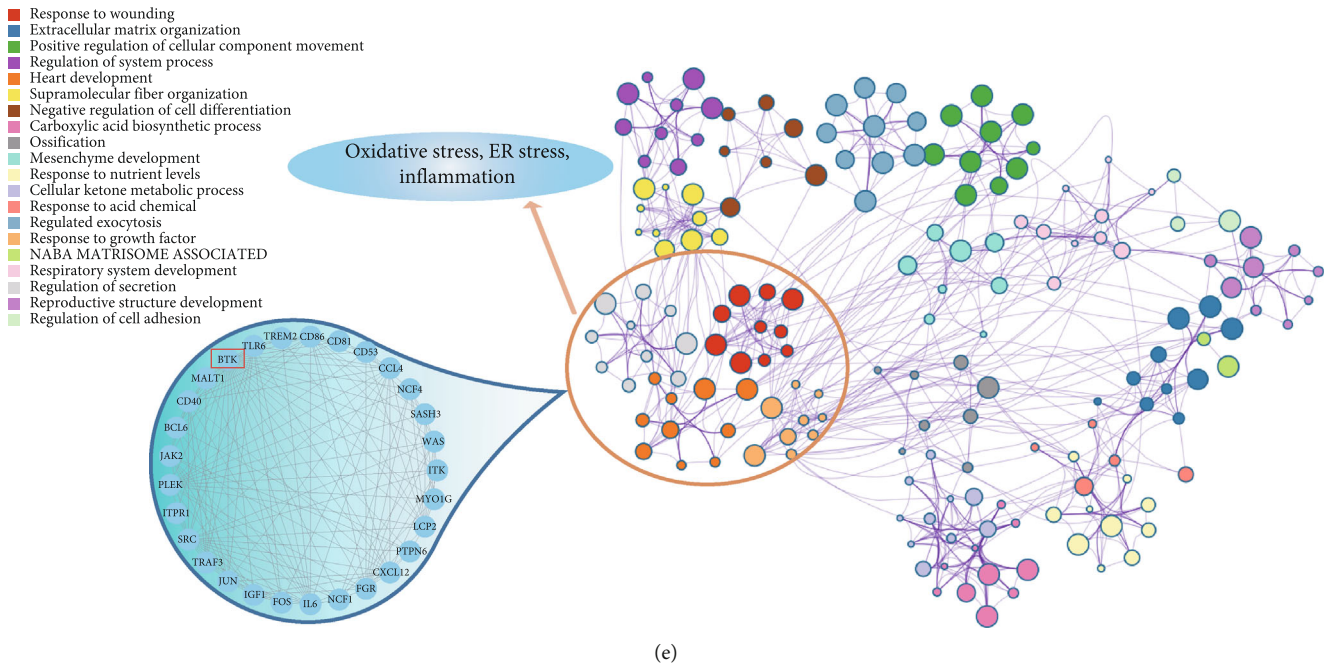


FIGURE 2: BTK was determined as the hub gene related to oxidative stress, ER stress, and inflammation in macrophage-induced AS. (a) The volcano plot indicated 592 upregulated DEGs and 533 downregulated DEGs. (b) The heat map and cluster analysis. (c) STRING and Cytoscape software programs were used to construct the PPI network, and we obtained 19 hub genes through the MCODE application, of which BTK had a high score. (d) By using the cytoHubba application, the hub gene network following core gene scores was built. (e) The functional clustering network from the Metascape database indicated that BTK was closely related to oxidative stress, ER stress, and inflammation.

for proinflammatory factor ELISA; and 24 h for fluorescent staining). The expression level of BTK was upregulated in ox-LDL-induced macrophages, including mRNA and protein expression (Figures 3(c) and 3(d)). Moreover, siRNA-mediated inhibition of BTK was performed in macrophages, and the ELISA results indicated that BTK knockdown could attenuate the cytokine levels of TNF- α and IL-6 (Figure 3(e)). Consistent with the ELISA results, the fluorescent intensities of TNF- α and IL-6 in ox-LDL-induced macrophages were also restrained by the knockdown of BTK (Figure 3(f)).

3.4. BTK Knockdown Suppressed the ox-LDL-Induced $\text{NK-}\kappa\text{B}$ Signaling in Macrophages, Inhibited M1 Macrophage Polarization, and Facilitated M2 Polarization. As shown in Figure 4(a), the phosphorylation level of p65 protein, an important $\text{NK-}\kappa\text{B}$ signaling mediator, was significantly reduced by the knockdown of BTK. Moreover, we performed the fluorescent staining of p65 protein, and the results indicated that BTK knockdown inhibited the nucleus translocation of p65 in macrophages (Figure 4(b)). Macrophage polarization, which is closely related to the $\text{NF-}\kappa\text{B}$ pathway, was also determined by flow cytometry here. As shown in Figure 4(c), BTK knockdown decreased the number of M1 macrophages, which were considered a proinflammatory type. In contrast, M2 anti-inflammatory macrophages significantly increased caused by the knockdown of BTK. Besides, the expression of iNOS was downregulated, while the expression of COX-2 was upregulated on the mRNA level caused by BTK knockdown (Figure 4(d)). Consistently, the knockdown

of BTK significantly reduced the protein expression level of phosphorylated IRF3, which is an important transcription factor in the process of M1 polarization (Figure 4(e)).

3.5. BTK Knockdown Alleviated Oxidative Stress, Mitochondrial Injury, and ER Stress in ox-LDL-Induced Macrophages. In view of the ox-LDL-triggered oxidative stress that played an important role in AS, we next determined the effect of BTK knockdown on oxidative stress and mitochondrial injury. Flow cytometry results revealed that BTK knockdown significantly reduced the production levels of ROS (Figures 5(a) and 5(b)). The upregulation of the NRF2 nuclear protein level in ox-LDL-stimulated macrophages when BTK was knocked down is shown in Figure 5(c). Moreover, BTK knockdown attenuated the mitochondrial injury in macrophages, as shown in our fluorescent staining results (Figure 5(d)). Besides, the knockdown of BTK clearly suppressed the protein expression of DRP1 and FIS1, the two important mitochondrial fission factors (Figure 5(e)). To further determine the correlation between BTK knockdown and ER stress, we administered ox-LDL to macrophages for different periods. A fluorescent staining assay was carried out to clarify the activation of ATF6 protein, an ER stress-related transcription factor. The confocal microscope results showed that ox-LDL-stimulated nuclear translocation of ATF6 was attenuated by BTK knockdown (Figure 5(f)). Besides, the results demonstrated that the phosphorylation levels of PERK and IRE1 significantly decreased in the si-BTK group (Figure 5(g)).

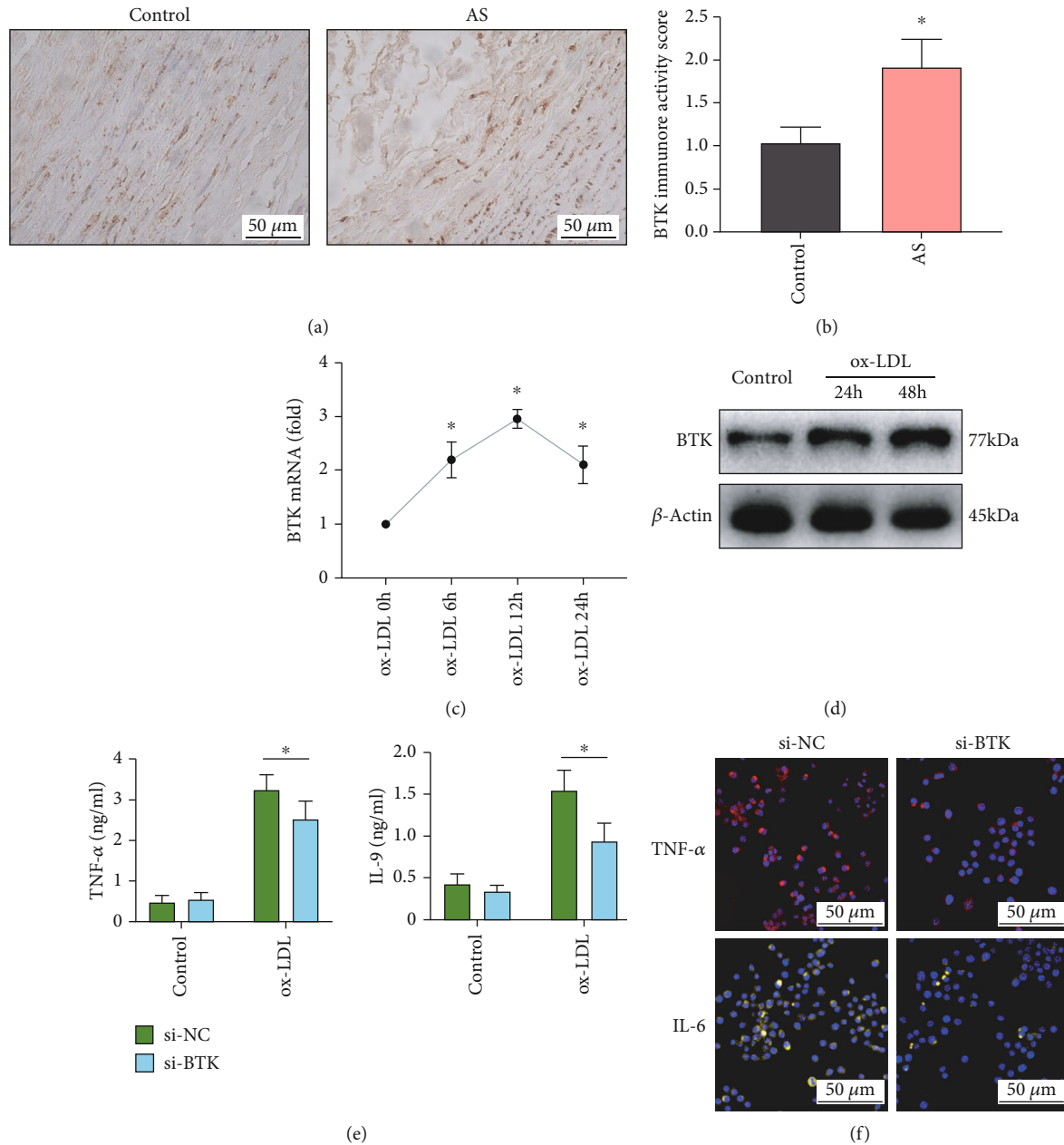


FIGURE 3: BTK knockdown suppressed the inflammatory responses of ox-LDL-induced macrophages. (a) IHC staining and (b) immunoreactivity score of BTK in specimens from the control group and AS group. (c, d) The mRNA and protein expression levels of BTK were upregulated in ox-LDL-induced macrophages. (e) The siRNA-mediated inhibition of BTK was performed in macrophages, and the ELISA results indicated that TNF- α and IL-6 were reduced by BTK knockdown. (f) The fluorescent intensities of TNF- α and IL-6 were restrained by the knockdown of BTK in ox-LDL-induced macrophages. The threshold of statistical significance was set at $*P < 0.05$.

3.6. *sh-BTK Adenovirus Injection Reduced the Progression of AS Lesions in ApoE^{-/-} Mice*. The therapeutic roles of BTK in atherogenesis were determined in ApoE^{-/-} mice, which were fed with a Western diet for 12 weeks. Then, the tail vein injection of adenovirus-mediated sh-BTK and sh-NC was performed. We observed that the Oil Red O area within the aortic tree was significantly attenuated in the sh-BTK group, which indicated that sh-BTK adenovirus injection effectively attenuated the progression of AS (Figures 6(a) and 6(b)). Consistently, the H&E staining results showed that the necrotic core area in ApoE^{-/-} mice decreased in the sh-BTK

group (Figures 6(c) and 6(d)). Besides, the foam cells in the cross-sections of ApoE^{-/-} mouse aortas were stained with Oil Red O, and the results showed that the lesion area significantly decreased in the sh-BTK group (Figures 6(e) and 6(f)). Hence, our results indicated that the knockdown of BTK reduced the development of AS in ApoE^{-/-} mice.

4. Discussion

AS is a progressive chronic inflammatory condition shared by several cardiovascular diseases, bringing immense burdens on

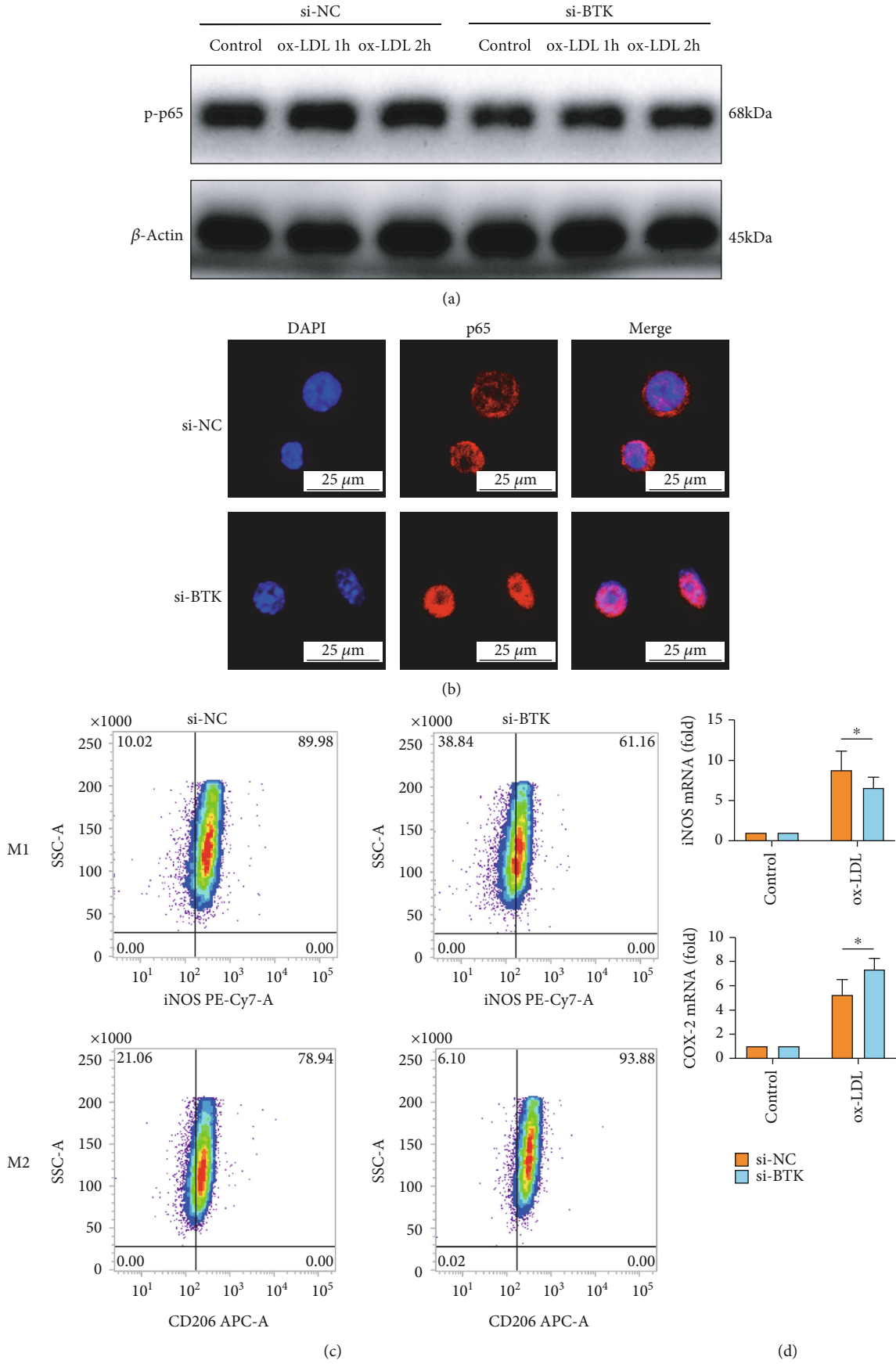


FIGURE 4: Continued.

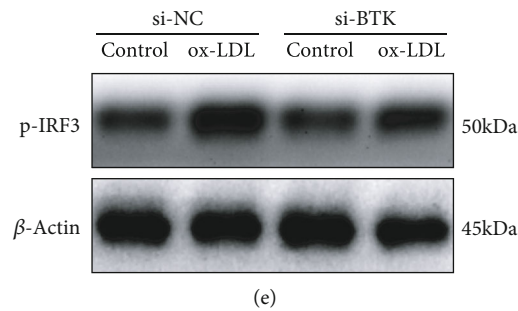


FIGURE 4: BTK knockdown suppressed the ox-LDL-induced NF- κ B activation and inhibited M1 polarization. (a) The phosphorylation level of p65 protein was significantly reduced by the knockdown of BTK. (b) BTK knockdown inhibited the nucleus translocation of p65 in macrophages. (c) BTK knockdown reduced the number of M1 macrophages and significantly increased the M2 anti-inflammatory macrophages. (d) iNOS was downregulated, while COX-2 was upregulated on the mRNA level caused by BTK knockdown. (e) The knockdown of BTK significantly reduced the protein expression level of phosphorylated IRF3. The threshold of statistical significance was set at $*P < 0.05$.

health and economy worldwide [49, 50]. Using genetically engineered mice, our results suggested that the knockdown of BTK inhibited the development of AS in ApoE^{-/-} mice, and one of the mechanisms is through releasing ox-LDL-induced inflammatory response, oxidative stress, and ER stress in macrophages and promoting macrophage polarization to the M2 type. It is well recognized that the biochemical cascade of atherogenesis is inseparable from the foam cell formation and inflammatory responses of macrophages [51]. ox-LDL, an atherogenic factor, contributes to AS progression by promoting the inflammatory response in macrophages [52]. Consistently, we found that the NF- κ B signaling pathway and IRF3 were activated by ox-LDL in macrophages. NF- κ B was considered a first responder to regulate the central cellular response to inflammation [19]. And activation of the interferon regulatory factor 3 (IRF3), a downstream factor that induced the type I interferon production and initiated inflammation, suggested the increase of the ox-LDL-induced M1 phenotype macrophages [53]. Inflammation and polarization of macrophages play an important role in AS. In our previous report, we also found that atherosclerotic lesions can be alleviated when inflammatory responses of ox-LDL-induced macrophages were released [28].

Nevertheless, the exact mechanisms of how ox-LDL stimulated macrophages have not been clarified. Single-cell RNA-seq of aortic macrophages in murine AS identified that inflammatory macrophages (enriched in M1 proinflammatory genes) accounted for a large part of the overall macrophage subpopulations [54]. In our current study, RNA-seq analysis has been applied in foam cell macrophages. After analysis of DEGs and the PPIN, we performed a detailed comparison of gene expression. BTK was considered a hub gene related to oxidative stress, ER stress, and inflammation in macrophage-induced AS. Consistently, we showed that the protein level of BTK in the AS group increased significantly than that in the control group, and the knockdown of BTK significantly suppressed the proinflammatory factor secretion and the phosphorylation level of p65 protein, indicating that BTK positively regulated the inflammatory responses of ox-LDL-stimulated macrophages. Thus, these results implicated BTK as a candidate causal gene for AS

and pointed to future directions to treatment for AS, using pharmacological or genetic inhibition of BTK.

Former investigators indicated that BTK positively regulated TLR4-mediated activation of the NF- κ B signaling pathway in the monocytic cell line [15, 55]. These data are consistent with our results that BTK knockdown decreased NF- κ B signaling pathway activation in ox-LDL-induced macrophages. Another study reported that BTK also made sense on lipopolysaccharide-induced sepsis and negatively regulated the lipopolysaccharide-induced canonical NF- κ B signaling pathway in mast cells [56]. This discrepancy may be caused by different cell types and stimuli. The role of BTK might be cell type-specific. The activation of the NF- κ B signaling pathway and the secretion of proinflammatory factors have a strong association with the macrophage polarization to the M1 type [57]. Since BTK positively regulates the NF- κ B signaling pathway in our current study, BTK knockdown inhibited M1 macrophage polarization and facilitated M2 polarization, which was validated by the flow cytometry analysis. Phosphorylation levels of IRF3 were significantly decreased accompanied by fewer M1 macrophages.

Previous studies have shown that ER stress and oxidative stress were extremely significant in macrophage polarization and proinflammatory factor secretion [58–60]. ER stress, oxidative stress, and inflammatory response together make up defense networks of the cells that react to outside stimuli [8, 61]. Risk factors related to AS, such as hyperlipidemia, hypertension, and obesity, activated the ER stress-related proteins, such as IRE1, PERK, and ATF6, and aggravated the inflammatory response in macrophages [62, 63]. UPR activation and ER stress had been identified in atherosclerotic lesions. ER stress inhibitors could relieve inflammation and decreased IL-6 secretion in macrophages via inhibition of the ER stress-related PERK-AFT4 pathway [7]. Additionally, AS development was closely related to oxidative stress and mitochondrial injury. Suppression of mitochondrial oxidative stress in macrophages attenuated AS in mice. The imbalanced mitochondrial homeostasis and excessive ROS production in macrophages would activate the NF- κ B signaling pathway and promote the release of proinflammatory factors such as TNF- α and IL-6 [10, 64]. The interaction between ROS and proinflammatory factors

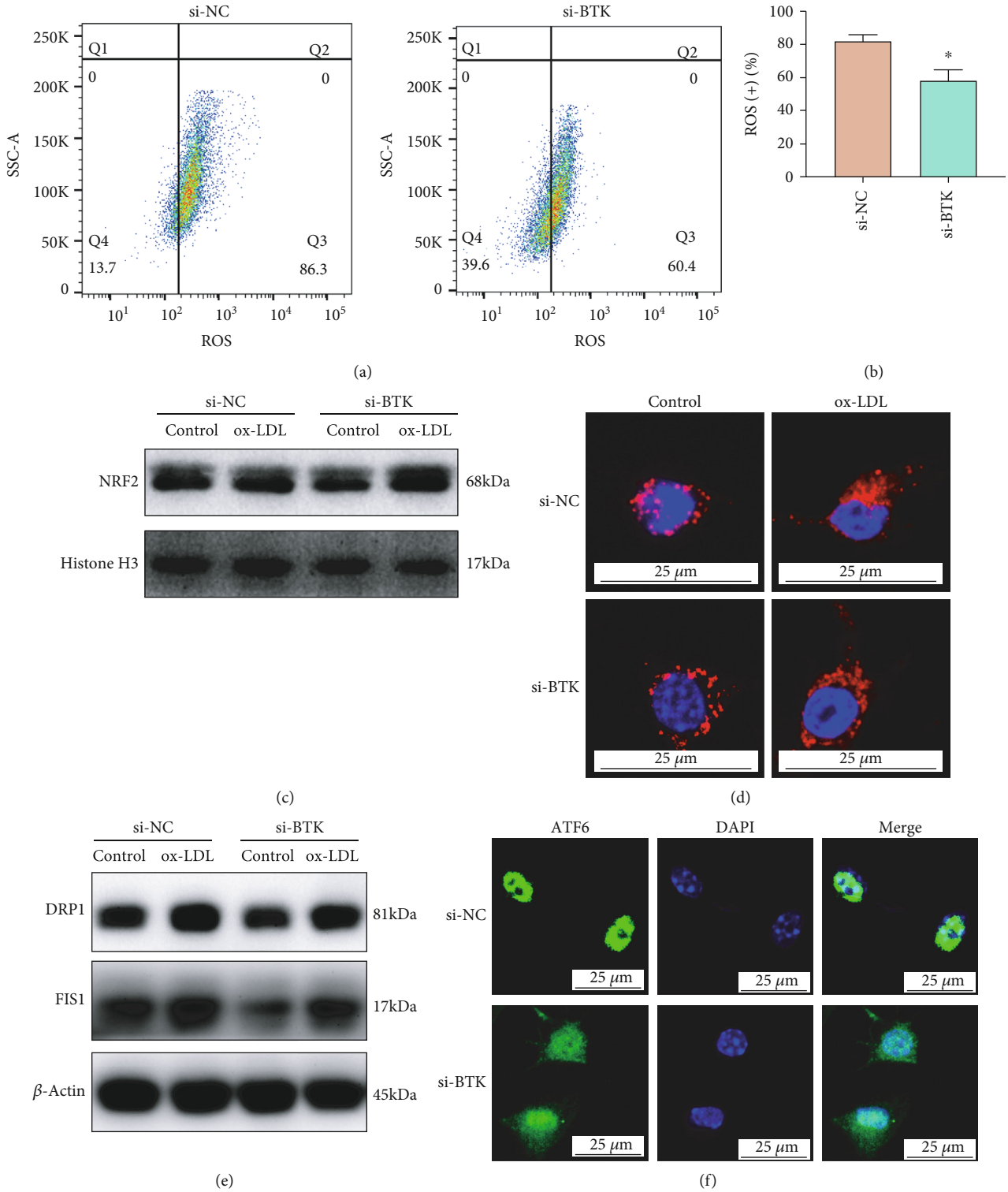


FIGURE 5: Continued.

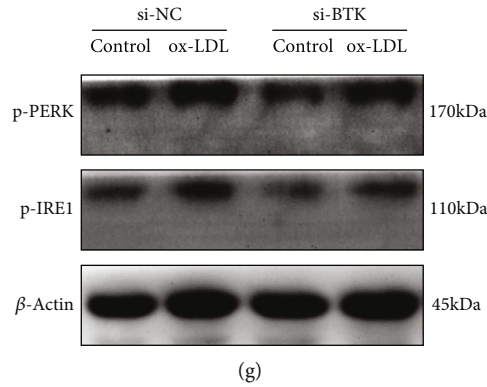


FIGURE 5: BTK knockdown alleviated oxidative stress, mitochondrial injury, and ER stress in ox-LDL-induced macrophages. (a, b) The flow cytometry results showed that BTK knockdown significantly reduced the production levels of ROS. (c) The upregulation of the NRF2 nuclear protein level in ox-LDL-stimulated macrophages when BTK was knocked down. (d) BTK knockdown attenuated the mitochondrial injury in macrophages. (e) The knockdown of BTK suppressed the protein expression of DRP1 and FIS1. (f) The confocal microscope results revealed that ox-LDL-induced nuclear translocation of ATF6 was attenuated by BTK knockdown. (g) The phosphorylation levels of PERK and IRE1 significantly decreased in the si-BTK group. The threshold of statistical significance was set at $*P < 0.05$.

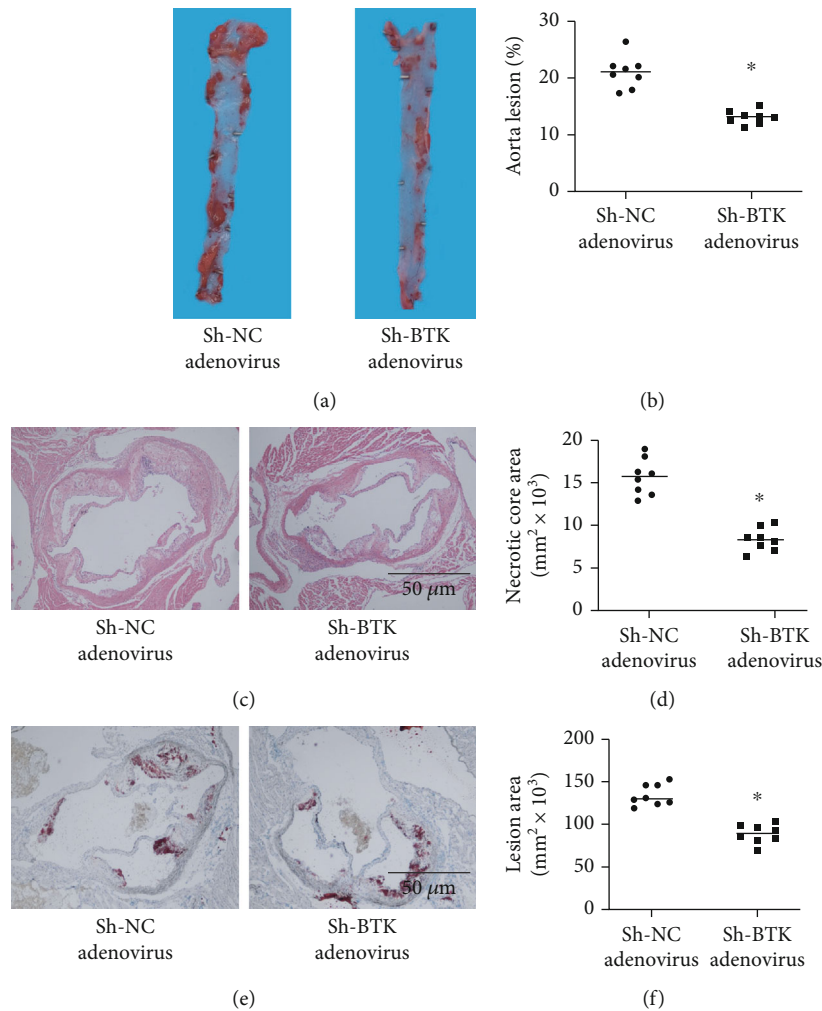


FIGURE 6: sh-BTK adenovirus injection reduced the development of AS lesions in ApoE^{-/-} mice. (a, b) The Oil Red O area within the aortic tree was significantly attenuated in the sh-BTK group. The lesion coverage of the entire aorta (%) was assessed by ImageJ software. (c, d) The H&E staining results showed that the necrotic core area in ApoE^{-/-} mice decreased in the sh-BTK group. The necrotic core area was assessed by ImageJ software. (e, f) The lesion area significantly decreased in the sh-BTK group. The lesion area was assessed by ImageJ software. The threshold of statistical significance was set at $*P < 0.05$.

would also enhance the damage and aggravate the inflammation, implicating the pathogenesis of the atherosclerotic lesion [11]. Researchers revealed that MAMs, associated with the mitochondria with ER, made sense on several metabolic diseases, including diabetes, stroke, and coronary artery diseases [65, 66]. And this association between ER and mitochondria was considered a potential target for many cardiovascular diseases. We show in the current study that the knockdown of BTK could attenuate the ER stress and mitochondrial oxidative stress. Our findings advanced our understanding of the association between MAMs and metabolic disorders in AS.

Finally, we had reported that the injection of ZBTB20 knockdown adenovirus in the tail vein of ApoE^{-/-} mice fed with a Western diet could alleviate AS, indicating that the tail vein adenovirus injection is a potential method for treatment of cardiovascular diseases [28]. In our current study, ApoE^{-/-} mice injected with BTK knockdown adenovirus presented a smaller AS lesion area in the aorta. BTK knockdown attenuates the progression of AS and foam cell formation in mice, suggesting that BTK positively regulates the development of AS in ApoE^{-/-} mice fed with the Western diet. Despite our rigorous experimental design, there are some limitations in our study. Although adenovirus vectors have recently emerged as attractive vectors for cardiovascular gene therapy due to their high transduction efficiency, direct distribution of the adenovirus in mice could not be identified. Moreover, adenovirus tail vein injection cannot definitively prove the effector cell types. Therefore, the cell-specific BTK knockdown ApoE^{-/-} mice need to be addressed in future research. The present study showed that the knockdown of the BTK led to the attenuation of the oxidative stress, mitochondrial stress, ER stress, and inflammation in macrophages induced by ox-LDL, which were consistent with the decreased ROS production levels, alleviated mitochondrial injury, inhibited ATF6 nuclear translocation, decreased M1 macrophages, and reduced proinflammatory cytokine secretion. Additionally, the progression of AS of the Western diet-fed ApoE^{-/-} mice was attenuated by intravenous injection of BTK knockdown adenovirus, suggesting that BTK inhibitors may make a difference in AS treatment as a powerful therapeutic target.

All in all, we clarified that BTK knockdown reduced the AS lesion area and attenuated the progression of AS in mice, and BTK positively regulated inflammatory responses of ox-LDL-induced macrophages in AS by regulating oxidative stress, mitochondrial injury, and ER stress.

Data Availability

All the datasets were available from the corresponding authors.

Conflicts of Interest

No conflicts of interest need to be declared by the authors.

Authors' Contributions

Junxiong Qiu, Yuan Fu, and Zhiteng Chen are the co-first authors and contributed equally to this work.

Acknowledgments

The source of funding in this study was from the Guangdong Science and Technology Department (project number 2020B1212060018) and the National Natural Science Foundation of China (project number 81702618).

References

- [1] H. W. Kim, H. Shi, M. A. Winkler, R. Lee, and N. L. Weintraub, "Perivascular adipose tissue and vascular perturbation/atherosclerosis," *Arteriosclerosis, Thrombosis, and Vascular Biology*, vol. 40, no. 11, pp. 2569–2576, 2020.
- [2] P. K. Shah, "Inflammation, infection and atherosclerosis," *Trends in Cardiovascular Medicine*, vol. 29, no. 8, pp. 468–472, 2019.
- [3] J. Khalou-Laschet, A. Varthaman, G. Fornasa et al., "Macrophage plasticity in experimental atherosclerosis," *PLoS One*, vol. 5, no. 1, article e8852, 2010.
- [4] L. Galle-Treger, M. Moreau, R. Ballaire et al., "Targeted inactivation of SR-B1 in macrophages reduces macrophage apoptosis and accelerates atherosclerosis," *Cardiovascular Research*, vol. 116, no. 3, pp. 554–565, 2020.
- [5] P. A. Mueller, L. Zhu, H. Tavori et al., "Deletion of macrophage low-density lipoprotein receptor-related protein 1 (LRP1) accelerates atherosclerosis regression and increases C-C chemokine receptor type 7 (CCR7) expression in plaque macrophages," *Circulation*, vol. 138, no. 17, pp. 1850–1863, 2018.
- [6] R. Wang, Y. Zhang, L. Xu et al., "Protein Inhibitor of Activated STAT3 Suppresses Oxidized LDL-induced Cell Responses during Atherosclerosis in Apolipoprotein E-deficient Mice," *Scientific Reports*, vol. 6, no. 1, 2016.
- [7] S. Chen, Y. Chen, Y. Chen, and Z. Yao, "InP/ZnS quantum dots cause inflammatory response in macrophages through endoplasmic reticulum stress and oxidative stress," *International Journal of Nanomedicine*, vol. 14, pp. 9577–9586, 2019.
- [8] A. Dandekar, R. Mendez, and K. Zhang, "Cross talk between ER stress, oxidative stress, and inflammation in health and disease," *Methods in Molecular Biology*, vol. 1292, pp. 205–214, 2015.
- [9] Y. Liao, T. Hussain, C. Liu et al., "Endoplasmic reticulum stress induces macrophages to produce IL-1 β during *Mycobacterium bovis* infection via a positive feedback loop between mitochondrial damage and inflammasome activation," *Frontiers in Immunology*, vol. 10, p. 268, 2019.
- [10] N. R. Madamanchi and M. S. Runge, "Mitochondrial dysfunction in atherosclerosis," *Circulation Research*, vol. 100, no. 4, pp. 460–473, 2007.
- [11] S. Missiroli, S. Patergnani, N. Caroccia et al., "Mitochondria-associated membranes (MAMs) and inflammation," *Cell Death & Disease*, vol. 9, no. 3, p. 329, 2018.
- [12] A. A. Momtazi-Borojeni, E. Abdollahi, B. Nikfar, S. Chaichian, and M. Ekhlas-Hundrieser, "Curcumin as a potential modulator of M1 and M2 macrophages: new insights in atherosclerosis therapy," *Heart Failure Reviews*, vol. 24, no. 3, pp. 399–409, 2019.
- [13] Y. Liu, X. Wang, J. Pang et al., "Attenuation of Atherosclerosis by Protocatechuic Acid via Inhibition of M1 and Promotion of M2 Macrophage Polarization," *Journal of Agricultural and Food Chemistry*, vol. 67, no. 3, pp. 807–818, 2019.

- [14] J. Afaghani and J. Taylor, "A moving target: inactivating BTK mutations as drivers of follicular lymphoma," *Clinical Cancer Research*, vol. 27, no. 8, pp. 2123–2125, 2021.
- [15] C. Yue, M. Niu, Q. Q. Shan et al., "High expression of Bruton's tyrosine kinase (BTK) is required for EGFR-induced NF- κ B activation and predicts poor prognosis in human glioma," *Journal of Experimental & Clinical Cancer Research*, vol. 36, no. 1, p. 132, 2017.
- [16] P. Bhargava, S. Kim, A. A. Reyes et al., "Imaging meningeal inflammation in CNS autoimmunity identifies a therapeutic role for BTK inhibition," *Brain*, 2021.
- [17] M. Pontoriero, G. Fiume, E. Vecchio et al., "Activation of NF- κ B in B cell receptor signaling through Bruton's tyrosine kinase-dependent phosphorylation of I κ B- α ," *Journal of Molecular Medicine (Berlin, Germany)*, vol. 97, no. 5, pp. 675–690, 2019.
- [18] J. Choi, J. D. Phelan, G. W. Wright et al., "Regulation of B cell receptor-dependent NF- κ B signaling by the tumor suppressor KLHL14," *Proceedings of the National Academy of Sciences*, vol. 117, no. 11, pp. 6092–6102, 2020.
- [19] I. Pateras, C. Giaginis, C. Tsigris, E. Patsouris, and S. Theocharis, "NF- κ B signaling at the crossroads of inflammation and atherogenesis: searching for new therapeutic links," *Expert Opinion on Therapeutic Targets*, vol. 18, no. 9, pp. 1089–1101, 2014.
- [20] A. Papin, B. Tessoulin, C. Bellanger et al., "CSF1R and BTK inhibitions as novel strategies to disrupt the dialog between mantle cell lymphoma and macrophages," *Leukemia*, vol. 33, no. 10, pp. 2442–2453, 2019.
- [21] A. Colado, M. Genoula, C. Cougoule et al., "Effect of the BTK inhibitor ibrutinib on macrophage- and $\gamma\delta$ T cell-mediated response against *Mycobacterium tuberculosis*," *Blood Cancer Journal*, vol. 8, no. 11, p. 100, 2018.
- [22] M. Feng, J. Y. Chen, R. Weissman-Tsukamoto et al., "Macrophages eat cancer cells using their own calreticulin as a guide: roles of TLR and Btk," *Proceedings of the National Academy of Sciences of the United States of America*, vol. 112, no. 7, pp. 2145–2150, 2015.
- [23] S. Herbst, A. Shah, M. Mazon Moya et al., "Phagocytosis-dependent activation of a TLR9-BTK-calcineurin-NFAT pathway co-ordinates innate immunity to *Aspergillus fumigatus*," *EMBO Molecular Medicine*, vol. 7, no. 3, pp. 240–258, 2015.
- [24] K. Busygina, J. Jamasbi, T. Seiler et al., "Oral Bruton tyrosine kinase inhibitors selectively block atherosclerotic plaque-triggered thrombus formation in humans," *Blood*, vol. 131, no. 24, pp. 2605–2616, 2018.
- [25] M. von Scheidt, Y. Zhao, Z. Kurt et al., "Applications and limitations of mouse models for understanding human atherosclerosis," *Cell Metabolism*, vol. 25, no. 2, pp. 248–261, 2017.
- [26] J. Bai, M. Khajavi, L. Sui et al., "Angiogenic responses in a 3D micro-engineered environment of primary endothelial cells and pericytes," *Angiogenesis*, vol. 24, no. 1, pp. 111–127, 2021.
- [27] N. Abbas, F. Perbellini, and T. Thum, "Non-coding RNAs: emerging players in cardiomyocyte proliferation and cardiac regeneration," *Basic Research in Cardiology*, vol. 115, no. 5, p. 52, 2020.
- [28] J. Tao, J. Qiu, L. Lu et al., "ZBTB20 Positively Regulates Oxidative Stress, Mitochondrial Fission, and Inflammatory Responses of ox-LDL-Induced Macrophages in Atherosclerosis," *Oxidative Medicine and Cellular Longevity*, vol. 2021, Article ID 5590855, 18 pages, 2021.
- [29] R. K. Adapala, A. K. Kanugula, S. Paruchuri, W. M. Chilian, and C. K. Thodeti, "TRPV4 deletion protects heart from myocardial infarction-induced adverse remodeling via modulation of cardiac fibroblast differentiation," *Basic Research in Cardiology*, vol. 115, no. 2, p. 14, 2020.
- [30] J. Qiu, P. Peng, M. Xin et al., "ZBTB20-mediated titanium particle-induced peri-implant osteolysis by promoting macrophage inflammatory responses," *Biomaterials Science*, vol. 8, no. 11, pp. 3147–3163, 2020.
- [31] O. Bakhta, A. Pascaud, X. Dieu et al., "Tryptophane-kynurenine pathway in the remote ischemic conditioning mechanism," *Basic Research in Cardiology*, vol. 115, no. 2, p. 13, 2020.
- [32] L. Li, Z. Bi, Y. Hu et al., "Silver nanoparticles and silver ions cause inflammatory response through induction of cell necrosis and the release of mitochondria in vivo and in vitro," *Cell Biology and Toxicology*, vol. 37, no. 2, pp. 177–191, 2021.
- [33] E. Bridges, H. Sheldon, E. Kleibeuker et al., "RHOQ is induced by DLL4 and regulates angiogenesis by determining the intracellular route of the Notch intracellular domain," *Angiogenesis*, vol. 23, no. 3, pp. 493–513, 2020.
- [34] J. Wang and H. Zhou, "Mitochondrial quality control mechanisms as molecular targets in cardiac ischemia-reperfusion injury," *Acta Pharmaceutica Sinica B*, vol. 10, no. 10, pp. 1866–1879, 2020.
- [35] S. Li, J. Qiu, L. Qin et al., "NOD2 negatively regulated titanium particle-induced osteolysis in mice," *Biomaterials Science*, vol. 7, no. 7, pp. 2702–2715, 2019.
- [36] D. B. Buglak, E. J. Kushner, A. P. Marvin, K. L. Davis, and V. L. Bautch, "Excess centrosomes disrupt vascular lumenization and endothelial cell adherens junctions," *Angiogenesis*, vol. 23, no. 4, pp. 567–575, 2020.
- [37] M. M. Bekhite, A. G. Delgado, F. Menz et al., "Longitudinal metabolic profiling of cardiomyocytes derived from human-induced pluripotent stem cells," *Basic Research in Cardiology*, vol. 115, no. 4, p. 37, 2020.
- [38] Y. Tan, D. Mui, S. Toan, P. Zhu, R. Li, and H. Zhou, "SERCA overexpression improves mitochondrial quality control and attenuates cardiac microvascular ischemia-reperfusion injury," *Molecular Therapy-Nucleic Acids*, vol. 22, pp. 696–707, 2020.
- [39] J. Wang, P. Zhu, R. Li, J. Ren, and H. Zhou, "Fundc1-dependent mitophagy is obligatory to ischemic preconditioning-conferred renoprotection in ischemic AKI via suppression of Drp1-mediated mitochondrial fission," *Redox Biology*, vol. 30, article 101415, 2020.
- [40] F. Cao, M. L. Maguire, D. J. McAndrew et al., "Overexpression of mitochondrial creatine kinase preserves cardiac energetics without ameliorating murine chronic heart failure," *Basic Research in Cardiology*, vol. 115, no. 2, p. 12, 2020.
- [41] J. Wang, S. Toan, R. Li, and H. Zhou, "Melatonin fine-tunes intracellular calcium signals and eliminates myocardial damage through the IP3R/MCU pathways in cardiorenal syndrome type 3," *Biochemical Pharmacology*, vol. 174, article 113832, 2020.
- [42] M. Lobo-Gonzalez, C. Galán-Arriola, X. Rossello et al., "Metoprolol blunts the time-dependent progression of infarct size," *Basic Research in Cardiology*, vol. 115, no. 5, p. 55, 2020.
- [43] A. C. Dudley, "Introduction to special issue: vascular cooption in cancer," *Angiogenesis*, vol. 23, no. 1, pp. 1–2, 2020.
- [44] G. Fang, Y. Fu, S. Li et al., "The USP14-NLRC5 pathway inhibits titanium particle-induced osteolysis in mice by

- suppressing NF- κ B and PI3K/AKT activities,” *The Journal of Biological Chemistry*, vol. 295, no. 20, pp. 7018–7032, 2020.
- [45] P. Fournier, C. Viallard, A. Dejda, P. Sapieha, B. Larrivée, and I. Royal, “The protein tyrosine phosphatase PTPRJ/DEP-1 contributes to the regulation of the Notch-signaling pathway and sprouting angiogenesis,” *Angiogenesis*, vol. 23, no. 2, pp. 145–157, 2020.
- [46] M. Lindner, H. Mehel, A. David et al., “Fibroblast growth factor 23 decreases PDE4 expression in heart increasing the risk of cardiac arrhythmia; Klotho opposes these effects,” *Basic Research in Cardiology*, vol. 115, no. 5, p. 51, 2020.
- [47] S. K. Lahiri, A. P. Quick, B. Samson-Couterie et al., “Nuclear localization of a novel calpain-2 mediated junctophilin-2 C-terminal cleavage peptide promotes cardiomyocyte remodeling,” *Basic Research in Cardiology*, vol. 115, no. 4, p. 49, 2020.
- [48] N. Ludwig, S. S. Yerneni, J. H. Azambuja et al., “Tumor-derived exosomes promote angiogenesis via adenosine A_{2B} receptor signaling,” *Angiogenesis*, vol. 23, no. 4, pp. 599–610, 2020.
- [49] Authors/Task Force members, R. Erbel, V. Aboyans et al., “2014 ESC Guidelines on the diagnosis and treatment of aortic diseases,” *European Heart Journal*, vol. 35, no. 41, pp. 2873–2926, 2014.
- [50] E. J. Benjamin, M. J. Blaha, S. E. Chiuve et al., “Correction to: Heart Disease and Stroke Statistics—2017 Update: A Report From the American Heart Association,” *Circulation*, vol. 135, no. 10, p. e646, 2017.
- [51] D. Wang, Y. Yang, Y. Lei et al., “Targeting foam cell formation in atherosclerosis: therapeutic potential of natural products,” *Pharmacological Reviews*, vol. 71, no. 4, pp. 596–670, 2019.
- [52] A. Pirillo, G. D. Norata, and A. L. Catapano, “LOX-1, OxLDL, and Atherosclerosis,” *Mediators of Inflammation*, vol. 2013, Article ID 152786, 12 pages, 2013.
- [53] X. Chen, Y. Xu, W. Tu et al., “Ubiquitin E3 ligase MID1 inhibits the innate immune response by ubiquitinating IRF3,” *Immunology*, 2021.
- [54] C. Cochain, E. Vafadarnejad, P. Arampatzi et al., “Single-cell RNA-seq reveals the transcriptional landscape and heterogeneity of aortic macrophages in murine atherosclerosis,” *Circulation Research*, vol. 122, no. 12, pp. 1661–1674, 2018.
- [55] C. A. Jefferies, S. Doyle, C. Brunner et al., “Bruton’s Tyrosine Kinase Is a Toll/Interleukin-1 Receptor Domain-binding Protein That Participates in Nuclear Factor κ B Activation by Toll-like Receptor 4,” *Journal of Biological Chemistry*, vol. 278, no. 28, pp. 26258–26264, 2003.
- [56] W. Huang, J. L. Morales, V. P. Gazivoda, and A. August, “Non-receptor tyrosine kinases ITK and BTK negatively regulate mast cell proinflammatory responses to lipopolysaccharide,” *The Journal of Allergy and Clinical Immunology*, vol. 137, no. 4, pp. 1197–1205, 2016.
- [57] M. Sun, Z. Deng, F. Shi et al., “Rebamipide-loaded chitosan nanoparticles accelerate prostatic wound healing by inhibiting M1 macrophage-mediated inflammation via the NF- κ B signaling pathway,” *Biomaterials Science*, vol. 8, no. 3, pp. 912–925, 2020.
- [58] C. He, S. Jiang, H. Yao et al., “Endoplasmic reticulum stress mediates inflammatory response triggered by ultra-small superparamagnetic iron oxide nanoparticles in hepatocytes,” *Nanotoxicology*, vol. 12, no. 10, pp. 1198–1214, 2018.
- [59] K. Shenderov, N. Riteau, R. Yip et al., “Cutting edge: endoplasmic reticulum stress licenses macrophages to produce mature IL-1 β in response to TLR4 stimulation through a caspase-8- and TRIF-dependent pathway,” *Journal of Immunology*, vol. 192, no. 5, pp. 2029–2033, 2014.
- [60] C. Veith, D. Neghabian, H. Luitel et al., “FHL-1 is not involved in pressure overload-induced maladaptive right ventricular remodeling and dysfunction,” *Basic Research in Cardiology*, vol. 115, no. 2, p. 17, 2020.
- [61] E. H. Moon, Y. H. Kim, P. N. Vu et al., “TMEM100 is a key factor for specification of lymphatic endothelial progenitors,” *Angiogenesis*, vol. 23, no. 3, pp. 339–355, 2020.
- [62] M. R. Hamczyk, R. Villa-Bellosta, V. Quesada et al., “Progerin accelerates atherosclerosis by inducing endoplasmic reticulum stress in vascular smooth muscle cells,” *EMBO Molecular Medicine*, vol. 11, no. 4, article e9736, 2019.
- [63] E. Di Pasquale and G. Condorelli, “Endoplasmic reticulum stress at the crossroads of progeria and atherosclerosis,” *EMBO Molecular Medicine*, vol. 11, no. 4, 2019.
- [64] Y. Wang, W. Wang, N. Wang, A. R. Tall, and I. Tabas, “Mitochondrial Oxidative Stress Promotes Atherosclerosis and Neutrophil Extracellular Traps in Aged Mice,” *Arteriosclerosis, Thrombosis, and Vascular Biology*, vol. 37, no. 8, pp. e99–e107, 2017.
- [65] C. Li, L. Li, M. Yang, L. Zeng, and L. Sun, “PACS-2: a key regulator of mitochondria-associated membranes (MAMs),” *Pharmacological Research*, vol. 160, article 105080, 2020.
- [66] C. Margadant, “Positive and negative feedback mechanisms controlling tip/stalk cell identity during sprouting angiogenesis,” *Angiogenesis*, vol. 23, no. 2, pp. 75–77, 2020.

Research Article

The Downregulation of ADAM17 Exerts Protective Effects against Cardiac Fibrosis by Regulating Endoplasmic Reticulum Stress and Mitophagy

Chang Guan,^{1,2} Hai-Feng Zhang ,^{1,2} Ya-Jing Wang,³ Zhi-Teng Chen,^{1,2} Bing-Qing Deng,¹ Qiong Qiu,¹ Si-Xu Chen,^{1,2} Mao-Xiong Wu,^{1,2} Yang-Xin Chen ,^{1,2} and Jing-Feng Wang ^{1,2}

¹Department of Cardiology, Sun Yat-sen Memorial Hospital, Sun Yat-sen University, Guangzhou, China

²Laboratory of Cardiac Electrophysiology and Arrhythmia in Guangdong Province, Guangzhou, China

³Department of Otolaryngology, Sun Yat-sen Memorial Hospital, Sun Yat-sen University, Guangzhou, China

Correspondence should be addressed to Yang-Xin Chen; chenyx39@mail.sysu.edu.cn and Jing-Feng Wang; wjingt@mail.sysu.edu.cn

Received 14 February 2021; Revised 27 March 2021; Accepted 9 April 2021; Published 6 May 2021

Academic Editor: Yun-dai Chen

Copyright © 2021 Chang Guan et al. This is an open access article distributed under the Creative Commons Attribution License, which permits unrestricted use, distribution, and reproduction in any medium, provided the original work is properly cited.

Background. A disintegrin and metalloproteinase 17 (ADAM17) is a transmembrane protein that is widely expressed in various tissues; it mediates the shedding of many membrane-bound molecules, involving cell-cell and cell-matrix interactions. We investigated the role of ADAM17 within mouse cardiac fibroblasts (mCFs) in heart fibrosis. **Methods.** mCFs were isolated from the hearts of neonatal mice. Effects of ADAM17 on the differentiation of mCFs towards myofibroblasts and their fibrotic behaviors following induction with TGF- β 1 were examined. The expression levels of fibrotic proteins, such as collagen I and α -SMA, were assessed by qRT-PCR analysis and western blotting. Cell proliferation and migration were measured using the CCK-8 and wound healing assay. To identify the target gene for ADAM17, the protein levels of the components of endoplasmic reticulum (ER) stress and the PINK1/Parkin pathway were assessed following ADAM17 silencing. The effects of ADAM17 silencing or treatment with thapsigargin, a key stimulator of acute ER stress, on mCFs proliferation, migration, and collagen secretion were also examined. **In vivo**, we used a mouse model of cardiac fibrosis established by left anterior descending artery ligation; the mice were administered oral gavage with a selective ADAM17 inhibitor (TMI-005) for 4 weeks after the operation. **Results.** We found that the ADAM17 expression levels were higher in fibrosis heart tissues and TGF- β 1-treated mCFs. The ADAM17-specific siRNAs decreased TGF- β 1-induced increase in the collagen secretion, proliferation, and migration of mCFs. Knockdown of ADAM17 reduces the activation of mCFs by inhibiting the ATF6 branch of ER stress and further activating mitophagy. Moreover, decreased ADAM17 expression also ameliorated cardiac fibrosis and improved heart function. **Conclusions.** This study highlights that mCF ADAM17 expression plays a key role in cardiac fibrosis by regulating ER stress and mitophagy, thereby limiting fibrosis and improving heart function. Therefore, ADAM17 downregulation, within the physiological range, could exert protective effects against cardiac fibrosis.

1. Introduction

Cardiac fibrosis is a common pathophysiological process that exists in various heart diseases such as myocardial infarction, hypertension, and cardiac hypertrophy, and it is characterized by excessive deposition of extracellular matrix (ECM) proteins [1, 2]. This process is a strategy to protect heart function in the early stage, and it can repair, replace, and strengthen the

severely or chronically damaged tissue. However, long-term excessive deposition of ECM will reduce the compliance of the ventricle and the contractile function of cardiomyocytes, eventually leading to heart failure and increasing mortality [3, 4]. It is an inappropriate transformation process of quiescent cardiac fibroblasts (CFs) to myofibroblasts (CMFs), leading to the disproportionate accumulation of ECM proteins [4–6]. Due to the clear association between cardiac fibrosis and its

adverse outcomes, understanding the mechanisms responsible for the pathogenesis of cardiac fibrosis and formulating new antifibrotic strategies for treating patients with heart diseases are issues requiring urgent attention.

A disintegrin and metalloproteases (ADAMs) is a newly discovered protein family in recent years. Numerous members of this family have been reported to be involved in the regulation of cardiovascular diseases [7, 8]. A disintegrin and metalloproteinase 17 (ADAM17), as one of the most well-studied proteins in the ADAMs family, is widely expressed in various tissues including the heart, kidney, liver, and lung. As a transmembrane protein, its main function is to cleave extracellular domains of various substrate proteins, such as TNF α , TNF receptors (TNFR1 and TNFR2), and several epidermal growth factor receptor (EGFR) ligands [9, 10]. The cells also contain a large amount of ADAM17, but the mechanism of its action remains unclear [11]. It plays an important role in biologic processes involving cell-cell and cell-matrix interactions. Many studies have shown that ADAM17 can participate in the regulation of the occurrence and development of tumors, inflammatory diseases, nervous system, and cardiovascular diseases. In the cardiovascular system, a short-term increase in ADAM17 expression after acute myocardial infarction can aggravate cardiac dysfunction [12]. The deficiency of ADAM17 in vascular smooth muscle cells can inhibit the progression of thoracic aortic aneurysms [13]. ADAM17 in blood vessels can aggravate angiotensin II-induced vascular remodeling and peritubular fibrosis [14, 15]. In fibrotic diseases, ADAM17 and connective tissue growth factor (CTGF) participate in the formation of pulmonary fibrosis [16]. The expression of ADAM17 is increased in glomerular sclerosis and interstitial fibrosis and correlated positively with the progression of renal fibrosis [17–19]. However, whether ADAM17 plays functional roles during the development of cardiac fibrosis is still unknown.

As important intracellular organelles, the endoplasmic reticulum (ER) and mitochondria are widely involved in the regulation of protein, lipid, and energy metabolism and maintain the normal function of cells. Many studies have shown that there is a physical and functional interaction between the ER and mitochondria. This interaction is involved in the regulation of atherosclerosis, myocardial hypertrophy, heart failure, and other cardiovascular diseases [20]. ER stress is a condition that is accelerated by the accumulation of unfolded/misfolded proteins after disturbances owing to a variety of physiological and pathological phenomena [21]. Mitophagy, i.e., selective mitochondrial degradation through autophagy, is a conserved cellular process used to eliminate damaged mitochondria. Under various pathological stimuli, ER stress and mitophagy are activated. ER stress leads to increased synthesis of molecular chaperones (such as GRP78) through three pathways (IRE1/XBP1s, PERK/ATF4, and ATF6), decreased protein synthesis, and increased degradation. Mitophagy degrades impaired mitochondria through the classic PINK1/Parkin pathway [22]. Excessive ER stress will aggravate abnormal Ca²⁺ and ROS regulation and further damage mitochondria, aggravate mitophagy, and eventually lead to cell death [21–23]. ER stress and mitophagy likely contribute to the development and progression of cardiovascular

diseases such as heart failure and atherosclerosis [24–26]. Furthermore, excessive ER stress and the absence of mitophagy both lead to the aggravation of cardiac fibrosis, and both of them are key mechanisms in cardiac fibrosis [27–30]. Recent studies have shown that ADAM17 can affect the progression of vascular remodeling, perivascular fibrosis, and differentiation and drug resistance of cancer cells through ER stress and mitophagy [14, 31]. However, the role of ADAM17, ER stress, and mitophagy in cardiac fibrosis remains unclear.

In this research, we speculated the potential effects of ADAM17 on cardiac fibrosis. To address this question, the present study examined the function of ADAM17 with ER stress and mitophagy in cardiac fibrosis. We found that reduction of ADAM17 expression is associated with beneficial effects against activation of mCFs by regulating the ATF6 branch of ER stress and the PINK1/Parkin pathway of mitophagy. Furthermore, inhibition of ADAM17 in mice could ameliorate left anterior descending artery (LAD) ligation-induced cardiac fibrosis and improve heart function.

2. Methods

2.1. Induction of Myocardial Infarction (MI) and Treatment. All animal care and experimental protocols were performed in accordance with the Institutional Animal Care and were approved by the Ethics Committee of the Sun Yat-sen University. Male C57BL/6 mice (6–8 weeks old, 20–25 g) were subjected to the induction of MI by LAD ligation, as described previously [32]. Briefly, the mice were anesthetized with sodium pentobarbital (intraperitoneal injection, 50 mg/kg; Merck) and mechanically ventilated using the HX-101E ventilator (Chengdu Tai Meng Software Ltd.). Their chests were opened through the 4th left intercostal space, and then, the LAD was ligated with 8-0 polyester sutures. Mice in the sham group were subjected to the same experimental procedures but without LAD constriction. The mice were randomly divided into four groups ($n = 6$ per group): control/MI groups receiving vehicle buffer (2% Tween 80 and 0.5% methylcellulose) by oral gavage twice daily and TMI-005/MI+TMI-005 groups receiving 10 mg/kg ADAM17 inhibitor (TMI-005, Glpbio, GC35377) by oral gavage twice daily. After 4 weeks of intragastric administration (endpoint), cardiac function was assessed by echocardiography analysis, and then, the hearts were harvested.

2.2. Isolation and Culture of CFs. First, mouse cardiac fibroblasts (mCFs) were isolated and cultured as described in a previous study [33]. mCFs were isolated from 1- to 3-day-old neonatal mice obtained from the Animal Centre of the Sun Yat-sen University. Briefly, the hearts of mice were quickly excised and digested with 0.1% trypsin/D-Hanks solution at 4°C with gentle rotation for 12 hours. Then, the hearts were digested with 0.8 mg/mL collagenase II/D-Hanks solution at 37°C for 10 minutes and were repeated 2–3 times. Cells were collected and suspended in Dulbecco's modified Eagle medium: Nutrient Mixture F12 (DMEM/F12, Gibco, Thermo Fisher Scientific) containing 10% fetal bovine serum. After plating at 37°C for 0.5 h, mCFs adhered onto the culture plates, and the nonadherent cells in the supernatant were

removed by washing with PBS. Then, the mCFs were cultured with DMEM/F12 containing 10% FBS (Invitrogen, Carlsbad) and 1% penicillin/streptomycin (Gibco, Thermo Fisher Scientific) at 37°C in humid air containing 5% CO₂, until they reached confluence; then, they were passaged further. The identity of mCFs was confirmed by immunofluorescence staining with vimentin. mCFs at the second or third passages were used in the subsequent experiments. After starvation in the serum-free medium for 12 h, the mCFs were treated with 5 ng/mL recombinant mouse TGF- β 1 protein (R&D Systems, #7666-MB) for 48 h.

2.3. Transfection Procedure and TGF- β 1 Administration. ADAM17-specific siRNAs were purchased from RiboBio (Guangzhou, China). mCFs were seeded on 6-well plates at 50–60% confluence before transfection. Each siADAM17 (50 nM) (Table s1) and Lipofectamine[®] RNAiMAX (Invitrogen) were mixed, incubated at room temperature for 10–15 min, and then added to the cell cultures. Twenty-four hours after transfection, the mCFs were treated with TGF- β 1 (5 ng/mL) for 48 h or thapsigargin (TG, 1 μ M, Sigma-Aldrich, T9033) for 24 h.

2.4. Wound Healing Assay. To verify the migration ability of the mCFs, a wound healing assay was performed. Transfected mCFs (2×10^5 cells/well) left untreated or those treated with TGF- β 1 or thapsigargin were seeded into 6-well plates and grown until subconfluence. A scratch was then created in each well using a 200 μ L pipette tip, and the wounded monolayers were washed twice with PBS to remove the cell debris and floating cells. The wounds were photographed at the beginning (time 0 h) and then after 24 h under an inverted microscope, and the width of the wound area was measured at the reference points ImageJ software.

2.5. CCK-8 Assay. The CCK-8 method was used to analyze the proliferation of mCFs according to the manufacturer's instructions. The mCFs, transfected with siADAM17 as described above, were seeded into 96-well plates at a density of 5×10^3 cells/well and treated with TGF- β 1 or thapsigargin for a total of 24, 48, and 72 hours, respectively. Then, 100 μ L of fresh medium containing 10 μ L CCK-8 (DOJINDO) was added into the wells, followed by incubation in the presence of 5% CO₂ at 37°C for 2 h; next, the absorbance readings of the samples were obtained at 450 nm using a microplate reader (Invitrogen).

2.6. Quantitative Real-Time RT-PCR. Total RNA was extracted from the mouse heart tissues or mCFs using the Trizol reagent (Invitrogen). A PrimeScript[™] RT Master Mix Kit (Takara Bio, RR036A) was used to reverse-transcribe 1 μ g of RNA into cDNA, as described previously [4]. Quantitative real-time polymerase chain reaction (qRT-PCR) was performed using the SYBR method (Takara Bio, RR420A) in a LightCycler[®] 96 Real-Time PCR System (Roche). The qRT-PCR analysis was performed using the primers listed in Table s2. Normalization of gene expression was achieved by comparing the expression of the target genes to that GAPDH in the corresponding samples.

2.7. Western Blotting. Total proteins were extracted from the mCFs or mouse heart tissues using a radio immunoprecipitation assay (RIPA) buffer (CST) containing protease and phosphatase inhibitors (Roche, 04906845001, 04693124001). The mitochondrial and cytosolic fractions were isolated from cells using a commercially available kit (Thermo Fisher Scientific, #89874) according to the manufacturer's instructions. Total protein or mitochondrial protein concentrations were measured using a BCA Protein Assay Kit (Pierce, Thermo Fisher Scientific, 23227). Equal amounts of the total protein samples were separated by 10% sodium dodecyl sulfate-polyacrylamide gel electrophoresis; the resultant bands were transferred to 0.2 μ m PVDF membranes (Millipore). Then, the membranes were blocked with 5% BSA diluted with tris-buffered saline tween-20 at room temperature for 1 h and incubated overnight at 4°C with the following primary antibodies: antibodies against collagen I (1:1000, Abcam), α -SMA (1:1000, Abcam), ADAM17 (1:1000, Abcam), Smad2/3 (1:1000, CST), p-Smad2/3 (1:1000, CST), p-PERK (1:1000, CST), ATF4 (1:1000, Abcam), p-IRE1 (1:1000, Abcam), XBP1s (1:1000, Abcam), ATF6 (1:1000, Proteintech), GRP78 (1:1000, Abcam), and GAPDH (1:1000, CST). They were then washed with TBST ($\times 3$) and incubated with horseradish peroxidase-conjugated secondary antibody (1:5000, CST) for 1 h at room temperature. Next, the membranes were washed with TBST ($\times 3$), followed by the detection of the protein bands using ECL reagents (Merck Millipore, WBULS050). The intensity of the protein bands was quantified using the ImageJ software and normalized to the intensity of GAPDH.

2.8. ADAM17 Enzymatic Activity Assay. The ADAM17 activity assay was performed using the InnoZyme TACE Activity Kit (Sigma-Aldrich, CBA042) following the manufacturer's protocol. The activity of ADAM17 was measured using an internally quenched fluorescent substrate, MCA-KPLGL-Dpa-AR-NH₂. The resultant fluorescence was measured at an excitation wavelength of 320 nm and an emission wavelength of 405 nm. The ADAM17 activity was expressed as relative fluorescence units per milligrams of protein.

2.9. Echocardiography. Echocardiography was performed to assess the left ventricular end systolic diameter (LVESD), left ventricular end diastolic diameter (LVEDD), left ventricular ejection fraction (LVEF), and left ventricular fractional shortening (LVFS) using a VisualSonics Echo System (Vevo 2100, VisualSonics, Inc.) equipped with a MicroScan Transducer (MS-400, 30 MHz, VisualSonics, Inc.). The mice were slightly anesthetized via inhalation of 1% isoflurane, and their heart rate was maintained at >400 bpm. The hearts' short axis views were obtained in B-mode and M-mode. The LVESD, LVEDD, LVEF, and LVFS were calculated from the M-mode measurements; the measurements represented the mean of three successive cardiac cycles, as described previously [34].

2.10. Masson's Trichrome Staining. The mouse hearts were dissected and fixed in 4% paraformaldehyde for 24 h; then,

they were embedded in paraffin and stained with Masson's trichrome stain, as previously described [3]. The area occupied by collagen was calculated using the ImageJ software. The percentage of fibrosis was measured using the following formula: (fibrotic areas/total left ventricular areas) \times 100%.

2.11. Statistical Analysis. All data are presented as the mean \pm SEM. Statistical analysis was performed using Student's *t*-test for the comparison of two groups and one-way ANOVA followed by Bonferroni test for the comparison of multiple groups, and the significance was set at $P < 0.05$. The statistical graphs were prepared using GraphPad Prism Software (version 7).

3. Results

3.1. ADAM17 is Upregulated in Fibrosis Heart Tissues and MCFs Treated with TGF- β 1. To determine the potential mechanistic link between ADAM17 and cardiac fibrosis *in vivo*, a murine model of MI was established using a previously described protocol. The expression levels of fibrotic proteins, such as collagen I and α -SMA, were increased in the MI group. Meanwhile, ADAM17 mRNA and protein levels were significantly higher in fibrosis hearts than in normal hearts (Figures 1(a) and 1(b)). *In vitro*, mCFs isolated from neonatal mice hearts were incubated with TGF- β 1 (5 ng/mL, for 48 h). The mRNA and protein levels of collagen I and α -SMA were increased, indicating that the mCFs were effectively differentiated into myofibroblasts. Consistent with our results in the fibrosis heart tissues, the ADAM17 expression levels were higher in TGF- β 1-treated mCFs than in those not subjected to TGF- β 1 stimulation (Figures 1(c) and 1(d)). Taken together, these data indicate that ADAM17 may be involved in the regulation of cardiac fibrosis and activation of mCFs.

3.2. ADAM17 Knockdown Attenuated TGF- β 1-Induced MCF Activation and the Upregulation of ECM Proteins. To further identify the important role of ADAM17 in activation of mCFs, the cells were transfected with ADAM17-specific siRNA or scramble siRNA as a negative control (NC) for 24 h before treatment; qRT-PCR was used to confirm the knockdown efficiency of ADAM17. We found that transfection with siRNA3 reduced the ADAM17 levels by nearly 80%, compared to those in the NC groups (Figure 2(a)). Following the TGF- β 1-induced activation of mCFs, the transcript and protein levels of the ECM protein collagen I, as well as those of the myofibroblast marker α -SMA, were increased. Further, siRNA3 successfully inhibited the expression of ADAM17, α -SMA, and collagen I (Figures 2(b) and 2(c)). Our data revealed that knockdown of ADAM17 not only inhibited mCF differentiation but also reduced the synthesis and secretion of collagen I. Next, we assessed the mCF migration and proliferation abilities using wound healing and CCK-8 assays, respectively. We found that TGF- β 1 significantly increased the proliferation and migration abilities of mCFs; the knockdown of ADAM17 partially reversed these phenomena (Figures 2(d) and 2(e)). Thus, our results suggested that ADAM17 enhances the collagen synthesis

and secretion, migration, and proliferation abilities of mCFs; that is, it promotes the activation of mCFs.

3.3. ADAM17 Regulates ER Stress and Mitophagy to Promote the Activation of MCFs. It is well-known that TGF- β 1 signal through the activation of Smad2/3 (canonical pathway) to promote mCF differentiation, migration, and proliferation and the deposition of ECM proteins during the formation of pathological cardiac fibrosis [35, 36]. Therefore, we investigated the effects of ADAM17 on the TGF- β 1/Smad2/3 pathway in mCFs. Western blotting analysis revealed that the phosphorylation levels of Smad2/3 were increased significantly after stimulation with TGF- β 1, but they were unaltered between the NC and ADAM17 knockdown groups. These data indicated that ADAM17 had no effect on the canonical Smad2/3 pathway. In addition, TGF- β 1 is known to trigger an increase in ER stress and the unfolded protein response. After the TGF- β 1-induced activation of mCFs, the downstream signaling molecules associated with ER stress, phosphorylated PERK, and IRE1 (p-PERK and p-IRE1), ATF4, XBP1s, ATF6, and GRP78 were markedly upregulated. Then, we found that the activity of the ATF6 was further reduced after the silencing of ADAM17, compared to the case in the NC groups (Figure 3(a)). These results indicate that the ATF6, but not the PERK/ATF4 and IRE1/XBP1 pathways associated with ER stress, may mediate ADAM17-induced activation of mCFs.

To further investigate whether the ATF6 is involved in the activation of mCFs, we employ thapsigargin (TG), a key stimulator of acute ER stress. Compared with those in the TGF- β 1 treatment groups, the administration of the TGF- β 1 and TG groups not only increased the expression levels of ATF6 and GRP78, as expected, but also upregulated the expression levels of collagen I and α -SMA. However, after adding TG, there was no significant difference in the expression levels of collagen I, α -SMA, ATF6, and GRP78 between the siRNA3 group and the NC group (Figure 3(b)). Next, migration and proliferation abilities of mCFs also showed similar changes, according to the results of the wound healing and CCK-8 assays, respectively. Knockdown of ADAM17 inhibited mCF migration and proliferation abilities, but this difference disappeared after using TG (Figures 3(c) and 3(d)). Collectively, these data suggested that the decreased expression of ADAM17 protects against mCF activation via the inhibition of the ATF6 in ER stress.

A recent study reported that ADAM17 and mitophagy are involved in the occurrence and development of tumors [31]. To clarify whether mitophagy is involved in the regulation of mCF activation by ADAM17, we observed the mitophagy response in the process of mCF activation. PINK1/Parkin pathway acts as a classical regulation pathway in mitophagy and plays an important role in cardiac fibrosis [26, 37]. We found that the protein levels of PINK1 and Parkin were enhanced after TGF- β 1 stimulation, and their protein levels were further increased after the knocking down ADAM17 (Figure 3(e)). These data showed that ADAM17 may regulate mCF activation by affecting mitophagy.

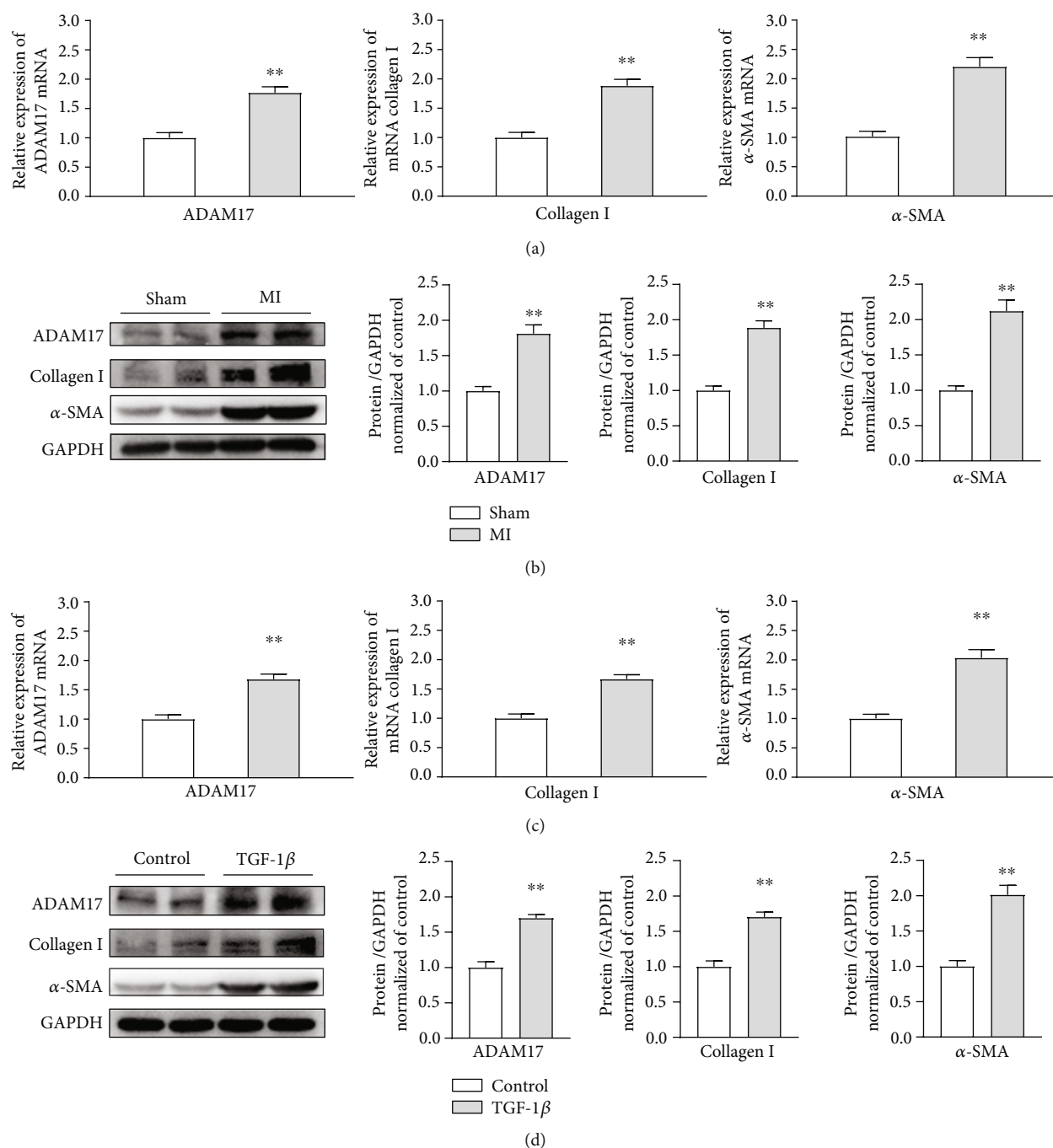


FIGURE 1: ADAM17 is upregulated in fibrosis heart tissues and mCFs treated with TGF- β 1. Mice were divided into two groups: sham and MI. (a, b) The mRNA and protein levels of ADAM17, collagen I, and α -SMA in fibrosis heart tissues ($n = 4$). (c, d) mCFs were divided into two groups: control and TGF- β 1 treatment (5 ng/mL, 48 h). The mRNA and protein levels of ADAM17, collagen I, and α -SMA in the process of mCF activation ($n = 5$). Data in (a–d) are expressed as mean \pm SEM. * indicates $P < 0.05$ and ** indicates $P < 0.01$ vs. sham or control groups.

3.4. Inhibition of ADAM17 with TMI-005 Reduced the Degree of Post-MI Fibrosis and Enhanced Cardiac Function in Vivo. To assess whether ADAM17 mediates post-MI cardiac fibrosis *in vivo*, we employed TMI-005, a pharmacological selective inhibitor of ADAM17. The 8-week-old mice were subjected to MI via permanent LAD ligation and then administered 10 mg/kg TMI-005 by oral gavage twice daily for 4 weeks, as depicted in Figure 4(a). We performed echo-

cardiography and Masson's trichrome staining analyses to assess collagen deposition and cardiac function, respectively. After TMI-005 treatment alone for 4 weeks, ADAM17 activity was remarkably inhibited in the heart, and there was no significant difference in collagen deposition and cardiac function, compared to those in the control group (Figures 4(b)–4(d)). Then, we observed the heart function and degree of fibrosis in the mice post-MI after they were

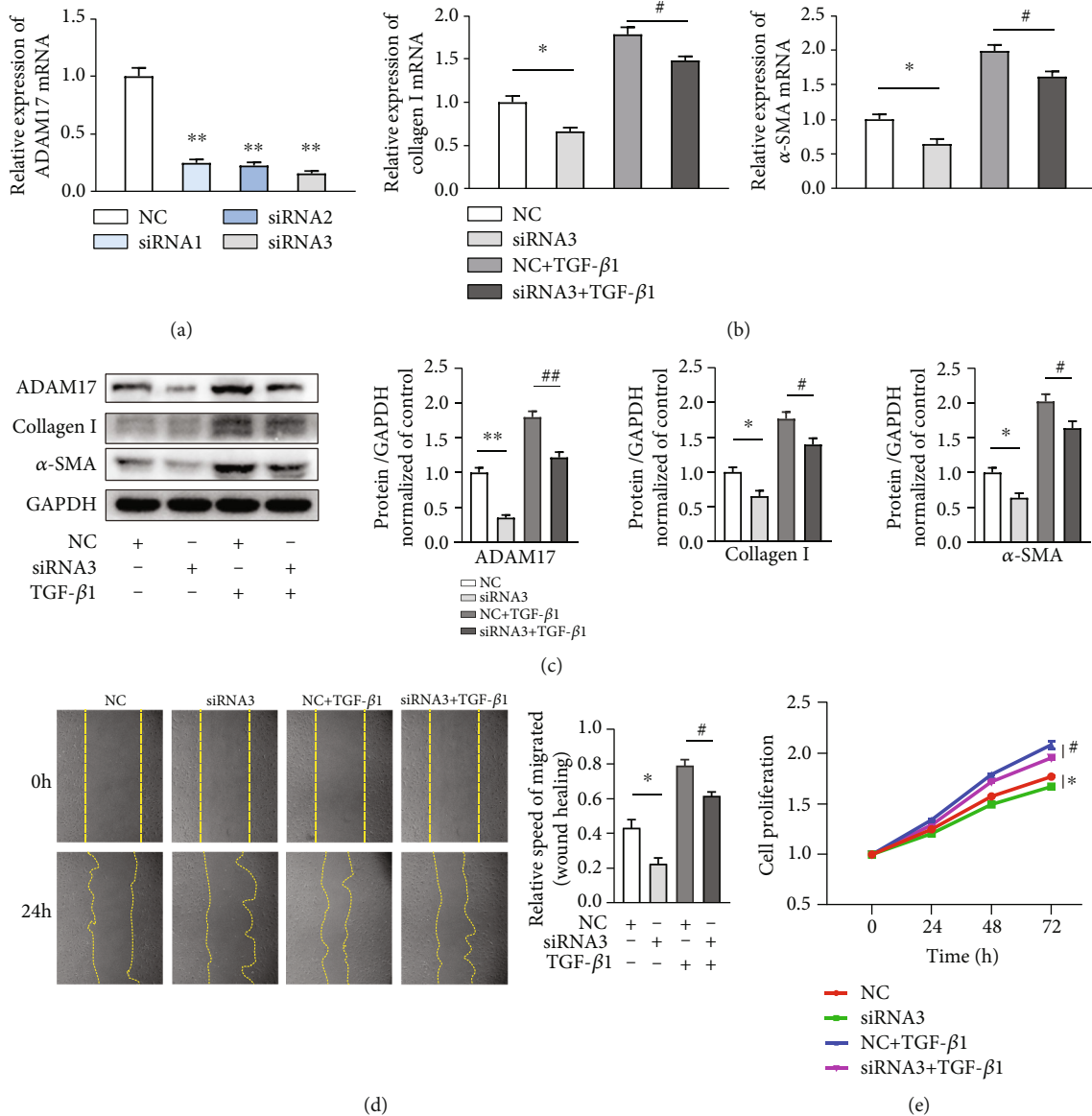


FIGURE 2: ADAM17 knockdown attenuated TGF- β 1-induced mCF activation and the upregulation of ECM proteins. (a) The mRNA expression of ADAM17 after three siRNA chain transfections ($n=3$); siRNA3 was the most efficient chain. (b, c) NC or siRNA3 transfection in the presence or absence of TGF- β 1 (5 ng/mL, 48 h). The mRNA and protein levels of ADAM17, collagen I, and α -SMA in activated mCFs after transfection with NC or siRNA3 ($n=5$). (d) The migration of mCFs (determined by the areas of cells protruding from the wound border) after transduction with NC or siRNA3 ($n=3$). (e) The proliferation of mCFs was assayed using CCK-8 ($n=5$). Data in (a–e) are expressed as mean \pm SEM. * indicates $P < 0.05$, and ** indicates $P < 0.01$ vs. the NC group; # indicates $P < 0.05$, and ## indicates $P < 0.01$ vs. the NC+TGF- β 1 group.

treated with TMI-005 for 28 days. The Masson's trichrome staining results showed that the ADAM17 inhibitor prevented MI-associated increase in the area of cardiac fibrosis (Figure 4(e)). In Figure 4(f), compared with the MI group, although the TMI-005 administration group had no obvious difference in LVESD and LVEDD, the LVEF and LVFS were improved. And the western blotting results also showed that the levels of the fibrotic proteins collagen I and α -SMA were reduced in the hearts of the mice treated with the ADAM17 inhibitor (Figure 4(g)). Thus, the ADAM17 inhibitor TMI-005 notably improved cardiac function after MI. These find-

ings support the speculation that ADAM17 inhibition exerts protective effects on fibrosis post-MI and cardiac function.

4. Discussion

Despite the rising prevalence and the adverse prognosis associated with cardiac fibrosis in both men and women, there is still no effective treatment for this condition. Although ADAM17 exerts potential regulatory effects in cardiovascular diseases, including cardiac hypertrophy, coronary microvascular dysfunction, and thoracic aortic aneurysm [12, 13, 15,

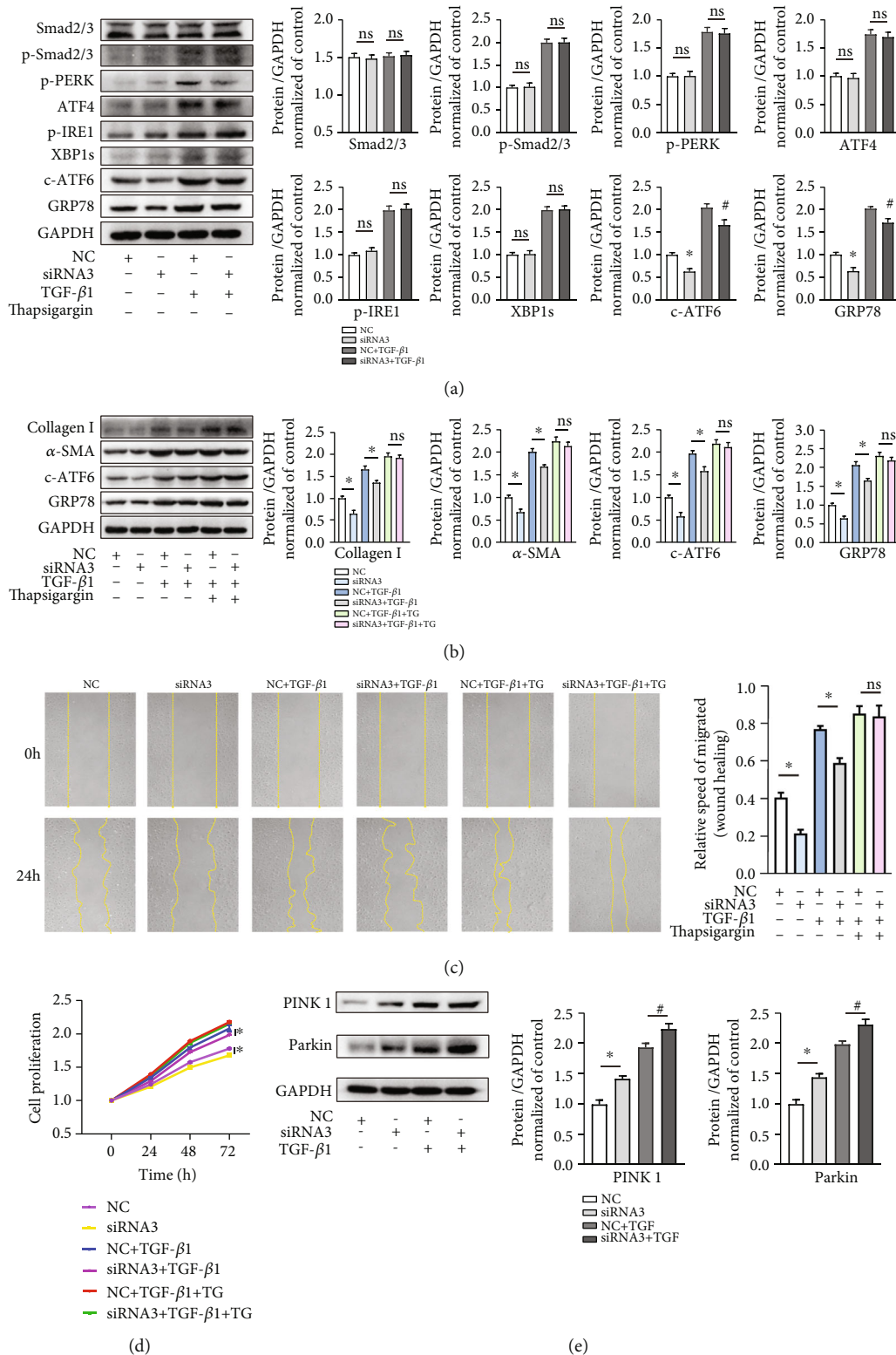


FIGURE 3: ADAM17 regulates ER stress and mitophagy to promote the activation of mCFs. (a) Protein expressions of Smad2/3, p-Smad2/3, p-PERK, ATF4, p-IRE1, XBP1s, c-ATF6, and GRP78 in mCFs with NC or siRNA3 transfection in the presence or absence of TGF- β 1 ($n = 5$). (b) The protein levels of the ER stress branch, the ATF6 and GRP78, after transfection of NC or siRNA3 in the presence or absence of TGF- β 1 or TG ($n = 5$). (c, d) Wound healing and CCK-8 assays for migration and proliferation in mCFs transfected with NC or siRNA3 in the presence or absence of TGF- β 1 or TG ($n = 5$). (e) Protein expression of PINK1 and Parkin with NC or siRNA3 transfection in the presence or absence of TGF- β 1 in mCFs ($n = 5$). Data in (a–e) are expressed as mean \pm SEM. ns: not statistically significant; * indicates $P < 0.05$, and ** indicates $P < 0.01$ vs. the NC or NC+TGF- β 1 groups.

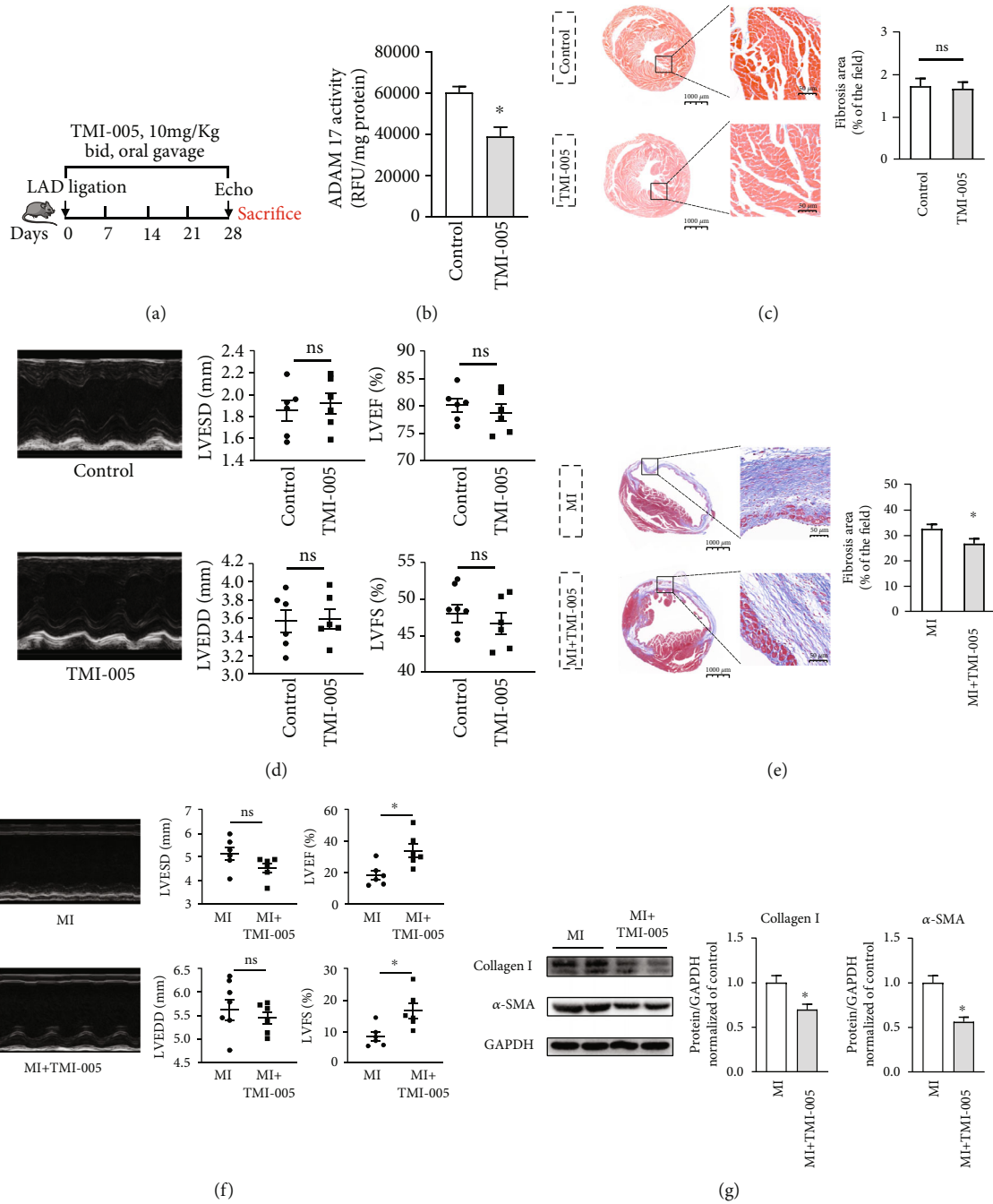


FIGURE 4: Inhibition of ADAM17 with TMI-005 reduced the degree of post-MI fibrosis and enhanced cardiac function *in vivo*. C57BL/6 mice were randomly divided into 4 groups, including control, TMI-005, MI, and MI treated with TMI-005. MI groups had left anterior descending ligation for 28 days to induced cardiac fibrosis. (a) Schema of the TMI-005 treatment protocol. (b) ADAM 17 activity in heart tissues was determined by measuring cleavage of the internally quenched fluorogenic substrate MCA-KPLGLDpa-AR-NH2 ($n = 6$). (c, d) In the control and TMI-005 groups, Masson's trichrome staining and M-mode images were used to assess the collagen deposition and cardiac function. LVESD, LVEDD, LVEF, and LVFS were quantified via echocardiography. (e, f) In the MI and MI treated with TMI-005 groups, Masson's trichrome staining and M-mode images were used to assess the degree of fibrosis and cardiac function. LVESD, LVEDD, LVEF, and LVFS were quantified via echocardiography. (g) Collagen I and α -SMA expression levels were quantified using western blotting. $n = 6$ in each group. Data in (a–g) are expressed as mean \pm SEM. * indicates $P < 0.05$, and ** indicates $P < 0.01$ vs. the control or MI groups.

38–40], its precise function in cardiac fibrosis remains unknown. In this study, we demonstrate the key role of ADAM17 in mCF activation and heart fibrosis progression, which can provide a new direction for antifibrosis therapies. We first found that ADAM17 was upregulated in RNA and

protein levels in both fibrosis heart tissue and activated mCFs. To verify the role of ADAM17 in fibrosis, we transfected mCFs with specific siRNA to knock down the expression of ADAM17; we found that silencing of ADAM17 in the mCFs further prevented the deposition of ECM proteins and

abrogated the TGF- β 1-induced increase in the proliferation and migration abilities *in vitro*. Consistent with existing studies in other systems, increased expression of ADAM17 can promote lung and kidney fibrosis [41, 42]. Therefore, we speculate that the upregulated expression of ADAM17 in cardiac fibrosis is harmful to mCFs.

ADAM17 is well known as a membrane-bound enzyme that can regulate growth and development by mediating the catalytic shedding of various growth factors and cytokines. However, an immunohistochemical study found that most of the active form of ADAM17 were also localized in the cellular perinuclear region, with a small amount present in the plasma membrane [11]. Whether the ADAM17 in the cytoplasm affects the activation of mCFs is still unclear. The major finding of the present study is that the ATF6 branch of ER stress contributes to the development of ADAM17-related cardiac fibrosis. As we know, *in vitro* and *in vivo* evidences have shown that the TGF- β 1-induced increase in ECM protein synthesis occurs mainly through the canonical Smad2/3 pathway [35, 36]. The present study showed that the downregulation of ADAM17 via siRNAs further alleviated mCF activation via the ATF6 branch, but not the PERK/ATF4, IRE1/XBP1s, and canonical Smad2/3 pathway. Interestingly, a recent study also found that vascular ADAM17 is indirectly related to ER stress with regard to regulating Ang II-induced cardiovascular remodeling [15]. Based on the observations of the present study, we suggest that the downregulation of ADAM17 attenuates the degree of mCF activation by inhibiting the ATF6 branch of ER stress. However, the specific mechanism between ATF6 and ADAM17 is still unclear and needs further study.

Mitophagy is essential for the clearance of dysfunctional mitochondria to maintain the mitochondrial integrity; dysregulation of mitophagy is associated with many cardiovascular diseases [26]; the absence of mitophagy leads to the aggravation of cardiac fibrosis [43]. It is regulated through multiple pathways, and the most well studied in the cardiovascular system is the canonical PINK1/Parkin pathway. Enhanced Pink/Parkin-mediated mitophagy can decrease the degree of fibrosis, as well as improved cardiac function, and stabilize the microvascular network [30]. Other reports demonstrate that the PINK1/Parkin pathway involved in heart repair following MI [37]. Our study showed that ADAM17 affects mitophagy to regulate the activation of mCFs. Consistent with previous studies, we found that the knockdown of ADAM17 reduced the degree of mCF activation by further activating the PINK1/Parkin pathway. However, the specific mechanism between mitophagy and ADAM17 is still unclear and needs further study.

Numerous studies have shown that there is a physical and functional interaction between the ER and mitochondria, and this interaction is involved in the regulation of cardiovascular diseases. Excessive ER stress will aggravate abnormal Ca²⁺ and ROS regulation, further damage mitochondria, exacerbate dysregulation of mitophagy, lead to cell death, and eventually promote cardiac fibrosis [21–23]. Bueno et al. found that in aging lung epithelial cells, PINK1 can be activated by ER stress, which can damage mitochondrial function and aggravate pulmonary fibrosis [44]. When

Zhang et al. studied brain tissue ischemia-reperfusion injury, they also found that moderate ER stress can activate mitophagy through ATF4 to protect the tissues [45]. In a study of pulmonary arterial hypertension, Dromparis et al. found that ATF6 produced by ER stress in pulmonary artery smooth muscle cells can improve mitochondrial function by reducing abnormal ER and mitochondrial Ca²⁺ transfer and inhibiting key calcium-sensitive mitochondrial enzymes [23]. All the above studies suggest that there is a complex relationship between ER stress and mitophagy. This study is the first to indicate that ADAM17, ER stress, and mitophagy play an important role in the regulation of cardiac fibrosis, but the specific mechanism between them requires further study.

Since ADAM17 was discovered in 1997, many inhibitors have been developed that work through the following mechanisms: (1) inhibition of ADAM17 expression and induction, (2) inhibition of ADAM17 maturation, (3) inhibition of ADAM17 activation, (4) inhibition at the active site by small molecules, (5) inhibitory prodomains, and (6) inhibition of substrate recognition. Among the above inhibitors, most of them were developed in the early stage, had poor targeting, and were only used *in vitro*, while some of them used in the mouse had been proved to damage in other organs [46–48]. Recently, a phase II trial with TMI-5 for treatment of rheumatoid arthritis showed no toxicity of this compound [49]. Therefore, we chose TMI-005 as the inhibitor *in vivo*. In this study, we used a cardiac fibrosis model established via LAD ligation for 28 days; decreased heart function and collagen deposition are common features of this model. We administered TMI-005 to the mice by oral gavage daily to inhibit ADAM17 in their heart tissues. Continuous oral ADAM17 inhibitors can markedly inhibit the activity of ADAM17 and do not affect the collagen deposition and cardiac function in normal hearts. In cardiac fibrosis models, inhibiting ADAM17 expression can alleviate cardiac fibrosis and improve cardiac function. This phenomenon may be due to the fact that ADAM17 is not the main molecule regulating ECM deposition and cardiac function under a physiological state. Collectively, our *in vivo* and *in vitro* experiments revealed that the deficiency of ADAM17 inhibited the activation of mCFs, protected against cardiac fibrosis, and improved heart function.

5. Conclusion

Our indirect evidence indicates that ADAM17 plays a key role in cardiac fibrosis. Knockdown of ADAM17 inhibits the activation of cardiac fibroblasts by regulating the ATF6 branch of ER stress and the PINK1/Parkin pathway of mitophagy. Inhibition of ADAM17 is associated with beneficial effects of against post-MI cardiac fibrosis and improving heart function. These data provide insights into novel mechanisms with potential treatment strategies for cardiac fibrosis.

Data Availability

The data used to support the findings of this study are available from the corresponding author upon request.

Conflicts of Interest

The authors declare no conflict of interest.

Authors' Contributions

CG and HFZ contributed to the conception and design of the experiments. CG, HFZ, YJW, ZTC, BQD, QQ, SXC, and WMX collected, analyzed, and interpreted data and drafted and revised the manuscript. CG, HFZ, and YJW contributed to the analysis and interpretation of data and drafting and revising the manuscript. All authors approved the manuscript and agree to be accountable for all aspects of the work. Chang Guan, Hai-Feng Zhang, and Ya-Jing Wang contributed equally to this work.

Acknowledgments

This work was supported by grants from the National Natural Science Foundation of China to Hai-Feng Zhang (Grant nos. 81300071 and 81870334), Jing-Feng Wang (Grant nos. 81570213 and 81870170), Yang-Xin Chen (Grant nos. 81770229 and 81970200), Bing-Qing Deng (Grant no. 81700261), and Qiong Qiu (Grant no. 81700359); the Guangdong Basic and Applied Basic Research Foundation to Hai-Feng Zhang (Grant no. 2020A151501886) and Mao-Xiong Wu (Grant no. 2019A1515110129); the Natural Science Foundation of Guangdong Province of China to Yang-Xin Chen (Grant no. 2016A030313263); and the Science and Technology Program of Guangzhou City of China to Yang-Xin Chen (Grant no. 201707010206) and Jing-Feng Wang (Grant no. 201803040010). All experiments were performed in the Laboratory of Cardiac Electrophysiology and Arrhythmia, Department of Cardiology, Sun Yat-sen Memorial Hospital.

Supplementary Materials

Table s1: sequences of siRNAs. Table s2: sequences of primers. (*Supplementary Materials*)


References

- [1] M. Disertori, M. Masè, and F. Ravelli, "Myocardial fibrosis predicts ventricular tachyarrhythmias," *Trends in Cardiovascular Medicine*, vol. 27, no. 5, pp. 363–372, 2017.
- [2] C. Jellis, J. Martin, J. Narula, and T. H. Marwick, "Assessment of nonischemic myocardial fibrosis," *Journal of the American College of Cardiology*, vol. 56, no. 2, pp. 89–97, 2010.
- [3] D. C. Rockey, P. D. Bell, and J. A. Hill, "Fibrosis—a common pathway to organ injury and failure," *The New England Journal of Medicine*, vol. 372, no. 12, pp. 1138–1149, 2015.
- [4] M. Sweeney, B. Corden, and S. A. Cook, "Targeting cardiac fibrosis in heart failure with preserved ejection fraction: mirage or miracle?," *EMBO Molecular Medicine*, vol. 12, no. 10, article e10865, 2020.
- [5] N. G. Frangogiannis, "Cardiac fibrosis: cell biological mechanisms, molecular pathways and therapeutic opportunities," *Molecular Aspects of Medicine*, vol. 65, pp. 70–99, 2019.
- [6] J. G. Travers, F. A. Kamal, J. Robbins, K. E. Yutzey, and B. C. Blaxall, "Cardiac fibrosis: the fibroblast awakens," *Circulation Research*, vol. 118, no. 6, pp. 1021–1040, 2016.
- [7] K. Reiss and S. Bhakdi, "The plasma membrane: penultimate regulator of ADAM sheddase function," *Biochimica et Biophysica Acta (BBA) - Molecular Cell Research*, vol. 1864, no. 11, pp. 2082–2087, 2017.
- [8] N. Saha, D. Robev, J. P. Himanen, and D. B. Nikolov, "ADAM proteases: emerging role and targeting of the non-catalytic domains," *Cancer Letters*, vol. 467, pp. 50–57, 2019.
- [9] J. Grötzinger, I. Lorenzen, and S. Düsterhöft, "Molecular insights into the multilayered regulation of ADAM17: the role of the extracellular region," *Biochimica et Biophysica Acta (BBA) - Molecular Cell Research*, vol. 1864, no. 11, pp. 2088–2095, 2017.
- [10] T. Kawai, K. J. Elliott, R. Scalia, and S. Eguchi, "Contribution of ADAM17 and related ADAMs in cardiovascular diseases," *Cellular and Molecular Life Sciences*, 2021.
- [11] J. Schlöndorff, J. D. Becherer, and C. P. Blobel, "Intracellular maturation and localization of the tumour necrosis factor α convertase (TACE)," *Biochemical Journal*, vol. 347, no. 1, pp. 131–138, 2000.
- [12] D. Y. Zheng, J. Zhao, J. M. Yang, M. Wang, and X. T. Zhang, "Enhanced ADAM17 expression is associated with cardiac remodeling in rats with acute myocardial infarction," *Life Sciences*, vol. 151, pp. 61–69, 2016.
- [13] M. Shen, M. Hu, P. W. M. Fedak, G. Y. Oudit, and Z. Kassiri, "Cell-specific functions of ADAM17 regulate the progression of thoracic aortic aneurysm," *Circulation Research*, vol. 123, no. 3, pp. 372–388, 2018.
- [14] T. Takayanagi, T. Kawai, S. J. Forrester et al., "Role of epidermal growth factor receptor and endoplasmic reticulum stress in vascular remodeling induced by angiotensin II," *Hypertension*, vol. 65, no. 6, pp. 1349–1355, 2015.
- [15] T. Takayanagi, S. J. Forrester, T. Kawai et al., "Vascular ADAM17 as a novel therapeutic target in mediating cardiovascular hypertrophy and perivascular fibrosis induced by angiotensin II," *Hypertension*, vol. 68, no. 4, pp. 949–955, 2016.
- [16] H. Y. Chen, C. H. Lin, and B. C. Chen, "ADAM17/EGFR-dependent ERK activation mediates thrombin-induced CTGF expression in human lung fibroblasts," *Experimental Cell Research*, vol. 370, no. 1, pp. 39–45, 2018.
- [17] E. Kefaloyianni, M. L. Muthu, J. Kaeppeler et al., "ADAM17 substrate release in proximal tubule drives kidney fibrosis," *JCI Insight*, vol. 1, no. 13, 2016.
- [18] G. M. Mulder, W. B. W. H. Melenhorst, J. W. A. M. Celie et al., "ADAM17 up-regulation in renal transplant dysfunction and non-transplant-related renal fibrosis," *Nephrology, Dialysis, Transplantation*, vol. 27, no. 5, pp. 2114–2122, 2012.
- [19] V. Palau, J. Pascual, M. J. Soler, and M. Riera, "Role of ADAM17 in kidney disease," *American Journal of Physiology. Renal Physiology*, vol. 317, no. 2, pp. F333–F342, 2019.
- [20] P. Gao, Z. Yan, and Z. Zhu, "Mitochondria-associated endoplasmic reticulum membranes in cardiovascular diseases," *Frontiers in Cell and Development Biology*, vol. 8, article 604240, 2020.
- [21] M. Q. Liu, Z. Chen, and L. X. Chen, "Endoplasmic reticulum stress: a novel mechanism and therapeutic target for cardiovascular diseases," *Acta Pharmacologica Sinica*, vol. 37, no. 4, pp. 425–443, 2016.

- [22] M. Z. Springer and K. F. Macleod, "In brief: Mitophagy: mechanisms and role in human disease," *The Journal of Pathology*, vol. 240, no. 3, pp. 253–255, 2016.
- [23] P. Dromparis, R. Paulin, T. H. Stenson, A. Haromy, G. Sutendra, and E. D. Michelakis, "Attenuating endoplasmic reticulum stress as a novel therapeutic strategy in pulmonary hypertension," *Circulation*, vol. 127, no. 1, pp. 115–125, 2013.
- [24] X. Chen, X. Guo, Q. Ge, Y. Zhao, H. Mu, and J. Zhang, "ER stress activates the NLRP3 inflammasome: a novel mechanism of atherosclerosis," *Oxidative Medicine and Cellular Longevity*, vol. 2019, Article ID 3462530, 18 pages, 2019.
- [25] C. D. Ochoa, R. F. Wu, and L. S. Terada, "ROS signaling and ER stress in cardiovascular disease," *Molecular Aspects of Medicine*, vol. 63, pp. 18–29, 2018.
- [26] C. Vásquez-Trincado, I. García-Carvajal, C. Pennanen et al., "Mitochondrial dynamics, mitophagy and cardiovascular disease," *The Journal of Physiology*, vol. 594, no. 3, pp. 509–525, 2016.
- [27] M. Galán, M. Kassin, S. K. Choi et al., "A novel role for epidermal growth factor receptor tyrosine kinase and its downstream endoplasmic reticulum stress in cardiac damage and microvascular dysfunction in type 1 diabetes mellitus," *Hypertension*, vol. 60, no. 1, pp. 71–80, 2012.
- [28] A. Hoshino, Y. Okawa, M. Ariyoshi et al., "Cytosolic p53 inhibits Parkin-mediated mitophagy and promotes mitochondrial dysfunction in the mouse heart," *Nature Communications*, vol. 4, no. 1, 2013.
- [29] Y. Liu, J. Wang, S. Y. Qi et al., "Reduced endoplasmic reticulum stress might alter the course of heart failure via caspase-12 and JNK pathways," *The Canadian Journal of Cardiology*, vol. 30, no. 3, pp. 368–375, 2014.
- [30] T. Wei, G. Huang, J. Gao et al., "Sirtuin 3 deficiency accelerates hypertensive cardiac remodeling by impairing angiogenesis," *Journal of the American Heart Association*, vol. 6, no. 8, 2017.
- [31] P. P. Naik, S. Mukhopadhyay, P. K. Panda et al., "Autophagy regulates cisplatin-induced stemness and chemoresistance via the upregulation of CD44, ABCB1 and ADAM17 in oral squamous cell carcinoma," *Cell Proliferation*, vol. 51, no. 1, 2018.
- [32] L. Tao, Y. Bei, P. Chen et al., "Crucial role of miR-433 in regulating cardiac fibrosis," *Theranostics*, vol. 6, no. 12, pp. 2068–2083, 2016.
- [33] J. Soppert, S. Kraemer, C. Beckers et al., "Soluble CD74 reroutes MIF/CXCR4/AKT-mediated survival of cardiac myofibroblasts to necroptosis," *Journal of the American Heart Association*, vol. 7, no. 17, article e009384, 2018.
- [34] H. Y. Fu, S. Sanada, T. Matsuzaki et al., "Chemical endoplasmic reticulum chaperone alleviates doxorubicin-induced cardiac dysfunction," *Circulation Research*, vol. 118, no. 5, pp. 798–809, 2016.
- [35] M. Bujak, G. Ren, H. J. Kweon et al., "Essential role of Smad 3 in infarct healing and in the pathogenesis of cardiac remodeling," *Circulation*, vol. 116, no. 19, pp. 2127–2138, 2007.
- [36] H. Khalil, O. Kanisicak, V. Prasad et al., "Fibroblast-specific TGF- β -Smad 2/3 signaling underlies cardiac fibrosis," *The Journal of Clinical Investigation*, vol. 127, no. 10, pp. 3770–3783, 2017.
- [37] H. Qiao, H. Ren, H. du, M. Zhang, X. Xiong, and R. Lv, "Liraglutide repairs the infarcted heart: the role of the SIRT1/Parkin/mitophagy pathway," *Molecular Medicine Reports*, vol. 17, no. 3, pp. 3722–3734, 2018.
- [38] H. Dou, A. Feher, A. C. Davila et al., "Role of adipose tissue endothelial ADAM17 in age-related coronary microvascular dysfunction," *Arteriosclerosis, Thrombosis, and Vascular Biology*, vol. 37, no. 6, pp. 1180–1193, 2017.
- [39] Y. Xie, A. Ma, B. Wang et al., "Rare mutations of ADAM17 from TOFs induce hypertrophy in human embryonic stem cell-derived cardiomyocytes via HB-EGF signaling," *Clinical Science (London, England)*, vol. 133, no. 2, pp. 225–238, 2019.
- [40] C. G. Zhai, Y. Y. Xu, Y. Y. Tie et al., "DKK3 overexpression attenuates cardiac hypertrophy and fibrosis in an angiotensin-perfused animal model by regulating the ADAM17/ACE2 and GSK-3 β / β -catenin pathways," *Journal of Molecular and Cellular Cardiology*, vol. 114, pp. 243–252, 2018.
- [41] E. Kefaloyianni, M. R. Keerthi Raja, J. Schumacher et al., "Proximal tubule-derived amphiregulin amplifies and integrates profibrotic EGF receptor signals in kidney fibrosis," *J Am Soc Nephrol*, vol. 30, no. 12, pp. 2370–2383, 2019.
- [42] M. Stolarczyk and B. J. Scholte, "The EGFR-ADAM17 axis in chronic obstructive pulmonary disease and cystic fibrosis lung pathology," *Mediators of Inflammation*, vol. 2018, Article ID 1067134, 22 pages, 2018.
- [43] A. A. Gibb, M. P. Lazaropoulos, and J. W. Elrod, "Myofibroblasts and fibrosis: mitochondrial and metabolic control of cellular differentiation," *Circulation Research*, vol. 127, no. 3, pp. 427–447, 2020.
- [44] M. Bueno, J. Brands, L. Voltz et al., "ATF3 represses PINK1 gene transcription in lung epithelial cells to control mitochondrial homeostasis," *Aging Cell*, vol. 17, no. 2, article e12720, 2018.
- [45] X. Zhang, Y. Yuan, L. Jiang et al., "Endoplasmic reticulum stress induced by tunicamycin and thapsigargin protects against transient ischemic brain injury: involvement of PARK2-dependent mitophagy," *Autophagy*, vol. 10, no. 10, pp. 1801–1813, 2014.
- [46] P. R. Murumkar, R. Giridhar, and M. R. Yadav, "Novel methods and strategies in the discovery of TACE inhibitors," *Expert Opin Drug Discov*, vol. 8, no. 2, pp. 157–181, 2013.
- [47] D. Drey Mueller and A. Ludwig, "Considerations on inhibition approaches for proinflammatory functions of ADAM proteases," *Platelets*, vol. 28, no. 4, pp. 354–361, 2017.
- [48] M. L. Moss and D. Minond, "Recent advances in ADAM17 research: a promising target for cancer and inflammation," *Mediators of Inflammation*, vol. 2017, Article ID 9673537, 21 pages, 2017.
- [49] M. M. Thabet and T. W. Huizinga, "Drug evaluation: apratastat, a novel TACE/MMP inhibitor for rheumatoid arthritis," *Current Opinion in Investigational Drugs*, vol. 7, no. 11, pp. 1014–1019, 2006.

Research Article

Mitochondrial Dysfunction Contributes to Aging-Related Atrial Fibrillation

Chuanbin Liu,^{1,2} Jing Bai,¹ Qing Dan,³ Xue Yang,^{2,4} Kun Lin,³ Zihao Fu,¹ Xu Lu,¹ Xiaoye Xie,^{1,2} Jianwei Liu,^{2,4} Li Fan,^{2,4} and Yang Li³ 

¹Medical School of Chinese PLA, Beijing, China

²National Clinical Research Center for Geriatric Disease, Chinese PLA General Hospital, Beijing, China

³Department of Cardiology, The Sixth Medical Center, Chinese PLA General Hospital, Beijing, China

⁴The Second Medical Center, Chinese PLA General Hospital, Beijing, China

Correspondence should be addressed to Yang Li; liyangbsh@163.com

Received 28 January 2021; Revised 4 April 2021; Accepted 15 April 2021; Published 29 April 2021

Academic Editor: Sang-Bing Ong

Copyright © 2021 Chuanbin Liu et al. This is an open access article distributed under the Creative Commons Attribution License, which permits unrestricted use, distribution, and reproduction in any medium, provided the original work is properly cited.

The incidence of atrial fibrillation (AF) increases with age, and telomere length gradually shortens with age. However, whether telomere length is related to AF is still inconclusive, and the exact mechanism by which aging causes the increased incidence of AF is still unclear. We hypothesize that telomere length is correlated with aging-related AF and that mitochondrial dysfunction plays a role in this. This research recruited 96 elderly male patients with AF who were admitted to the Second Medical Center of Chinese PLA General Hospital from April to October 2018. After matching by age and gender, 96 non-AF elderly male patients who were admitted to the hospital for physical examination during the same period were selected as controls. Anthropometric, clinical, and laboratory analyses were performed on all subjects. The mitochondrial membrane potential (MMP) of peripheral blood leukocytes was detected as the indicator of mitochondrial function. Compared with the control group, the leukocyte telomere length (LTL) was significantly shorter ($P < 0.001$), and the level of PGC-1 α in serum was significantly lower in AF patients. Additionally, in subjects without any other diseases, the AF patients had lower MMP when compared with the control. Multivariate logistic regression confirmed that LTL (OR 0.365; 95% CI 0.235-0.568; $P < 0.001$) and serum PGC-1 α (OR 0.993; 95% CI 0.988-0.997; $P = 0.002$) were inversely associated with the presence of AF. In addition, ROC analysis indicated the potential diagnostic value of LTL and serum PGC-1 α with AUC values of 0.734 and 0.633, respectively. This research concludes that LTL and serum PGC-1 α are inversely correlated with the occurrence of aging-related AF and that mitochondrial dysfunction plays a role in this.

1. Introduction

Atrial fibrillation (AF) is the most common cardiac arrhythmia and contributes to a high prevalence of mortality and morbidity [1]. Studies have shown that the prevalence of AF increases with advancing age, reaching 5% between 60 and 70 years old and as high as 8% at over 80 years old [2]. Furthermore, the incidence of AF in males is higher than in females [3].

The shortening of telomere length has been found to be common with age in the majority of tissues and cells; thus, it is often used as a biomarker of aging [4]. Research efforts have argued that leukocyte telomere length (LTL) shortening

is related to a variety of cardiovascular diseases, including atherosclerosis, left ventricular hypertrophy, and heart failure, but the relevance to AF is still controversial [5–7]. In the Cardiovascular Health Study, researchers found no relationship between mean telomere length and AF in human atrial tissue [8]. However, Carlquist et al. found that shortened LTL was related to the presence of paroxysmal AF among cardiovascular patients [9]. In addition, recent studies have argued that shortened LTL is associated with the recurrence of AF and is an independent risk factor in humans [10].

The mechanisms of AF remain incompletely understood. Mitochondria play an important role in oxidative stress, calcium homeostasis, and energy metabolism. Studies have

shown that mitochondrial dysfunction can cause insufficient ATP production and excessive reactive oxygen species (ROS), which damages the homeostasis of Ca^{2+} in myocardial cells and the excitability of membranes, in turn leading to AF [11, 12]. Peroxisome proliferator-activated receptor γ coactivator-1 (PGC-1) is an important nuclear transcription coactivator that contains PGC-1 α , PGC-1 β , and PGC-1-related coactivator (PRC) [13]. Accumulating evidence has argued that PGC-1 α is a key molecule of mitochondrial function because it participates in the regulation of mitochondrial biogenesis and energy metabolism and is closely related to oxidative stress and inflammation [14, 15]. It plays an important role in the occurrence and development of atherosclerosis, coronary heart disease, heart failure, and other cardiovascular diseases [15, 16]. Some researchers have put forward the concept of a “telomere-p53-PGC axis”: that is, that the shortening of telomere will activate p53 expression, thereby inhibiting PGC-1 and causing mitochondrial dysfunction and a series of reactions such as oxidative stress and intracellular Ca^{2+} overload, eventually inducing AF [11, 12, 17, 18].

It is not clearly known whether telomere shortening is associated with aging-related AF and whether mitochondrial dysfunction is involved in this process. Therefore, we measured the LTL, telomere-associated molecules, and mitochondrial membrane potential (MMP) of leukocytes to ascertain if they are correlated with aging-related AF and if they could be used as novel biomarkers for it.

2. Materials and Methods

2.1. Ethics Approval of the Research Protocol. The study protocol was approved by the Human Ethics Review Committee of Chinese PLA General Hospital, and a signed consent form was obtained from each subject.

2.2. Participants. A total of 143 male patients with AF were admitted to the Second Medical Center of Chinese PLA General Hospital from April to October 2018. The inclusion criteria were (i) patients aged 60 years or older and diagnosed as having AF by electrocardiogram or 24 h dynamic electrocardiogram according to the guidelines established by the European Society of Cardiology in 2010 [19] and (ii) patients with a complete clinical data record. According to the inclusion criteria, 118 patients were enrolled in the study. The exclusion criteria were valvular heart disease, acute coronary syndrome, dilated or hypertrophic cardiomyopathy, congenital heart disease, previous cardiac surgery, heart failure (including heart failure with preserved ejection fraction and heart failure with reduced ejection fraction), hyperthyroidism, inflammatory diseases, systemic disease, and moderate-to-severe renal dysfunction (estimated glomerular filtration rate (eGFR) < 60 mL/min/1.73 m²). Considering the effect of diseases on AF, 10 patients with heart failure, 8 patients with renal dysfunction, and 1 patient with hyperthyroidism were excluded. After excluding another 3 patients with previous cardiac surgery, 96 participants with AF were enrolled in the study as an AF group. At the same time, we selected 96 non-AF elderly males who were admitted to the hospital for

physical examination during the same period as controls after matching for age and gender. LTL was associated with AF with a hazard ratio (HR) of 3.17 in a previous study [10]. According to the sample size calculation formula for a paired case-control study, the sample size required was calculated to be 85 patients by using PASS 11 software (proportioning; tests for two correlated proportions in a matched case-control design). Consequently, having 96 subjects in each group met the sample size requirements; therefore, 192 elderly males were selected as the study cohort. Among them, 96 AF patients (mean age 77.81 years, range 61-97 years) were in the AF group, and 96 elderly males (mean age 78.61 years, range 60-103 years) were in the control group (Figure 1). The subjects were divided into the elderly age group (60-74 years), the senile age group (75-89 years), and the long-living group (≥ 90 years) [20]. AF patients were then divided into the paroxysmal AF group ($n = 36$), the persistent AF group ($n = 37$), and the permanent AF group ($n = 23$).

2.3. Clinical Data Collection. Patients' demographic characteristics, lifestyle information, and medication use were obtained by reviewing their medical records. The age value was the age recorded at admission. The definition of “smoking” was having smoked more than 1 cigarette per day for over 1 year. Patients' body mass index (BMI) was also calculated, and blood pressure was measured using the right arms of seated participants by an automated blood pressure monitor (J710, Omron Corporation, Kyoto, Japan) in the morning. Transthoracic echocardiography was performed by experienced echocardiologists on all subjects to evaluate the characteristics of their left atrial diameter (LAD) and left ventricular ejection fraction (LVEF).

2.4. Biochemical Index Determination. Blood samples were obtained with anticoagulation between 6:00 and 7:00 a.m. after patients fasted overnight. Samples were stored at 4°C for less than 1 hour. Some samples were used for testing, and others were centrifuged to obtain white blood cells and plasma and frozen at -80°C. Concentrations of fasting blood glucose (FBG), uric acid (UA), blood lipid, blood urea nitrogen (BUN), and C-reactive protein (CRP) were measured by enzymatic assays (Roche Diagnostics, Mannheim, Germany). The concentration of creatinine was determined by an enzymatic assay (Roche Diagnostics) on an autoanalyzer (7600, Hitachi, Tokyo, Japan). The glycated hemoglobin (GHb) level was tested using high-performance liquid chromatography.

2.5. Leukocyte Isolation and Mitochondrial Membrane Potential Detection. The blood samples were diluted with an equal volume of buffer. Then, an appropriate amount of Ficoll-Hypaque (Solarbio, Beijing, China) was added to a tube, and the diluted blood was also carefully added to it. 800 g was centrifuged for 20 minutes at room temperature to isolate leukocytes. The cells in the middle layer were carefully pipetted into a new centrifuge tube and diluted with PBS. Then, 250 g was centrifuged for 10 minutes. The pellet was treated with PBS, and 250 g was centrifuged for 10

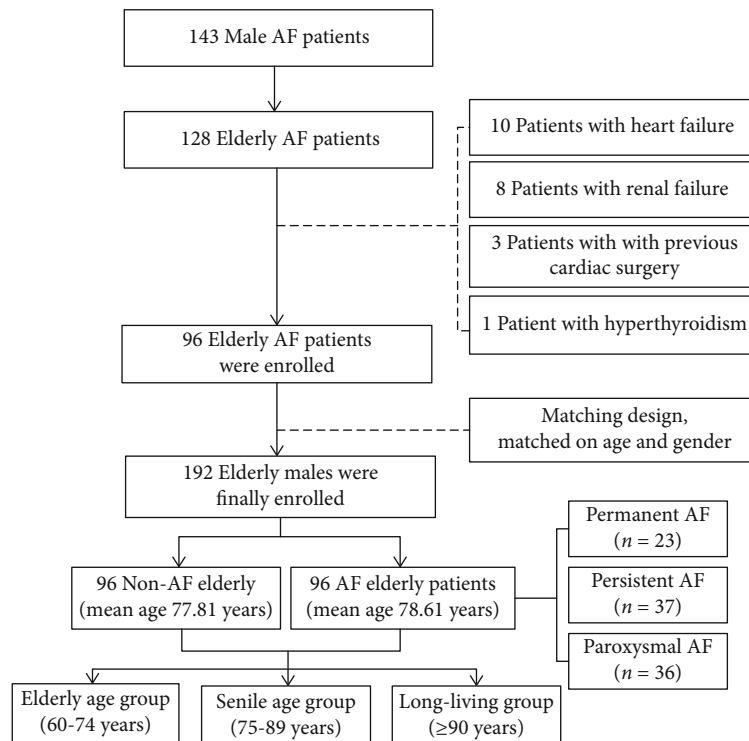


FIGURE 1: Study frame diagram. AF: atrial fibrillation.

minutes, and peripheral blood mononuclear cells were achieved [21]. After being washed and resuspended in PBS, cells were treated with 500X MitoTell™ Orange (AAT Bioquest, Sunnyvale, USA) for 15-30 minutes at 37°C in the dark [22]. After washing, the fluorescence was measured using a flow cytometer at an emission of 590 nm and 540 nm. The data was analyzed using the software FlowJo V10.

2.6. Measurement of Telomere Length. The leukocytes were obtained from blood samples by centrifugation and stored at -80°C until analysis. Telomere length in genomic DNA was extracted directly from peripheral blood leukocytes according to the instructions of the DNA extraction kit (TIANGEN Biotech Corporation, China) and was measured by applying a quantitative real-time PCR method (GenePool Biotech Corporation, China). Telomere length was measured according to the ratio of the telomere repeat copy number (T) to the single-copy gene copy number (S) in each given sample. The relative LTL was calculated as the ratio of telomere repeats to single-copy gene copies (T/S ratio) [10]. DNA samples were amplified in 10 μ L PCR reactions with StepOnePlus Real Time PCR System (Applied Biosystems, Foster City, CA, USA). The primers used for the telomere repeat and the single-copy gene copy number amplification were as follows: telomere forward—ACACTAAGGTTTGGGT TTGGGTTTGGGTTTGGGTTAGTGT, telomere reverse—TGTTAGGTATCCCTATCCCTATCCCTATCCCTAT CCCTAACA; single-copy gene forward—CTTCATCCACG TTCACCTTG, single-copy gene reverse—GAGGAGAAG TCTGCCGTT [10]. Both PCRs were activated in a final volume of 10 μ L that contained SYBR Green Master Mix none-ROX (2x) (TaKaRa, Shiga, Japan), 3.12 ng of DNA template,

and 0.5 nM of telomere primers or 0.5 nM of single-copy gene primers. The thermal cycling profile for both telomere and single-copy gene primers started with 95°C incubation for 10 minutes, followed by 40 cycles of 15 seconds at 95°C and 1 minute at 54°C. All amplification specificity was regulated by employing melting curve analysis. In each sample, the quantities of telomere repeats and single-copy genes were normalized to a reference DNA. The same reference DNA sample (from a single individual) was included in each measurement to control interassay variability [9]. All measurements were performed blinded with respect to clinical data.

2.7. RNA Isolation and mRNA Expression Analysis. The leukocytes were obtained from blood samples by centrifugation and stored at -80°C until analysis. Total RNA was extracted from leukocytes by RNeasy Pure Blood Kit (TIANGEN Biotech Corporation, China) according to the standard protocol. Absorption spectrophotometry, using NanoDrop-1000 (Thermo Fisher Scientific, Yokohama, Japan), was used to determine RNA concentrations and purity (260/280 ratio above 1.8 was used). RNA (1 μ g per sample) was reverse transcribed using the High-Capacity cDNA Reverse Transcription Kit (Applied Biosystems, CA, USA) in a total reaction volume of 40 μ L. For a quantitative estimate of p53 and PGC-1 α mRNA levels, the StepOnePlus Real Time PCR System was used. The primers were as follows: p53 forward—C-CATCCTCACCATCATCACACT, p53 reverse—GCACAA ACACGCACCTCAA; PGC-1 α forward—TGACGACGA AGCAGACAAGAC, PGC-1 α reverse—GAACAAGAAGG AGACACATTGAACA; Actin forward—ACTTAGTTGCG TTACACCCTT, and Actin reverse—GTCACCTTCAC CGTTCCA. The relative expression level of p53 or PGC-1 α

TABLE 1: Clinical and biochemical characteristics of AF patients and controls.

Characteristic	The controls ($n = 96$)	AF patients ($n = 96$)	<i>P</i> value
Clinical parameters			
Age (years)	77.81 ± 11.30	78.61 ± 11.64	0.629
Male, n (%)	96 (100)	96 (100)	1.000
BMI (kg/m ²)	23.60 ± 2.83	24.25 ± 2.74	0.106
Smoking, n (%)	16 (16.67)	21 (21.88)	0.363
History of CHD, n (%)	21 (21.88)	18 (18.75)	0.593
Hypertension, n (%)	42 (43.75)	47 (48.96)	0.472
Diabetes mellitus, n (%)	15 (15.62)	17 (17.71)	0.700
Hyperlipidemia	24 (25.00)	20 (20.83)	0.495
Antihypertensive medication, n (%)	42 (43.75)	46 (47.92)	0.565
Glucose lowering treatment, n (%)	14 (14.58)	15 (15.63)	0.841
Lipid-lowering medication, n (%)	41 (42.71)	34 (35.42)	0.303
SBP (mmHg)	127.54 ± 11.10	129.02 ± 12.25	0.382
DBP (mmHg)	68.35 ± 8.74	70.42 ± 9.00	0.109
Laboratory parameters			
TC (mmol/L)	3.67 ± 0.73	3.59 ± 0.73	0.464
TG (mmol/L)	1.22 ± 0.49	1.34 ± 0.58	0.107
LDL-C (mmol/L)	2.33 ± 0.71	2.21 ± 0.68	0.236
HDL-C (mmol/L)	1.26 ± 0.33	1.21 ± 0.30	0.283
Cr (mmol/L)	84.03 ± 15.88	88.82 ± 21.12	0.077
BUN (mmol/L)	6.30 ± 1.56	6.55 ± 1.83	0.299
UA (mmol/L)	311.02 ± 58.10	333.08 ± 76.18	0.025
FBG (mmol/L)	6.18 ± 0.96	6.15 ± 0.99	0.829
GHb (%)	6.02 ± 0.57	6.11 ± 0.66	0.311
CRP (mg/dL)	0.71 ± 0.46	0.84 ± 0.51	0.077
Echocardiographic parameters			
LVEF (%)	60.06 ± 4.23	58.94 ± 3.87	0.056
LAD (mm)	37.54 ± 3.02	38.68 ± 4.02	0.028

Abbreviations: BMI: body mass index; CHD: coronary heart disease; SBP: systolic blood pressure; DBP: diastolic blood pressure; TC: total cholesterol; TG: triglyceride; LDL-C: low-density lipoprotein cholesterol; HDL-C: high-density lipoprotein cholesterol; Cr: creatinine; BUN: blood urea nitrogen; UA: uric acid; FBG: fasting blood glucose; GHb: glycated hemoglobin; CRP: C-reactive protein; LVEF: left ventricular ejection fraction; LAD: left atrial diameter. *P* < 0.05 with italic font means statistically significant.

mRNA was determined by comparison, with the housekeeping gene Actin serving as an internal standard. Relative mRNA levels were calculated via the $2^{-\Delta\Delta CT}$ method using StepOne software (Applied Biosystems) [23]. We averaged the fold changes from three wells for each sample (in triplicate) and used this average value for statistical analyses.

2.8. ELISA Measurement of Serum PGC-1 α . An enzyme-linked immunosorbent assay kit (Jianglai Biotech Corporation, China) was utilized to evaluate serum PGC-1 α concentrations. An anti-human PGC-1 α monoclonal coating antibody adsorbed onto microwells and a lyophilized HRP-conjugated monoclonal anti-human PGC-1 α were incubated with 100 μ L of diluted (1 : 20) sample serum at room temperature for 3 hours on a microplate shaker at 100 rpm. Following three washes, the unbound enzyme conjugate anti-human sPGC-1 α was removed and 100 μ L of TMB (tetrame-

tylbenzidine) substrate solution reactive with HRP was added to the wells. After incubation at room temperature for 10 minutes, the reaction was terminated by the addition of acid, and absorbance was measured at 450 nm. A standard curve was prepared from seven human PGC-1 α standard dilutions, and human PGC-1 α sample concentration was determined [24]. All measurements were performed blinded with respect to clinical data.

2.9. Definition of Variables. Paroxysmal AF was defined as AF terminating spontaneously within 7 days, especially within 48 hours. Persistent AF was defined as AF that lasted longer than 7 days (regardless of whether it terminated spontaneously or by cardioversion). Permanent AF was defined as AF that fails to terminate using cardioversion or is terminated but relapses within 24 hours [25, 26]. Hypertension was defined as systolic blood pressure (SBP) of ≥ 140 mmHg,

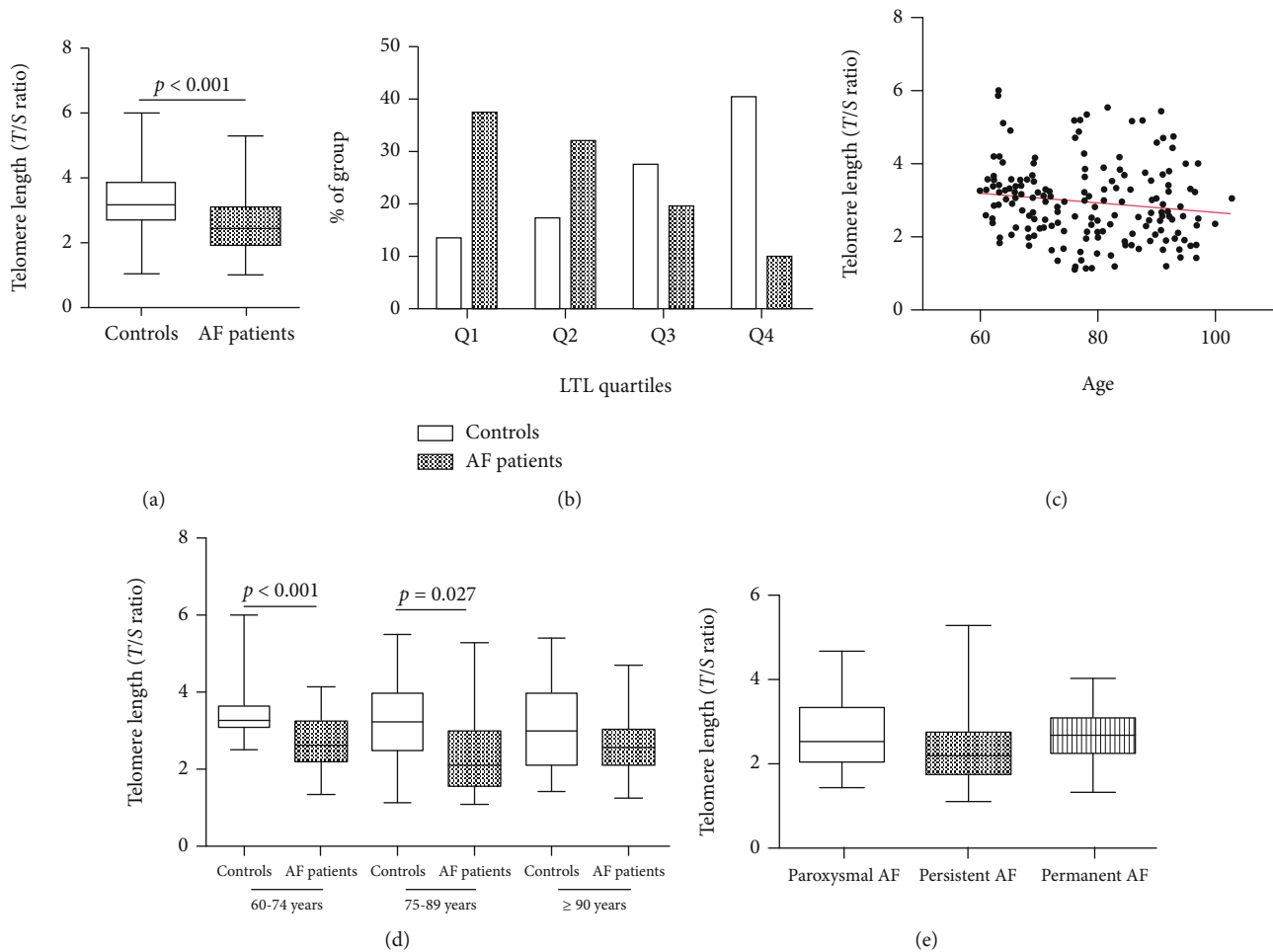


FIGURE 2: LTL in AF patients and the controls. (a) AF patients showed significantly shorter LTL compared with controls; (b) quartile distribution of LTL; (c) LTL in elderly males was significantly negatively correlated with age; (d) LTL was significantly shorter in AF patients in the elderly age group and senile age group; (e) there were no significant differences of LTL among the paroxysmal AF, persistent AF, and permanent AF groups. LTL: leukocyte telomere length; AF: atrial fibrillation; Q: quartile.

diastolic blood pressure (DBP) of ≥ 90 mmHg, or taking anti-hypertensive medication.

2.10. Statistical Analysis. Statistical analyses were performed with the SPSS statistical package, version 20.0 (SPSS Inc., Chicago, USA). The continuous variables were exhibited as means \pm standard errors, and categorical variables were expressed as percentages. The Student *t*-test and the chi-square test were utilized to determine the parameter differences between the AF patients and controls. Simple and multiple logistic regression analyses were performed to determine the correlation of LTL with the presence of AF. Chi-square tests, one-way ANOVA, or Kruskal-Wallis tests were utilized to determine the parameter differences between different age and AF subgroups. Pearson correlation analysis was used to analyze the correlation of LTL with age. The correlation between LTL and other parameters was analyzed using simple linear regression analysis. Then, a multiple stepwise linear regression analysis was used to determine the contribution of various factors to LTL. Receiver operating characteristic (ROC) curves were constructed to evaluate the specificity and sensitivity of predicting AF using LTL as

well as the serum PGC-1 α and CRP values, and the area under curve (AUC) was calculated. A *P* value of less than 0.05 was statistically significant.

3. Results

3.1. Baseline Clinical Characteristics. A total of 192 subjects were enrolled in this study, and their characteristics are summarized in Table 1. The AF patients showed higher UA and LAD compared with the controls. There were no significant differences in other characteristics between the two groups.

3.2. AF Patients Had Shorter LTL. AF patients showed significantly shorter LTL compared with controls (2.54 ± 0.85 vs. 3.33 ± 1.01 , $P < 0.001$) (Figure 2(a)). All subjects are separated into quartiles (Q) according to the LTL. The distribution of AF patients and controls from Q1 to Q4 is shown in Figure 2(b). As shown, the LTL of AF patients is mostly located in Q1 (37.50%) and Q2 (32.29%), while the controls' LTL is mostly located in Q3 (28.13%) and Q4 (40.63%). This indicates an inverse relationship between LTL and AF prevalence.

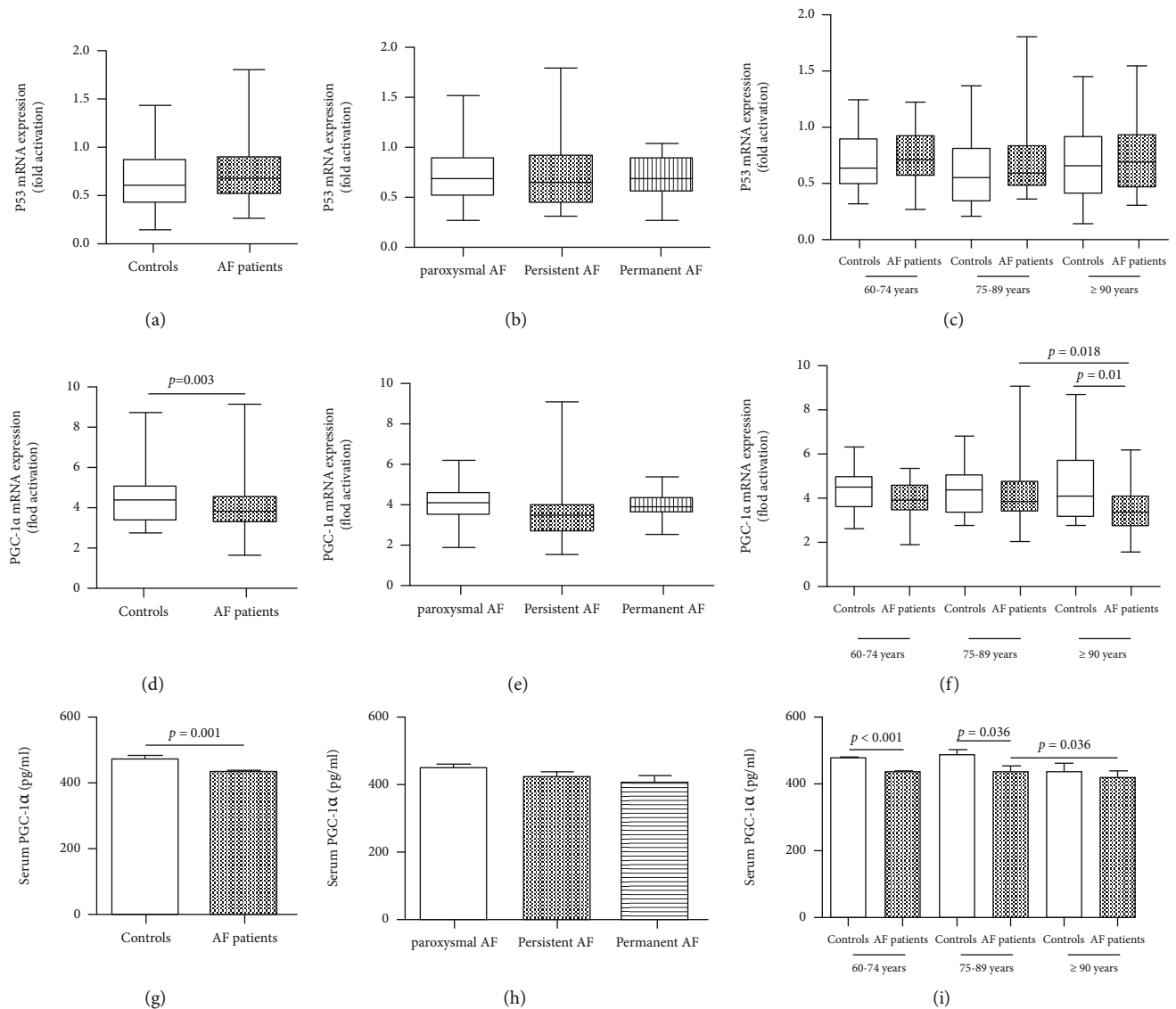


FIGURE 3: Telomere-associated molecules in AF patients. (a) p53 mRNA in AF patients was higher than controls and without statistical differences; (b, c) no significant differences of p53 mRNA among different types of AF and different age groups; (d) the expression of PGC-1 α mRNA in leukocytes was significantly reduced in AF patients; (e) no significant differences of PGC-1 α mRNA among different types of AF; (f) the expression of PGC-1 α mRNA was significantly lower in AF patients in the long-living age group; (g) the serum PGC-1 α concentration was significantly reduced in AF patients; (h) no significant differences of serum PGC-1 α concentration among different types of AF; (i) the serum PGC-1 α concentration was significantly reduced in AF patients in the elderly age group and senile age group. AF: atrial fibrillation.

A Pearson correlation analysis showed that LTL in elderly males was significantly negatively correlated with age ($r = -0.151$, $P = 0.037$) (Figure 2(c)). In the control group, LTL was significantly shortened with age ($r = -0.202$, $P = 0.048$). However, in AF patients, LTL was also negatively correlated with age, but with no statistical difference ($r = -0.089$, $P = 0.389$).

Then, the elderly males were divided into three groups according to the WHO's guidelines [20]. The LTL in AF patients was significantly shorter in the elderly age group (60-74 years) ($P < 0.001$) and the senile age group (75-89 years) ($P = 0.027$) than in the controls. It was also shorter in AF patients in the long-living group (≥ 90 years), but with-

out being statistically significant (Figure 2(d)). In the AF patient group and the control group, analysis of variance on the LTL of the three age groups showed no statistical difference. In the AF subgroups, there were no significant differences in LTL among the paroxysmal AF, persistent AF, and permanent AF groups (Figure 2(e)).

3.3. Telomere-Associated Molecules. The expression of p53 mRNA in leukocytes in AF patients was higher than that in the controls, but there was no statistical difference (Figure 3(a)). Compared with the controls, the expression of PGC-1 α mRNA in leukocytes was significantly lower (4.38 ± 1.17 vs. 3.87 ± 1.15 , $P = 0.003$) (Figure 3(d)), as was

TABLE 2: Clinical and biochemical characteristics of subjects without other diseases.

Characteristic	The controls (<i>n</i> = 26)	AF patients (<i>n</i> = 23)	<i>P</i> value
Clinical parameters			
Age (years)	77.54 ± 9.82	76.52 ± 12.11	0.530
Male, <i>n</i> (%)	26 (100)	23 (100)	1.000
BMI (kg/m ²)	23.80 ± 2.75	24.12 ± 2.65	0.684
SBP (mmHg)	128.23 ± 10.58	124.96 ± 10.75	0.289
DBP (mmHg)	69.54 ± 8.12	69.13 ± 9.75	0.874
Laboratory parameters			
TC (mmol/L)	3.95 ± 0.61	3.71 ± 0.62	0.170
TG (mmol/L)	1.20 ± 0.54	1.40 ± 0.54	0.201
LDL-C (mmol/L)	2.42 ± 0.81	2.05 ± 0.61	0.078
HDL-C (mmol/L)	1.36 ± 0.33	1.20 ± 0.30	0.083
Cr (mmol/L)	79.27 ± 11.68	86.70 ± 22.32	0.145
BUN (mmol/L)	6.06 ± 1.08	6.61 ± 2.18	0.256
UA (mmol/L)	307.50 ± 49.88	301.61 ± 68.70	0.731
FBG (mmol/L)	6.03 ± 0.80	6.21 ± 1.13	0.518
GHb (%)	6.10 ± 0.69	6.10 ± 0.76	0.998
CRP(mg/dL)	0.65 ± 0.37	1.00 ± 0.56	<i>0.011</i>
Echocardiographic parameters			
LVEF (%)	61.31 ± 3.36	59.70 ± 3.32	0.098
LAD (mm)	37.35 ± 3.15	39.04 ± 3.39	0.076
Telomere-associated molecules			
LTL (<i>T/S</i> ratio)	3.23 ± 0.76	2.30 ± 0.73	< <i>0.001</i>
Leukocyte p53 mRNA	0.63 ± 0.28	0.69 ± 0.24	0.395
Leukocyte PGC-1 α mRNA	4.35 ± 1.00	3.52 ± 0.89	<i>0.004</i>
Serum PGC-1 α (pg/mL)	488.69 ± 65.94	420.56 ± 84.79	<i>0.003</i>

Abbreviations: BMI: body mass index; SBP: systolic blood pressure; DBP: diastolic blood pressure; TC: total cholesterol; TG: triglyceride; LDL-C: low-density lipoprotein cholesterol; HDL-C: high-density lipoprotein cholesterol; Cr: creatinine; BUN: blood urea nitrogen; UA: uric acid; FBG: fasting blood glucose; GHb: glycated hemoglobin; CRP: C-reactive protein; LVEF: left ventricular ejection fraction; LAD: left atrial diameter. *P* < 0.05 with italic font means statistically significant.

the serum PGC-1 α concentration (470.41 ± 84.13 vs. 428.56 ± 86.07 , *P* = 0.001) (Figure 3(g)). Interestingly, in AF patients, the p53 mRNA, PGC-1 α mRNA, and serum PGC-1 α levels had no significant differences among the paroxysmal AF, persistent AF, and permanent AF (Figures 3(b), 3(e), and 3(h)). Via subgroup analysis based on age, we found that the expression of PGC-1 α mRNA was significantly lower in the long-living age group, and the serum PGC-1 α concentration was significantly reduced in the elderly age group and the senile age groups in AF patients (Figures 3(f) and 3(i)). However, no significant differences were found in p53 mRNA among the different age groups (Figure 3(c)).

3.4. Subgroup Analysis for the Subjects without Other Diseases. In order to reduce the impact of other diseases that may affect telomere length on the results of the study, we conducted a subgroup analysis of all nonsmoking subjects without comorbidities and measured the MMP of their peripheral blood leukocytes. Among these subjects, there was no signifi-

cant difference in baseline data except CRP between the AF group and the control group (Table 2). The AF patients showed significantly shorter LTL and lower expression of PGC-1 α mRNA and serum PGC-1 α (Figures 4(a)–4(c)). In addition, the MMP of the AF patients was significantly decreased when compared with that of the controls, which indicates that AF patients have poor mitochondrial function (Figures 4(d) and 4(e)).

3.5. The Correlation of LTL with the Presence of AF. Simple logistic regression analysis demonstrated that UA, CRP, LAD, LTL, and serum PGC-1 α showed a trend toward an association with the presence of AF (Table 3). All of these parameters were then entered into a multiple logistic regression model, and the LTL (OR 0.404, 95% CI 0.278–0.587; *P* < 0.001), CRP (OR 1.971, 95% CI 1.023–3.799; *P* = 0.043), and serum PGC-1 α (OR 0.994, 95% CI 0.989–0.998; *P* = 0.003) remained to be significantly associated with the presence of AF (Table 3). Drawing from previous studies, variables that were considered clinically relevant such as age,

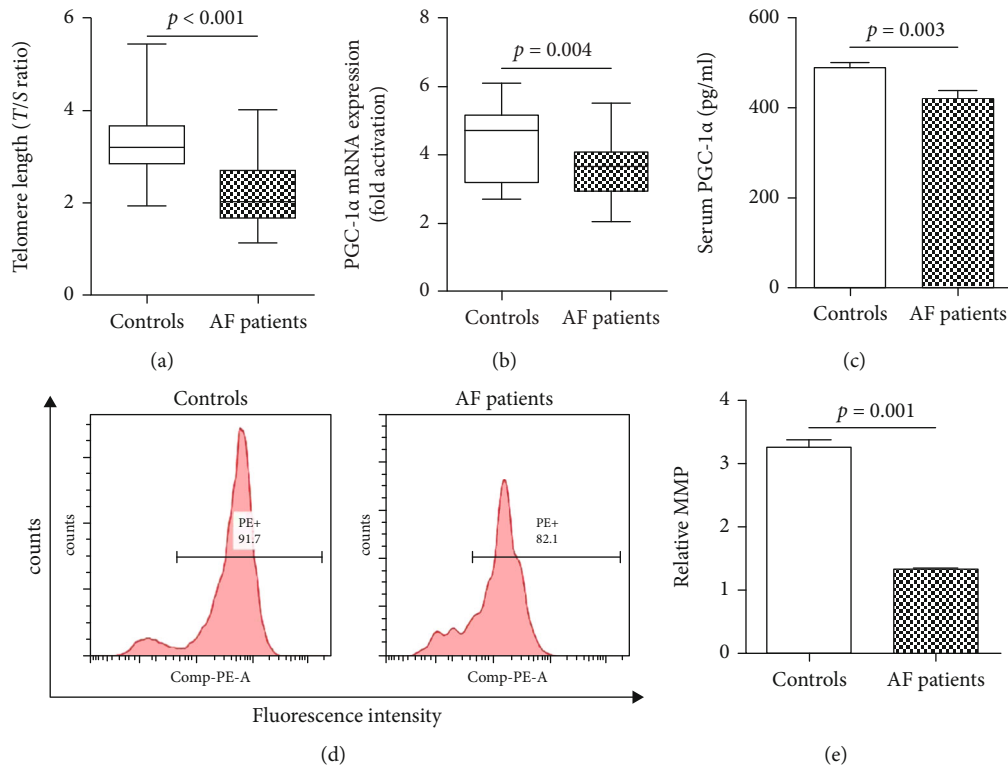


FIGURE 4: LTL, PGC-1 α expression, and MMP in subgroup of patients without other diseases. (a) AF patients showed significantly shorter LTL compared with controls; (b) the expression of PGC-1 α mRNA in leukocytes was significantly reduced in AF patients; (c) the serum PGC-1 α concentration was significantly reduced in AF patients; (d) representative pictures of MMP detected by flow cytometry; (e) the MMP of AF patients was significantly decreased when compared with controls. AF: atrial fibrillation; MMP: mitochondrial membrane potential.

BMI, diabetes, SBP, DBP, TG, and HDL-C were entered into a multivariate logistic regression model. LTL (OR 0.365, 95% CI 0.235-0.568; $P < 0.001$), CRP (OR 2.250, 95% CI 1.143-4.428; $P = 0.019$), and serum PGC-1 α (OR 0.993, 95% CI 0.988-0.997; $P = 0.002$) were still significantly associated with the presence of AF (Figure 5).

In the subgroup of subjects without other diseases, we incorporated age, CRP, LTL, leukocyte PGC-1 α mRNA expression, and serum PGC-1 α into the multivariate logistic regression model and also found that LTL and serum PGC-1 α were significantly associated with the presence of AF (Table 4).

3.6. The Correlation of LTL with Other Parameters. Simple linear regression analyses showed that LTL was negatively correlated with age ($r = -0.151$, $P = 0.037$), CRP ($r = -0.200$, $P = 0.005$), and LAD ($r = -0.196$, $P = 0.006$) and positively correlated with PGC-1 α mRNA ($r = 0.168$, $P = 0.020$) and serum PGC-1 α ($r = 0.176$, $P = 0.014$). Multiple stepwise regression analysis showed that CRP ($\beta = -0.167$, $P = 0.017$) and LAD ($\beta = -0.165$, $P = 0.018$) remain to be inversely associated with LTL (Table 5).

3.7. LTL and Serum PGC-1 α Has a Potential Predictive Role in Elderly AF. The corrected multivariate logistic regression model has argued that LTL, CRP, and serum PGC-1 α are sig-

nificantly related to the presence of AF in the elderly. ROC analysis was used to determine if LTL, CRP, and serum PGC-1 α could predict AF. As shown in Figure 6, the AUC was 0.734 (95% CI: 0.663-0.806, $P < 0.001$) for LTL in the prediction of AF. The optimum cutoff value of LTL on the ROC curve was 2.830 with a sensitivity of 67.7% and a specificity of 74.0%. Serum PGC-1 α showed a potential predictive value of AF with an AUC of 0.633 (95% CI: 0.555-0.711; $P = 0.001$), and the optimum cutoff value was 463.5 with a sensitivity of 65.6% and a specificity of 57.3%. Further, the AUC for CRP in the prediction of AF was 0.599 (95% CI: 0.519-0.679; $P = 0.018$), and the optimum cutoff value was 0.6150 with a sensitivity of 68.8% and a specificity of 51.0% (Figure 6).

4. Discussion

This study found that LTL and serum PGC-1 α are inversely correlated with the occurrence of aging-related AF and that the MMP of AF patients was significantly decreased, indicating that mitochondrial dysfunction plays a role in this. In addition, ROC analysis revealed the potential diagnostic value of LTL and serum PGC-1 α for AF patients, indicating that LTL and serum PGC-1 α could possibly be novel predictive biomarkers for the occurrence or outcome of aging-related AF.

TABLE 3: Logistic regression analysis for the presence of AF.

	Simple regression		Multiple regression	
	OR (95% CI)	<i>P</i> value	OR (95% CI)	<i>P</i> value
Clinical parameters				
Age (years)	1.006 (0.982-1.031)	0.627		
BMI (kg/m ²)	1.089 (0.982-1.207)	0.107		
Smoking, <i>n</i> (%)	0.714 (0.347-1.471)	0.361		
History of CHD, <i>n</i> (%)	0.824 (0.407-1.668)	0.591		
Hypertension, <i>n</i> (%)	1.233 (0.699-2.177)	0.470		
Diabetes mellitus, <i>n</i> (%)	1.162 (0.543-2.486)	0.699		
Hyperlipidemia	0.789 (0.402-1.551)	0.493		
Antihypertensive medication, <i>n</i> (%)	1.183 (0.670-2.088)	0.562		
Glucose lowering treatment, <i>n</i> (%)	1.085 (0.492-2.391)	0.840		
Lipid-lowering medication, <i>n</i> (%)	0.736 (0.411-1.316)	0.301		
SBP (mmHg)	1.011 (1.008-1.061)	0.380		
DBP (mmHg)	1.027 (0.994-1.061)	0.110		
Laboratory parameters				
TC (mmol/L)	0.864 (0.584-1.277)	0.462		
TG (mmol/L)	1.562 (0.904-2.700)	0.110		
LDL-C (mmol/L)	0.780 (0.517-1.176)	0.236		
HDL-C (mmol/L)	0.607 (0.244-1.509)	0.282		
Cr (mmol/L)	1.015 (0.998-1.031)	0.084		
BUN (mmol/L)	1.095 (0.923-1.298)	0.300		
UA (mmol/L)	1.005 (1.001-1.009)	0.027	1.004 (0.999-1.009)	0.130
FBG (mmol/L)	0.968 (0.723-1.296)	0.828		
GHb (%)	1.272 (0.798-2.026)	0.311		
CRP (mg/dL)	2.250 (1.277-3.965)	0.005	1.971 (1.023-3.799)	0.043
Echocardiographic parameters				
LVEF (%)	0.933 (0.869-1.002)	0.058		
LAD (mm)	1.095 (1.009-1.187)	0.030	1.084 (0.984-1.195)	0.103
Telomere-associated molecules				
LTL (<i>T/S</i> ratio)	0.388 (0.269-0.560)	<0.001	0.404 (0.278-0.587)	<0.001
Leukocyte p53 mRNA	2.340 (0.848-6.457)	0.101		
Leukocyte PGC-1 α mRNA	2.340 (0.848-6.457)	0.101		
Serum PGC-1 α (pg/mL)	0.994 (0.991-0.998)	0.001	0.994 (0.989-0.998)	0.003

Abbreviations: CI: confidence interval; BMI: body mass index; CHD: coronary heart disease; SBP: systolic blood pressure; DBP: diastolic blood pressure; TC: total cholesterol; TG: triglyceride; LDL-C: low-density lipoprotein cholesterol; HDL-C: high-density lipoprotein cholesterol; Cr: creatinine; BUN: blood urea nitrogen; UA: uric acid; FBG: fasting blood glucose; GHb: glycated hemoglobin; CRP: C-reactive protein; LVEF: left ventricular ejection fraction; LAD: left atrial diameter; *T/S* ratio: the ratio of telomere repeats to single-copy gene copies; PGC-1 α : peroxisome proliferator-activated receptor γ coactivator-1 α . *P* < 0.05 with italic font means statistically significant.

Telomere shortening has been suggested to be susceptible to age-related cardiovascular diseases, including atherosclerosis and heart failure [5, 7]. Many studies have shown that LTL predicts cardiovascular disease and all-cause mortality [27–30]. However, it is not clear whether telomere shortening is related to the occurrence of AF. In the current study, we found that LTL was significantly shorter in elderly male AF patients compared with the controls, and the multivariate logistic regression analysis confirmed that LTL was significantly related to AF. Our finding is consistent with an analysis of the Intermountain Heart Collaborative Study investigators in a 63% male cohort with a mean age of 62.9 \pm 13.47 years [9]. However, Siland et al. [31] found that

shorter LTL was not independently associated with incident AF in a community-based, 50% male cohort with a mean age of 49 \pm 13 years (range between 29 and 74 years). Roberts et al. [8] found no evidence of an association between LTL and incident AF in a cohort with the mean age of 72.2 years that was 41.3% male at baseline. In our opinion, this difference in results may come from the choice of subjects, as the subjects were not elderly or had a lower ratio of males. In the subgroup analysis of age, we found that the LTL of patients with AF in the elderly age group and the senile age group was significantly shorter when compared with that of the controls, while there was no statistical difference in the long-living group, indicating that the rate of telomere

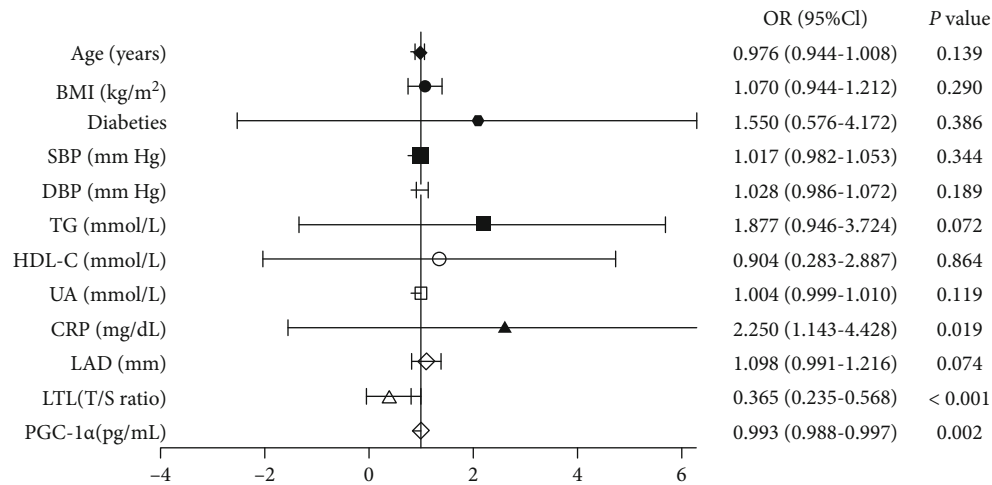


FIGURE 5: Multiple logistic regression analysis for the presence of AF. BMI: body mass index; SBP: systolic blood pressure; DBP: diastolic blood pressure; TG: triglyceride; HDL-C: high-density lipoprotein cholesterol; UA: uric acid; CRP: C-reactive protein; LAD: left atrial diameter; LTL: leukocyte telomere length.

TABLE 4: Logistic regression analysis in subgroup.

	Simple regression		Multiple regression	
	OR (95% CI)	P value	OR (95% CI)	P value
Age (years)	1.017 (0.965-1.072)	0.521	0.996 (0.917-1.081)	0.920
CRP(mg/dL)	6.021 (1.319-27.485)	0.020	9.163 (0.772-108.764)	0.790
LTL (T/S ratio)	0.162 (0.054-0.488)	0.001	0.188 (0.046-0.766)	0.020
Leukocyte PGC-1α mRNA	0.405 (0.208-0.788)	0.008	0.460 (0.196-1.080)	0.075
Serum PGC-1α (pg/mL)	0.987 (0.978-0.997)	0.008	0.983 (0.968-0.998)	0.031

Abbreviations: CI, confidence interval; CRP: C-reactive protein; T/S ratio: the ratio of telomere repeats to single-copy gene copies; PGC-1α: peroxisome proliferator-activated receptor γ coactivator-1 α . *P* < 0.05 with italic font means statistically significant.

shortening is different at different ages and that telomere may shorten faster in the early stages of aging [32].

The mechanisms of aging-related AF remain incompletely understood, but atrial electrical and structural remodeling and disturbed calcium homeostasis may be involved [33, 34]. Mitochondrial function is the core of energy metabolism, which is involved in oxidative stress, the regulation of intracellular calcium homeostasis, and intracellular signal transduction. Studies have shown that mitochondrial dysfunction causes energy metabolism disorders and decreased membrane potential, leading to myocardial abnormal local electrical activity [35]. In addition, mitochondrial dysfunction can cause oxidative stress and calcium overload, thereby promoting the occurrence of AF [36]. Studies have argued that telomere shortening consequently contributes to mitochondrial dysfunction, and the “telomere-p53-PGC axis” plays an important role in this [37]. Thus, telomere shortening will activate p53, thereby inhibiting PGC-1 and inducing mitochondrial dysfunction as well as a series of reactions such as oxidative stress and Ca²⁺ overload [11, 17]. Researchers had also found that the telomere of left ventricular cardiomyocytes of TERC^{-/-} mice at 6-8 months was shorter than that of 2-4 months (*P* < 0.0001); further, the expression of p53 was higher, while the expression of PGC

was lower [38]. The existence and effects of the “telomere-p53-PGC axis” have also been verified by other scholars [39, 40]. Accumulating evidence has shown that PGC-1 α participate in the regulation of mitochondrial biogenesis and energy metabolism, which can directly reduce intracellular Ca²⁺ and indirectly reduce intracellular Ca²⁺ by inhibiting oxidative stress [12, 41, 42]. A recent study has argued that LTL is negatively associated with inflammation and oxidative status in humans [43]. In this study, we found that AF patients had a significantly lower level of PGC-1 α mRNA expression and serum PGC-1 α as well as decreased MMP when compared with controls, which indicate that telomere shortening and mitochondrial dysfunction are associated with the occurrence of aging-related AF. Interestingly, compared with the controls, the expression of leukocytes p53 mRNA was higher but without statistical difference; we assumed that this was because of the selected types of peripheral blood cells and the p53 expression being affected by many factors, as it is involved in multiple signaling pathways. Meanwhile, multivariate logistic regression confirmed that LTL and serum PGC-1 α were inversely associated with the presence of AF, and linear regression analysis confirmed that LTL was significantly correlated with CRP and LAD. Therefore, we can reasonably speculate that telomere may regulate

TABLE 5: The correlation of LTL with other clinical characteristics.

	Simple linear regression		Multiple linear regression	
	<i>r</i>	<i>P</i>	β	<i>P</i>
Clinical parameters				
Age (years)	-0.151	0.037	-0.111	0.110
BMI (kg/m ²)	-0.079	0.274		
Smoking, <i>n</i> (%)	0.119	0.099		
History of CHD, <i>n</i> (%)	-0.013	0.861		
Hypertension, <i>n</i> (%)	-0.046	0.529		
Diabetes mellitus, <i>n</i> (%)	0.115	0.114		
Hyperlipidemia	0.128	0.077		
Antihypertensive medication, <i>n</i> (%)	-0.045	0.532		
Glucose lowering treatment, <i>n</i> (%)	0.103	0.155		
Lipid-lowering medication, <i>n</i> (%)	-0.025	0.726		
SBP (mmHg)	0.068	0.352		
DBP (mmHg)	-0.071	0.331		
Laboratory parameters				
TC (mmol/L)	0.015	0.836		
TG (mmol/L)	-0.046	0.523		
LDL-C (mmol/L)	0.041	0.571		
HDL-C (mmol/L)	0.097	0.180		
Cr (mmol/L)	0.020	0.785		
BUN (mmol/L)	0.040	0.577		
UA (mmol/L)	-0.138	0.057		
FBG (mmol/L)	0.071	0.329		
GHB (%)	0.047	0.519		
CRP (mg/dL)	-0.200	0.005	-0.167	0.017
Echocardiographic parameters				
LVEF (%)	0.021	0.771		
LAD (mm)	-0.196	0.006	-0.165	0.018
Telomere-associated molecules				
Leukocyte p53 mRNA	0.059	0.417		
Leukocyte PGC-1 α mRNA	0.168	0.020	0.131	0.160
Serum PGC-1 α (pg/mL)	0.176	0.014	0.109	0.122

Abbreviations: BMI: body mass index; CHD: coronary heart disease; SBP: systolic blood pressure; DBP: diastolic blood pressure; TC: total cholesterol; TG: triglyceride; LDL-C: low-density lipoprotein cholesterol; HDL-C: high-density lipoprotein cholesterol; Cr: creatinine; BUN: blood urea nitrogen; UA: uric acid; FBG: fasting blood glucose; GHB: glycated hemoglobin; CRP: C-reactive protein; LVEF: left ventricular ejection fraction; LAD: left atrial diameter; PGC-1 α : peroxisome proliferator-activated receptor γ coactivator-1 α . *P* < 0.05 with italic font means statistically significant.

mitochondrial function, oxidative stress, calcium balance, and inflammation through downstream molecular PGC-1 α , causing atrial electrical and structural remodeling, eventually inducing AF. The specific mechanism remains to be further studied.

AF is a global public-health challenge with increased mortality and major morbidity, including stroke and heart failure [1, 2]. With the aging of the population, an increasing

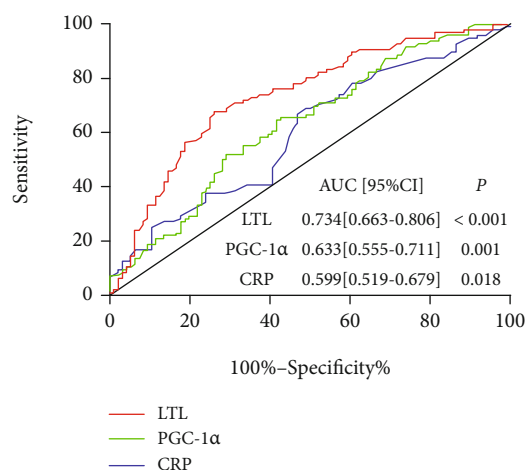


FIGURE 6: ROC curves of LTL, PGC-1 α , and CRP to predict AF. ROC analysis was performed to determine the sensitivity and specificity of the value. ROC: receiver operator characteristic; AUC: area under the curve; CI: confidence interval; LTL: leukocyte telomere length; CRP: C-reactive protein.

segment is being directly or indirectly impacted by this common arrhythmia. Studies have shown that about 70% of AF occurs between 65 and 80 years of age. The incidence of AF increases with age, and males have a higher rate of it than females, which means that elderly males are at the highest risk for developing AF. Studies have confirmed that extensive asymptomatic AF screening in the elderly can reduce the incidence of stroke and related disabilities [44]. However, many elderly asymptomatic AF people cannot be diagnosed early due to a lack of effective biomarkers. Our study revealed that LTL and serum PGC-1 α are negatively correlated with AF and confirmed that they have potential value in the early diagnosis of AF in the elderly male, which could provide new strategies for the screening of asymptomatic AF. In addition, PGC-1 α is an important regulator of mitochondrial metabolism, which is a protective factor for AF in the elderly population; thus, PGC-1 α may even be a possible novel target for AF intervention.

This study has several potential limitations. First, our study was an observational study, unable to establish a causal relationship. Second, many AF patients also presented with multiple age-related diseases such as hypertension, diabetes, and CHD; despite our best efforts to adjust for established and potential comorbidities, therefore, residual confounding by other unmeasured or unknown factors remains possible. Third, LTL was detected at one time point, while LTL declines throughout life, and the rate of telomere shortening could affect the incidence of AF. Fourth, due to various reasons, we were unable to detect the mitochondrial function indicators such as mitochondrial permeability transition pore (mPTP), mitochondrial calcium, and ROS for all subjects, and the specific mechanism remains to be further studied. Lastly, the subjects who we ultimately enrolled in our study were elderly males. More studies are warranted to compare these results with those of other populations.

In conclusion, LTL and serum PGC-1 α are inversely correlated with the occurrence of aging-related AF, and

mitochondrial dysfunction plays a role in this. These findings suggest that LTL and serum PGC-1 α could possibly be novel predictive biomarkers for the occurrence or outcomes of aging-related AF.

Data Availability

The data used to support the findings of this study are available from the corresponding authors upon request.

Conflicts of Interest

The authors declare that the research was conducted in the absence of any commercial or financial relationships that could be construed as potential conflicts of interest.

Acknowledgments

This work was supported by the National Nature Science Foundation of China (82070328 and 81870249).

References

- [1] J. Kornej, C. S. Börschel, E. J. Benjamin, and R. B. Schnabel, "Epidemiology of atrial fibrillation in the 21st century: novel methods and new insights," *Circulation Research*, vol. 127, no. 1, pp. 4–20, 2020.
- [2] V. Fuster, L. E. Rydén, D. S. Cannom et al., "2011 ACCF/AHA/HRS Focused Updates Incorporated Into the ACC/AHA/ESC 2006 Guidelines for the Management of Patients With Atrial Fibrillation," *Journal of the American College of Cardiology*, vol. 57, no. 11, pp. e101–e198, 2011.
- [3] S.-R. Lee, E.-K. Choi, K.-D. Han, M.-J. Cha, and S. Oh, "Trends in the incidence and prevalence of atrial fibrillation and estimated thromboembolic risk using the Cha2ds₂-Vasc score in the entire Korean population," *International Journal of Cardiology*, vol. 236, pp. 226–231, 2017.
- [4] D. Révész, Y. Milaneschi, J. E. Verhoeven, and B. W. J. H. Penninx, "Telomere length as a marker of cellular aging is associated with prevalence and progression of metabolic syndrome," *Journal of Clinical Endocrinology & Metabolism*, vol. 99, no. 12, pp. 4607–4615, 2014.
- [5] J. M. Fernández-Alvira, V. Fuster, B. Dorado et al., "Short telomere load, telomere length, and subclinical atherosclerosis," *Journal of the American College of Cardiology*, vol. 67, no. 21, pp. 2467–2476, 2016.
- [6] F. Z. Marques, S. A. Booth, P. R. Prestes et al., "Telomere dynamics during aging in polygenic left ventricular hypertrophy," *Physiological Genomics*, vol. 48, no. 1, pp. 42–49, 2016.
- [7] E. Silver, A. Ras, C. Cosgrove et al., "Telomere length as a biomarker and potential contributor of heart failure progression," *Journal of Cardiac Failure*, vol. 21, no. 8, pp. S28–S28, 2015.
- [8] J. D. Roberts, T. A. Dewland, J. Longoria et al., "Telomere length and the risk of atrial fibrillation: insights into the role of biological versus chronological aging," *Circulation. Arrhythmia and Electrophysiology*, vol. 7, no. 6, pp. 1026–1032, 2014.
- [9] J. F. Carlquist, S. Knight, R. M. Cawthon et al., "Shortened telomere length is associated with paroxysmal atrial fibrillation among cardiovascular patients enrolled in the intermountain heart collaborative study," *Heart Rhythm*, vol. 13, no. 1, pp. 21–27, 2016.
- [10] C. Su, Z. Liu, Y. Gao et al., "Study on the relationship between telomere length changes and recurrence of atrial fibrillation after radiofrequency catheter ablation," *Journal of Cardiovascular Electrophysiology*, vol. 30, no. 7, pp. 1117–1124, 2019.
- [11] J. Moslehi, R. A. Depinho, and E. Sahin, "Telomeres and mitochondria in the aging heart," *Circulation Research*, vol. 110, no. 9, pp. 1226–1237, 2012.
- [12] C. Allison and M. Núria, "The crosstalk between the gut microbiota and mitochondria during exercise," *Frontiers in Physiology*, vol. 8, 2017.
- [13] G. Uguccioni and D. A. Hood, "The importance of Pgc-1 α in contractile activity-induced mitochondrial adaptations," *American Journal of Physiology. Endocrinology and Metabolism*, vol. 300, no. 2, pp. E361–E371, 2011.
- [14] K. Chandrasekaran, M. Anjaneyulu, T. Inoue et al., "Mitochondrial transcription factor A regulation of mitochondrial degeneration in experimental diabetic neuropathy," *Neurobiology of Disease*, vol. 309, no. 2, pp. E132–E141, 2015.
- [15] J. Jeganathan, R. Saraf, F. Mahmood et al., "Mitochondrial dysfunction in atrial tissue of patients developing postoperative atrial fibrillation," *Annals of Thoracic Surgery*, vol. 104, no. 5, pp. 1547–1555, 2017.
- [16] Ó. Fabregat-Andrés, F. Ridocci-Soriano, J. Estornell-Erill et al., "Los niveles en sangre de PGC-1 α predice miocardio salvado y remodelado ventricular tras infarto agudo de miocardio con elevación del segmento ST," *Revista Espanola De Cardiologia*, vol. 68, no. 5, pp. 408–416, 2015.
- [17] E. Sahin, S. Colla, M. Liesa et al., "Telomere dysfunction induces metabolic and mitochondrial compromise," *Nature*, vol. 470, no. 7334, pp. 359–365, 2011.
- [18] S. Summermatter, G. Santos, J. Perez-Schindler, and C. Handschin, "Skeletal muscle PGC-1 controls whole-body lactate homeostasis through estrogen-related receptor - dependent activation of Ldh B and repression of Ldh A," *PNAS*, vol. 110, no. 21, pp. 8738–8743, 2013.
- [19] G. Y. H. Lip, J. L. Halperin, and H.-F. Tse, "The 2010 European Society of Cardiology guidelines on the management of atrial fibrillation: an evolution or revolution?," *Chest*, vol. 139, no. 4, pp. 738–741, 2011.
- [20] O. V. Tatarinova, I. P. Nikitin, V. N. Neustroeva, L. V. Shcherbakova, and Z. P. Gorokhova, "Arterial blood pressure in persons of elderly, senile age and long-livers of Yakutsk: population screening," *Uspekhi Gerontologii*, vol. 26, no. 1, pp. 82–88, 2013.
- [21] S. López-Domènech, C. Bañuls, N. Díaz-Morales et al., "Obesity impairs leukocyte-endothelium cell interactions and oxidative stress in humans," *European Journal of Clinical Investigation*, vol. 48, no. 8, p. e12985, 2018.
- [22] C. S. Stein, P. Jadiya, X. Zhang et al., "Mitoregulin: a lncRNA-encoded microprotein that supports mitochondrial supercomplexes and respiratory efficiency," *Cell Reports*, vol. 23, no. 13, pp. 3710–3720.e8, 2018.
- [23] R. Marrakchi, S. Ouerhani, S. Benammar et al., "Detection of cytokeratin 19 Mrna and Cyfra 21–1 (cytokeratin 19 fragments) in blood of Tunisian women with breast cancer," *The International Journal of Biological Markers*, vol. 23, no. 4, pp. 238–243, 2008.
- [24] N. S. Alavizadeh, A. Rashidlamir, and S. M. Hejazi, "Effect of eight weeks aerobic and combined training on serum levels of sirtuin 1 and Pgc-1 α in coronary artery bypass graft

- patients,” *Medical Laboratory Journal*, vol. 12, no. 5, pp. 50–56, 2018.
- [25] T. Yamada, Y. Murakami, T. Okada et al., “Plasma brain natriuretic peptide level after radiofrequency catheter ablation of paroxysmal, persistent, and permanent atrial fibrillation,” *Europace*, vol. 9, pp. 770–774, 2007.
- [26] A. D. Margulescu and L. M. Girbau, “Persistent atrial fibrillation vs paroxysmal atrial fibrillation: differences in management,” *Expert Review of Cardiovascular Therapy*, vol. 15, no. 8, pp. 601–618, 2017.
- [27] Y. Jih-Kai and C.-Y. Wang, “Telomeres and telomerase in cardiovascular diseases,” *Genes*, vol. 7, no. 9, p. 58, 2016.
- [28] Q. Wang, Y. Zhan, N. L. Pedersen, F. Fang, and S. Hägg, “Telomere length and all-cause mortality: a meta-analysis,” *Ageing Research Reviews*, vol. 48, pp. 11–20, 2018.
- [29] M. Allende, E. Molina, J. R. González-Porras, E. Toledo, R. Lecumberri, and J. Hermida, “Short leukocyte telomere length is associated with cardioembolic stroke risk in patients with atrial fibrillation,” *Stroke; a journal of cerebral circulation*, vol. 47, no. 3, 2016.
- [30] M. Margaritis, S. Patel, A. S. Antonopoulos, L. Herdman, M. Petrou, and R. Sayeed, “Telomere length predicts post-operative atrial fibrillation in patients undergoing cabg independently of chronological age,” *Circulation*, vol. 30, article A17369, 2014.
- [31] J. E. Siland, B. Geelhoed, I. C. Van Gelder, P. Van Der Harst, and M. Rienstra, “Telomere length and incident atrial fibrillation – data of the PREVEND cohort,” *Plos One*, vol. 12, no. 2, 2017.
- [32] W. Herrmann and M. Herrmann, “The importance of telomere shortening for atherosclerosis and mortality,” *Journal of Cardiovascular Development and Disease*, vol. 7, 2020.
- [33] S. Ravassa, G. Ballesteros, and J. Díez, “Aging and atrial fibrillation: a matter of fibrosis,” *Aging (Albany NY)*, vol. 11, no. 22, pp. 9965–9966, 2019.
- [34] L. Mikael, W. Victor, K. Paul, and N. Stanley, “Age as a critical determinant of atrial fibrillation: a two-sided relationship,” *Canadian Journal of Cardiology*, vol. 34, no. 11, pp. 1396–1406, 2018.
- [35] G. Bisaccia, F. Ricci, S. Gallina, A. Di Baldassarre, and B. Ghinassi, “Mitochondrial dysfunction and heart disease: critical appraisal of an overlooked association,” *International Journal of Molecular Sciences*, vol. 22, no. 2, p. 614, 2021.
- [36] J. N. Peoples, A. Saraf, N. Ghazal, T. T. Pham, and J. Q. Kwong, “Mitochondrial dysfunction and oxidative stress in heart disease,” *Experimental and Molecular Medicine*, vol. 51, no. 12, pp. 1–13, 2019.
- [37] Y. Zhu, X. Liu, X. Ding, F. Wang, and X. Geng, “Telomere and its role in the aging pathways: telomere shortening, cell senescence and mitochondria dysfunction,” *Biogerontology*, vol. 20, no. 1, pp. 1–16, 2019, Epub 2018 Sep 18.
- [38] A. Leri, “Ablation of telomerase and telomere loss leads to cardiac dilatation and heart failure associated with P53 upregulation,” *EMBO Journal*, vol. 22, no. 1, pp. 131–139, 2003.
- [39] N. Pieters, B. G. Janssen, L. Valeri et al., “Molecular responses in the telomere-mitochondrial axis of ageing in the elderly: a candidate gene approach,” *Mechanisms of Ageing & Development*, vol. 145, pp. 51–57, 2015.
- [40] B. Sui, C. Hu, and Y. Jin, “Mitochondrial metabolic failure in telomere attrition-provoked aging of bone marrow mesenchymal stem cells,” *Biogerontology*, vol. 17, no. 2, pp. 267–279, 2016.
- [41] Q. Li, S. Di, B. O’Rourke, S. M. Pogwizd, and L. Zhou, “Mitochondria-derived ROS bursts disturb Ca cycling and induce abnormal automaticity in guinea pig cardiomyocytes: a theoretical study,” *American Journal of Physiology Heart & Circulatory Physiology*, vol. 308, no. 6, 2015.
- [42] H. Eshima, S. Miura, N. Senoo, K. Hatakeyama, and Y. Kano, “Improved skeletal muscle Ca²⁺ regulation in vivo following contractions in mice overexpressing Pgc-1 α ,” *Ajp Regulatory Integrative & Comparative Physiology*, vol. 312, no. 6, 2017.
- [43] H. G. Simões, S. S. Aguiar, L. A. Deus, C. V. Souza, and T. S. Rosa, “Leucocyte telomere length, inflammation and oxidative stress in master athletes: the interplay,” *Medicine & Science in Sports & Exercise*, vol. 51, no. 6S, p. 987, 2019.
- [44] B. Freedman, J. Camm, H. Calkins, J. S. Healey, and B. P. Yan, “Screening for atrial fibrillation a report of the AF-Screen International Collaboration,” *Circulation*, vol. 135, no. 19, 2017.

Research Article

Ketogenic Diet Suppressed T-Regulatory Cells and Promoted Cardiac Fibrosis via Reducing Mitochondria-Associated Membranes and Inhibiting Mitochondrial Function

Jun Tao,¹ Hao Chen,² Ya-Jing Wang,³ Jun-Xiong Qiu,¹ Qing-Qi Meng,⁴ Rong-Jun Zou,⁵ Ling Li,¹ Jun-Gang Huang,¹ Zong-Kai Zhao,¹ Yu-Li Huang ,⁶ Hai-Feng Zhang ,⁷ and Jun-Meng Zheng ^{1,8}

¹Department of Cardiovascular surgery, Sun Yat-Sen Memorial Hospital, Sun Yat-sen University, Guangzhou, China

²Department of Gastroenterology, Guangdong Provincial People's Hospital, Guangdong Academy of Medical Sciences, Guangzhou, China

³Department of Otorhinolaryngology-Head and Neck Surgery, Sun Yat-sen Memorial Hospital, Sun Yat-sen University, Guangzhou, China

⁴Department of Orthopedics of Guangzhou Red Cross Hospital, Medical College, Jinan University, Guangzhou, China

⁵Heart Center, Guangdong Provincial Key Laboratory of Research in Structural Birth Defect Disease, Guangzhou Women and Children's Medical Center, Guangzhou Medical University, Guangzhou, China

⁶Department of Cardiology, Shunde Hospital, Southern Medical University, Foshan, China

⁷Department of Cardiology, Sun Yat-sen Memorial Hospital, Sun Yat-sen University, Guangzhou, Guangdong, China

⁸Department of surgery, Kiang Wu Hospital, Macau SAR, China

Correspondence should be addressed to Yu-Li Huang; hyuli821@smu.edu.cn, Hai-Feng Zhang; zhanghf9@mail.sysu.edu.cn, and Jun-Meng Zheng; zhengjm27@mail.sysu.edu.cn

Received 2 February 2021; Revised 28 February 2021; Accepted 22 March 2021; Published 19 April 2021

Academic Editor: Yun-dai Chen

Copyright © 2021 Jun Tao et al. This is an open access article distributed under the Creative Commons Attribution License, which permits unrestricted use, distribution, and reproduction in any medium, provided the original work is properly cited.

Ketogenic diet (KD) is popular in diabetic patients but its cardiac safety and efficiency on the heart are unknown. The aim of the present study is to determine the effects and the underlined mechanisms of KD on cardiac function in diabetic cardiomyopathy (DCM). We used db/db mice to model DCM, and different diets (regular or KD) were used. Cardiac function and interstitial fibrosis were determined. T-regulatory cell (Treg) number and functions were evaluated. The effects of ketone body (KB) on fatty acid (FA) and glucose metabolism, mitochondria-associated endoplasmic reticulum membranes (MAMs), and mitochondrial respiration were assessed. The mechanisms *via* which KB regulated MAMs and Tregs were addressed. KD improved metabolic indices in db/db mice. However, KD impaired cardiac diastolic function and exacerbated ventricular fibrosis. Proportions of circulatory CD4⁺CD25⁺Foxp3⁺ cells in whole blood cells and serum levels of IL-4 and IL-10 were reduced in mice fed with KD. KB suppressed the differentiation to Tregs from naive CD4⁺ T cells. Cultured medium from KB-treated Tregs synergically activated cardiac fibroblasts. Meanwhile, KB inhibited Treg proliferation and productions of IL-4 and IL-10. Treg MAMs, mitochondrial respiration and respiratory complexes, and FA synthesis and oxidation were all suppressed by KB while glycolytic levels were increased. L-carnitine reversed Treg proliferation and function inhibited by KB. Proportions of ST2L⁺ cells in Tregs were reduced by KB, as well as the production of ST2L ligand, IL-33. Reinforcement expressions of ST2L in Tregs counteracted the reductions in MAMs, mitochondrial respiration, and Treg proliferations and productions of Treg cytokines IL-4 and IL-10. Therefore, despite the improvement of metabolic indices, KD impaired Treg expansion and function and promoted cardiac fibroblast activation and interstitial fibrosis. This could be mainly mediated by the suppression of MAMs and fatty acid metabolism inhibition *via* blunting IL-33/ST2L signaling.

1. Introduction

Diabetic individuals suffer from much more cardiovascular complications than nondiabetic patients. Besides coronary artery disease, ventricular damage is also frequently evident in diabetic patients, which refers to a term of “diabetic cardiomyopathy” (DCM). The incidence of DCM greatly contributes to heart failure, which is the main complication leading to life and health loss in diabetic patients. In clinical aspect, DCM is characterized by the impairment of diastolic function while the systolic function remained unchanged, especially in the early stage of the disease. From the microcosmic view, cardiomyocyte hypertrophy and interstitial cardiac fibrosis are the fundamental changes [1].

Ketogenic diet (KD) is a very low-carbohydrate, high-fat diet that typically includes plenty of meats, eggs, cheeses, fish, and nuts, which is a therapy to epilepsy in clinical practice. It has been shown to improve blood sugar control for patients with type 2 diabetes (T2DM) and thus widely used in these patients. Moreover, it has been proposed to be a preventive or therapeutic strategy for metabolic disorders [2]. However, on the other hand, it has been linked to vascular insult recently [3]. In the field of cardiac remodeling, KD is reported to be associated with improved cardiac function, cardiomyocyte survival, and attenuated cardiac fibrosis in both T2DM and aging mice [4, 5]. In contrast, ketogenic diet was shown to be associated with cardiac remodeling in hypertensive rats [6]. Besides, *in vitro* study directly showed that the ketone body strengthened cardiac fibroblast activation induced by transforming growth factor- β 1, which is a hallmark of the enhanced interstitial fibrosis [6]. Therefore, more studies are needed in order to clarify the detailed roles of KD on DCM.

Besides the heart itself, KD could modify the innate immune system that is closely related to the development of DCM. For example, KD regulates the T cell subset and group 2 innate lymphoid cells [7–11]. However, the alterations of KD on the innate immune system during DCM are also unknown. On the other hand, the ketone body was found to be associated with enhanced mitochondrial respiratory function and substrate metabolism, [12, 13] which is crucial to T cell subset differentiation and function [14, 15]. Among various factors critically involved in mitochondrial respiratory function and substrate metabolism, mitochondria-associated endoplasmic reticulum membranes (MAMs) are an important one [16, 17].

IL-33 acts through its receptor ST2. The membrane ST2 (ST2L) mediates the biological effects of IL-33 while the soluble ST2 (sST2) acts as the decoy receptor that restricts the effects of IL-33 [18]. We recently demonstrated that interleukin-33 (IL-33) protected diabetic mice from DCM and reduced cardiac fibrosis [19]. However, the role of changes of endogenous IL-33/ST2L signaling and their potential roles in Tregs and KD-treated diabetes are unknown.

Thus, to link KD and DCM development, we demonstrated the effects of KD on cardiac fibrosis of DCM and Tregs. We found that KD impaired cardiac function and addressed the roles of MAMs, Treg substrate metabolism, and IL-33/ST2L signaling in this process.

2. Methods

2.1. Animals and Cells. Male C57BLKsJ-db/db mice were used to establish the spontaneous T2DM and DCM as our previous report [19]. Age-matched male C57BLKsJ-m/m mice were used as the control [19]. Mice were kept in a 12 h light/dark cycle with free access to chow and water. Eight-week-old db/db mice were randomly assigned to receive either regular chow diet (RD, % of total kcal, 18% protein, 65% carbohydrate, and 17% fat) or KD (% of total kcal, 10% protein, <1% carbohydrate, and 89% fat) for 12 weeks. The nutritional composition of the ketogenic diet was shown in Table 1. After 12 weeks of treatment, mice were subjected to echocardiography and invasive hemodynamic assessment. After that, mice were anesthetized by intraperitoneal injection of ketamine (80 mg/kg body weight) and xylazine (5 mg/kg body weight) and then were sacrificed. The left ventricular was acquired and cut, which were then fixed in 4% paraformaldehyde or cryopreserved in liquid nitrogen according to different further assessments. All the animals were purchased from the Model Animal Research Center of Nanjing University. All the animal procedures were conformed to the Guide for the Care and Use of Laboratory Animals published by the US National Institutes of Health and were approved by the Institutional Animal Care and Use Committee of Sun Yat-sen University.

Peripheral blood mononuclear cell (PBMC) or CD4⁺ T cells were used in the *in vitro* study. PBMCs were isolated by the density gradient centrifugation method with Ficoll (TBD science, density: 1.079 g/ml, Tianjin, China) as previously reported [20]. Briefly, for isolation, whole blood samples were collected in the heparin anticoagulation condition. Blood samples were diluted with the same volume of PBS, which were then overlaid on Ficoll. PBMCs were isolated in the middle layer after centrifugation, which were collected for further analysis. For CD4⁺ T cells and CD4⁺CD25⁺Foxp3⁺ Treg isolations, the mouse spleen were obtained and splenocytes were retrieved by mechanical dissociation of the spleen on 70 μ m Cell strainer filter (BD Falcon™, New Jersey, USA) [21]. Cell suspensions were then transferred for isolation using the commercially available kits (EasySep™, StemCell Tech, Vancouver, Canada) under the manufacturer's instructions. Isolated CD4⁺ T cells were then resuspended and cultured in the RPMI-1640 medium (Thermo Fisher, Massachusetts, USA) containing 10% FBS (Thermo Fisher, Massachusetts, USA), 2 mM L-glutamine (Sigma-Aldrich, Missouri, USA), 1% penicillin/streptomycin, and 50 μ M mercaptoethanol (Sigma-Aldrich, Missouri, USA). The ketone bodies used in the current study are 25 mM β -hydroxybutyrate (Sigma-Aldrich, Missouri, USA).

2.2. Echocardiogram and Invasive Hemodynamic Assessments. Echocardiogram and invasive hemodynamic assessment were used to assess *in vivo* cardiac function. Animals were anesthetized as mentioned above. Left ventricular ejection function (LVEF) and left ventricular end diastolic dimension (LVEDd) were measured by the Visual Sonics Echo System (Vevo2100, VisualSonics, Toronto, Canada) and MicroScan Transducer (MS-400, 30 MHz, VisualSonics, Toronto, Canada) [19].

Hemodynamic assessment was performed before sacrifice following anesthesia according to the previous report

TABLE 1: Nutritional composition of ketogenic diet (g/1000 g).

Ingredients	
Vitamins, mixed	10.0
Choline	—
Minerals, mixed	35.0
Fibers	50.0
Sucrose	—
Casein	200.0
Maize starch	—
Soya oil	—
Maize oil	102.0
Lard	424.7
Margarine	178.3
Total	1000

[22]. Briefly, a percutaneous puncture of the carotid was performed under sterile conditions. After the Millar catheter (Mikro-Tip®, Millar Instruments, Houston) insertion, heparin (100 IU/kg, iv) was administered. $\pm dp/dt_{\max}$ was obtained by MPVS Ultra™ pressure-volume unit and PowerLab data acquisition system (ADInstruments, Sydney, Australia). All measurements were performed after the confirmation of hemodynamic stability for 2 min. An average of 3 respiratory cycles was used for analysis.

2.3. Isolation of MAMs, Western Blot, and Polymerase Chain Reaction (PCR). MAMs were isolated using the modified protocol according to the previous reports [23]. Briefly, Tregs were ultrasonically fragmented, which were centrifuged for 5 min at 750 g for 2 times. Supernatants were collected and were subjected to high-speed centrifugations (10 min for 9000 g \times 1 and 10000 g \times 2). Pellets were collected and resuspended in solution (250 mM mannitol, 0.5 mM EGTA, and 5 mM HEPES; pH 7.4), which were then subjected to ultra-speed centrifugation (100000 g, 30 min). The middle layers were collected for centrifugations (6300 g, 10 min), and the supernatants were collected for final centrifugations for 1 h at 100000 g. All centrifugations were done in 4°C. Protein quantification analysis using BCA methods according to the manufacturer's instructions (Cell Signaling Technology, Massachusetts, USA) was adopted to represent the amounts of MAMs. The pure mitochondria isolated using the commercially available kit (Thermo Fisher, Massachusetts, USA) as our previous report [24] were used as the inner control.

Western blot was performed as our previous report [25]. Briefly, samples were collected and washed. Totally proteins were extracted and quantified using the BCA methods. The amount of 60 μ g total proteins was subjected to SDS-PAGE electrophoresis, which was then transferred to a PVDF membrane (Millipore, Massachusetts, USA). Finally, PVDF membranes were incubated with respective antibodies (all were from Abcam, Cambridge, UK) and electrochemiluminescence (Millipore, Massachusetts, USA) was added to visualize bands. The ImageJ software was used for densitometry measurements.

To assess mtDNA copy number, quantified PCR was performed. Briefly, DNA was extracted and the short segment of

mtDNA was amplified, which was compared to the amplification of the short segment of nuclear DNA (β -globin) [26]. Primers used were also listed in the previous report [26].

2.4. Masson's Trichrome Staining and Hydroxyproline Assay. Masson's Trichrome staining and hydroxyproline assessment were used to evaluate contents of ventricular collagen. For Masson's Trichrome staining, ventricular tissues fixed in 4% paraformaldehyde were embedded in paraffin, which were then subjected to cut into 5 μ m slices. Slices were deparaffinized and rehydrated. After that, slices were stained using Trichrome Stain (Masson) kit (Sigma-Aldrich, Missouri, USA) under the manufacturer's instructions. Collagen, muscle, and nuclei are stained in blue, red, and black, respectively.

2.5. Flow Cytometry. Flow cytometry was used to detect fatty acid absorption, intracellular fatty acid, and CD4⁺CD25⁺Foxp3⁺ Tregs. For fatty acid absorption, BODIPY (BODIPY 503/512, Thermo Fisher Scientific, Massachusetts, USA) was used. It is a green fluorescent fatty acid, which could be used to monitor fatty acid absorption by cells [27]. For the detection of intracellular fatty acid, another BODIPY (BODIPY 505/515, Thermo Fisher Scientific, Massachusetts, USA), a cell membrane permeant fluorophore and a stain for natural lipids, was used. Flow cytometry was used to detect the fluorescence by BODIPY. All the flow cytometry data were acquired by LSR Fortessa flow cytometer (BD, New Jersey, USA) and were analyzed with FlowJo software (Version 10, Tree Star Inc.).

2.6. Cell Viability and Treg Cytokine Assessment. Cell viability of Tregs were reflected by CCK-8 levels determined using Cell Counting Kit-8 (CCK-8, Dojindo Molecular Technologies, Kumamoto, Japan). Interleukin-4 (IL-4) and interleukin-10 (IL-10) are the main cytokines represented by Treg functions. They were determined by enzyme-linked immunosorbent assay (ELISA). Procedures of CCK-8 measurements and levels of IL-4 and IL-10 determination were performed under the manufacturer's instructions (kits of ELISA, R&D Systems, Minnesota, USA).

2.7. Seahorse Analysis. Oxygen consumption rate (OCR) was measured using Seahorse XF96 (Agilent, Delaware, USA) as our previous report [28]. Briefly, cells were cultured in the working medium (Seahorse XF basal medium, Catalog, 103335-100, Agilent, Delaware, USA). Basal oxidative phosphorylation (OXPHOS) and ATP-linked OXPHOS were calculated from the OCR profile to represent mitochondrial respiratory function.

2.8. Statistical Analysis. Normally distributed data are expressed as mean \pm SEM. One-way ANOVA, followed by SNK test for multiple post hoc comparisons, was adopted to test the statically differences among groups. A *P* value < 0.05 indicated the statistical significance. All the statistical analyses were done with the OriginLab software (version2019b, Massachusetts, USA).

TABLE 2: Metabolic indices of mice.

	m/m	db/db	db/db+KD	db/db+PBS	P value
Body weight (g)	28.72 ± 3.72	40.12 ± 3.47*	43.48 ± 3.66 [#]	34.26 ± 5.87	<0.01
Heart weight (g)	0.26 ± 0.02	0.41 ± 0.03*	0.46 ± 0.03 [#]	0.393 ± 0.042	<0.01
Fasting glucose (mM)	10.06 ± 0.57	23.01 ± 3.56*	17.43 ± 3.15 [#]	23.11 ± 3.79	<0.01
TC (mg/dl)	216.37 ± 15.37	240.58 ± 20.75	225.48 ± 35.05	234.57 ± 20.59	0.35
TG (mg/dl)	116.13 ± 10.35	132.68 ± 12.84	114.25 ± 15.48 [§]	135.54 ± 12.84	0.02
LDL-c (mg/ml)	153.59 ± 5.78	157.15 ± 8.39	152.89 ± 10.60	154.99 ± 13.67	0.89
Fasting insulin (mIU/l)	21.59 ± 4.60	49.333 ± 9.522*	31.47 ± 6.36 [#]	50.32 ± 11.94	<0.01
HOMA-IR	9.70 ± 2.30	49.83 ± 8.60*	24.35 ± 6.68 [#]	52.30 ± 17.57	<0.01

KD: ketogenic diet; PBS: phosphate-buffered solution; TC: total cholesterol; TG: triglyceride; LDL-c: low-density lipoprotein cholesterol; HOMA-IR: homeostasis model assessment-insulin resistance; *compared with m/m, $P < 0.01$; [#]compared with db/db+PBS, $P < 0.01$; [§]compared with db/db+PBS, $P < 0.05$; P values were derived from ANOVA.

3. Results

3.1. KD Promoted Cardiac Fibrosis and Worsened Diastolic Function despite Metabolic Improvements. We examined the effects of KD on metabolic dysfunction in mice first. Metabolic indices were listed in Table 2. In summary, body weight, heart weight, serum fasting glucose, and cholesterol levels were improved by KD. Besides, serum insulin was decreased, and the insulin sensitivity, as indicated by HOMA-IR, was improved by KD (Table 2).

We next assessed ventricular performance and function in mice. Unexpectedly, as results measured by the hemodynamic methods, cardiac contractile function (dp/dt_{max} , Figure 1(a)) was mildly decreased while the diastolic function ($-dp/dt_{max}$, Figure 1(b)) were obviously reduced in KD-treated mice. Results from UCG measurements showed that mice treated with KD, compared with those either with PBS control or with pre-KD treatment, showed a decreased E/A ratio (Figure 1(c)), while nonsignificant changes of LVEF (Figure 1(d)) and LVEDd (Figure 1(e)) could be observed.

Diastolic dysfunction may be due to cardiomyocyte hypertrophy and/or declined ventricular compliance. However, heart weight was not significantly different among mice with different treatments, which might not support the significant role of hypertrophy during this process. Interstitial fibrosis is the key for ventricular compliance; therefore, we sought for the evidence of cardiac interstitial fibrosis in mice. As expected, Masson's Trichrome staining revealed that ventricular collagen levels were much more obvious in mice fed with KD (Figures 1(f) and 1(g)). All these results showed that KD worsened diastolic function and promoted interstitial fibrosis despite improvements of serum glucose.

3.2. KD Resulted in Circulating Treg Reduction and Cardiac Fibroblast Activation. The reason of the exacerbated cardiac fibrosis elicited by KD is unknown, and Tregs played an important role in cardiac fibrosis. We therefore continued to explore the changes of Tregs upon KD treatment. As shown in Figure 2(a), KD resulted in a reduced proportion of $CD4^+CD25^+Foxp3^+$ cells in whole blood cells. Besides, serum levels of Treg cytokines, IL-4 and IL-10, were also decreased in KD-treated mice (Figures 2(b) and 2(c)). *In*

vitro, KB, compared with PBS control, significantly reduced the proportion of $CD4^+CD25^+Foxp3^+$ cells induced from spleen $CD4^+$ T cells (Figure 2(d)). IL-4 and IL-10 productions in supernatants of these cells were also decreased (Figures 2(e) and 2(f)).

The results shown in Figure 1 supported the role of interstitial fibrosis in DCM diastolic dysfunction, and we therefore focused on the activation of cardiac fibroblasts. However, the roles of suppressing Treg differentiation from T cells by KD/KB on cardiac fibroblasts activation is unknown and we therefore continued to explore them. Results found that cultured medium from KB-treated Tregs dramatically activated cardiac fibroblasts, as manifested by α -SMA and POSTN expressions assessed by Western blotting (Figure 2(g)). Proliferation assays also supported cardiac fibroblast activation. Compared with the cultured medium from Tregs that received PBS treatment, CCK-8 levels were increased in cells treated with the medium from KB-treated Tregs (Figure 2(h)). All these results supported that the regulation on Treg expansion and function are critical in cardiac fibroblast activation.

3.3. KB Orchestrated FA and Glycolysis Metabolisms and Suppressed Tregs. The mechanism that KB regulates Tregs is unknown, and the metabolisms of fatty acid and glucose are crucial for Treg expansion and function. Therefore, we continued to investigate the changes of fatty acid and glucose metabolism under KB treatment.

We investigated the levels of glycolysis and mitochondrial respiration first. As shown in Figure 3(a), ECAR was increased in cells treated with KB, indicating the increased levels of glycolysis. However, OCR was decreased in cells administered with KB, showing a decreased level of OXPHOS (Figures 3(b) and 3(c)). Accordingly, ATP productions were also reduced (Figure 3(c)).

As for intracellular fatty acid contents, Tregs were separated from the spleen and intracellular fatty acid was determined by BODIPY, a membrane-permeable fluorophore for lipids. As shown in Figure 3(c), compared with regular diet mice, Tregs from KD-treated mice represented a less BODIPY staining (Figure 3(d)), indicating a reduced level of intracellular fatty acid. We next tested whether the

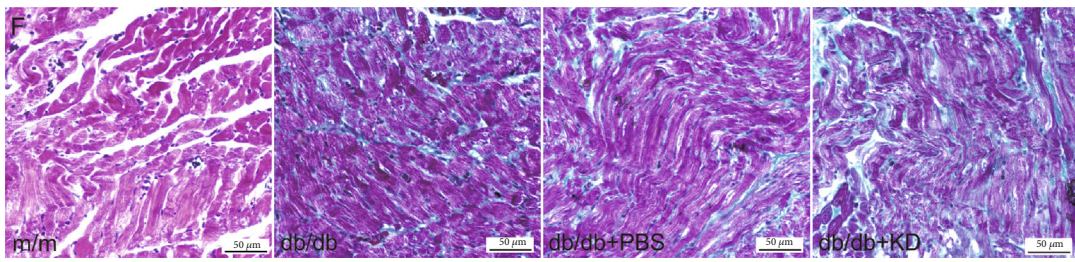
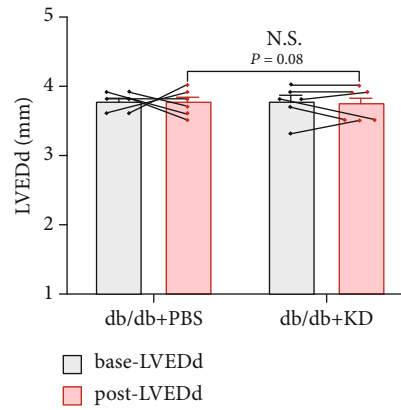
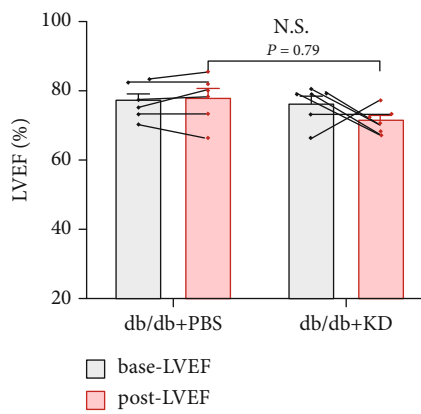
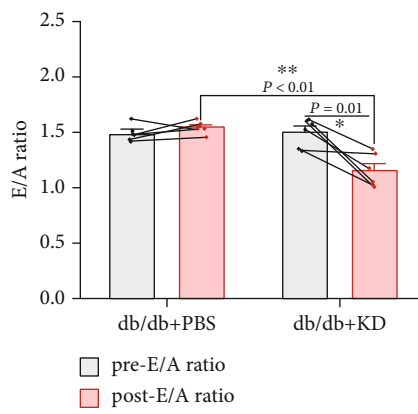
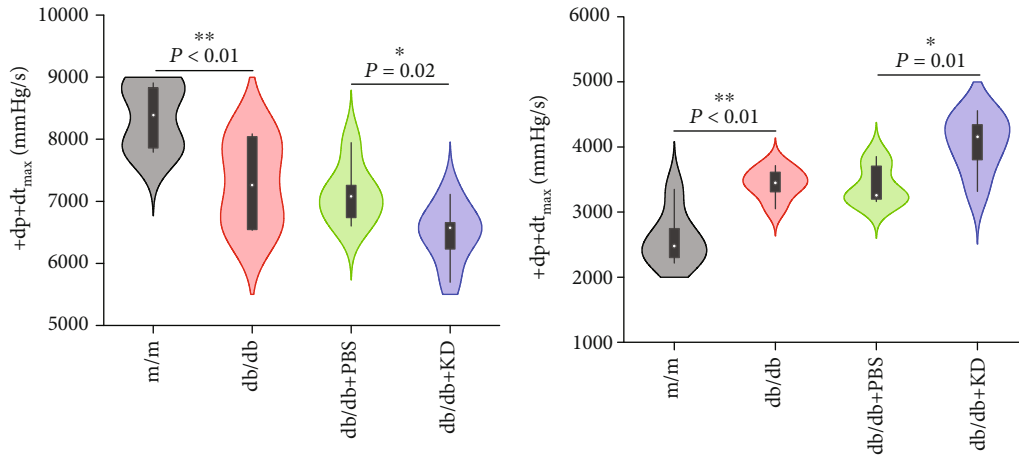


FIGURE 1: Continued.

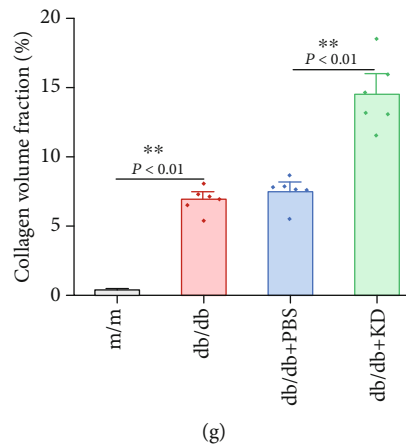


FIGURE 1: Effects of ketogenic diet on cardiac functions, left ventricular size, and collagen contents. Cardiac functions were represented as $+dp/dt_{\max}$ (a), $-dp/dt_{\max}$ (b), E/A ratio (c), LVEF (d) and LVEDd (e). Left ventricular size was represented as LVEDd. Collagen contents were represented as Masson's Trichrome staining (f) quantified as collagen volume fraction (g). KD: ketogenic diet; LVEF: left ventricular ejection fraction; LVEDd: left ventricular end-diastolic diameter.

absorption of fatty acid by Tregs was also decreased. Unexpectedly, we found that KB treatment resulted in a mildly increased green fluorescence, indicating an upregulated fatty acid absorption (Figure 3(e)). We therefore continued to explore whether, instead, intracellular FA metabolic routes were involved in lipid accumulation and Treg proliferation and function. FA synthesis and oxidation were analyzed, respectively.

The expressions of FA synthesis rate-limiting enzymes, FAS and ACACB, were detected by Western blotting. As shown in Figure 3(f), both the expressions of FAS and ACACB were moderately decreased upon KB treatment. CPT1a is the critical enzyme of mitochondrial FA oxidation; the expressions of which were also investigated. Unexpectedly, CPT1a expressions were decreased to a more extent compared with those of ACACB (Figure 3(f)). Therefore, we continued to explore the role of decreased FA oxidation in Treg suppression by using L-carnitine to facilitate FA oxidation. As shown in Figure 3(g), L-carnitine significantly increased Treg proportions. All these results indicated that FA oxidation inhibition is the key event in KB-induced Treg suppression.

3.4. KB Dismissed MAMs and Respiratory Complexes in Tregs *In Vitro*. The mitochondria are the main organelle that FA oxidation occurs. Thus, the above results implied the role of mitochondrial respiration in KB-dependent Treg regulation. MAMs are the key structure that controls mitochondrial respiratory function, and we therefore examined the alterations of MAMs first. As shown in Figure 4(a), the reduction of MAMs was found in AGEs-treated Tregs, as determined by the quantitative analysis of MAM protein levels relative to those of pure mitochondria. Moreover, compared with AGEs alone, MAMs were further decreased in the presence of KB. The MAM proteins, Sigma-1 receptor, and FACLA, as determined by Western blot were also decreased upon KB treatment (Figure 4(b)).

Mitochondrial respiratory complexes are the main proteins that charge OXPHOS, and we also investigated the

changes of these respiratory complexes. As shown in Figure 4(c), complexes I, II, and IV were barely detected in all Tregs. Complex III were mostly expressed, followed by complex IV. Both the contents of complexes III and V were decreased by AGEs, which were further decreased in the presence of KB (Figure 4(c)).

Besides MAMs and respiratory complexes, mitochondrial quantity was also examined. As shown in Figure 4(d), Tregs under KB treatment represented less mitochondrial DNA, which supported the reduction of intracellular mitochondrial contents. All these results showed that both mitochondrial functions were significantly impaired in AGEs-treated Tregs, which were exacerbated in the presence of KB.

3.5. Attenuation of IL-33/ST2L Signaling Is Essential in KB-Induced MAM Reduction and Treg Inhibition. Despite the fact that the suppression of MAMs could explain the effects of KB on FA oxidation and mitochondrial respiration, it is still unclear how KB inhibits MAMs. The transmembrane receptor, ST2L, is crucial in Treg expansion and function, and we therefore detected the alterations of ST2L in Tregs under KB treatment.

As shown in the results of flow cytometry in Figure 5(a), the proportions of ST2L⁺ Tregs were obviously decreased in KB-treated Tregs. We tried to examine the supernatant contents of IL-33, the only ST2L ligand discovered, which could also activate Tregs, but it was hardly to be detected in the supernatants of Tregs unless NP-40 was added (Figure 5(b)). However, levels of the decoy receptor of IL-33 and sST2, despite the expression levels of which being relatively low, were statistically significantly increased in the supernatant of Tregs treated by KB (Figure 5(c)). Besides, it also should be noted that IL-33 and sST2 productions were even less in ST2L⁺ Tregs (Figures 5(d) and 5(e)). These results showed that KB suppressed IL-33/ST2L signaling in Tregs.

We continued to ask whether the depressed IL-33/ST2L signaling mediated KB-induced MAM suppression and Treg expansion. Expressions of ST2L in Tregs were restored, and the quantities of Tregs and their MAMs were examined.

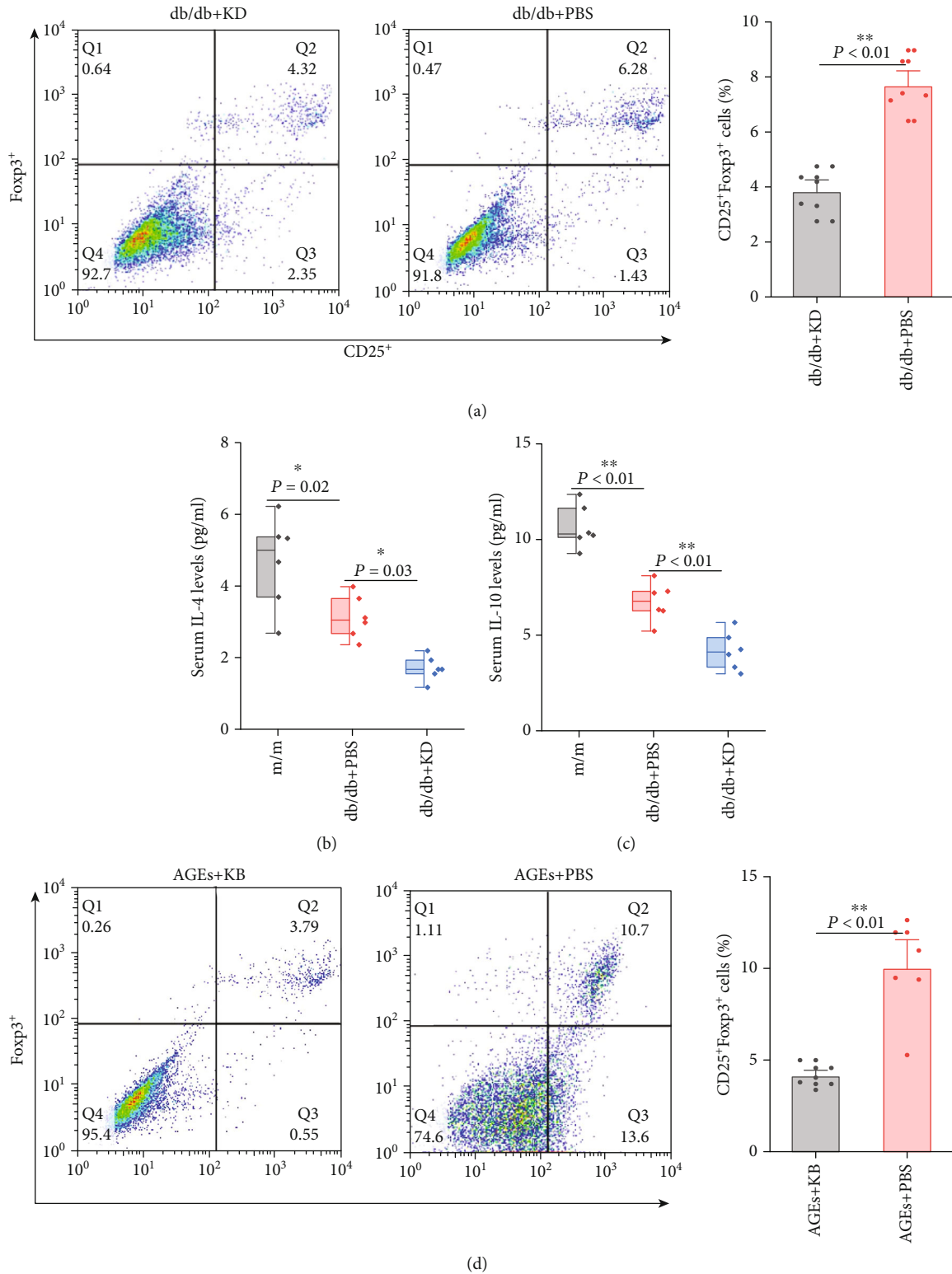


FIGURE 2: Continued.

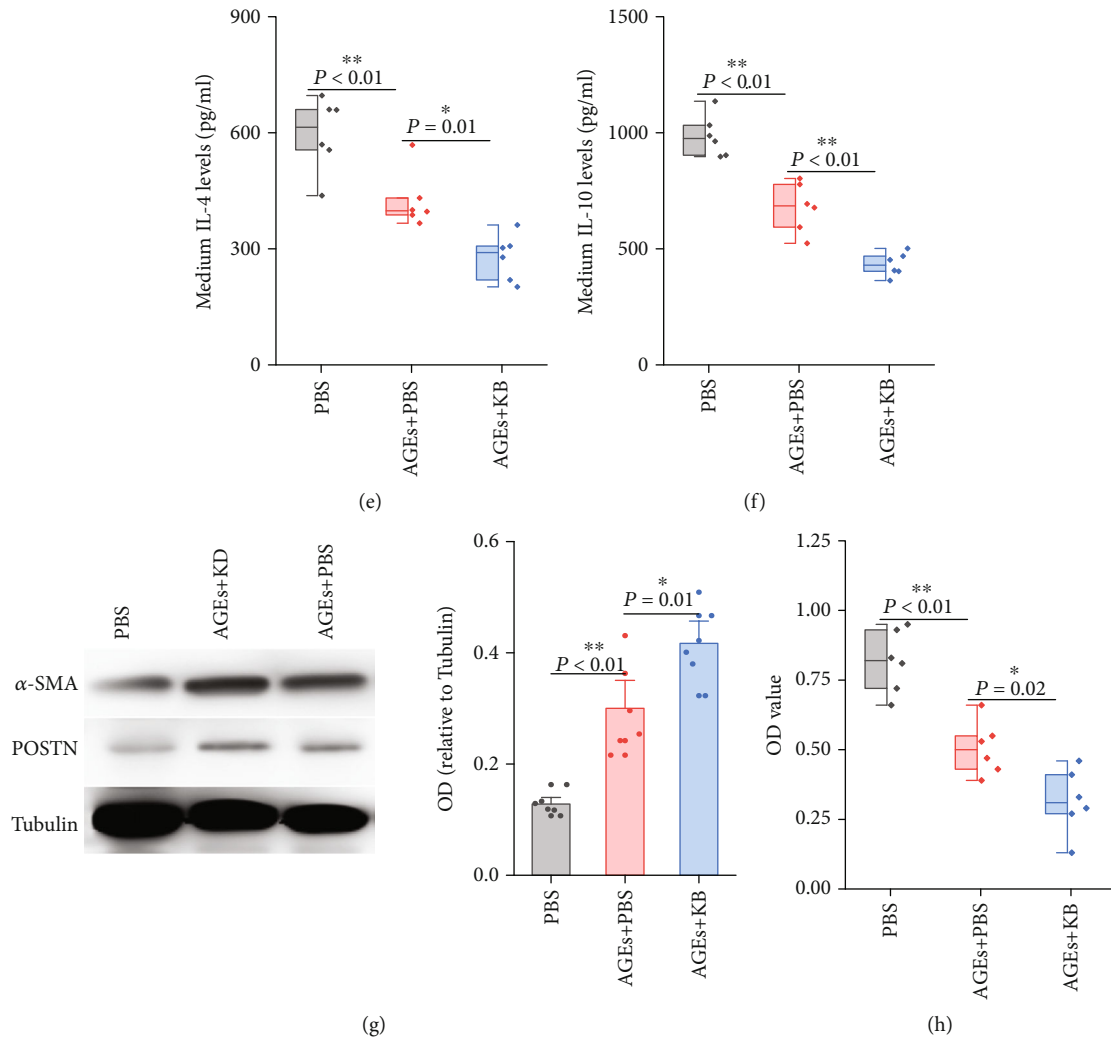


FIGURE 2: Ketogenic diet suppressed Treg functions which promoted cardiac fibroblast activation. Effects of ketogenic diet on Treg proportions in whole blood cells (a) and serum Treg cytokines (b, c). Effects of ketogenic diet on Treg proportions in $CD4^+$ T cells derived from the spleen (d) and medium Treg cytokines (e, f). Effects of spleen-derived $CD4^+CD25^+Foxp3^+$ Treg cultured medium from different treatments on activation markers (g) and cell vitality (h). *P* values were derived either from the *t*-test (a, d) or the ANOVA followed by SNK for multiple comparisons (b, c, e–h).

Results found that, compared with the vector control, reinforcement of ST2L in Tregs prevented the loss of MAMs (Figure 5(f)) in KB-treated $CD4^+CD25^+Foxp3^+$ Tregs (Figure 5(g)). All these results indicated that the depressed IL-33/ST2L signaling is crucial for KB-induced MAM reduction and Treg suppression.

4. Discussion

The potential benefits of KB were recognized recently, and the adoption of this diet style is becoming more and more popular. However, the safety and efficiency of KB in the heart function during diabetes are still under sharp debating. In the present study, we demonstrated that KB, despite improved metabolic profiles, resulted in worse heart function and more severe ventricular remodeling in DCM. Our study implied that the inhibition of Tregs could be the underline mechanism mediating the cardiac insults exacerbated by KB. Fur-

thermore, we revealed that the reduction of MAMs and mitochondrial respiration, which was caused by the blunt IL-33/ST2L signaling, could be the reason of KB-induced Treg suppression.

The current study did not support the regular and wide adoption of KD in diabetes patients. Despite KD being able to confer potential benefits in metabolic indices in this situation, KD, in fact, impaired heart function. Our results were supported by a recent population-based study, which concluded a deleterious result on the coronary artery conferred by low-carbohydrate diet that is similar to KD [3]. However, the findings of the current study supporting the unflavored role of KD in diabetes is sharply in contrast to the previous study, showing beneficial effects of KD in cardiomyocyte survival and interstitial fibrosis [4]. The differences of animal characteristics could be the most plausible explanation of this discrepancy. The hallmark of typical DCM, especially during the early stage, is the impairment of diastolic dysfunction

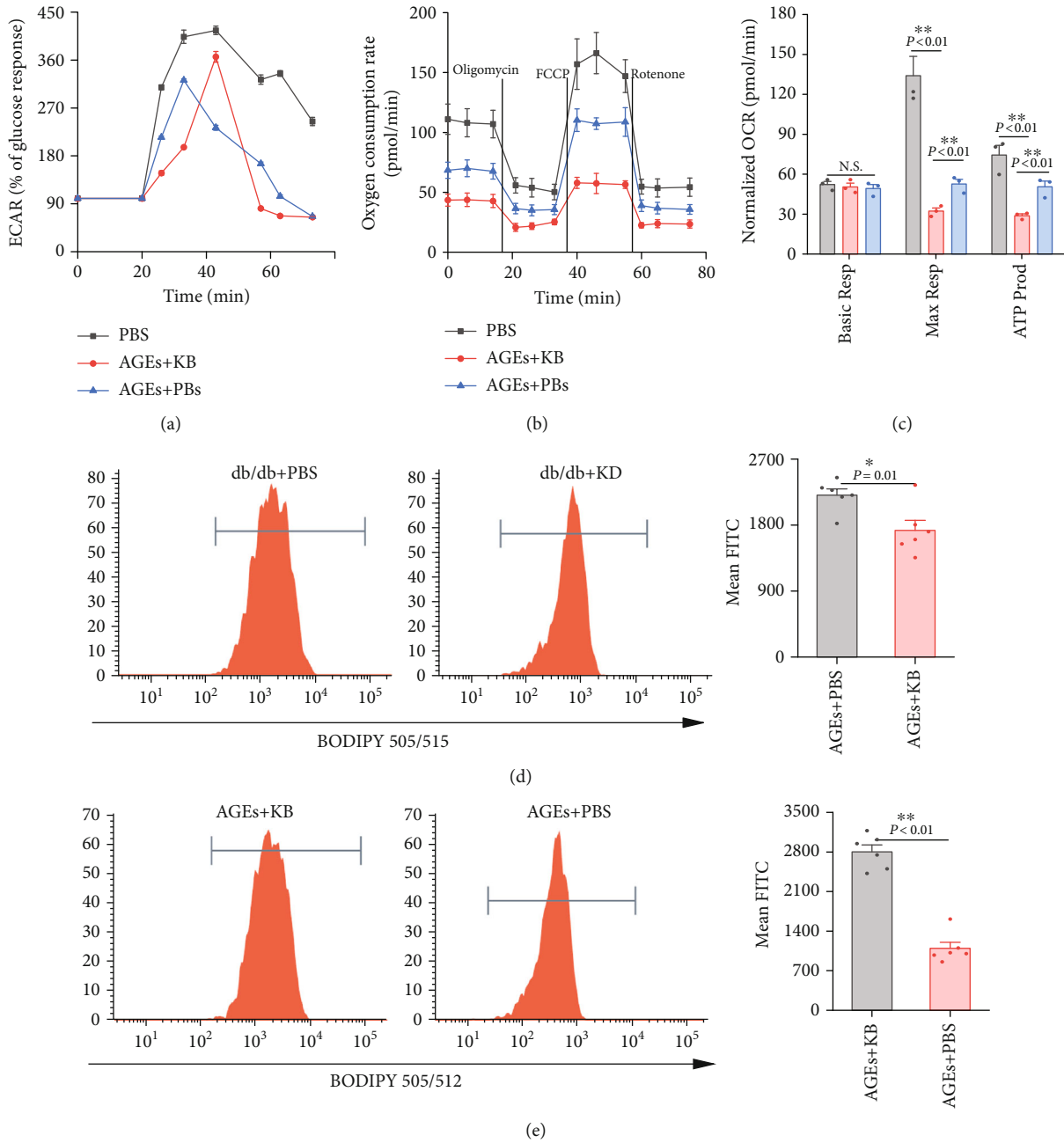


FIGURE 3: Continued.

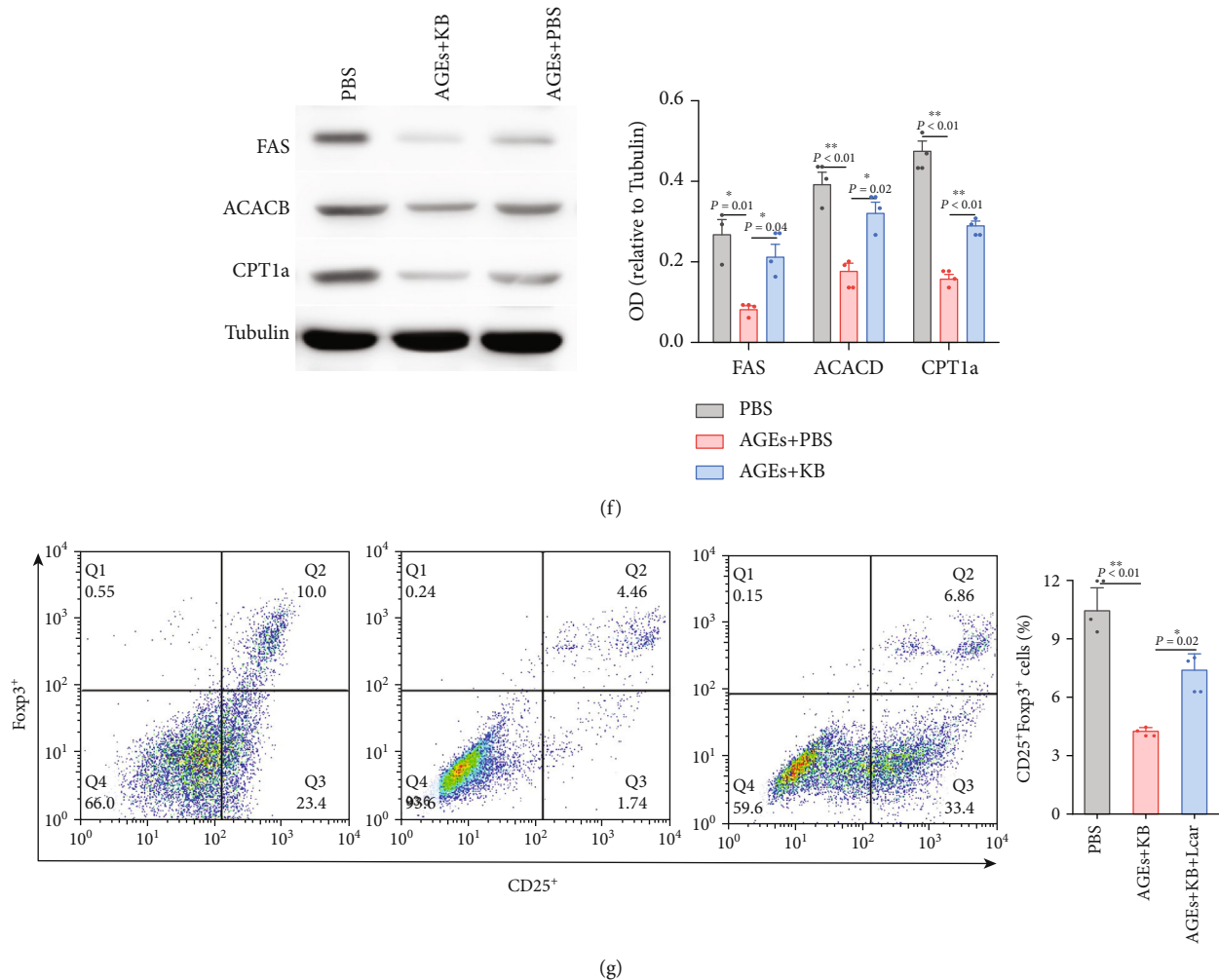


FIGURE 3: Effects of KB on glucose and FA metabolism in Tregs. Effects of KB on extracellular acidification rates (a) and oxygen consumption (b, c) in CD4⁺CD25⁺Foxp3⁺ cells derived from the spleen. Effects of KB on intracellular FA contents (d) and absorption (e) in CD4⁺CD25⁺Foxp3⁺ cells. Effects of KB on key genes involved in FA synthesis and oxidation (f). Effects of KB on CD25⁺Foxp3⁺ cells derived from CD4⁺ T cells (g). *P* values were derived either from the ANOVA followed by SNK for multiple comparisons (a–c, f, g) or the *t*-test (d, e). Basic Resp: basic respiration; Max Resp: maximum respiration; ATP Prod: ATP production.

without concurrent systolic defects [19]. However, the above-mentioned study showed a significant reduction of LVEF in db/db mice [4], which implied a late stage of DCM or other coexistent causes of cardiac insults. The serum insulin levels also supported the distinct characteristics of the animal used in our and the previous study. Levels of serum insulin were dramatically decreased in db/db mice in the study by Guo et al. [4], while it is well acknowledged that hyperinsulin is one of the basic characteristics of db/db mice as found in the current and many other studies [19, 29, 30], which is the basic pathophysiological alterations of T2DM. Therefore, the animal used in the current study, which reflects the canonical T2DM leading to cardiac remodeling, is distinct from the previous one and this could cause different responses to KD treatment. Besides, it should be noted that treatment was started earlier in the current study (6 weeks vs. 8 weeks) and last for a longer time (12 weeks vs. 8 weeks). Thus, the influence of therapeutic duration could not be neglected since KD could correct metabolic dysfunction, which may confound its intrinsic effects on the heart and lon-

ger time may be needed to investigate the real and long-time effects of KD. Other studies reported both beneficial and detrimental effects of KD on the heart [5, 6]. *In vitro* study showed an unflavored role of KD in cardiac fibroblast activation [6] and prevention of cardiomyocyte loss [5]. Besides, KD is also found to be related to live fibrosis [31]. These studies indicated a complex effect of KD, and the adoption of this kind of diet should be cautious.

T cell function may be a key and novel modulator during the development of T2DM and DCM. Interestingly, T cells were also closely related to cardiomyopathy, especially cardiac fibrosis. Alcaide et al. reported that during the development of myocardial infarction, T cells played a central role in the process of myocardial scarring after infarction and directly modulated the phenotypes and functions of cardiac fibroblasts [32]. Furthermore, T cells within the heart could direct the remote fibrosis and scarring in the left ventricle during the chronic remodeling process [32]. Similar to our current findings, one study has reported a reduced circulating CD4⁺CD25⁺ T cell proportion and a suppression of Foxp3 expression in high-fat

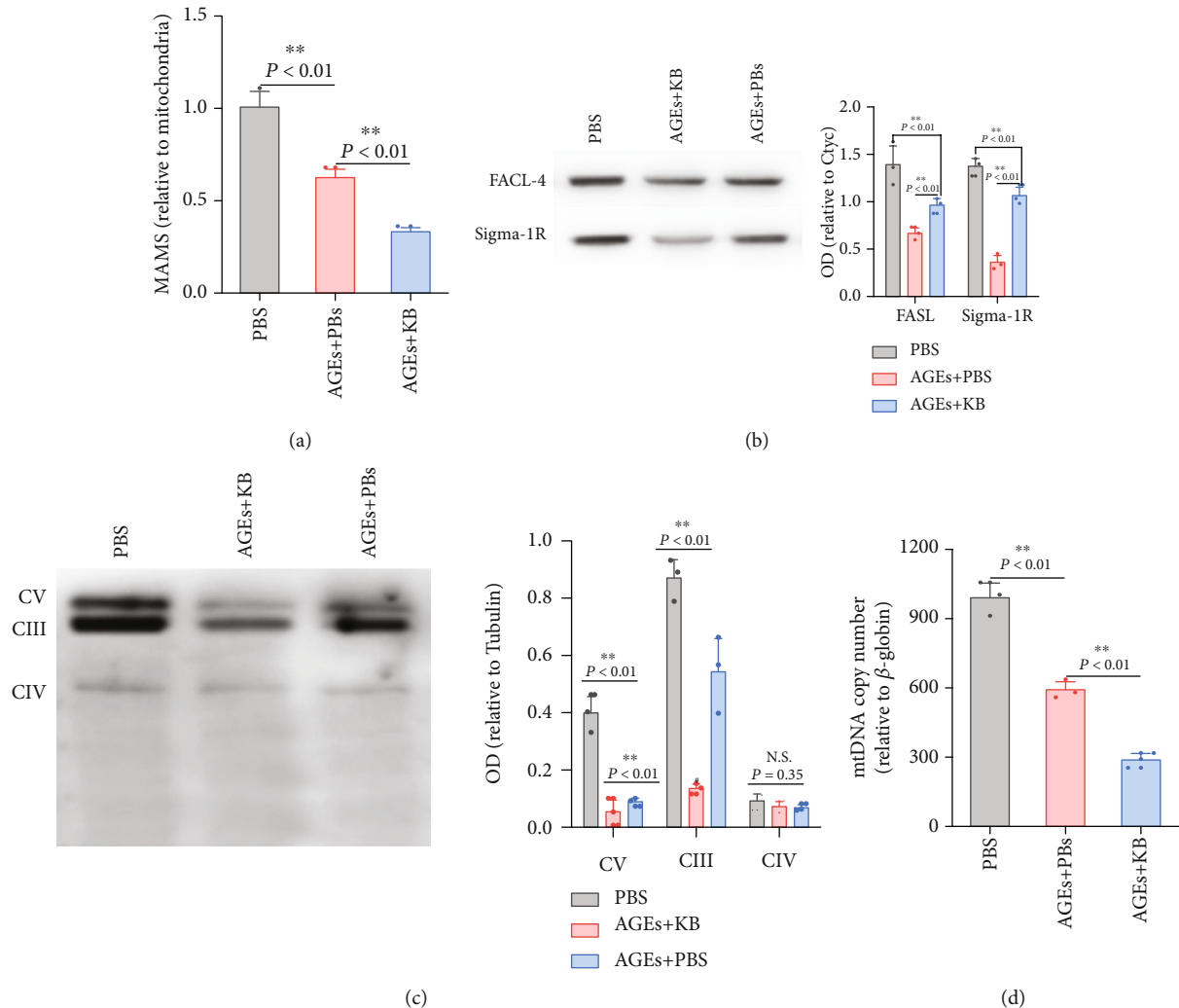


FIGURE 4: Effects of KB on MAMs (a, b) and mitochondrial respiratory complex (c) contents and mitochondrial number (d). MAMs: mitochondria-associated endoplasmic reticulum membranes; FACL-4: long-chain fatty-acid CoA synthases-4; Sigma-1R: Sigma-1 receptor; OD: optical density; Ctyc: cytochrome C; CV: complex V; CIII: complexes III; CIV: complexes. Other abbreviations were the same as the above.

diet-induced DCM [33]. We discovered that the subset of Tregs, namely, those with ST2L expressing on the membrane, was dramatically reduced upon KD treatment. ST2L⁺ Tregs are highly activated and robust in function, especially in the presence of IL-33, the only discovered ligand of ST2L [34, 35]. On the other hand, the activated Tregs are an important source of IL-33 production. Therefore, it may be plausible to infer that KD treatment blunt IL-33/ST2L signaling result in a positive feedback loop maintaining Treg suppression and contribute to cardiac fibrosis.

MAMs are specific subcellular structure charging calcium, lipid, and metabolite exchange between the endoplasmic reticulum and mitochondria, which are crucial to proper mitochondrial function. It is well known that MAMs are closely connected with cardiovascular diseases. Ikeda et al. revealed that the suppression of mitochondrial dynamics resulted in diminished survival, cardiac hypertrophy, and fibrosis in mice [36]. Moreover, Giorgi et al. found that MAMs promoted the development of infarctions and myocardial fibrosis via recruit-

ing NLRP3 protein and mediating the activation of NLRP3 inflammasome [37]. Besides, MAMs are essential for proper mitochondrial respiration [38]. Some researchers found that excessive Ca²⁺ transfer via MAMs promoted ROS generation and oxidative stress and augmented MAM formation could lead to elevated Ca²⁺ transfer from the ER to mitochondria, resulting in enhanced oxidative stress and mtROS overgeneration [39]. Data on the changes of MAMs in Tregs were scarce but most studies investigating MAMs reported reduction of MAMs, which contributed to disease development in diabetes [40, 41] while reinforcement of MAM conferred protective effects [41]. However, excessive MAMs also impaired mitochondrial oxidative capacity [42]. On the other hand, it should be noted that despite alterations of MAMs being able to explain the reduction of mitochondrial respiration in the current study, MAM reduction did not necessary directly induce mitochondria loss [43]. Therefore, the potential mechanisms leading to mitochondria reduction in response to KB treatment and more studies are merited.

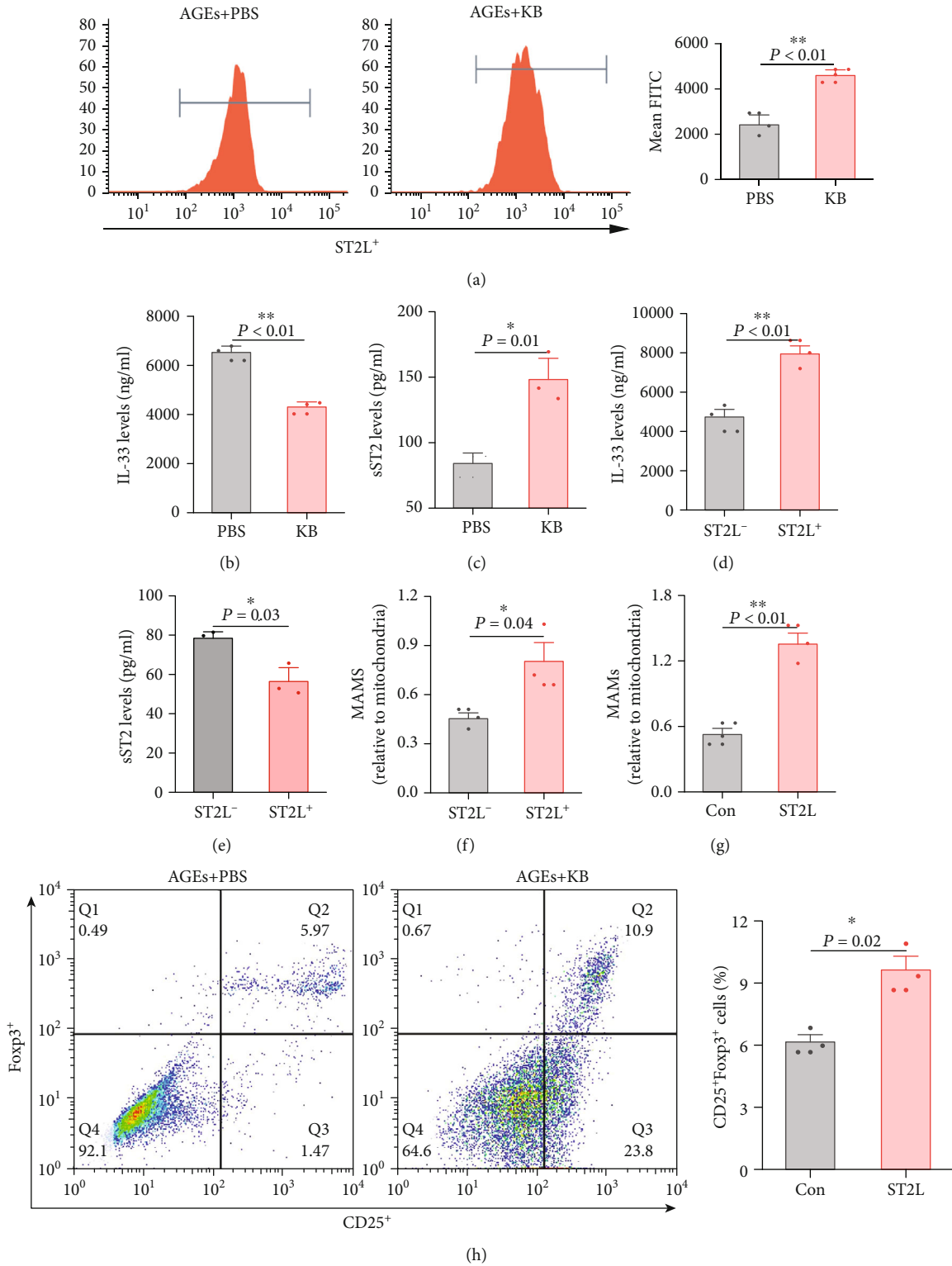


FIGURE 5: Effects of KB on IL-33/ST2L signaling and its role in KB-induced MAMs and Treg alterations. Flow cytometry detected the changes of membrane ST2L expression in CD4⁺CD25⁺Foxp3⁺ Tregs (a). Cultured medium levels of IL-33 and sST2 PBS-/KB-treated Tregs (b, c). Cultured medium levels of IL-33 and sST2 and MAMs in membrane-ST2L-negative/positive Tregs (d, e). Reinforcement of membrane-ST2L expression on Treg MAMs and Treg proportions in CD4⁺ T cells (f, g, h). sST2: soluble ST2; ST2L⁻: ST2L⁻ Tregs; ST2L⁺: ST2L⁺ Tregs; Con: control vector; ST2L: ST2L vector. Levels of IL-33 were detected by ELISA after NP-40 treatment.

Some limitations of the current study should be acknowledged. Firstly, we did not explore the effects of KD on other key cell types closely related to the development of DCM. As for T cells, Goldberg et al. demonstrated that KD expanded metabolically protective $\gamma\delta$ T cells and suppressed inflammatory responses [44]. In the cardiomyocytes, You et al. found that KD contributes to the profibrotic actions in fibroblasts possibly via the mTOR signaling pathway in hypertension [6]. Besides, diabetes could modulate a wide range of cellular processes (e.g., autophagy, oxidative stress, and ferroptosis) in cardiomyocytes and endothelial cells, which could be important in the regulations of fibrosis during DCM development [45, 46]. A lack of evidence on these aspects has restricted us to provide full information assessing the way that KD regulates DCM *in vivo*. Secondly, despite the current study focus on DCM and animal model is a canonical DCM, based on the sharp contrast conclusion induced by KD as described above, the conclusions of the current study could be interpreted cautiously if extended to the field outside DCM.

Despite limitations, the current study has explicitly showed an unfavorable effect of KD on ventricular function and cardiac remodeling during the development of DCM, which is partly mediated by regulatory T cell modulation due to altered IL-33/ST2L signaling. There is a great need for studies exploring the effects of KD on other crucial cell types (e.g., cardiac fibroblast and cardiomyocyte) to reveal the molecular mechanism of DCM development. Besides, studies investigating the role of KD on other cardiovascular disorders are also merited to provide a full landscape of KD adoption and cardiovascular outcomes.

Data Availability

The authors declare that all data supporting the findings of this study are available within the paper.

Conflicts of Interest

All authors declare no potential conflict of interest.

Authors' Contributions

Jun Tao, Hao Chen, and Ya-Jing Wang contributed equally to this work and should be considered co-first authors.

Acknowledgments

This work was supported by the National Natural Science Foundation of China (Grant Nos. 81870334, 81300071, 81741067, and 81300279), Science and Technology Program of Guangdong Province (Grant No. 2020A1515011237), Science and Technology Program of Guangzhou (Grant No. 201804010050), High-level Hospital Construction Project (Grant Nos. DFJH201803 and KJ012019099), and Natural Science Foundation for Distinguished Young Scholars of Guangdong Province (2021B1515020003).

References

- [1] S. P. Levick and A. Widiapradja, "The diabetic cardiac fibroblast: mechanisms underlying phenotype and function," *International Journal of Molecular Sciences*, vol. 21, no. 3, p. 970, 2020.
- [2] S. Kumar, T. Behl, M. Sachdeva et al., "Implicating the effect of ketogenic diet as a preventive measure to obesity and diabetes mellitus," *Life Sciences*, vol. 264, article 118661, 2021.
- [3] J.-W. Gao, Q.-Y. Hao, H.-F. Zhang et al., "Low-carbohydrate diet score and coronary artery calcium progression: results from the CARDIA Study," *Arteriosclerosis, Thrombosis, and Vascular Biology*, 2020, [cited 2020 Oct 29]; Available from: <https://www.ahajournals.org/doi/10.1161/ATVBAHA.120.314838>.
- [4] Y. Guo, C. Zhang, F.-F. Shang et al., "Ketogenic diet ameliorates cardiac dysfunction via balancing mitochondrial dynamics and inhibiting apoptosis in type 2 diabetic mice," *Aging and Disease*, vol. 11, no. 2, pp. 229–240, 2020.
- [5] Y. Yu, F. Wang, J. Wang, D. Zhang, and X. Zhao, "Ketogenic diet attenuates aging-associated myocardial remodeling and dysfunction in mice," *Experimental Gerontology*, vol. 140, p. 111058, 2020.
- [6] Y. You, Y. Guo, P. Jia et al., "Ketogenic diet aggravates cardiac remodeling in adult spontaneously hypertensive rats," *Nutrition and Metabolism*, vol. 17, no. 1, p. 91, 2020.
- [7] D. M. Lussier, E. C. Woolf, J. L. Johnson, K. S. Brooks, J. N. Blattman, and A. C. Scheck, "Enhanced immunity in a mouse model of malignant glioma is mediated by a therapeutic ketogenic diet," *BMC Cancer*, vol. 16, no. 1, p. 310, 2016.
- [8] C. Wright and N. L. Simone, "Obesity and tumor growth: inflammation, immunity, and the role of a ketogenic diet," *Current Opinion in Clinical Nutrition and Metabolic Care*, vol. 19, no. 4, pp. 294–299, 2016.
- [9] Q. Y. Ang, M. Alexander, J. C. Newman et al., "Ketogenic diets alter the gut microbiome resulting in decreased intestinal Th17 cells," *Cell*, vol. 181, no. 6, pp. 1263–1275.e16, 2020.
- [10] F. Karagiannis, S. K. Masouleh, K. Wunderling et al., "Lipid droplet formation drives pathogenic group 2 innate lymphoid cells in airway inflammation," *Immunity*, vol. 52, no. 4, pp. 620–634.e6, 2020.
- [11] H. Zhang, K. Tang, J. Ma et al., "Ketogenesis-generated β -hydroxybutyrate is an epigenetic regulator of CD8⁺ T-cell memory development," *Nature Cell Biology*, vol. 22, no. 1, pp. 18–25, 2020.
- [12] J. T. Mey, M. L. Erickson, C. L. Axelrod, W. T. King, and C. A. Flask, " β -Hydroxybutyrate is reduced in humans with obesity-related NAFLD and displays a dose-dependent effect on skeletal muscle mitochondrial respiration *in vitro*," *American Journal of Physiology-Endocrinology and Metabolism*, vol. 319, no. 1, pp. E187–E195, 2020.
- [13] V. J. Miller, R. A. LaFountain, E. Barnhart et al., "A ketogenic diet combined with exercise alters mitochondrial function in human skeletal muscle while improving metabolic health," *American Journal of Physiology. Endocrinology and Metabolism*, vol. 319, no. 6, pp. E995–E1007, 2020.
- [14] M. D. Buck, D. O'Sullivan, and E. L. Pearce, "T cell metabolism drives immunity," *The Journal of Experimental Medicine*, vol. 212, no. 9, pp. 1345–1360, 2015.
- [15] R. J. Kishon, M. Sukumar, and N. P. Restifo, "Metabolic regulation of T cell longevity and function in tumor immunotherapy," *Cell Metabolism*, vol. 26, no. 1, pp. 94–109, 2017.

- [16] E. Area-Gomez, A. de Groof, E. Bonilla et al., "A key role for MAM in mediating mitochondrial dysfunction in Alzheimer disease," *Cell Death & Disease*, vol. 9, no. 3, p. 335, 2018.
- [17] F. Dingreville, B. Panthu, C. Thivolet et al., "Differential effect of glucose on ER-mitochondria Ca²⁺ exchange participates in insulin secretion and glucotoxicity-mediated dysfunction of β -cells," *Diabetes*, vol. 68, no. 9, pp. 1778–1794, 2019.
- [18] H.-F. Zhang, S.-L. Xie, Y.-X. Chen et al., "Altered serum levels of IL-33 in patients with advanced systolic chronic heart failure: correlation with oxidative stress," *Journal of Translational Medicine*, vol. 10, no. 1, p. 120, 2012.
- [19] M. Wu, S. Wang, Y. Xie et al., "Interleukin-33 alleviates diabetic cardiomyopathy through regulation of endoplasmic reticulum stress and autophagy via insulin-like growth factor-binding protein 3," *Journal of Cellular Physiology*, vol. 236, no. 6, pp. 4403–4419, 2020.
- [20] Y. Rao, Y. Fang, W. Tan et al., "Delivery of long non-coding RNA NEAT1 by peripheral blood mononuclear cells-derived exosomes promotes the occurrence of rheumatoid arthritis via the microRNA-23a/MDM2/SIRT6 axis," *Frontiers in Cell and Development Biology*, vol. 8, p. 551681, 2020.
- [21] I. Pacella, C. Procaccini, C. Focaccetti et al., "Fatty acid metabolism complements glycolysis in the selective regulatory T cell expansion during tumor growth," *Proceedings of the National Academy of Sciences*, vol. 115, no. 28, pp. E6546–E6555, 2018.
- [22] K. Ishikawa, E. R. Chemaly, L. Tilemann et al., "Assessing left ventricular systolic dysfunction after myocardial infarction: are ejection fraction and dP/dt_{max} complementary or redundant?," *Am J Physiol-Heart Circ Physiol*, vol. 302, no. 7, pp. H1423–H1428, 2012.
- [23] M. R. Wieckowski, C. Giorgi, M. Lebedzinska, J. Duszynski, and P. Pinton, "Isolation of mitochondria-associated membranes and mitochondria from animal tissues and cells," *Nature Protocols*, vol. 4, no. 11, pp. 1582–1590, 2009.
- [24] Q.-Y. Gao, H.-F. Zhang, J. Tao et al., "Mitochondrial fission and mitophagy reciprocally orchestrate cardiac fibroblasts activation," *Frontiers in Cell and Development Biology*, vol. 8, p. 629397, 2021.
- [25] H.-F. Zhang, M.-X. Wu, Y.-Q. Lin et al., "IL-33 promotes IL-10 production in macrophages: a role for IL-33 in macrophage foam cell formation," *Experimental & Molecular Medicine*, vol. 49, no. 11, article e388, 2017.
- [26] E. P. K. Yu, J. Reinhold, H. Yu et al., "Mitochondrial respiration is reduced in atherosclerosis, promoting necrotic core formation and reducing relative fibrous cap thickness highlights," *Arteriosclerosis, Thrombosis, and Vascular Biology*, vol. 37, no. 12, pp. 2322–2332, 2017.
- [27] G. C. Atella and M. Shahabuddin, "Differential partitioning of maternal fatty acid and phospholipid in neonate mosquito larvae," *The Journal of Experimental Biology*, vol. 205, pp. 3623–3630, 2002.
- [28] Z.-T. Chen, H.-F. Zhang, M. Wang et al., "Long non-coding RNA Linc00092 inhibits cardiac fibroblast activation by altering glycolysis in an ERK-dependent manner," *Cellular Signaling*, vol. 74, p. 109708, 2020.
- [29] L. Koranyi, D. James, M. Mueckler, and M. A. Permutt, "Glucose transporter levels in spontaneously obese (db/db) insulin-resistant mice," *The Journal of Clinical Investigation*, vol. 85, no. 3, pp. 962–967, 1990.
- [30] S. M. Hofmann, H.-J. Dong, Z. Li et al., "Improved insulin sensitivity is associated with restricted intake of dietary glycoxidation products in the db/db mouse," *Diabetes*, vol. 51, no. 7, pp. 2082–2089, 2002.
- [31] Q. Zhang, F. Shen, W. Shen et al., "High-intensity interval training attenuates ketogenic diet-induced liver fibrosis in type 2 diabetic mice by ameliorating TGF- β 1/Smad signaling," *Diabetes, Metabolic Syndrome and Obesity: Targets and Therapy*, vol. 13, pp. 4209–4219, 2020.
- [32] R. M. Blanton, F. J. Carrillo-Salinas, and P. Alcaide, "T-cell recruitment to the heart: friendly guests or unwelcome visitors?," *American Journal of Physiology. Heart and Circulatory Physiology*, vol. 317, no. 1, pp. H124–H140, 2019.
- [33] Y. Han, J. Lai, J. Tao et al., "Sustaining circulating regulatory T cell subset contributes to the therapeutic effect of paroxetine on mice with diabetic cardiomyopathy," *Circulation Journal*, vol. 84, no. 9, pp. 1587–1598, 2020.
- [34] J. Biton, S. Khaleghparast Athari, A. Thiolat et al., "In vivo expansion of activated Foxp3⁺ regulatory T cells and establishment of a type 2 immune response upon IL-33 treatment protect against experimental arthritis," *Journal of Immunology*, vol. 197, no. 5, pp. 1708–1719, 2016.
- [35] J. Siede, A. Fröhlich, A. Datsi et al., "IL-33 receptor-expressing regulatory T cells are highly activated, Th2 biased and suppress CD4 T cell proliferation through IL-10 and TGF β release," *PLoS One*, vol. 11, no. 8, article e0161507, 2016.
- [36] Y. Ikeda, A. Shirakabe, Y. Maejima et al., "Endogenous Drp1 mediates mitochondrial autophagy and protects the heart against energy stress," *Circulation Research*, vol. 116, no. 2, pp. 264–278, 2015.
- [37] S. Missiroli, S. Patergnani, N. Carocchia et al., "Mitochondria-associated membranes (MAMs) and inflammation," *Cell Death & Disease*, vol. 9, no. 3, p. 329, 2018.
- [38] J. Rieusset, "The role of endoplasmic reticulum-mitochondria contact sites in the control of glucose homeostasis: an update," *Cell Death & Disease*, vol. 9, no. 3, p. 388, 2018.
- [39] X. Wei, X. Wei, Z. Lu et al., "Activation of TRPV1 channel antagonizes diabetic nephropathy through inhibiting endoplasmic reticulum-mitochondria contact in podocytes," *Metabolism*, vol. 105, p. 154182, 2020.
- [40] J. Rieusset, J. Fauconnier, M. Paillard et al., "Disruption of calcium transfer from ER to mitochondria links alterations of mitochondria-associated ER membrane integrity to hepatic insulin resistance," *Diabetologia*, vol. 59, no. 3, pp. 614–623, 2016.
- [41] E. Tubbs, S. Chanon, M. Robert et al., "Disruption of mitochondria-associated endoplasmic reticulum membrane (MAM) integrity contributes to muscle insulin resistance in mice and humans," *Diabetes*, vol. 67, no. 4, pp. 636–650, 2018.
- [42] A. P. Arruda, B. M. Pers, G. Parlakgöl, E. Güney, K. Inouye, and G. S. Hotamisligil, "Chronic enrichment of hepatic endoplasmic reticulum-mitochondria contact leads to mitochondrial dysfunction in obesity," *Nature Medicine*, vol. 20, no. 12, pp. 1427–1435, 2014.
- [43] R. Bravo, J. M. Vicencio, V. Parra et al., "Increased ER-mitochondrial coupling promotes mitochondrial respiration and bioenergetics during early phases of ER stress," *Journal of Cell Science*, vol. 124, no. 13, pp. 2143–2152, 2011.
- [44] E. L. Goldberg, I. Shchukina, J. L. Asher, S. Sidorov, M. N. Artyomov, and V. D. Dixit, "Ketogenesis activates metabolically protective $\gamma\delta$ T cells in visceral adipose tissue," *Nature Metabolism*, vol. 2, no. 1, pp. 50–61, 2020.

- [45] I. D. Kyriazis, M. Hoffman, L. Gaignebet et al., “KLF5 is induced by FOXO1 and causes oxidative stress and diabetic cardiomyopathy,” *Circulation Research*, vol. 128, no. 3, pp. 335–357, 2021.
- [46] H. Zang, W. Wu, L. Qi et al., “Autophagy inhibition enables Nrf2 to exaggerate the progression of diabetic cardiomyopathy in mice,” *Diabetes*, vol. 69, no. 12, pp. 2720–2734, 2020.

Research Article

Quercetin Improves Cardiomyocyte Vulnerability to Hypoxia by Regulating SIRT1/TMBIM6-Related Mitophagy and Endoplasmic Reticulum Stress

Xing Chang ^{1,2}, Tian Zhang ³, Qingyan Meng³, Shiyuan Wang³, Peizheng Yan ³,
Xue Wang⁴, Duosheng Luo ^{5,6}, XiuTeng Zhou ^{1,5} and Ruifeng Ji ^{5,6}

¹State Key Laboratory of Dao-di Herbs, National Resource Center for Chinese Materia Medica, China Academy of Chinese Medical Sciences, Beijing 100700, China

²Guang'anmen Hospital of Chinese Academy of Traditional Chinese Medicine, Beijing 100053, China

³Shandong University of Traditional Chinese Medicine, Jinan 250355, China

⁴School of Business, Macau University of Science and Technology, Taipa, Macau 999078, China

⁵School of Traditional Chinese Medicine, Guangdong Pharmaceutical University, Guangzhou 510006, China

⁶Institute of Chinese Medicine, Guangdong Pharmaceutical University, Guangzhou 510006, China

Correspondence should be addressed to Duosheng Luo; lds0901@163.com, XiuTeng Zhou; zxt_0508@163.com, and Ruifeng Ji; jiruifeng0708@163.com

Received 13 January 2021; Revised 21 February 2021; Accepted 1 March 2021; Published 30 March 2021

Academic Editor: Yun-dai Chen

Copyright © 2021 Xing Chang et al. This is an open access article distributed under the Creative Commons Attribution License, which permits unrestricted use, distribution, and reproduction in any medium, provided the original work is properly cited.

Cardiomyocyte apoptosis is an important pathological mechanism underlying cardiovascular diseases and is commonly caused by hypoxia. Moreover, hypoxic injury occurs not only in common cardiovascular diseases but also following various treatments of heart-related conditions. One of the major mechanisms underlying hypoxic injury is oxidative stress. Quercetin has been shown to exert antioxidant stress and vascular protective effects, making it a promising candidate for treating cardiovascular diseases. Therefore, we examined the protective effect of quercetin on human cardiomyocytes subjected to hypoxia-induced oxidative stress damage and its underlying mechanism. Human cardiomyocytes were subjected to hypoxia/reoxygenation (H/R) *in vitro* with or without quercetin pretreatment; thereafter, flow cytometry, Cell Counting Kit-8 assay, laser scanning confocal microscopy, quantitative PCR, western blotting, and enzyme-linked immunosorbent assay were performed to analyze the effects of quercetin on cardiomyocytes. We found that H/R induced reactive oxygen species overproduction and endoplasmic reticulum stress, as well as inhibited the function of the mitochondria/endoplasmic reticulum and mitophagy, eventually leading to apoptosis and decreasing the viability of human cardiomyocytes. Quercetin pretreatment inhibited H/R-mediated overproduction of reactive oxygen species and damage caused by oxidative stress, increased mitophagy, regulated mRNA and protein expression of transmembrane BAX inhibitor-1 motif-containing 6 (TMBIM6), regulated endoplasmic reticulum stress, and improved the vulnerability of human cardiomyocytes to H/R. Furthermore, transfection with short interfering RNA against silent information regulator protein 1 (SIRT1) counteracted the protective effects of quercetin on cardiomyocytes. Thus, quercetin was predicted to regulate mitophagy and endoplasmic reticulum stress through SIRT1/TMBIM6 and inhibit H/R-induced oxidative stress damage. These findings may be useful for developing treatments for hypoxic injury-induced cardiovascular diseases and further highlight the potential of quercetin for regulating mitochondrial quality control and endoplasmic reticulum function.

1. Introduction

Myocardial hypoxia refers to abnormal changes in myocardial function induced in response to an insufficient O₂ supply

or metabolic disorders and is the primary cause of death [1, 2]. When cardiomyocytes cannot adapt to the lack of O₂ supply, reactive oxygen species (ROS) are overproduced, leading to the development of mitochondrial quality control

disorders and cardiomyocyte apoptosis. Hypoxia can also lead to dysfunctions in mitochondrial oxidative phosphorylation [3]. Moreover, excessive production of mitochondrial ROS because of mitochondrial respiratory chain dysfunction can affect signal transduction pathways, resulting in lipid peroxidation of the cell membrane and an imbalance in G protein and effector coupling [4]. Mitochondrial dysfunction and disruptions in homeostasis of the intracellular environment are accompanied by endoplasmic reticulum (ER) stress, which further reduces cell viability and accelerates apoptosis [5].

Quercetin (Que) is found in the flowers, leaves, and fruits of many plants, mostly in the form of glycosides [6]. As a natural antioxidant, Que exerts pharmacological effects such as regulating mitochondrial quality control and ER function, reducing capillary fragility, lowering blood lipids, and increasing coronary blood flow. Although Que has been demonstrated to protect cardiomyocytes [7], its underlying mechanism, particularly in the mitochondria and ER, is unclear.

Mitophagy is one of the most important pathways by which mitochondria maintain homeostasis [8], and a two-way regulatory mechanism is associated with hypoxia during cell metabolic stress [9]. Hypoxia activates mitophagy in various manners. Mitophagy can degrade damaged proteins to maintain cell survival [10]; however, when mitophagy is excessive, the cells are damaged and can undergo type II programmed cell death [11]. Studies have shown that mild hypoxia (1% or 0.1% O₂) induces autophagy to promote cell survival but does not cause apoptosis [12]. Therefore, early stage hypoxia can induce protective autophagy and moderate apoptosis [13]. However, long-term exposure to hypoxia or extremely low O₂ concentrations (0.1% or 0% O₂) causes the death of numerous cells [14].

Hypoxia affects the function of multiple organelles, including the mitochondria and ER. In eukaryotic cells, the ER is the site of protein synthesis, modification, and folding [15]. Mitochondria are the most important organelles for supplying energy and regulating cell survival [16]. The ER and mitochondria share an interconnected region in which the molecular components are involved in an interaction mechanism to create a stable environment [17]. Homeostasis of this local environment enhances signal exchange between organelles and regulates the structure and function of mitochondria and the ER in the cardiovascular system [18].

Mitochondria interact with the ER structurally and functionally and are closely related to the survival of cardiomyocytes [17,19]. The adaptive response of the ER and mitophagy, as an intrinsic protective mechanism, promotes protein renewal and timely removal of harmful components, such as damaged proteins and mitochondria [20]. An imbalance in ROS-mediated redox signaling leads to the development of mitophagy disorder and ER stress, and the ability of the ER to fold proteins decreases, causing the accumulation of unfolded proteins and increased production of ROS [21]. These events eventually lead to apoptosis, necrosis, or inflammation [22].

Silent information regulator protein 1 (SIRT1) can regulate apoptosis, oxidative stress, mitochondrial constitution,

and the ER [23]. Although Que can ameliorate myocardial ischemia-reperfusion-induced cardiomyocyte apoptosis via the SIRT1 pathway [24], the specific regulatory mechanism is unclear. TMBIM6 is an inhibitor of ER stress and was originally named as Bax inhibitor- (BI-) 12 [25]. TMBIM6, as a calcium channel-like protein, can reduce the calcium release balance on the ER membrane and plays an important role in regulating ER function and calcium homeostasis. TMBIM6 can play a protective role against various types of cell death caused by numerous stimuli [26]. Studies have shown that overexpression of TMBIM6 in cells can inhibit the activation of Bax, but its regulatory mechanism is unclear. As TMBIM6 and SIRT1 can regulate programmed cell death and autophagy, we predicted that TMBIM6 and SIRT1 are related in the regulation of mitophagy and ER stress.

Therefore, in this study, we examined the protective mechanism of Que against hypoxia/reoxygenation (H/R) stress in human cardiomyocytes and verified whether this antioxidant can improve the vulnerability of cardiomyocytes by regulating mitochondrial and ER functions through SIRT1/TMBIM6.

2. Materials and Methods

2.1. Cell Culture. Human cardiomyocytes were provided by the Chinese Academy of Medical Sciences (Institute of Basic Medicine, Beijing, China). Que (purity $\geq 98\%$) was provided by the Chinese Medicine Resource Center of the Chinese Academy of Traditional Chinese Medicine (Beijing, China). The cells were cultured in Dulbecco's modified Eagle medium (Gibco, Grand Island, NY, USA) containing 10% fetal bovine serum (Gibco) and penicillin-streptomycin (1%, Gibco) at 37°C (95% humidity and 5% CO₂). The medium was exchanged every 2 days.

Before use in experiments, human cardiomyocytes were divided into four groups: (1) control group cells cultured under the abovementioned conditions; (2) H/R group cells cultured in fresh hypoxia medium (mM): CaCl₂ 1.8, HEPES 20, KCl 10, MgSO₄ 1.2, NaCl 98.5, NaHCO₃ 6, NaH₂PO₄ 0.9, and sodium lactate 40 at 37°C; placed in an anoxic chamber for 3 h to induce hypoxia; then cultured in reoxygenation medium (mM): CaCl₂ 1.8, glucose 5.5, HEPES 20, KCl 5, MgSO₄ 1.2, NaCl 129.5, NaHCO₃ 20, and NaH₂PO₄ 0.9 at 37°C; and finally exposed to an atmosphere of 95% O₂ and 5% CO₂ for 2 h; (3) Que group cells were treated with Que (50, 100, 150, 200, and 250 mg/L) for 24 h before H/R treatment; and (4) Que+SIRT1 short interfering RNA (siRNA) group cells transfected with SIRT1 siRNA for 36 h and then treated with 150 mg/L Que for 24 h before H/R treatment.

2.2. Measurement of Cardiomyocyte Viability. Human cardiomyocytes were healthy and grown to a confluence of $>90\%$. Cells were digested with trypsin (0.25%; Sigma, St. Louis, MO, USA) for 10 min. Trypsin activity was terminated by adding Dulbecco's modified Eagle's medium, and cell counting was performed. The cells were then seeded into 12-well plates (50,000 cells/well), cultured for 12 h, and observed

under an inverted microscope. Cell viability was measured by the Cell Counting Kit-8 (CCK-8) method.

2.3. Evaluation of Apoptosis. The different groups of cardiomyocytes were washed with phosphate-buffered saline. Using an apoptosis detection kit, the percentage of nonapoptotic cells was determined after biopsy staining. Cytomics FC 500 with CXP software (Beckman, Brea, CA, USA) was used for flow cytometric analysis.

2.4. Measurement of ROS Levels. Cells from different groups were collected and incubated with 2',7'-dichlorofluorescein (10 μ M) at 37°C (20 min). ROS production was measured by flow cytometry.

2.5. Measurement of Mitochondrial Membrane Potential (MMP). The MMP was measured in human cardiomyocytes by staining with JC-1 in the dark for 30 min. Images were acquired using a confocal microscope (Olympus, Tokyo, Japan).

2.6. Measurement of Antioxidant Enzyme Activity in Mitochondria. The activities of superoxide dismutase (SOD), glutathione (GSH), glutathione peroxidase (GPX), catalase (CAT), malondialdehyde (MDA), interleukin-10, interleukin-18, and tumor necrosis factor- α were determined using a total analysis kit.

2.7. Measurement of Mitochondrial Energy Metabolism. The mitochondrial O₂ consumption rate was analyzed in real time in intact cells using an XFp Extracellular Flux Analyzer (Agilent Technologies, Santa Clara, CA, USA). Human cardiomyocytes were seeded at a density of 5×10^5 cells/well, and mitochondrial energy metabolism was measured.

2.8. Western Blotting. Total protein was extracted from the cells in each group and resolved by electrophoresis (SDS-PAGE). The resolved peptides were electrotransferred onto polyvinylidene fluoride membranes and probed with primary antibodies against SIRT1, LC3A/B, Beclin-1, and Bcl-2 (Abcam, Cambridge, UK; diluted in 5% skim milk powder prepared in Tris-buffered saline) and TMBIM6 (Thermo Fisher Scientific Waltham, MA, USA; diluted in 5% skim milk powder prepared in Tris-buffered saline) at room temperature for 30 min and then at 4°C overnight. Goat anti-mouse IgG (H+L) conjugated with horseradish peroxidase (diluted 1 : 5000 in Tris-buffered saline) (Abcam, Cambridge, UK) served as the secondary antibody. The membrane was washed three times with Tris-buffered saline and incubated with electrochemiluminescence reagent for 3–5 min. An eBlot exposure instrument was used to expose the film for 60 s; images acquired after an appropriate exposure time were selected and analyzed using the ImageJ software (NIH, Bethesda, MD, USA).

2.9. Quantitative PCR. Total RNA extraction reagent (Trizol, Invitrogen, Carlsbad, CA, USA) was used to extract RNA from the cells. A NanoDrop® ND-2000 spectrometer (Wilmington, DE, USA) was used to determine the concentration and purity of RNA, and a PrimeScript™ RT reagent

Kit with gDNA Eraser was used to reverse transcribe the RNA into cDNA. The cDNA was used as a template for real-time PCR, and the data were analyzed using the 2- Δ CT method [27].

2.10. Statistical Analysis. All experimental data are expressed as the mean \pm standard error of the mean, and analysis of variance was used for overall evaluation. The *t*-test was used to analyze the differences between groups, and one-way or two-way analysis of variance and Tukey-test were used to analyze differences between multiple groups. *p* < 0.05 indicated a significant difference.

3. Results

3.1. Que Improves the Vulnerability of Human Cardiomyocytes to H/R. Hypoxia was established by treating human cardiomyocytes with H/R, and the effect of Que on cell viability and apoptosis was evaluated. The CCK-8 assay showed that the viability of H/R-treated human cardiomyocytes was decreased significantly compared to that of the control group (Figure 1(a)). However, treatment of the cells with 50, 100, 150, 200, and 250 mg/L Que improved the viability of human cardiomyocytes after H/R treatment, with 150 mg/L Que inducing the most significant improvement (Figure 1(b)). Therefore, 150 mg/L Que was used in the apoptosis experiment. H/R increased the number of apoptotic human cardiomyocytes; 150 mg/L Que pretreatment significantly reversed this effect (Figures 1(c) and 1(d)). Moreover, transfection with *SIRT1* siRNA further reduced the viability of human cardiomyocytes and increased apoptosis (Figures 1(c) and 1(d)). These results indicate that H/R treatment promotes apoptosis and seriously reduces the viability of human cardiomyocytes, whereas Que can reverse these effects, ameliorating their vulnerability to H/R. Notably, the protective effect of Que was eliminated after *SIRT1* knockdown, suggesting that *SIRT1* mediates Que-induced protection of human cardiomyocytes.

3.2. Que Regulates Mitochondrial Homeostasis in H/R-Treated Human Cardiomyocytes through *SIRT1*. Energy metabolism in cardiomyocytes mainly occurs in mitochondria, which can synthesize ATP through oxidative phosphorylation. As defects in mitochondrial energy metabolism and respiratory function may affect mitochondrial homeostasis, quality control of these organelles is critical. Therefore, we examined whether Que improved mitochondrial quality control through *SIRT1* to ameliorate cardiomyocyte vulnerability to H/R. Cells treated with H/R exhibited increased mitochondrial ROS production compared to that in cells in the control group, a phenomenon that was inhibited upon pretreatment with Que (Figures 2(a) and 2(b)). Furthermore, H/R treatment reduced MMP levels, whereas pretreatment with Que reversed these effects (Figures 2(c) and 2(d)). H/R also inhibited the activity of mitochondrial respiratory complexes I/III (Figures 2(e) and 2(f)). Pretreatment with Que prevented these phenomena in a *SIRT1*-dependent manner, and *SIRT1* knockdown eliminated the effect of Que on mitochondrial function (Figures 2(e) and 2(f)). Our results demonstrate that disruption of mitochondrial homeostasis

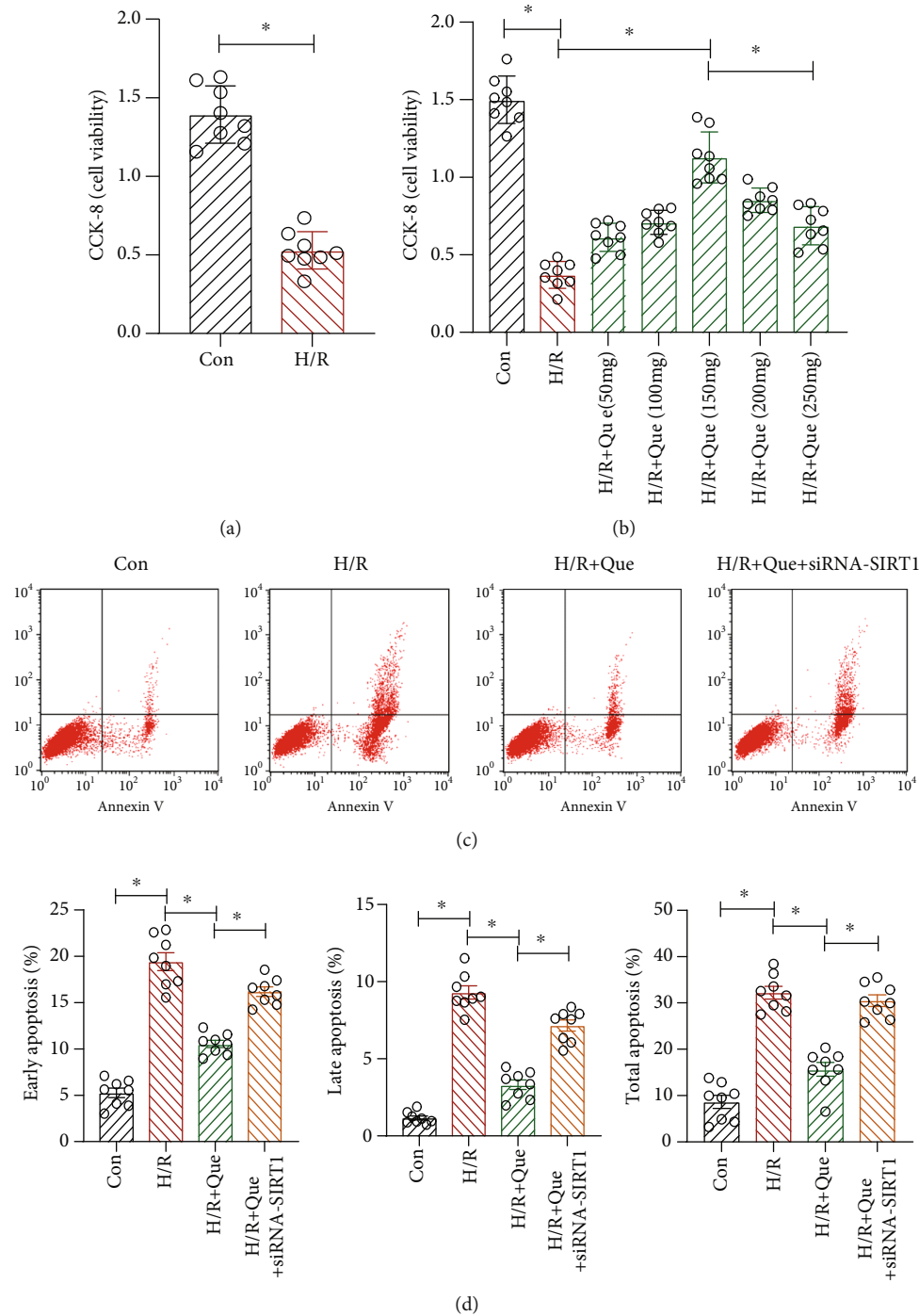


FIGURE 1: Quercetin (Que) ameliorates the vulnerability of human cardiomyocytes to hypoxia/reoxygenation (H/R): (a) viability of human cardiomyocytes; (b) viability of human cardiomyocytes with different concentrations of Que; (c, d) apoptosis of human cardiomyocytes before and after treatment. * $p < 0.05$. Con: control; *SIRT1* siRNA: *SIRT1* short interfering RNA.

triggered by H/R results in an imbalance in the levels of mitochondrial respiratory complexes, further disturbing mitochondrial homeostasis, decreasing human cardiomyocyte viability, and enhancing apoptosis. Thus, Que regulates mitochondrial homeostasis in human cardiomyocytes under H/R conditions through *SIRT1*.

3.3. Que Improves Mitochondrial Respiratory Function under Conditions of H/R through *SIRT1*. Mitochondria are extremely sensitive to changes in their environment, such as nutrition and O_2 supplies, and respond through metabolic adaptations, eventually inducing an imbalance in mitochondrial homeostasis. When accompanied by abnormal

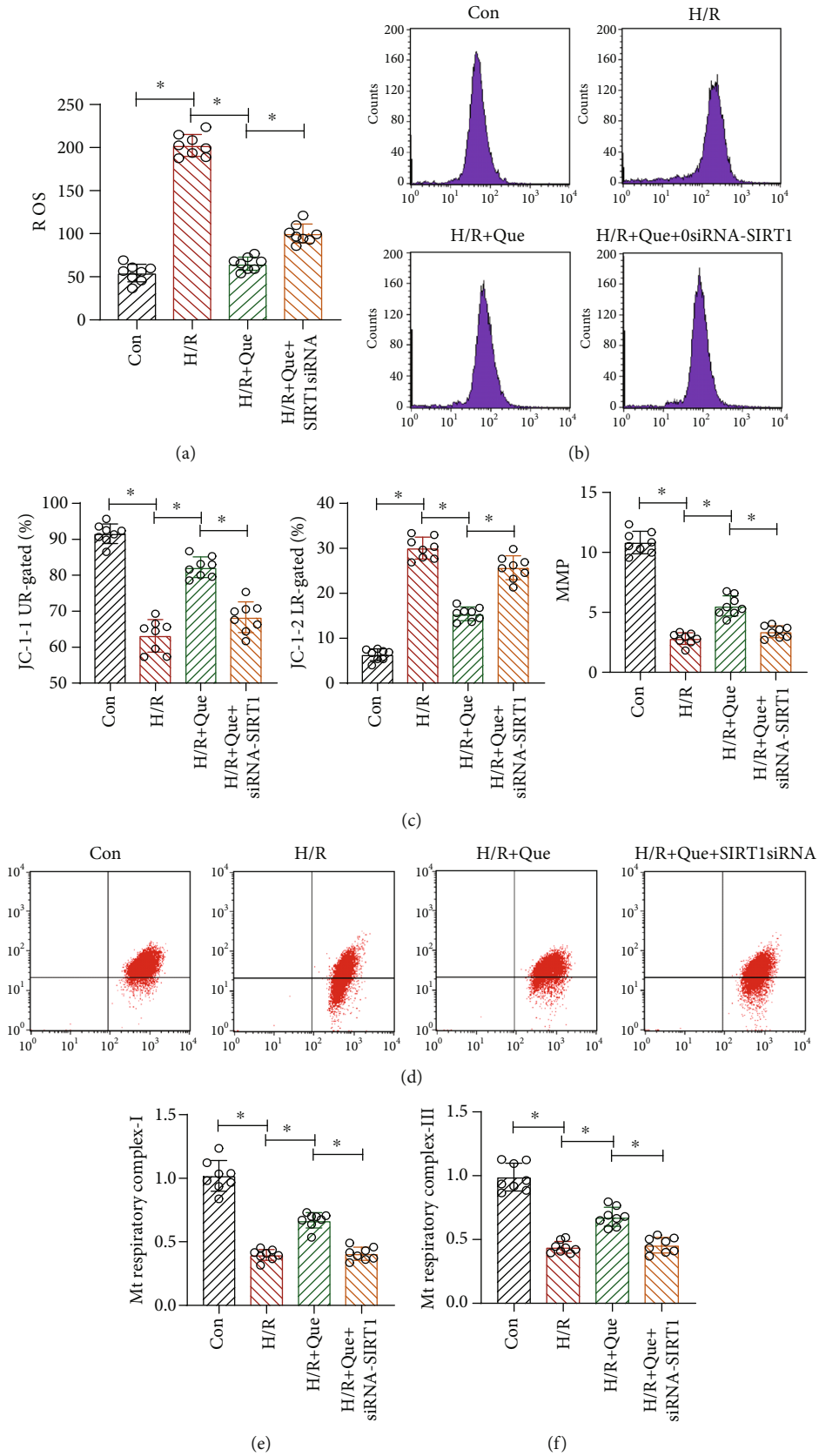


FIGURE 2: Quercetin (Que) regulates mitochondrial homeostasis in hypoxia/reoxygenation- (H/R-) stimulated human cardiomyocytes through SIRT1: (a, b) ROS level analysis; (c, d) MMP analysis; (e, f) activity of mitochondrial (Mt) respiratory complexes I/III. * $p < 0.05$. Con: control; SIRT1 siRNA: SIRT1 short interfering RNA.

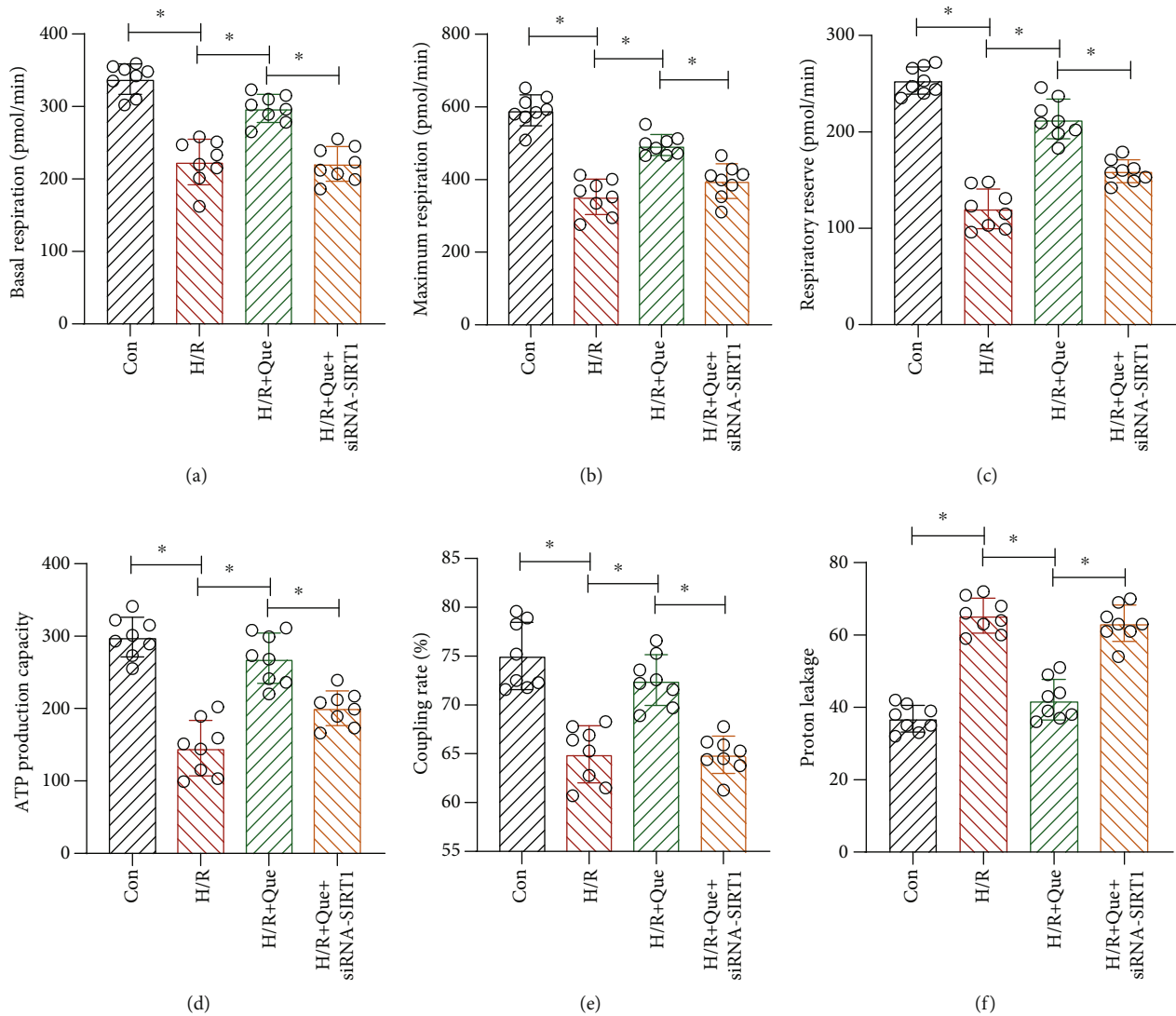


FIGURE 3: Quercetin (Que) ameliorates mitochondrial respiratory function under conditions of hypoxia/reoxygenation (H/R) through SIRT1: (a) basal mitochondrial respiration; (b) maximum respiration; (c) respiratory reserve; (d) ATP production capacity; (e) coupling rate; (f) proton leakage. * $p < 0.05$. Con: control; SIRT1 siRNA: SIRT1 short interfering RNA.

respiratory chain function, mitochondrial respiratory function progressively declines, which culminates in ATP depletion, extensive cardiomyocyte damage, and apoptosis. To determine whether Que ameliorates mitochondrial respiratory function under conditions of H/R, we performed a mitochondrial stress test. The results revealed that compared to the control group, basal mitochondrial respiration (Figure 3(a)), maximum respiration (Figure 3(b)), respiratory reserve (Figure 3(c)), ATP production capacity (Figure 3(d)), and coupling rate (Figure 3(e)) were all significantly inhibited in human cardiomyocytes exposed to H/R. Moreover, proton leakage was significantly increased upon H/R exposure (Figure 3(f)). However, Que pretreatment reversed these effects (Figures 3(a)–3(f)). Interestingly, SIRT1 knockdown abrogated the effects of Que on mitochondrial respiratory function in H/R-exposed human cardiomyocytes (Figures 3(a)–3(f)). These data indicate that Que improves mitochondrial respiratory function and protects

mitochondria in human cardiomyocytes through SIRT1. Mitochondrial respiration is central to energy production because it controls the coupling reaction of electron transfer in the respiratory chain complex in the inner mitochondrial membrane. ROS are by-products of electron transfer and the main cause of oxidative stress.

3.4. Que Ameliorates Mitochondrial Oxidative Stress Damage in H/R-Exposed Human Cardiomyocytes. ROS-induced oxidative stress can induce the development of mitochondrial quality control disorders, which in turn lead to excessive mitochondrial lysis and mitophagy imbalance, inducing cardiomyocyte apoptosis. Next, we verified whether Que affects oxidative stress damage through SIRT1 under H/R by enzyme-linked immunosorbent assay. We found that Que reduced oxidative stress damage in human cardiomyocytes. Compared to the control group, the activities of SOD, CAT, GSH, and GPX in the H/R group decreased (Figures 4(a)–

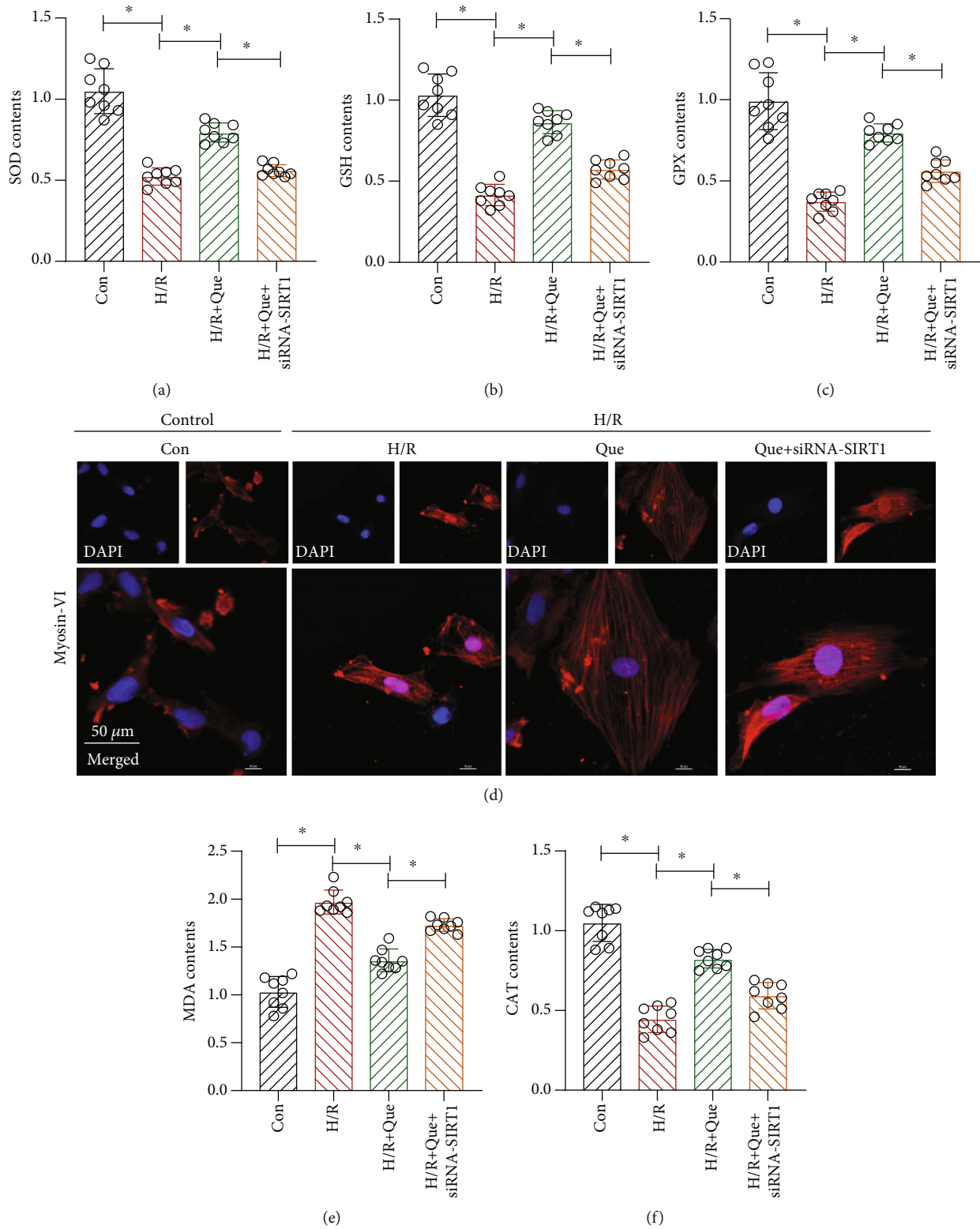


FIGURE 4: Quercetin (Que) ameliorates mitochondrial oxidative stress damage in hypoxia/reoxygenation- (H/R) treated human cardiomyocytes: (a) antioxidant activity of superoxide dismutase (SOD), (b) glutathione (GSH), and (c) glutathione peroxidase (GPX); (d) myosin-VI detection by laser confocal microscopy; (e) activity of malondialdehyde (MDA); (f) antioxidant activity of catalase (CAT). $*p < 0.05$. Con: control; SIRT1 siRNA: SIRT1 short interfering RNA.

4(c) and 4(f)) and those of MDA increased (Figure 4(e)) in cells treated with H/R. Pretreatment of cells with Que inhibited these H/R-induced effects (Figures 4(a)–4(c), 4(e), and 4(f)); however, SIRT1 knockdown blocked Que-induced amelioration of oxidative stress damage (Figures 4(a)–4(c), 4(e), and 4(f)). Moreover, under hypoxia, myosin expression in cardiomyocytes decreased significantly after H/R, but Que reversed this phenomenon. The expression of myosin further decreased after transfection with si-SIRT1 (Figure 4(d)). These results suggest that H/R inhibits the activity of the above-mentioned antioxidant enzymes and causes oxidative stress damage and that Que regulates the mitochondrial redox state in hypoxic cardiomyocytes by activating SIRT1. Que may regulate myosin expression by maintaining mitochondrial/endoplasmic reticulum function, but further experiments are needed to verify this.

3.5. Que Regulates Human Cardiomyocyte Mitophagy under Conditions of H/R through SIRT1. Mitophagy is related to energy metabolism in human cardiomyocytes. Under physiological conditions, mitophagy can directly regulate mitochondrial numbers and ensure their normal function by clearing damaged and dysfunctional mitochondria from cells. These actions affect the physiological function of the mitochondrial respiratory chain and energy metabolism. In addition, mitophagy enables the removal of endogenous ROS produced by mitochondria. To explore the protective mechanism of Que in mitophagy, quantitative PCR was used to analyze the expression of *PINK1*/parkin and *ATG5/12*, which encode mitophagy-related proteins, and SIRT1. The results revealed that the expression of *PINK1*/parkin, *ATG5/12*, and *SIRT1* in the H/R group was lower than that in the control group (Figures 5(a)–5(c), 5(g), and 4(h)). However, under conditions of Que pretreatment, the expression of these mRNA was significantly increased (Figures 5(a)–5(c), 5(g), and 5(h)). Transmission electron microscopy revealed that the number of mitochondria in cells from the H/R group was lower than that in cells from the control group; Que pretreatment significantly increased this number (Figure 5(f)). Moreover, western blotting revealed that the levels of SIRT1, LC3-I/II, Beclin-1, and Bcl-2 were lower in the H/R group than in the control group, but Que reversed the expression of these proteins (Figures 5(d) and 5(e)). Notably, *SIRT1* knockdown eliminated the regulatory effect of Que on mitophagy (Figures 5(a)–5(h)).

3.6. Que Improves ER Stress in Human Cardiomyocytes under H/R Conditions through SIRT1/TMBIM6. The above experimental results suggest that Que can enhance mitophagy and energy metabolism, inhibit oxidative stress damage, and ameliorate the vulnerability of cardiomyocytes to H/R. Additionally, the results demonstrate that SIRT1 plays a key role in Que-mediated regulation of mitochondrial function. To verify whether mitophagy inhibition under H/R conditions affects ER function and if Que-induced amelioration of cardiomyocyte vulnerability to H/R involves the regulation of ER function, we analyzed the mRNA levels of *PERK* and *CHOP*, which are closely related to ER stress, and caspase-12, which mediates ER stress-induced apoptosis. As shown

in Figures 6(b)–6(d), compared to the control group levels, the mRNA and protein levels of *PERK*, *CHOP*, and caspase-12 were increased in human cardiomyocytes from the H/R group, whereas pretreatment of cells with Que inhibited this upregulation (Figures 6(b)–6(d)). Nevertheless, *SIRT1* knockdown countered the protective effect of Que (Figures 6(b)–6(d)). These results suggest that H/R upregulates ER stress-related proteins. As shown in Figure 6(a), H/R intervention can promote calcium release and lead to an imbalance in calcium homeostasis. However, Que inhibited calcium release from cardiomyocytes, and *SIRT1* siRNA abolished the ability of Que to regulate calcium homeostasis. TMBIM6 is an independent protein that can play a very important role in regulating ER function and Ca^{2+} homeostasis. TMBIM6 can interact with Ca^{2+} signaling proteins, inhibit apoptosis of the ER pathway, and regulate cell life and death. As shown in Figure 6(h), the mRNA and protein expression of TMBIM6, determined by qPCR and western blotting, respectively, decreased significantly under the influence of H/R. Pretreatment with Que reversed the effect of TMBIM6, and *SIRT1* siRNA inhibited the regulatory function of Que on TMBIM6. These results demonstrate that Que-mediated regulation of ER stress in human cardiomyocytes involves SIRT1/TMBIM6. However, the interaction mechanism between SIRT1 and TMBIM6 needs to be further clarified.

4. Discussion

We found that hypoxia increases ROS production and further induces oxidative stress damage, resulting in mitophagy dysfunction and ER stress and culminating in decreased myocardial cell viability. Que pretreatment can ameliorate mitophagy and mitochondrial function, regulate ER stress and ROS-mediated oxidative stress damage, and restore myocardial cell viability. To understand the effect of Que on mitochondrial/ER function and to investigate whether its protective effect on cardiomyocytes involves the SIRT1 signaling pathway, we transfected cells with SIRT1 siRNA. Depletion of SIRT1 blocked the Que-induced regulation of mitochondrial/ER function and the protection of cardiomyocytes from H/R. Thus, we showed that Que regulates mitophagy through the SIRT1 signaling pathway and ameliorates the activity of cardiomyocytes under hypoxia conditions. Furthermore, H/R inhibited the mRNA and protein expression of TMBIM6. Que restored the expression of TMBIM6, whereas siSIRT1 further inhibited it. Therefore, Que may regulate mitophagy and the ER through SIRT1/TMBIM6 to stabilize intracellular calcium homeostasis and improve cardiomyocyte activity.

Under physiological conditions in the vascular system, ROS levels can be increased through mitochondrial and non-mitochondrial pathways. Cells can then eliminate excessive ROS through the antioxidant system [28], resulting in reduced oxidative stress with respect to mitochondrial DNA, respiratory chain complex proteins, and other important molecules [29]. However, under hypoxic conditions, mitochondrial/ER dysfunction induces increased mitochondrial damage and excessive ROS production, resulting in

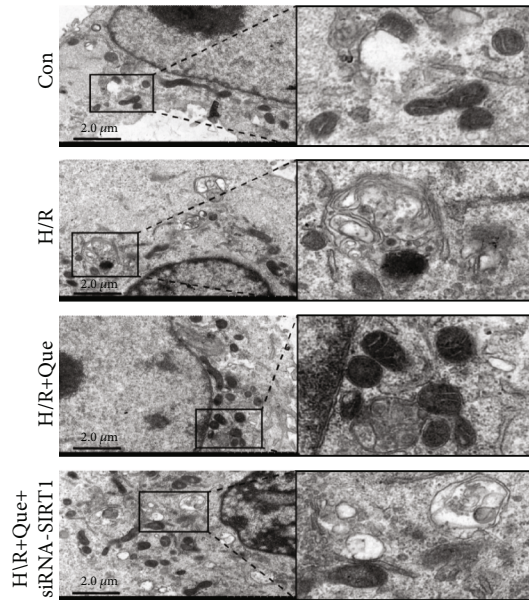
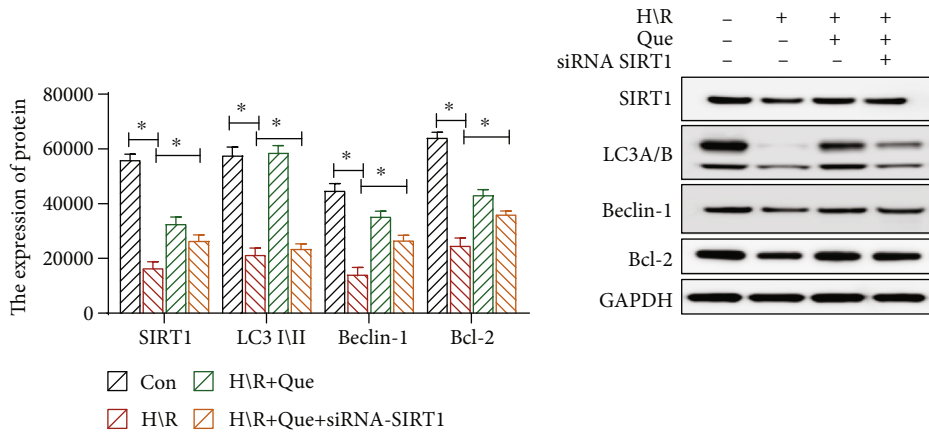
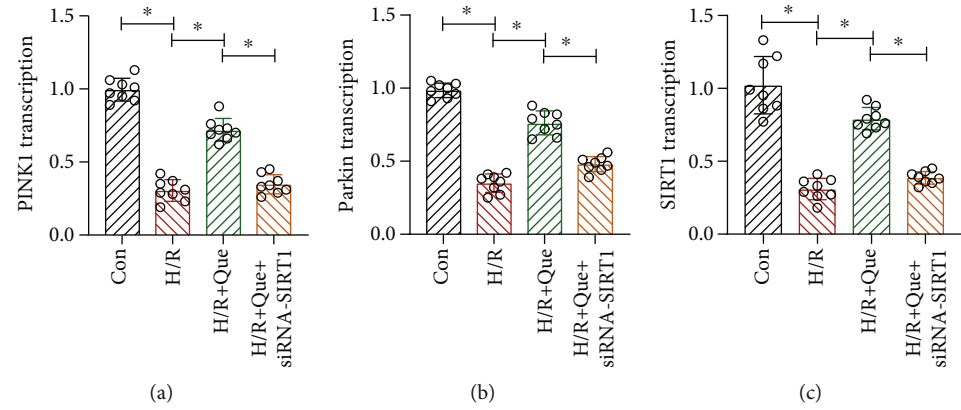


FIGURE 5: Continued.

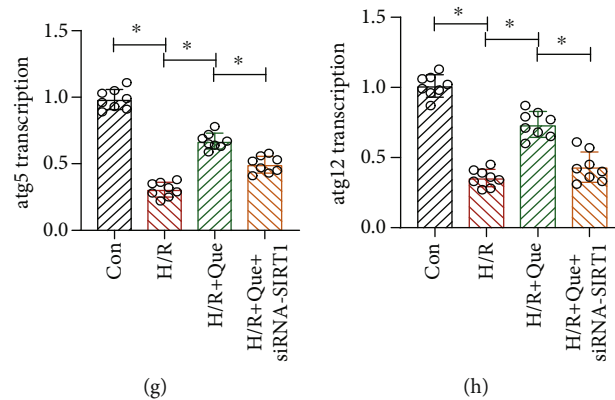


FIGURE 5: Quercetin (Que) regulates human cardiomyocyte mitophagy under conditions of hypoxia/reoxygenation (H/R): (a, b, c, g, h) levels of the *SIRT1*, *PINK1*/parkin, *ATG5*, and *ATG12* mRNAs determined by qPCR; (d, e) protein levels of *SIRT1*, LC3-I/II, Beclin-1, Bcl-2, and GAPDH determined by western blotting; (f) mitochondria observed by transmission electron microscopy. * $p < 0.05$. Con: control; *SIRT1* siRNA: *SIRT1* short interfering RNA.

MMP loss, along with the release of caspase and other apoptosis signaling molecules [30]. This is consistent with our findings showing that hypoxia-mediated oxidative stress damage increased ROS production, indirectly leading to mitochondrial/ER dysfunction and further damage in human cardiomyocytes.

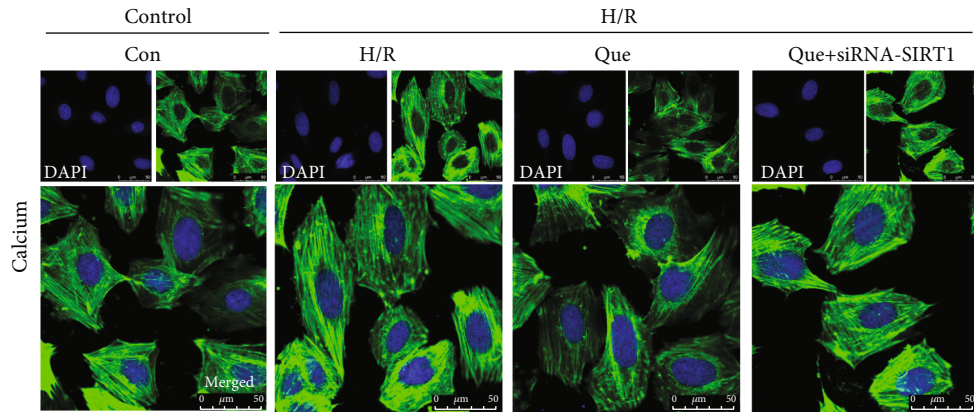
Mitophagy is an autophagic process that selectively removes excess or damaged mitochondria [31]. Overexpression of *ATG5*, *ATG12*, and LC3-II (mitophagy-related proteins) significantly prolongs the lifespan of endothelial cells. These effects are closely related to increased MMP and ATP production, reduced mitochondrial DNA damage, and improved mitochondrial function [32]. Moreover, autophagy and mitophagy dysfunction may result in abnormal cardiac and endothelial cell function, including vascular aging and calcification [9]. Autophagy and selective mitophagy reverse endothelium-dependent diastolic dysfunction by regulating the total redox state of blood vessels, inhibiting ROS production, and increasing arterial stiffness [33].

These studies indicate that mitophagy plays a regulatory role in vascular and myocardial tissues and cells. A study of endothelial cells from elderly and young populations and aged and young mice found that *ATG* and Beclin-1 in the elderly groups were significantly decreased, suggesting decreased autophagy in aged vessels. Furthermore, autophagy inducers can reverse some changes in aging arteries and inhibit oxidative stress by increasing the bioavailability of nitric oxide [34]. In a mouse model of diabetic cardiomyopathy induced by a high-fat diet, parkin-mediated mitophagy reduced myocardial hypertrophy and diastolic dysfunction and protected cardiac function. In addition, pretreatment with Tat-Beclin-1 (a mitophagy inducer) reduced myocardial hypertrophy and diastolic dysfunction induced by continuous high-fat diet feeding. In this study, we found that Que upregulates Beclin-1 and LC3-I/II by regulating *ATG*, restoring the mitophagy level and energy metabolism function, and inhibiting ER stress and oxidative stress damage. These findings also corroborate the protective mechanism of mitophagy in cardiovascular diseases.

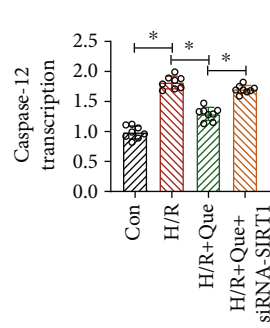
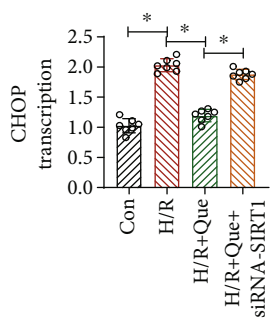
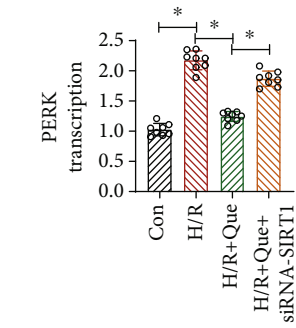
In addition to mitophagy dysfunction, ER dysfunction is an important factor leading to cardiomyocyte apoptosis [35]. Combined ER stress and mitophagy disorders lead to an imbalance in intracellular homeostasis [36]. When hypoxia-induced excessive ROS production mediates oxidative stress damage, unfolded proteins accumulate in the ER, exceeding the ability to perform the unfolded protein reaction, affecting mitophagy, and finally leading to increased myocardial apoptosis [37]. Que was found to inhibit ER stress, promote mitophagy, reduce mitochondrial dysfunction, and effectively maintain the homeostasis of myocardial cells by regulating *SIRT1*/TMBIM6 related to ER stress.

Previous research showed that Que regulates the *SIRT1*, JNK/c-JUN/CYP7A1, MAPK, and PI3K/AKT pathways [38]. Although this study preliminarily confirmed that Que can protect cardiomyocytes by regulating mitophagy and ER stress, its specific molecular mechanism is unclear. Another study showed that the axial shear stress of *SIRT1*-FOXO induces upregulation of *SIRT1* and activates autophagy [39]. Moreover, *SIRT1* can play a protective role in various cardiovascular diseases through diverse cellular functions. For instance, the *SIRT1* activator SRT1720 can activate AMPK, enhance autophagy, and reduce myocardial apoptosis, whereas treatment with the *SIRT1* inhibitor EX527 reverses the increase in autophagy. These findings suggest that *SIRT1* promotes mitophagy, reduces hypoxia-induced apoptosis, and protects cardiomyocytes from oxidative stress. To further verify the regulatory pathway of the effects of Que on the ER through *SIRT1*, we examined the ability of Que to regulate TMBIM6.

As an important organelle, the ER can activate multiple ER stress signaling pathways to regulate protein folding, synthesis, protein degradation, gene expression, apoptosis, and bioenergy efficiency. Under various physiological and pathological conditions, unfolded proteins can accumulate in the ER, a cellular state known as ER stress. TMBIM6, as an important regulatory protein of ER stress, can participate in regulating ER stress signaling pathways. TMBIM6 can directly inhibit IRE1- α activity by binding to its cytoplasmic



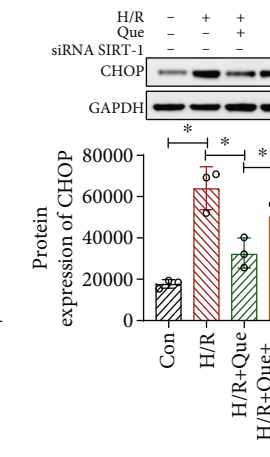
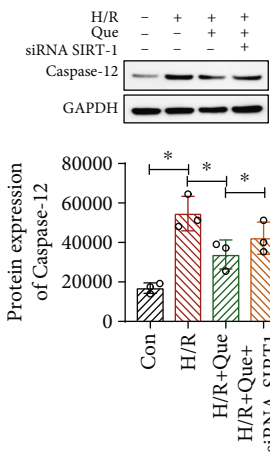
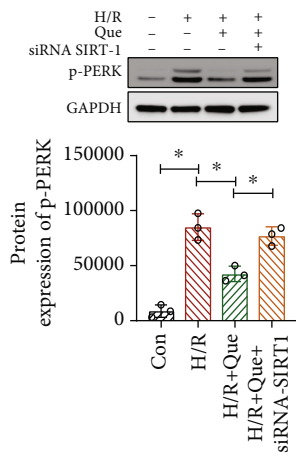
(a)



(b)

(c)

(d)



(e)

(f)

(g)

FIGURE 6: Continued.

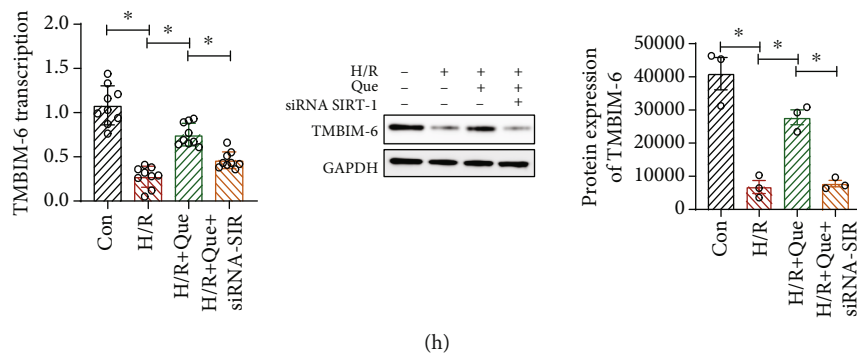


FIGURE 6: Quercetin (Que) ameliorates ER stress in human cardiomyocytes under conditions of hypoxia/reoxygenation (H/R): (a) calcium released from cardiomyocytes, as observed by laser confocal microscopy; (b–d) levels of the *PERK*, *CHOP*, and caspase-12 mRNAs determined by qPCR; (e–g) protein levels of p-PERK, CHOP, caspase-12, and GAPDH determined by western blotting; (h) mRNA and protein levels of TMBIM6 determined by qPCR and western blotting, respectively. * $p < 0.05$. Con: control; SIRT1 siRNA: SIRT1 short interfering RNA.

domain [40]. This protein is also responsible for controlling calcium release and the ER apoptosis pathway in the ER region [41]. Our results confirm that Que regulates mitophagy and ER stress through SIRT1/TMBIM6 and that the protective effect of Que on cardiomyocytes under oxidative stress damage caused by hypoxia is accomplished by SIRT-1/TMBIM6.

Nevertheless, this study had some limitations. First, although we inferred that Que regulates mitochondrial function and ER stress through SIRT1/TMBIM6 activation, the SIRT1–TMBIM6 interaction mechanism is not well-understood. Whether TMBIM6, as a regulatory protein of ER function, can directly regulate mitophagy is unknown. Further studies of the molecular mechanisms underlying these effects are needed to clarify the upstream and downstream processes regulating SIRT1/TMBIM6 expression. Second, the mechanism by which Que inhibits oxidative stress-induced damage in cardiomyocytes was only discussed in the context of mitophagy and ER stress; phenomena such as mitochondria–ER contact and calcium signal transduction were not explored. Therefore, in-depth studies are needed to determine the potential involvement of mitochondria–ER contact disorders in cardiomyocyte or vascular endothelial cell apoptosis. Finally, the therapeutic relevance of our in vitro findings must be verified in vivo and in clinical trials.

5. Conclusions

Our research shows that Que ameliorates the vulnerability of cardiomyocytes to H/R by inhibiting ROS production and oxidative stress damage, thereby improving mitophagy and energy metabolism, regulating mitochondrial/ER function, and ultimately reducing apoptosis. Under Que pretreatment, SIRT-1 and TMBIM6, which are closely related to the functions of mitochondria and ER, both showed significant improvement. The protective effect of Que on cardiomyocytes can be eliminated by depleting SIRT1, suggesting that Que regulates mitophagy and ER stress by activating SIRT1/TMBIM6 and inhibiting oxidative stress damage. These findings provide insights into the treatment of hypoxic

injury-induced cardiovascular diseases and the potential of natural antioxidants for regulating mitochondrial and ER function.

Data Availability

The data used to support the findings of this study are available from the corresponding author upon request.

Conflicts of Interest

The authors declare that there is no conflict of interest regarding the publication of this paper.

Acknowledgments

We would like to thank Editage (<http://www.editage.cn/>) for English language editing. This work was supported by the Guangdong Natural Science Basic Level Project, Study on “Calcification paradox” via SphK1/S1P and the mechanism of THF (grant number 2020A1515010245); National Natural Science Youth Fund (grant number 82004233); and Natural Science Foundation of Shandong Province (grant number ZR2020MH352).

References

- [1] H. Abe, H. Semba, and N. Takeda, “The roles of hypoxia signaling in the pathogenesis of cardiovascular diseases,” *Journal of Atherosclerosis and Thrombosis*, vol. 24, no. 9, p. 884, 2017.
- [2] G. Heusch, “Coronary microvascular obstruction: the new frontier in cardioprotection,” *Basic Research In Cardiology*, vol. 114, no. 6, 2019.
- [3] Q. Y. Qin, X. W. Lu, Q. Wu, P. Lu, and W. K. Zhao, “6-Gingerol pretreatment alleviates hypoxia/reoxygenation-induced H9C2 cardiomyocyte injury by inhibiting oxidative stress and inflammation,” *Sichuan Da Xue Xue Bao Yi Xue Ban*, vol. 51, no. 5, pp. 658–663, 2020.
- [4] Q. Zhao, H. Li, L. Chang et al., “Qiliqiangxin Attenuates Oxidative Stress-Induced Mitochondrion-Dependent Apoptosis in Cardiomyocytes via PI3K/AKT/GSK3 β Signaling Pathway,”

- Biological & Pharmaceutical Bulletin*, vol. 42, no. 8, pp. 1310–1321, 2019.
- [5] Z. Yang, J. Wang, S. Ai, J. Sun, X. Mai, and W. Guan, “Self-generating oxygen enhanced mitochondrion-targeted photodynamic therapy for tumor treatment with hypoxia scavenging,” *Theranostics*, vol. 9, no. 23, pp. 6809–6823, 2019.
 - [6] Y. Zhao, B. Chen, J. Shen et al., “The beneficial effects of quercetin, curcumin, and resveratrol in obesity,” *Oxidative Medicine and Cellular Longevity*, vol. 2017, Article ID 1459497, 8 pages, 2017.
 - [7] L. Cui, Z. Li, X. Chang, G. Cong, and L. Hao, “Quercetin attenuates vascular calcification by inhibiting oxidative stress and mitochondrial fission,” *Vascular pharmacology*, vol. 88, pp. 21–29, 2017.
 - [8] W. E. Hughes, A. M. Beyer, and D. D. Gutterman, “Vascular autophagy in health and disease,” *BASIC RESEARCH IN CARDIOLOGY*, vol. 115, no. 4, 2020.
 - [9] J. M. Bravo-San Pedro, G. Kroemer, and L. Galluzzi, “Autophagy and mitophagy in cardiovascular disease,” *CIRCULATION RESEARCH*, vol. 120, no. 11, pp. 1812–1824, 2017.
 - [10] M. Akbari, T. Kirkwood, and V. A. Bohr, “Mitochondria in the signaling pathways that control longevity and health span,” *AGEING RESEARCH REVIEWS*, vol. 54, article 100940, 2019.
 - [11] M. Manevski, T. Muthumalage, D. Devadoss et al., “Cellular stress responses and dysfunctional mitochondrial-cellular senescence, and therapeutics in chronic respiratory diseases,” *Redox Biology*, vol. 33, article 101443, 2020.
 - [12] K. Palikaras, E. Lionaki, and N. Tavernarakis, “Mechanisms of mitophagy in cellular homeostasis, physiology and pathology,” *NATURE CELL BIOLOGY*, vol. 20, no. 9, pp. 1013–1022, 2018.
 - [13] N. M. Mazure and J. Pouyssegur, “Hypoxia-induced autophagy: cell death or cell survival?,” *CURRENT OPINION IN CELL BIOLOGY*, vol. 22, no. 2, pp. 177–180, 2010.
 - [14] B. Loos, S. Genade, B. Ellis, A. Lochner, and A. M. Engelbrecht, “At the core of survival: autophagy delays the onset of both apoptotic and necrotic cell death in a model of ischemic cell injury,” *EXPERIMENTAL CELL RESEARCH*, vol. 317, no. 10, pp. 1437–1453, 2011.
 - [15] C. Zhang, Y. Li, J. Zhao et al., “Endoplasmic reticulum stress regulates cardiomyocyte apoptosis in myocardial fibrosis development via PERK-mediated autophagy,” *Cardiovascular Toxicology*, vol. 20, no. 6, article 9586, pp. 618–626, 2020.
 - [16] A. P. Magalhães Rebelo, F. Dal Bello, T. Knedlik et al., “Chemical modulation of mitochondria-endoplasmic reticulum contact sites,” *Cells*, vol. 9, no. 7, p. 1637, 2020.
 - [17] C. Dong, W. Tu, M. He et al., “Role of endoplasmic reticulum and mitochondrion in proton microbeam radiation-induced bystander effect,” *RADIATION RESEARCH*, vol. 193, no. 1, pp. 63–72, 2020.
 - [18] D. Martinvalet, “The role of the mitochondria and the endoplasmic reticulum contact sites in the development of the immune responses,” *Cell Death & Disease*, vol. 9, no. 3, p. 336, 2018.
 - [19] R. Aishwarya, S. Alam, C. S. Abdullah et al., “Pleiotropic effects of mdivi-1 in altering mitochondrial dynamics, respiration, and autophagy in cardiomyocytes,” *Redox Biology*, vol. 36, article 101660, 2020.
 - [20] H. M. Zeeshan, G. H. Lee, H. R. Kim, and H. J. Chae, “Endoplasmic reticulum stress and associated ROS,” *INTERNATIONAL JOURNAL OF MOLECULAR SCIENCES*, vol. 17, no. 3, p. 327, 2016.
 - [21] Y. Qiu, R. Cheng, C. Liang et al., “MicroRNA-20b Promotes Cardiac Hypertrophy by the Inhibition of Mitofusin 2-Mediated Inter-organelle Ca²⁺ Cross-Talk,” *Molecular Therapy-Nucleic Acids*, vol. 19, pp. 1343–1356, 2020.
 - [22] G. Guan, L. Yang, W. Huang et al., “Mechanism of interactions between endoplasmic reticulum stress and autophagy in hypoxia/reoxygenation-induced injury of H9c2 cardiomyocytes,” *Molecular Medicine Reports*, vol. 20, no. 1, pp. 350–358, 2019.
 - [23] W. Zhang, Y. Zhang, X. Guo et al., “Sirt1 protects endothelial cells against LPS-induced barrier dysfunction,” *Oxidative Medicine and Cellular Longevity*, vol. 2017, Article ID 4082102, 14 pages, 2017.
 - [24] J. Tang, L. Lu, Y. Liu et al., “Quercetin improve ischemia/reperfusion-induced cardiomyocyte apoptosis in vitro and in vivo study via SIRT1/PGC-1 α signaling,” *JOURNAL OF CELLULAR BIOCHEMISTRY*, vol. 120, no. 6, pp. 9747–9757, 2019.
 - [25] D. Doycheva, H. Kaur, J. Tang, and J. H. Zhang, “The characteristics of the ancient cell death suppressor, TMBIM6, and its related signaling pathways after endoplasmic reticulum stress,” *JOURNAL OF NEUROSCIENCE RESEARCH*, vol. 98, no. 1, pp. 77–86, 2020.
 - [26] H. K. Kim, G. H. Lee, K. R. Bhattarai et al., “TMBIM6 (transmembrane BAX inhibitor motif containing 6) enhances autophagy through regulation of lysosomal calcium,” *Autophagy*, pp. 1–18, 2020.
 - [27] C. Li, Y. Tan, J. Wu et al., “Resveratrol improves Bnip3-related mitophagy and attenuates high-fat-induced endothelial dysfunction,” *Frontiers in Cell and Developmental Biology*, vol. 8, 2020.
 - [28] Z. W. Zhang, X. C. Xu, T. Liu, and S. Yuan, “Mitochondrion-permeable antioxidants to treat ROS-burst-mediated acute diseases,” *Oxidative Medicine and Cellular Longevity*, vol. 2016, Article ID 6859523, 10 pages, 2016.
 - [29] B. Paital and G. B. Chainy, “Effects of temperature on complexes I and II mediated respiration, ROS generation and oxidative stress status in isolated gill mitochondria of the mud crab *Scylla serrata*,” *JOURNAL OF THERMAL BIOLOGY*, vol. 41, pp. 104–111, 2014.
 - [30] F. J. Meng, Z. W. Hou, Y. Li, Y. Yang, and B. Yu, “The protective effect of picoside II against hypoxia/reoxygenation injury in neonatal rat cardiomyocytes,” *PHARMACEUTICAL BIOLOGY*, vol. 50, no. 10, pp. 1226–1232, 2012.
 - [31] M. Li, D. Yuan, Y. Liu, H. Jin, and B. Tan, “Dietary puerarin supplementation alleviates oxidative stress in the small intestines of diquat-challenged piglets,” *Animals (Basel)*, vol. 10, no. 4, p. 631, 2020.
 - [32] Y. Z. Li, X. D. Wu, X. H. Liu, and P. F. Li, “Mitophagy imbalance in cardiomyocyte ischaemia/reperfusion injury,” *Acta Physiologica*, vol. 225, no. 4, article e13228, 2019.
 - [33] T. J. LaRocca, G. D. Henson, A. Thorburn, A. L. Sindler, G. L. Pierce, and D. R. Seals, “Translational evidence that impaired autophagy contributes to arterial ageing,” *The Journal of physiology*, vol. 590, no. 14, pp. 3305–3316, 2012.
 - [34] T. J. LaRocca, R. A. Gioscia-Ryan, C. J. Heaton, and D. R. Seals, “The autophagy enhancer spermidine reverses arterial aging,” *MECHANISMS OF AGEING AND DEVELOPMENT*, vol. 134, no. 7-8, pp. 314–320, 2013.
 - [35] J. R. Lin, W. L. Shen, C. Yan, and P. J. Gao, “Downregulation of dynamin-related protein 1 contributes to impaired autophagic

- flux and angiogenic function in senescent endothelial cells,” *Arteriosclerosis, thrombosis, and vascular biology*, vol. 35, no. 6, pp. 1413–1422, 2015.
- [36] D. Spratt, D. M. Poitz, I. Korovina et al., “Endothelial-specific deficiency of ATG5 (autophagy protein 5) attenuates ischemia-related angiogenesis,” *Arteriosclerosis, thrombosis, and vascular biology*, vol. 39, no. 6, pp. 1137–1148, 2019.
- [37] Z. Zha, J. Wang, X. Wang, M. Lu, and Y. Guo, “Involvement of PINK1/Parkin-mediated mitophagy in AGE-induced cardiomyocyte aging,” *INTERNATIONAL JOURNAL OF CARDIOLOGY*, vol. 227, pp. 201–208, 2017.
- [38] J. Q. Ma, J. Ding, H. Zhao, and C. M. Liu, “Puerarin attenuates carbon tetrachloride-induced liver oxidative stress and hyperlipidaemia in mouse by JNK/c-Jun/CYP7A1 pathway,” *Basic Clin Pharmacol Toxicol*, vol. 115, no. 5, pp. 389–395, 2014.
- [39] G. Luo, Z. Jian, Y. Zhu et al., “Sirt1 promotes autophagy and inhibits apoptosis to protect cardiomyocytes from hypoxic stress,” *INTERNATIONAL JOURNAL OF MOLECULAR MEDICINE*, vol. 43, no. 5, pp. 2033–2043, 2019.
- [40] R. P. Junjappa, H. K. Kim, S. Y. Park et al., “Expression of TMBIM6 in Cancers: The Involvement of Sp1 and PKC,” *Cancers (Basel)*, vol. 11, no. 7, p. 974, 2019.
- [41] D. Doycheva, N. Xu, H. Kaur et al., “Adenoviral TMBIM6 vector attenuates ER-stress-induced apoptosis in a neonatal hypoxic-ischemic rat model,” *Disease Models & Mechanisms*, vol. 12, no. 11, p. dmm040352, 2019.

Research Article

RIPK3 Induces Cardiomyocyte Necroptosis via Inhibition of AMPK-Parkin-Mitophagy in Cardiac Remodelling after Myocardial Infarction

Pingjun Zhu ¹, Kun Wan,² Ming Yin,³ Peng Hu,⁴ Yifan Que,⁴ Xin Zhou,⁴ Lei Zhang,⁴ Tianzhi Li,⁴ Yingzhen Du ¹, Guogang Xu ⁴, and Xiangqun Fang ¹

¹Department of Respiratory and Critical Care Medicine, The Second Medical Center & National Clinical Research Center for Geriatric Diseases, Chinese PLA General Hospital, Beijing, China

²Medical Supplies Center of Chinese PLA General Hospital, Beijing, China

³Department of Emergency, The Second Medical Center & National Clinical Research Center for Geriatric Diseases, Chinese PLA General Hospital, Beijing, China

⁴The Second Medical Center & National Clinical Research Center for Geriatric Diseases, Chinese PLA General Hospital, Beijing, China

Correspondence should be addressed to Yingzhen Du; zhenzhen52@163.com, Guogang Xu; guogang_xu@qq.com, and Xiangqun Fang; fangxiangquntg@sina.com

Received 7 January 2021; Revised 15 February 2021; Accepted 10 March 2021; Published 28 March 2021

Academic Editor: Daniele Vergara

Copyright © 2021 Pingjun Zhu et al. This is an open access article distributed under the Creative Commons Attribution License, which permits unrestricted use, distribution, and reproduction in any medium, provided the original work is properly cited.

Receptor-interacting protein 3- (RIPK3-) modulated necroptosis plays a critical role in cardiac remodelling after myocardial infarction (MI). However, the precise regulatory mechanism is not fully elucidated yet. In the present study, we showed that RIPK3 expression was upregulated in myocardial tissue after MI in a mouse model by coronary artery ligation, as well as in the cardiomyocytes following hypoxic injury *in vitro*. The increase of RIPK3 expression was found to be accompanied by severe cardiac remodelling, cardiac dysfunction, and higher mortality. Elevated RIPK3 expression subsequently abrogated the AMPK pathway that was accompanied by inhibition of Parkin-mediated mitophagy. Loss of mitophagy increased the opening of mitochondrial permeability transition pore (mPTP), which ultimately induced the cardiomyocyte necroptosis. In contrast, genetic ablation of *Ripk3* induced the AMPK/Parkin-mitophagy pathway, favouring a prosurvival state that eventually inhibited mPTP opening and induced the necroptosis of cardiomyocytes in the post-MI cardiac remodelling. In conclusion, our results revealed a key mechanism by which necroptosis could be mediated by RIPK3 via the AMPK/Parkin-mitophagy/mPTP opening axis, which provides a potential therapeutic target in the management of heart failure after MI.

1. Introduction

Today, ischemic heart failure remains a major health concern, accounting for high morbidity and mortality globally [1]. Myocardial infarction (MI) has been found to be the leading cause of ischemic heart failure. The loss of cardiomyocytes is confirmed as essential in the pathogenesis of cardiac remodelling following MI [2, 3], which is mainly due to necroptosis [4]. Thus, reducing cardiomyocyte necroptosis represents a very promising strategy in treating ischemic heart failure.

Necroptosis is one subtype of necrosis that is regulated by a specific pathway of cell death [5]. Specifically, the receptor-interacting protein 3- (RIPK3-) mediated mitochondrial permeability transition pore (mPTP) opening signalling pathways are key in regulating necroptosis of cardiomyocyte under different stimuli [4, 6, 7]. The mPTP opening causes proton gradient dissipation, which thereby modulates the oxidative phosphorylation and ATP synthesis, mitochondrial swelling and rupture, and eventually cardiomyocyte necroptosis [8, 9]. However, the precise mechanism by which RIPK3

regulates mPTP opening in post-MI cardiac remodelling remains elusive.

Mitochondria are intracellular organelles that are critical in certain intracellular processes that are fundamental in energy transformation with ATP [10]. Mitochondria are also important in cell life and fate as they play key roles in initiating apoptosis. Maintaining homeostatic control of the mitochondria, in terms of both quantity and quality, is essential for cell fate and function [11]. Mitophagy is a protective mechanism which degrades those damaged mitochondria in the lysosomes under exposure to different stimuli [12–14]. Recent studies have confirmed that mitophagy is critically involved in the regulation of cellular necroptosis. In neuroblastic SH-SY5Y cells, activation of mitophagy by UNBS1450 inhibited the dissipation of mitochondrial membrane potential, mPTP opening, and cellular necroptosis. However, another study showed that mitophagy can also activate cellular necroptosis. During the progression in chronic obstructive pulmonary disease (COPD), inhibition of mitophagy was also shown to reduce the number of human pulmonary arterial endothelial cells undergoing necroptosis due to smoke exposure [15–17]. Thus, mitophagy appears to play different roles in the regulation of cell necroptosis in different contexts, which may be related to the cell type and pathological environment [18]. Accordingly, we were interested in determining the role of mitophagy in cardiomyocyte necroptosis during post-MI cardiac remodelling.

Numerous studies have shown that activation of mitophagy can inhibit mPTP opening [19–21]. The PINK1-dependent recruitment of Parkin to damaged mitochondria is crucial in the process of mitophagy [22, 23]. Parkin phosphorylation is necessary for the full activation of the protein's E3 ligase activity, which increases the capacity of Parkin to interact with LC3. At the molecular level, Parkin-mediated mitophagy inhibits mPTP opening by catalysing ubiquitination of CypD, a key component of the mPTP complex [24]. Furthermore, Parkin-dependent mitophagy was shown to be essential for cardiomyocyte repair in ischemia and reperfusion (I/R) injury [25], hypoxic injury [26], and cardiac hypertrophy [27], as well as diabetic cardiomyopathy [28].

Thus, we hypothesized that RIPK3 may cause Parkin-dependent mitophagy to provoke mPTP opening and cardiomyocyte necroptosis in the pathogenesis of cardiac remodelling after MI. To test this hypothesis, RIPK3-deficient mice (*Ripk3*^{-/-}) were selected to establish an MI model with coronary artery ligation. We also established an *in vitro* model of hypoxic injury by using of cardiomyocytes from wild-type (WT) and *Ripk3*^{-/-} mice cultured in hypoxic conditions. The impact of RIPK3 after MI on mPTP opening and the expression of inflammatory factors were assessed. To explore the mechanisms underlying the influence of RIPK3 on post-MI heart remodelling, we evaluated the effects on angiogenesis, inflammation, oxidative stress, and cardiomyocyte necroptosis and the potential role of Parkin-mediated mitophagy on these effects.

2. Materials and Methods

2.1. Establishment of Animal Models. The present study was officially approved by the Institutional Animal Care and

Use Committee, Chinese PLA General Hospital, Beijing. Gene knockout mice (*Ripk3*^{-/-}) with a C57BL/6 background (male, 12 wk old, *n* = 60) were generated as previously described [19]. MI mouse models were established according to a standard protocol: prior to surgery, wild-type (WT, male, 12 wk old, *n* = 60) and *Ripk3*^{-/-} mice were administered with inhalation anaesthesia by using 1–2% isoflurane. The ligation surgical procedure of left anterior descending coronary artery was done as reported [29]. As a control, the specific artery remained intact in the sham group in the operation. Blood samples were collected 28 days after the surgery, emulating MI. The size of infarction was measured in the post-MI hearts using Masson's trichrome staining. Interstitial fibrosis in the noninfarct area was also investigated.

2.2. Determination of Cardiac Function. To monitor the cardiac function (*n* = 6/group) of animal models, echocardiography of all the mice was carefully examined by using a 14.0 MHz echocardiogram (Sequoia C512; Acuson) from Germany as reported in our previous study [19, 30].

2.3. Isolation of Cardiomyocytes and Primary Cell Culture, *In Vitro* I/R Injury Induction. Primary cardiomyocytes were all isolated from both *Ripk3*^{-/-} and wild-type (WT) mice according to our previous protocol [6]. The cells were subsequently proliferated in the high glucose-containing Dulbecco's modified Eagle medium (DMEM; Gibco) with 20% foetal bovine serum (FBS, HyClone, USA) in a 37°C incubation chamber supplied with 5% CO₂ and 95% air. For the cardiomyocytes under *in vitro* I/R injury induction, cells were incubated in pure DMEM with no FBS and other ingredients in a hypoxia chamber (95% N₂ and 5% CO₂) for 24 h. The adenovirus plasmid (Ad-Parkin) and control adenovirus plasmid (Ad-ctrl) were purchased from Vigene Biosciences. The Ad-Parkin and Ad-ctrl were used to infect the cardiomyocytes.

2.4. Cellular Necroptosis Detection. Cell suspension was seeded in 6-well cell-culture plates at a density of 10⁶ cells/well and incubated at 37°C for 24 h. To identify cells that had undergone necroptosis, cardiomyocytes were stained with 5 μL of FITC Annexin V and PI at RT (25°C) for 15 min in the dark with the FITC Annexin V Apoptosis Detection Kit (556547, BD Bioscience) [6].

2.5. Reactive Oxygen Species (ROS) Assays. ROS were measured after staining with dihydroethidium (DHE; Invitrogen, USA) [31]. The fluorescence was observed under microscopes and further analysed by flow cytometry. DHE was excited at 300 nm and 535 nm based on the standard protocol. The malondialdehyde (MDA) and the total superoxide dismutase (SOD) were detected as indicated by manufacturer (Biotin, Shanghai, China).

2.6. Enzyme-Linked Immunosorbent Assay (ELISA) of Cytokines. In addition to serum tumour necrosis factor-α (TNF-α) and interleukin-6 (IL-6), monocyte chemoattractant protein-1 (MCP-1) were also identified with commercially available ELISA kits from Technology Co., Ltd., Boster Bio, China.

2.7. RNA Isolation and Reverse Transcription-Quantitative PCR. RNA samples were extracted from the blood of mice or cells after treatment with hypoxia with routine laboratory protocol [32]. Total RNA (1 mg) was used for reverse transcription to synthesise cDNA (Invitrogen). Quantitative PCR was then run on a LightCycler 480 II system (Roche) with the LightCycler 480 Probes Master kit (Roche, 04887301001) and TaqMan primer-probe mix for each target gene. The reference gene 18S was used as an internal control.

2.8. Immunoblotting. For immunoblotting analysis, equal amounts (20–35 μ g) of total protein were fractionated by electrophoresis under denaturing conditions on a 4–20% sodium dodecyl sulphate- (SDS-) polyacrylamide gel (PAGE). The entire gel with protein bands was then transferred onto a piece of Immobilon-P polyvinylidene fluoride (PVDF) membrane (EMD Millipore, IPV00010). Since a gradient gel usually provides better separation of proteins with a wide range of molecular weights, we aimed to blot 2–3 proteins from the same membrane by cutting the membrane into small pieces. The target proteins were therefore ensured to fall into the middle of truncated membranes. In brief, the membranes were prestained with Pierce reversible protein stain kit and cut into 2–3 pieces based on the predicted molecular weights of target proteins according to direct visualization using a prestained protein ladder as reference. The PVDF membrane with proteins was blocked in 3% bovine serum albumin (BSA) for 1 h at RT. The membranes were further soaked overnight in primary antibodies at the desired dilution ratio in 3% BSA/TBST at 4°C. Primary antibodies for immunoblotting were as follows: PAGM5 (1:1000, Abcam, #ab126534), GADPH (1:1000, Abcam, #ab8245), p-MLKL (1:1000, Abcam, #ab196436), MLKL (1:1000, Cell Signaling Technology, #37705), Ripk3 (1:1000, Cell Signaling Technology, #95702), LC3II (1:1000, Cell Signaling Technology, #3868), p62 (1:1000, Abcam, #ab56416), Beclin1 (1:1000, Cell Signaling Technology, #3495), Atg5 (1:1000, Cell Signaling Technology, #12994), phospho-AMPK (Thr172, 1:500, Cell Signaling Technology, #2535), AMPK (1:1000, Cell Signaling Technology, #2532), Parkin (1:500, Abcam, #ab15954), phospho-Parkin (Ser65) (1:1000, Abcam, ab154995), and VDAC (1:1000, Abcam, #ab14734). They were subsequently washed in 1x TBST 5 min each for three times before incubating for 1 h with species-relevant horseradish peroxidase-conjugated secondary antibodies (1:5000–10,000) at RT. The PVDF membrane was washed again before being incubated in an Amersham ECL Prime Western Blotting Detection Reagent (GE Healthcare, RPN2232) or Clarity Max Western ECL Substrate (Bio-Rad, 1705062) as per the manufacturer's protocols, and target bands were detected on the ImageQuant LAS 400 system (GE Healthcare). The intensity of protein bands was quantified with the built-in ImageQuant TL software (Version 7.0 GE Healthcare) and normalized to the level of GADPH.

2.9. Immunofluorescence. Immunofluorescence analysis was performed on the cells as described previously. In brief, the cells were washed in phosphate-buffered saline (PBS) for three times prior to being fixed in 4% paraformaldehyde for

1 h at RT. Primary antibodies soaked with the cells were incubated overnight at 4°C. Afterwards, washout of excess primary antibodies (3×10 min with 0.1% Triton-X100 in PBS), the cells were further incubated for 2 h with secondary antibodies diluted in 5% NDS buffer at RT. The cover slips were subsequently washed with PBS-T (3×10 min) and PBS (1×10 min) in the dark and mounted onto slides using Fluoromount-G (SouthernBioTech, Birmingham, AL, USA). Immunostained preparations were analysed using a Nikon A1R confocal microscope (Melville, NY, USA) to determine protein expression.

2.10. Determination of mPTP Opening. mPTP opening was visualized by the rapid dissipation of tetramethylrhodamine ethyl ester (TMRE) fluorescence. We determined the arbitrary time of mPTP opening as the time when the TMRE fluorescence intensity was detected half-reduced between the initial and residual fluorescence intensities as reported. Cyclosporin A (CsA, 2 μ g/ml, Sigma Aldrich) was used as the inhibitor for mPTP opening in the negative control [33].

2.11. Statistical Analysis. One-way analysis of variance and the Student-Newman-Keuls test for post hoc comparisons were used to test for differences between the means of three or more independent groups. In addition, the Mann-Whitney *U* test was applied between the two experimental groups. The difference in the survival between two groups after MI was determined by the Mantel-Cox test. Data were all expressed as mean \pm SEM. The statistical differences were cut off at $p < 0.05$.

3. Results

3.1. RIPK3 Aggravated Cardiac Remodelling after MI. As shown in Figures 1(a) and 1(b), the western blot results demonstrated that expression of the myocardial RIPK3 protein was significantly upregulated in the peri-infarct heart tissue at 4 weeks after surgery compared to that of the sham-operated mice. Masson's trichrome staining of samples collected 4 weeks after MI showed that loss of *Ripk3* reduced the infarct size and the degree of fibrosis compared with those of the WT group after MI (Figures 1(c)–1(f)). Furthermore, *Ripk3* genetic ablation led to a lower level of heart weight-to-body weight ratio and lung weight-to-body weight ratio (Figures 1(g) and 1(h)). Gene knockout of *Ripk3* downregulated the mRNA expression in myocardial atrial natriuretic peptide (ANP), brain natriuretic peptide (BNP), and plasma BNP (Figures 1(i)–1(k)).

Compared with the WT group, deletion of the *Ripk3* gene induced lower mRNA expression levels of some proinflammatory cytokines such as TNF- α and IL-6 in the peri-infarcted areas of the heart tissue after MI (Figures 1(l) and 1(m)). DHE staining showed that the ROS content was elevated in the WT group but was restored to normal levels in the *Ripk3*^{-/-} group after MI (Figure 1(n)). In addition, decreased SOD enzymatic activity and increased content of MDA in remodelled hearts was reversed by *Ripk3* deletion (Supplemental Fig. 1A–B). *Ripk3* genetic deletion was also found to show effects of attenuating cardiac necroptosis, as

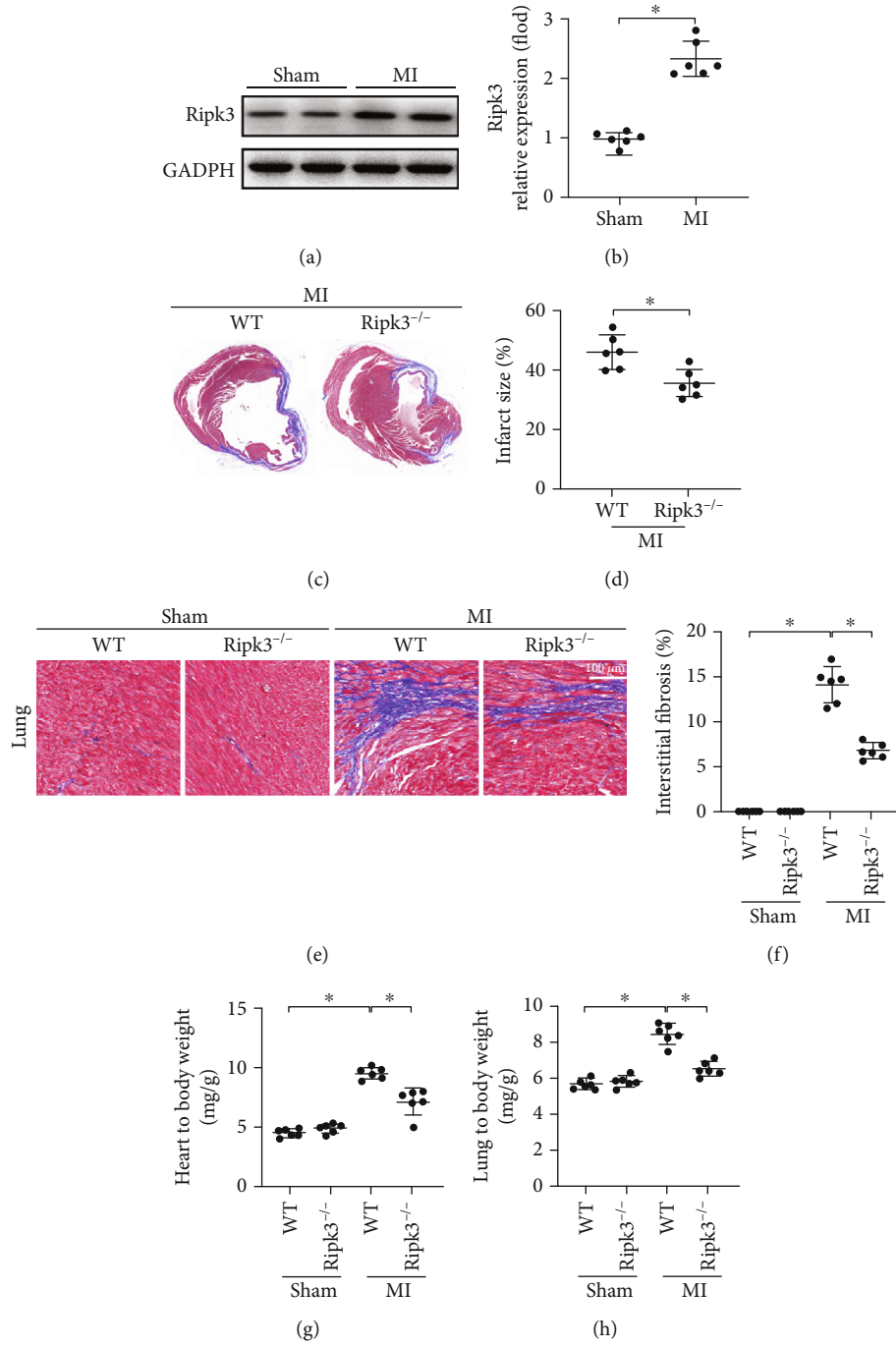


FIGURE 1: Continued.

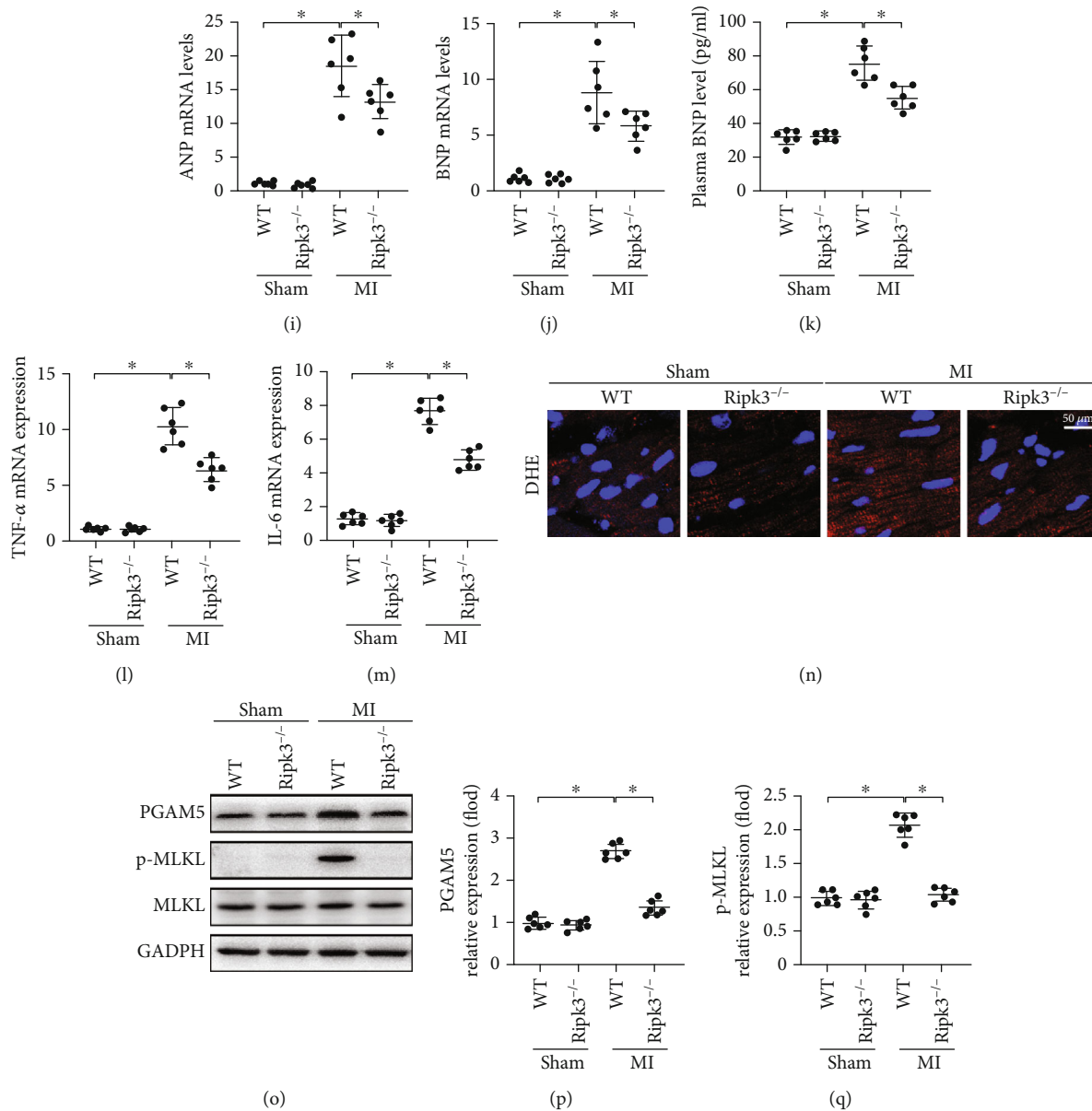


FIGURE 1: RIPK3 upregulation promoted cardiac remodelling after MI ($n = 6/\text{group}$). (a, b) The change of RIPK3 expression after MI. The infarct size (c, d) and the degree of fibrosis (e, f) of mice hearts were performed by Masson's trichrome staining. *Ripk3* genetic ablation reduced both the heart weight-to-body weight ratio (g) and the lung weight-to-body weight ratio (h). (i, j) The mRNA expression levels of myocardial atrial natriuretic peptide (ANP) and brain natriuretic peptide (BNP) were performed by RT-PCR. (k) The change of plasma BNP levels was detected by ELISA. (l, m) Loss of *Ripk3* reduced the mRNA levels of proinflammatory cytokines TNF- α and IL-6 in the peri-infarcted areas of the heart tissue. (n) ROS content in the heart tissue was detected by DHE staining. (o–q) The change of protein levels of phosphoglycerate mutase 5 (PGAM5) and phosphorylated mixed-lineage kinase domain-like protein (p-MLKL). Data are shown as the means \pm SEM, * $p < 0.05$.

confirmed by the decreased levels of phosphoglycerate mutase 5 (PGAM5) and phosphorylated mixed-lineage kinase domain-like protein (p-MLKL) (Figures 1(o)–1(q)). Collectively, these results indicated that RIPK3 contributed to post-MI heart remodelling.

3.2. Ablation of *Ripk3* Gene Enhanced the Cardiac Function and Survival of MI Mice. Echocardiography analysis at 4 weeks after MI confirmed that knockout of *Ripk3* significantly improved the left ventricular ejection fraction (LVEF)

and left ventricular fractional shortening (LVFS) and also reduced the internal diameter of the left ventricle at the end of systole and diastole (Figures 2(a)–2(d)). In sham-operated mice, the ablation of *Ripk3* had no effects on the above parameters in echocardiography scans. Furthermore, *Ripk3*^{-/-} mice had higher survival rates after MI compared with that of WT mice (Figure 2(e)). Taken together, our results strongly indicate that knockout of the *Ripk3* gene would help maintain the cardiac performance and survival during the chronic phase of MI.

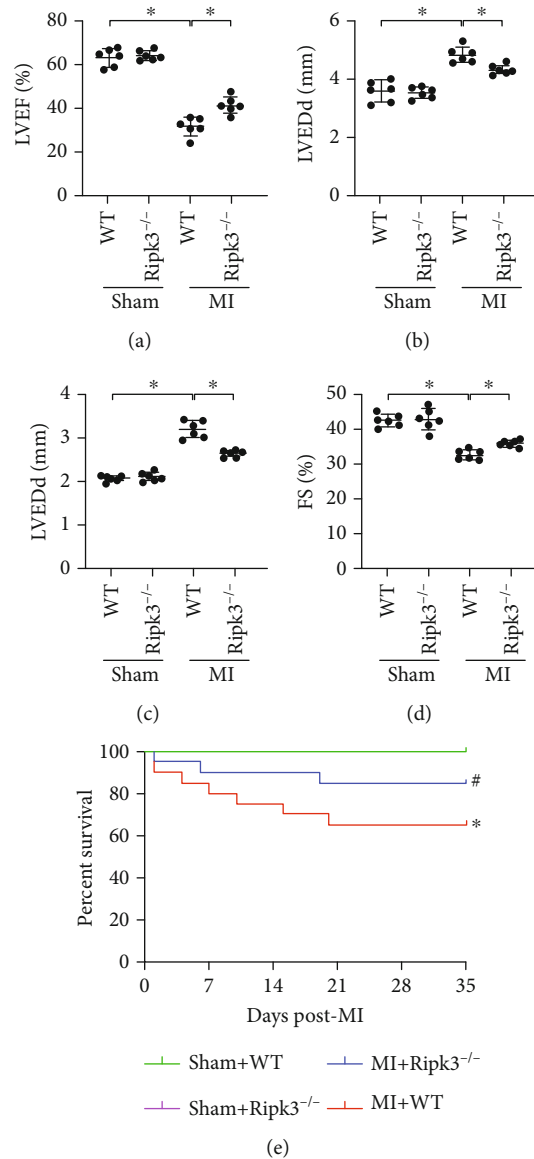


FIGURE 2: Genetic ablation of *Ripk3* enhanced the cardiac function and survival of MI mice. (a–d) Cardiac function is evaluated through echocardiography ($n = 6/\text{group}$). Data are shown as the means \pm SEM, $*p < 0.05$. LVEF: left-ventricular ejection fraction; LVFS: left-ventricular fractional shortening; LVEDd: left ventricular end-diastolic diameter; LVESd: left ventricular end-systolic diameter. (e) Survival of WT or *Ripk3*^{-/-} mice treated with sham or MI surgery ($n = 20/\text{group}$), $*p < 0.05$ vs. Sham+WT group, $\#p < 0.05$ vs. MI+WT group.

3.3. RIPK3-Induced Necroptosis Is Mediated by mPTP Opening in Cardiomyocytes. As shown in Figures 3(a) and 3(b), the cardiomyocyte necroptosis index was increased by hypoxia treatment for 24 h, based on the elevated expression of PGAM5 and p-MLKL. However, this effect was reversed in cardiomyocytes from *Ripk3*^{-/-} mice. To probe the underlying mechanism of *Ripk3*-mediated cardiomyocyte necroptosis, we first evaluated the rate of mitochondrial mPTP opening. Hypoxia treatment increased the mPTP opening time in WT cells, which was reversed in the case of *Ripk3* deficiency (Figure 3(d)). Inhibition of mPTP opening with CsA reduced necroptosis of WT cells under hypoxic stress, reaching a similar level to that as observed under *Ripk3* deletion (Figures 3(e) and 3(f)). Thus, mPTP opening plays a role in *Ripk3*-induced cardiomyocyte necroptosis.

3.4. RIPK3 Promoted mPTP Opening via Reducing Parkin-Related Mitophagy. As shown in Figures 4(a)–4(f), hypoxia reduced the levels of mitophagy markers in WT cells, including mito-LC3II, Atg5, Beclin1, and p62, compared with those of the control group cultured under normoxic conditions. However, these changes were reversed by *Ripk3* deletion. Since Parkin is essential for cardiac repair in post-MI heart remodeling, we further focused on the role of Parkin-related mitophagy in the *Ripk3*-mediated regulation of mitophagy under hypoxic stress. A gain-of-function Parkin assay was performed by overexpressing Parkin in the cardiomyocytes via transfection with an adenovirus vector (Ad-Parkin). Overexpression of Parkin reduced the hypoxic-induced mPTP opening following hypoxia injury in WT cells, which was consistent with the effect of *Ripk3* ablation

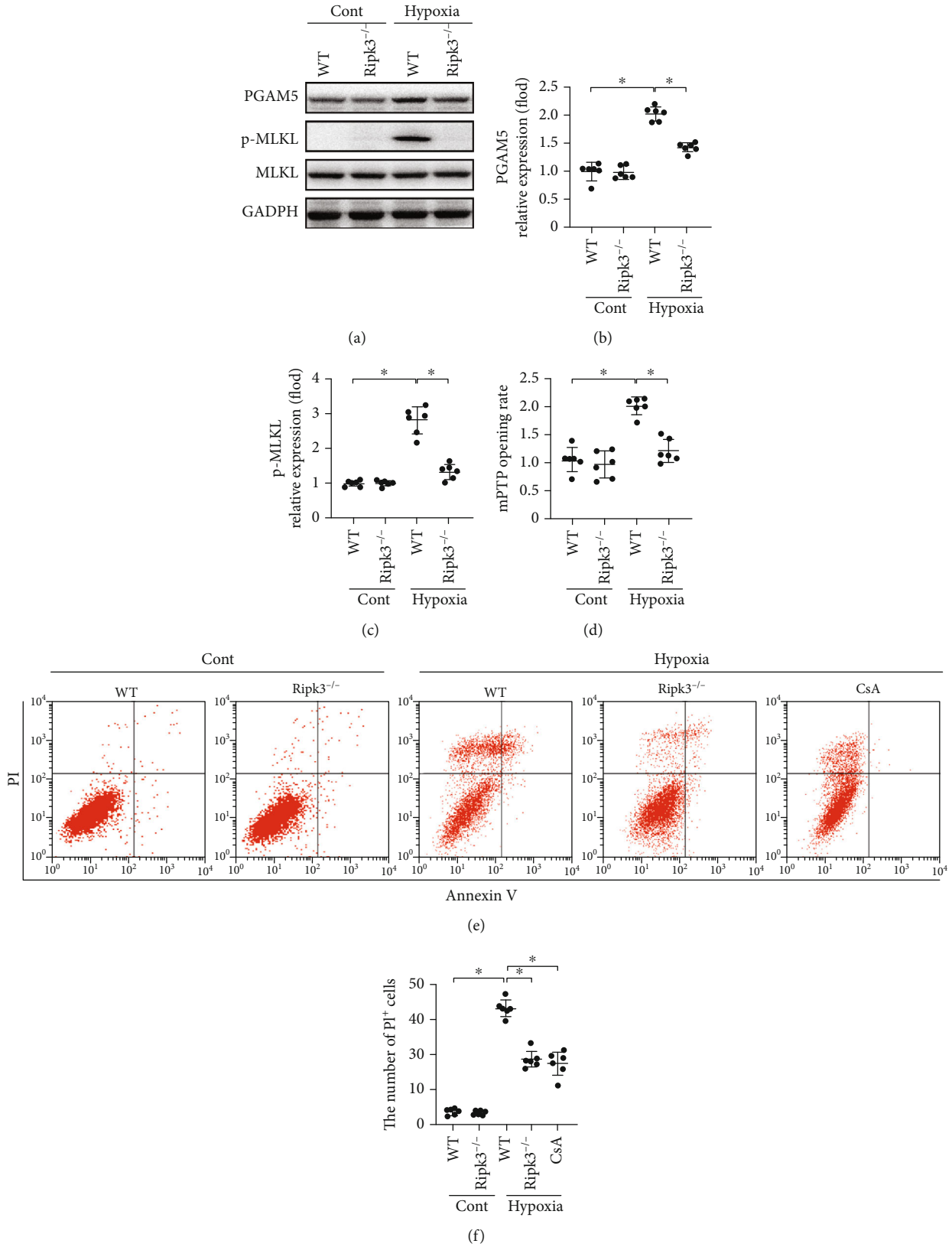


FIGURE 3: RIPK3 initiated necroptosis via promoting mPTP opening ($n = 6/\text{group}$). (a-c) The expression change of PGAM5 and p-MLKL was determined by western blot in vitro. (d) The change of mPTP opening time. (e) The cardiomyocyte necroptosis was measured flow cytometry with Annexin V/PI staining. Necroptosis group: the percentage of PI⁺ cells. Data are shown as the means \pm SEM, * $p < 0.05$.

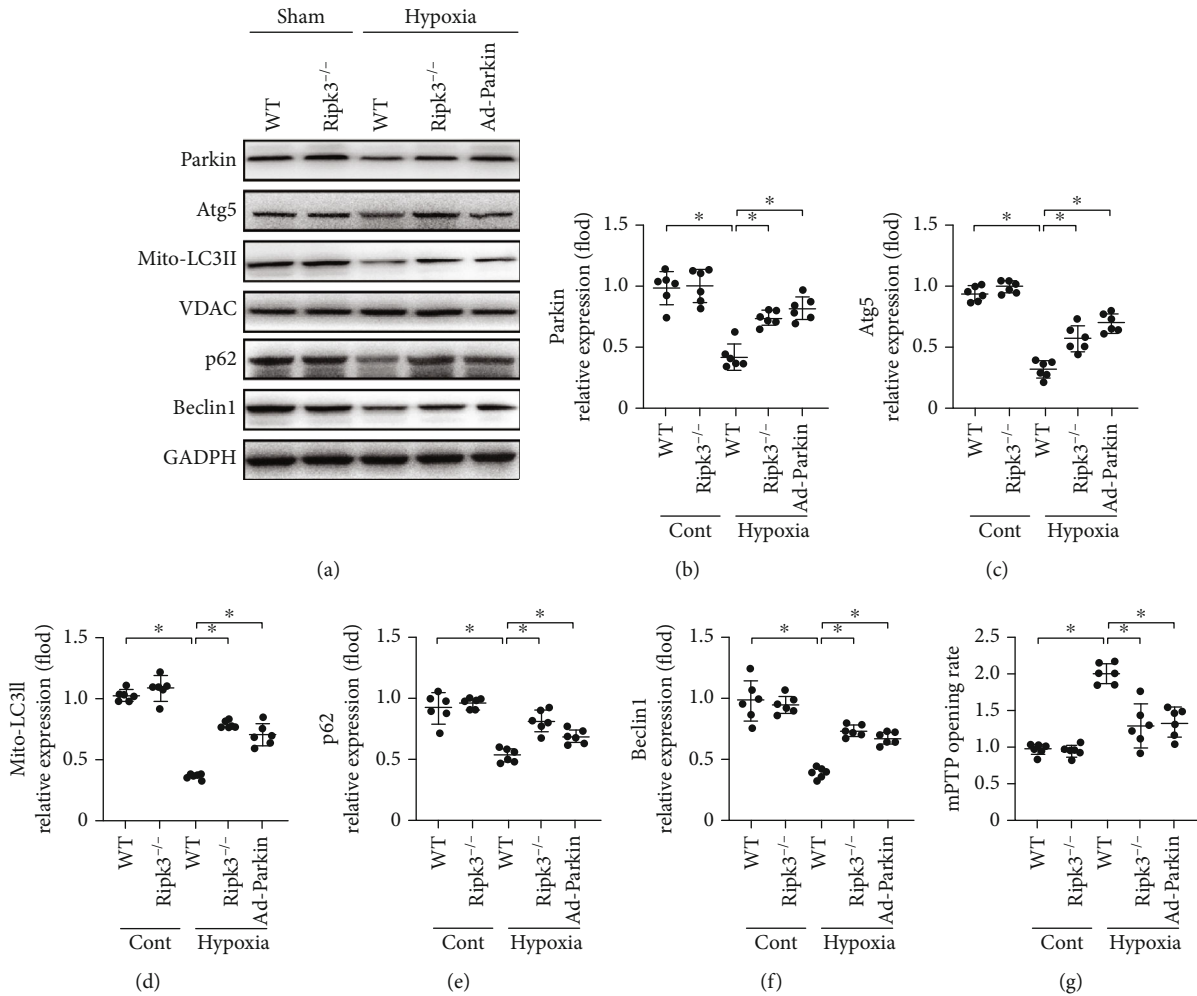


FIGURE 4: RIPK3 induced mPTP opening via Parkin-related mitophagy ($n = 6/\text{group}$). (a–f) Western blots were used to analyse the protein related to mitophagy. The gain-of-function assay about Parkin was carried out via adenovirus vector (Ad-Parkin) transfection. (g) The change of mPTP opening time. Data are shown as the means \pm SEM, * $p < 0.05$.

(Figure 4(g)). These data confirmed that RIPK3 regulates mPTP opening via Parkin-related mitophagy.

3.5. RIPK3 Regulated Parkin-Related Mitophagy via the AMPK Pathway. Hypoxic injury reduced the level of Parkin phosphorylation. However, this change was prevented with *Ripk3* deletion. To further investigate AMPK regulation of Parkin phosphorylation, we also observed the levels of AMPK activation under hypoxia. As shown in Figure 5(a), AMPK phosphorylation was suppressed under hypoxic conditions; this was reversed by *Ripk3* knockout. Treatment of the cardiomyocytes with the AMPK pathway activator (AICAR, AI) facilitated the phosphorylation of AMPK in the hypoxia group, together with increased Parkin phosphorylation (Figures 5(a)–5(c)). Costaining of the mitochondria and lysosome revealed that AMPK activation declined the association between the mitochondria and lysosome under hypoxic injury (Figure 5(d)). These data confirmed our hypothesis that RIPK3 regulates Parkin-related mitophagy via the AMPK pathway.

4. Discussion

Loss of cardiomyocytes after myocardial infarction promotes cardiac remodelling. RIPK3 supposedly plays a key role in cardiomyocyte necroptosis after MI. In our study, it was found that (i) RIPK3 could be activated after MI and would facilitate the development of post-MI cardiac remodelling; (ii) genetic ablation of *Ripk3* alleviated cardiac remodelling and promoted the cardiac function and survival of MI mice; (iii) *Ripk3* upregulation in cardiomyocytes inhibited AMPK phosphorylation, which reduced Parkin activation, thereby inhibiting mitophagy; and (iv) inactivation of mitophagy promoted opening of the mPTP, leading to cardiomyocyte necroptosis.

Mechanistically, formation of the “necrosome” by RIPK1, RIPK3, and p-MLKL results in necroptosis in various types of cells. However, myocardial necroptosis was reported to be the prominent mode of cell death, which is dependent on RIPK3 and mPTP opening [4, 6, 19]. Although the potential mechanism of how the mPTP opening triggers

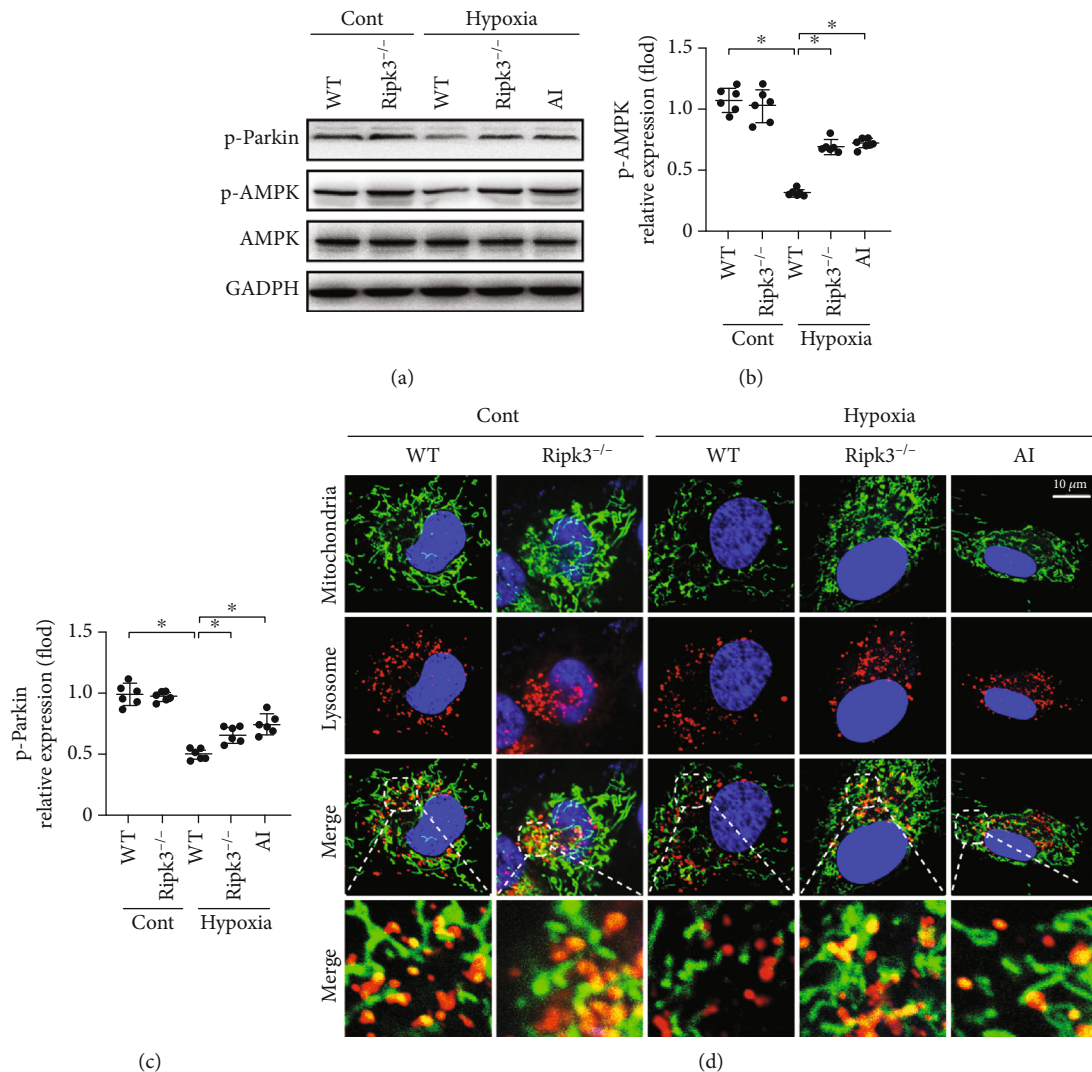


FIGURE 5: RIPK3 inactivated Parkin via inhibiting AMPK-mediated Parkin phosphorylation ($n = 6/\text{group}$). (a–c) Parkin and AMPK phosphorylation was analysed by western blots. AICAR (AI), the AMPK pathway activator, was used to activate AMPK pathways in WT cell under hypoxia injury. (d) The coimmunofluorescence of mitochondria and lysosomes in cardiomyocyte. AMPK activation facilitated the disassociation between the mitochondria and lysosome under hypoxia injury. Data are shown as the means \pm SEM, * $p < 0.05$.

cardiomyocyte necroptosis is well understood due to extensive research, the precise mechanism by which RIPK3 triggers mPTP opening has remained elusive, especially during cardiac remodelling after MI. Therefore, this study fills this gap in knowledge by confirming that RIPK3 induces necroptosis via the AMPK/Parkin-mitophagy/mPTP opening pathway, representing a novel signalling pathway involving post-MI cardiac remodelling as well as cardiomyocyte necroptosis.

The current study identified that mitophagy could act as a negative regulator of cardiomyocyte necroptosis in post-MI cardiac remodelling. Although accumulating evidence has hinted at a potential association between mitophagy and necroptosis, the regulatory role of mitophagy in necroptosis activation remains controversial. In patients with COPD, activation of both mitophagy and necroptosis has been observed in lung epithelial cells under persistent cigarette smoke extract (CSE) stimulation [34]. However, in Crohn's disease, activation of mitophagy was found to inhibit

RIPK3-dependent necroptosis in the intestinal epithelium [35]. Therefore, the cross-talk between mitophagy and necroptosis might differ depending on the stimulus exposure and disease model.

Extensive research on Parkin-dependent mitophagy has been carried out in the field of cardiac injury [24, 36]. Our results demonstrated that an increase in Parkin-related mitophagy was accompanied by a decrease in mPTP opening and cardiomyocyte death, which was consistent with previous studies. In addition, mitophagy could be activated by specific receptors such as Fundc1, Bnip3, and Parkin [37, 38]. The role of other mitophagy-related receptors in regulating cardiomyocyte necroptosis should be taken into consideration for further research.

In addition, AMPK plays a protective role in a variety of pathophysiological processes in cardiac functions [39]. AMPK activates Parkin-mediated mitophagy through the phosphorylation of PINK1 and thus modulates Parkin

recruitment/activation from the cytoplasm to the outer membrane of mitochondria [18, 40, 41]. In the current study, we identified RIPK3 as a negative regulator of Parkin-mediated mitophagy via inhibiting the AMPK pathway in cardiomyocytes, thereby revealing a novel myocardial necroptosis regulation model. However, the regulation mechanism of AMPK by RIPK3 warrants further investigation.

5. Conclusion

In conclusion, hypoxic injury and MI were associated with increased RIPK3 expression, leading to inactivation of AMPK. The reduction in AMPK in turn inhibited Parkin activation, which suppressed mitophagy and promoted mPTP opening and cellular necroptosis after MI. Thus, genetic ablation of *Ripk3* could activate the AMPK/Parkin-mitophagy pathway and subsequently prevent mPTP opening and cardiomyocyte necroptosis, ultimately preventing cardiac remodelling. Our results provide a potential therapeutic target to treat ischemic heart failure after MI.

Data Availability

The original data presented in the study are included in the article; further inquiries can be directed to the corresponding author/s.

Disclosure

The funders had no role in the study design, data collection and analysis, decision to publish, or preparation of the manuscript.

Conflicts of Interest

The authors declare no conflict of interest.

Authors' Contributions

GX, TL, and XF conceived the project and designed the research. PH, YQ, XZ, LZ, and YD performed the experiments. PZ, KW, and MY analysed the data, discussed the research, and wrote the manuscript. All authors contributed to the article and approved the submitted version. Pingjun Zhu, Kun Wan, and Ming Yin contributed equally to this work.

Acknowledgments

This study was financially supported by grants from the National Natural Science Foundation of China (No. 81900254 and No. 82000004) and National Key Research and Development Program of China (No. 2020YFC2002706).

Supplementary Materials

Supplemental Figure: total SOD activity (A) and MDA level (B) in hearts ($n = 6/\text{group}$); data are shown as the means \pm SEM, $*p < 0.05$. (*Supplementary Materials*)

References

- [1] A. Adameova, E. Goncalvesova, A. Szobi, and N. S. Dhalla, "Necroptotic cell death in failing heart: relevance and proposed mechanisms," *Heart Failure Reviews*, vol. 21, no. 2, pp. 213–221, 2016.
- [2] S. Guerra, A. Leri, X. Wang et al., "Myocyte death in the failing human heart is gender dependent," *Circulation Research*, vol. 85, no. 9, pp. 856–866, 1999.
- [3] A. M. Orogó and A. B. Gustafsson, "Cell death in the myocardium: my heart won't go on," *IUBMB Life*, vol. 65, no. 8, pp. 651–656, 2013.
- [4] T. Zhang, Y. Zhang, M. Cui et al., "CaMKII is a RIP3 substrate mediating ischemia- and oxidative stress-induced myocardial necroptosis," *Nature Medicine*, vol. 22, no. 2, pp. 175–182, 2016.
- [5] A. Degtarev, W. Zhou, J. L. Maki, and J. Yuan, "Assays for necroptosis and activity of RIP kinases," *Methods in Enzymology*, vol. 545, pp. 1–33, 2014.
- [6] P. Zhu, S. Hu, Q. Jin et al., "Ripk3 promotes ER stress-induced necroptosis in cardiac IR injury: a mechanism involving calcium overload/XO/ROS/mPTP pathway," *Redox Biology*, vol. 16, pp. 157–168, 2018.
- [7] G. Kung, K. Konstantinidis, and R. N. Kitsis, "Programmed necrosis, not apoptosis, in the heart," *Circulation Research*, vol. 108, no. 8, pp. 1017–1036, 2011.
- [8] S. Y. Lim, D. J. Hausenloy, S. Arjun et al., "Mitochondrial cyclophilin-D as a potential therapeutic target for post-myocardial infarction heart failure," *Journal of Cellular and Molecular Medicine*, vol. 15, no. 11, pp. 2443–2451, 2011.
- [9] H. Zhou, D. Li, P. Zhu et al., "Inhibitory effect of melatonin on necroptosis via repressing the Ripk3-PGAM5-CypD-mPTP pathway attenuates cardiac microvascular ischemia-reperfusion injury," *Journal of Pineal Research*, vol. 65, no. 3, article e12503, 2018.
- [10] D. R. Green and G. Kroemer, "The pathophysiology of mitochondrial cell death," *Science*, vol. 305, no. 5684, pp. 626–629, 2004.
- [11] H. Zhou and S. Toan, "Pathological roles of mitochondrial oxidative stress and mitochondrial dynamics in cardiac microvascular ischemia/reperfusion injury," *Biomolecules*, vol. 10, no. 1, p. 85, 2020.
- [12] R. J. Youle and D. P. Narendra, "Mechanisms of mitophagy," *Nature Reviews. Molecular Cell Biology*, vol. 12, no. 1, pp. 9–14, 2011.
- [13] H. Zhou, S. Wang, P. Zhu, S. Hu, Y. Chen, and J. Ren, "Empagliflozin rescues diabetic myocardial microvascular injury via AMPK-mediated inhibition of mitochondrial fission," *Redox Biology*, vol. 15, pp. 335–346, 2018.
- [14] R. Li, S. Toan, and H. Zhou, "Role of mitochondrial quality control in the pathogenesis of nonalcoholic fatty liver disease," *Aging (Albany NY)*, vol. 12, no. 7, pp. 6467–6485, 2020.
- [15] S. Ito, J. Araya, Y. Kurita et al., "PARK2-mediated mitophagy is involved in regulation of HBEC senescence in COPD pathogenesis," *Autophagy*, vol. 11, no. 3, pp. 547–559, 2015.

- [16] K. Mizumura, M. J. Justice, K. S. Schweitzer et al., "Sphingolipid regulation of lung epithelial cell mitophagy and necroptosis during cigarette smoke exposure," *The FASEB Journal*, vol. 32, no. 4, pp. 1880–1890, 2018.
- [17] K. Mizumura, S. M. Cloonan, K. Nakahira et al., "Mitophagy-dependent necroptosis contributes to the pathogenesis of COPD," *The Journal of Clinical Investigation*, vol. 124, no. 9, pp. 3987–4003, 2014.
- [18] R. Q. Yao, C. Ren, Z. F. Xia, and Y. M. Yao, "Organelle-specific autophagy in inflammatory diseases: a potential therapeutic target underlying the quality control of multiple organelles," *Autophagy*, vol. 11, pp. 1–17, 2020.
- [19] H. Zhou, P. Zhu, J. Guo et al., "Ripk3 induces mitochondrial apoptosis via inhibition of FUNDC1 mitophagy in cardiac IR injury," *Redox Biology*, vol. 13, pp. 498–507, 2017.
- [20] H. Zhu, Y. Tan, W. Du et al., "Phosphoglycerate mutase 5 exacerbates cardiac ischemia-reperfusion injury through disrupting mitochondrial quality control," *Redox Biology*, vol. 38, p. 101777, 2021.
- [21] H. Zhou, P. Zhu, J. Wang, H. Zhu, J. Ren, and Y. Chen, "Pathogenesis of cardiac ischemia reperfusion injury is associated with CK2 α -disturbed mitochondrial homeostasis via suppression of FUNDC1-related mitophagy," *Cell Death and Differentiation*, vol. 25, no. 6, pp. 1080–1093, 2018.
- [22] T. M. Durcan and E. A. Fon, "The three 'P's of mitophagy: PARKIN, PINK1, and post-translational modifications," *Genes & Development*, vol. 29, no. 10, pp. 989–999, 2015.
- [23] L. Liu, K. Sakakibara, Q. Chen, and K. Okamoto, "Receptor-mediated mitophagy in yeast and mammalian systems," *Cell Research*, vol. 24, no. 7, pp. 787–795, 2014.
- [24] T. Sun, W. Ding, T. Xu et al., "Parkin regulates programmed necrosis and myocardial ischemia/reperfusion injury by targeting cyclophilin-D," *Antioxidants & Redox Signaling*, vol. 31, no. 16, pp. 1177–1193, 2019.
- [25] T. Kitada, S. Asakawa, N. Hattori et al., "Mutations in the parkin gene cause autosomal recessive juvenile parkinsonism," *Nature*, vol. 392, no. 6676, pp. 605–608, 1998.
- [26] H. Qiao, H. Ren, H. du, M. Zhang, X. Xiong, and R. Lv, "Liraglutide repairs the infarcted heart: the role of the SIRT1/Parkin/mitophagy pathway," *Molecular Medicine Reports*, vol. 17, no. 3, pp. 3722–3734, 2018.
- [27] B. P. Woodall, A. M. Orogo, R. H. Najor et al., "Parkin does not prevent accelerated cardiac aging in mitochondrial DNA mutator mice," *JCI Insight*, vol. 4, no. 10, 2019.
- [28] S. Wang, Z. Zhao, X. Feng et al., "Melatonin activates Parkin translocation and rescues the impaired mitophagy activity of diabetic cardiomyopathy through Mst1 inhibition," *Journal of Cellular and Molecular Medicine*, vol. 22, no. 10, pp. 5132–5144, 2018.
- [29] F. Li, Y. Yang, C. Xue et al., "Zinc finger protein ZBTB20 protects against cardiac remodelling post-myocardial infarction via ROS-TNF α /ASK1/JNK pathway regulation," *Journal of Cellular and Molecular Medicine*, vol. 24, no. 22, pp. 13383–13396, 2020.
- [30] H. Zhou, S. Toan, P. Zhu, J. Wang, J. Ren, and Y. Zhang, "DNA-PKcs promotes cardiac ischemia reperfusion injury through mitigating BI-1-governed mitochondrial homeostasis," *Basic Research in Cardiology*, vol. 115, no. 2, 2020.
- [31] C. Li, Q. Ma, S. Toan, J. Wang, H. Zhou, and J. Liang, "SERCA overexpression reduces reperfusion-mediated cardiac microvascular damage through inhibition of the calcium/M-CU/mPTP/necroptosis signaling pathways," *Redox Biology*, vol. 36, p. 101659, 2020.
- [32] J. Wang, P. Zhu, R. Li, J. Ren, and H. Zhou, "Fundc1-dependent mitophagy is obligatory to ischemic preconditioning-conferred renoprotection in ischemic AKI via suppression of Drp1-mediated mitochondrial fission," *Redox Biology*, vol. 30, p. 101415, 2020.
- [33] S. W. Cho, J.-S. Park, H. J. Heo et al., "Dual modulation of the mitochondrial permeability transition pore and redox signaling synergistically promotes cardiomyocyte differentiation from pluripotent stem cells," *Journal of the American Heart Association*, vol. 3, no. 2, article e000693, 2014.
- [34] A. A. Dera, M. al Fayi, H. Otifi, M. Alshyarba, M. Alfhili, and P. Rajagopalan, "Thymoquinone (Tq) protects necroptosis induced by autophagy/mitophagy-dependent oxidative stress in human bronchial epithelial cells exposed to cigarette smoke extract (CSE)," *Journal of Food Biochemistry*, vol. 44, no. 9, article e13366, 2020.
- [35] Y. Matsuzawa-Ishimoto, Y. Shono, L. E. Gomez et al., "Autophagy protein ATG16L1 prevents necroptosis in the intestinal epithelium," *The Journal of Experimental Medicine*, vol. 214, no. 12, pp. 3687–3705, 2017.
- [36] U. A. Mukherjee, S. B. Ong, S. G. Ong, and D. J. Hausenloy, "Parkinson's disease proteins: novel mitochondrial targets for cardioprotection," *Pharmacology & Therapeutics*, vol. 156, pp. 34–43, 2015.
- [37] J. Wang and H. Zhou, "Mitochondrial quality control mechanisms as molecular targets in cardiac ischemia-reperfusion injury," *Acta Pharmaceutica Sinica B*, vol. 10, no. 10, pp. 1866–1879, 2020.
- [38] M. A. Lampert, A. M. Orogo, R. H. Najor et al., "BNIP3L/NIX and FUNDC1-mediated mitophagy is required for mitochondrial network remodeling during cardiac progenitor cell differentiation," *Autophagy*, vol. 15, no. 7, pp. 1182–1198, 2019.
- [39] Y. Feng, Y. Zhang, and H. Xiao, "AMPK and cardiac remodeling," *Science China. Life Sciences*, vol. 61, no. 1, pp. 14–23, 2018.
- [40] S. B. Lee, J. J. Kim, S. A. Han et al., "The AMPK-Parkin axis negatively regulates necroptosis and tumorigenesis by inhibiting the necrosome," *Nature Cell Biology*, vol. 21, no. 8, pp. 940–951, 2019.
- [41] T. Wang, Q. Zhu, B. Cao, Y. Yuan, S. Wen, and Z. Liu, "Cadmium induces mitophagy via AMP-activated protein kinases activation in a PINK1/Parkin-dependent manner in PC12 cells," *Cell Proliferation*, vol. 53, no. 6, article e12817, 2020.

Review Article

Novel Insight into the Role of Endoplasmic Reticulum Stress in the Pathogenesis of Myocardial Ischemia-Reperfusion Injury

Hang Zhu¹ and Hao Zhou ^{1,2}

¹*Institute of Geriatric Cardiovascular Disease, Medical School of Chinese People's Liberation Army, China*

²*Center for Cardiovascular Research and Alternative Medicine, University of Wyoming College of Health Sciences, USA*

Correspondence should be addressed to Hao Zhou; zhouhao@plagh.org

Received 7 February 2021; Revised 28 February 2021; Accepted 17 March 2021; Published 28 March 2021

Academic Editor: Daniele Vergara

Copyright © 2021 Hang Zhu and Hao Zhou. This is an open access article distributed under the Creative Commons Attribution License, which permits unrestricted use, distribution, and reproduction in any medium, provided the original work is properly cited.

Impaired function of the endoplasmic reticulum (ER) is followed by evolutionarily conserved cell stress responses, which are employed by cells, including cardiomyocytes, to maintain and/or restore ER homeostasis. ER stress activates the unfolded protein response (UPR) to degrade and remove abnormal proteins from the ER lumen. Although the UPR is an intracellular defense mechanism to sustain cardiomyocyte viability and heart function, excessive activation initiates ER-dependent cardiomyocyte apoptosis. Myocardial ischemia/reperfusion (I/R) injury is a pathological process occurring during or after revascularization of ischemic myocardium. Several molecular mechanisms contribute to the pathogenesis of cardiac I/R injury. Due to the dual protective/degradative effects of ER stress on cardiomyocyte viability and function, it is of interest to understand the basic concepts, regulatory signals, and molecular processes involved in ER stress following myocardial I/R injury. In this review, therefore, we present recent findings related to the novel components of ER stress activation. The complex effects of ER stress and whether they mitigate or exacerbate myocardial I/R injury are summarized to serve as the basis for research into potential therapies for cardioprotection through control of ER homeostasis.

1. Introduction

Myocardial ischemia/reperfusion (I/R) injury occurs when myocardial tissues or cardiomyocytes are resupplied with fresh blood flow following a period of ischemia. In that situation, tissues/cells not only fail to recover from the ischemic damage but also develop additional injury caused by the reperfusion itself [1, 2]. This phenomenon is particularly prominent in the heart, liver, and brain [3–5]. Clinically, cardiac surgery and coronary artery bypass graft may cause myocardial I/R injury [6–8]. It is now generally believed that the main mechanisms of reperfusion injury are excessive formation of free radicals within the tissue and intracellular calcium overload [9–11]. Among the various biochemical mechanisms and signal pathways that may be involved [12–14], endoplasmic reticulum (ER) stress has been found to be associated with reperfusion-mediated oxidative stress and cardiomyocyte death [15, 16]. ER stress refers to a pathological process associated with hypoxia, starvation, calcium imbalance, and free radical overproduction that disrupts the

physiological functions of the ER [17, 18]. These stimuli may cause signaling from the ER to the cytoplasm and nucleus, where adaptive responses or the apoptotic program will be ultimately activated [19, 20].

Recent studies have reported a close relationship between ER stress and cardiac I/R injury [21, 22]. This suggests reducing ER stress through genetic approaches or pharmacological treatments could potentially reduce myocardial I/R injury [23–25], thereby bringing clinical benefits on many patients with cardiovascular disease. This review focuses on the current research investigating the role played by ER stress in myocardial I/R injury with the aim of identifying clinical approaches that may be applied to reduce cardiac I/R injury in the future.

2. Overview of Myocardial I/R Injury

Nutrients are supplied to tissues and metabolic waste carried away by the circulation. Insufficient blood flow to a tissue, such as the myocardium, results in ischemia [26, 27], which

can lead to cell death and tissue damage. Myocardial ischemia is usually caused by occlusion of one or more coronary arteries, which is followed by a decline in oxygen tension within the myocardium [2, 28, 29]. Myocardial ischemia severely hinders oxidative metabolism of fatty acids, glucose, pyruvate, and lactic acid, which causes energetic stress within cardiomyocytes [30, 31]. It also slows or even stops mitochondrial respiration [32, 33], diminishing oxidative phosphorylation and ATP production. In the absence of sufficient oxygen, ATP production through glycolysis is enhanced, which leads to overproduction of lactic acid [34, 35] and, in turn, intracellular acidosis. In addition, ischemia interrupts β -oxidation of fatty acids and thus promotes accumulation of incomplete fatty acid metabolites in the cytoplasm [36, 37]. The most important change within the ischemic myocardium is the reduced generation of high-energy phosphoric compounds (e.g., ATP) and cardiomyocyte death due to ATP deficiency [38, 39]. As a result of the ATP undersupply, the calcium pump within cardiomyocytes cannot effectively remove calcium from the cytoplasm, resulting into calcium overload [40, 41]. The resultant abnormal calcium signal blunts ventricular contraction and promotes the development of cardiac dysfunction [42–44].

From the perspective of treatment, timely restoration of blood flow to the myocardium is an effective way to relieve tissue ischemia and insufficient nutrient supply [45, 46]. Interestingly, however, reperfusion of ischemic tissue can cause additional damage due to I/R injury [47, 48]. This concept was first proposed in 1955 by Sewell et al., based on observations made in dogs after coronary artery ligation [49]. They reported that removing the coronary ligation, and thus restoring of myocardial perfusion, induced ventricular fibrillation and death [50, 51]. This concept was further validated in 1960 by Jennings et al. [52], who reported that when tissue or cells regain a blood supply after transient ischemia, they undergo I/R injury. It was also shown that myocardial ischemia and subsequent reperfusion injury are independent but interrelated pathophysiological processes [53, 54]. Consequently, the prevention and treatment of reperfusion injury should start during the ischemic period, and the ischemia must be removed as soon as possible [55, 56]. The shorter the duration of ischemia, the smaller are the ischemic changes and the possibility of injury after reperfusion [57, 58]. At present, there is no particularly effective way to cope with myocardial I/R injury [59–61]. Several studies have been conducted to understand the molecular mechanisms underlying myocardial I/R injury. Oxidative stress, microvascular damage, inflammatory responses, autophagy inhibition, immune disorders, platelet activation, cardiomyocyte metabolic disturbance, ER stress, and mitochondrial dysfunction are all reported to be potential pathological factors contributing to the development of cardiac I/R injury [62–66].

3. Molecular Basis of ER Stress

3.1. Overview of the ER. The ER is a membranous tubular organelle within eukaryotic cells [67]. It is found in two

forms: rough and smooth [68]. Rough ER localizes with ribosomes and is mainly responsible for protein folding and post-translational modification [69, 70]. Smooth ER, on the other hand, functions to maintain lipid biosynthesis and calcium storage [71]. ER stress is a state in which an external stimulus disrupts ER homeostasis and triggers the accumulation of unfolded or misfolded proteins within the ER lumen [72]. Calcium overload and abnormal lipid metabolism, due to ER dysregulation, will further promote ER stress [73]. The stimuli thought to cause ER stress include nutritional deficiency, hypoxia, ischemia, oxidative stress, and DNA damage [74–76]. When ER stress occurs, the cell reduces protein synthesis and promotes degradation of misfolded proteins [77]. However, under continuous strong stimulation, excessive ER stress is associated with cell apoptosis [78].

3.2. Activation of ER Stress. ER stress in mammals has four components: inhibition of protein translation, upregulation of molecular chaperones, activation of the protein degradative program, and induction of apoptosis [79]. ER stress signal transduction is mediated via three crucial enzymes (Figure 1) [80]: protein kinase R-link ER kinase (PERK), activating transcription factor-6 (ATF-6), and inositol-requiring enzyme-1 (IRE1). ER molecular chaperones acting as sensors of ER homeostasis play a key role in monitoring the accumulation of unfolded proteins within the ER [81]. Under physiological conditions, GRP78 (also known as binding immunoglobulin protein; BiP) binds to PERK, ATF-6, and IRE1 [82] within the ER. However, GRP78 has greater affinity for unfolded proteins; consequently, when ER homeostasis is disrupted, leading to accumulation of unfolded proteins within the ER, GRP78 dissociates from PERK, ATF-6, and IRE1, which results in the activation of ER stress signaling transduction pathways [83].

3.3. The Transduction Pathways of ER Stress

3.3.1. PERK Pathway. PERK is a transmembrane protein in the ER membrane [84]. After dissociation of GRP78, it forms a homodimer and is then activated by autophosphorylation. Phosphorylated PERK catalyzes the phosphorylation of eukaryotic initiation factor-2 α (eIF2 α) [85], which inactivates eIF2 α -mediated translation. This effect significantly represses the transcription of most mRNA and, in turn, protein synthesis, which reduces the protein load on the ER [86]. Interestingly, eIF2 α phosphorylation is associated with an increase in the transcription of activating transcription factor-4 (ATF-4), which, after translation, translocates the cell nucleus and functions to upregulate ER molecular chaperones [87]. However, if ER homeostasis cannot be restored, the continuous overexpression of ATF-4 will promote the upregulation of C/EBP homologous protein (CHOP), a potential proapoptotic protein regulating cell death [88].

3.3.2. ATF-6 Pathway. Like PERK, ATF-6 is an ER transmembrane protein [89]. After dissociation of GRP78, ATF-6 translocates to the Golgi apparatus where it is cleaved and activated by the proteases Sit-1/2. The activated ATF-6 migrates into the nucleus where it forms homodimers or

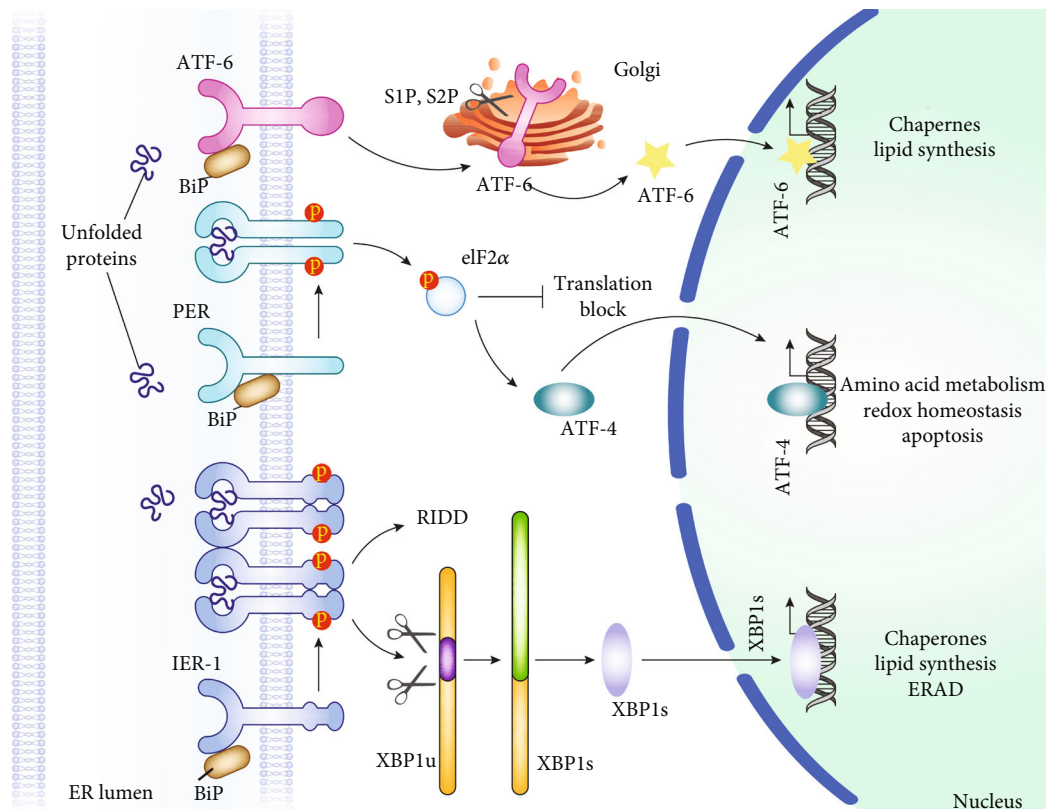


FIGURE 1: The regulatory mechanisms of endoplasmic reticulum (ER) stress. ER stress in mammals has four components: inhibition of protein translation, upregulation of molecular chaperones, activation of the protein degradative program, and induction of apoptosis [79]. ER stress signal transduction is mediated via three crucial enzymes [80]: protein kinase R-link ER kinase (PERK), activating transcription factor-6 (ATF-6), and inositol-requiring enzyme-1 (IRE1). ER molecular chaperones acting as sensors of ER homeostasis play a key role in monitoring the accumulation of unfolded proteins within the ER.

heterodimers with other transcription factors, leading to the upregulation of ER chaperone genes [90].

3.3.3. IRE1 Pathway. Upon dissociation of GRP78, the ER transmembrane protein IRE1 forms a homodimer and undergoes autophosphorylation activation [91]. Activated IRE1 has endoribonuclease activity [92], which can cut the mRNA encoding XBP1 (x-box binding protein-1) to form a new transcript encoding a second XBP1 isoform [93]. When abundant, the translated XBP1 protein migrates into the nucleus, where it upregulates the expression of genes related to ER stress [94]. Long-term activation of the IRE1 is associated with apoptosis activated via the TRAF2/ASK1/JNK pathway.

3.4. Unfolded Protein Response. After synthesis on the ribosomes, proteins must be folded and packaged correctly within the ER. Protein folding is carried out under redox conditions and requires two ER stress reactive proteins [95]: ER stress oxidoreductase (ERO) and disulfide proteolytic enzyme. After dissociation of GRP78 and their autoactivation (as described above), IRE1, ATF-6, and PERK respond to the presence of incorrectly folded proteins associated with ER stress [96, 97]. This is called the “unfolded protein response” (UPR) [98]. A key function of the ER is identification, control, and correction of protein quality. Proteins that

cannot be folded correctly will be transferred from ER to the cytoplasm for degradation by the 26S proteasome [99]. The early stage of the UPR is the activation of proteasome-induced degradation of unfolded proteins and the upregulation of XBP1 and ATF-4 [100]. These alterations are aimed at reducing the load of unfolded or misfolded proteins within ER. Later, an inflammatory response is activated via NF- κ B and JNK [101], which enhances defensive responses within the cytoplasm. If these responses are unable to restore ER function or cell homeostasis, the cell apoptosis program will be activated as the final stage of the UPR.

4. Role of ER Stress in Myocardial I/R Injury

4.1. ER Stress and Calcium Overload. Myocardial contraction relies on the oscillation of cytoplasmic free calcium concentration. Within cardiomyocytes, smooth ER (termed sarcoplasmic reticulum; SR) contains the primary calcium store. Excessive calcium release from SR into the cytoplasm leads to intracellular calcium overload, which is closely associated with cardiomyocyte contraction dysfunction and cell death [102–104]. ER dysfunction-mediated calcium overload plays an important role in myocardial I/R injury. During reperfusion, the function of the sodium-calcium exchanger and L-type calcium channels is impaired as a result of the insufficient oxygen supply during the ischemia [105]. By

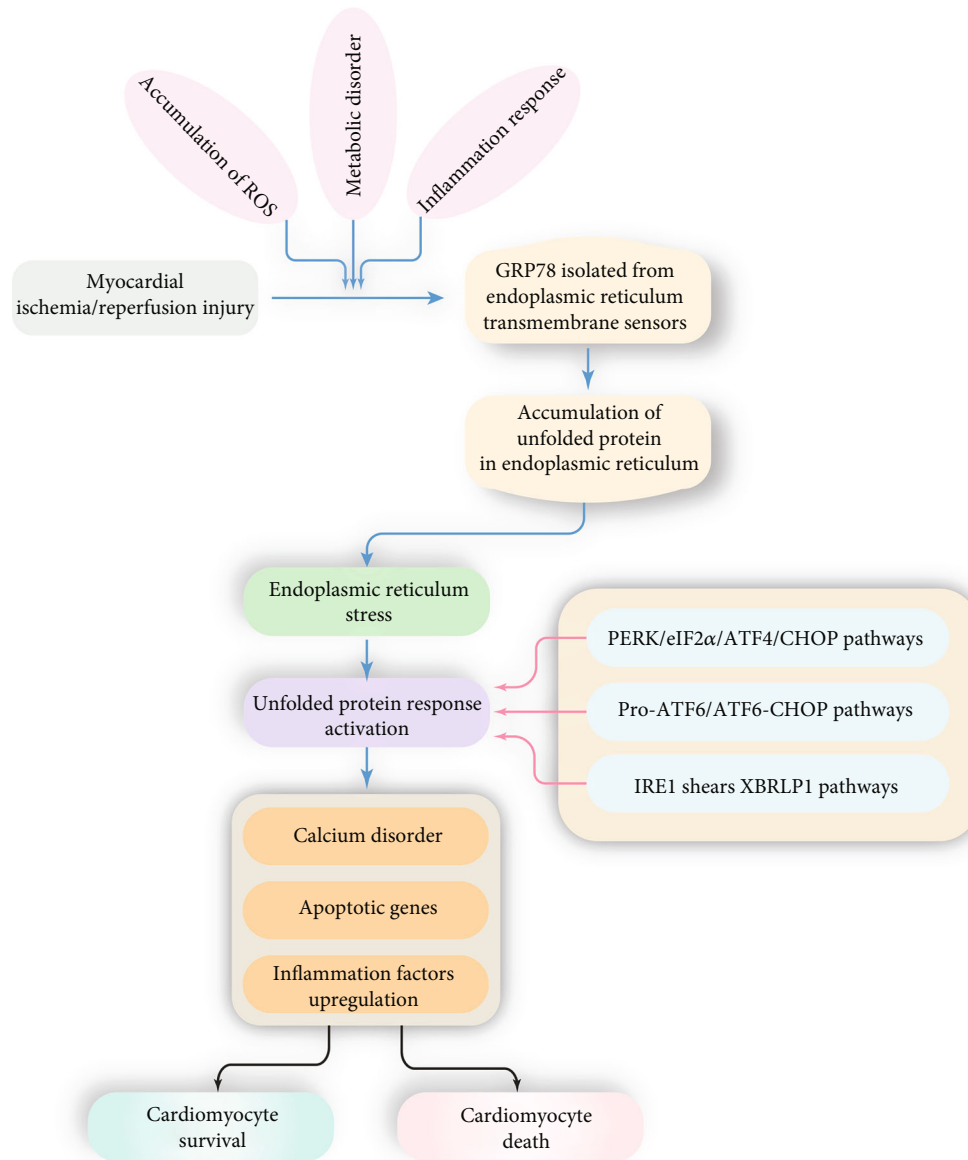


FIGURE 2: Role of endoplasmic reticulum (ER) stress in myocardial ischemia/reperfusion injury. ER stress is activated by accumulation of ROS, metabolic disorder, or inflammation response, which is featured by GRP78 isolation from ER. Then, unfolded protein accumulation in ER will activate the unfolded protein response (UPR) which is followed by calcium disorder, apoptotic gene upregulation, and inflammation response, resulting into cardiomyocyte death or survival dependent on the extent of ER stress.

contrast, the expression of calcium-sensitive receptors, such as 1,4,5-inositol trisphosphate receptor (IP3R), is significantly increased due to hypoxic stress or upregulation of hypoxia-inducible factor-1 (HIF1) [106]. These effects enhance calcium release from SR into the cytoplasm under conditions where physiological extrusion of calcium from the cell is suppressed. Thus, ER stress is an upstream trigger of cardiomyocyte calcium overload.

4.2. ER Stress and Cardiomyocyte Apoptosis. Once UPR fails to control the level of unfolded or misfolded proteins, ER stress will trigger the activation of apoptotic signaling. It is currently believed that ER stress can cause cardiomyocyte apoptosis via three pathways (Figure 2).

4.2.1. CHOP Pathway. CHOP is a transcription factor belonging to the C/EBP family. Under normal circumstances, CHOP expression is very low. The transcription and translation of CHOP are primarily regulated by IRE1 α , ATF-6, and PERK [107, 108], and CHOP plays a key role in ER-induced apoptosis, such as that induced by I/R injury [109]. Upregulation of CHOP induces the expression of a variety of downstream proapoptotic and antiapoptotic genes, including Bcl-2, Bax, Bim, growth arrest and DNA damage-inducible protein 34 (GADD34), ER oxidoreductase-1 α (ERO1 α), and the death receptor 5 (DR5) [110]. Among those, GADD34 promotes the expression of protein phosphatase-1 (PP1), which in turn augments transcription of genes related to UPR [111]; ERO1 α triggers calcium leakage from

the ER through IP3Rs, which leads to calcium overload-dependent cell apoptosis [112, 113]; and DR5 triggers apoptosis through activation of caspase-8 [114].

4.2.2. IRE1 α /JNK Pathway. IRE1 α is a component of the most conserved pathway in mammalian UPR [115]. It has two active enzyme domains: a serine/threonine kinase domain and an endoribonuclease (RNase) domain. When ER stress is induced, unfolded or misfolded proteins in the ER lumen directly bind to and activate IRE1 α . Once activated, IRE1 α recruits tumor necrosis factor receptor-related factor-2 (TRAF2) and apoptotic-signaling kinase-1 (ASK1) [116], after which JNK is phosphorylated by the resultant IRE1 α -TRAF2-ASK1 signaling complex [117, 118]. Following cardiac I/R injury, activated JNK may promote cardiomyocyte apoptosis through phosphorylation of various members of the Bcl-2 family [119, 120]. For example, JNK catalyzes phosphorylation of the antiapoptotic protein Bcl-2, which impairs its activity. At the same time JNK catalyzed, phosphorylation enhances the proapoptotic activity of Bim [121]. These alterations work together to mediate apoptosis in cardiomyocytes.

4.2.3. The Caspase-12 Pathway. The caspase-12 pathway is considered to be an ER-specific, nonmitochondrial-dependent apoptotic pathway [122]. Caspase-12 activation is also a feature of ER stress-mediated cardiomyocyte apoptosis [123]. Under normal circumstances, caspase-12 binds to the ER membrane and forms a complex with TRAF2. ER stress directly induces caspase-12 dissociation from the ER membrane, enabling it to be activated by calpain [124, 125] or the IRE1 α -TRAF2 complex [126]. Once activated, caspase-12 cleaves and activates caspase-9, which in turn cleaves and activates caspase-3 to promote apoptosis [127].

5. Summary and Outlook

ER stress arises via multiple signaling pathways, expression of multiple genes, and participation of multiple stress factors. In cases of mild or early myocardial injury, ER stress involves a variety of protective proteins, which reduce the pathological stress on cardiomyocytes. However, excessive ER stress is associated with protein quality control disorder, resulting in the upregulation of apoptotic proteins. Notably, the role of ER stress during ischemia differs from that during reperfusion. It remains unclear whether ER stress is protective in the ischemic heart and only becomes lethal following reperfusion. In addition, although the molecular mechanisms underlying ER stress and its role in I/R injury have been characterized, the interactive effects of ER stress and other pathological alterations that occur during cardiac I/R injury, such as oxidative stress and mitochondrial dysfunction, are still not fully understood. Moreover, there are still no specific drugs targeting ER stress available in clinical practice. Additional investigations are therefore required to help us better understand the role of ER stress in myocardial I/R injury.

Data Availability

All data generated or analyzed during this study are included in this published article.

Conflicts of Interest

All the authors declare that they have no conflicts of interest.

References

- [1] G. Heusch, "Coronary microvascular obstruction: the new frontier in cardioprotection," *Basic Research in Cardiology*, vol. 114, no. 6, p. 45, 2019.
- [2] J. Wang and H. Zhou, "Mitochondrial quality control mechanisms as molecular targets in cardiac ischemia ** - ** reperfusion injury," *Acta Pharmaceutica Sinica B*, vol. 10, no. 10, pp. 1866–1879, 2020.
- [3] J. Oliva, "Proteasome and organs ischemia-reperfusion injury," *International Journal of Molecular Sciences*, vol. 19, no. 1, p. 106, 2018.
- [4] H. Zhou, J. Wang, P. Zhu et al., "NR4A1 aggravates the cardiac microvascular ischemia reperfusion injury through suppressing FUNDC1-mediated mitophagy and promoting Mff-required mitochondrial fission by CK2 α ," *Basic Research in Cardiology*, vol. 113, no. 4, p. 23, 2018.
- [5] J. Wang, P. Zhu, S. Toan, R. Li, J. Ren, and H. Zhou, "Pum2-Mff axis fine-tunes mitochondrial quality control in acute ischemic kidney injury," *Cell Biology and Toxicology*, vol. 36, no. 4, pp. 365–378, 2020.
- [6] M. Aghaei, M. Motallebnezhad, S. Ghorghanlu et al., "Targeting autophagy in cardiac ischemia/reperfusion injury: a novel therapeutic strategy," *Journal of Cellular Physiology*, vol. 234, no. 10, pp. 16768–16778, 2019.
- [7] Z. J. Mao, H. Lin, F. Y. Xiao, Z. Q. Huang, and Y. H. Chen, "Melatonin against myocardial ischemia-reperfusion injury: a meta-analysis and mechanism insight from animal studies," *Oxidative Medicine and Cellular Longevity*, vol. 2020, Article ID 1241065, 11 pages, 2020.
- [8] T. Carbonell and A. V. Gomes, "MicroRNAs in the regulation of cellular redox status and its implications in myocardial ischemia-reperfusion injury," *Redox Biology*, vol. 36, article 101607, 2020.
- [9] N. B. Liu, M. Wu, C. Chen et al., "Novel molecular targets participating in myocardial ischemia-reperfusion injury and cardioprotection," *Cardiology Research and Practice*, vol. 2019, Article ID 6935147, 16 pages, 2019.
- [10] K. Boengler, J. Bornbaum, K. D. Schlüter, and R. Schulz, "P66shc and its role in ischemic cardiovascular diseases," *Basic Research in Cardiology*, vol. 114, no. 4, p. 29, 2019.
- [11] S. An, X. Wang, H. Shi et al., "Apelin protects against ischemia-reperfusion injury in diabetic myocardium via inhibiting apoptosis and oxidative stress through PI3K and p38-MAPK signaling pathways," *Aging (Albany NY)*, vol. 12, no. 24, pp. 25120–25137, 2020.
- [12] E. Chen, C. Chen, Z. Niu et al., "Poly(I:C) preconditioning protects the heart against myocardial ischemia/reperfusion injury through TLR3/PI3K/Akt-dependent pathway," *Signal Transduction and Targeted Therapy*, vol. 5, no. 1, p. 216, 2020.
- [13] L. Zhang, S. Cai, S. Cao et al., "Diazoxide protects against myocardial ischemia/reperfusion injury by moderating ERs

- via regulation of the miR-10a/IRE1 pathway," *Oxidative Medicine and Cellular Longevity*, vol. 2020, Article ID 4957238, 16 pages, 2020.
- [14] Y. Tan, D. Mui, S. Toan, P. Zhu, R. Li, and H. Zhou, "SERCA overexpression improves mitochondrial quality control and attenuates cardiac microvascular ischemia-reperfusion injury," *Mol Ther Nucleic Acids*, vol. 22, pp. 696–707, 2020.
- [15] D. Han, Y. Wang, J. Chen et al., "Activation of melatonin receptor 2 but not melatonin receptor 1 mediates melatonin-conferred cardioprotection against myocardial ischemia/reperfusion injury," *Journal of Pineal Research*, vol. 67, article e12571, 2019.
- [16] L. M. Yu, X. Dong, J. Zhang et al., "Naringenin attenuates myocardial ischemia-reperfusion injury via cGMP-PKG α signaling and in vivo and in vitro studies," *Oxidative Medicine and Cellular Longevity*, vol. 2019, Article ID 7670854, 15 pages, 2019.
- [17] J. Sandoval, D. J. Orlicky, A. Allawzi et al., "Toxic acetaminophen exposure induces distal lung ER stress, proinflammatory signaling, and emphysematous changes in the adult murine lung," *Oxidative Medicine and Cellular Longevity*, vol. 2019, Article ID 7595126, 15 pages, 2019.
- [18] Z. W. Chen, C. Y. Huang, J. F. Cheng, S. Y. Chen, L. Y. Lin, and C. K. Wu, "Stress echocardiography-derived E/e' predicts abnormal exercise hemodynamics in heart failure with preserved ejection fraction," *Frontiers in Physiology*, vol. 10, p. 1470, 2019.
- [19] O. Moltedo, P. Remondelli, and G. Amodio, "The mitochondria-endoplasmic reticulum contacts and their critical role in aging and age-associated diseases," *Frontiers in Cell and Development Biology*, vol. 7, p. 172, 2019.
- [20] J. Zhong, Y. Tan, J. Lu et al., "Therapeutic contribution of melatonin to the treatment of septic cardiomyopathy: a novel mechanism linking Ripk3-modified mitochondrial performance and endoplasmic reticulum function," *Redox Biology*, vol. 26, p. 101287, 2019.
- [21] X. Zhang, C. S. Gibhardt, T. Will et al., "Redox signals at the ER-mitochondria interface control melanoma progression," *The EMBO Journal*, vol. 38, no. 15, article e100871, 2019.
- [22] R. C. Yue, S. Z. Lu, Y. Luo et al., "Calpain silencing alleviates myocardial ischemia-reperfusion injury through the NLRP3/ASC/Caspase-1 axis in mice," *Life Sciences*, vol. 233, p. 116631, 2019.
- [23] S. Wang, W. Bian, J. Zhen, L. Zhao, and W. Chen, "Melatonin-mediated Pak2 activation reduces cardiomyocyte death through suppressing hypoxia reoxygenation injury-induced endoplasmic reticulum stress," *Journal of Cardiovascular Pharmacology*, vol. 74, no. 1, pp. 20–29, 2019.
- [24] D. Shen, R. Chen, L. Zhang et al., "Sulodexide attenuates endoplasmic reticulum stress induced by myocardial ischemia/reperfusion by activating the PI3K/Akt pathway," *Journal of Cellular and Molecular Medicine*, vol. 23, no. 8, pp. 5063–5075, 2019.
- [25] G. Zhang, X. Wang, T. G. Gillette, Y. Deng, and Z. V. Wang, "Unfolded protein response as a therapeutic target in cardiovascular disease," *Current Topics in Medicinal Chemistry*, vol. 19, no. 21, pp. 1902–1917, 2019.
- [26] J. Wang, S. Toan, and H. Zhou, "Mitochondrial quality control in cardiac microvascular ischemia-reperfusion injury: new insights into the mechanisms and therapeutic potentials," *Pharmacological Research*, vol. 156, p. 104771, 2020.
- [27] J. Wang, S. Toan, and H. Zhou, "New insights into the role of mitochondria in cardiac microvascular ischemia/reperfusion injury," *Angiogenesis*, vol. 23, no. 3, pp. 299–314, 2020.
- [28] J. Wang, P. Zhu, R. Li, J. Ren, Y. Zhang, and H. Zhou, "Bax inhibitor 1 preserves mitochondrial homeostasis in acute kidney injury through promoting mitochondrial retention of PHB2," *Theranostics*, vol. 10, no. 1, pp. 384–397, 2020.
- [29] H. Zhou, P. Zhu, J. Wang, H. Zhu, J. Ren, and Y. Chen, "Pathogenesis of cardiac ischemia reperfusion injury is associated with CK2 α -disturbed mitochondrial homeostasis via suppression of FUNDC1-related mitophagy," *Cell Death and Differentiation*, vol. 25, no. 6, pp. 1080–1093, 2018.
- [30] W. E. Hughes, A. M. Beyer, and D. D. Gutterman, "Vascular autophagy in health and disease," *Basic Research in Cardiology*, vol. 115, no. 4, p. 41, 2020.
- [31] P. Kleinbongard, "Cardioprotection by early metoprolol-attenuation of ischemic vs. reperfusion injury?," *Basic Research in Cardiology*, vol. 115, no. 5, p. 54, 2020.
- [32] X. Yang, N. An, C. Zhong et al., "Enhanced cardiomyocyte reactive oxygen species signaling promotes ibuprofen-induced atrial fibrillation," *Redox Biology*, vol. 30, article 101432, 2020.
- [33] M. Matzinger, K. Fischhuber, D. Pölöske, K. Mechtler, and E. H. Heiss, "AMPK leads to phosphorylation of the transcription factor Nrf2, tuning transactivation of selected target genes," *Redox Biology*, vol. 29, p. 101393, 2020.
- [34] M. Manevski, T. Muthumalage, D. Devadoss et al., "Cellular stress responses and dysfunctional mitochondrial-cellular senescence, and therapeutics in chronic respiratory diseases," *Redox Biology*, vol. 33, p. 101443, 2020.
- [35] F. Cao, M. L. Maguire, D. J. McAndrew et al., "Overexpression of mitochondrial creatine kinase preserves cardiac energetics without ameliorating murine chronic heart failure," *Basic Research in Cardiology*, vol. 115, no. 2, p. 12, 2020.
- [36] H. Li and N. Xia, "The role of oxidative stress in cardiovascular disease caused by social isolation and loneliness," *Redox Biology*, vol. 37, article 101585, 2020.
- [37] H. Jiang, D. Jia, B. Zhang et al., "Exercise improves cardiac function and glucose metabolism in mice with experimental myocardial infarction through inhibiting HDAC4 and upregulating GLUT1 expression," *Basic Research in Cardiology*, vol. 115, no. 3, p. 28, 2020.
- [38] A. J. Causer, J. K. Shute, M. H. Cummings et al., "Circulating biomarkers of antioxidant status and oxidative stress in people with cystic fibrosis: a systematic review and meta-analysis," *Redox Biology*, vol. 32, p. 101436, 2020.
- [39] A. R. Ednie and E. S. Bennett, "Intracellular O-linked glycosylation directly regulates cardiomyocyte L-type Ca²⁺ channel activity and excitation-contraction coupling," *Basic Research in Cardiology*, vol. 115, no. 6, p. 59, 2020.
- [40] Y. Zhang, H. Zhou, W. Wu et al., "Liraglutide protects cardiac microvascular endothelial cells against hypoxia/reoxygenation injury through the suppression of the SR-Ca²⁺-XO-ROS axis via activation of the GLP-1R/PI3K/Akt/survivin pathways," *Free Radical Biology & Medicine*, vol. 95, pp. 278–292, 2016.
- [41] F. E. Mason, J. R. D. Pronto, K. Alhussini, C. Maack, and N. Voigt, "Cellular and mitochondrial mechanisms of atrial fibrillation," *Basic Research in Cardiology*, vol. 115, no. 6, p. 72, 2020.

- [42] H. Zhou, J. Wang, P. Zhu, S. Hu, and J. Ren, "Ripk3 regulates cardiac microvascular reperfusion injury: The role of IP3R-dependent calcium overload, XO-mediated oxidative stress and F-actin/filopodia-based cellular migration," *Cellular Signalling*, vol. 45, pp. 12–22, 2018.
- [43] K. Éva Sikura, Z. Combi, L. Potor et al., "Hydrogen sulfide inhibits aortic valve calcification in heart via regulating RUNX2 by NF- κ B, a link between inflammation and mineralization," *Journal of Advanced Research*, vol. 27, pp. 165–176, 2021.
- [44] M. Dia, L. Gomez, H. Thibault et al., "Reduced reticulum-mitochondria Ca²⁺ transfer is an early and reversible trigger of mitochondrial dysfunctions in diabetic cardiomyopathy," *Basic Research in Cardiology*, vol. 115, no. 6, p. 74, 2020.
- [45] R. K. Adapala, A. K. Kanugula, S. Paruchuri, W. M. Chilian, and C. K. Thodeti, "TRPV4 deletion protects heart from myocardial infarction-induced adverse remodeling via modulation of cardiac fibroblast differentiation," *Basic Research in Cardiology*, vol. 115, no. 2, p. 14, 2020.
- [46] C. Maldonado, M. D. Nguyen, P. Bauer et al., "Rapid lipid modification of endothelial cell membranes in cardiac ischemia/reperfusion injury: a novel therapeutic strategy to reduce infarct size," *Cardiovascular Drugs and Therapy*, vol. 35, no. 1, pp. 113–123, 2021.
- [47] Y. J. Zhang, M. Zhang, X. Zhao et al., "NAD(+) administration decreases microvascular damage following cardiac ischemia/reperfusion by restoring autophagic flux," *Basic Research in Cardiology*, vol. 115, no. 5, p. 57, 2020.
- [48] M. V. Basalay, D. M. Yellon, and S. M. Davidson, "Targeting myocardial ischaemic injury in the absence of reperfusion," *Basic Research in Cardiology*, vol. 115, no. 6, p. 63, 2020.
- [49] W. H. Sewell, D. R. Koth, and C. E. Huggins, "Ventricular fibrillation in dogs after sudden return of flow to the coronary artery," *Surgery*, vol. 38, no. 6, pp. 1050–1053, 1955.
- [50] M. Kohlhauer, V. R. Pell, N. Burger et al., "Protection against cardiac ischemia-reperfusion injury by hypothermia and by inhibition of succinate accumulation and oxidation is additive," *Basic Research in Cardiology*, vol. 114, no. 3, p. 18, 2019.
- [51] L. A. Bienvenu, A. Maluenda, J. D. McFadyen et al., "Combined antiplatelet/anticoagulant drug for cardiac ischemia/reperfusion injury," *Circulation Research*, vol. 127, no. 9, pp. 1211–1213, 2020.
- [52] R. B. Jennings, H. M. Sommers, G. A. Smyth, H. A. Flack, and H. Linn, "Myocardial necrosis induced by temporary occlusion of a coronary artery in the dog," *Archives of Pathology*, vol. 70, pp. 68–78, 1960.
- [53] Y. Guo, Y. Nong, D. N. Tukaye et al., "Inducible cardiac-specific overexpression of cyclooxygenase-2 (COX-2) confers resistance to ischemia/reperfusion injury," *Basic Research in Cardiology*, vol. 114, no. 5, p. 32, 2019.
- [54] Y. Li, P. Liang, B. Jiang et al., "CARD9 promotes autophagy in cardiomyocytes in myocardial ischemia/reperfusion injury via interacting with Rybicon directly," *Basic Research in Cardiology*, vol. 115, no. 3, p. 29, 2020.
- [55] X. M. Gao, Y. Su, S. Moore et al., "Relaxin mitigates microvascular damage and inflammation following cardiac ischemia-reperfusion," *Basic Research in Cardiology*, vol. 114, no. 4, p. 30, 2019.
- [56] Y. Sawashita, N. Hirata, Y. Yoshikawa, H. Terada, Y. Tokinaga, and M. Yamakage, "Remote ischemic preconditioning reduces myocardial ischemia-reperfusion injury through unacylated ghrelin-induced activation of the JAK/STAT pathway," *Basic Research in Cardiology*, vol. 115, no. 4, p. 50, 2020.
- [57] S. Lahnwong, S. Palee, N. Apajai et al., "Acute dapagliflozin administration exerts cardioprotective effects in rats with cardiac ischemia/reperfusion injury," *Cardiovascular Diabetology*, vol. 19, no. 1, p. 91, 2020.
- [58] M. Lobo-Gonzalez, C. Galán-Arriola, X. Rossello et al., "Metoprolol blunts the time-dependent progression of infarct size," *Basic Research in Cardiology*, vol. 115, no. 5, p. 55, 2020.
- [59] Z. He, S. Davidson, and D. Yellon, "The importance of clinically relevant background therapy in cardioprotective studies," *Basic Research in Cardiology*, vol. 115, no. 6, p. 69, 2020.
- [60] A. Clementi, G. M. Virzi, A. Brocca et al., "Advances in the pathogenesis of cardiorenal syndrome type 3," *Oxidative Medicine and Cellular Longevity*, vol. 2015, Article ID 148082, 8 pages, 2015.
- [61] H. Bøtker, "The changing face after acute myocardial infarction," *Basic Research in Cardiology*, vol. 115, p. 5, 2020.
- [62] B. Chan, A. Roczowski, W. J. Cho et al., "Junctophilin-2 is a target of matrix metalloproteinase-2 in myocardial ischemia-reperfusion injury," *Basic Research in Cardiology*, vol. 114, no. 6, p. 42, 2019.
- [63] Y. Yang, G. Yang, L. Yu et al., "An interplay between MRTFA and the histone acetyltransferase TIP60 mediates hypoxia-reoxygenation induced iNOS transcription in macrophages," *Frontiers in Cell and Development Biology*, vol. 8, p. 484, 2020.
- [64] M. Wallert, M. Ziegler, X. Wang et al., " α -Tocopherol preserves cardiac function by reducing oxidative stress and inflammation in ischemia/reperfusion injury," *Redox O Biologica*, vol. 26, article 101292, 2019.
- [65] C. Xiao, M. L. Xia, J. Wang et al., "Luteolin attenuates cardiac ischemia/reperfusion injury in diabetic rats by modulating Nrf2 antioxidative function," *Oxidative Medicine and Cellular Longevity*, vol. 2019, Article ID 2719252, 9 pages, 2019.
- [66] T. Alakoski, J. Ulvila, R. Yrjölä et al., "Inhibition of cardiomyocyte Sprouty1 protects from cardiac ischemia-reperfusion injury," *Basic Research in Cardiology*, vol. 114, no. 2, p. 7, 2019.
- [67] E. Bovo, R. Nikolaienko, S. Bhayani et al., "Novel approach for quantification of endoplasmic reticulum Ca(2+) transport," *American Journal of Physiology. Heart and Circulatory Physiology*, vol. 316, no. 6, pp. H1323–h1331, 2019.
- [68] Y. Ji, Y. Ge, X. Xu et al., "Vildagliptin reduces stenosis of injured carotid artery in diabetic mouse through inhibiting vascular smooth muscle cell proliferation via ER stress/NF- κ B pathway," *Frontiers in Pharmacology*, vol. 10, p. 142, 2019.
- [69] J. Lin, P. Walter, and T. Yen, "Endoplasmic reticulum stress in disease pathogenesis," *Annual Review of Pathology*, vol. 3, no. 1, pp. 399–425, 2008.
- [70] C. Xu, B. Bailly-Maitre, and J. Reed, "Endoplasmic reticulum stress: cell life and death decisions," *The Journal of Clinical Investigation*, vol. 115, no. 10, pp. 2656–2664, 2005.
- [71] C. Adams, M. Kopp, N. Larburu, P. Nowak, and M. Ali, "Structure and molecular mechanism of ER stress signaling by the unfolded protein response signal activator IRE1," *Frontiers in Molecular Biosciences*, vol. 6, p. 11, 2019.
- [72] H. Zhu, Q. Jin, Y. Li et al., "Melatonin protected cardiac microvascular endothelial cells against oxidative stress injury via suppression of IP3R-[Ca(2+)]c/VDAC-[Ca(2+)]m axis by activation of MAPK/ERK signaling pathway," *Cell Stress & Chaperones*, vol. 23, no. 1, pp. 101–113, 2018.

- [73] C. Costa, W. Manaa, E. Duplan, and F. Checler, "The endoplasmic reticulum stress/unfolded protein response and their contributions to Parkinson's disease pathophysiology," *Cells*, vol. 9, no. 11, p. 2495, 2020.
- [74] K. Meyerovich, F. Ortis, F. Allagnat, and A. Cardozo, "Endoplasmic reticulum stress and the unfolded protein response in pancreatic islet inflammation," *Journal of Molecular Endocrinology*, vol. 57, no. 1, pp. R1–R17, 2016.
- [75] M. Kitamura, "Endoplasmic reticulum stress and unfolded protein response in renal pathophysiology: Janus faces," *American Journal of Physiology. Renal Physiology*, vol. 295, no. 2, pp. F323–F334, 2008.
- [76] K. Bhattarai, M. Chaudhary, H. Kim, and H. Chae, "Endoplasmic reticulum (ER) stress response failure in diseases," *Trends in Cell Biology*, vol. 30, no. 9, pp. 672–675, 2020.
- [77] H. Hemingway, A. Moore, A. Olivencia-Yurvati, and S. Romero, "Effect of endoplasmic reticulum stress on endothelial ischemia-reperfusion injury in humans," *American journal of physiology. Regulatory, integrative and comparative physiology*, vol. 319, no. 6, pp. R666–R672, 2020.
- [78] J. Ayyappan, K. Lizardo, S. Wang, E. Yurkow, and J. Nagajothi, "Inhibition of SREBP improves cardiac lipidopathy, improves endoplasmic reticulum stress, and modulates chronic Chagas cardiomyopathy," *Journal of the American Heart Association*, vol. 9, no. 3, article e014255, 2020.
- [79] J. Hong, K. Kim, J. H. Kim, and Y. Park, "The role of endoplasmic reticulum stress in cardiovascular disease and exercise," *International Journal of Vascular Medicine*, vol. 2017, 9 pages, 2017.
- [80] S. Wang, P. Binder, Q. Fang et al., "Endoplasmic reticulum stress in the heart: insights into mechanisms and drug targets," *British Journal of Pharmacology*, vol. 175, no. 8, pp. 1293–1304, 2018.
- [81] M. L. Battson, D. M. Lee, and C. L. Gentile, "Endoplasmic reticulum stress and the development of endothelial dysfunction," *American Journal of Physiology. Heart and Circulatory Physiology*, vol. 312, no. 3, pp. H355–h367, 2017.
- [82] A. Cimellaro, M. Perticone, T. V. Fiorentino, A. Sciacqua, and M. L. Hribal, "Role of endoplasmic reticulum stress in endothelial dysfunction," *Nutrition, Metabolism, and Cardiovascular Diseases*, vol. 26, no. 10, pp. 863–871, 2016.
- [83] W. S. Lee, W. H. Yoo, and H. J. Chae, "ER stress and autophagy," *Current Molecular Medicine*, vol. 15, no. 8, pp. 735–745, 2015.
- [84] L. Cominacini, C. Mozzini, U. Garbin et al., "Endoplasmic reticulum stress and Nrf2 signaling in cardiovascular diseases," *Free Radical Biology & Medicine*, vol. 88, pp. 233–242, 2015.
- [85] E. Sozen, B. Karademir, and N. K. Ozer, "Basic mechanisms in endoplasmic reticulum stress and relation to cardiovascular diseases," *Free Radical Biology & Medicine*, vol. 78, pp. 30–41, 2015.
- [86] X. Zhou, B. Lu, D. Fu, M. Gui, L. Yao, and J. Li, "Huoxue Qianyang decoction ameliorates cardiac remodeling in obese spontaneously hypertensive rats in association with ATF6-CHOP endoplasmic reticulum stress signaling pathway regulation," *Biomedicine & Pharmacotherapy*, vol. 121, p. 109518, 2020.
- [87] J. Nie, N. Ta, L. Liu, G. Shi, T. Kang, and Z. Zheng, "Activation of CaMKII via ER-stress mediates coxsackievirus B3-induced cardiomyocyte apoptosis," *Cell Biology International*, vol. 44, no. 2, pp. 488–498, 2019.
- [88] J. Zhang, L. Wang, W. Xie et al., "Melatonin attenuates ER stress and mitochondrial damage in septic cardiomyopathy: a new mechanism involving BAP31 upregulation and MAPK-ERK pathway," *Journal of Cellular Physiology*, vol. 235, no. 3, pp. 2847–2856, 2020.
- [89] R. Lenin, P. G. Nagy, K. A. Jha, and R. Gangaraju, "GRP78 translocation to the cell surface and O-GlcNAcylation of VE-cadherin contribute to ER stress-mediated endothelial permeability," *Scientific Reports*, vol. 9, no. 1, p. 10783, 2019.
- [90] M. di Somma, M. Vliora, E. Grillo et al., "Role of VEGFs in metabolic disorders," *Angiogenesis*, vol. 23, no. 2, pp. 119–130, 2020.
- [91] S. Mohan, M. R. Preetha Rani, L. Brown, P. Ayyappan, and K. G. Raghu, "Endoplasmic reticulum stress: a master regulator of metabolic syndrome," *European Journal of Pharmacology*, vol. 860, article 172553, 2019.
- [92] P. Fournier, C. Viillard, A. Dejda, P. Sapieha, B. Larrivée, and I. Royal, "The protein tyrosine phosphatase PTPRJ/DEP-1 contributes to the regulation of the Notch-signaling pathway and sprouting angiogenesis," *Angiogenesis*, vol. 23, no. 2, pp. 145–157, 2020.
- [93] M. Navas-Madroñal, C. Rodriguez, M. Kassin et al., "Enhanced endoplasmic reticulum and mitochondrial stress in abdominal aortic aneurysm," *Clinical Science (London, England)*, vol. 133, no. 13, pp. 1421–1438, 2019.
- [94] A. Domingues, C. Boisson-Vidal, P. Marquet de Rouge et al., "Targeting endothelial thioredoxin-interacting protein (TXNIP) protects from metabolic disorder-related impairment of vascular function and post-ischemic revascularisation," *Angiogenesis*, vol. 23, no. 2, pp. 249–264, 2020.
- [95] J. I. Abe, K. A. Ko, S. Kotla et al., "MAGI1 as a link between endothelial activation and ER stress drives atherosclerosis," *JCI Insight*, vol. 4, no. 7, 2019.
- [96] M. Thamsen, R. Ghosh, V. C. Auyeung et al., "Small molecule inhibition of IRE1 α kinase/RNase has anti-fibrotic effects in the lung," *PLoS One*, vol. 14, no. 1, article e0209824, 2019.
- [97] X. Wu, L. Zhang, Y. Miao et al., "Homocysteine causes vascular endothelial dysfunction by disrupting endoplasmic reticulum redox homeostasis," *Redox Biology*, vol. 20, pp. 46–59, 2019.
- [98] T. Ji, X. Zhang, Z. Xin et al., "Does perturbation in the mitochondrial protein folding pave the way for neurodegeneration diseases?," *Ageing Research Reviews*, vol. 57, p. 100997, 2020.
- [99] O. M. Amen, S. D. Sarker, R. Ghildyal, and A. Arya, "Endoplasmic reticulum stress activates unfolded protein response signaling and mediates inflammation, obesity, and cardiac dysfunction: therapeutic and molecular approach," *Frontiers in Pharmacology*, vol. 10, p. 977, 2019.
- [100] V. Tang, S. Fu, B. S. Rayner, and C. L. Hawkins, "8-Chloroadenosine induces apoptosis in human coronary artery endothelial cells through the activation of the unfolded protein response," *Redox Biology*, vol. 26, p. 101274, 2019.
- [101] C. Hofmann, H. A. Katus, and S. Doroudgar, "Protein misfolding in cardiac disease," *Circulation*, vol. 139, no. 18, pp. 2085–2088, 2019.
- [102] E. L. Wilson and E. Metzakopian, "ER-mitochondria contact sites in neurodegeneration: genetic screening approaches to

- investigate novel disease mechanisms,” *Cell Death and Differentiation*, 2020.
- [103] H. N. Cha, C. H. Woo, H. Y. Kim, and S. Y. Park, “Methionine sulfoxide reductase B3 deficiency inhibits the development of diet-induced insulin resistance in mice,” *Redox Biology*, vol. 38, p. 101823, 2021.
- [104] S. Sharma, P. Chaudhary, R. Sandhir et al., “Heat-induced endoplasmic reticulum stress in soleus and gastrocnemius muscles and differential response to UPR pathway in rats,” *Cell Stress & Chaperones*, vol. 26, no. 2, pp. 323–339, 2021.
- [105] B. A. Niemeyer, “TRICKing SOCE into altered oscillations,” *Cell Calcium*, vol. 92, p. 102290, 2020.
- [106] A. A. Mohsin, J. Thompson, Y. Hu, J. Hollander, E. J. Lesnefsky, and Q. Chen, “Endoplasmic reticulum stress-induced complex I defect: central role of calcium overload,” *Archives of Biochemistry and Biophysics*, vol. 683, p. 108299, 2020.
- [107] M. L. O’Byrne, J. Huang, I. Asztalos et al., “Pediatric/congenital cardiac catheterization quality: an analysis of existing metrics,” *JACC. Cardiovascular Interventions*, vol. 13, no. 24, pp. 2853–2864, 2020.
- [108] T. L. Capasso, B. Li, H. J. Volek et al., “BMP10-mediated ALK1 signaling is continuously required for vascular development and maintenance,” *Angiogenesis*, vol. 23, no. 2, pp. 203–220, 2020.
- [109] Y. Miyazaki, K. Kaikita, M. Endo et al., “C/EBP homologous protein deficiency attenuates myocardial reperfusion injury by inhibiting myocardial apoptosis and inflammation,” *Arteriosclerosis, Thrombosis, and Vascular Biology*, vol. 31, no. 5, pp. 1124–1132, 2011.
- [110] B. Dong, H. Zhou, C. Han et al., “Ischemia/reperfusion-induced CHOP expression promotes apoptosis and impairs renal function recovery: the role of acidosis and GPR4,” *PLoS One*, vol. 9, no. 10, article e110944, 2014.
- [111] X. F. Guo and X. J. Yang, “Endoplasmic reticulum stress response in spontaneously hypertensive rats is affected by myocardial ischemia reperfusion injury,” *Experimental and Therapeutic Medicine*, vol. 9, no. 2, pp. 319–326, 2015.
- [112] M. R. Noh, J. I. Kim, S. J. Han, T. J. Lee, and K. M. Park, “C/EBP homologous protein (CHOP) gene deficiency attenuates renal ischemia/reperfusion injury in mice,” *Biochimica et Biophysica Acta*, vol. 1852, no. 9, pp. 1895–1901, 2015.
- [113] J. Bai, M. Khajavi, L. Sui et al., “Angiogenic responses in a 3D micro-engineered environment of primary endothelial cells and pericytes,” *Angiogenesis*, vol. 24, no. 1, pp. 111–127, 2021.
- [114] M. Chen, Y. Y. Zheng, Y. T. Song et al., “Pretreatment with low-dose gadolinium chloride attenuates myocardial ischemia/reperfusion injury in rats,” *Acta Pharmacologica Sinica*, vol. 37, no. 4, pp. 453–462, 2016.
- [115] T. Wu, N. Jiang, Z. Ji, and G. Shi, “The IRE1 signaling pathway is involved in the protective effect of low-dose LPS on myocardial ischemia-reperfusion injury,” *Life Sciences*, vol. 231, p. 116569, 2019.
- [116] E. Sozen, B. Yazgan, O. E. Tok et al., “Cholesterol induced autophagy via IRE1/JNK pathway promotes autophagic cell death in heart tissue,” *Metabolism*, vol. 106, p. 154205, 2020.
- [117] H. Chen, H. Yang, L. Pan et al., “The molecular mechanisms of XBP-1 gene silencing on IRE1 α -TRAF2-ASK1-JNK pathways in oral squamous cell carcinoma under endoplasmic reticulum stress,” *Biomedicine & Pharmacotherapy*, vol. 77, pp. 108–113, 2016.
- [118] A. L. Bayliss, A. Sundararaman, C. Granet, and H. Mellor, “Raflin is recruited by neuropilin-1 to the activated VEGFR2 complex to control proangiogenic signaling,” *Angiogenesis*, vol. 23, no. 3, pp. 371–383, 2020.
- [119] Q. Jin, R. Li, N. Hu et al., “DUSP1 alleviates cardiac ischemia/reperfusion injury by suppressing the Mff- required mitochondrial fission and Bnip3-related mitophagy via the JNK pathways,” *Redox Biology*, vol. 14, pp. 576–587, 2018.
- [120] W. Xu, L. Zhang, Y. Zhang, K. Zhang, Y. Wu, and D. Jin, “TRAF1 exacerbates myocardial ischemia reperfusion injury via ASK1-JNK/p38 signaling,” *Journal of the American Heart Association*, vol. 8, no. 21, article e012575, 2019.
- [121] H. H. Su, J. M. Liao, Y. H. Wang et al., “Exogenous GDF11 attenuates non-canonical TGF- β signaling to protect the heart from acute myocardial ischemia-reperfusion injury,” *Basic Research in Cardiology*, vol. 114, no. 3, p. 20, 2019.
- [122] M. Liu, Y. Wang, Q. Zhu et al., “Protective effects of circulating microvesicles derived from ischemic preconditioning on myocardial ischemia/reperfusion injury in rats by inhibiting endoplasmic reticulum stress,” *Apoptosis*, vol. 23, no. 7–8, pp. 436–448, 2018.
- [123] J. G. Xia, F. F. Xu, Y. Qu, D. D. Song, H. Shen, and X. H. Liu, “Atorvastatin post-conditioning attenuates myocardial ischemia reperfusion injury via inhibiting endoplasmic reticulum stress-related apoptosis,” *Shock*, vol. 42, no. 4, pp. 365–371, 2014.
- [124] J. Guo, Y. Bian, R. Bai, H. Li, M. Fu, and C. Xiao, “Globular adiponectin attenuates myocardial ischemia/reperfusion injury by upregulating endoplasmic reticulum Ca²⁺-ATPase activity and inhibiting endoplasmic reticulum stress,” *Journal of Cardiovascular Pharmacology*, vol. 62, no. 2, pp. 143–153, 2013.
- [125] E. H. Moon, Y. H. Kim, P. N. Vu et al., “TMEM100 is a key factor for specification of lymphatic endothelial progenitors,” *Angiogenesis*, vol. 23, no. 3, pp. 339–355, 2020.
- [126] T. Yoneda, K. Imaizumi, K. Oono et al., “Activation of caspase-12, an endoplasmic reticulum (ER) resident caspase, through tumor necrosis factor receptor-associated factor 2-dependent mechanism in response to the ER stress,” *The Journal of Biological Chemistry*, vol. 276, no. 17, pp. 13935–13940, 2001.
- [127] D. Datta, A. Singh, D. R. Saha et al., “_Mycobacterium fortuitum_ -induced ER-Mitochondrial calcium dynamics promotes calpain/caspase-12/caspase-9 mediated apoptosis in fish macrophages,” *Cell Death Discovery*, vol. 4, no. 1, p. 30, 2018.

Research Article

Bevacizumab-Induced Mitochondrial Dysfunction, Endoplasmic Reticulum Stress, and ERK Inactivation Contribute to Cardiotoxicity

Yue Li,¹ Wei Tian,² Dongsheng Yue,¹ Chen Chen,¹ Chenguang Li,¹ Zhenfa Zhang,¹ and Changli Wang¹ 

¹Department of Lung Cancer, Tianjin Medical University Cancer Institute and Hospital, National Clinical Research Center for Cancer, Key Laboratory of Cancer Prevention and Therapy, Tianjin's Clinical Research Center for Cancer, Tianjin Lung Cancer Center, Tianjin 300060, China

²Department of General Surgery, The Second Affiliated Hospital of Tianjin University of Traditional Chinese Medicine, Tianjin 300060, China

Correspondence should be addressed to Changli Wang; wangchangli@tjmuch.com

Received 14 February 2021; Revised 1 March 2021; Accepted 11 March 2021; Published 23 March 2021

Academic Editor: Yun-dai Chen

Copyright © 2021 Yue Li et al. This is an open access article distributed under the Creative Commons Attribution License, which permits unrestricted use, distribution, and reproduction in any medium, provided the original work is properly cited.

The molecular mechanisms underlying the cardiotoxicity associated with bevacizumab, a first-line immunotherapeutic agent used to treat lung cancer, are not fully understood. Here, we examined intracellular signal transduction in cardiomyocytes after exposure to different doses of bevacizumab *in vitro*. Our results demonstrated that bevacizumab significantly and dose-dependently reduces cardiomyocyte viability and increases cell apoptosis. Bevacizumab treatment also led to mitochondrial dysfunction in cardiomyocytes, as evidenced by the decreased ATP production, increased ROS production, attenuated antioxidative enzyme levels, and reduced respiratory complex function. In addition, bevacizumab induced intracellular calcium overload, ER stress, and caspase-12 activation. Finally, bevacizumab treatment inhibited the ERK signaling pathway, which, in turn, significantly reduced cardiomyocyte viability and contributed to mitochondrial dysfunction. Together, our results demonstrate that bevacizumab-mediated cardiotoxicity is associated with mitochondrial dysfunction, ER stress, and ERK pathway inactivation. These findings may provide potential treatment targets to attenuate myocardial injury during lung cancer immunotherapy.

1. Introduction

Bevacizumab is a first-line immunotherapeutic agent used for the treatment of lung cancer [1]. The cancer-suppressing effects of bevacizumab are associated with inhibition of vascular endothelial growth factor signaling, which leads to decreased tumor growth and impaired invasion [2, 3]. However, bevacizumab is also associated with cardiovascular toxicities, including decreased left ventricular ejection fraction, vasculitis, hypertension, arrhythmias, vascular bed degeneration, and limited angiogenesis response [4–8]. Several mechanisms, including accumulation of toxic metabolites, cardiac microvascular vasospasm, and excessive activation of the renin-angiotensin system, might underlie the adverse effects of bevacizumab on the heart [4–7]. However, the intracellular

molecular mechanisms underlying bevacizumab-associated cardiotoxicity are not fully understood.

At the molecular level, cardiomyocyte viability and function are greatly affected by mitochondrial performance [9, 10]. Mitochondria regulate cardiomyocyte contraction and relaxation by controlling ATP production [11, 12]. As the primary site of protein manufacturing, the endoplasmic reticulum (ER) controls protein synthesis, folding, and release [13, 14]. Previous studies have reported that targeted cancer therapies, such as doxorubicin [15], anthracycline [16], and cantharidin [17], can result in cardiovascular toxicities. The adverse effects of chemotherapy drugs may result from impaired mitochondrial function, increased oxidative stress [15, 18], increased mitochondria-proteasome interactions [19], impaired mitochondrial autophagy [20, 21],

activation of mitochondrial inflammation signaling pathways such as NF- κ B [22], mitochondrial energy metabolic dysfunction [23], and mitochondrial apoptosis [24]. In addition, ER-mediated abnormalities in intracellular calcium signaling, protein misfolding as a result of ER stress, and ER-dependent cell apoptosis [25–27] can also contribute to cardiomyocyte damage during chemotherapy. Whether bevacizumab-mediated cardiovascular disorders are attributable to mitochondrial damage and/or ER stress remains to be determined.

The MAPK/ERK signaling pathway plays an important role in cardiomyocyte survival under stress conditions [28, 29]. Activated ERK attenuates oxidative stress in cardiomyocytes by promoting the transcription of antioxidative stress genes [30]. In addition, ERK alleviated chronic cardiac hypertrophy by improving mitochondrial metabolism [31]. As in cardiomyocytes, ERK promotes growth during tumor proliferation and invasion, and upregulation of the ERK pathway increased angiogenesis [32]. The ERK pathway also affects immune response in various tumors [33, 34]. In this study, we examined whether mitochondrial dysfunction, ER stress, and the ERK pathway are involved in bevacizumab-induced cardiotoxicity.

2. Materials and Methods

2.1. Cell Culture. H9C2 cell lines purchased from ATCC were grown in DMEM supplemented with 10% fetal bovine serum. The cells were maintained at 37°C and 5% carbon dioxide in a humidified environment. Cardiomyocytes were incubated with 0.1 or 5 mM bevacizumab as described in previous studies. Cardiomyocytes were also incubated with PD98059, an ERK pathway inhibitor, as described in previous reports to examine the influence of ERK inhibition on cardiomyocyte viability.

2.2. Cell Viability Assay. A total of 3000 treated cells per well were seeded in 96-well culture plates and incubated with or without bevacizumab for the indicated times; fresh media containing 50 μ l of CCK8 solution (5 mg/ml) (Dojindo Laboratories, Kumamoto, Japan) was then added followed by incubation at 37°C for 3 hours according to the manufacturer's protocol [35]. Absorbance was measured at 450 nm using an enzyme e-linked immunosorbent assay reader [36].

2.3. Mitochondrial ROS Detection. Cardiomyocytes were treated with bevacizumab and then washed with cold PBS three times. Then, 0.5 ng/ml MitoSOX Red mitochondrial superoxide indicator (Molecular Probes, USA) was added to the cardiomyocyte medium and incubated for 30 minutes in the dark. Cells were then washed with cold PBS three times [37]. Mitochondrial ROS production was observed under a confocal laser scanning microscope (LSM780; Carl Zeiss, Oberkochen, Germany, or TCS SP8; Leica, Wetzlar, Germany) and an Axio Zoom V16 stereo microscope (Carl Zeiss) [38].

2.4. Intracellular Calcium Content. Intracellular calcium measurements were performed as previously described with minor modifications [39]. Briefly, H9C2 cells were loaded

with 5 μ M Fluo4-AM calcium probe for 30 minutes at 37°C [40]. Cells were then washed with PBS, and intracellular calcium was observed under a confocal laser scanning microscope (LSM780; Carl Zeiss, Oberkochen, Germany, or TCS SP8; Leica, Wetzlar, Germany) and an Axio Zoom V16 stereo microscope (Carl Zeiss) [41].

2.5. Immunofluorescence. For fluorescence microscopy-based detection of target proteins, 5 μ m thick cryosections were deparaffinized in xylene and rehydrated through graded ethanol [42]. Antigen retrieval was performed for 20 min at 95°C with 0.1% sodium citrate buffer (pH 6.0). After endogenous peroxidase activity was quenched with 3% H₂O₂-dH₂O and nonspecific binding was blocked with 1% bovine serum albumin buffer, sections were incubated overnight at 4°C with primary antibodies using an Alexa 594 TSA Kit (Invitrogen) according to the manufacturer's instructions [43]. Stained sections were observed under a confocal laser scanning microscope (LSM780; Carl Zeiss, Oberkochen, Germany, or TCS SP8; Leica, Wetzlar, Germany) and an Axio Zoom V16 stereo microscope (Carl Zeiss) [44].

2.6. Detection of GSH, SOD, and GPX Activities. GSH, SOD, and GPX activities were detected using a Zymography Assay Kit (Applygen Technologies, China) according to the manufacturer's protocol [45]. GSH, SOD, and GPX were separated by SDS-PAGE. SDS was then extracted from the gel by incubating with Triton X-100 for 48 hours at 37°C. Finally, the gels were stained with Coomassie Brilliant Blue G250 and decolorized. A bright band against the blue background indicated the activity of targeted proteins. A Gel Image System (image master 1D analysis software, Pharmacia) was used to image the band [46].

2.7. Western Blot Analysis. Cell lysate was boiled in a sample buffer (62.5 mM Tris-HCl, pH 6.8, 2% sodium dodecyl sulfate, 20% glycerol, and 10% 2-mercaptoethanol), and protein concentration was determined using a Bradford protein assay kit (Thermo Fisher Scientific, Waltham, MA, USA) with bovine serum albumin as the standard [47]. Following protein transfer, the membrane was blocked with 5% skim milk in PBS Tween- (PBST-) 20 for 2 h at room temperature and then incubated overnight with antibodies at 4°C (the primary antibodies include Bcl2, 1 : 1000, Cell Signaling Technology, #3498; Bax, 1 : 1000, Cell Signaling Technology, #2772; caspase-9, 1 : 1000, Cell Signaling Technology, #9504; c-IAP, 1 : 1000, Cell Signaling Technology, #4952). The membranes were then washed with PBST containing 0.1% Tween. After three washes in PBST, each blot was incubated with peroxidase-conjugated secondary antibody for 1 h at 37°C. Labeled proteins were visualized using the Odyssey infrared scanner (LI-COR, Lincoln, NB, USA) [48]. Signals were densitometrically assessed and normalized to the β -actin signals, and an enhanced chemiluminescence detection system (Amersham, Piscataway, NJ, USA) was used to visualize the antibody-specific proteins in accordance with the manufacturer's recommended protocol [49].

2.8. Reverse Transcription-Quantitative Polymerase Chain Reaction (RT-qPCR). Total RNA was isolated from samples

according to miRNeasy Mini Kit (217004, Qiagen Company, Hilden, Germany) instructions [50]. All primers were synthesized by Takara Holdings Inc., Kyoto, Japan. RNA was then reverse transcribed into cDNA using the PrimeScript RT kit (RR036A, Takara). Next, fluorescence quantitative PCR was conducted using the SYBR® Premix ExTaq™ II kit (RR820A, Takara) on an ABI 7500 quantitative PCR instrument (7500, ABI Company, Oyster Bay, N.Y., USA). All samples were normalized to U6 and GAPDH using the $2^{-\Delta\Delta CT}$ method [51].

2.9. Mitochondrial Respiratory Chain Complex Activity Analysis. Mitochondrial respiratory chain activity was assessed using the Mitochondrial Respiratory Chain Complex Activity Assay Kit (Solarbio, Beijing, China) according to the manufacturer's instructions [52]. Briefly, the mitochondrial complex was extracted from cells and 10 μ l of the extract was added to each well of a 96-well plate. Detection reagents were then added to the wells followed by gentle mixing and incubation at 37°C for 2 min. Absorbance values were measured before and after the reaction using a microplate reader (BioTek, Vermont, VT), and the difference was calculated [53]. Respiratory complex enzyme activity was then calculated using the formula provided in the kit manual [54].

2.10. Measurement of ATP Levels. ATP production was measured using the luminometric ATP Assay kit (AAT Bioquest, Sunnyvale, CA) according to the manufacturer's instructions [55]. Briefly, H9C2 cells were seeded in a 96-well white plate and 200 μ l ATP assay solution was added. After mixing gently and incubating for 20 min at room temperature, luminescence intensity was measured using the luminometer mode on a plate reader (Tecan, Zurich, Switzerland) [56]. The readings were normalized to the total protein content.

2.11. Statistical Analysis. All results were confirmed in three independent experiments, and all quantitative data are expressed as the mean \pm SD. Differences in quantitative variables between two groups were analyzed using Student's *t*-test, and differences in quantitative variables for three or more groups were analyzed by one-way ANOVA. $p < 0.05$ was considered statistically significant.

3. Results

3.1. Bevacizumab Reduces Cardiomyocyte Viability and Function. After H9C2 cells were treated with low and high concentrations of bevacizumab, cell viability was measured through a CCK-8 assay. As shown in Figure 1(a), compared to the control group, bevacizumab treatment significantly reduced cardiomyocyte viability in a dose-dependent manner. Moreover, an LDH release assay, which measures levels of LDH released into the culture medium as a result of cell membrane breakage, showed that bevacizumab-treated H9C2 cells released more LDH than control cells (Figure 1(b)). Because decreased cardiomyocyte viability is strongly associated with impaired cardiomyocyte function, we next examined single-cell contraction function in primary cardiomyocytes. While the average length of primary cardiomyocytes was not affected by bevacizumab

(Figures 1(c)–1(h)), peak heights and maximal shortening velocity decreased after bevacizumab treatment, suggesting that bevacizumab disturbs cardiomyocyte contraction (Figures 1(c)–1(h)). In addition, maximal relengthening velocity and time-to-peak values increased after bevacizumab treatment (Figures 1(c)–1(h)), suggesting that bevacizumab also inhibits cardiomyocyte relaxation. Together, these results indicate that bevacizumab treatment dose-dependently reduces cardiomyocyte viability and impairs cardiomyocyte contraction/relaxation index.

3.2. Bevacizumab Induces Cell Apoptosis. Next, we examined alterations in cardiomyocyte apoptosis after bevacizumab treatment. First, TUNEL staining was used to observe cell apoptotic rate. As shown in Figures 2(a) and 2(b), compared to the control group, bevacizumab treatment significantly increased the number of TUNEL-positive cells in a dose-dependent manner; the low concentration of bevacizumab increased cardiomyocyte apoptosis rates to ~15%, while the high concentration increased rates to ~30%. Western blots were also performed to analyze changes in proapoptotic protein levels in cardiomyocytes. As shown in Figures 2(c)–2(e), compared to the control group, Bax, Bad, and caspase-9 protein levels increased dramatically in response to bevacizumab treatment in a dose-dependent manner (Figures 2(c)–2(e)). In contrast, Bcl-2 and c-IAP1 levels decreased significantly after bevacizumab treatment in a dose-dependent manner (Figures 2(f)–2(h)). Together, these results indicate that bevacizumab induces cardiomyocyte apoptosis.

3.3. Bevacizumab Treatment Is Associated with Mitochondrial Dysfunction. Mitochondrial dysfunction is considered the primary mechanism underlying chemotherapy-mediated myocardial injury. The subsequent experiments were therefore performed to analyze the effects of bevacizumab on mitochondrial function. Mitochondrial metabolism was examined first due to the importance of ATP production for cardiomyocyte viability and function. Bevacizumab treatment significantly decreased ATP production in a dose-dependent manner (Figure 3(a)). Reduced mitochondrial ATP production can result from oxidative stress and respiration dysfunction. A mitochondrial ROS probe was therefore used to analyze changes in mitochondrial oxidative stress. As shown in Figures 3(b) and 3(c), compared to the control group, mitochondrial ROS levels were significantly increased after bevacizumab treatment in a dose-dependent manner. In contrast, concentrations of antioxidative enzymes such as GSH and SOD were significantly lower after bevacizumab treatment (Figures 3(d) and 3(e)), confirming increased oxidative stress within mitochondria. In addition to mitochondrial oxidative stress, an ELISA assay also demonstrated that mitochondrial respiration complex activity (including COX-I and COX-III) decreased significantly in cardiomyocytes treated with bevacizumab (Figures 3(f) and 3(g)). These findings indicate that bevacizumab induces mitochondrial dysfunction characterized by ROS production, respiration impairments, and reduced metabolism in cardiomyocytes.

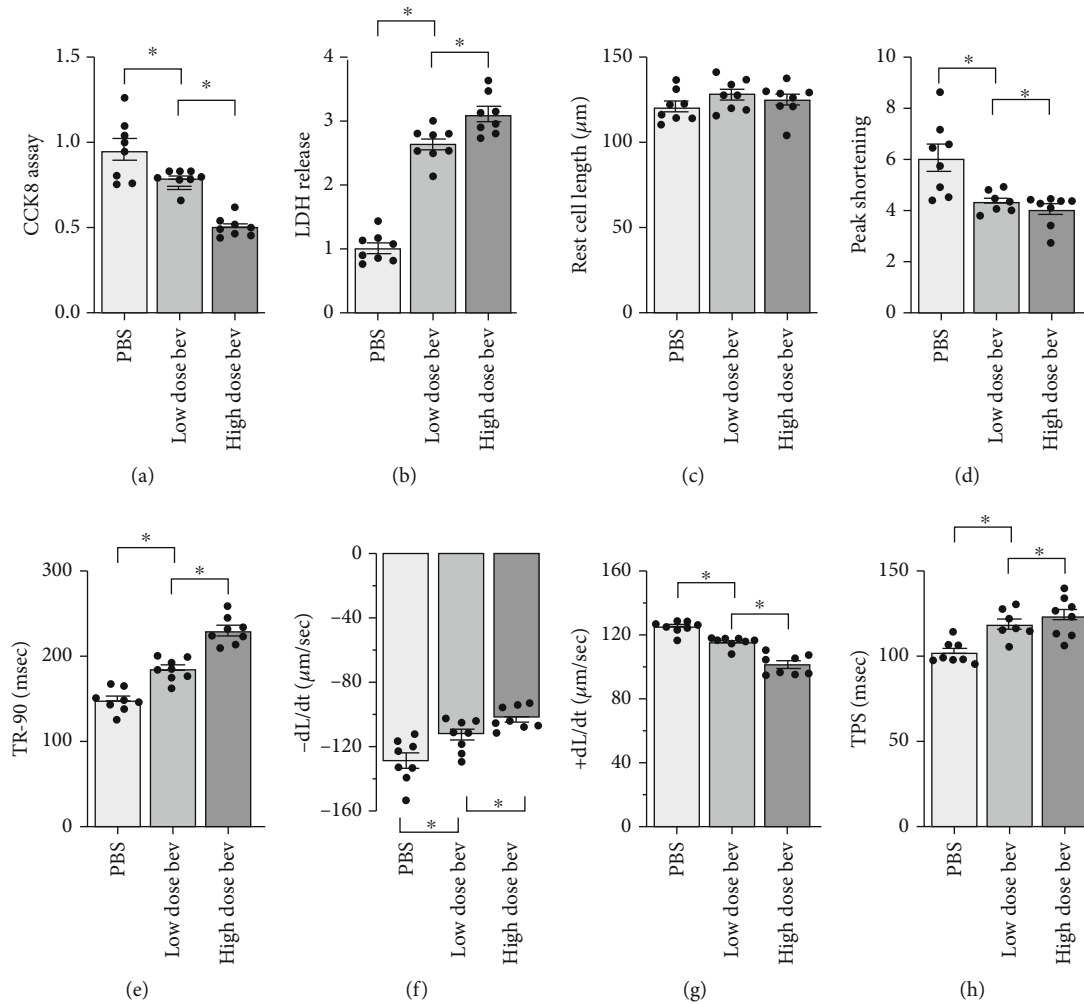


FIGURE 1: Bevacizumab reduces cardiomyocyte viability and function. (a) Cell viability was determined using a CCK-8 assay. (b) An LDH release assay was performed to examine whether bevacizumab induced cardiomyocyte damage. (c–h) The following single cardiomyocyte contractile properties were measured: peak height, maximal shortening velocity, maximal relengthening velocity, and time-to-peak. $*p < 0.05$.

3.4. Bevacizumab Treatment Induces ER Stress in Cardiomyocytes. Next, we examined alterations in ER stress in cardiomyocytes treated with bevacizumab. ER stress is associated with intracellular calcium overload. An immunofluorescence assay was therefore used to examine alterations in intracellular calcium concentration. As shown in Figures 4(a) and 4(b), compared to the control group, bevacizumab treatment significantly increased intracellular calcium concentration in a dose-dependent manner. Abnormal calcium signaling activates ER stress, which is characterized by increased expression of CHOP and PERK. qPCR demonstrated that CHOP and PERK expression increased significantly in response to bevacizumab treatment (Figures 4(c) and 4(d)), indicative of ER stress activation. Excessive ER damage activates caspase-12, an upstream activator of caspase-3. An ELISA showed that caspase-12 activity increased dramatically after bevacizumab treatment in a dose-dependent manner (Figure 4(e)). Taken together, these results demonstrate that bevacizumab can induce ER stress in cardiomyocytes.

3.5. Bevacizumab Inactivates the ERK Pathway in Cardiomyocytes. The ERK pathway, a classical signaling pathway responsible for cardiomyocyte survival, is a potential target of many chemotherapy drugs. We therefore examined whether ERK pathway activity was affected by bevacizumab. Western blots demonstrated that the ERK pathway was inactivated, as indicated by decreased ERK phosphorylation, in cardiomyocytes after bevacizumab treatment (Figures 5(a) and 5(b)). These results demonstrated that the ERK pathway was a downstream target of bevacizumab. To understand whether ERK inactivation contributed to bevacizumab-induced cardiomyocyte death and mitochondrial dysfunction, cardiomyocytes were incubated with an ERK inhibitor (PD98059). Cell viability was measured using a CCK-8 assay, and mitochondrial function was examined by measuring ATP production. As shown in Figure 5(c), compared to the control group, PD98059 treatment significantly reduced cardiomyocyte viability, and this effect was accompanied by a drop in mitochondrial ATP production (Figure 5(d)). This finding confirmed that ERK

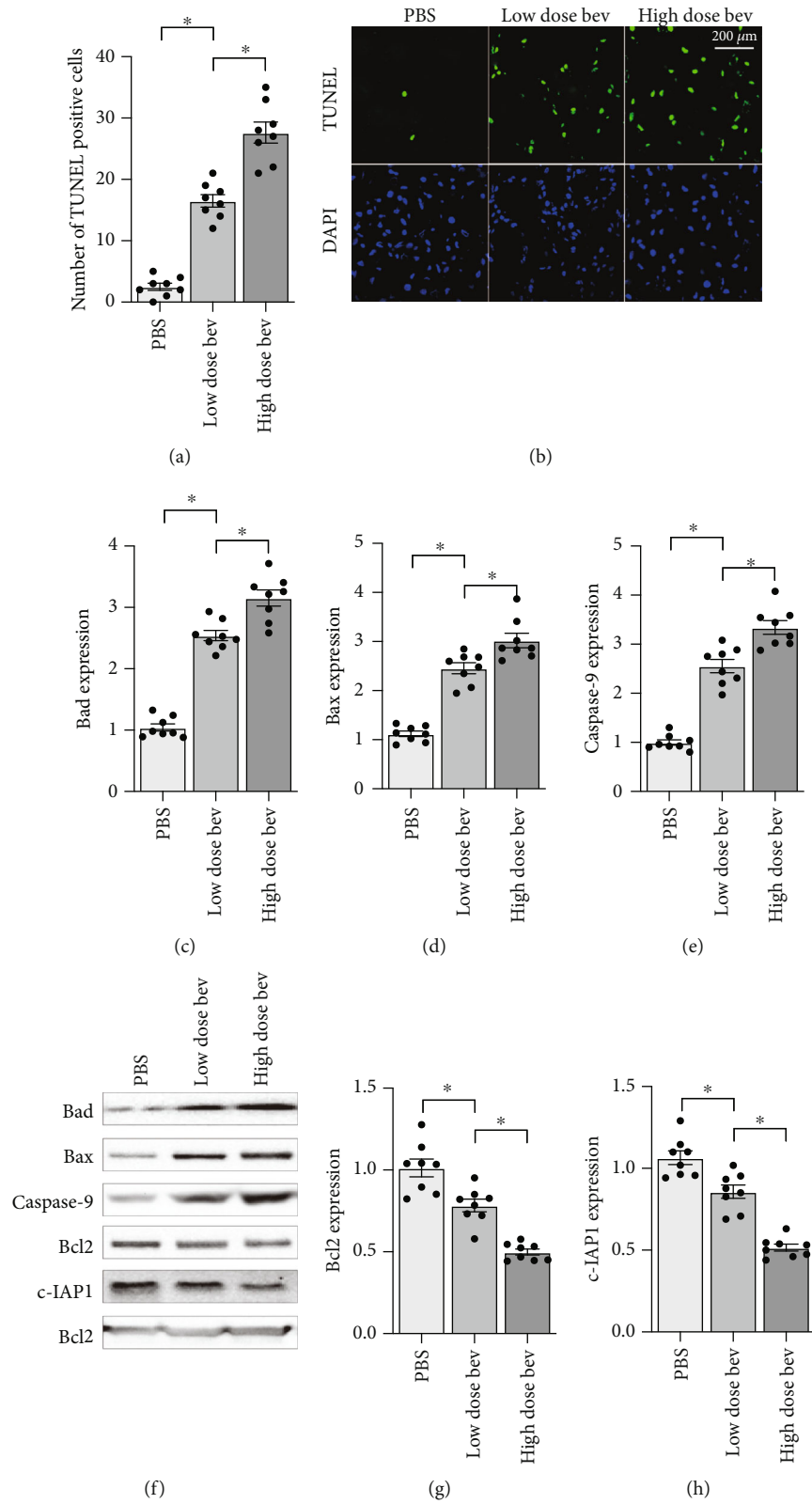


FIGURE 2: Bevacizumab induces cell apoptosis. (a, b) TUNEL staining was used to observe cell apoptosis. (c–h) Western blots were used to analyze alterations in expression of apoptosis-related proteins such as Bax, Bad, caspase-9, Bcl-2, and c-IAP1. * $p < 0.05$.

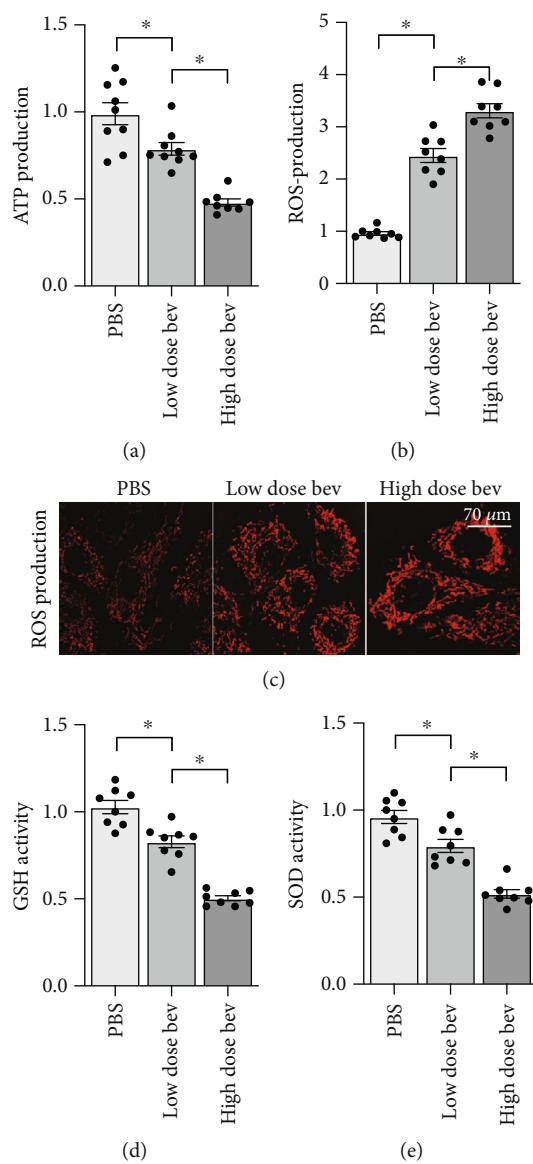


FIGURE 3: Continued.

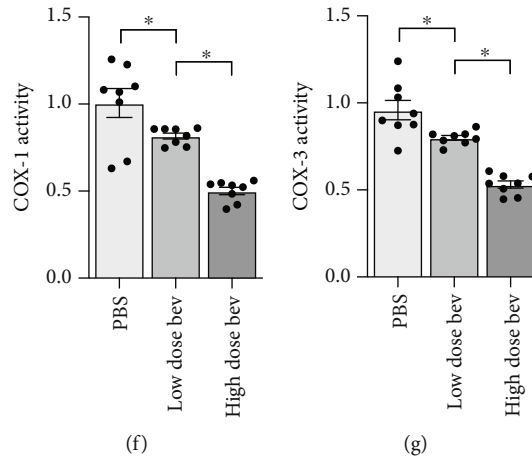


FIGURE 3: Bevacizumab treatment is associated with mitochondrial dysfunction. (a) ATP production was measured via ELISA in cardiomyocytes treated with bevacizumab. (b, c) Immunofluorescence staining was used to quantify mitochondrial ROS levels. (d, e) Changes in GSH, SOD, and GPX levels were analyzed in an ELISA. (f, g) Mitochondrial respiration complex activity was examined in an ELISA. * $p < 0.05$.

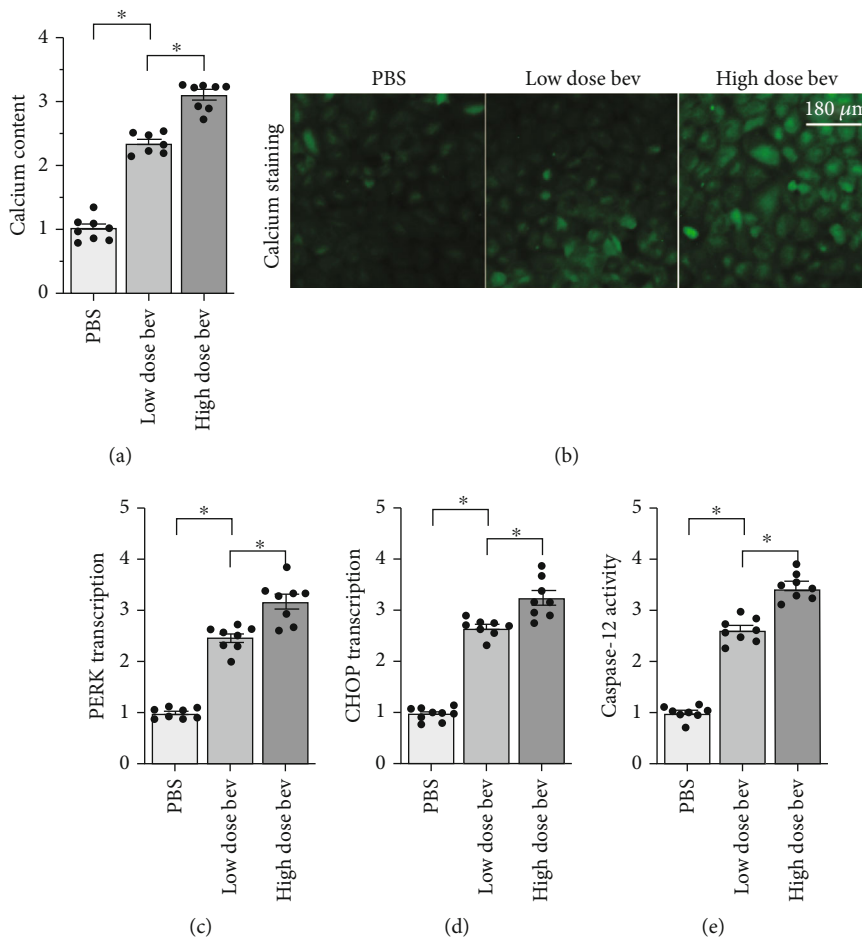


FIGURE 4: Bevacizumab treatment induces ER stress in cardiomyocytes. (a, b) Intracellular calcium levels were measured using immunofluorescence. (c, d) qPCR was used to analyze changes in CHOP and PERK levels. (e) ELISA was used to detect changes in caspase-12 activity. * $p < 0.05$.

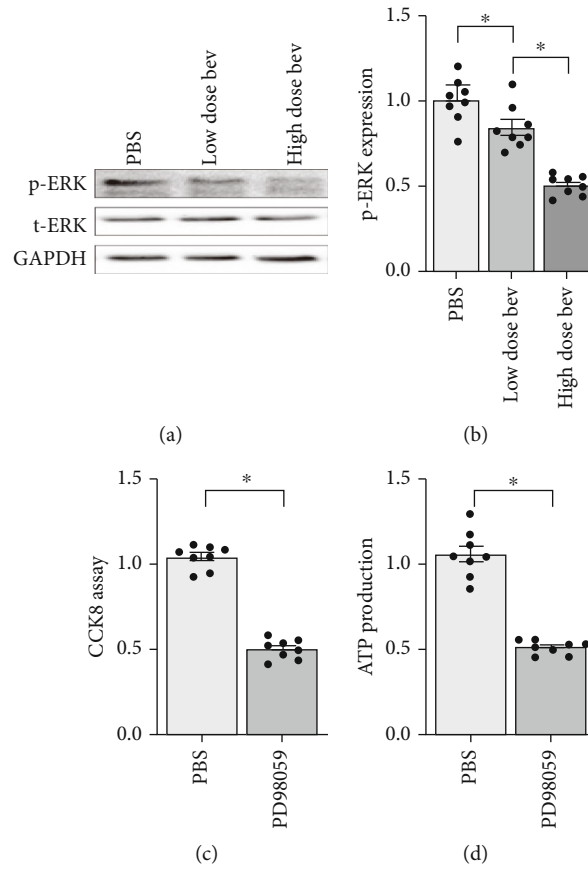


FIGURE 5: The ERK pathway is inactivated in cardiomyocytes treated with bevacizumab. (a, b) Western blots were used to analyze changes in ERK phosphorylation. (c) Cell viability was measured in a CCK-8 assay. Cardiomyocytes were treated with PD98059 to inhibit ERK activity. (d) ATP production was measured using an ELISA after PD98059 treatment. * $p < 0.05$.

inhibition plays a role in cardiomyocyte damage associated with bevacizumab treatment.

4. Discussion

The cardiotoxic effects of chemotherapy have been well documented. Although chemotherapy and immunotherapy improve the prognoses of lung cancer patients, these treatments also significantly increase the risk of myocardial injury and heart failure. In the present study, we found that bevacizumab treatment induces cardiomyocyte damage as indicated by decreased cell viability, impaired contraction/relaxation, attenuated ATP production, elevated mitochondrial ROS production, decreased mitochondrial respiration complex transcription, increased intracellular calcium concentration, and activation of ER stress. These alterations are similar to pathological changes observed in various cardiovascular disorders such as myocardial infarction, heart failure, diabetic cardiomyopathy, and hypertension, suggesting that common molecular mechanisms and signaling pathways may be involved. Furthermore, we found that the ERK pathway is inactivated by bevacizumab, and decreased ERK activity promotes cardiomyocyte death and mitochondrial damage. Overall, this study helps to explain the intracellular molecular mechanisms, including

mitochondrial dysfunction, ER stress, and inhibition of the ERK pathway, that underlie bevacizumab-induced cardiovascular toxicity.

Mitochondrial damage has been proposed as the primary cause of cardiomyocyte death and dysfunction [57]. Induction of mitochondrial fission promotes cardiomyocyte death by activating the caspase-9-related mitochondrial apoptotic pathway [58]. Additionally, inhibition of mitophagy leads to the accumulation of damaged mitochondria [59]. Chemotherapy drugs also contribute to cardiomyocyte dysfunction and death by affecting mitochondrial function. For example, doxorubicin-induced upregulation of p53 inhibits protective mechanisms in cardiac fibroblast mitochondria [20], and administration of mitochondria-associated protein LRPPRC protects against doxorubicin-induced cardiac injury by inhibiting ROS production [60]. Anthracycline-mediated cardiotoxicity is also associated with dysregulation of mitochondrial metabolism, although the detailed molecular mechanisms involved are not fully understood [23]. In the present study, bevacizumab treatment resulted in mitochondrial injury associated with metabolic dysregulation in cardiomyocytes. As far as we know, this is the first study to explore the influence of bevacizumab on mitochondrial homeostasis. While recent studies have examined the relationship between morphological

alterations in mitochondria and chemotherapy-induced cardiovascular damage, additional studies are required to determine whether bevacizumab also alters mitochondrial morphology.

ER stress can act as an adaptive response in cardiomyocytes [61]. Mild ER stress is characterized by increased intracellular calcium levels, which accelerate calcium-dependent ATP metabolism [62]. However, excessive ER stress is associated with the activation of CHOP and PERK, transcription factors that promote expression of apoptosis-related genes such as Bax and Bad [63]. Irreversible ER stress promotes the activation of caspase-12, which in turn directly induces caspase-3 cleavage that ultimately leads to cell apoptosis [64]. ER stress has also been identified as a potential intracellular signaling transduction mechanism underlying cardiotoxicity associated with chemotherapy drugs [65, 66]. In the present study, we found that bevacizumab treatment is associated with intracellular calcium overload, ER stress, and caspase-12 activation, suggesting that ER stress contributes to bevacizumab-mediated cardiomyocyte damage. Notably, while our data do not establish a causal relationship between ER stress and mitochondrial dysfunction, many studies have reported that ER stress may contribute to mitochondrial damage [67]. We also did not explore the possibility of interactive effects between ER stress and mitochondrial dysfunction.

Taken together, our results demonstrate that bevacizumab-mediated myocardial injury is associated with mitochondrial damage, ER stress, and ERK pathway inactivation. However, some limitations of this study should be considered when interpreting these results. First, only *in vitro* experiments were performed, and *in vivo* studies are needed to confirm our findings on the cardiotoxic effects of bevacizumab. Second, although we found that ERK inactivation is associated with cardiomyocyte death and mitochondrial damage, it remains unclear whether bevacizumab induces mitochondrial damage and ER stress specifically by directly inhibiting the ERK pathway. Third, additional bevacizumab concentrations beyond those tested here may have different effects on cardiomyocyte viability and function, and further study is needed to determine the dose threshold beyond which bevacizumab triggers cardiomyocyte damage.

Data Availability

The analyzed datasets that were generated during the study are available from the corresponding author upon reasonable request.

Conflicts of Interest

All authors declare that there are no conflicts of interest associated with this study.

Authors' Contributions

Yue Li and Wei Tian contributed to this article equally.

References

- [1] H. Akamatsu, Y. Toi, H. Hayashi et al., "Efficacy of osimertinib plus bevacizumab vs osimertinib in patients with EGFR T790M-mutated non-small cell lung cancer previously treated with epidermal growth factor receptor-tyrosine kinase inhibitor," *JAMA Oncology*, vol. 8, 2021.
- [2] N. Yamamoto, T. Seto, M. Nishio et al., "Erlotinib plus bevacizumab vs erlotinib monotherapy as first-line treatment for advanced EGFR mutation-positive non-squamous non-small-cell lung cancer: survival follow-up results of the randomized JO25567 study," *Lung Cancer*, vol. 151, pp. 20–24, 2021.
- [3] M. di Somma, M. Vliora, E. Grillo et al., "Role of VEGFs in metabolic disorders," *Angiogenesis*, vol. 23, no. 2, pp. 119–130, 2020.
- [4] M. T. van Leeuwen, S. Luu, H. Gurney et al., "Cardiovascular toxicity of targeted therapies for cancer: an overview of systematic reviews," *JNCI Cancer Spectrum*, vol. 4, no. 6, 2020.
- [5] B. Yetkin-Arik, A. W. Kastelein, I. Klaassen et al., "Angiogenesis in gynecological cancers and the options for anti-angiogenesis therapy," *Biochimica Et Biophysica Acta. Reviews on Cancer*, vol. 1875, no. 1, article 188446, 2021.
- [6] H. Huang, Y. Cao, Y. Dong et al., "Cardiac hemodynamic response to the 6-minute walk test in patients with intestinal carcinoma undergoing bevacizumab treatment," *Annals of Palliative Medicine*, vol. 10, no. 2, pp. 1362–1369, 2021.
- [7] M. P. Winter, S. Sharma, J. Altmann et al., "Interruption of vascular endothelial growth factor receptor 2 signaling induces a proliferative pulmonary vasculopathy and pulmonary hypertension," *Basic Research in Cardiology*, vol. 115, no. 6, p. 58, 2020.
- [8] D. B. Buglak, E. J. Kushner, A. P. Marvin, K. L. Davis, and V. L. Bautch, "Excess centrosomes disrupt vascular lumenization and endothelial cell adherens junctions," *Angiogenesis*, vol. 23, no. 4, pp. 567–575, 2020.
- [9] J. Ghaemi Kerahrodi and M. Michal, "The fear-defense system, emotions, and oxidative stress," *Redox Biology*, vol. 37, article 101588, 2020.
- [10] B. Kalyanaraman, "Teaching the basics of the mechanism of doxorubicin-induced cardiotoxicity: have we been barking up the wrong tree?," *Redox Biology*, vol. 29, p. 101394, 2020.
- [11] H. Zhou and S. Toan, "Pathological roles of mitochondrial oxidative stress and mitochondrial dynamics in cardiac microvascular ischemia/reperfusion injury," *Biomolecules*, vol. 10, no. 1, p. 85, 2020.
- [12] J. Wang, S. Toan, and H. Zhou, "Mitochondrial quality control in cardiac microvascular ischemia-reperfusion injury: new insights into the mechanisms and therapeutic potentials," *Pharmacological Research*, vol. 156, p. 104771, 2020.
- [13] M. Yuan, M. Gong, Z. Zhang et al., "Hyperglycemia induces endoplasmic reticulum stress in atrial cardiomyocytes, and mitofusin-2 downregulation prevents mitochondrial dysfunction and subsequent cell death," *Oxidative Medicine and Cellular Longevity*, vol. 2020, Article ID 6569728, 14 pages, 2020.
- [14] X. Nie, W. Tang, Z. Zhang et al., "Procyanidin B2 mitigates endothelial endoplasmic reticulum stress through a PPAR δ -dependent mechanism," *Redox Biology*, vol. 37, p. 101728, 2020.
- [15] A. Z. Ahmed, S. M. Satyam, P. Shetty, and M. R. D'Souza, "Methyl gallate attenuates doxorubicin-induced cardiotoxicity

- in rats by suppressing oxidative stress," *Scientifica*, vol. 2021, 12 pages, 2021.
- [16] P. Xia, J. Chen, Y. Liu, M. Fletcher, B. C. Jensen, and Z. Cheng, "Doxorubicin induces cardiomyocyte apoptosis and atrophy through cyclin-dependent kinase 2-mediated activation of forkhead box O1," *The Journal of Biological Chemistry*, vol. 295, no. 13, pp. 4265–4276, 2020.
 - [17] H. Shao, L. Dong, Y. Feng, C. Wang, and H. Tong, "The protective effect of L-glutamine against acute cantharidin-induced cardiotoxicity in the mice," *BMC Pharmacology and Toxicology*, vol. 21, no. 1, p. 71, 2020.
 - [18] L. C. Dieterich, C. Tacconi, F. Menzi et al., "Lymphatic MAFB regulates vascular patterning during developmental and pathological lymphangiogenesis," *Angiogenesis*, vol. 23, no. 3, pp. 411–423, 2020.
 - [19] L. Brandolini, A. Antonosante, C. Giorgio et al., "NSAIDs-dependent adaptation of the mitochondria-proteasome system in immortalized human cardiomyocytes," *Scientific Reports*, vol. 10, no. 1, article 18337, 2020.
 - [20] T. R. Mancilla, L. R. Davis, and G. J. Aune, "Doxorubicin-induced p53 interferes with mitophagy in cardiac fibroblasts," *PLoS One*, vol. 15, no. 9, article e0238856, 2020.
 - [21] F. Cao, M. L. Maguire, D. J. McAndrew et al., "Overexpression of mitochondrial creatine kinase preserves cardiac energetics without ameliorating murine chronic heart failure," *Basic Research in Cardiology*, vol. 115, no. 2, p. 12, 2020.
 - [22] A. Xu, F. Deng, Y. Chen et al., "NF- κ B pathway activation during endothelial-to-mesenchymal transition in a rat model of doxorubicin-induced cardiotoxicity," *Biomedicine & Pharmacotherapy*, vol. 130, article 110525, 2020.
 - [23] A. Murabito, E. Hirsch, and A. Ghigo, "Mechanisms of anthracycline-induced cardiotoxicity: is mitochondrial dysfunction the answer?," *Frontiers in Cardiovascular Medicine*, vol. 7, p. 35, 2020.
 - [24] B. Yang, H. Li, Y. Qiao et al., "Tetramethylpyrazine attenuates the endotheliotoxicity and the mitochondrial dysfunction by doxorubicin via 14-3-3 γ /Bcl-2," *Oxidative Medicine and Cellular Longevity*, vol. 2019, Article ID 5820415, 20 pages, 2019.
 - [25] H. Bae, J. Y. Lee, C. Yang, G. Song, and W. Lim, "Fucoidan derived from Fucus vesiculosus inhibits the development of human ovarian cancer via the disturbance of calcium homeostasis, endoplasmic reticulum stress, and angiogenesis," *Marine Drugs*, vol. 18, no. 1, p. 45, 2020.
 - [26] R. Lage, M. Cebro-Márquez, M. Rodríguez-Mañero, J. R. González-Juanatey, and I. Moscoso, "Omentin protects H9c2 cells against docetaxel cardiotoxicity," *PLoS One*, vol. 14, no. 2, article e0212782, 2019.
 - [27] L. Wang, J. Y. Chan, X. Zhou et al., "A novel agent enhances the chemotherapeutic efficacy of doxorubicin in MCF-7 breast cancer cells," *Frontiers in Pharmacology*, vol. 7, p. 249, 2016.
 - [28] S. Lama, V. Monda, M. R. Rizzo et al., "Cardioprotective effects of Taurisolo® in cardiomyoblast H9c2 cells under high-glucose and trimethylamine N-oxide treatment via de novo sphingolipid synthesis," *Oxidative Medicine and Cellular Longevity*, vol. 2020, Article ID 2961406, 11 pages, 2020.
 - [29] T. Xin, W. Lv, D. Liu, Y. Jing, and F. Hu, "Opa1 reduces hypoxia-induced cardiomyocyte death by improving mitochondrial quality control," *Frontiers in Cell and Development Biology*, vol. 8, p. 853, 2020.
 - [30] G. Shi, Y. Wang, J. Yang et al., "Effect of cryptotanshinone on measures of rat cardiomyocyte oxidative stress and gene activation associated with apoptosis," *Cardiorenal Medicine*, vol. 11, no. 1, pp. 18–26, 2021.
 - [31] Y. Shen, X. Zhang, C. Li et al., "Pressure overload promotes cystatin C secretion of cardiomyocytes to regulate the MAPK signaling pathway and mediate cardiac hypertrophy," *Annals of Translational Medicine*, vol. 8, no. 22, p. 1514, 2020.
 - [32] A. Russignan, G. Dal Collo, A. Bagnato et al., "Targeting the endothelin-1 receptors curtails tumor growth and angiogenesis in multiple myeloma," *Frontiers in Oncology*, vol. 10, article 600025, 2021.
 - [33] F. Wang, H. Wang, X. Liu et al., "Neuregulin-1 alleviate oxidative stress and mitigate inflammation by suppressing NOX4 and NLRP3/caspase-1 in myocardial ischaemia-reperfusion injury," *Journal of Cellular and Molecular Medicine*, vol. 25, no. 3, pp. 1783–1795, 2021.
 - [34] Z. Zhao, L. Zhu, Y. Xing, and Z. Zhang, "Praja2 suppresses the growth of gastric cancer by ubiquitylation of KSR1 and inhibiting MEK-ERK signal pathways," *Aging*, vol. 13, pp. 3886–3897, 2021.
 - [35] J. Chen, F. L. Lin, J. Y. K. Leung et al., "A drug-tunable Flt23k gene therapy for controlled intervention in retinal neovascularization," *Angiogenesis*, vol. 24, no. 1, pp. 97–110, 2021.
 - [36] R. K. Adapala, A. K. Kanugula, S. Paruchuri, W. M. Chilian, and C. K. Thodeti, "TRPV4 deletion protects heart from myocardial infarction-induced adverse remodeling via modulation of cardiac fibroblast differentiation," *Basic Research in Cardiology*, vol. 115, no. 2, p. 14, 2020.
 - [37] H. Zhou, S. Toan, P. Zhu, J. Wang, J. Ren, and Y. Zhang, "DNA-PKcs promotes cardiac ischemia reperfusion injury through mitigating BI-1-governed mitochondrial homeostasis," *Basic Research in Cardiology*, vol. 115, no. 2, p. 11, 2020.
 - [38] M. Escoll, D. Lastra, M. Pajares et al., "Transcription factor NRF2 uses the Hippo pathway effector TAZ to induce tumorigenesis in glioblastomas," *Redox Biology*, vol. 30, article 101425, 2020.
 - [39] N. Lubos, S. van der Gaag, M. Gerçek, S. Kant, R. E. Leube, and C. A. Krusche, "Inflammation shapes pathogenesis of murine arrhythmogenic cardiomyopathy," *Basic Research in Cardiology*, vol. 115, no. 4, p. 42, 2020.
 - [40] Y. Tan, D. Mui, S. Toan, P. Zhu, R. Li, and H. Zhou, "SERCA overexpression improves mitochondrial quality control and attenuates cardiac microvascular ischemia-reperfusion injury," *Molecular Therapy Nucleic Acids*, vol. 22, pp. 696–707, 2020.
 - [41] J. Lyu, M. Wang, X. Kang et al., "Macrophage-mediated regulation of catecholamines in sympathetic neural remodeling after myocardial infarction," *Basic Research in Cardiology*, vol. 115, no. 5, p. 56, 2020.
 - [42] J. Wang, S. Toan, R. Li, and H. Zhou, "Melatonin fine-tunes intracellular calcium signals and eliminates myocardial damage through the IP3R/MCU pathways in cardiorenal syndrome type 3," *Biochemical Pharmacology*, vol. 174, p. 113832, 2020.
 - [43] J. Wang, P. Zhu, S. Toan, R. Li, J. Ren, and H. Zhou, "Pum2-Mff axis fine-tunes mitochondrial quality control in acute ischemic kidney injury," *Cell Biology and Toxicology*, vol. 36, no. 4, pp. 365–378, 2020.
 - [44] E. García-Martínez, A. Redondo, J. M. Piulats, A. Rodríguez, and A. Casado, "Are antiangiogenics a good 'partner' for immunotherapy in ovarian cancer?," *Angiogenesis*, vol. 23, no. 4, pp. 543–557, 2020.

- [45] K. L. Kuo, J. F. Zhao, P. H. Huang, B. C. Guo, D. C. Tarnag, and T. S. Lee, "Indoxyl sulfate impairs valsartan-induced neovascularization," *Redox Biology*, vol. 30, p. 101433, 2020.
- [46] H. Li and N. Xia, "The role of oxidative stress in cardiovascular disease caused by social isolation and loneliness," *Redox Biology*, vol. 37, article 101585, 2020.
- [47] Y. S. Ma, K. J. Chu, C. C. Ling et al., "Long noncoding RNA OIP5-AS1 promotes the progression of liver hepatocellular carcinoma via regulating the hsa-miR-26a-3p/EPHA2 axis," *Molecular Therapy Nucleic Acids*, vol. 21, pp. 229–241, 2020.
- [48] E. Kong, H. D. Kim, and J. Kim, "Deleting key autophagy elongation proteins induces acquirement of tumor-associated phenotypes via ISG15," *Cell Death and Differentiation*, vol. 27, no. 8, pp. 2517–2530, 2020.
- [49] H. Zhou, P. Zhu, J. Wang, S. Toan, and J. Ren, "DNA-PKcs promotes alcohol-related liver disease by activating Drp1-related mitochondrial fission and repressing FUNDC1-required mitophagy," *Signal Transduction and Targeted Therapy*, vol. 4, no. 1, article 56, 2019.
- [50] Y. Yang, L. Ma, C. Wang et al., "Matrix metalloproteinase-7 in platelet-activated macrophages accounts for cardiac remodeling in uremic mice," *Basic Research in Cardiology*, vol. 115, no. 3, p. 30, 2020.
- [51] Q. L. Nguyen, N. Okuno, T. Hamashima et al., "Vascular PDGFR- α protects against BBB dysfunction after stroke in mice," *Angiogenesis*, vol. 24, no. 1, pp. 35–46, 2021.
- [52] J. Wang, P. Zhu, R. Li, J. Ren, Y. Zhang, and H. Zhou, "Bax inhibitor 1 preserves mitochondrial homeostasis in acute kidney injury through promoting mitochondrial retention of PHB2," *Theranostics*, vol. 10, no. 1, pp. 384–397, 2020.
- [53] J. Liu, Q. Cai, W. Wang et al., "Ginsenoside Rh2 pretreatment and withdrawal reactivated the pentose phosphate pathway to ameliorate intracellular redox disturbance and promoted intratumoral penetration of adriamycin," *Redox Biology*, vol. 32, p. 101452, 2020.
- [54] J. Wang, Z. Chen, Q. Dai et al., "Intravenously delivered mesenchymal stem cells prevent microvascular obstruction formation after myocardial ischemia/reperfusion injury," *Basic Research in Cardiology*, vol. 115, no. 4, p. 40, 2020.
- [55] J. Wang, P. Zhu, R. Li, J. Ren, and H. Zhou, "Fundc1-dependent mitophagy is obligatory to ischemic preconditioning-conferred renoprotection in ischemic AKI via suppression of Drp1-mediated mitochondrial fission," *Redox Biology*, vol. 30, p. 101415, 2020.
- [56] J. M. Mulcahy Levy and A. Thorburn, "Autophagy in cancer: moving from understanding mechanism to improving therapy responses in patients," *Cell Death and Differentiation*, vol. 27, no. 3, pp. 843–857, 2020.
- [57] J. Wang, S. Toan, and H. Zhou, "New insights into the role of mitochondria in cardiac microvascular ischemia/reperfusion injury," *Angiogenesis*, vol. 23, no. 3, pp. 299–314, 2020.
- [58] Q. Jin, R. Li, N. Hu et al., "DUSP1 alleviates cardiac ischemia/reperfusion injury by suppressing the Mff-required mitochondrial fission and Bnip3-related mitophagy via the JNK pathways," *Redox Biology*, vol. 14, pp. 576–587, 2018.
- [59] H. Zhou, P. Zhu, J. Wang, H. Zhu, J. Ren, and Y. Chen, "Pathogenesis of cardiac ischemia reperfusion injury is associated with CK2 α -disturbed mitochondrial homeostasis via suppression of FUNDC1-related mitophagy," *Cell Death and Differentiation*, vol. 25, no. 6, pp. 1080–1093, 2018.
- [60] Q. Tang, W. Xiong, X. Ke, J. Zhang, Y. Xia, and D. Liu, "Mitochondria-associated protein LRPPRC exerts cardioprotective effects against doxorubicin-induced toxicity, potentially via inhibition of ROS accumulation," *Experimental and Therapeutic Medicine*, vol. 20, pp. 3837–3845, 2020.
- [61] H. Zhou, S. Wang, S. Hu, Y. Chen, and J. Ren, "ER-mitochondria microdomains in cardiac ischemia-reperfusion injury: a fresh perspective," *Frontiers in Physiology*, vol. 9, p. 755, 2018.
- [62] J. Li, C. Xu, Y. Liu et al., "Fibroblast growth factor 21 inhibited ischemic arrhythmias via targeting miR-143/EGR1 axis," *Basic Research in Cardiology*, vol. 115, no. 2, p. 9, 2020.
- [63] G. Heusch, "Coronary microvascular obstruction: the new frontier in cardioprotection," *Basic Research in Cardiology*, vol. 114, no. 6, p. 45, 2019.
- [64] W. E. Hughes, A. M. Beyer, and D. D. Gutterman, "Vascular autophagy in health and disease," *Basic Research in Cardiology*, vol. 115, no. 4, p. 41, 2020.
- [65] R. Kerkelä, L. Grazette, R. Yacobi et al., "Cardiotoxicity of the cancer therapeutic agent imatinib mesylate," *Nature Medicine*, vol. 12, no. 8, pp. 908–916, 2006.
- [66] M. Lu, S. Merali, R. Gordon et al., "Prevention of doxorubicin cardiopathic changes by a benzyl styryl sulfone in mice," *Genes & Cancer*, vol. 2, no. 10, pp. 985–992, 2012.
- [67] F. Giamogante, L. Barazzuol, M. Brini, and T. Cali, "ER-mitochondria contact sites reporters: strengths and weaknesses of the available approaches," *International Journal of Molecular Sciences*, vol. 21, no. 21, p. 8157, 2020.

Research Article

ZBTB20 Positively Regulates Oxidative Stress, Mitochondrial Fission, and Inflammatory Responses of ox-LDL-Induced Macrophages in Atherosclerosis

Jun Tao,^{1,2} Junxiong Qiu,^{1,2} Liuyi Lu,^{1,2} Lisui Zhang,² Yuan Fu,² Meng Wang,² Jingjun Han,³ Maomao Shi,² Ling Li,² Zongkai Zhao,² Feng Wei,² Chao Wang,² Haifeng Zhang^{4,5}, Shi Liang^{1,2}, and Junmeng Zheng^{1,2}

¹Guangdong Provincial Key Laboratory of Malignant Tumor Epigenetics and Gene Regulation, Sun Yat-sen Memorial Hospital, Sun Yat-sen University, Guangzhou, China 510120

²Department of Cardiovascular Surgery, Sun Yat-sen Memorial Hospital, Sun Yat-sen University, Guangzhou, China 510120

³Department of Thoracic and Cardiac Surgery, The Eighth Affiliated Hospital, Sun Yat-sen University, Shenzhen, China 518033

⁴Department of Cardiology, Sun Yat-sen Memorial Hospital, Sun Yat-sen University, Guangzhou, China 510120

⁵Laboratory of Cardiac Electrophysiology and Arrhythmia in Guangdong Province, Guangzhou, China 510120

Correspondence should be addressed to Haifeng Zhang; zhanghf9@mail.sysu.edu.cn, Shi Liang; md02ls@mail2.sysu.edu.cn, and Junmeng Zheng; zhengjm27@mail.sysu.edu.cn

Received 6 January 2021; Revised 26 January 2021; Accepted 9 February 2021; Published 11 March 2021

Academic Editor: Yun-dai Chen

Copyright © 2021 Jun Tao et al. This is an open access article distributed under the Creative Commons Attribution License, which permits unrestricted use, distribution, and reproduction in any medium, provided the original work is properly cited.

Atherosclerosis (AS) is one of the most serious and common cardiovascular diseases affecting human health. AS is featured by the accumulation of plaques in vessel walls. The pathophysiology of AS is relevant in the low-density lipoprotein (LDL) uptake by macrophages, as well as the conversion of macrophages to foam cells. However, the mechanisms about how macrophages regulate AS have not been fully elucidated. In this study, we aimed to illuminate the roles of ZBTB20 and to excavate the underlying regulative mechanisms of ZBTB20 in AS. The microarray analysis revealed that ZBTB20 was a hub gene in the oxidative stress and inflammatory responses induced by oxidized LDL (ox-LDL) in AS. Correspondingly, our validation studies showed that ZBTB20 increased in either the human atherosclerotic lesion or the ox-LDL-stimulated macrophages. Moreover, the knockdown of ZBTB20 decreased M1 polarization, suppressed the proinflammatory factors, inhibited mitochondrial fission, and reduced the oxidative stress level of macrophages induced by ox-LDL. The mechanistic studies revealed that the ZBTB20 knockdown suppressed NF- κ B/MAPK activation and attenuated the mitochondrial fission possibly via regulating the nucleus translocation of NRF2, a pivotal transcription factor on redox homeostasis. Our *in vivo* studies showed that the sh-ZBTB20 adenovirus injection could reduce the progression of AS in apolipoprotein E-deficient (ApoE^{-/-}) mice. All in all, these results suggested that ZBTB20 positively regulated the oxidative stress level, mitochondrial fission, and inflammatory responses of macrophages induced by ox-LDL, and the knockdown of ZBTB20 could attenuate the development of AS in ApoE^{-/-} mice.

1. Introduction

AS is a chronic vascular disease featured by the accumulation of plaques within the vessel wall of the large- and middle-sized arteries [1, 2]. Up to date, various factors including hypertension, diabetes mellitus, high cholesterol level, smoking, and adiposity have been found to be associated with the development of AS [3, 4]. The pathophysiology of AS is

closely related to the LDL uptake by macrophages and subsequent differentiation into foam cells. The plaques formed by macrophages have different subtypes based on the activation stimuli and protein expression patterns. Thus, macrophages may exert either harmful effects or beneficial effects in the progression of AS [5, 6]. Recent studies have proposed that targeting of the macrophage may be a crucial target to ameliorate vulnerable plaques and subsequently alleviate AS [7].

However, the underlying mechanistic role of macrophages in the pathophysiology remains unclear. Hence, it is of paramount importance to further elucidate the underlying mechanisms of macrophage-mediated AS, which may provide novel therapies for the treatment.

Recently, studies demonstrated that mitochondria not only can regulate innate immune responses [8] but also can modulate the level of reactive oxygen species (ROS) to affect the homeostasis and inflammatory status of macrophages [9]. There is growing evidence showing that AS may be associated with the dysregulated mitochondrial function and bioenergetics [10]. Chen et al. demonstrated that CD36 signaling regulated mitochondrial metabolic reprogramming, which subsequently drives macrophage inflammatory responses in AS [11]. Besides, Dicer in macrophages was found to prevent AS by promoting mitochondrial oxidative metabolism [12]. Recently, myeloperoxidase-derived oxidant hypothiocyanous acid (HOSCN) was found to induce mitochondrial dysfunction in macrophages, which may be associated with the pathophysiology of AS [13]. Xin et al. also demonstrated that ox-LDL activates the dynamin-related protein 1 (DRP1) level as well as the mitochondrial fission status of macrophages [14].

ZBTB20, mainly known as a transcriptional repressor, is a member of the POZ and Krüppel family, with a zinc finger domain and an intact BTB domain [15, 16]. Up to date, the diverse functions of ZBTB20 have been reported, and studies demonstrated that ZBTB20 could regulate ion channels, remodeling, immunity, and inflammation [17–20]. In vascular diseases, especially in the development of AS, NF- κ B signaling functions as a key modulator in AS plaque initiation and evolution [21]. Emerging evidence suggests that the NF- κ B pathway was activated during the transformation of cholesterol-rich foam cells after taking in LDL, as well as the oxidation of LDL [22]. As for ZBTB20, in vascular diseases, it can regulate cardiac remodeling after myocardial infarction via ROS/TNF- α signaling [23]. Recently, a study by Liu et al. showed that ZBTB20 was able to inhibit the transcription of the *I κ B α* gene, which is a key element in NF- κ B signaling. Our study has also found that during the macrophage-mediated osteolysis, ZBTB20 could adjust the inflammatory response and polarization of macrophages via regulating *I κ B α* transcription and NF- κ B activation [18]. However, the roles of macrophage ZBTB20 during the progression of AS remain to be examined.

Here, we examined the expression of ZBTB20 in the macrophages stimulated by ox-LDL and the human AS lesions. Furthermore, the loss-of-function studies were carried out to determine the roles of ZBTB20 on the inflammatory responses, oxidative stress, and mitochondrial fission of the ox-LDL-stimulated macrophages. Besides, the subsequent signaling pathways were also examined. Finally, the effects of ZBTB20 on the AS progression were evaluated in the ApoE^{-/-} mice. In brief, the present study may provide novel insights into the roles of ZBTB20 in the pathophysiology and progression of AS.

2. Materials and Methods

2.1. Clinical Samples. Clinical samples were collected from 16 patients, including 9 males and 7 females (average age: 57.1

\pm 13.1 years). These patients have accepted bypass operation of the coronary artery because of coronary diseases from 2017 to 2019. Those coronary artery tissues containing AS were collected. The internal mammary artery tissues without AS were used as the control group. All procedures were carried out with the approval of the Ethics Committee of Sun Yat-sen University, Sun Yat-sen Memorial Hospital (SYSEC-KY-KS-2020-090).

2.2. Cell Lines and Cell Culture. The macrophages, RAW264.7, were from Procell Life Science & Technology. The RAW264.7 macrophages were cultured in high-glucose DMEM, containing 10% fetal bovine serum (FBS) [24]. Cells were cultured at 37°C and 5% CO₂. The macrophages were seeded 24 h before the experiments.

2.3. Small Interfering RNA (siRNA), Cell Transfections, and Treatments. The siRNA targeting ZBTB20 was synthesized by the RiboBio company (Guangzhou, China), and the scrambled siRNA was served as the negative control (NC). For the cell transfections, the ZBTB20-siRNA or the scrambled siRNA was transfected into the macrophages with RNAiMAX (Thermo Fisher Scientific) [25]. Forty-eight hours later, the transfected macrophages were collected for further experimentation.

The ox-LDL was from Yeasen Biotech Co., Ltd., and a concentration of 50 μ g/ml was adopted for respective time durations. After that, the macrophages were subjected to further experimental assays. The NRF2 inhibitor (ML385) was purchased from Selleck, and a concentration/duration of 5 μ M/24 h was used before further experimental assays [26].

2.4. Oil Red O Staining. After treatment, the RAW264.7 macrophages were treated with 4% PFA for 15 min and stained with oil red O solution for 60 min. For the mouse aortas, the adipose tissues were stripped from the aortas [27]. After washing with PBS three times, the aortas were stained with oil red O solution for 60 min. The stained macrophages and tissues were imaged using a biomicroscope (DM2000, Leica).

2.5. Dil-ox-LDL Uptake of Macrophages. The macrophages were incubated with red fluorescence-labeled Dil-ox-LDL (50 μ g/ml; Yeasen Biotech Co., Ltd.) for 24 h at 37°C [28]. After that, the macrophages were washed by PBS three times, and a biomicroscope (DM2000, Leica) was used.

2.6. PPI Network Construction and Identification of Hub Genes. A microarray data of the GSE54666 dataset was obtained from the GEO database. The STRING database and Cytoscape software were used to construct a protein-protein interaction network (PPIN) of differentially expressed genes (DEGs). The topology property of the network was analyzed using the MCODE application of Cytoscape software. The functional clustering of the DEGs was performed using the Metascape online tool (<https://metascape.org>).

2.7. RNA Extraction and qRT-PCR. RNAiso Plus (TaKaRa) was used to collect the RNA of RAW264.7 macrophages. A NanoDrop instrument was used to measure the concentrations of RNA [29]. After that, cDNA was obtained by reverse-transcribing RNA with PrimeScript RT Mix (TaKaRa). Then,

qRT-PCR was carried out on a Roche Real-Time PCR System using SYBR Green Mix (Yeasen Biotech Co., Ltd.). Table 1 shows the primers used.

2.8. Western Blot Assay and ELISA. The total protein from RAW264.7 macrophages was obtained by using the RIPA buffer (Beyotime). A nuclear and cytoplasmic extraction kit (CWbiotech) was used to, respectively, obtain the cytosolic protein and nuclear protein. A total of 30 μ g protein in each lane was prepared, followed by separating in a 10% polyacrylamide SDS-PAGE gel [30]. After transferring, the PVDF membranes were then blocked with 5% BSA, then incubated with different antibodies including NRF2, Histone H3, p-JNK, KEAP1, DRP1, p-ERK, FIS1, ZBTB20, p-p65, I κ B α , p-p38, IRF3, p-IRF3, and GAPDH (Cell Signaling Technology) [31]. After the incubation, a secondary antibody with linked HRP (Cell Signaling Technology), an ECL detection kit (Yeasen Biotech Co., Ltd.), and a digital imaging system (Kodak) were used.

To detect the cytokines, including TNF- α , IL-6, and IFN- β , the macrophage supernatants were collected, followed by detection with ELISA kits (Neobioscience Technology Co., Ltd.).

2.9. Flow Cytometry for Macrophage Polarization and ROS Detection. For the detection of macrophage polarization, iNOS and CD206 were adopted as M1 and M2 polarization markers [32]. Briefly, after incubating in the fixation buffer and washing by the perm/wash buffer, the RAW264.7 macrophages were then incubated in the iNOS antibody or CD206 antibody for 20 min, respectively. After that, these macrophages were washed three times, resuspended in 200 μ l PBS for each sample, and analyzed with BD Biosciences flow cytometry.

The ROS production was evaluated using a 2',7'-DHE-DA staining kit (KeyGen Biotech). A concentration of 2 μ M and an incubation duration of 20 min were adopted [33]. After the incubation, the ROS-positive cell numbers were detected by BD Biosciences flow cytometry, and the fluorescence intensity of the ROS probe was observed on an Olympus fluorescence microscope.

2.10. Mitochondrial Staining of Macrophages. The mitochondrial staining of the macrophages was performed using the MitoTracker Red CMXRos reagent (Beyotime). Briefly, RAW264.7 macrophages after different treatments were incubated with the MitoTracker Red CMXRos reagent for 30 min [34]. Then, the cells were counterstained with DAPI for 10 min and imaged under an Olympus fluorescence microscope.

2.11. In Vivo Animal Models of Atherosclerosis and Atherosclerotic Lesion Analysis. Adenovirus expressing sh-ZBTB20 or sh-NC was purchased from GeneChem. The ApoE^{-/-} mice (20-30 grams, 8-10 weeks) were purchased from GemPharmatech Co. Ltd. To study the effects of the ZBTB20 knockdown on the AS mouse model, the animals were injected with adenovirus expressing sh-ZBTB20 or sh-NC via the tail, and then the ApoE^{-/-} mice were fed with a high-fat diet for 12 weeks. At the end of the experiments [35], the animals were killed by an overdose of pentobarbi-

TABLE 1: Primers used in this study.

ZBTB20	Forward	GTGGACCGAATCTACTCCGC
	Reverse	CATGAATGCGTGTGATCCAGC
iNOS	Forward	GGAGTGACGGCAAACATGACT
	Reverse	TCGATGCACAACCTGGGTGAAC
COX-2	Forward	TGCACTATGGTTACAAAAGCTGG
	Reverse	TCAGGAAGCTCCTTATTTCCCTT
GAPDH	Forward	TGTGTCCGTCGTGGATCTGA
	Reverse	TTGCTGTTGAAGTCGCAGGAG

tone (80 mg/kg, intravenous injection), and the tissues were collected for further experimental assays. All the guidelines of the Institutional Animal Care and Use Committee of Sun Yat-sen University were followed during the animal experiments [36].

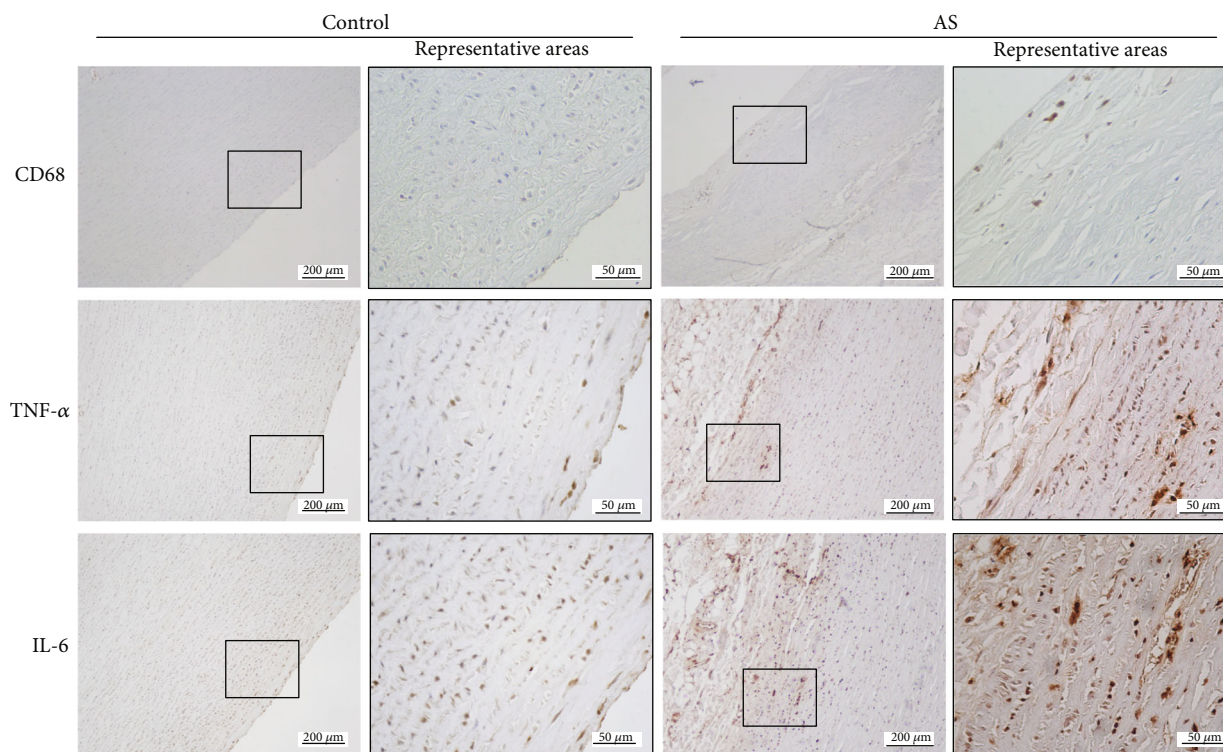
The collected tissues were fixed and embedded, then sliced into sections using a microtome. The sections were then dewaxed using the xylene. The H&E staining kit (Beyotime), CD68 antibody (Servicebio), Masson stain kit (Solarbio), α -SMA antibody (Beyotime), and EVG stain kit (Abcam) were used to evaluate the AS lesions [37].

2.12. Immunofluorescent Staining of Macrophages. For the immunofluorescent staining of the macrophages, the macrophages with different treatments were fixed with 4% PFA, followed by incubation with 0.1% Triton X-100 and blocking with 1% BSA. Then, the macrophages were incubated with TNF- α , IL-6, p65, IRF3, or NRF2 antibodies (Cell Signaling Technology) overnight at 4°C [38]. Alexa Fluor 555 conjugate immunofluorescent secondary antibodies and a Carl Zeiss confocal microscope were used to observe the macrophages.

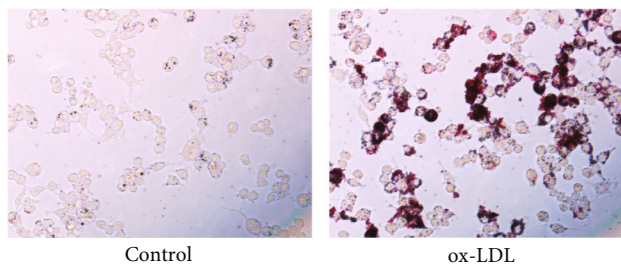
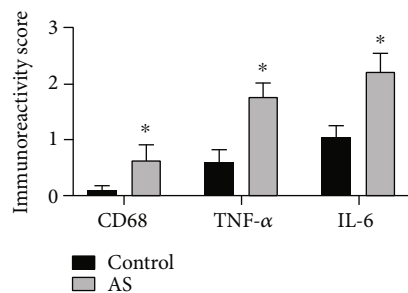
2.13. Statistical Analysis. Data are presented as mean \pm standard deviation. The data normality was analyzed by the Kolmogorov-Smirnov test. Two-sided Student's *t*-test and one-way analysis of variance followed by Fisher's least significant difference test were performed with the SPSS 20.0 software. The differences between means were considered significant when $P < 0.05$.

3. Results

3.1. TNF- α and IL-6 Were Upregulated in the AS Lesions and the ox-LDL-Stimulated Macrophages. Firstly, we examined the expression levels of CD68, TNF- α , and IL-6 in the lesion area from the patients with AS by IHC staining. The protein expression of CD68, TNF- α , and IL-6 was significantly upregulated in the lesion area from the patients with AS compared to the control group (Figures 1(a) and 1(b)). We further treated the macrophages with ox-LDL for 24 h, and the differentiation of macrophages into foam cells was observed by oil red O staining (Figure 1(c)). In addition, the fluorescence microscope showed that the macrophages could directly take in Dil-ox-LDL, which was red fluorescence-labeled (Figure 1(d)). The ELISA results showed that inflammatory cytokines were also significantly elevated in the macrophages induced by ox-LDL



(a)

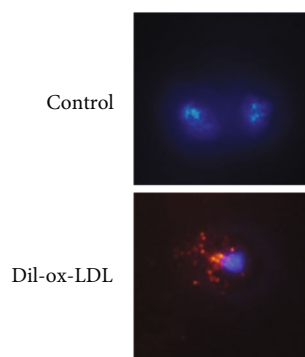


Control

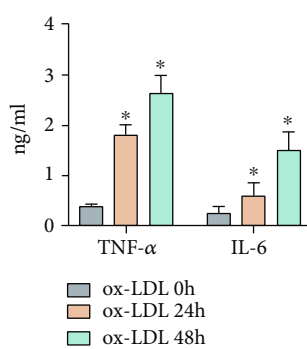
ox-LDL

(b)

(c)



(d)



(e)

FIGURE 1: Continued.

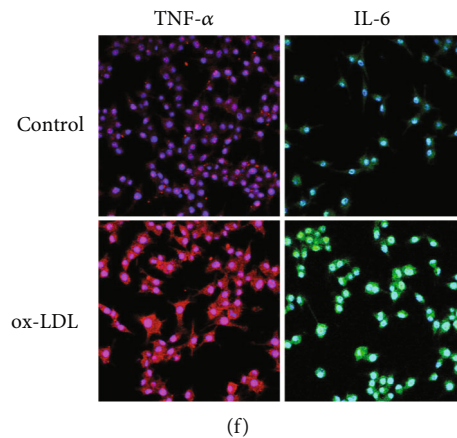


FIGURE 1: TNF- α and IL-6 were upregulated in the atherosclerotic aorta and the ox-LDL-stimulated macrophages. (a) The protein expression of CD68, TNF- α , and IL-6 in the normal aorta and atherosclerotic aorta was determined by immunofluorescent staining. (b) The immunostaining scores in the normal aorta and atherosclerotic aorta were determined. (c) The uptake of ox-LDL by macrophages was assessed by oil red O staining. (d) The uptake of Dil-ox-LDL by macrophages was assessed by immunofluorescent staining. (e) The TNF- α and IL-6 cytokines secreted by macrophages after being treated with ox-LDL for 0, 24, and 48 h, respectively, were determined by ELISA. (f) The TNF- α and IL-6 protein expression levels in the macrophages after being treated with ox-LDL for 24 h were determined by immunofluorescent staining. $N = 3$; significant differences between treatment groups were shown as $*P < 0.05$.

for 24 h and 48 h (Figure 1(e)). In addition, the mRNA levels of TNF- α and IL-6 were upregulated and induced by ox-LDL (Fig. S1A). Consistently, the fluorescent signaling intensities of these two inflammatory proteins significantly increased in macrophages because of the treatment of ox-LDL (Figure 1(f)).

3.2. ox-LDL Increased the Oxidative Stress and Mitochondrial Injury via Modulating NRF2. Here, ox-LDL treatment significantly enhanced the ROS production in the macrophages and also raised the number of ROS-positive macrophages (Figures 2(a) and 2(b) and Fig. S1B). The Western blot results showed that ox-LDL stimulation significantly raised the protein level of NRF2 in the nucleus of macrophages but decreased NRF2 and KEAP1 protein levels in the cytoplasm of the macrophages (Figures 2(c) and 2(d) and Fig. S1C-S1D). Moreover, the MitoTracker staining showed that ox-LDL stimulation significantly induced the mitochondrial injury of the macrophages (Figure 2(e)). Besides, the ox-LDL stimulation for 4 and 8 h both increased the protein levels of DRP1 and FIS1 in the macrophages (Figure 2(f) and Fig. S1E).

3.3. ZBTB20 Was Identified as the Hub Gene Associated with Oxidative Stress and Inflammation in ox-LDL-Stimulated Macrophages. The DEGs between the treatment group and the control group from the GSE54666 dataset were illustrated in the volcano plot and heat map, respectively (Figures 3(a) and 3(b)). A total of 642 DEGs were identified, including 357 upregulated DEGs and 285 downregulated DEGs. The DEGs were then subjected to the PPI network construction by using the STRING database, and a total of 538 nodes and 2037 edges were identified in the PPI network. The top 15 significant GO terms and KEGG pathways from the GO categories and KEGG database were shown in Fig. S2A, and the four most significant KEGG pathways analyzed with GSEA were shown in Fig. S2B. Furthermore, the hub genes

were extracted using the MCODE application in the Cytoscape software. Eighty-six hub genes were identified, and the ZBTB20 gene had a high score among them (Figure 3(c)). Besides, the hub gene network was obtained according to the core gene scores by the cytoHubba plug-in (Figure 3(d)). The functional clustering of the hub genes showed that ZBTB20 was associated with oxidative stress, inflammation, and cytokines (Figure 3(e)).

3.4. ZBTB20 Promoted the Inflammatory Responses of the ox-LDL-Stimulated Macrophages. The expression of ZBTB20 as illustrated by the IHC staining was significantly upregulated in the lesion area from the patients with AS compared to the control group (Figure 4(a)). Western blot as well as qRT-PCR showed that ox-LDL time-dependently increased the expression of ZBTB20 in the macrophages not only in the mRNA level but also in the protein level (Figures 4(b) and 4(c) and Fig. S3A). The Western blot result of ZBTB20-siRNA knockdown efficiency was shown in Fig. S3B. The ELISA results showed that the knockdown of ZBTB20 significantly reduced the inflammatory cytokine levels secreted by ox-LDL-induced macrophages (Figure 4(d)). Consistently, the ZBTB20 knockdown significantly reduced the fluorescent signaling intensities of TNF- α and IL-6 proteins in ox-LDL-induced macrophages (Figure 4(e)).

3.5. ZBTB20 Knockdown Suppressed the NK- κ B and MAPK Signaling Activities in the ox-LDL-Stimulated Macrophages. Here, the effects of the ZBTB20 knockdown on the ox-LDL uptake of macrophages were determined by fluorescent staining and flow cytometry. As shown in Figures 5(a) and 5(b) and Fig. S3C, the ZBTB20 knockdown had no significant effects on the Dil-ox-LDL-positive macrophage ratios as determined by flow cytometry. Consistently, there was no significant difference in the fluorescent signaling intensity of Dil-ox-LDL in the macrophages between the NC-siRNA

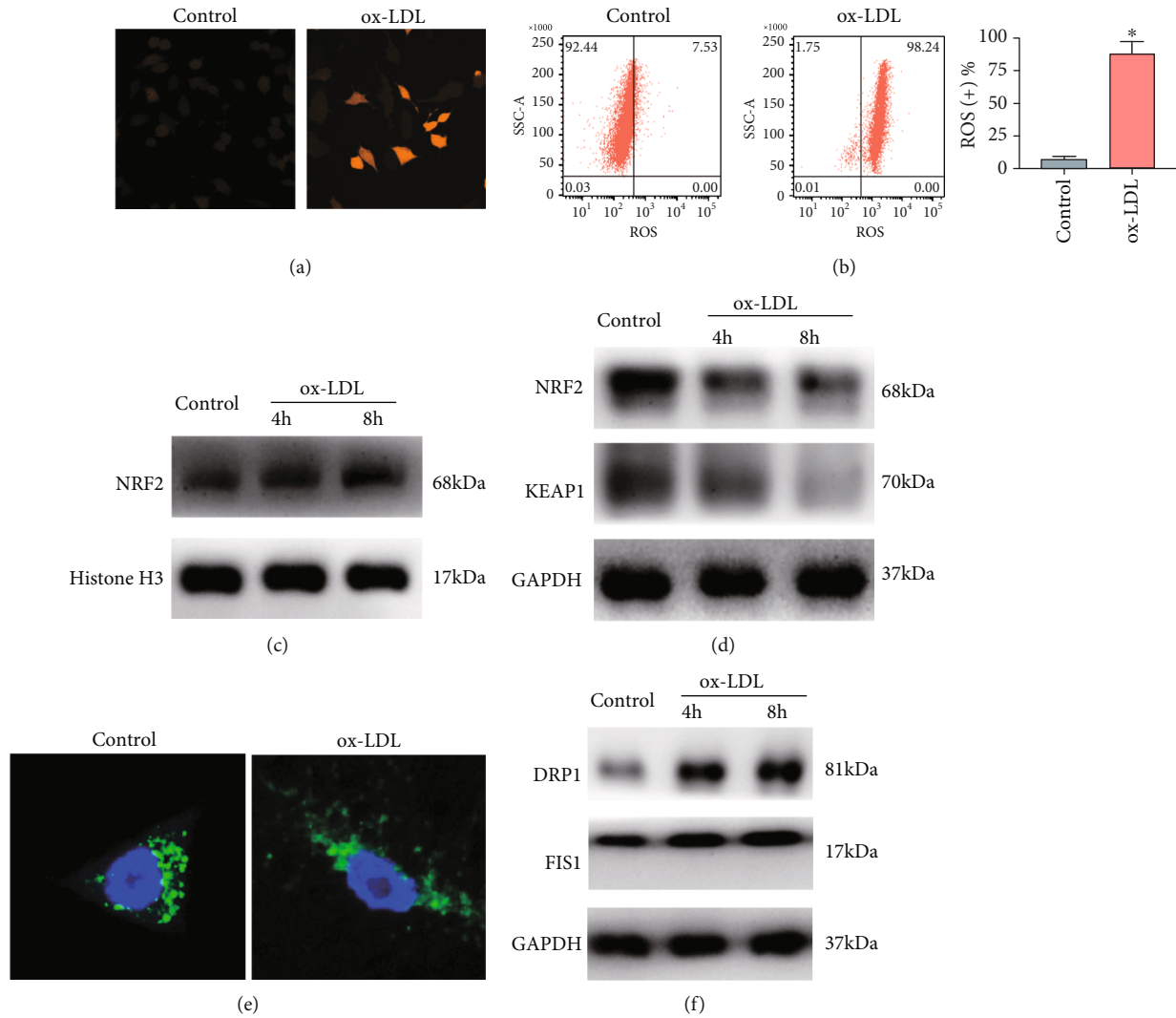


FIGURE 2: ox-LDL increased the oxidative stress and mitochondrial injury via modulating NRF2. (a) The ROS level of the PBS- or ox-LDL-treated macrophages was determined by immunofluorescent staining. (b) The ROS-positive rates of the PBS- or ox-LDL-treated macrophages with different treatments were determined by flow cytometry. (c) The protein level of NRF2 in the nucleus of the PBS- or ox-LDL-treated macrophages was assessed by Western blot assay. (d) The protein level of NRF2 and KEAP1 in the cytoplasm of the PBS- or ox-LDL-treated macrophages was assessed by Western blot assay. (e) The mitochondrial injury of the PBS- or ox-LDL-treated (6 h) macrophages was assessed by MitoTracker staining. (f) The protein level of DRP1 and FIS1 in the PBS- or ox-LDL-treated (6 h) macrophages with respective treatments was assessed by Western blot assay. $N = 3$; significant differences between treatment groups were shown as $^*P < 0.05$.

and ZBTB20-siRNA groups as determined by flow cytometry (Figure 5(c)).

The effects of the ZBTB20 knockdown on the protein levels of the $\text{NK-}\kappa\text{B}$ -related mediators in the macrophages were determined by the Western blot assay. Interestingly, the ZBTB20 knockdown significantly reduced the protein level of p-p65 but increased that of $\text{I}\kappa\text{B}\alpha$ in the ox-LDL-stimulated macrophages when compared to the PBS-treated macrophages (Figure 5(d) and Fig. S3D). Consistently, the fluorescent staining showed that the ZBTB20 knockdown suppressed the nucleus translocation of p65 in the ox-LDL-stimulated macrophages (Figure 5(e)). In addition, the MAPK-related mediators were also examined, and as shown in Figure 5(f) and Fig. S3E, the ZBTB20 knockdown signifi-

cantly downregulated the phosphorylation levels of JNK, ERK, and p38 induced by ox-LDL in macrophages.

3.6. ZBTB20 Knockdown Suppressed M1 Polarization, Increased M2 Polarization, and Inhibited the Phosphorylation and Nucleus Translocation of IRF3. Here, the effects of the ZBTB20 knockdown on M1/M2 polarization of macrophages were determined by flow cytometry, and as presented in Figure 6(a) and Fig. S4A-S4B, the percentage of macrophages with M1 polarization significantly decreased, and the percentage of macrophages with M2 polarization increased in the ZBTB20-siRNA group compared to the NC-siRNA group. The qRT-PCR results showed that the ZBTB20 knockdown downregulated the mRNA level of iNOS, an M1 polarization

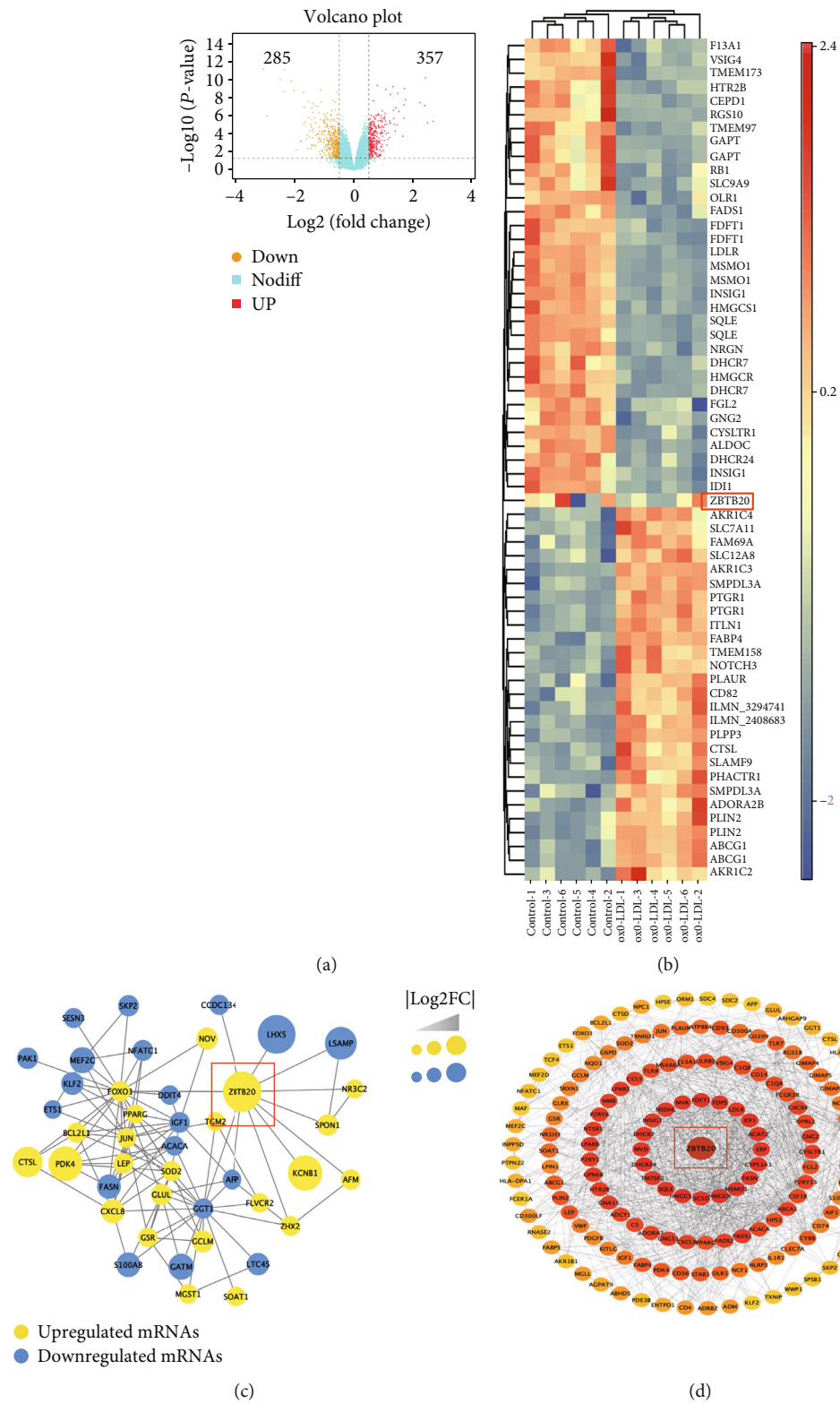


FIGURE 3: Continued.

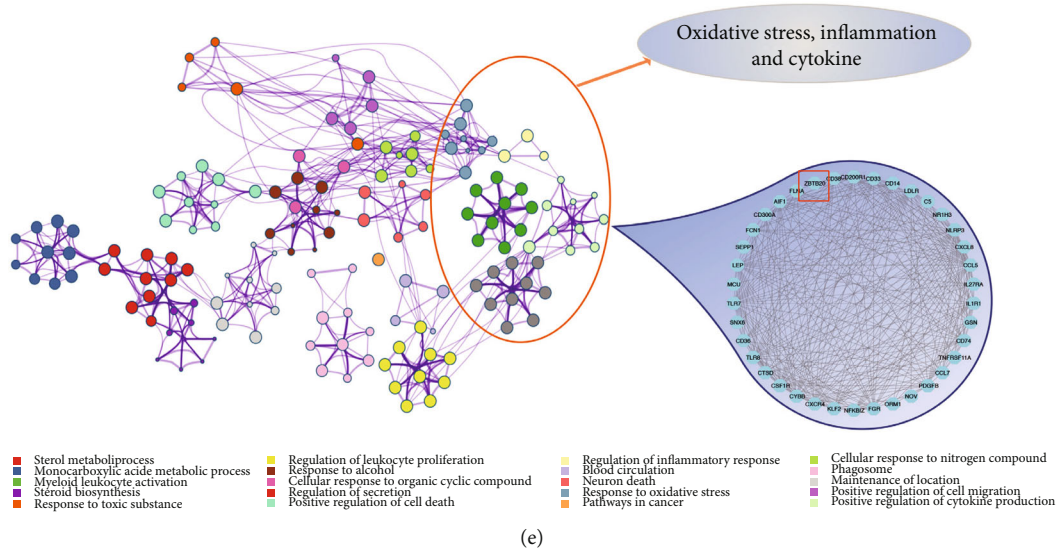


FIGURE 3: ZBTB20 was identified as the hub gene associated with oxidative stress, inflammation, and cytokines in the ox-LDL-stimulated macrophages. (a) Volcano plots and (b) heat map illustration of the differentially expressed genes between control macrophages and ox-LDL-stimulated macrophages. (c) The hub genes from the PPI network were further identified using the MCODE app from Cytoscape software. (d) The cytoHubba plug-in from Cytoscape software was used, and the hub gene network was obtained according to the core gene scores. (e) The functional clustering of genes associated with oxidative stress, inflammation, and cytokines was performed using the Metascape database.

marker, but upregulated the mRNA level of COX-2, an M2 polarization marker, in the ox-LDL-stimulated macrophages (Figure 6(b)). Interestingly, the Western blot results showed that the ZBTB20 knockdown significantly suppressed the phosphorylation of the IRF3 in the ox-LDL-stimulated macrophages, but not in the PBS-treated macrophages (Figure 6(c) and Fig. S4C). In addition, the fluorescent staining results showed that the ZBTB20 knockdown repressed the nucleus translation of IRF3 in the ox-LDL-stimulated macrophages (Figure 6(d)). ELISA showed that the ZBTB20 knockdown reduced the cytokine levels of IFN- β in the ox-LDL-stimulated macrophages (Figure 6(e)).

3.7. ZBTB20 Regulated Oxidative Stress and Mitochondrial Fission in ox-LDL-Stimulated Macrophages via Modulating NRF2. The ROS production in the macrophages with respective treatments was analyzed using fluorescent staining and flow cytometry. The fluorescent staining results showed that the treatment of ox-LDL significantly increased the ROS level in the macrophages, which was significantly attenuated by the ZBTB20 knockdown (Figure 7(a)). Consistently, the ZBTB20 knockdown attenuated the ox-LDL-induced increase of ROS-positive macrophages, and more importantly, the effects of the ZBTB20 knockdown on the number of ROS-positive macrophages were antagonized by the treatment of ML385, a novel NRF2 inhibitor (Figures 7(b) and 7(c) and Fig. S4D). The fluorescent staining results showed that the knockdown of ZBTB20 enhanced the nucleus translocation of NRF2 induced by ox-LDL, which was also attenuated by ML385 treatment (Figure 7(d)). Consistently, the ZBTB20 knockdown increased the nuclear expression level of NRF2 protein in ox-LDL-stimulated macrophages as determined by the Western blot

assay (Figure 7(e) and Fig. S4E). Furthermore, MitoTracker staining showed that the ZBTB20 knockdown prevented the mitochondrial injury in the macrophages (Figure 7(f)), and the increased protein expression levels of DRP1 and FIS1 induced by ox-LDL were significantly attenuated by the ZBTB20 knockdown as well (Figure 7(g) and Fig. S4F-S4G).

3.8. Knockdown of ZBTB20 Attenuates the Development of AS in ApoE^{-/-} Mice. The effects of the ZBTB20 knockdown on the progression of AS were evaluated in ApoE^{-/-} mice, which were fed with a high-fat diet for 12 weeks. As shown in Figure 8(a), the tail vein injection of the adenovirus expressing sh-ZBTB20 significantly reduced the aorta lesion in the ApoE^{-/-} mice when compared to animals treated with control adenovirus. The H&E staining showed consistent results (Figure 8(b)). Furthermore, the foam cells in the aorta were stained by the oil red, and the lesion area significantly decreased in the sh-ZBTB20 group (Figure 8(c)). Besides, we performed Masson staining for collagen content, IHC staining for smooth muscle cell (SMC) content (α -SMA (α -smooth muscle actin)), and macrophage accumulation (CD68) in whole aortas from sh-NC-treated ApoE^{-/-} mice and sh-ZBTB20-treated ApoE^{-/-} mice (Figure 8(d)), and the results showed that the knockdown of ZBTB20 attenuated the macrophage accumulation in the progression of AS but had no effects on collagen or SMC content.

4. Discussion

AS progression is closely related to proinflammatory and proatherogenic mediators, which can promote plaque formation and stenosis progression [39]. In the initiation of AS, high levels of ox-LDL can recruit monocytes, promoting the

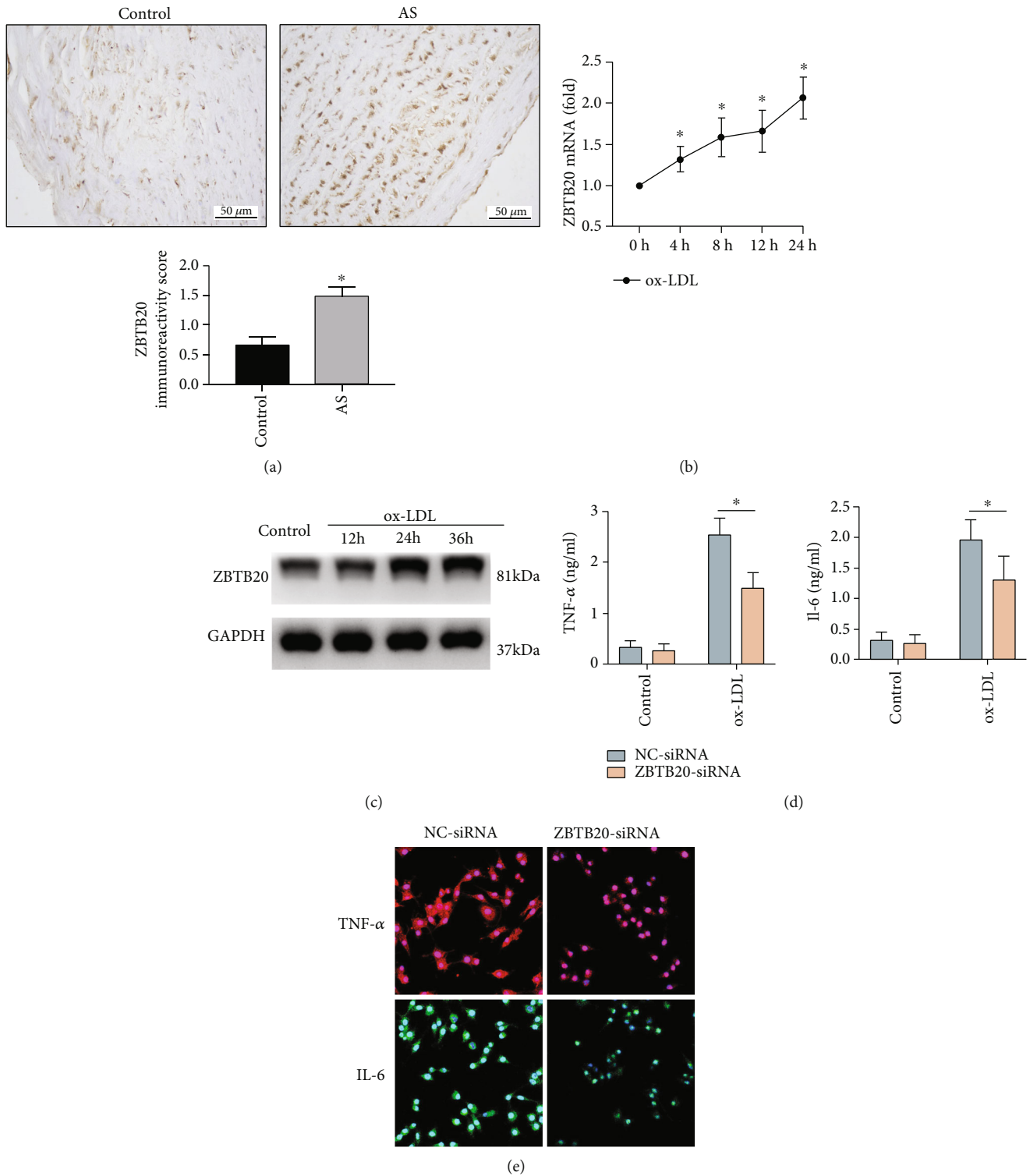


FIGURE 4: ZBTB20 promotes the inflammatory responses of the ox-LDL-stimulated macrophages. (a) The protein expression of ZBTB20 in the normal aorta and atherosclerotic aorta was determined by immunofluorescent staining. The (b) mRNA and (c) protein expression levels of ZBTB20 in the macrophages after being treated with ox-LDL for 0, 4, 8, or 24 h were determined by qRT-PCR and Western blot assays, respectively. (d) The TNF- α and IL-6 protein expression levels in the PBS- or ox-LDL-treated macrophages after being transfected with scrambled siRNA (NC) or si-ZBTB20 were determined by ELISA. (e) The TNF- α and IL-6 protein expression levels in the ox-LDL-treated macrophages after being transfected with scrambled siRNA (NC) or si-ZBTB20 were evaluated by immunofluorescent staining. $N = 3$; significant differences between treatment groups were shown as $*P < 0.05$.

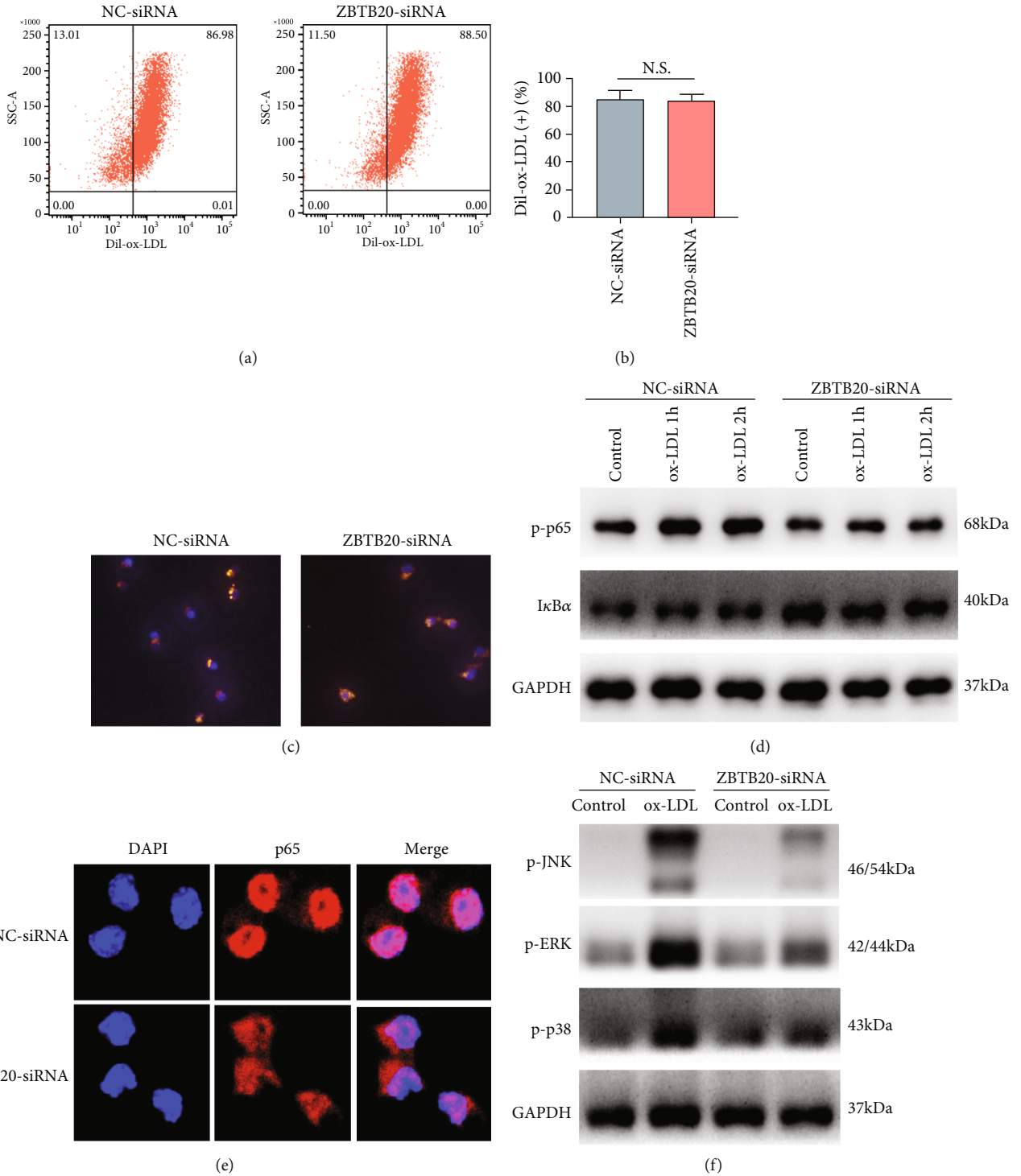


FIGURE 5: ZBTB20 knockdown suppresses the NF- κ B and MAPK signaling activities in the ox-LDL-stimulated macrophages. (a, b) The ox-LDL uptake of macrophages after being transfected with scrambled siRNA (NC) or si-ZBTB20 was determined by flow cytometry. (c) The ox-LDL uptake of macrophages after being transfected with scrambled siRNA (NC) or si-ZBTB20 was determined by immunofluorescent staining. (d) The protein expression levels of the NF- κ B-related mediators in the PBS- or ox-LDL-treated macrophages after being transfected with scrambled siRNA (NC) or si-ZBTB20 were determined by Western blot assay. (e) The protein expression level of p65 in ox-LDL-treated (1 h) macrophages after being transfected with scrambled siRNA (NC) or si-ZBTB20 was determined by immunofluorescent staining. (f) The protein expression levels of the MAPK-related mediators in the PBS- or ox-LDL-treated (1 h) macrophages after being transfected with scrambled siRNA (NC) or si-ZBTB20 were determined by Western blot assay. $N = 3$.

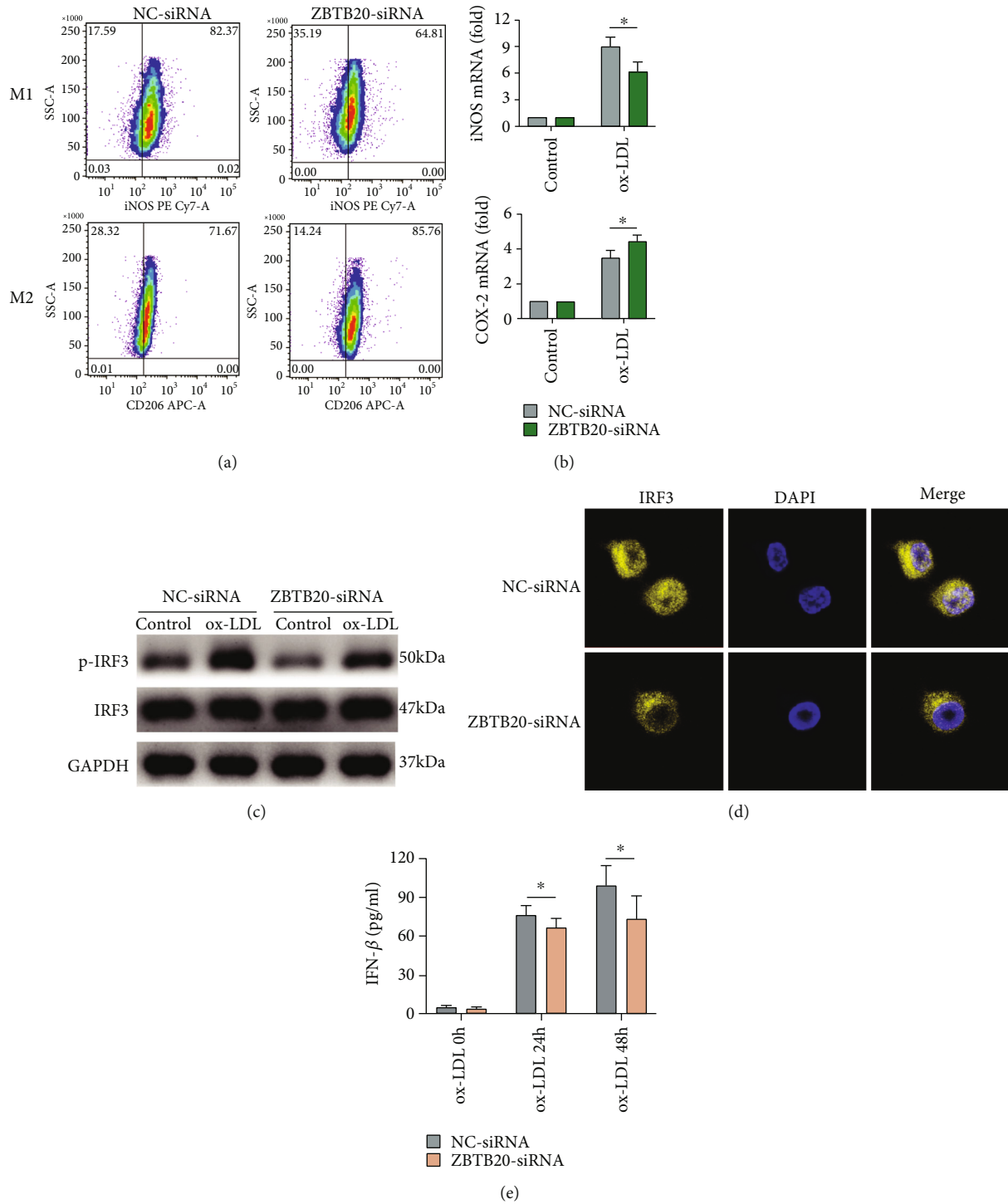


FIGURE 6: ZBTB20 knockdown suppresses the M1 polarization, increases the M2 polarization, and inhibits the phosphorylation and nucleus translocation of IRF3 in the ox-LDL-stimulated macrophages. (a) The M1 and M2 polarization of the ox-LDL-treated (24 h) macrophages after being transfected with scrambled siRNA (NC) or si-ZBTB20 was determined by flow cytometry. (b) The mRNA expression level of the iNOS in the PBS- or ox-LDL-treated (24 h) macrophages after being transfected with scrambled siRNA (NC) or si-ZBTB20 was determined by qRT-PCR. (c) The phosphorylation level of the IRF3 in the PBS- or ox-LDL-treated (8 h) macrophages after being transfected with scrambled siRNA (NC) or si-ZBTB20 was determined by Western blot assay. (d) The nucleus translocation of IRF3 in the ox-LDL-treated (8 h) macrophages after being transfected with scrambled siRNA (NC) or si-ZBTB20 was determined by immunofluorescent staining. (e) The cytokine level of IFN- β in the ox-LDL-treated macrophages after being transfected with scrambled siRNA (NC) or si-ZBTB20 was determined by ELISA. $N = 3$; significant differences between treatment groups were shown as * $P < 0.05$.

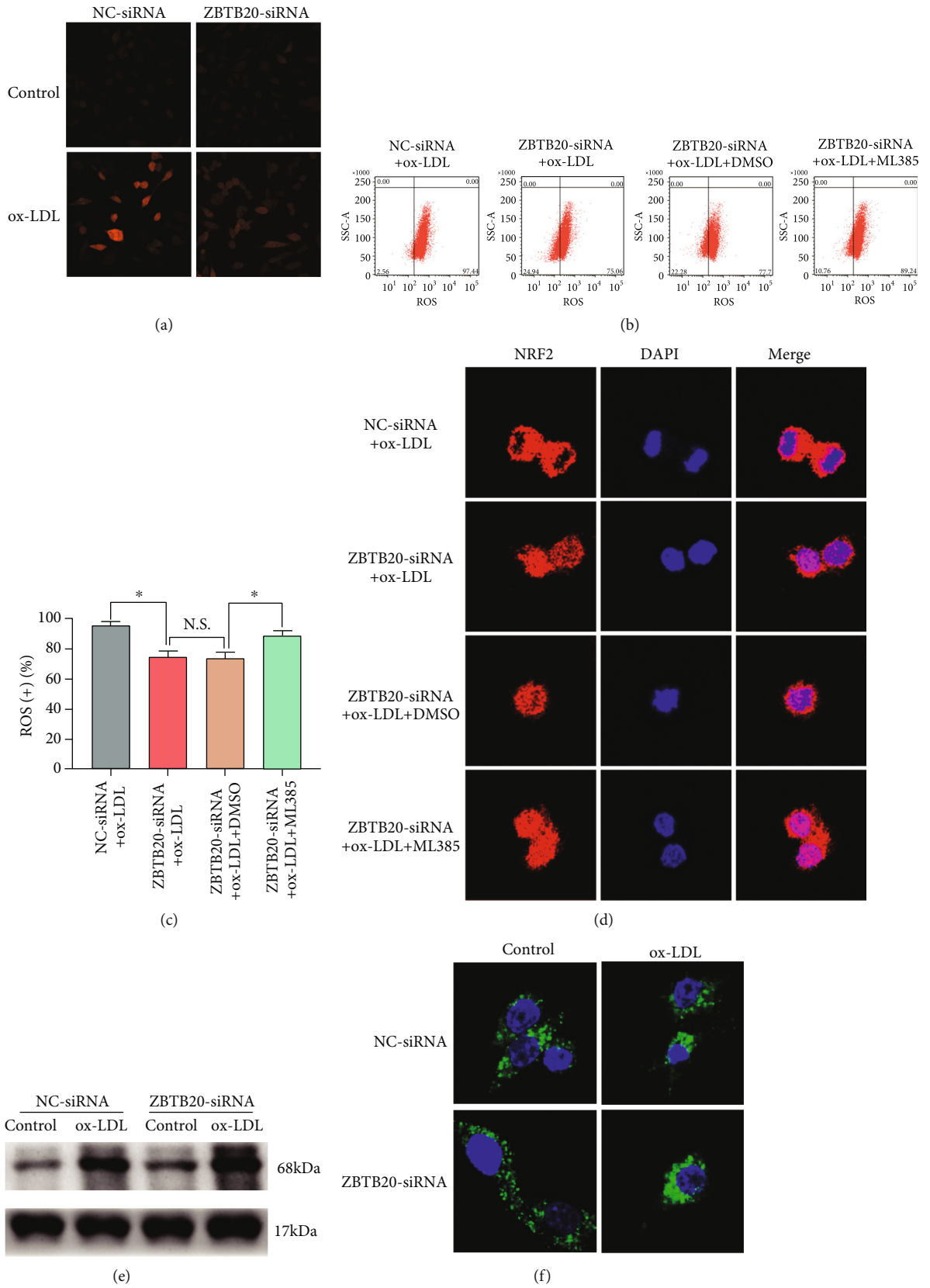


FIGURE 7: Continued.

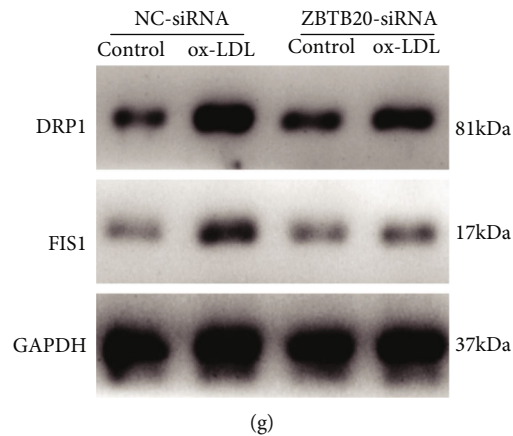


FIGURE 7: ZBTB20 positively regulates oxidative stress and mitochondrial fission in ox-LDL-stimulated macrophages via modulating NRF2. (a) The ROS level in the PBS- or ox-LDL-treated macrophages after being transfected with scrambled siRNA (NC) or si-ZBTB20 was determined by immunofluorescent staining. (b, c) The ROS-positive rates of the macrophages with different treatments were determined by flow cytometry. (d) The nucleus translation of NRF2 in the ox-LDL-stimulated macrophages with respective treatments was determined by immunofluorescent staining. (e) The protein level of NRF2 in the nucleus of the macrophages with respective treatments was assessed by Western blot assay. (f) The mitochondrial injury of the macrophages with respective treatments was assessed by MitoTracker staining. (g) The protein level of DRP1 and FIS1 in the macrophages with respective treatments was assessed by Western blot assay. $N = 3$; significant differences between treatment groups were shown as $*P < 0.05$.

adhesion molecule expression on the endothelium and the subsequent adhesion of the monocytes to the intima [40]. Here, our microarray analysis revealed that ZBTB20 was identified as the hub gene in the ox-LDL-stimulated macrophages. The validation studies showed that ZBTB20 was upregulated in the human AS lesions and ox-LDL-stimulated macrophages. The loss-of-function studies showed that the ZBTB20 knockdown suppressed the proinflammatory cytokine levels, decreased the M1 polarization, and reduced the oxidative stress and mitochondrial fission in the ox-LDL-stimulated macrophages. The mechanistic studies showed that the ZBTB20 knockdown not only suppressed the NF- κ B and MAPK signaling activities but also inhibited the nucleus translocation of NRF2 in the ox-LDL-stimulated macrophages. Our *in vivo* data showed that the ZBTB20 knockdown attenuated the development of AS in ApoE^{-/-} mice.

The present study showed the increased expression levels of proinflammatory factors in the human AS lesions and ox-LDL-stimulated macrophages, which was consistent with previous studies [41, 42]. These results indicated the increased inflammatory response in the macrophages during AS. The upregulation of ZBTB20 in human AS lesions and ox-LDL-stimulated macrophages suggested that ZBTB20 may promote the initiation and progression of AS. Thus, we performed the loss-of-function studies by silencing the ZBTB20 gene. In this study, the knockdown of ZBTB20 suppressed proinflammatory protein levels in ox-LDL-induced macrophages, which was consistent with studies by Qiu et al., showing that ZBTB20 silencing suppressed the inflammatory responses in titanium particle-stimulated or lipopolysaccharide- (LPS-) stimulated macrophages [18]. In addition, the ZBTB20 knockout was reported to decrease the serum levels of IL-6 and TNF- α in LPS-treated mice [20]. AS is an inflammatory disease, and NF- κ B functions as a major transcription factor in inflamma-

tory and immune responses [43, 44]. Thus, we further examined the roles of the ZBTB20 knockdown on NF- κ B activities, and we found that the ox-LDL stimulation increased the activities of macrophage NF- κ B signaling, which was consistent with findings from previous studies [45, 46]. ZBTB20 was also found to promote the activity of NF- κ B in the gastric cancer cells and human dental pulp stem cells [47, 48]. Besides, the present study showed that ox-LDL enhanced the activity of MAPK, another inflammatory signaling, in macrophages, which was consistent with previous reports from Taketa et al. [49]. Here, our further results revealed that the ZBTB20 knockdown reduced MAPK activity in ox-LDL-stimulated macrophages. However, studies from Liu et al. showed that ZBTB20 had no effects on Toll-like receptor-triggered activation of MAPK [20]. The inconsistent effects of ZBTB20 on the activity of MAPK in macrophages among different studies might be attributed to the different stimuli used. Collectively, in this study, the inhibitory effects of the ZBTB20 knockdown on the inflammatory responses in the macrophages may be related to the impaired activity of NF- κ B and MAPK.

Macrophages can be divided into M1 or M2 type, depending on the polarization state, all of which were derived from monocytes [50]. Recent studies showed that M2 macrophages could clear dying cells and debris and secrete anti-inflammatory factors, which can attenuate the formation of AS plaques [51]. Our results showed that the ZBTB20 knockdown increased the M2 macrophage polarization but decreased the M1 macrophage polarization, implying that the ZBTB20 knockdown may attenuate AS by activating M2 macrophages. IRF3 is a key interferon-regulator factor in regulating the M2 polarization of macrophages, and IRF3 can cooperate with NF- κ B to launch IFN- β gene transcription [52]. Consistently, our data showed that the

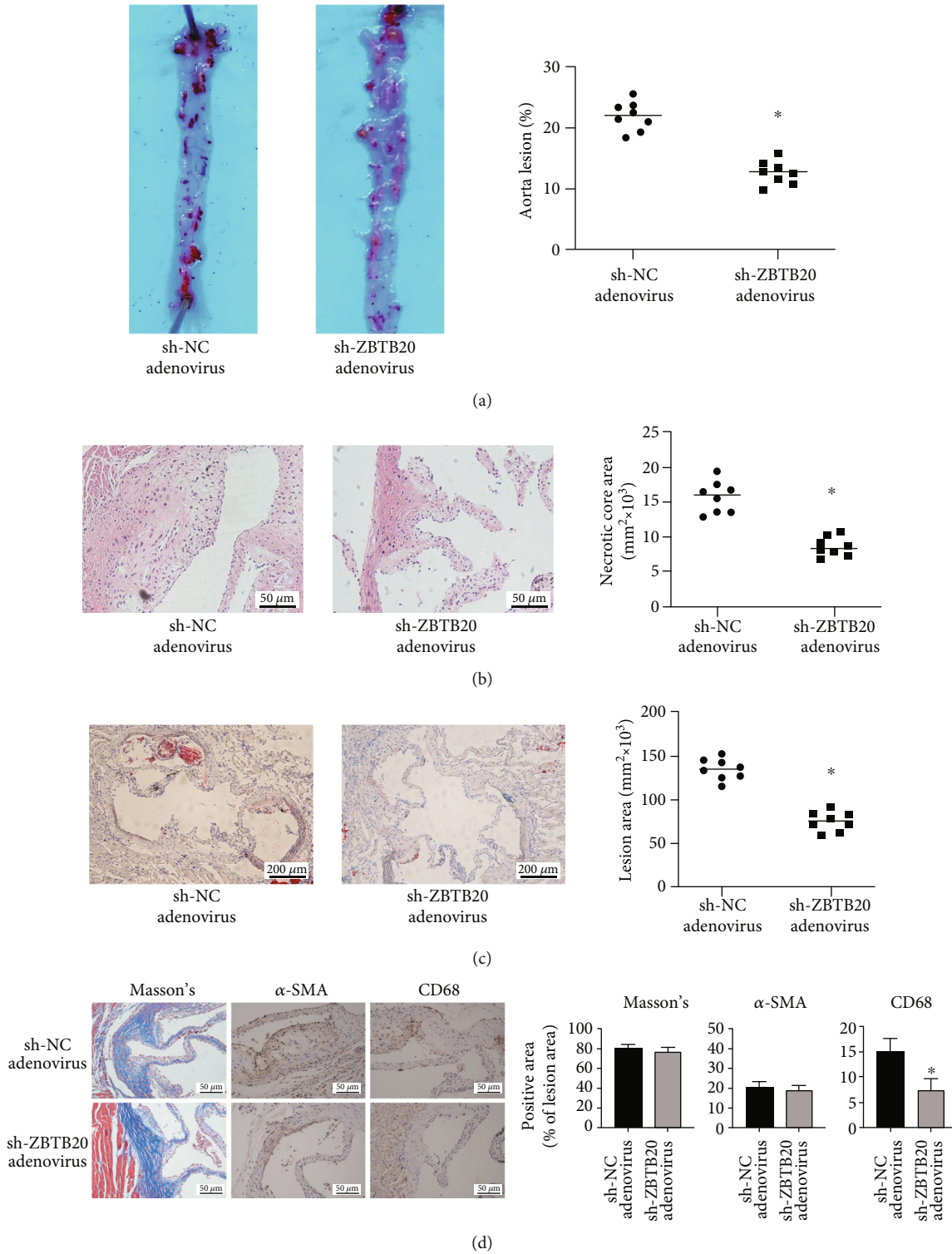


FIGURE 8: Knockdown of ZBTB20 attenuates the progression of the atherosclerosis of the ApoE^{-/-} mice. (a) Representative images of the oil red O staining in whole aortas from sh-NC-treated ApoE^{-/-} mice or sh-ZBTB20-treated ApoE^{-/-} mice fed with a high-fat diet for 16 weeks. ImageJ software was used to quantify the lesion coverage of the entire aorta (%). (b) Representative images of H&E staining in cross-sections of the aortic root from mice in different groups. ImageJ software was used to quantify areas of the necrotic core. (c) Representative images of oil red O staining in cross-sections of the aortic root from mice in different groups. ImageJ software was used to assess the lesion areas. (d) Representative images of Masson staining for collagen content, IHC staining for SMC content, and macrophage accumulation (CD68) in whole aortas from sh-NC-treated ApoE^{-/-} mice or sh-ZBTB20-treated ApoE^{-/-} mice fed with a high-fat diet for 16 weeks. *N* = 8; significant differences between treatment groups were shown as **P* < 0.05.

ZBTB20 knockdown suppressed the phosphorylation and nucleus translocation of IRF3 and reduced the IFN- β cytokine level in the ox-LDL-stimulated macrophages, suggesting that ZBTB20 regulated the phenotype switching of macrophages by targeting IRF3 and regulating IFN- β . Similarly, in the clinic, it may be possible to use macrophage polarization as a target to treat macrophage-related inflammatory diseases, such as aseptic loosening and immune rejection.

It has been widely reported that ox-LDL induced oxidative stress in macrophages [53, 54], and our results consistently elucidated that ox-LDL increased the ROS production and DRP1/FIS1 protein. NRF2 is a crucial transcription factor that regulates oxidative stress responses, and it is required for the antioxidant responses in macrophages [47]. Our results showed that the ZBTB20 knockdown attenuated the ox-LDL-induced ROS production and increased the nucleus translocation of NRF2 in the macrophages, which was significantly antagonized by the NRF2 inhibitor ML385. In addition, the ZBTB20 knockdown also rescued the ox-LDL-induced mitochondrial injury in the macrophages. Collectively, these results suggested that the ZBTB20 knockdown exerted antioxidative stress effects via enhancing the nucleus translocation of NRF2 and preventing the mitochondrial injury in macrophages. Some previous studies suggested that ZBTB20 ablation could protect mice from liver steatosis and improve hepatic lipid metabolism, the dysregulation of which may lead to AS [55]. Here, our *in vivo* data showed that the knockdown of ZBTB20 attenuated AS in ApoE^{-/-} mice. Hence, it is possible to selectively target ZBTB20 using novel viral vectors, such as adenovirus and adeno-associated virus, to slow the progression of clinical immune-inflammatory diseases. However, the *in vivo* effects of ZBTB20 on the AS progression, as well as how ZBTB20 regulates other cell types in AS, such as endothelial cells, still require further investigations.

Mitochondria are well known for their roles in integrating redox, efferocytosis, epigenetic, and apoptotic regulations [56]. How mitochondria function will depend on the shape and density, which are modulated by the fusion/fission balances [57, 58]. These functions have been found to be disturbed in macrophages from the AS plaques [59]. In this study, we found that ox-LDL stimulation caused ROS production and mitochondrial injury, which were significantly attenuated by ZBTB20 silencing. Our findings were consistent with studies from Peng et al., showing that ox-LDL induced mitophagy in mitochondria [60]. DRP1 and FIS1 are two key mediators relevant to the mitochondrial fission process [61, 62], and our results showed that the ZBTB20 knockdown attenuated the ox-LDL-induced activation of DRP1/FIS1 protein. Besides, our results showed that the knockdown of ZBTB20 enhanced the nucleus translocation of NRF2 in the ox-LDL-stimulated macrophages, which was counteracted by ML385, a novel NRF2 inhibitor. Nevertheless, the NRF2 transcription factor might be one of the signaling pathways through which ZBTB20 regulated the oxidative stress level, and the deeper mechanisms remain to be explored.

Collectively, our results may imply that ZBTB20 silencing reduced oxidative stress by reducing ROS production and mitochondrial injury via NRF2 signaling. In the clinic, it may be possible to use adenovirus or adeno-associated virus targeting ZBTB20 to prevent and treat AS.

5. Conclusions

In conclusion, this study demonstrated that the ZBTB20 knockdown could attenuate the progression of AS, and ZBTB20 mediated ox-LDL-induced AS possibly via modulating the inflammatory responses, oxidative stress, and mitochondrial fission of macrophages.

Data Availability

All the datasets were available from the corresponding authors.

Conflicts of Interest

The authors declare no conflict of interest.

Authors' Contributions

Jun Tao, Junxiong Qiu, and Liuyi Lu contributed equally to this work.

Acknowledgments

This work was supported by the National Natural Science Foundation of China (81702618) and the Guangdong Science and Technology Department (2020B1212060018).

Supplementary Materials

Fig. S1: (A) The mRNA levels of TNF- α and IL-6 after being treated with ox-LDL for 0, 12, 24, and 48 h were determined by qRT-PCR. (B) The blank control of Figure 2(b). (C) Quantitative analysis of Western blot results in Figure 2(c). (D) Quantitative analysis of Western blot results in Figure 2(d). (E) Quantitative analysis of Western blot results in Figure 2(f). Significant differences between treatment groups were shown as $*P < 0.05$. Fig. S2: (A) The top 15 significant GO terms and KEGG pathways from the GO categories and KEGG database. (B) The four most significant KEGG pathways analyzed with GSEA. Fig. S3: (A) Quantitative analysis of Western blot results in Figure 4(c). (B) The Western blot result of ZBTB20-siRNA knockdown efficiency. (C) The blank control of Figure 5(a). (D) Quantitative analysis of Western blot results in Figure 5(d). (E) Quantitative analysis of Western blot in Figure 5(f). Significant differences between treatment groups were shown as $*P < 0.05$. Fig. S4: (A) The isotype controls of Figure 6(a). (B) Quantitative analysis of flow cytometry results in Figure 6(a). (C) Quantitative analysis of Western blot results in Figure 6(c). (D) The blank control of Figure 7(b). (E) Quantitative analysis of Western blot results in Figure 7(e). (F, G) Quantitative analysis of Western blot results in Figure 7(g). Significant differences between treatment groups were shown as $*P < 0.05$. (*Supplementary Materials*)

References

- [1] K. Kobiyama and K. Ley, "Atherosclerosis," *Circulation Research*, vol. 123, no. 10, pp. 1118–1120, 2018.

- [2] G. Heusch, "Coronary microvascular obstruction: the new frontier in cardioprotection," *Basic Research in Cardiology*, vol. 114, no. 6, p. 45, 2019.
- [3] P. Libby, P. M. Ridker, and G. K. Hansson, "Progress and challenges in translating the biology of atherosclerosis," *Nature*, vol. 473, no. 7347, pp. 317–325, 2011.
- [4] D. J. Tyrrell and D. R. Goldstein, "Ageing and atherosclerosis: vascular intrinsic and extrinsic factors and potential role of IL-6," *Nature Reviews. Cardiology*, vol. 18, no. 1, pp. 58–68, 2021.
- [5] D. A. Chistiakov, A. A. Melnichenko, V. A. Myasoedova, A. V. Grechko, and A. N. Orekhov, "Mechanisms of foam cell formation in atherosclerosis," *Journal of molecular medicine (Berlin, Germany)*, vol. 95, no. 11, pp. 1153–1165, 2017.
- [6] A. J. Kattoor, S. H. Kanuri, and J. L. Mehta, "Role of Ox-LDL and LOX-1 in atherogenesis," *Current medicinal chemistry*, vol. 26, no. 9, pp. 1693–1700, 2019.
- [7] W. Martinet, I. Coornaert, P. Puylaert, and G. R. Y. De Meyer, "Macrophage death as a pharmacological target in atherosclerosis," *Frontiers in Pharmacology*, vol. 10, p. 306, 2019.
- [8] A. P. West, W. Khoury-Hanold, M. Staron et al., "Mitochondrial DNA stress primes the antiviral innate immune response," *Nature*, vol. 520, no. 7548, pp. 553–557, 2015.
- [9] E. L. Mills, B. Kelly, A. Logan et al., "Succinate dehydrogenase supports metabolic repurposing of mitochondria to drive inflammatory macrophages," *Cell*, vol. 167, no. 2, pp. 457–470.e13, 2016.
- [10] W. Peng, G. Cai, Y. Xia et al., "Mitochondrial dysfunction in atherosclerosis," *DNA and cell biology*, vol. 38, no. 7, pp. 597–606, 2019.
- [11] Y. Chen, M. Yang, W. Huang et al., "Mitochondrial metabolic reprogramming by CD36 signaling drives macrophage inflammatory responses," *Circulation Research*, vol. 125, no. 12, pp. 1087–1102, 2019.
- [12] Y. Wei, J. Corbalán-Campos, R. Gurung et al., "Dicer in macrophages prevents atherosclerosis by promoting mitochondrial oxidative metabolism," *Circulation*, vol. 138, no. 18, pp. 2007–2020, 2018.
- [13] D. T. Love, C. Guo, E. I. Nikelshparg, N. A. Brazhe, O. Sosnovtseva, and C. L. Hawkins, "The role of the myeloperoxidase-derived oxidant hypothiocyanous acid (HOSCN) in the induction of mitochondrial dysfunction in macrophages," *Redox Biology*, vol. 36, p. 101602, 2020.
- [14] T. Xin, C. Lu, J. Zhang et al., "Oxidized LDL disrupts metabolism and inhibits macrophage survival by activating a miR-9/Drp1/mitochondrial fission signaling pathway," *Oxidative Medicine and Cellular Longevity*, vol. 2020, Article ID 8848930, 16 pages, 2020.
- [15] F. Mattioli, A. Piton, B. Gérard, A. Superti-Furga, J. L. Mandel, and S. Unger, "Novel de novo mutations in ZBTB20 in Primrose syndrome with congenital hypothyroidism," *American journal of medical genetics Part A*, vol. 170, no. 6, pp. 1626–1629, 2016.
- [16] M. L. Peterson, C. Ma, and B. T. Spear, "Zhx2 and Zbtb20: novel regulators of postnatal alpha-fetoprotein repression and their potential role in gene reactivation during liver cancer," *Seminars in cancer biology*, vol. 21, no. 1, pp. 21–27, 2011.
- [17] Y. Sun, N. K. Preiss, K. B. Valenteros et al., "Zbtb20 restrains CD8 T cell immunometabolism and restricts memory differentiation and antitumor immunity," *Journal of Immunology*, vol. 205, no. 10, pp. 2649–2666, 2020.
- [18] J. Qiu, P. Peng, M. Xin et al., "ZBTB20-mediated titanium particle-induced peri-implant osteolysis by promoting macrophage inflammatory responses," *Biomaterials Science*, vol. 8, no. 11, pp. 3147–3163, 2020.
- [19] A. J. Ren, K. Wang, H. Zhang et al., "ZBTB20 regulates nociception and pain sensation by modulating TRP channel expression in nociceptive sensory neurons," *Nature Communications*, vol. 5, no. 1, p. 4984, 2014.
- [20] X. Liu, P. Zhang, Y. Bao et al., "Zinc finger protein ZBTB20 promotes Toll-like receptor-triggered innate immune responses by repressing I κ B α gene transcription," *Proceedings of the National Academy of Sciences of the United States of America*, vol. 110, no. 27, pp. 11097–11102, 2013.
- [21] I. Pateras, C. Giaginis, C. Tsigris, E. Patsouris, and S. Theocharis, "NF- κ B signaling at the crossroads of inflammation and atherogenesis: searching for new therapeutic links," *Expert Opinion on Therapeutic Targets*, vol. 18, no. 9, pp. 1089–1101, 2014.
- [22] A. Schwarz, G. A. Bonaterra, H. Schwarzbach, and R. Kinscherf, "Oxidized LDL-induced JAB1 influences NF- κ B independent inflammatory signaling in human macrophages during foam cell formation," *Journal of Biomedical Science*, vol. 24, no. 1, p. 12, 2017.
- [23] F. Li, Y. Yang, C. Xue et al., "Zinc finger protein ZBTB20 protects against cardiac remodelling post-myocardial infarction via ROS-TNF α /ASK1/JNK pathway regulation," *Journal of Cellular and Molecular Medicine*, vol. 24, no. 22, pp. 13383–13396, 2020.
- [24] M. Wagner, E. Bertero, A. Nickel et al., "Selective NADH communication from α -ketoglutarate dehydrogenase to mitochondrial transhydrogenase prevents reactive oxygen species formation under reducing conditions in the heart," *Basic Research in Cardiology*, vol. 115, no. 5, p. 53, 2020.
- [25] A. Vasseur, L. Cabel, O. Tredan et al., "Prognostic value of CEC count in HER2-negative metastatic breast cancer patients treated with bevacizumab and chemotherapy: a prospective validation study (UCBG COMET)," *Angiogenesis*, vol. 23, no. 2, pp. 193–202, 2020.
- [26] J. Wang, Z. Chen, Q. Dai et al., "Intravenously delivered mesenchymal stem cells prevent microvascular obstruction formation after myocardial ischemia/reperfusion injury," *Basic Research in Cardiology*, vol. 115, no. 4, p. 40, 2020.
- [27] D. E. Vatner, M. Oydanich, J. Zhang, D. Babici, and S. F. Vatner, "Secreted frizzled-related protein 2, a novel mechanism to induce myocardial ischemic protection through angiogenesis," *Basic Research in Cardiology*, vol. 115, no. 4, p. 48, 2020.
- [28] M. P. Winter, S. Sharma, J. Altmann et al., "Interruption of vascular endothelial growth factor receptor 2 signaling induces a proliferative pulmonary vasculopathy and pulmonary hypertension," *Basic Research in Cardiology*, vol. 115, no. 6, p. 58, 2020.
- [29] Z. Radak, K. Suzuki, A. Posa, Z. Petrovszky, E. Koltai, and I. Boldogh, "The systemic role of SIRT1 in exercise mediated adaptation," *Redox Biology*, vol. 35, p. 101467, 2020.
- [30] Y. Yang, L. Ma, C. Wang et al., "Matrix metalloproteinase-7 in platelet-activated macrophages accounts for cardiac remodeling in uremic mice," *Basic Research in Cardiology*, vol. 115, no. 3, p. 30, 2020.
- [31] E. Bridges, H. Sheldon, E. Kleibeuker et al., "RHOQ is induced by DLL4 and regulates angiogenesis by determining the

- intracellular route of the Notch intracellular domain," *Angiogenesis*, vol. 23, no. 3, pp. 493–513, 2020.
- [32] Y. Tan, D. Mui, S. Toan, P. Zhu, R. Li, and H. Zhou, "SERCA overexpression improves mitochondrial quality control and attenuates cardiac microvascular ischemia-reperfusion injury," *Mol Ther Nucleic Acids*, vol. 22, pp. 696–707, 2020.
- [33] T. C. Chen, J. Y. Chuang, C. Y. Ko et al., "AR ubiquitination induced by the curcumin analog suppresses growth of temozolomide-resistant glioblastoma through disrupting GPX4-mediated redox homeostasis," *Redox Biology*, vol. 30, p. 101413, 2020.
- [34] J. Cao, X. Liu, Y. Yang et al., "Decylubiquinone suppresses breast cancer growth and metastasis by inhibiting angiogenesis via the ROS/p53/ BAI1 signaling pathway," *Angiogenesis*, vol. 23, no. 3, pp. 325–338, 2020.
- [35] N. Abbas, F. Perbellini, and T. Thum, "Non-coding RNAs: emerging players in cardiomyocyte proliferation and cardiac regeneration," *Basic Research in Cardiology*, vol. 115, no. 5, p. 52, 2020.
- [36] S. Deng, K. Essandoh, X. Wang et al., "Tsg101 positively regulates P62-Keap1-Nrf2 pathway to protect hearts against oxidative damage," *Redox Biology*, vol. 32, p. 101453, 2020.
- [37] K. Fukada and K. Kajiya, "Age-related structural alterations of skeletal muscles and associated capillaries," *Angiogenesis*, vol. 23, no. 2, pp. 79–82, 2020.
- [38] X. Lu, Y. He, C. Tang et al., "Triad3A attenuates pathological cardiac hypertrophy involving the augmentation of ubiquitination-mediated degradation of TLR4 and TLR9," *Basic Research in Cardiology*, vol. 115, no. 2, p. 19, 2020.
- [39] R. Khan, V. Spagnoli, J. C. Tardif, and P. L. L'Allier, "Novel anti-inflammatory therapies for the treatment of atherosclerosis," *Atherosclerosis*, vol. 240, no. 2, pp. 497–509, 2015.
- [40] C. Khatana, N. K. Saini, S. Chakrabarti et al., "Mechanistic insights into the oxidized low-density lipoprotein-induced atherosclerosis," *Oxidative Medicine and Cellular Longevity*, vol. 2020, Article ID 5245308, 14 pages, 2020.
- [41] M. Kurano, N. Iso-O, M. Hara et al., "Plant sterols increased IL-6 and TNF- α secretion from macrophages, but to a lesser extent than cholesterol," *Journal of atherosclerosis and thrombosis*, vol. 18, no. 5, pp. 373–383, 2011.
- [42] N. Haddy, C. Sass, S. Drosch et al., "IL-6, TNF- α and atherosclerosis risk indicators in a healthy family population: the STANISLAS cohort," *Atherosclerosis*, vol. 170, no. 2, pp. 277–283, 2003.
- [43] M. P. de Winther, E. Kanters, G. Kraal, and M. H. Hofker, "Nuclear factor κ B signaling in atherogenesis," *Arteriosclerosis, thrombosis, and vascular biology*, vol. 25, no. 5, pp. 904–914, 2005.
- [44] S. Li, J. Qiu, L. Qin et al., "NOD2 negatively regulated titanium particle-induced osteolysis in mice," *Biomaterials Science*, vol. 7, no. 7, pp. 2702–2715, 2019.
- [45] L. Zhang, L. Lu, X. Zhong et al., "Metformin reduced NLRP3 inflammasome activity in Ox-LDL stimulated macrophages through adenosine monophosphate activated protein kinase and protein phosphatase 2A," *European journal of pharmacology*, vol. 852, pp. 99–106, 2019.
- [46] X. Cao, N. Zhu, L. Li et al., "Y-box binding protein 1 regulates ox-LDL mediated inflammatory responses and lipid uptake in macrophages," *Free radical biology & medicine*, vol. 141, pp. 10–20, 2019.
- [47] Y. Zhang, X. Zhou, M. Zhang, L. Cheng, Y. Zhang, and X. Wang, "ZBTB20 promotes cell migration and invasion of gastric cancer by inhibiting I κ B α to induce NF- κ B activation," *Artif Cells Nanomed Biotechnol.*, vol. 47, no. 1, pp. 3862–3872, 2019.
- [48] S. Gu, S. Ran, F. Qin et al., "Human dental pulp stem cells via the NF- κ B pathway," *Cellular Physiology and Biochemistry*, vol. 36, no. 5, pp. 1725–1734, 2015.
- [49] K. Taketa, T. Matsumura, M. Yano et al., "Oxidized low density lipoprotein activates peroxisome proliferator-activated receptor- α (PPAR α) and PPAR γ through MAPK-dependent COX-2 expression in macrophages*," *The Journal of Biological Chemistry*, vol. 283, no. 15, pp. 9852–9862, 2008.
- [50] Y. Bi, J. Chen, F. Hu, J. Liu, M. Li, and L. Zhao, "M2 macrophages as a potential target for antiatherosclerosis treatment," *Neural plasticity*, vol. 2019, article 6724903, 21 pages, 2019.
- [51] J. Liao, X. An, X. Yang et al., "Deficiency of LMP10 attenuates diet-induced atherosclerosis by inhibiting macrophage polarization and inflammation in apolipoprotein E deficient mice," *Frontiers in Cell and Development Biology*, vol. 8, p. 592048, 2020.
- [52] D. A. Chistiakov, V. A. Myasoedova, V. V. Revin, A. N. Orekhov, and Y. V. Bobryshev, "The impact of interferon-regulatory factors to macrophage differentiation and polarization into M1 and M2," *Immunobiology*, vol. 223, no. 1, pp. 101–111, 2018.
- [53] L. Håversen, J. P. Sundelin, A. Mardinoglu et al., "Vimentin deficiency in macrophages induces increased oxidative stress and vascular inflammation but attenuates atherosclerosis in mice," *Scientific Reports*, vol. 8, no. 1, p. 16973, 2018.
- [54] D. D. Chen, L. L. Hui, X. C. Zhang, and Q. Chang, "NEAT1 contributes to ox-LDL-induced inflammation and oxidative stress in macrophages through inhibiting miR-128," *Journal of Cellular Biochemistry*, vol. 120, no. 2, pp. 2493–2501, 2018.
- [55] G. Liu, L. Zhou, H. Zhang et al., "Regulation of hepatic lipogenesis by the zinc finger protein Zbtb20," *Nature Communications*, vol. 8, no. 1, p. 14824, 2017.
- [56] A. Shteinifer-Kuzmine, A. Verma, T. Arif, O. Aizenberg, A. Paul, and V. Shoshan-Barmaz, "Mitochondria and nucleus cross-talk: signaling in metabolism, apoptosis, and differentiation, and function in cancer," *IUBMB Life*, 2020.
- [57] H. Xian and Y. C. Liou, "Functions of outer mitochondrial membrane proteins: mediating the crosstalk between mitochondrial dynamics and mitophagy," *Cell Death and Differentiation*, 2020.
- [58] J. Wang, S. Toan, and H. Zhou, "Mitochondrial quality control in cardiac microvascular ischemia-reperfusion injury: new insights into the mechanisms and therapeutic potentials," *Pharmacological Research*, vol. 156, p. 104771, 2020.
- [59] A. Dumont, M. Lee, T. Barouillet, A. Murphy, and L. Yvan-Charvet, "Mitochondria orchestrate macrophage effector functions in atherosclerosis," *Molecular aspects of medicine*, p. 100922, 2020.
- [60] X. Peng, H. Chen, Y. Li, D. Huang, B. Huang, and D. Sun, "Effects of NIX-mediated mitophagy on ox-LDL-induced macrophage pyroptosis in atherosclerosis," *Cell biology international*, vol. 44, no. 7, pp. 1481–1490, 2020.

- [61] A. U. Joshi, N. L. Saw, M. Shamloo, and D. Mochly-Rosen, "Drp1/Fis1 interaction mediates mitochondrial dysfunction, bioenergetic failure and cognitive decline in Alzheimer's disease," *Oncotarget*, vol. 9, no. 5, pp. 6128–6143, 2018.
- [62] J. Wang and H. Zhou, "Mitochondrial quality control mechanisms as molecular targets in cardiac ischemia ** – ** reperfusion injury," *Acta Pharmaceutica Sinica B*, vol. 10, no. 10, pp. 1866–1879, 2020.

Research Article

Ndufs1 Deficiency Aggravates the Mitochondrial Membrane Potential Dysfunction in Pressure Overload-Induced Myocardial Hypertrophy

Rongjun Zou ¹, Jun Tao,² Junxiong Qiu,² Wanting Shi ³, Minghui Zou ¹,
Weidan Chen ¹, Wenlei Li ¹, Na Zhou ¹, Shaoli Wang ⁴, Li Ma ¹ and Xinxin Chen ¹

¹Heart Center, Guangdong Provincial Key Laboratory of Research in Structural Birth Defect Disease, Guangzhou Women and Children's Medical Center, Guangzhou Medical University, Guangzhou 510623, China

²Department of Cardiovascular Surgery, Sun Yat-sen Memorial Hospital, Sun Yat-sen University, Guangzhou, Guangdong 510120, China

³Department of Paediatrics, Guangdong Provincial Key Laboratory of Research in Structural Birth Defect Disease, Guangzhou Women and Children's Medical Center, Guangzhou Medical University, Guangzhou 510623, China

⁴Department of Surgical Nursing, Guangzhou Women and Children's Medical Center, Guangzhou Medical University, Guangzhou 510623, China

Correspondence should be addressed to Li Ma; limagz@163.com and Xinxin Chen; xinxinchengz@163.com

Received 9 January 2021; Revised 3 February 2021; Accepted 18 February 2021; Published 4 March 2021

Academic Editor: Yun-dai Chen

Copyright © 2021 Rongjun Zou et al. This is an open access article distributed under the Creative Commons Attribution License, which permits unrestricted use, distribution, and reproduction in any medium, provided the original work is properly cited.

Mitochondrial dysfunction has been suggested to be the key factor in the development and progression of cardiac hypertrophy. The onset of mitochondrial dysfunction and the mechanisms underlying the development of cardiac hypertrophy (CH) are incompletely understood. The present study is based on the use of multiple bioinformatics analyses for the organization and analysis of scRNA-seq and microarray datasets from a transverse aortic constriction (TAC) model to examine the potential role of mitochondrial dysfunction in the pathophysiology of CH. The results showed that NADH:ubiquinone oxidoreductase core subunit S1- (Ndufs1-) dependent mitochondrial dysfunction plays a key role in pressure overload-induced CH. Furthermore, *in vivo* animal studies using a TAC mouse model of CH showed that Ndufs1 expression was significantly downregulated in hypertrophic heart tissue compared to that in normal controls. In an *in vitro* model of angiotensin II- (Ang II-) induced cardiomyocyte hypertrophy, Ang II treatment significantly downregulated the expression of Ndufs1 in cardiomyocytes. *In vitro* mechanistic studies showed that Ndufs1 knockdown induced CH; decreased the mitochondrial DNA content, mitochondrial membrane potential (MMP), and mitochondrial mass; and increased the production of mitochondrial reactive oxygen species (ROS) in cardiomyocytes. On the other hand, Ang II treatment upregulated the expression levels of atrial natriuretic peptide, brain natriuretic peptide, and myosin heavy chain beta; decreased the mitochondrial DNA content, MMP, and mitochondrial mass; and increased mitochondrial ROS production in cardiomyocytes. The Ang II-mediated effects were significantly attenuated by overexpression of Ndufs1 in rat cardiomyocytes. In conclusion, our results demonstrate downregulation of Ndufs1 in hypertrophic heart tissue, and the results of mechanistic studies suggest that Ndufs1 deficiency may cause mitochondrial dysfunction in cardiomyocytes, which may be associated with the development and progression of CH.

1. Introduction

Cardiac hypertrophy (CH) is a pathophysiological response characterized by increased thickness of the ventricular wall, greater myocardial cell volume, and enhanced myocardial

contractility during the early stage of overload pressure [1]. Primarily, CH is the compensatory response for preservation of cardiac function; however, persistent CH is often associated with disturbed energy metabolism, deteriorated cardiac function, and interstitial fibrosis, which will eventually

progress into heart failure [2, 3]. Heart failure caused by CH has been shown to be an independent risk factor for various cardiovascular diseases [4, 5]. To date, the pathophysiology underlying the progression of myocardial hypertrophy remains elusive. Thus, determination of potential molecular mechanisms is necessary for identification of novel and effective therapies to attenuate myocardial hypertrophy.

The contraction and relaxation of cardiomyocytes require a sufficient energy supply to meet the workload demand, and mitochondria are important primary organelles for energy production in cardiomyocytes [6–8]. Mitochondrial dysfunction was shown to be closely associated with the development of heart failure [9–11]. Under pathological conditions of CH, the activities of ATP synthase and mitochondrial oxidative phosphorylation complex are attenuated, which results in reduced production of ATP [12, 13]. Moreover, attenuated mitochondrial dynamics, reduced mitochondrial volume, and abnormal mitochondrial morphology were detected in cardiomyocytes in CH [14, 15]. Mitochondrial dysfunction was shown to increase the production of reactive oxygen species (ROS) via impaired electron transport chains, which can lead to increased oxidative stress and decreased energy production in cardiomyocytes [9, 16, 17]. Thus, restoration of impaired mitochondrial functions will provide novel strategies to attenuate the progression of CH. NADH:ubiquinone oxidoreductase core subunit S1 (Ndufs1) is one of the core subunits of mitochondrial complex I that regulates mitochondrial oxidative phosphorylation and ROS production [18–20]. However, the detailed role of Ndufs1 in the pathophysiology of CH is largely unknown.

In the present study, we initially demonstrated the deregulation of Ndufs1 in heart tissue of mice with CH by analyzing the GSE95140 scRNA-seq dataset. The expression of Ndufs1 was confirmed in heart tissue in a mouse model of CH. Furthermore, *in vitro* studies determined the molecular mechanisms of Ndufs1-mediated CH. The present study may provide novel insight into the role of Ndufs1 in the pathophysiology of CH.

2. Materials and Methods

2.1. Analysis of scRNA-seq and Microarray Datasets. RNA sequencing data for single cardiomyocytes were downloaded from the GSE95140 dataset of the GEO database [21]. This dataset is based on the GPL17021 platform and contains 396 single-cardiomyocyte transcriptomes of mice after transverse aortic constriction (TAC) or sham operation assayed on day 3 (D3), week 1 (W1), week 2 (W2), week 4 (W4), and week 8 (W8). The expression in each cell was detected by using the “DropletUtils” package. Gene expression in the cells was calculated using the “QC-Metrics” function in the “scater” package [22]. Ribosomal genes $\geq 10\%$ and mitochondrial genes $\leq 5\%$ were used for subsequent filtering. After filtering, the expression matrix of each sample was normalized by using the “NormalizeData” function of the “Seurat” package (version 3.0) [23]. The genes with the most pronounced differences between the cells were selected using the “FindVariableFeatures” function of the “Seurat” package.

The “ScaleData” function was used to convert the expression data to linear scale. Then, principal component analysis (PCA) was performed using the “RunPCA” function of the “Seurat” package. Principal components (PCs) with standard deviations $> 70\%$ were selected. “RunUMAP” of the “Seurat” package was employed to perform UMAP dimensionality reduction analysis. The “FindAllMarkers” function of the “Seurat” package was used to define the criteria for identification of differentially expressed genes (DEGs) as follows: cell population expression ratio > 0.25 , \log_2 fold change (FC) > 0.25 , and $p \leq 0.05$.

The differentially expressed genes were validated using the GSE24454 microarray dataset. In this dataset, mice were sacrificed 4 weeks after aortic banding (AB) or sham procedure (sAB) and subsequent debanding, including banding and subsequent debanding (DB3) or sham procedure and subsequent debanding (sDB3); the data were obtained at various time points up to day 3 [24]. Thus, the CEL raw data and corresponding annotation platform file were downloaded and preprocessed by background adjustment, normalization, probe summarization, and \log_2 transformation of the expression values using the “Affy” package in R.

2.2. Gene Ontology (GO) Term Enrichment Analysis. GO enrichment analysis was performed using the “clusterProfiler” package in R [25]. Notably, the major GO terms of DE genes in biological processes, molecular functions, cellular components, and pathways were evaluated. The Benjamini-Hochberg method was used to adjust the original p values. The GO terms corresponding to the DE genes were enriched with the threshold of correction p value < 0.05 . Additionally, the enrichment analyses of the biological processes of the hub genes were carried out with the ToppGene tool (<https://toppgene.cchmc.org/>), which is a web-based analytic tool used for functional enrichment analysis of the gene lists [26]. Additionally, the cellular compartment-specific protein-protein interaction network was constructed by the ComPPI database (<https://comppi.linkgroup.hu/>) [27].

2.3. Gene Set Enrichment Analysis (GSEA). GSEA was used to assess the Kyoto Encyclopedia of Genes and Genomes (KEGG) maps involved in TCA-induced CH development based on time series analysis [28]. Initially, the Kolmogorov-Smirnov method was used to determine the enrichment score (ES); then, the statistical significance of ES was assessed using the empirical phenotype replacement test procedure. The enrichment score (NES) was derived by normalization of ES for each gene set. The false discovery rate (FDR) of each NES was determined.

2.4. Gene Set Variation Analysis (GSVA). The GSVA package of R was used to analyze the activation of the gene sets by unsupervised and nonparametric scoring calculations [29]. The hub pathway-related scores were calculated by the GSVA method in each cell based on the transcription expression matrix after assigning various groups in the TAC model. Significant differences in GSVA scores between various groups were assessed by one-way ANOVA.

2.5. Animals and Surgical Intervention. All animal experiments were approved by the Animal Ethics Committee of Sun Yat-sen University (SYSU-IACUC-2020-000469). Sixteen male C57BL/6 mice (8 weeks old) were purchased from Sun Yat-sen University, and the mice were randomly divided into two groups, including the sham ($n = 8$) and TAC groups ($n = 8$). Before operation, the animals were anaesthetized by intraperitoneal injection with 100 mg/kg ketamine + 5 mg/kg xylazine. After the animals reached general anesthesia, a small incision was made in the second intercostal space at the left upper sternal border to open the chest cavity, and the animals were subjected to respiratory ventilation. After exposure of the aortic arch, TAC was performed by tying a 7-0 nylon suture ligature against a 27-gauge needle between the left common carotid artery and the brachiocephalic artery. Then, the needle was quickly retracted to complete the partial constriction procedure. Sham-operated mice were subjected to the same surgical procedures without transverse aortic constriction. The chest was closed with 5-0 nonabsorbable sutures. Postoperatively, the animals were subcutaneously injected with 1.0 mg/kg buprenorphine to relieve postoperative pain every 12 h for 3 consecutive days. The mice were closely monitored every day for body weight and any signs of labored breathing or postoperative pain.

2.6. Echocardiography. Four weeks after ascending TAC operation, the animals from the sham and TAC groups were subjected to echocardiography examination. Briefly, the mice were anaesthetized by 3% isoflurane using an anesthesia machine. The hair on the left chest was carefully removed, and cardiac geometry was determined from the parasternal long axis view with a probe frequency of 30 MHz using a small animal color ultrasonic diagnostic apparatus (Vevo 2100, VisualSonics, Toronto, Canada). The images of the left ventricular area were captured using M-type echocardiography. The interventricular septum (IVS) thickness and left ventricular posterior wall (LVPW) thickness were measured.

2.7. Evaluation of Cardiac Index. After assessment by echocardiography, the animals were sacrificed by an overdose of 5% isoflurane. The heart was immediately dissected and rinsed with ice-cold saline to remove blood clots. After draining the heart tissue on sterile paper, the whole weight of the heart was measured using a digital balance. The left ventricular weight (LVW) was determined by removing the atrium and right ventricle from the whole heart. The heart mass index (HMI) and left ventricular mass index (LVMI) were calculated as follows: $HMI = LVW/body\ weight$; $LVMI = LVW/body\ weight$. The length of the medial malleolar distance on the right hindlimb to the tibial plateau edge was defined as the tibia length (TL). The ratios of LVW to TL were used as an index of cardiac hypertrophy.

2.8. Hematoxylin and Eosin (H&E) Staining. After animals were sacrificed by an overdose of 5% isoflurane, a part of the heart tissue was fixed with 4% paraformaldehyde and embedded in paraffin. The paraffin-embedded heart tissue was sectioned into 5 μm sections and stained by hematoxylin

and eosin. The stained sections were examined under a light microscope (Nikon, Tokyo, Japan).

2.9. Transmission Electron Microscopy (TEM). The mitochondria in the heart tissue were evaluated by TEM. Briefly, the heart tissue was sectioned into 1 mm³ pieces, which were fixed with 4% glutaraldehyde and 1% osmic acid. Then, the tissue was dehydrated with acetone, embedded in Epon 821, and cut into 70 nm sections. Then, the sections were double stained with uranyl acetate and lead citrate. The mitochondria were examined using TEM (JEM-1230, Tokyo, Japan). Mitochondrial volume and mitochondrial number were evaluated based on the TEM images.

2.10. Rat Cardiomyocyte Culture. Neonatal Sprague-Dawley rats (1-2 days old) were sacrificed by cervical dislocation, and the heart was immediately dissected under sterile conditions. Ventricular tissue was isolated from the atria and digested in Hanks balanced salt solution containing 0.25% trypsin (Sigma-Aldrich, St. Louis, USA) at 37°C for 5 min, and the digestion cycle was repeated 10 times. After digestion, the supernatants were pooled and mixed with an equal volume of DMEM supplemented with 10% fetal bovine serum (FBS; Thermo Fisher Scientific, Waltham, USA). After centrifugation at 1,000 $\times g$ for 5 min, the supernatant was discarded, and the cell pellet was resuspended in DMEM supplemented with 10% FBS. After incubation for 4 h at 37°C in a humidified 5% CO₂ incubator, cardiomyocytes were collected from the medium. Cardiac fibroblasts adhered to the walls of the dishes. Cardiomyocytes were cultured in 6-well plates for 24 h and in fresh DMEM supplemented with 10% FBS for 2-3 days before *in vitro* assays.

2.11. Construction of the Ndsf1 siRNA and Overexpression Vectors and Ang II Treatment. The siRNAs targeting Ndsf1 (si-Ndsf1) and the corresponding scrambled siRNAs were designed and synthesized by RiboBio (Guangzhou, China). The vector for Ndsf1 overexpression was constructed by cloning the full-length Ndsf1 sequence into the pcDNA3.1 vector, and the empty pcDNA3.1 vector was used as the corresponding negative control. All plasmids were purchased from RiboBio. For transfections, rat cardiomyocytes were seeded in 12-well plates and cultured for 24 h; then, cardiomyocytes were transfected with various plasmids or siRNAs by using Lipofectamine 2000 reagent (Invitrogen, Carlsbad, USA) according to the manufacturer's protocol. Cardiomyocytes were collected for the experiments 24 h after the transfection. For angiotensin II (Ang II; Sigma-Aldrich) treatment, cardiomyocytes were seeded in 12-well plates and cultured for 24 h; then, cardiomyocytes were treated with 100 nM Ang II for 24 h and harvested for subsequent experiments.

2.12. Quantitative Real-Time PCR (qRT-PCR). Total RNA from cardiomyocytes and heart tissue was extracted using TRIzol reagent (Invitrogen, Carlsbad, USA) according to the manufacturer's protocol. RNA was reverse transcribed using a PrimerScript RT kit with gDNA eraser (Takara, Dalian, USA). Real-time PCR was performed using a SYBR Premix Ex Taq II kit (Takara) on an ABI7900 instrument

(Applied Biosystems, Foster City, USA). The parameters for thermal cycling were as follows: 95°C for 15 s, 55°C for 15 s, and 72°C for 15 s for 40 cycles. The relative mRNA expression levels were determined by the comparative Ct method, and β -actin was used as the internal control.

2.13. Western Blot Assay. Proteins from cardiomyocytes or heart tissue were isolated using RIPA buffer supplemented with proteinase inhibitors (Sigma-Aldrich). The concentrations of the protein samples were measured by the BCA method. Equal amounts of proteins (50 μ g) were resolved by gel electrophoresis and transferred to a polyvinylidene difluoride (PVDF) membrane. After blocking with 5% nonfat milk at room temperature for 1 h, the membranes were incubated with primary antibodies against NDUFS1 (1:1,000; CST, Danvers, USA), atrial natriuretic peptide (ANP; 1:1,000; CST), brain natriuretic peptide (BNP; 1:1,000; CST), myosin heavy chain beta (β -MHC; 1:1,000; CST), and β -actin (1:2,000; CST) at 4°C overnight. Then, the membrane was incubated with horseradish peroxidase-conjugated secondary antibodies (1:2,000; CST) for 2 h at room temperature. The immunoreactive bands were analyzed by using a chemiluminescence system (Bio-Rad).

2.14. Assessment of mtDNA Copy Number. The mtDNA/nDNA ratio was evaluated by using the qRT-PCR assay as described previously. The primers were designed to target mtDNA (NADH dehydrogenase: 1,5'-AAACGC CTAACAACCAT-3' and 5'-GGATAGGATGC TCGG ATT-3') and nDNA (β -actin: 5'-ATGGTGGGAATGGG TCAGAA-3' and 5'-CTTTTCACG GTTGGCCTTAG-3'). The relative mtDNA copy number was calculated by normalizing the mtDNA content to the expression of the β -actin gene.

2.15. Assessment of Mitochondrial Membrane Potential (MMP). MMP of cardiomyocytes was evaluated using a JC-1 mitochondria staining kit (Thermo Fisher Scientific). Briefly, cardiomyocytes (5×10^3 cells/well) were plated in 96-well plates, treated for 24, and incubated with JC-1 fluorescent dye for 20 min at room temperature in the dark. The fluorescent staining by JC-1 was evaluated by fluorescence microscopy. JC-1 monomers were imaged at excitation and emission wavelengths of 490 nm and 530 nm, respectively; JC-1 aggregates were imaged at excitation and emission wavelengths of 525 nm and 590 nm, respectively.

2.16. Detection of Mitochondrial ROS. The production of mitochondrial ROS was determined by using a MitoSOX fluorescent staining kit (Thermo Fisher Scientific, Waltham, USA) according to the manufacturer's protocol. Confocal laser scanning microscopy was used to capture fluorescent images, which were further analyzed using ImageJ software.

2.17. Flow Cytometry Analysis of ROS-Positive Cells. ROS production in cardiomyocytes was evaluated using the 2',7'-dichlorofluorescein diacetate (DCF-DA) staining assay (Thermo Fisher Scientific). Briefly, the cells were incubated with DCF-DA for 30 min at 37°C in the dark, washed, resus-

pending in PBS, and maintained on ice for immediate assay by flow cytometry (BD Biosciences). The data were analyzed using FACSDiva software (BD) to calculate the number of ROS-positive cardiomyocytes.

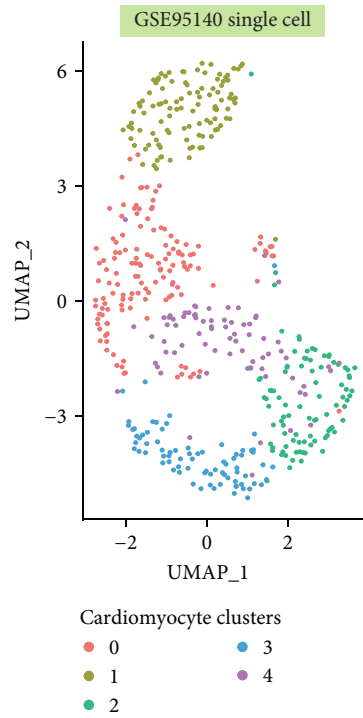
2.18. Mitochondrial Mass Analysis Using MitoTracker Red Staining. MitoTracker Red staining was performed to assess mitochondrial mass. Briefly, cardiomyocytes were incubated with 100 nM MitoTracker Red for 30 min at 37°C. Fluorescence was detected at excitation and emission wavelengths of 490 and 516 nm, respectively, using an ELx-800 microplate reader (BioTek; Winooski, VT, USA).

2.19. Statistical Analysis. The data are presented as the mean \pm standard deviation. All data analyses were performed using GraphPad Prism software (version 8; GraphPad Software, La Jolla, USA). Statistical significance of differences between various treatment groups was assessed using unpaired Student's *t*-test or one-way ANOVA followed by the Bonferroni multiple comparison test. $p < 0.05$ indicated statistical significance.

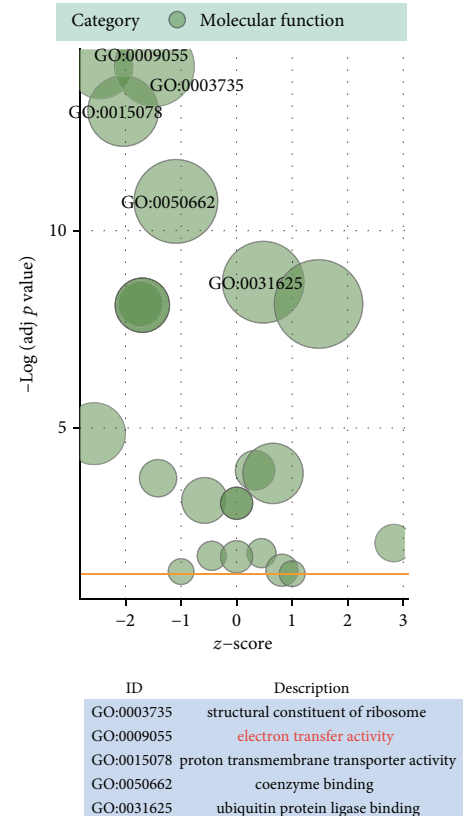
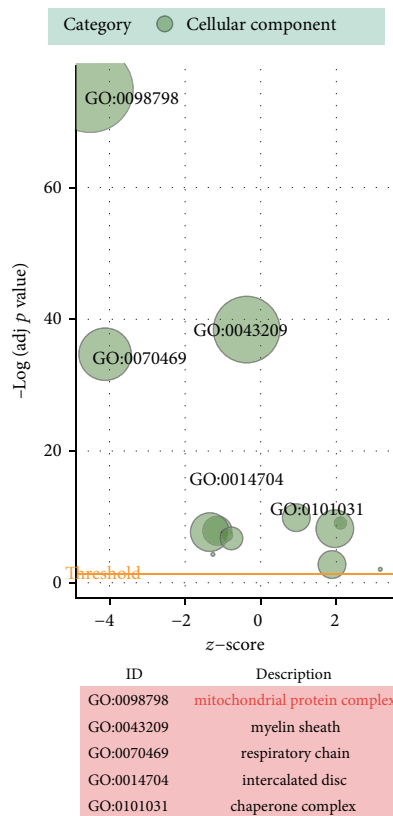
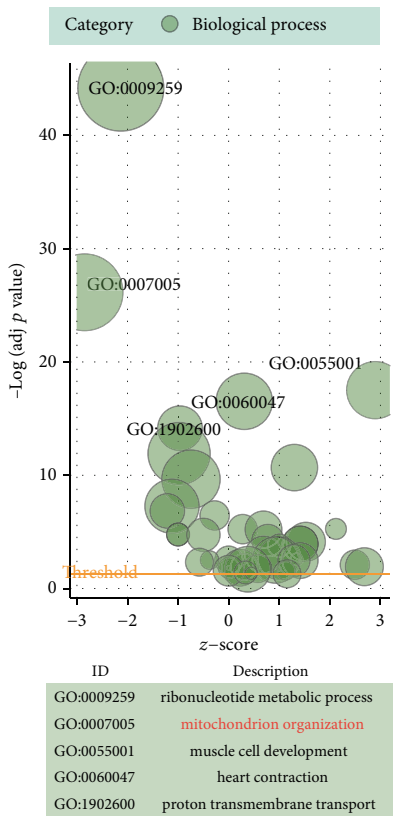
3. Results

3.1. scRNA-seq Clustering by the Seurat Package and Functional Enrichment Analysis. The number of principal components was set as 12, and cardiomyocytes were classified into six clusters based on UMAP visualization after batch correction (Figure 1(a)). A total of 3,408 highly variable genes were detected after normalization. Consequently, a total of 288 markers were identified by the Wilcoxon signed-rank test. These markers were then subjected to GO enrichment analysis. As shown in Figure 1(b) and Table S1, the genes were significantly enriched in "ribonucleotide metabolic process" (enriched genes = 97, p value = $1.44E - 48$), "mitochondrion organization" (enriched genes = 77, p value = $3.35E - 29$), "muscle cell development" (enriched genes = 43, p value = $1.72E - 20$), "heart contraction" (enriched genes = 42, p value = $2.16E - 19$), and "proton transmembrane transport" (enriched genes = 77, p value = $7.66E - 17$) in the biological process category. Additionally, DE genes were significantly enriched in "mitochondrial protein complex" (enriched genes = 104, p value = $2.18E - 78$), "myelin sheath" (enriched genes = 65, p value = $4.38E - 41$), "respiratory chain" (enriched genes = 43, p value = $2.76E - 37$), "intercalated disc" (enriched genes = 18, p value = $6.72E - 12$), and "chaperone complex" (enriched genes = 11, p value = $4.69E - 11$) in the cellular component category. For molecular function, the terms "structural constituent of ribosome" (enriched genes = 37, p value = $2.43E - 17$), "electron transfer activity" (enriched genes = 24, p value = $2.73E - 17$), "proton transmembrane transporter activity" (enriched genes = 29, p value = $5.49E - 16$), "coenzyme binding" (enriched genes = 41, p value = $1.63E - 13$), and "ubiquitin protein ligase binding" (enriched genes = 39, p value = $2.34E - 11$) were also enriched.

As shown in Figure 1(c) and Table S2, GSEA was used to analyze the CH-related KEGG pathways, and the KEGG: oxidative phosphorylation pathway was significantly enriched in



(a)



(b)

FIGURE 1: Continued.

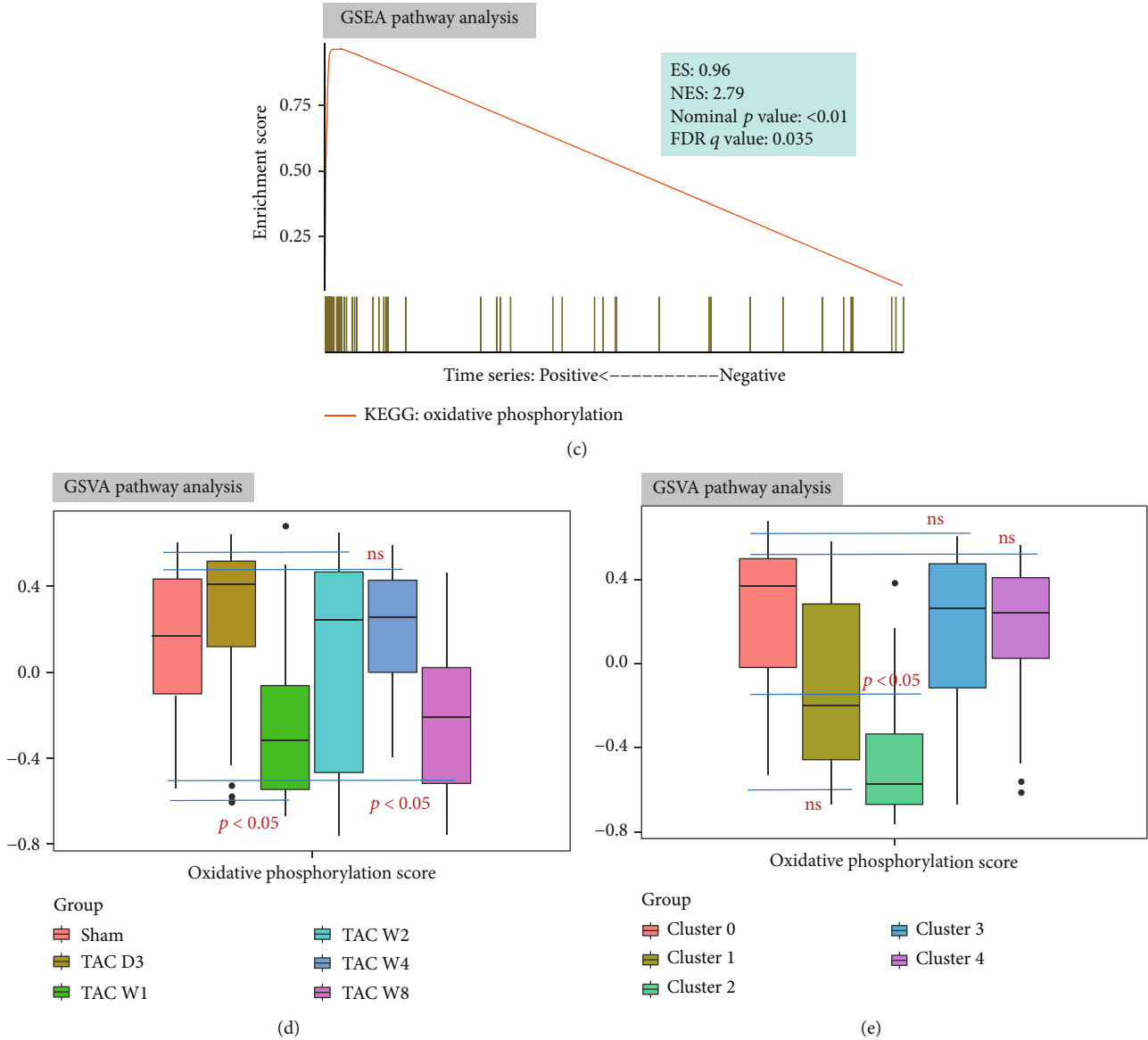


FIGURE 1: scRNA-seq clustering by the Seurat package and functional enrichment analysis. (a) UMAP visualization after batch correction. Cells are colored according to the clusters. (b) GO enrichment analysis of differentially expressed genes, including biological process, cellular component, and molecular function categories. (c) KEGG: oxidative phosphorylation pathway enrichment map of time series analysis during the development of a TAC model. (d) The patterns of the GSEA-calculated scores of the KEGG: oxidative phosphorylation pathway at various stages of cardiac hypertrophy and after sham operation. (e) The patterns of the GSEA-calculated scores of the KEGG: oxidative phosphorylation pathway across various cell clusters.

the progression of CH based on time series analysis (ES = 0.96, $S = 2.79$, nominal p value < 0.01 , FDR q value = 0.035). Furthermore, the GSEA calculated scores of the KEGG: oxidative phosphorylation (OxP score) pathway at various stages of CH were distinctly different from those in the sham operation group. Specifically, CH-related scores were significantly lower in the TAC W1 and W4 groups compared to those in the sham group (all p value < 0.05 ; Figure 1(d) and Table S3). Moreover, the patterns of GSEA calculated based on the corresponding OxP scores across various cell clusters showed that the scores were significantly lower in cluster 2 than those in cluster 0 (p value < 0.05 ; Figure 1(e)).

3.2. Identification of Candidate Biomarkers Involved in TAC-Induced CH. DE genes in cluster 2 are illustrated by a volcano plot (Nduzf1: average LogFC = 2.21, adjusted p value = 1.78 $E - 38$; Figure 2(a)). These genes included genes with log fold change > 1 , which were used for Spearman correlation analysis; the results showed that Nduzf1 was highly correlated with the OxP score ($R = 0.74$, p value < 0.05 ; Figure 2(b)). The validation of Nduzf1 using GSE24454 showed that Nduzf1 was significantly downregulated in the heart tissue from aortic banding mice compared to that in sham-operated mice (Figure 2(c)). Additionally, NDUSF1 was identified as a key interactor in the protein-protein

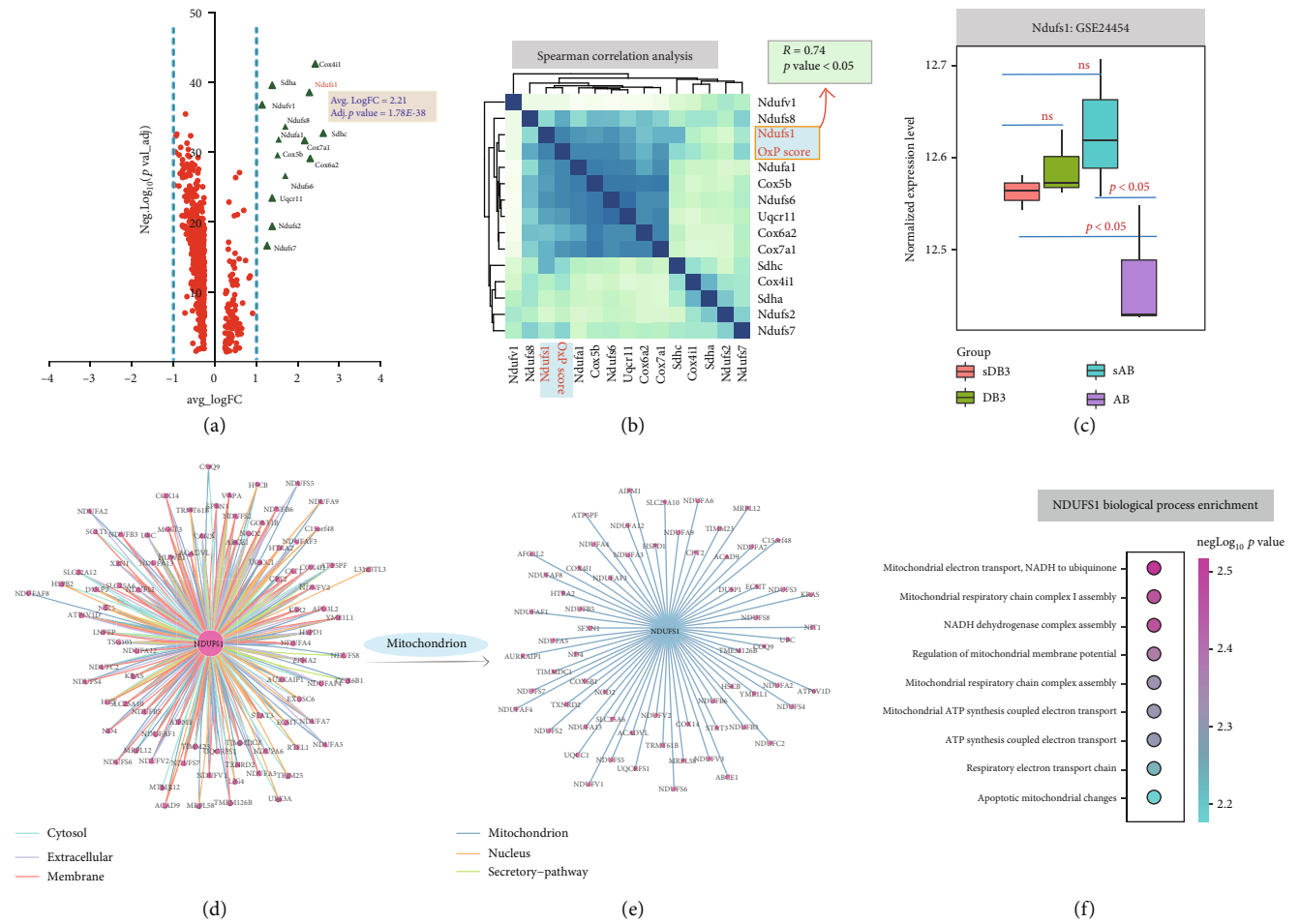


FIGURE 2: Identification of candidate biomarkers involved in TAC-induced CH. (a) Volcano plot of the differentially expressed genes in cluster 2 based on the p value and expression fold changes. (b) Spearman correlation analysis of genes from cluster 2 and GSEA scores of the KEGG: oxidative phosphorylation pathway in cluster 2. OxP score: GSEA scores of KEGG: oxidative phosphorylation. (c) The expression of Ndufs1 in mouse cardiac tissue based on the data of GSE24454. Mice were subjected to 4 weeks of aortic banding (AB) or sham procedure (sAB), banding and subsequent debanding (DB3), or sham procedure and subsequent debanding (sDB3) and sacrificed 3 days after debanding. (d) Protein-protein interaction network analysis of NDUFS1 based on the CompPPI database. (e) Protein-protein interaction network analysis of NDUFS1 in mitochondria. (f) Functional enrichment analysis of mitochondrial proteins interacting with NDUFS1.

interaction network using CompPPI analysis and shared a close relationship with mitochondrial functional proteins, including STAT3, COX6B1, and ATP5PF (Figure 2(d), Figure 2(e), and Table S4). The biological process enrichment analysis showed that proteins that potentially interact with Ndufs1 were significantly associated with key mitochondrial functions, such as “mitochondrial electron transport, NADH to ubiquinone” ($p\text{-value} = 2.78E-4$), “mitochondrial respiratory chain complex I assembly” ($p\text{-value} = 1.52E-3$), and “NADH dehydrogenase complex assembly” ($p\text{-value} = 1.15E-2$) (Figure 2(f) and Table S5). Based on the results of bioinformatics analysis, Ndufs1 was selected for subsequent validation and functional analysis.

3.3. Ndufs1 Was Downregulated in the Hypertrophic Mouse Heart. As shown in Figures 3(a) and 3(b), the results of H&E staining indicated that cardiomyocytes were significantly enlarged in the TAC group compared to those in

the sham group ($p < 0.05$). Examination of the dissected heart tissue indicated that the heart weight, HMI, LVMI, and LV/TL were significantly higher in the TAC group than those in the sham group (Figures 3(c)–3(f); all $p < 0.05$). The results of echocardiography examination showed that the thickness of IVS and LVPW was significantly higher in the TAC group than that in the sham group (Figures 3(g)–3(i); all $p < 0.05$). qRT-PCR analysis showed that the mRNA expression levels of ANP, BNP, and β -MHC were significantly higher in heart tissue from the TAC group than those in the sham group (Figures 3(j)–3(l); all $p < 0.05$). Importantly, the expression levels of Ndufs1 mRNA and protein were significantly reduced in the heart tissue from the TAC group compared to those in the sham group (Figures 3(m) and 3(n); all $p < 0.05$). TEM examination showed that the mitochondrial volume was significantly increased, and the number of mitochondria was significantly decreased in the heart tissue from the TAC group compared

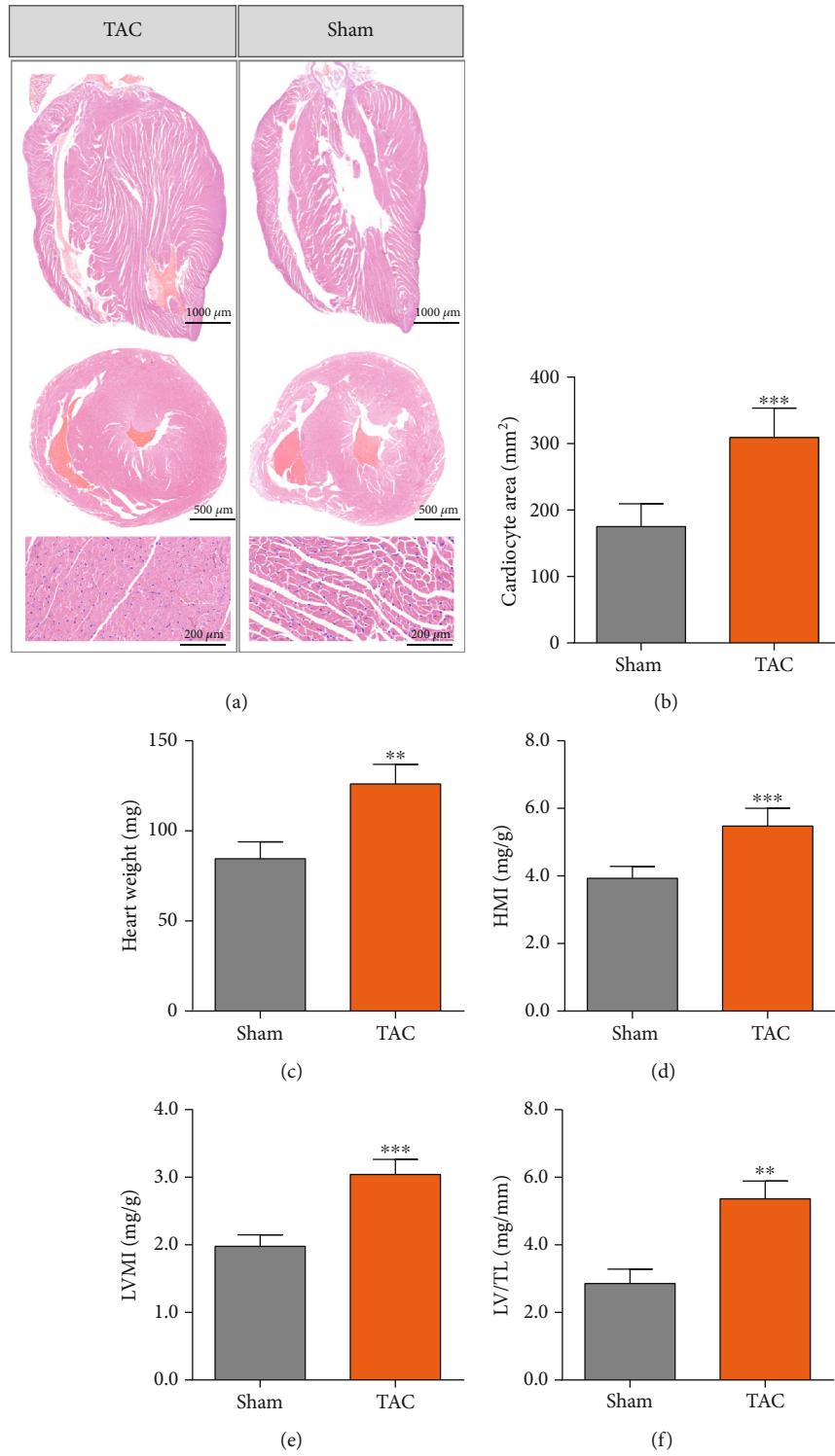


FIGURE 3: Continued.

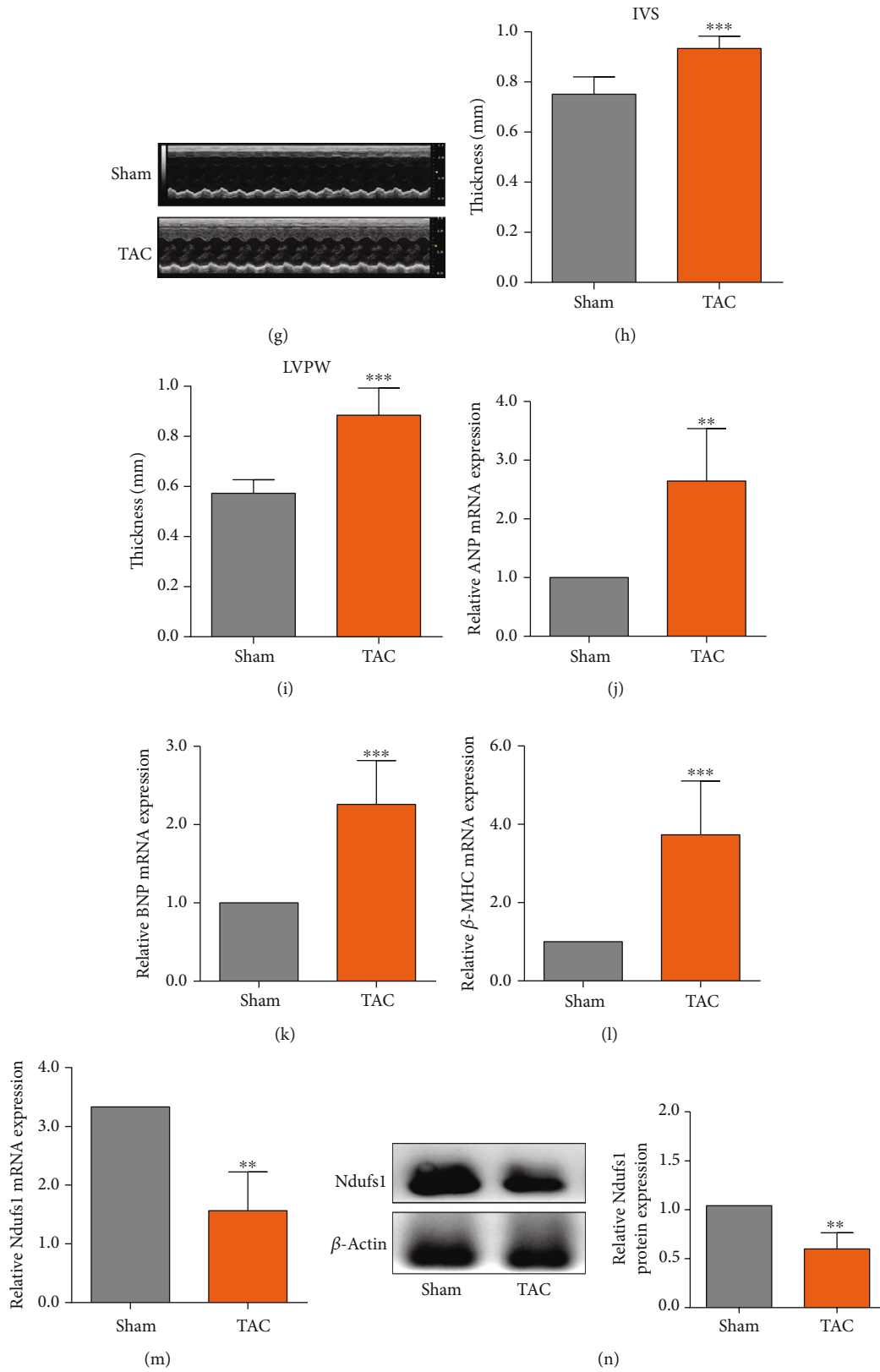


FIGURE 3: Continued.

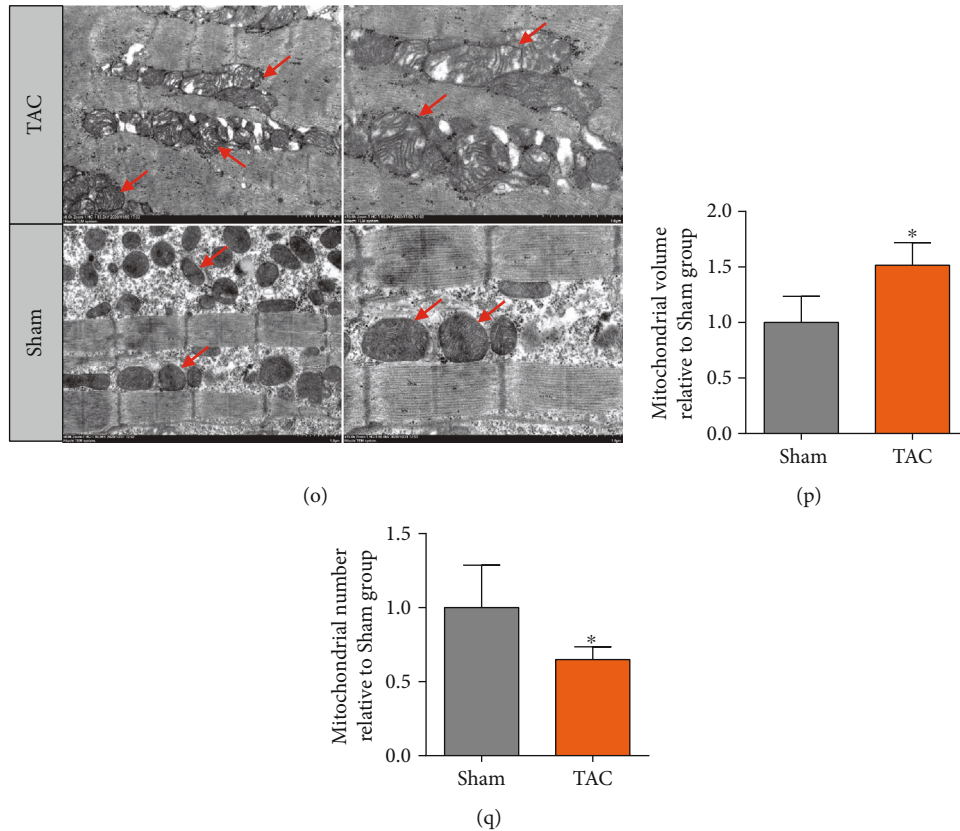


FIGURE 3: *Ndufs1* was downregulated in the hypertrophic heart of mice. (a) H&E staining of mouse heart tissue in the sham and TAC groups. (b) The cardiomyocyte area was evaluated in the sham and TAC groups. The heart was dissected, and the heart weight (c), HMI (d), LVMI (e), and LV/TL (f) in the sham and TAC groups were determined. (g) Representative images of echocardiography in the sham and TAC groups, and the thickness of IVS (h) and LVPW (i) in the sham and TAC groups according to echocardiography. (j–l) The mRNA expression levels of ANP, BNP, and β -MHC in the heart tissue of the sham and TAC groups determined by qRT-PCR. (m, n) The mRNA and protein expression levels of *Ndufs1* in the heart tissue of the sham and TAC groups were determined by qRT-PCR and western blot assays, respectively. (o) Representative TEM images of the heart tissue of the sham and TAC groups. (p, q) The mitochondrial volume and number were analyzed based on TEM images. $N = 6$. * $p < 0.05$, ** $p < 0.01$, and *** $p < 0.001$.

to those in the control group (Figures 3(o)–3(q); all $p < 0.05$). The sarcomeres were enlarged, and myofibrils were disordered in the TAC group. Comparison with the sham group indicated that mitochondria in TAC-induced CH cardiomyocytes showed mild to moderate swelling, intact adventitia, edema of the matrix, disappearance of partial cristae, and aggregation between myofibrils.

3.4. Effects of Ang II on the Expression Levels of ANP, BNP, β -MHC, and *Ndufs1*. As shown in Figure 4, Ang II treatment caused a significant increase in the mRNA and protein expression levels of ANP, BNP, and β -MHC in cardiomyocytes compared to those in the control group (Figures 4(a)–4(f); all $p < 0.05$). On the other hand, the mRNA and protein expression levels of *Ndufs1* in cardiomyocytes were significantly reduced by Ang II treatment compared to those in the control group (Figures 4(g) and 4(h); all $p < 0.05$). These results indicated that *Ndufs1* may have certain biological functions in Ang II-stimulated cardiomyocytes.

3.5. Effects of *Ndufs1* Knockdown on the Expression Levels of ANP, BNP, and β -MHC and on Mitochondrial Functions.

Ndufs1 was silenced by transient transfection of cardiomyocytes with *Ndufs1* siRNA. As shown in Figures 5(a) and 5(b), *Ndufs1* siRNA transfection (si-*Ndufs1*) significantly reduced the expression levels of *Ndufs1* mRNA and protein in cardiomyocytes compared to that in cells transfected with scrambled siRNA (si-NC; all $p < 0.05$). The size of cardiomyocytes was significantly increased in the si-*Ndufs1* group compared with that in the si-NC group (Figure 5(c); $p < 0.01$). The results of qRT-PCR and western blot indicated that the expression levels of mRNA and protein of ANP, BNP, and β -MHC were significantly downregulated in si-*Ndufs1*-transfected cardiomyocytes compared to those in si-NC-transfected cardiomyocytes (Figures 5(d)–5(i); all $p < 0.05$). Furthermore, the effects of *Ndufs1* knockdown on mitochondrial functions were determined by measuring mitochondrial DNA content, ROS production, and MMP. As shown in Figure 5(j), *Ndufs1* knockdown significantly reduced the mitochondrial DNA content in cardiomyocytes compared to that in the si-NC group ($p < 0.01$). Consistently, the levels of ROS production in cardiomyocytes were significantly elevated after *Ndufs1* silencing (Figures 5(k) and 5(l); all $p < 0.05$). Moreover, the fluorescent staining results showed that *Ndufs1* knockdown

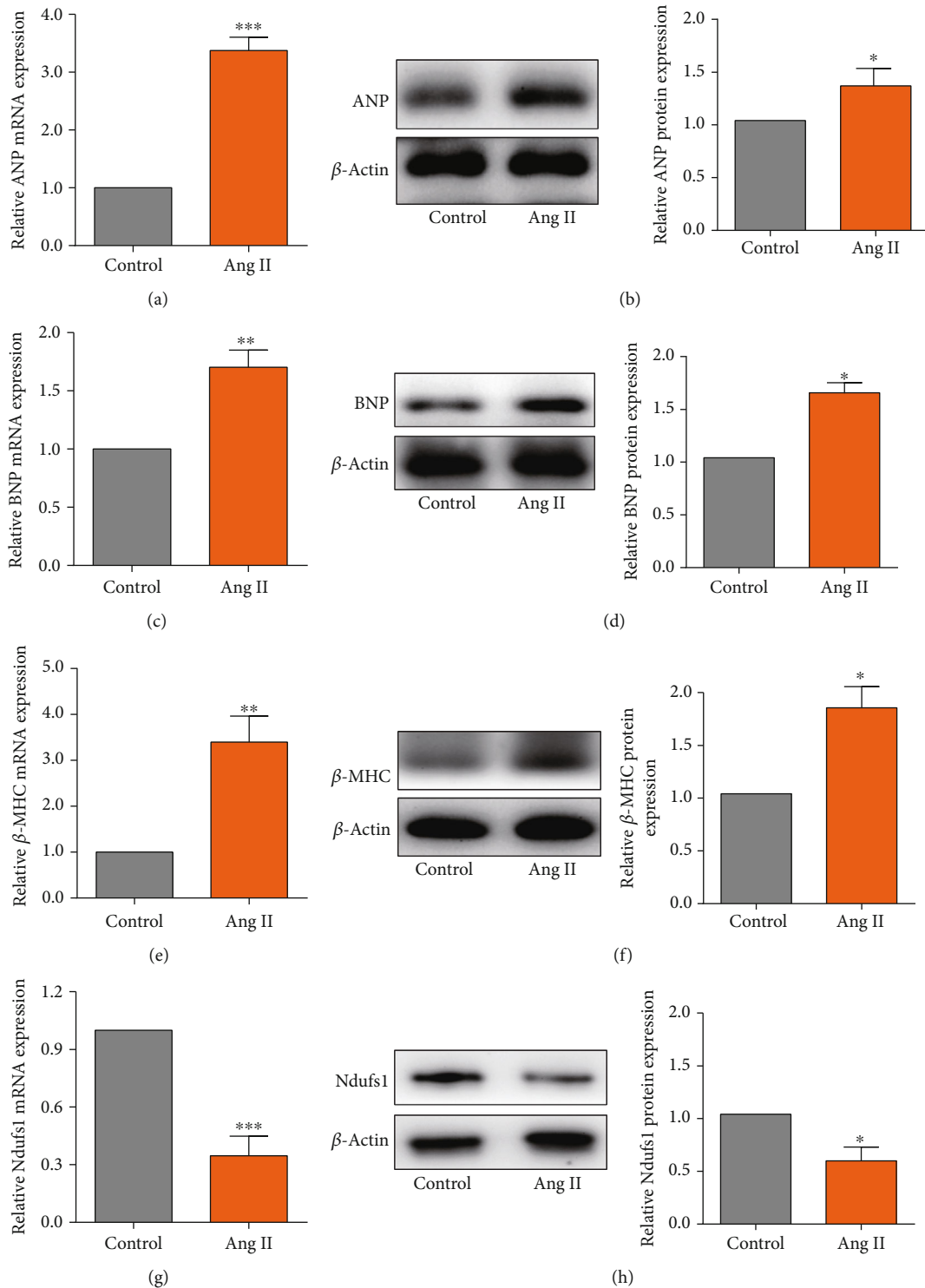


FIGURE 4: Ang II induced downregulation of Ndufs1 in rat cardiomyocytes. The mRNA and protein expression levels of ANP (a, b), BNP (c, d), β -MHC (e, f), and Ndufs1 (g, h) in control and Ang II-treated cardiomyocytes were determined by qRT-PCR and western blot assay. $N = 3$. * $p < 0.05$, ** $p < 0.01$, and *** $p < 0.001$.

dramatically increased MMP and mitochondrial mass of cardiomyocytes compared to those in the si-NC group (Figures 5(m) and 5(n); all $p < 0.05$). These results indicate that silencing Ndufs1 gene expression may aggravate MMP damage in Ang II-induced myocardial hypertrophy.

3.6. Effects of Ndufs1 Overexpression on Ang II-Induced Hypertrophy of Cardiomyocytes. Initially, we constructed the vector for Ndufs1 overexpression using the pcDNA3.1 plasmids. Cardiomyocytes transfected with the vector for Ndufs1 overexpression exhibited a significant increase in

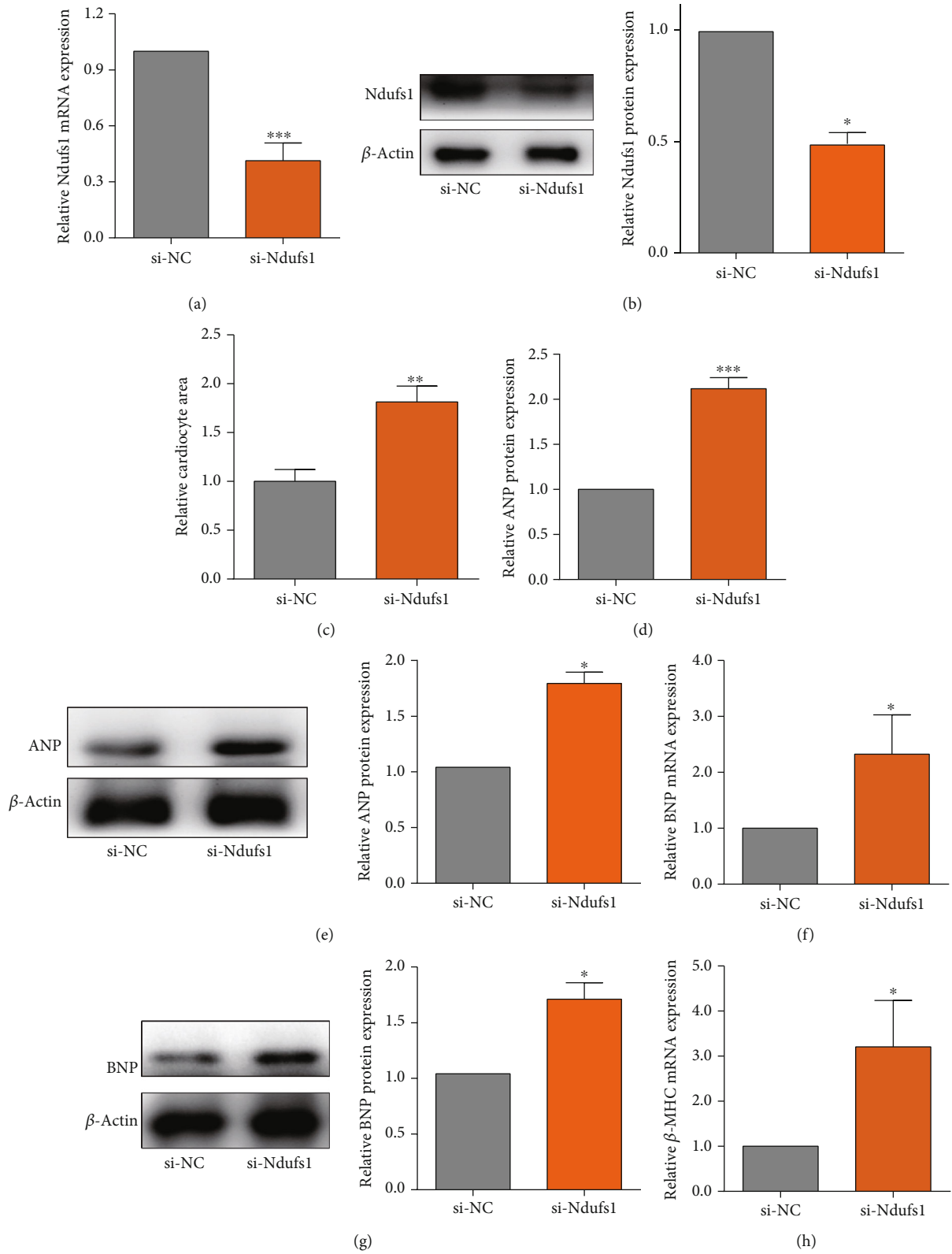


FIGURE 5: Continued.

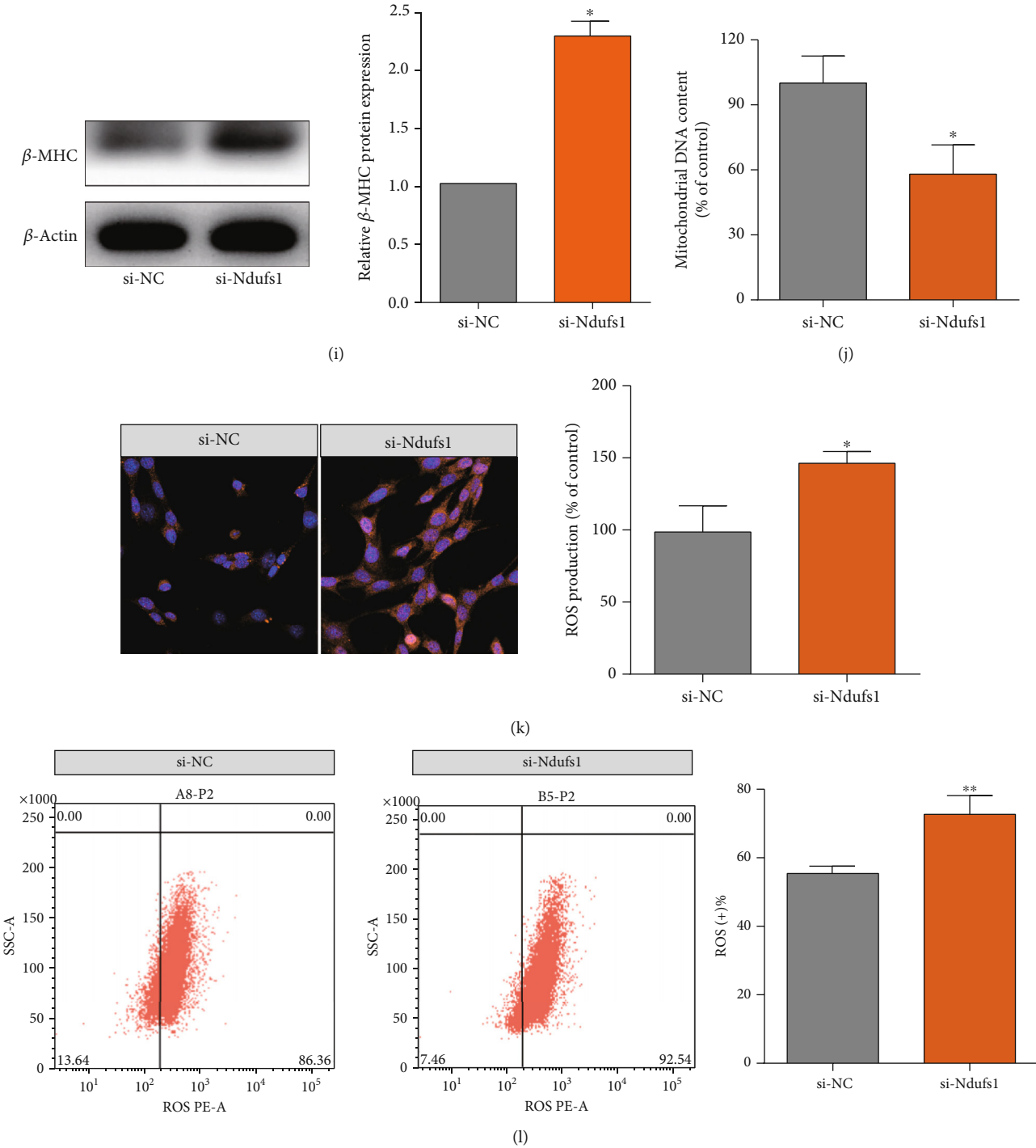


FIGURE 5: Continued.

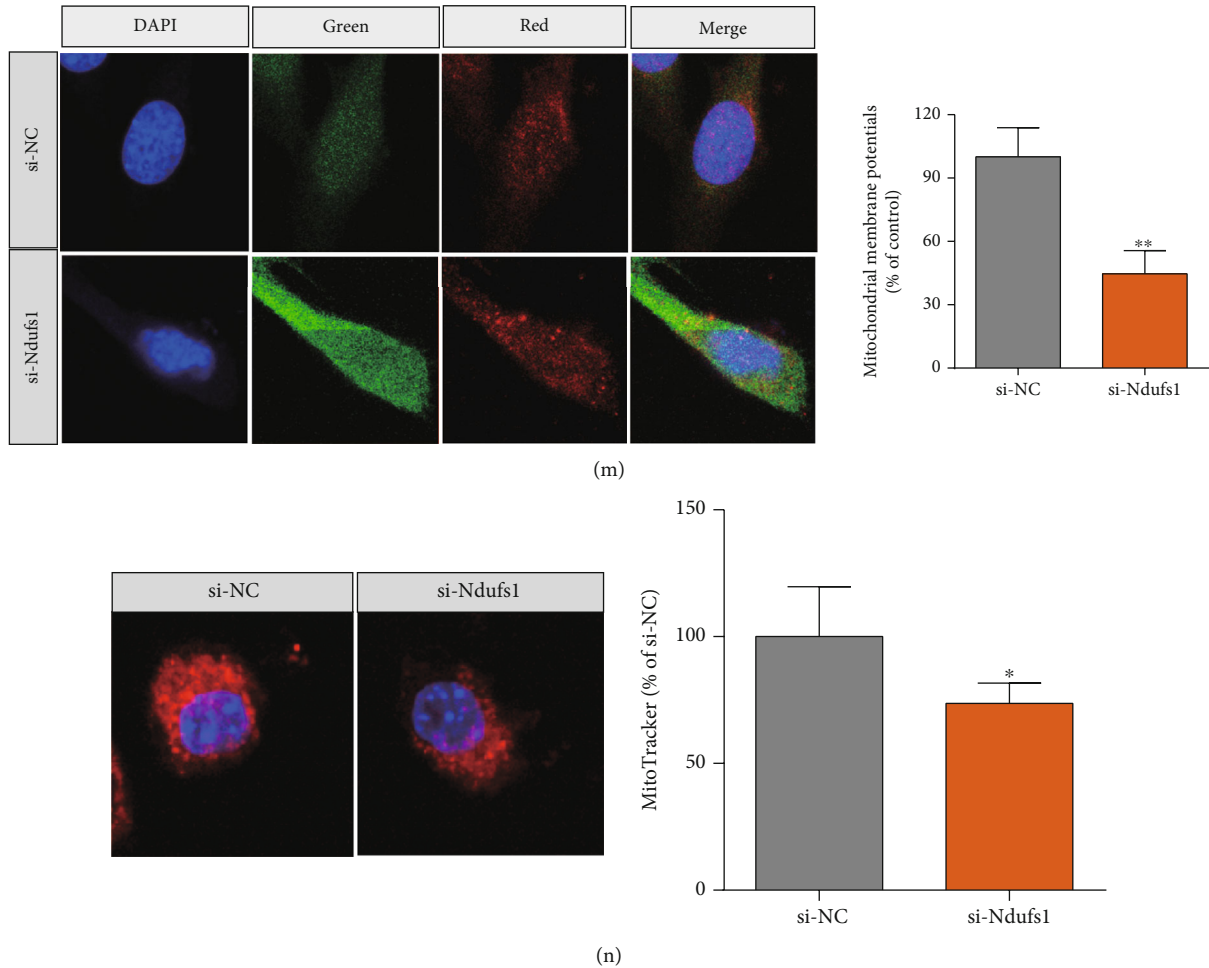


FIGURE 5: Effects of *Ndufs1* knockdown on the expression of hypertrophic markers and mitochondrial function. (a, b) The mRNA and protein expression levels of *Ndufs1* in cardiomyocytes transfected with scrambled siRNA or *Ndufs1* siRNA were determined by qRT-PCR and western blot assays. (c) The relative cardiomyocyte area was determined in cardiomyocytes transfected with scrambled siRNA or *Ndufs1* siRNA. The mRNA and protein expression levels of ANP (d, e), BNP (f, g), and β -MHC (h, i) in cardiomyocytes transfected with scrambled siRNA or *Ndufs1* siRNA were determined by qRT-PCR and western blot assays. The mitochondrial DNA content (j), mitochondrial ROS production (k), ROS-positive cardiomyocytes (l), MMP (m), and mitochondrial mass (n) were evaluated in cardiomyocytes transfected with scrambled siRNA or *Ndufs1* siRNA. $N = 3$. * $p < 0.05$, ** $p < 0.01$, and *** $p < 0.001$.

the levels of *Ndufs1* mRNA and protein compared with those in the cells transfected with pcDNA3.1 (NC group; Figures 6(a) and 6(b); all $p < 0.05$). As expected, Ang II treatment increased the cardiomyocyte area compared with that in the control group, and *Ndufs1* overexpression attenuated Ang II-induced increase in the cardiomyocyte area (Figure 6(c); $p < 0.05$). Consistently, Ang II treatment caused a significant increase in the levels of mRNA and protein of ANP, BNP, and β -MHC (all $p < 0.05$), and *Ndufs1* overexpression partially counteracted the stimulatory effects of Ang II on ANP, BNP, and β -MHC expression in cardiomyocytes (Figures 6(d)–6(i); all $p < 0.05$). The mitochondrial DNA content of cardiomyocytes was significantly reduced by Ang II, and this effect was attenuated by *Ndufs1* overexpression (Figure 6(j); all $p < 0.05$). Moreover, *Ndufs1* overexpression attenuated Ang II-induced elevation in the ROS production levels in cardiomyocytes (Figures 6(k) and 6(l); all $p < 0.05$). Importantly, Ang II treatment significantly repressed MMP and mitochondrial mass in cardiomyocytes,

and the effect was significantly alleviated by overexpression of *Ndufs1* (Figures 6(m) and 6(n)). In turn, these results indicate that *Ndufs1* overexpression may protect against MMP disorder in Ang II-induced mitochondrial dysfunction.

4. Discussion

CH is a pathophysiological response characterized by increased thickness of the ventricular wall, greater myocardial cell volume, and enhanced myocardial contractility in the early stage of overload pressure [1, 3]. The pathophysiology of CH is complex and involves multiple cellular events, and the mechanisms of the development of CH are not fully understood [1, 3, 30]. Growing evidence indicates that mitochondrial dysfunction is closely related to the development and progression of CH. In the present study, we explored the GSE95140 datasets by using integrated bioinformatics analysis and demonstrated downregulation of *Ndufs1* in heart tissue of mice with CH. The expression of *Ndufs1* was

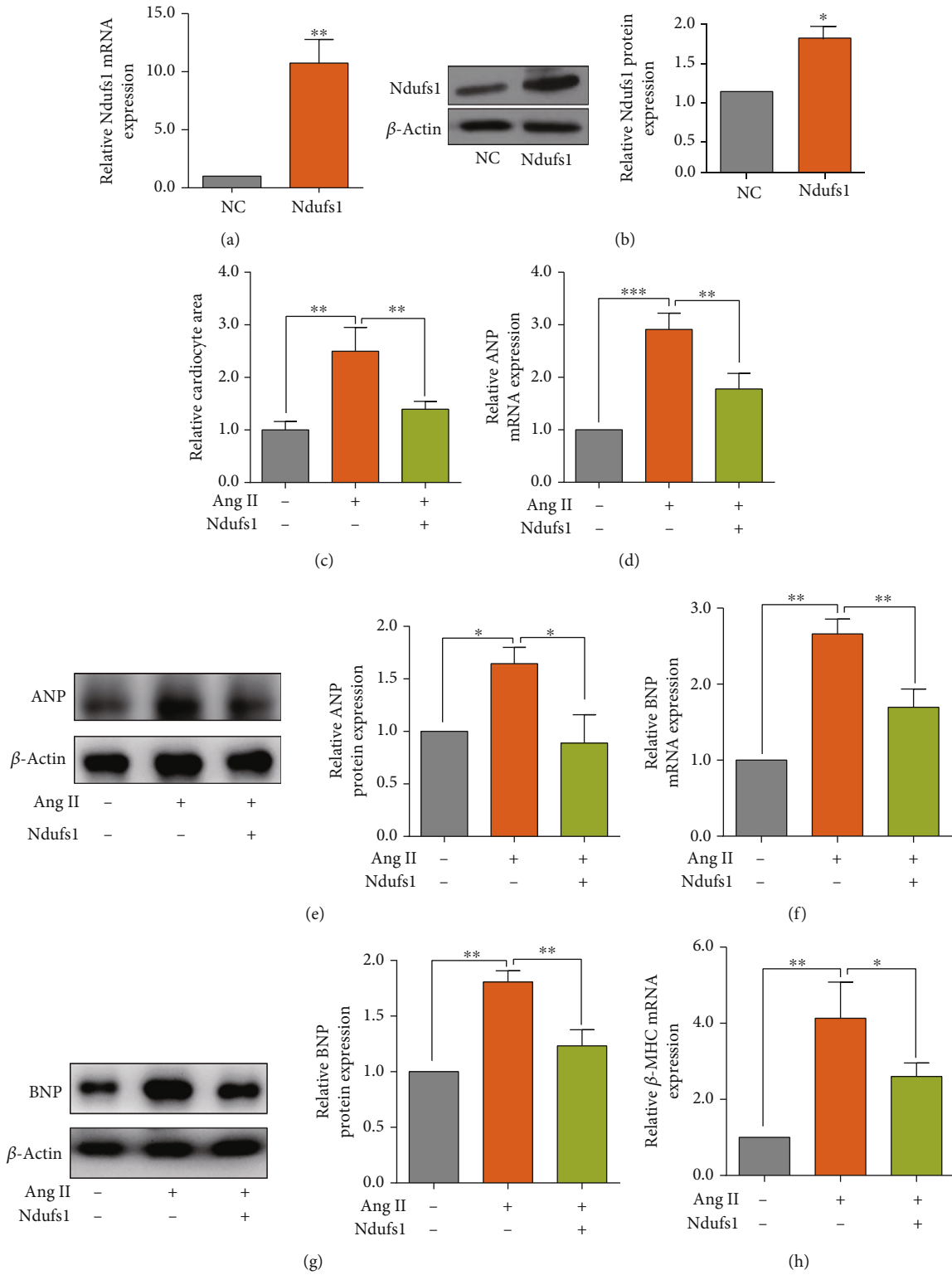


FIGURE 6: Continued.

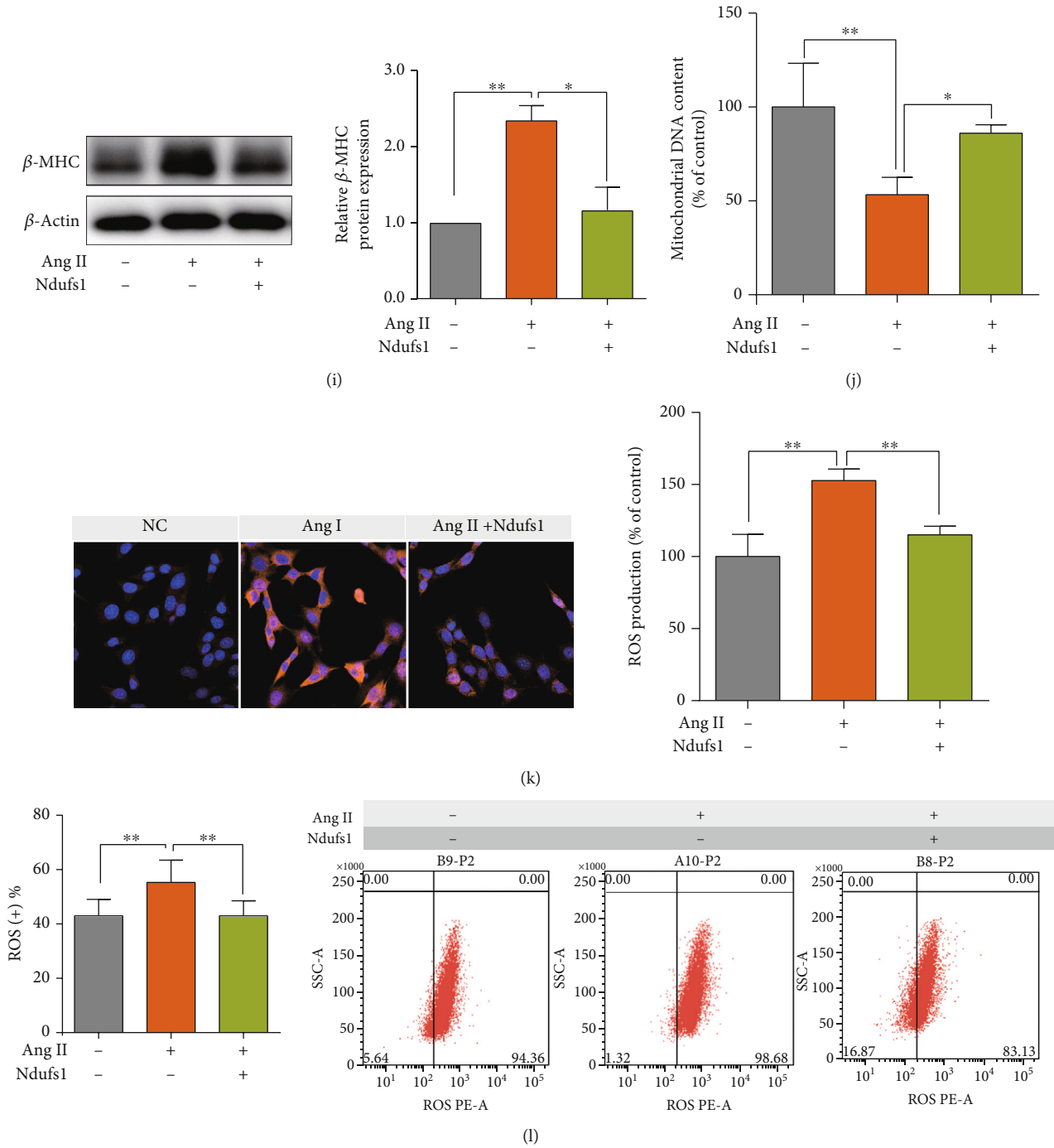


FIGURE 6: Continued.

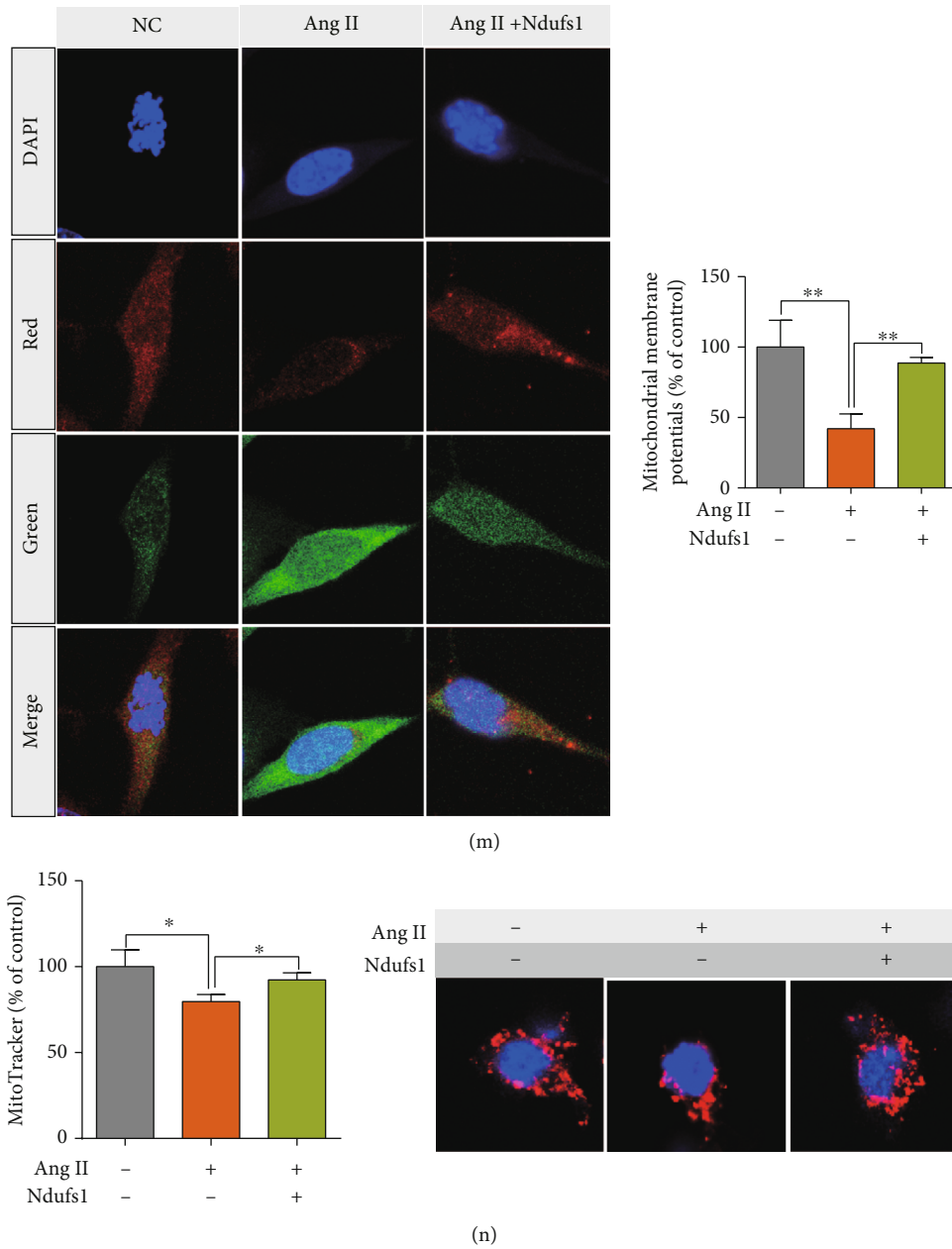


FIGURE 6: Ndufs1 overexpression attenuated Ang II-induced cardiac hypertrophy and mitochondrial dysfunction in cardiomyocytes. (a, b) The mRNA and protein expression levels of Ndufs1 in cardiomyocytes transfected with pcDNA3.1 or pcDNA3.1-Ndufs1 were determined by qRT-PCR and western blot assays. (c) The relative cardiomyocyte area was determined in cardiomyocytes subjected to various treatments. The mRNA and protein expression levels of ANP (d, e), BNP (f, g), and β -MHC (h, i) in cardiomyocytes subjected to various treatments were determined by qRT-PCR and western blot assays. The mitochondrial DNA content (j), mitochondrial ROS production (k), ROS-positive cardiomyocytes (l), MMP (m), and mitochondrial mass (n) were evaluated in cardiomyocytes subjected to various treatments. $N = 3$. * $p < 0.05$, ** $p < 0.01$, and *** $p < 0.001$.

further validated in a mouse TAC model; our data showed that Ndufs1 expression was significantly downregulated in hypertrophic heart tissue compared to that in normal controls. Moreover, *in vitro* mechanistic studies showed that Ndufs1 knockdown induced cardiomyocyte hypertrophy, decreased mitochondrial DNA content and MMP, and increased mitochondrial ROS production in cardiomyocytes. On the other hand, Ang II treatment upregulated the expression levels of ANP, BNP, and β -MHC, decreased mitochondrial DNA

content and MMP, and increased mitochondrial ROS production in cardiomyocytes; moreover, Ang II-mediated effects were significantly attenuated by overexpression of Ndufs1 in rat cardiomyocytes. Overall, our results indicate the important roles of Ndufs1 in the development and progression of CH.

In the present study, TAC surgery was performed to establish a CH mouse model. Enlarged cardiomyocytes and increases in the heart weight, HMI, LVMI, LV/TL, and

thickness of IVS and LVPW were detected in mice subjected to TAC compared with those in sham-operated mice; these findings are consistent with the results of previous studies [31]. Additionally, the mRNA expression levels of ANP, BNP, and β -MHC were elevated in the heart tissue of the mice with CH. ANP, BNP, and β -MHC are commonly used cardiac hypertrophic biomarkers, and elevated levels of these biomarkers have been demonstrated in heart tissue in clinical studies and animal models [32–35]. Overall, these results suggest successful establishment of CH in mice subjected to TAC treatment. Further validation by qRT-PCR and western blot showed that the expression levels of *Ndusf1* mRNA and protein were downregulated in hypertrophic heart tissue. The data suggest that *Ndusf1* may play an important role in CH.

Mitochondria are considered to be dynamic “energy stations”, and these morphological changes are characterized by fragmented disconnection and elongated interconnection of mitochondria, which are regulated by activation of mitochondrial fission and fusion proteases or posttranslational modifications of proteins during the development of CH [1, 36]. *Ndusf1* (NADH:ubiquinone oxidoreductase core subunit S1) is the largest subunit of complex I; the corresponding gene encodes a 75 kDa subunit of NADH-ubiquinone oxidoreductase [37] and thus has gained particular attention due to its significant role in the activity of mitochondrial oxidative phosphorylation. Mutations or deficiency of this gene can destabilize complex I assembly and result in defects of the activity of the electron transport chain (ETC) and elevated ATP production, which can cause mitochondrial fusion and fission to restore damaged mitochondrial DNA and remove damaged mitochondrial fragments, respectively [38–40]. However, the role of *Ndusf1* in the pathophysiology of CH has not been reported; however, the importance of *Ndusf1* in cardiovascular diseases has been emphasized by several research groups. Qi et al. showed that *Akap1* deficiency exacerbates diabetic cardiomyopathy in mice by *Ndusf1*-mediated mitochondrial dysfunction and apoptosis [19]. *Ndusf1* was shown to be upregulated in cardiac cells upon cyclic stretch, which may be associated with mitochondrial biogenesis [41]. Sato et al. showed that *Ndusf1* is associated with the cardiac response to iron deficiency [42]. Additionally, the cardiac levels of acetylated forms of *Ndusf1* are decreased in caloric restriction [43]. Impaired electron transport chains in mitochondria contribute to the development and progression of CH [44, 45]. *Ndusf1* is one of the key regulators of the electron transport chain; thus, we speculate that *Ndusf1* may be a key factor in CH. The results of our *in vitro* studies indicated that the Ang II-induced increase of the expression of hypertrophic biomarkers was accompanied by downregulation of *Ndusf1* in cardiomyocytes. Ang II is widely used to induce a cellular model of CH in cardiomyocytes [46, 47]. Schwartz et al. used serial analysis of gene expression to demonstrate that continuous Ang II treatment induces downregulation of *Ndusf1* in the mouse heart [48]. The activation of the endogenous renin-angiotensin aldosterone system increases the protein levels of *Ndusf1* in urine in hypertensive patients [49]. Additionally, Ang II exacerbates mitochondrial dysfunction and oxidative stress to cause heart

failure [50]. Thus, in combination with these findings, our results may imply that Ang II-induced CH in cardiomyocytes may be associated with downregulation of *Ndusf1*.

To gain additional insight into the mechanism of action of *Ndusf1* in Ang II-induced CH, we performed loss- and gain-of-function studies in cardiomyocytes. Our results showed that *Ndusf1* knockdown decreased the mitochondrial DNA content and MMP and increased mitochondrial ROS production; in addition, *Ndusf1* knockdown increased the expression levels of hypertrophic biomarkers in cardiomyocytes, possibly indicating that *Ndusf1* knockdown promoted CH by impairing mitochondrial functions. Downregulation of *Ndusf1* inhibits the neuroprotective effects of pyrroloquinoline against rotenone injury in cultured SH-SY5Y cells and cultured midbrain neurons, and rotenone can impair mitochondrial dysfunction [51]. Lopez-Fabuel et al. showed that *Ndusf1* knockdown impairs mitochondrial O_2 consumption and increases ROS production in neurons [52]. On the other hand, our results showed that overexpression of *Ndusf1* attenuated Ang II-mediated effects in cardiomyocytes. Thus, *Ndusf1* may be involved in Ang II-mediated CH by modulating mitochondrial functions in cardiomyocytes.

Balanced regulation of mitochondrial fusion and fission is very delicate and susceptible to the development of CH and heart failure; thus, efficient myocardial therapies that target mitochondrial lesions and dysfunction may be a new strategy to suppress susceptibility to myocardial remodeling and attenuate myocardial fibrosis; however, these possibilities are poorly characterized [1, 5, 11]. *Ndusf1* has been illustrated to play a central role in the regulation of morphological dynamics and oxidative stress and may play an important role in mitochondrial crista remodeling, cytochrome release, and mitochondrial respiration in the development of CH and heart failure. A decrease in the expression of *Ndusf1*, in turn, contributes to aggravated mitochondrial membrane potential disorder, mitochondrial ROS production, and mitochondrial DNA damage.

In conclusion, our results demonstrated downregulation of *Ndusf1* in hypertrophic heart tissue, and the results of the mechanistic studies suggest that *Ndusf1* deficiency causes mitochondrial dysfunction in cardiomyocytes, which may be associated with the development and progression of CH.

5. Limitations

There are several limitations in the present study. First, the expression of *Ndusf1* in the mouse cardiac tissue was determined 4 weeks after TAC surgery in mice, which cannot reflect the changes in *Ndusf1* during the progression of CH. Thus, future studies may determine the expression of *Ndusf1* at various time points to confirm the role of *Ndusf1* in the progression of CH. Second, the expression of *Ndusf1* was validated only in mouse cardiac tissue and cardiomyocytes, and future studies should determine the expression of *Ndusf1* in the clinical samples of hypertrophic hearts. Third, loss- and gain-of-function studies were only performed *in vitro*, and the functional role of *Ndusf1* *in vivo*

in the pathophysiology of CH should be determined. Fourth, the downstream signaling pathways mediated by Nduzf1 should be further explored.

Data Availability

Both of the GSE95140 and GSE24454 datasets were obtained from the GEO (<https://www.ncbi.nlm.nih.gov/geo/>) database, and the analysis scripts would be accessed from Dr. Rongjun Zou on a request.

Conflicts of Interest

The authors have no conflict of interest to disclose.

Authors' Contributions

RZ, JT, and JQ take the responsibility for all aspects of the reliability and freedom from bias of the data presented and their discussed interpretation, and drafting the article. WS, MZ, WC, WL, NZ, and SW take the responsibility for the statistical analyses and interpretation of data. LM and XC take the responsibility for the full-text evaluation and guidance and final approval of the version to be submitted. All authors read and approved the final manuscript.

Acknowledgments

This study was funded by the Guangdong Peak Project (DFJH201802) and the Key Project of the Natural Science Foundation of Guangdong Province (2017B030311010).

Supplementary Materials

Additional file 1 Table S1: Gene Ontology enrichment terms for differentially expressed genes identified based on the scRNA-seq of pressure overload-induced myocardial hypertrophy. Additional file 2: Table S2: pathways correlated with pressure overload-induced myocardial hypertrophy based on time series-related GSEA. Additional file 3: Table S3: the oxidative phosphorylation score of single cardiomyocytes was calculated by GSVA. Additional file 4: Table S4: the cellular compartment-specific protein-protein interaction network of NDUFS1. Additional file 5: Table S5: biological process enrichment analyses of NDUFS1. (*Supplementary Materials*)

References

- [1] M. Nakamura and J. Sadoshima, "Mechanisms of physiological and pathological cardiac hypertrophy," *Nature Reviews Cardiology*, vol. 15, no. 7, pp. 387–407, 2018.
- [2] M. Samak, J. Fatullayev, A. Sabashnikov et al., "Cardiac hypertrophy: an introduction to molecular and cellular basis," *Medical Science Monitor Basic Research*, vol. 22, pp. 75–79, 2016.
- [3] I. Shimizu and T. Minamino, "Physiological and pathological cardiac hypertrophy," *Journal of Molecular and Cellular Cardiology*, vol. 97, pp. 245–262, 2016.
- [4] Y. K. Tham, B. C. Bernardo, J. Y. Ooi, K. L. Weeks, and J. R. McMullen, "Pathophysiology of cardiac hypertrophy and heart failure: signaling pathways and novel therapeutic targets," *Archives of Toxicology*, vol. 89, no. 9, pp. 1401–1438, 2015.
- [5] C. J. Oldfield, T. A. Duhamel, and N. S. Dhalla, "Mechanisms for the transition from physiological to pathological cardiac hypertrophy," *Canadian Journal of Physiology and Pharmacology*, vol. 98, no. 2, pp. 74–84, 2020.
- [6] H. D. Facundo, R. E. Brainard, F. R. de Lemos Caldas, and A. M. Lucas, "Mitochondria and cardiac hypertrophy," *Advances in Experimental Medicine and Biology*, vol. 982, pp. 203–226, 2017.
- [7] M. G. Rosca, B. Tandler, and C. L. Hoppel, "Mitochondria in cardiac hypertrophy and heart failure," *Journal of Molecular and Cellular Cardiology*, vol. 55, pp. 31–41, 2013.
- [8] G. Heusch, "Coronary microvascular obstruction: the new frontier in cardioprotection," *Basic Research in Cardiology*, vol. 114, no. 6, 2019.
- [9] H. Tsutsui, S. Kinugawa, and S. Matsushima, "Oxidative stress and heart failure," *American Journal of Physiology. Heart and Circulatory Physiology*, vol. 301, no. 6, pp. H2181–H2190, 2011.
- [10] B. Zhou and R. Tian, "Mitochondrial dysfunction in pathophysiology of heart failure," *The Journal of Clinical Investigation*, vol. 128, no. 9, pp. 3716–3726, 2018.
- [11] W. E. Hughes, A. M. Beyer, and D. D. Gutterman, "Vascular autophagy in health and disease," *Basic Research in Cardiology*, vol. 115, p. 41, 2020.
- [12] T. Pham, D. Loiselle, A. Power, and A. J. Hickey, "Mitochondrial inefficiencies and anoxic ATP hydrolysis capacities in diabetic rat heart," *American Journal of Physiology. Cell Physiology*, vol. 307, no. 6, pp. C499–C507, 2014.
- [13] A. Power, N. Pearson, T. Pham, C. Cheung, A. Phillips, and A. Hickey, "Uncoupling of oxidative phosphorylation and ATP synthase reversal within the hyperthermic heart," *Physiological Reports*, vol. 2, no. 9, p. e12138, 2014.
- [14] J. Marín-García, A. T. Akhmedov, and G. W. Moe, "Mitochondria in heart failure: the emerging role of mitochondrial dynamics," *Heart Failure Reviews*, vol. 18, no. 4, pp. 439–456, 2013.
- [15] J. A. Garza-Cervantes, M. Ramos-González, O. Lozano, C. Jerjes-Sánchez, and G. García-Rivas, "Therapeutic applications of cannabinoids in cardiomyopathy and heart failure," *Oxidative Medicine and Cellular Longevity*, vol. 2020, Article ID 4587024, 17 pages, 2020.
- [16] B. Martín-Fernández and R. Gredilla, "Mitochondria and oxidative stress in heart aging," *Age (Dordrecht, Netherlands)*, vol. 38, no. 4, pp. 225–238, 2016.
- [17] T. L. Capasso, B. Li, H. J. Volek et al., "BMP10-mediated ALK1 signaling is continuously required for vascular development and maintenance," *Angiogenesis*, vol. 23, no. 2, pp. 203–220, 2020.
- [18] Y. Ni, M. A. Hagra, V. Konstantopoulou, J. A. Mayr, A. A. Stuchebrukhov, and D. Meierhofer, "Mutations in NDUFS1 cause metabolic reprogramming and disruption of the electron transfer," *Cell*, vol. 8, no. 10, p. 1149, 2019.
- [19] B. Qi, L. He, Y. Zhao et al., "Akap1 deficiency exacerbates diabetic cardiomyopathy in mice by NDUFS1-mediated mitochondrial dysfunction and apoptosis," *Diabetologia*, vol. 63, no. 5, pp. 1072–1087, 2020.
- [20] Y. Zhu, Z. Wang, J. Ni et al., "Genetic variant in NDUFS1 gene is associated with schizophrenia and negative symptoms in Han Chinese," *Journal of Human Genetics*, vol. 60, no. 1, pp. 11–16, 2015.

- [21] S. Nomura, M. Satoh, T. Fujita et al., “Cardiomyocyte gene programs encoding morphological and functional signatures in cardiac hypertrophy and failure,” *Nature Communications*, vol. 9, no. 1, p. 4435, 2018.
- [22] D. J. McCarthy, K. R. Campbell, A. T. Lun, and Q. F. Wills, “Scater: pre-processing, quality control, normalization and visualization of single-cell RNA-seq data in R,” *Bioinformatics*, vol. 33, no. 8, pp. 1179–1186, 2017.
- [23] A. Butler, P. Hoffman, P. Smibert, E. Papalexi, and R. Satija, “Integrating single-cell transcriptomic data across different conditions, technologies, and species,” *Nature Biotechnology*, vol. 36, no. 5, pp. 411–420, 2018.
- [24] J. L. Bjørnstad, I. Sjaastad, S. Nygård et al., “Collagen isoform shift during the early phase of reverse left ventricular remodeling after relief of pressure overload,” *European Heart Journal*, vol. 32, no. 2, pp. 236–245, 2011.
- [25] G. Yu, L. G. Wang, Y. Han, and Q. Y. He, “clusterProfiler: an R package for comparing biological themes among gene clusters,” *OMICS*, vol. 16, no. 5, pp. 284–287, 2012.
- [26] J. Chen, E. E. Bardes, B. J. Aronow, and A. G. Jegga, “ToppGene Suite for gene list enrichment analysis and candidate gene prioritization,” *Nucleic Acids Research*, vol. 37, pp. W305–W311, 2009.
- [27] D. V. Veres, D. M. Gyurkó, B. Thaler et al., “ComPPI: a cellular compartment-specific database for protein-protein interaction network analysis,” *Nucleic Acids Research*, vol. 43, no. D1, pp. D485–D493, 2015.
- [28] A. Subramanian, P. Tamayo, V. K. Mootha et al., “Gene set enrichment analysis: a knowledge-based approach for interpreting genome-wide expression profiles,” *Proceedings of the National Academy of Sciences of the United States of America*, vol. 102, no. 43, pp. 15545–15550, 2005.
- [29] S. Hänzelmann, R. Castelo, and J. Guinney, “GSVA: gene set variation analysis for microarray and RNA-seq data,” *BMC Bioinformatics*, vol. 14, no. 1, p. 7, 2013.
- [30] M. di Somma, M. Vliora, E. Grillo et al., “Role of VEGFs in metabolic disorders,” *Angiogenesis*, vol. 23, no. 2, pp. 119–130, 2020.
- [31] S. Mishra, H. Ling, M. Grimm, T. Zhang, D. M. Bers, and J. H. Brown, “Cardiac hypertrophy and heart failure development through Gq and CaM kinase II signaling,” *Journal of Cardiovascular Pharmacology*, vol. 56, no. 6, pp. 598–603, 2010.
- [32] A. Fulgencio-Covián, E. Alonso-Barroso, A. J. Guenzel et al., “Pathogenic implications of dysregulated miRNAs in propionic acidemia related cardiomyopathy,” *Translational Research*, vol. 218, pp. 43–56, 2020.
- [33] D. Kar and A. Bandyopadhyay, “Targeting peroxisome proliferator activated receptor α (PPAR α) for the prevention of mitochondrial impairment and hypertrophy in cardiomyocytes,” *Cellular Physiology and Biochemistry*, vol. 49, no. 1, pp. 245–259, 2018.
- [34] J. Yim, H. Cho, and S. W. Rabkin, “Gene expression and gene associations during the development of heart failure with preserved ejection fraction in the Dahl salt sensitive model of hypertension,” *Clinical and Experimental Hypertension*, vol. 40, no. 2, pp. 155–166, 2018.
- [35] C. Zhang, Y. Wang, Z. Ge et al., “GDF11 attenuated ANG II-induced hypertrophic cardiomyopathy and expression of ANP, BNP and beta-MHC through down-regulating CCL11 in mice,” *Current Molecular Medicine*, vol. 18, no. 10, pp. 661–671, 2018.
- [36] J. Wang, P. Zhu, R. Li, J. Ren, and H. Zhou, “Fundc1-dependent mitophagy is obligatory to ischemic preconditioning-conferred renoprotection in ischemic AKI via suppression of Drp1-mediated mitochondrial fission,” *Redox Biology*, vol. 30, article 101415, 2020.
- [37] A. Iuso, S. Scacco, C. Piccoli et al., “Dysfunctions of cellular oxidative metabolism in patients with mutations in the NDUFS1 and NDUFS4 genes of complex I,” *The Journal of Biological Chemistry*, vol. 281, no. 15, pp. 10374–10380, 2006.
- [38] J. Hirst, “Mitochondrial complex I,” *Annual Review of Biochemistry*, vol. 82, no. 1, pp. 551–575, 2013.
- [39] A. Jusic and Y. Devaux, “Mitochondrial noncoding RNA-regulatory network in cardiovascular disease,” *Basic Research in Cardiology*, vol. 115, no. 3, pp. 1–7, 2020.
- [40] M. G. Signorello, S. Ravera, and G. Leoncini, “Lectin-induced oxidative stress in human platelets,” *Redox Biology*, vol. 32, article 101456, 2020.
- [41] H. K. Kim, Y. G. Kang, S. H. Jeong et al., “Cyclic stretch increases mitochondrial biogenesis in a cardiac cell line,” *Biochemical and Biophysical Research Communications*, vol. 505, no. 3, pp. 768–774, 2018.
- [42] T. Sato, H. C. Chang, M. Bayeva et al., “mRNA-binding protein tristetraprolin is essential for cardiac response to iron deficiency by regulating mitochondrial function,” *Proceedings of the National Academy of Sciences of the United States of America*, vol. 115, no. 27, pp. E6291–e6300, 2018.
- [43] K. Shinmura, K. Tamaki, M. Sano et al., “Caloric restriction primes mitochondria for ischemic stress by deacetylating specific mitochondrial proteins of the electron transport chain,” *Circulation Research*, vol. 109, no. 4, pp. 396–406, 2011.
- [44] E. R. Griffiths, I. Friehs, E. Scherr, D. Poutias, F. X. McGowan, and P. J. Del Nido, “Electron transport chain dysfunction in neonatal pressure-overload hypertrophy precedes cardiomyocyte apoptosis independent of oxidative stress,” *The Journal of Thoracic and Cardiovascular Surgery*, vol. 139, no. 6, pp. 1609–1617, 2010.
- [45] M. Osterholt, T. D. Nguyen, M. Schwarzer, and T. Doent, “Alterations in mitochondrial function in cardiac hypertrophy and heart failure,” *Heart Failure Reviews*, vol. 18, no. 5, pp. 645–656, 2013.
- [46] Y. X. Luo, X. Tang, X. Z. An et al., “SIRT4 accelerates Ang II-induced pathological cardiac hypertrophy by inhibiting manganese superoxide dismutase activity,” *European Heart Journal*, vol. 38, no. 18, pp. 1389–1398, 2017.
- [47] L. Wang, Y. L. Zhang, Q. Y. Lin et al., “CXCL1-CXCR2 axis mediates angiotensin II-induced cardiac hypertrophy and remodelling through regulation of monocyte infiltration,” *European Heart Journal*, vol. 39, no. 20, pp. 1818–1831, 2018.
- [48] F. Schwartz, A. Duka, I. Duka, J. Cui, and H. Gavras, “Novel targets of ANG II regulation in mouse heart identified by serial analysis of gene expression,” *American Journal of Physiology-Heart and Circulatory Physiology*, vol. 287, no. 5, pp. H1957–H1966, 2004.
- [49] Y. Qi, X. Wang, K. L. Rose et al., “Activation of the endogenous renin-angiotensin-aldosterone system or aldosterone administration increases urinary exosomal sodium channel excretion,” *Journal of the American Society of Nephrology*, vol. 27, no. 2, pp. 646–656, 2016.
- [50] D. J. Hamilton, A. Zhang, S. Li et al., “Combination of angiotensin II and l-NG-nitroarginine methyl ester exacerbates mitochondrial dysfunction and oxidative stress to cause heart

failure,” *American Journal of Physiology-Heart and Circulatory Physiology*, vol. 310, no. 6, pp. H667–H680, 2016.

- [51] Q. Zhang, S. Chen, S. Yu et al., “Neuroprotective effects of pyrroloquinoline quinone against rotenone injury in primary cultured midbrain neurons and in a rat model of Parkinson’s disease,” *Neuropharmacology*, vol. 108, pp. 238–251, 2016.
- [52] I. Lopez-Fabuel, J. Le Douce, A. Logan et al., “Complex I assembly into supercomplexes determines differential mitochondrial ROS production in neurons and astrocytes,” *Proceedings of the National Academy of Sciences of the United States of America*, vol. 113, no. 46, pp. 13063–13068, 2016.

Research Article

Melatonin Attenuates ox-LDL-Induced Endothelial Dysfunction by Reducing ER Stress and Inhibiting JNK/Mff Signaling

Peng Li ^{1,2}, Changlian Xie,³ Jiankai Zhong,⁴ Zhongzhou Guo,⁵ Kai Guo ⁶,
and Qiuyun Tu ¹

¹Department of Gerontology, The Fifth Affiliated Hospital, Sun Yat-sen University, Zhuhai, Guangdong Province 519000, China

²Guangdong Provincial Key Laboratory of Biomedical Imaging, The Fifth Affiliated Hospital, Sun Yat-sen University, Zhuhai, Guangdong Province 519000, China

³Intensive Care Unit, The Traditional Chinese Medicine Hospital, Zhongshan, Guangdong Province 528400, China

⁴Department of Cardiology, Shunde Hospital, Southern Medical University (The First People's Hospital of Shunde), Foshan, Guangdong Province 528308, China

⁵Department of Cardiology, Nanfang Hospital, Southern Medical University, Guangzhou, Guangdong Province 510515, China

⁶Cardiovascular Medicine Department, Guangdong Second Provincial General Hospital, Guangzhou, Guangdong Province 510317, China

Correspondence should be addressed to Peng Li; lipeng_sysu@126.com, Kai Guo; guokai154556@i.smu.edu.cn, and Qiuyun Tu; 1147129858@qq.com

Received 5 January 2021; Revised 4 February 2021; Accepted 11 February 2021; Published 4 March 2021

Academic Editor: Yun-dai Chen

Copyright © 2021 Peng Li et al. This is an open access article distributed under the Creative Commons Attribution License, which permits unrestricted use, distribution, and reproduction in any medium, provided the original work is properly cited.

Endothelial dysfunction, which is characterized by damage to the endoplasmic reticulum (ER) and mitochondria, is involved in a variety of cardiovascular disorders. Here, we explored whether mitochondrial damage and ER stress are associated with endothelial dysfunction. We also examined whether and how melatonin protects against oxidized low-density lipoprotein- (ox-LDL-) induced damage in endothelial cells. We found that CHOP, GRP78, and PERK expressions, which are indicative of ER stress, increased significantly in response to ox-LDL treatment. ox-LDL also induced mitochondrial dysfunction as evidenced by decreased mitochondrial membrane potential, increased mitochondrial ROS levels, and downregulation of mitochondrial protective factors. In addition, ox-LDL inhibited antioxidative processes, as evidenced by decreased antioxidative enzyme activity and reduced Nrf2/HO-1 expression. Melatonin clearly reduced ER stress and promoted mitochondrial function and antioxidative processes in the presence of ox-LDL. Molecular investigation revealed that ox-LDL activated the JNK/Mff signaling pathway, and melatonin blocked this effect. These results demonstrate that ox-LDL induces ER stress and mitochondrial dysfunction and activates the JNK/Mff signaling pathway, thereby contributing to endothelial dysfunction. Moreover, melatonin inhibited JNK/Mff signaling and sustained ER homeostasis and mitochondrial function, thereby protecting endothelial cells against ox-LDL-induced damage.

1. Introduction

Endothelial dysfunction is associated with a variety of cardiovascular disorders such as ischemic heart disease, myocardial infarction, postinfarction heart remodeling, diabetic cardiomyopathy, and hypertension [1–3]. The cardioprotective effects of several clinical drugs, including statins, aspirin,

and clopidogrel, are reportedly associated with endothelial protection [4, 5]. In addition, many risk factors, such as oxidized low-density lipoprotein (ox-LDL), blood flow shear force, inflammation cytokines, oxidative stress, and septic shock, contribute to endothelial dysfunction. Among these risk factors, endothelial cells are particularly vulnerable to ox-LDL-induced stress through unknown mechanisms

[6–8]. Increases in ox-LDL result in decreased proliferative ability, impaired migratory response, increased apoptotic index, and reduced regenerative capability in endothelial cells [9–11]. Although many studies have examined the relationship between ox-LDL and pathological alterations in endothelial cells *in vivo* and *in vitro*, the key molecular mechanisms underlying ox-LDL-associated endothelial dysfunction have not been fully explained, and few effective therapeutic drugs are available for patients with endothelial dysfunction.

Endoplasmic reticulum (ER) stress is an adaptive response that regulates protein synthesis and folding within cells [6]. Moderate activation of ER stress is associated with timely removal of damaged or unfolded proteins, thereby contributing to protein quality control [12]. Interestingly, excessive induction of ER stress contributes to abnormal degradation of damaged proteins and activation of caspase-dependent cell apoptosis [13]. ER-related cell apoptosis is characterized by increased levels of CHOP and caspase-12 [14, 15]. In addition, previous studies have reported a close relationship between endothelial dysfunction and ER stress [16]. Excessive ER stress promotes calcium overload, leading to spasms in endothelial cells [17]. Migratory response and angiogenesis might also be affected by ER stress because of its connections to synthesis and secretion of proteins like vascular endothelial growth factor (VEGF), which is necessary for angiogenesis [18, 19]. In addition to the ER, the mitochondria are also responsible for energy supply and redox balance within endothelial cells [20, 21]. Impaired mitochondrial function resulting from mitochondrial fragmentation and decreased mitochondrial autophagy can act as an upstream regulator of endothelial dysfunction [22, 23]. Many physiological processes, such as endothelial cell movement, growth, proliferation, and regeneration, are highly dependent on mitochondrial function [24–26]. Mitochondrial damage reduces the available ATP in endothelial cells and therefore contributes to endothelial dysfunction. Recent studies report that mitochondrial damage is regulated by the JNK/Mff signaling pathway in the context of cardiac ischemia-reperfusion injury [27–29]. However, this mechanism has not been verified in ox-LDL-treated endothelial cells.

Melatonin is a classical cardioprotective drug with multiple effects on endothelial function. Melatonin treatment attenuates microvascular damage during ischemia-reperfusion injury [30, 31]. Melatonin also attenuates endothelial dysfunction in diabetic cardiomyopathy [32]. Furthermore, melatonin inhibits oxidative stress, calcium overload, and inflammation response in endothelial cells under different disease models [33, 34]. In the present study, we examined whether ox-LDL-induced endothelial dysfunction is associated with ER stress and JNK/Mff signaling pathway activation. We also conducted experiments to understand whether melatonin improves endothelial function by altering ER stress and the JNK/Mff signaling pathway.

2. Materials and Methods

2.1. Cell Line Culture. Human umbilical vein endothelial cells (HUVECs) were purchased from American Type Culture Collection (ATCC; Manassas, VA, USA). Cells were cultured

in RPMI 1640 (HyClone, Logan, UT, USA) containing 10% FBS (Gibco, Rockville, MD, USA) and maintained in a 37°C, 5% CO₂ incubator [35]. HUVECs were incubated with oxidized low-density lipoprotein (ox-LDL) at a concentration of 50 µg/mL according to a recent report [36]. To observe the protective effects of melatonin on ox-LDL-treated HUVECs, melatonin was added to the culture medium at a concentration of 5 µM based on a previous study [37].

2.2. 3-(4,5-Dimethyl-2-thiazolyl)-2,5-diphenyl-2-H-tetrazolium Bromide (MTT) Assay. HUVECs were plated on 96-well plates. After 24 h, 48 h, and 72 h of proliferation, 10 µL MTT (Beyotime, Shanghai, China) was added to each well for 4 h. The cells were then treated with 100 µL dimethyl sulfoxide (DMSO; Sigma) for 2 h. Finally, the optical density (OD) value at 490 nm was measured using a spectrophotometer [38].

2.3. CCK-8 Assay. HUVECs were seeded onto 96-well plates and then incubated for 24, 48, 72, or 96 h. The CCK-8 reagent was then added to each well and then incubated for 4 h. The absorbance value of each well was measured at 490 nm [39].

2.4. Enzyme-Linked Immunosorbent Assay (ELISA). HUVECs at a density of 1×10^5 cells/well were cultured in 96-well plates at 37°C with 5% CO₂ for 24 hours. Cell culture supernatant was then collected, and GSH, GPX, and SOD levels were quantified using the corresponding ELISA kits purchased from R&D (San Diego, CA, USA) [40]. OD values at 450 nm absorbance were measured using an ELX808 Absorbance Reader (BioTek, London, UK) [41].

2.5. Mitochondrial Membrane Potential (MMP) Assessment. MMP was assessed using the JC-1 mitochondrial membrane potential assay kit (C2006, Beyotime, Shanghai, China) as described in a previous study [42]. HUVECs were collected after treatment with melatonin in the presence of ox-LDL. The cells were then incubated with 5 µM JC-1 staining kit reagent at 37°C for 30 minutes in the dark [43]. Finally, cells were analyzed using the Guava easyCyte Benchtop Flow Cytometer (BR168323; Luminex, Austin, TX, USA) with Kaluza C Analysis Software (version 2.1, Beckman Coulter, Indianapolis, IN, USA) [44].

2.6. Western Blot. Protein expression levels were determined via western blot as previously described [45]. After cell collection, protein lysis and extraction were performed using RIPA lysis buffer (R0278, Sigma-Aldrich, USA), and the concentration of extracted protein was measured using the Bicinchoninic acid (BCA) protein assay kit (AR0146, Boster Bio, Pleasanton, CA, USA) [46]. Then, 20 µg protein lysates samples were subjected to sodium dodecyl sulfate-polyacrylamide gel electrophoresis (SDS-PAGE; P0012AC, Beyotime, China) and transferred onto polyvinylidene fluoride (PVDF) membranes (FFP36, Beyotime, China), which were blocked with fat-free milk (5%) for 2 hours and incubated with primary antibodies at 4°C overnight; β -actin was used as internal control [47, 48]. The membranes were then incubated in secondary horseradish peroxidase- (HRP-) conjugated antibodies at room temperature for 1 hour and washed three times using tris-buffered

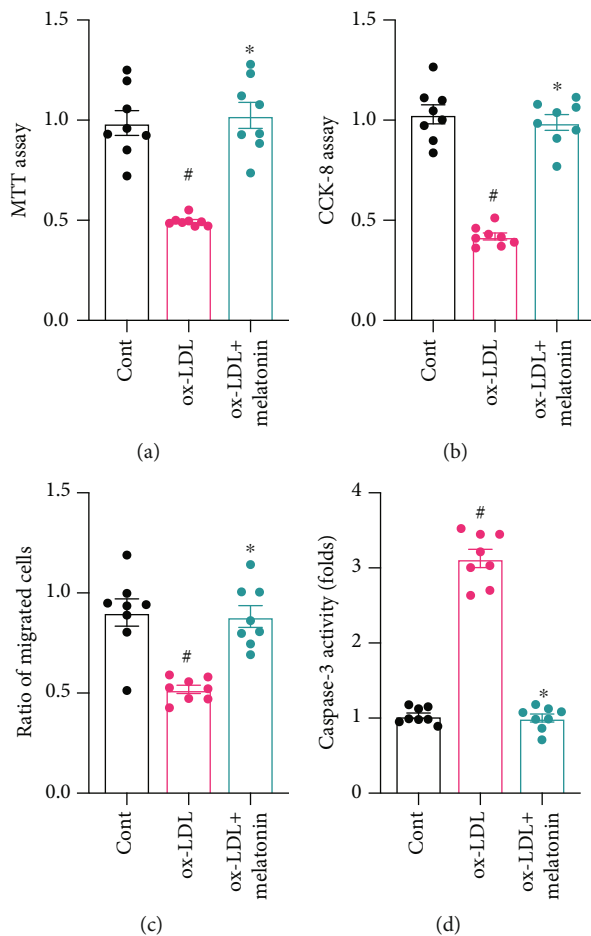


FIGURE 1: Melatonin attenuates ox-LDL-induced endothelial dysfunction. (a) HUVECs were treated with melatonin in the presence of ox-LDL. Cell viability was measured via MTT assay. (b) CCK-8 was used to measure the proliferative capacity of HUVECs after ox-LDL treatment. (c) A transwell assay was used to evaluate cell migratory response. (d) ELISA was used to analyze caspase-3 activity. [#] $p < 0.05$ vs. the control group, * $p < 0.05$ vs. the ox-LDL group.

saline Tween (TBST, T196393, Aladdin, China). Protein bands were visualized using the enhanced chemiluminescence (ECL) kit (P0018FS, Beyotime, China). Gray band density values were analyzed in the iBright CL1500 Imaging System (A44240, Thermo Fisher Scientific, USA) and calculated using ImageJ (version 5.0, Bio-Rad, Hercules, CA, USA) [49].

2.7. Detection of Caspase-3 Activity. Caspase-3 activity was evaluated using the caspase-3 activity assay kit (Beyotime) as previously described [50]. Briefly, HUVECs were seeded on 24-well plates and incubated with melatonin in the presence of ox-LDL for 48 h. The cells were then collected, and caspase-3 activity assay kit was measured [51].

2.8. Transwell Assay. For the migration assay, HUVECs were placed in the upper chamber of transwells [52]. For the invasion assay, the upper chamber was treated with Matrigel before cells were added. After incubation for 48 h,

cells that had migrated to or invaded the lower chamber were stained with 0.1% crystal violet and quantified using a microscope [53].

2.9. Quantitative Real-Time Polymerase Chain Reaction (qRT-PCR). Samples were incubated with TRIzol reagent (Invitrogen) to extract total RNA [54]. CRNDE, miR-4262, and ZEB1 cDNA were synthesized using the All-in-One™ cDNA Synthesis Kit (FulGen, Guangzhou, China) [55]. Subsequently, qRT-PCR was performed using SYBR green (Applied Biosystems, Foster City, CA, USA). Glyceraldehyde-3-phosphate dehydrogenase (GAPDH) was used as an internal reference (56).

2.10. Statistical Analysis. All experiments were repeated three times. Data are presented as means \pm standard deviation (SD). SPSS 17.0 software was used for statistical analyses. Student's *t*-tests and one-way analyses of variance (ANOVA) were used to identify differences between groups. $p < 0.05$ was considered statistically significant.

3. Results

3.1. Melatonin Attenuates ox-LDL-Induced Endothelial Dysfunction. After ox-LDL was administered to induce endothelial dysfunction, melatonin was added to the growth medium to evaluate any protective actions. First, cell viability was measured using an MTT assay. As shown in Figure 1(a), compared to the control group, endothelial cell viability was significantly reduced by exposure to ox-LDL. Interestingly, melatonin reversed this ox-LDL-induced cell damage. Endothelial cell proliferation capacity was also measured in a CCK-8 assay. As shown in Figure 1(b), compared to the control group, ox-LDL exposure progressively reduced endothelial cell proliferation. Again, melatonin reversed this ox-LDL-induced effect by increasing endothelial cell proliferative capacity. Migratory response in endothelial cells is also important for angiogenesis. A transwell assay was therefore used to analyze alterations in endothelial cell migratory response. As shown in Figure 1(c), compared to the control group, ox-LDL significantly reduced the number of endothelial cells that migrated, and melatonin reversed this effect. Finally, cell apoptosis was monitored using a caspase-3 activity assay. As shown in Figure 1(d), compared to the control group, caspase-3 activity in endothelial cells was significantly reduced in the ox-LDL group, suggesting that ox-LDL treatment induced cell apoptosis. Finally, melatonin treatment prevented ox-LDL-induced upregulation of caspase-3 activity, suggesting that melatonin has antiapoptotic effects in the presence of ox-LDL.

3.2. Melatonin Alleviates ox-LDL-Induced ER Stress. Changes in ER stress were evaluated to identify the molecular mechanism underlying ox-LDL-mediated endothelial dysfunction. First, ER stress biomarkers were analyzed by qPCR. As shown in Figures 2(a)–2(d), compared to the control group, transcription of CHOP, GRP78, and PERK was significantly elevated after ox-LDL treatment. However, melatonin inhibited this upregulation. To confirm that transcriptional activation of ER stress biomarkers is also associated with

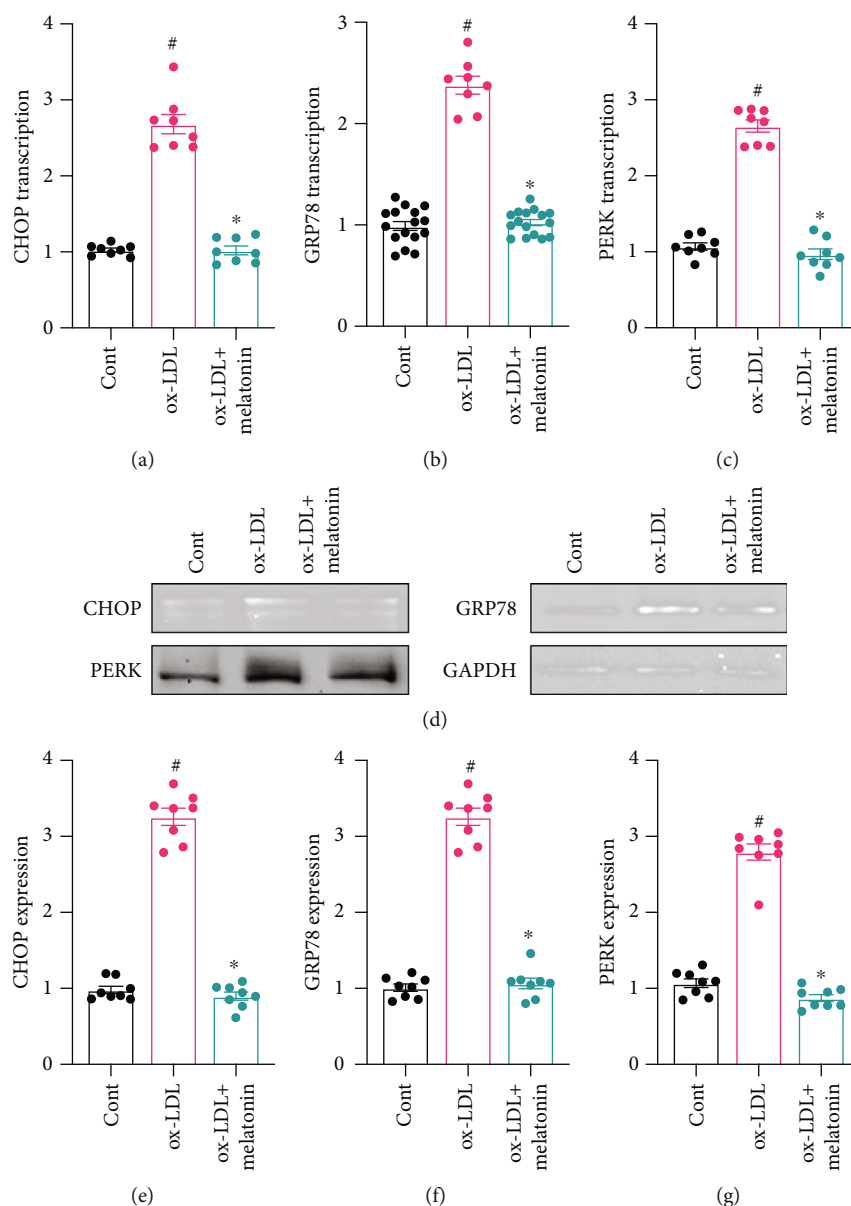


FIGURE 2: Melatonin alleviates ER stress during ox-LDL treatment. (a–c) HUVECs were treated with melatonin in the presence of ox-LDL. qPCR was then used to measure CHOP, GRP78, and PERK transcription. (d–g) Proteins were isolated from treated HUVECs, and expression of CHOP, GRP78, and PERK proteins was evaluated using western blots. # $p < 0.05$ vs. the control group, * $p < 0.05$ vs. the ox-LDL group.

upregulation of ER stress-related proteins, western blots were used to quantify expression of proteins involved in ER stress initiation, augmentation, and execution. As shown in Figures 2(e)–2(g), compared to the control group, CHOP, GRP78, and PERK protein expressions rapidly increased as a result of ox-LDL treatment. Furthermore, melatonin treatment inhibited upregulation of ER stress-related proteins, suggesting that melatonin can inhibit ER stress in ox-LDL-treated endothelial cells.

3.3. Melatonin Sustains Mitochondrial Function in ox-LDL-Treated Endothelial Cells. In addition to ER stress, we also examined the effects of ox-LDL on mitochondrial dysfunction. ox-LDL significantly increased mitochondrial oxidative stress as indicated by a mitochondrial ROS probe assay

(Figures 3(a) and 3(b)). Interestingly, melatonin treatment strongly inhibited mitochondrial ROS production in endothelial cells. Next, we examined the regulatory effects of melatonin on mitochondrial membrane potential. As shown in Figures 3(c) and 3(d), compared to the control group, ox-LDL treatment disrupted mitochondrial membrane potential, as indicated by decreased red JC-1 probe fluorescence. Interestingly, melatonin treatment significantly reversed this disruption of mitochondrial membrane potential. ox-LDL treatment also significantly decreased the expression of mitochondrial protective factors Bcl-2 and c-IAP1 (Figures 3(e) and 3(f)), and melatonin treatment again reversed this decrease. Taken together, these results indicate that melatonin protected mitochondrial function in endothelial cells.

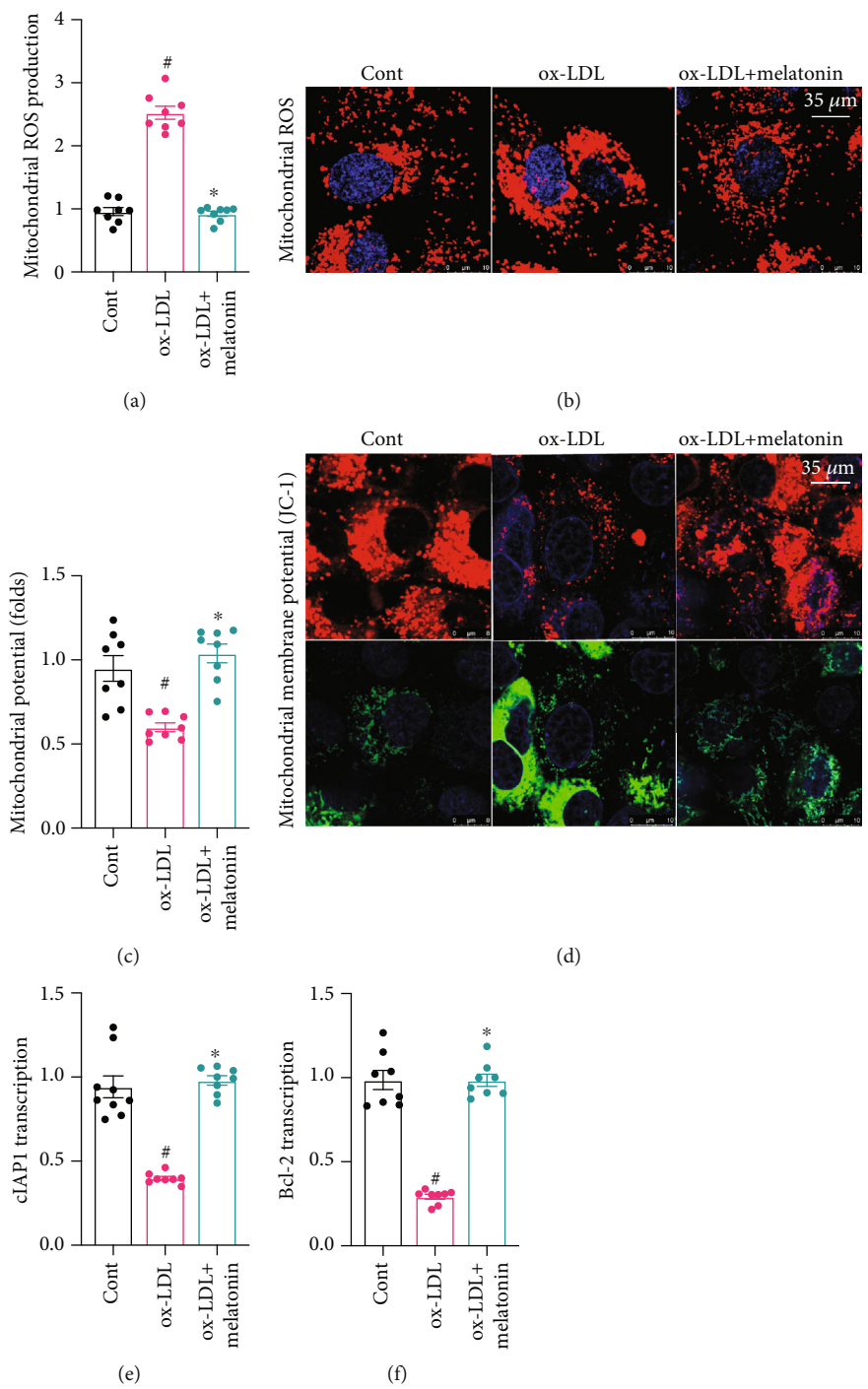


FIGURE 3: Melatonin sustains mitochondrial function in ox-LDL-treated endothelial cells. (a, b) Mitochondrial ROS production was examined using a mitochondrial ROS probe. HUVECs were treated with melatonin in the presence of ox-LDL. (c, d) Mitochondrial membrane potential was determined using the JC-1 probe. (e, f) qPCR was used to measure cIAP1 and Bcl-2 transcription in response to ox-LDL treatment with or without melatonin. [#]*p* < 0.05 vs. the control group, ^{*}*p* < 0.05 vs. the ox-LDL group.

3.4. Melatonin Inhibits Oxidative Stress in ox-LDL-Treated Endothelial Cells. In addition to ER stress and mitochondrial dysfunction, we also explored whether ox-LDL induces oxidative stress that contributes to endothelial dysfunction. As shown in Figures 4(a)–4(c), compared to the control group, ox-LDL significantly inhibited the activity of antioxidative enzymes. Interestingly, melatonin treatment reversed this

inhibition of antioxidative enzymes such as GSH, SOD, and GPX. Upstream regulatory mechanisms underlying melatonin-induced antioxidative effects were then examined further. Nrf2 and HO-1 have been identified as the primary antioxidative signaling molecules in endothelial cells. qPCR indicated that ox-LDL treatment significantly decreased Nrf2 and HO-1 transcription (Figures 4(d) and 4(e)), while

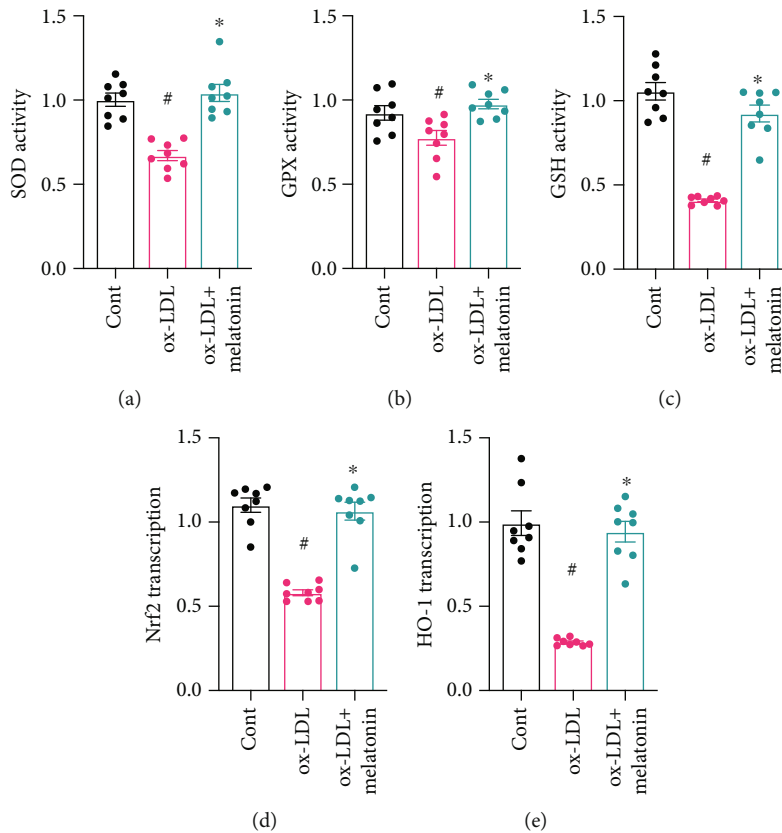


FIGURE 4: Melatonin inhibits oxidative stress in ox-LDL-treated endothelial cells. (a–c) ELSIAs were used to measure the activity of antioxidative enzymes such as GSH, GPX, and SOD. (d, e) qPCR was used to analyze Nrf2 and HO-1 transcription in response to ox-LDL treatment with or without melatonin. # $p < 0.05$ vs. the control group, * $p < 0.05$ vs. the ox-LDL group.

melatonin treatment restored Nrf2 and HO-1 levels. Taken together, these results demonstrate that melatonin could reduce oxidative stress in ox-LDL-treated endothelial cells.

3.5. Melatonin Inhibits the JNK/Mff Signaling Pathway in ox-LDL-Treated Endothelial Cells. Finally, we evaluated an upstream signaling pathway that might underlie ox-LDL-induced endothelial dysfunction. Recent studies indicate that the JNK/Mff signaling pathway is associated with inflammation response, cell apoptosis, and oxidative stress in endothelial cells in the context of cardiac ischemia-reperfusion injury. Based on this finding, we examined whether melatonin sustained endothelial function by inhibiting the JNK/Mff signaling pathway. As shown in Figures 5(a)–5(c), western blots demonstrated that ox-LDL activated the JNK pathway as evidenced by increased JNK phosphorylation in endothelial cells. Mff expression was also upregulated in ox-LDL-treated endothelial cells (Figures 5(a)–5(c)). These results indicate that ox-LDL treatment activates the JNK/Mff signaling pathway in endothelial cells. In addition, melatonin inhibited JNK phosphorylation and Mff upregulation in ox-LDL-treated endothelial cells. Immunofluorescence confirmed this finding. As shown in Figures 5(d)–5(f), compared to the control group, ox-LDL increased JNK and Mff immunofluorescence intensity, and melatonin returned both markers to near-normal levels. Overall, these data indicate

that melatonin can inhibit the JNK/Mff signaling pathway in ox-LDL-treated endothelial cells.

4. Discussion

In this study, we found that ox-LDL caused endothelial dysfunction characterized by decreases in cell viability, impaired proliferative capacity, blunted migratory ability, and increases in cell apoptosis rate. Endothelial dysfunction was associated with ER stress, mitochondrial damage, and oxidative stress. At the molecular level, expression of CHOP, PERK, and GRP78 was increased in ox-LDL-treated endothelial cells. Moreover, decreased mitochondrial membrane potential, increased mitochondrial ROS levels, and downregulation of mitochondrial protective factors were observed in ox-LDL-treated endothelial cells. In addition, ox-LDL reduced the activity of antioxidative enzymes and prevented activation of antioxidative signals. Interestingly, melatonin treatment attenuated ox-LDL-induced ER stress, as evidenced by decreased expression of CHOP, PERK, and GRP78. Mitochondrial function and oxidative stress also improved after melatonin administration in ox-LDL-treated endothelial cells. Finally, we found that melatonin protected endothelial cells against ER stress and mitochondrial dysfunction after ox-LDL treatment by inhibiting the JNK/Mff signaling pathway. Taken together, our results demonstrate

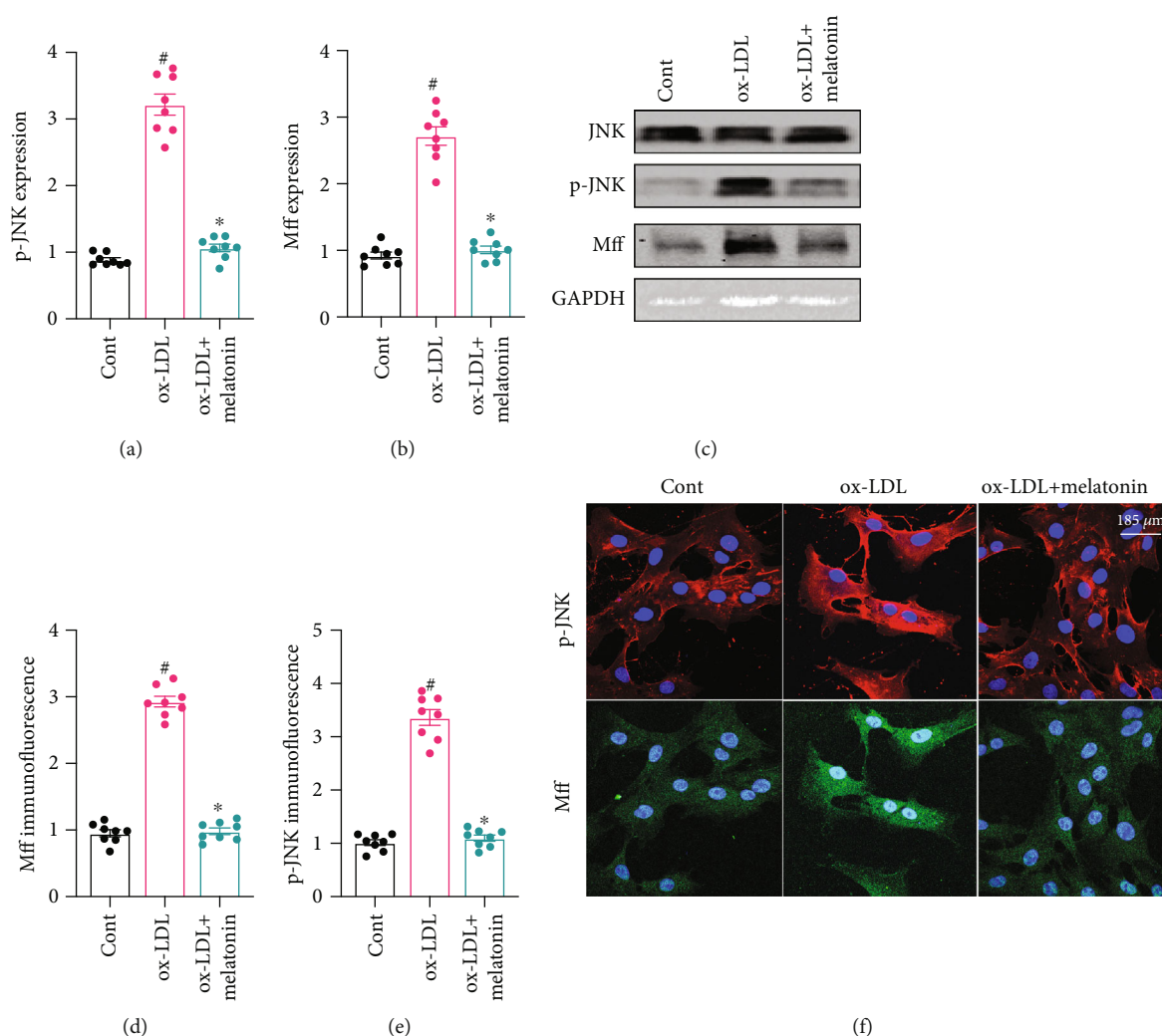


FIGURE 5: Melatonin inhibits the JNK/Mff signaling pathway in ox-LDL-treated endothelial cells. (a–c) Proteins were isolated from treated HUVECs and p-JNK and Mff levels were evaluated using western blots. (d, f) Immunofluorescence was used to measure o-JNK and Mff expression in HUVECs treated with melatonin in the presence of ox-LDL. # $p < 0.05$ vs. the control group, * $p < 0.05$ vs. the ox-LDL group.

that ox-LDL promoted endothelial dysfunction by activating ER stress, mitochondrial damage, oxidative stress, and the JNK/Mff signaling pathway. Furthermore, melatonin effectively sustained endothelial cell function by improving ER homeostasis, mitochondrial performance, redox balance, and JNK/Mff axis activity.

ER stress is an adaptive response that affects the quality and quantity of proteins within endothelial cells [57]. When the ER detects the presence of unfolded proteins, CHOP, PERK, and GRP78 expressions increase [58]. Those three proteins then migrate from the ER to the nucleus to interrupt protein transcription more broadly [59]. However, excessive ER stress promotes activation of stress-related proteins such as caspase-12, which is involved in the initiation of cell apoptosis [60]. The relationship between ER stress and endothelial dysfunction has been described in detail in previous studies. For example, ER stress induces interleukin-6 (IL-6) release from endothelial cells, which damages the endothelial barrier [61]. Hypoxia-mediated endothelial cell apoptosis also seems to be associated with ER stress [62]. Additionally,

laminar flow-mediated endothelial protection is associated with inhibition of ER stress through the PI3K/Akt signaling pathway [63]. Our present results further indicate that ER stress contributes to endothelial dysfunction when ox-LDL levels are elevated.

In addition to ER stress, mitochondrial damage or stress also may play a role in endothelial dysfunction. Mitochondria produce ATP to support endothelial cell growth and metabolism [64, 65]. Decreased mitochondrial function has been identified as an early event during endothelial dysfunction [66]. In addition, ATP produced by the mitochondria plays a key regulatory role in endothelia-dependent angiogenesis [67]. In the present study, we found that ox-LDL-induced mitochondrial damage was characterized by mitochondrial membrane potential disruption, mitochondrial ROS overproduction, and downregulation of mitochondrial protective factors. These findings are in accordance with the previous studies [68].

Our data also demonstrate that ER stress and mitochondrial damage could be attenuated by melatonin in endothelial

cells. At the molecular level, the JNK/Mff signaling pathway played a role in melatonin's ability to sustain ER homeostasis and mitochondrial function after ox-LDL treatment. Zhou et al. [27] were the first to report a role for the JNK/Mff signaling pathway in the context of cardiac ischemia-reperfusion injury. In that study, reperfusion injury induced JNK phosphorylation and thus promoted Mff transcription, which was followed by mitochondrial fragmentation, intracellular oxidative stress, and endothelial cell apoptosis [27]. In the present study, we found that the JNK/Mff axis was also activated by ox-LDL and might contribute to ox-LDL-induced endothelial dysfunction. In addition, melatonin treatment inhibited JNK/Mff signaling pathway activity. This finding provides novel insight into the pathological mechanisms underlying ox-LDL-related endothelial dysfunction as well as potential treatments.

In summary, we found that ox-LDL triggered endothelial dysfunction by inducing ER stress, mitochondrial damage, and oxidative stress. Furthermore, melatonin treatment was able to sustain endothelial viability by inhibiting the JNK/Mff signaling pathway and attenuating damage to the ER and mitochondria. Our study thus identified potential targets for clinical treatments that might protect endothelial function.

Data Availability

All data generated or analyzed during this study are included in the published article.

Conflicts of Interest

All authors declare that there are no conflicts of interest associated with this study.

Authors' Contributions

Peng Li and Changlian Xie designed this manuscript and conducted parts of the experiments. Jiankai Zhong and Zhongzhou Guo conducted parts of the experiments and analyzed all the data. Qiuyun Tu, Kai Guo, and Peng Li wrote the manuscript. All the authors approved the submission. Peng Li and Changlian Xie contributed equally to this work.

Acknowledgments

This work was supported by the National Natural Science Foundation Youth Program, China (Grant No. 81900398), Natural Science Foundation of Guangdong Province, China (Grant No. 2018A030313067), and Medical Scientific Research Foundation of Guangdong Province, China (Grant No. A2020206).

References

- [1] J. Wang, S. Toan, and H. Zhou, "New insights into the role of mitochondria in cardiac microvascular ischemia/reperfusion injury," *Angiogenesis*, vol. 23, no. 3, pp. 299–314, 2020.
- [2] G. Warpsinski, M. J. Smith, S. Srivastava et al., "Nrf2-regulated redox signaling in brain endothelial cells adapted to physiological oxygen levels: consequences for sulforaphane mediated protection against hypoxia-reoxygenation," *Redox Biology*, vol. 37, article 101708, 2020.
- [3] Y. Zhang, M. Zhang, X. Zhao et al., "NAD administration decreases microvascular damage following cardiac ischemia/reperfusion by restoring autophagic flux," *Basic Research in Cardiology*, vol. 115, no. 5, p. 57, 2020.
- [4] G. Heusch, "Coronary microvascular obstruction: the new frontier in cardioprotection," *Basic Research in Cardiology*, vol. 114, no. 6, p. 45, 2019.
- [5] W. E. Hughes, A. M. Beyer, and D. D. Gutterman, "Vascular autophagy in health and disease," *Basic Research in Cardiology*, vol. 115, no. 4, p. 41, 2020.
- [6] X. Nie, W. Tang, Z. Zhang et al., "Procyanidin B2 mitigates endothelial endoplasmic reticulum stress through a PPAR δ -dependent mechanism," *Redox Biology*, vol. 37, article 101728, 2020.
- [7] H. Zhang, Y. L. Wang, Y. Z. Tan, H. J. Wang, P. Tao, and P. Zhou, "Enhancement of cardiac lymphangiogenesis by transplantation of CD34+VEGFR-3+ endothelial progenitor cells and sustained release of VEGF-C," *Basic Research in Cardiology*, vol. 114, no. 6, p. 43, 2019.
- [8] D. Buglak, E. Kushner, A. Marvin, K. Davis, and V. Bautch, "Excess centrosomes disrupt vascular lumenization and endothelial cell adherens junctions," *Angiogenesis*, vol. 23, no. 4, pp. 567–575, 2020.
- [9] T. Xin, C. Lu, J. Zhang et al., "Oxidized LDL disrupts metabolism and inhibits macrophage survival by activating a miR-9/Drp1/mitochondrial fission signaling pathway," *Oxidative Medicine and Cellular Longevity*, vol. 2020, 16 pages, 2020.
- [10] C. Khatana, N. K. Saini, S. Chakrabarti et al., "Mechanistic insights into the oxidized low-density lipoprotein-induced atherosclerosis," *Oxidative Medicine and Cellular Longevity*, vol. 2020, Article ID 5245308, 14 pages, 2020.
- [11] K. Karolczak and C. Watala, "The mystery behind the pineal gland: melatonin affects the metabolism of cholesterol," *Oxidative Medicine and Cellular Longevity*, vol. 2019, Article ID 4531865, 8 pages, 2019.
- [12] D. Vatner, M. Oydanich, J. Zhang, D. Babici, and S. Vatner, "Secreted frizzled-related protein 2, a novel mechanism to induce myocardial ischemic protection through angiogenesis," *Basic Research in Cardiology*, vol. 115, no. 4, p. 48, 2020.
- [13] S. Yang, M. Wu, X. Li et al., "Role of endoplasmic reticulum stress in atherosclerosis and its potential as a therapeutic target," *Oxidative Medicine and Cellular Longevity*, vol. 2020, 15 pages, 2020.
- [14] K. T. Kubra, M. S. Akhter, M. A. Uddin, and N. Barabutis, "Unfolded protein response in cardiovascular disease," *Cellular Signalling*, vol. 73, article 109699, 2020.
- [15] N. Pastor-Cantizano, D. K. Ko, E. Angelos, Y. Pu, and F. Brandizzi, "Functional diversification of ER stress responses in Arabidopsis," *Trends in Biochemical Sciences*, vol. 45, no. 2, pp. 123–136, 2020.
- [16] H. Zhu, M. Zhao, Y. Chen, and D. Li, "Bcl-2-associated athanogene 5 overexpression attenuates catecholamine-induced vascular endothelial cell apoptosis," *Journal of Cellular Physiology*, vol. 236, no. 2, pp. 946–957, 2021.
- [17] R. Villalobos-Labra, M. Subiabre, F. Toledo, F. Pardo, and L. Sobrevia, "Endoplasmic reticulum stress and development of insulin resistance in adipose, skeletal, liver, and foetoplacental tissue in diabetes," *Molecular Aspects of Medicine*, vol. 66, pp. 49–61, 2019.

- [18] P. Zhu, S. Hu, Q. Jin et al., "Ripk3 promotes ER stress-induced necroptosis in cardiac IR injury: a mechanism involving calcium overload/XO/ROS/mPTP pathway," *Redox Biology*, vol. 16, pp. 157–168, 2018.
- [19] H. Zhou, J. Wang, P. Zhu, S. Hu, and J. Ren, "Ripk3 regulates cardiac microvascular reperfusion injury: the role of IP3R-dependent calcium overload, XO-mediated oxidative stress and F-actin/filopodia-based cellular migration," *Cellular Signalling*, vol. 45, pp. 12–22, 2018.
- [20] J. Wang, S. Toan, and H. Zhou, "Mitochondrial quality control in cardiac microvascular ischemia-reperfusion injury: new insights into the mechanisms and therapeutic potentials," *Pharmacological Research*, vol. 156, article 104771, 2020.
- [21] J. Wang and H. Zhou, "Mitochondrial quality control mechanisms as molecular targets in cardiac ischemia-reperfusion injury," *Acta Pharmaceutica Sinica B*, vol. 10, no. 10, pp. 1866–1879, 2020.
- [22] X. Wu, L. Zhang, Y. Miao et al., "Homocysteine causes vascular endothelial dysfunction by disrupting endoplasmic reticulum redox homeostasis," *Redox Biology*, vol. 20, pp. 46–59, 2019.
- [23] H. Zhou, Y. Zhang, S. Hu et al., "Melatonin protects cardiac microvasculature against ischemia/reperfusion injury via suppression of mitochondrial fission-VDAC1-HK2-mPTP-mitophagy axis," *Journal of Pineal Research*, vol. 63, no. 1, article e12413, 2017.
- [24] K. Rao, X. Shen, S. Pardue, and D. Krzywanski, "Nicotinamide nucleotide transhydrogenase (NNT) regulates mitochondrial ROS and endothelial dysfunction in response to angiotensin II," *Redox Biology*, vol. 36, article 101650, 2020.
- [25] M. Winkler, P. Müller, A. M. Sharifi et al., "Functional investigation of the coronary artery disease gene SVEP1," *Basic Research in Cardiology*, vol. 115, no. 6, p. 67, 2020.
- [26] E. Watanabe, T. Wada, A. Okekawa et al., "Stromal cell-derived factor 1 (SDF1) attenuates platelet-derived growth factor-B (PDGF-B)-induced vascular remodeling for adipose tissue expansion in obesity," *Angiogenesis*, vol. 23, no. 4, pp. 667–684, 2020.
- [27] Q. Jin, R. Li, N. Hu et al., "DUSP1 alleviates cardiac ischemia/reperfusion injury by suppressing the Mff-required mitochondrial fission and Bnip3-related mitophagy via the JNK pathways," *Redox Biology*, vol. 14, pp. 576–587, 2018.
- [28] H. Zhou, S. Hu, Q. Jin et al., "Mff-dependent mitochondrial fission contributes to the pathogenesis of cardiac microvasculature ischemia/reperfusion injury via induction of mROS-mediated cardiolipin oxidation and HK2/VDAC1 disassociation-involved mPTP opening," *Journal of the American Heart Association*, vol. 6, no. 3, 2017.
- [29] H. Zhou, J. Wang, P. Zhu et al., "NR4A1 aggravates the cardiac microvascular ischemia reperfusion injury through suppressing FUNDC1-mediated mitophagy and promoting Mff-required mitochondrial fission by CK2 α ," *Basic Research in Cardiology*, vol. 113, no. 4, p. 23, 2018.
- [30] Cochrane Anaesthesia Group, B. K. Madsen, D. Zetner, A. M. Møller, and J. Rosenberg, "Melatonin for preoperative and postoperative anxiety in adults," *Cochrane Database of Systematic Reviews*, vol. 12, article Cd009861, 2020.
- [31] M. Fernández-Ortiz, R. K. A. Sayed, J. Fernández-Martínez et al., "Melatonin/Nrf2/NLRP3 connection in mouse heart mitochondria during aging," *Antioxidants*, vol. 9, no. 12, p. 1187, 2020.
- [32] A. Albazal, A. A. Delshad, and M. Roghani, "Melatonin reverses cognitive deficits in streptozotocin-induced type 1 diabetes in the rat through attenuation of oxidative stress and inflammation," *Journal of Chemical Neuroanatomy*, vol. 112, article 101902, 2021.
- [33] S. W. Wang, H. C. Tai, C. H. Tang et al., "Melatonin impedes prostate cancer metastasis by suppressing MMP-13 expression," *Journal of Cellular Physiology*, 2020.
- [34] H. Zhou, D. Li, P. Zhu et al., "Melatonin suppresses platelet activation and function against cardiac ischemia/reperfusion injury via PPAR γ /FUNDC1/mitophagy pathways," *Journal of Pineal Research*, vol. 63, no. 4, 2017.
- [35] H. Zhou, Q. Jin, Y. Li et al., "Melatonin protected cardiac microvascular endothelial cells against oxidative stress injury via suppression of IP3R-[Ca $^{2+}$]_i/VDAC-[Ca $^{2+}$]_m axis by activation of MAPK/ERK signaling pathway," *Cell Stress & Chaperones*, vol. 23, no. 1, pp. 101–113, 2018.
- [36] G. R. Hinrichs, K. Weyer, U. G. Friis et al., "Sodium retention by uPA-plasmin-ENaC in nephrotic syndrome-authors reply," *Acta Physiologica (Oxford, England)*, vol. 228, no. 4, article e13432, 2020.
- [37] H. Zhou, D. Li, P. Zhu et al., "Inhibitory effect of melatonin on necroptosis via repressing the Ripk3-PGAM5-CypD-mPTP pathway attenuates cardiac microvascular ischemia-reperfusion injury," *Journal of Pineal Research*, vol. 65, no. 3, article e12503, 2018.
- [38] S. Liu, J. Chen, J. Shi et al., "M1-like macrophage-derived exosomes suppress angiogenesis and exacerbate cardiac dysfunction in a myocardial infarction microenvironment," *Basic Research in Cardiology*, vol. 115, no. 2, p. 22, 2020.
- [39] V. H. Ko, L. J. Yu, D. T. Dao et al., "Roxadustat (FG-4592) accelerates pulmonary growth, development, and function in a compensatory lung growth model," *Angiogenesis*, vol. 23, no. 4, pp. 637–649, 2020.
- [40] H. Zhou, S. Toan, P. Zhu, J. Wang, J. Ren, and Y. Zhang, "DNA-PKcs promotes cardiac ischemia reperfusion injury through mitigating BI-1-governed mitochondrial homeostasis," *Basic Research in Cardiology*, vol. 115, no. 2, p. 11, 2020.
- [41] J. Wang, P. Zhu, R. Li, J. Ren, and H. Zhou, "Fundc1-dependent mitophagy is obligatory to ischemic preconditioning-conferred renoprotection in ischemic AKI via suppression of Drp1-mediated mitochondrial fission," *Redox Biology*, vol. 30, article 101415, 2020.
- [42] Y. Tan, D. Mui, S. Toan, P. Zhu, R. Li, and H. Zhou, "SERCA overexpression improves mitochondrial quality control and attenuates cardiac microvascular ischemia-reperfusion injury," *Molecular Therapy-Nucleic Acids*, vol. 22, pp. 696–707, 2020.
- [43] S. Gunesch, M. Hoffmann, C. Kiermeier et al., "7-O-Esters of taxifolin with pronounced and overadditive effects in neuroprotection, anti-neuroinflammation, and amelioration of short-term memory impairment in vivo," *Redox Biology*, vol. 29, article 101378, 2020.
- [44] N. Lubos, S. van der Gaag, M. Gerçek, S. Kant, R. E. Leube, and C. A. Krusche, "Inflammation shapes pathogenesis of murine arrhythmogenic cardiomyopathy," *Basic Research in Cardiology*, vol. 115, no. 4, p. 42, 2020.
- [45] E. H. Moon, Y. H. Kim, P. N. Vu et al., "TMEM100 is a key factor for specification of lymphatic endothelial progenitors," *Angiogenesis*, vol. 23, no. 3, pp. 339–355, 2020.

- [46] F. Husain-Syed, M. H. Rosner, and C. Ronco, "Distant organ dysfunction in acute kidney injury," *Acta Physiologica*, vol. 228, article e13357, 2019.
- [47] J. Wang, Z. Chen, Q. Dai et al., "Intravenously delivered mesenchymal stem cells prevent microvascular obstruction formation after myocardial ischemia/reperfusion injury," *Basic Research in Cardiology*, vol. 115, no. 4, p. 40, 2020.
- [48] E. Steffen, W. B. E. Mayer von Wittgenstein, M. Hennig et al., "Murine sca1/flk1-positive cells are not endothelial progenitor cells, but B2 lymphocytes," *Basic Research in Cardiology*, vol. 115, no. 2, p. 18, 2020.
- [49] G. Seano and R. K. Jain, "Vessel co-option in glioblastoma: emerging insights and opportunities," *Angiogenesis*, vol. 23, no. 1, pp. 9–16, 2020.
- [50] H. Zhou, P. Zhu, J. Wang, S. Toan, and J. Ren, "DNA-PKcs promotes alcohol-related liver disease by activating Drp1-related mitochondrial fission and repressing FUNDC1-required mitophagy," *Signal Transduction and Targeted Therapy*, vol. 4, no. 1, p. 56, 2019.
- [51] J. Wang, P. Zhu, S. Toan, R. Li, J. Ren, and H. Zhou, "Pum2-Mff axis fine-tunes mitochondrial quality control in acute ischemic kidney injury," *Cell Biology and Toxicology*, vol. 36, no. 4, pp. 365–378, 2020.
- [52] I. Cuijpers, S. J. Simmonds, M. van Bilsen et al., "Microvascular and lymphatic dysfunction in HFpEF and its associated comorbidities," *Basic Res Cardiol*, vol. 115, no. 4, p. 39, 2020.
- [53] Y. Sawashita, N. Hirata, Y. Yoshikawa, H. Terada, Y. Tokinaga, and M. Yamakage, "Remote ischemic preconditioning reduces myocardial ischemia-reperfusion injury through unacylated ghrelin-induced activation of the JAK/STAT pathway," *Basic Research in Cardiology*, vol. 115, no. 4, p. 50, 2020.
- [54] C. Veith, D. Neghabian, H. Luitel et al., "FHL-1 is not involved in pressure overload-induced maladaptive right ventricular remodeling and dysfunction," *Basic Research in Cardiology*, vol. 115, no. 2, p. 17, 2020.
- [55] P. Villacampa, S. E. Liyanage, I. P. Klaska et al., "Stabilization of myeloid-derived HIFs promotes vascular regeneration in retinal ischemia," *Angiogenesis*, vol. 23, no. 2, pp. 83–90, 2020.
- [56] C. Schinner, S. Olivares-Florez, A. Schlipp et al., "The inotropic agent digitoxin strengthens desmosomal adhesion in cardiac myocytes in an ERK1/2-dependent manner," *Basic Research in Cardiology*, vol. 115, no. 4, p. 46, 2020.
- [57] M. Yuan, M. Gong, Z. Zhang et al., "Hyperglycemia induces endoplasmic reticulum stress in atrial cardiomyocytes, and mitofusin-2 downregulation prevents mitochondrial dysfunction and subsequent cell death," *Oxidative Medicine and Cellular Longevity*, vol. 2020, Article ID 6569728, 14 pages, 2020.
- [58] J. Zhang, J. Yang, C. Lin et al., "Endoplasmic reticulum stress-dependent expression of ERO1L promotes aerobic glycolysis in pancreatic cancer," *Theranostics*, vol. 10, no. 18, pp. 8400–8414, 2020.
- [59] J. Zhang, R. Saad, E. W. Taylor, and M. P. Rayman, "Selenium and selenoproteins in viral infection with potential relevance to COVID-19," *Redox Biology*, vol. 37, article 101715, 2020.
- [60] Y. Wang, Z. Chen, Y. Li et al., "Low density lipoprotein receptor related protein 6 (LRP6) protects heart against oxidative stress by the crosstalk of HSF1 and GSK3 β ," *Redox Biology*, vol. 37, article 101699, 2020.
- [61] E. Bernhart, N. Kogelnik, J. Prasch et al., "2-Chlorohexadecanoic acid induces ER stress and mitochondrial dysfunction in brain microvascular endothelial cells," *Redox Biology*, vol. 15, pp. 441–451, 2018.
- [62] H. Maekawa and R. Inagi, "Stress signal network between hypoxia and ER stress in chronic kidney disease," *Frontiers in Physiology*, vol. 8, p. 74, 2017.
- [63] S. Kim and C. H. Woo, "Laminar flow inhibits ER stress-induced endothelial apoptosis through PI3K/Akt-dependent signaling pathway," *Molecules and Cells*, vol. 41, no. 11, pp. 964–970, 2018.
- [64] A. Jusic, the EU-CardioRNA COST Action (CA17129), and Y. Devaux, "Mitochondrial noncoding RNA-regulatory network in cardiovascular disease," *Basic Research in Cardiology*, vol. 115, no. 3, pp. 1–17, 2020.
- [65] M. Ding, C. Liu, R. Shi et al., "Mitochondrial fusion promoter restores mitochondrial dynamics balance and ameliorates diabetic cardiomyopathy in an optic atrophy 1-dependent way," *Acta Physiologica (Oxford, England)*, vol. 229, no. 1, article e13428, 2020.
- [66] M. A. Kluge, J. L. Fetterman, and J. A. Vita, "Mitochondria and endothelial function," *Circulation Research*, vol. 112, no. 8, pp. 1171–1188, 2013.
- [67] R. Marcu, Y. Zheng, and B. J. Hawkins, "Mitochondria and angiogenesis," *Advances in Experimental Medicine and Biology*, vol. 982, pp. 371–406, 2017.
- [68] J. D. Marshall, I. Bazan, Y. Zhang, W. H. Fares, and P. J. Lee, "Mitochondrial dysfunction and pulmonary hypertension: cause, effect, or both," *American Journal of Physiology. Lung Cellular and Molecular Physiology*, vol. 314, no. 5, pp. L782–L796, 2018.

Research Article

Coronary Endothelium No-Reflow Injury Is Associated with ROS-Modified Mitochondrial Fission through the JNK-Drp1 Signaling Pathway

Yi Chen,¹ Chen Liu,¹ Peng Zhou,¹ Jiannan Li,¹ Xiaoxiao Zhao,¹ Ying Wang,¹ Runzhen Chen,¹ Li Song,¹ Hanjun Zhao,^{1,2} and Hongbing Yan ^{1,2}

¹Department of Cardiology, Fuwai Hospital, National Center for Cardiovascular Diseases, Peking Union Medical College, Chinese Academy of Medical Sciences, Beijing, China

²Fuwai Hospital, Chinese Academy of Medical Sciences, Shenzhen, China

Correspondence should be addressed to Hongbing Yan; hbyanfuwai2020@163.com

Received 22 December 2020; Revised 15 January 2021; Accepted 23 January 2021; Published 4 February 2021

Academic Editor: Yun-dai Chen

Copyright © 2021 Yi Chen et al. This is an open access article distributed under the Creative Commons Attribution License, which permits unrestricted use, distribution, and reproduction in any medium, provided the original work is properly cited.

Coronary artery no-reflow is a complex problem in the area of reperfusion therapy, and the molecular mechanisms underlying coronary artery no-reflow injury have not been fully elucidated. In the present study, we explored whether oxidative stress caused damage to coronary endothelial cells by inducing mitochondrial fission and activating the JNK pathway. The hypoxia/reoxygenation (H/R) model was induced *in vitro* to mimic coronary endothelial no-reflow injury, and mitochondrial fission, mitochondrial function, and endothelial cell viability were analyzed using western blotting, quantitative polymerase chain reaction (qPCR), enzyme-linked immunosorbent assay (ELISA), and immunofluorescence. Our data indicated that reactive oxygen species (ROS) were significantly induced upon H/R injury, and this was followed by decreased endothelial cell viability. Mitochondrial fission was induced and mitochondrial bioenergetics were impaired in cardiac endothelial cells after H/R injury. Neutralization of ROS reduced mitochondrial fission and protected mitochondrial function against H/R injury. Our results also demonstrated that ROS stimulated mitochondrial fission via JNK-mediated Drp1 phosphorylation. These findings indicate that the ROS-JNK-Drp1 signaling pathway may be one of the molecular mechanisms underlying endothelial cell damage during H/R injury. Novel treatments for coronary no-reflow injury may involve targeting mitochondrial fission and the JNK-Drp1 signaling pathway.

1. Introduction

Primary percutaneous coronary intervention (PPCI) is the gold standard for the treatment of ST segment elevation myocardial infarction (STEMI) because it results in the timely opening of the occluded coronary arteries [1]. Fresh blood flow is restored in >90% of STEMI patients after PPCI. However, there is still a small number of patients who develop severe microvascular obstruction (MVO) even though epicardial arteries are successfully opened following PPCI. This phenomenon is called coronary no-reflow injury [2]. The early clinical manifestation of patients with coronary no-reflow injury includes recurring angina pectoris, malignant arrhythmias (e.g., ventricular tachycardia, ventricular

fibrillation, and atrioventricular block), acute left heart failure, cardiogenic shock, and cardiac rupture or other malignant complications [3]. Although the incidence of coronary no-reflow varies between studies because of differences in evaluation methods and types of no-reflow injuries used [4], it is estimated that the incidence of no-reflow injury is ~26% in patients with anterior wall STEMI [5].

It is believed that the initial cause of coronary no-reflow injury is related to microvascular dysfunction [6]. The myocardial blood supply is composed of the subepicardial coronary artery and the capillaries that penetrate the myocardium [7], and microvessels form the main resistance to myocardial perfusion blood flow [8]. Further, coronary blood flow is inversely correlated with microvascular

resistance. Several mechanisms, including endothelial cell death, inflammation response, oxidative stress, and coronary spasm, have been introduced to explain microvascular damage after PPCI [9–12]. It was reported that the microvessel wall was thickened, the lumen became smaller, and the endothelial cells were swelling in patients undergoing myocardial biopsy [13]. It has also been reported that endothelial cell damage is primarily caused by oxidative stress; however, the detailed molecular mechanisms underlying this damage have not been fully elucidated [14].

Although previous studies have reported that excessive oxidative stress is associated with mitochondrial dysfunction [15] (as evidenced by decreased mitochondrial membrane potential and increased mitochondrial proapoptotic factor release), the mechanisms underlying ROS-induced mitochondrial damage in endothelial cells following coronary no-reflow injury remain unknown. Recent investigations have demonstrated that mitochondrial dynamics disorder may be an upstream regulator of mitochondrial function [16–18]. Excessive mitochondrial fission divides mitochondria into several fragmentations that contain damaged mitochondrial DNA [19]. Since these fragmented mitochondria cannot synthesize the normal mitochondrial respiration complex, the physiological mitochondrial membrane potential cannot be generated [20]. Additionally, a decreased mitochondrial membrane potential is associated with increased mitochondrial membrane hyperpermeability, which results in the leakage of proapoptotic proteins into the cytoplasm [21]. Interestingly, the relationship between ROS and mitochondrial dynamics disorders has not been fully elucidated [22]. A recent study illustrated that mitochondrial fission was mainly regulated by Drp1, which was activated through posttranscriptional phosphorylation following activation of the JNK pathway [23]. In the present study, we investigated whether ROS mediated endothelial cell damage by inducing mitochondrial fission via the JNK pathway. Specifically, the purpose of this study was to investigate the role of ROS-modified mitochondrial fission through the JNK-Drp1 pathway in cultured endothelial cells using a hypoxia/reoxygenation (H/R) injury model.

2. Materials and Methods

2.1. Cardiac Endothelial Cells (CECs). Murine CECs were purchased from CELLutions Biosystems Inc. (Ontario, Canada) and cultured according to the supplier's instructions [24]. CECs were maintained in Dulbecco's Modified Eagle's Medium (glucose [4500 mg/L], L-glutamine [0.584 g/L], sodium bicarbonate [3.7 g/L], without sodium pyruvate [Sigma-Aldrich]) that was supplemented with penicillin (100 U/mL) and streptomycin (100 µg/mL; both from GIBCO), 10 mmol/L HEPES (HyClone, Thermo Fisher Scientific), and 5% fetal bovine serum (FBS; Sigma-Aldrich). When confluent (2–3 days after plating), the CECs were harvested using a 0.25% trypsin/EDTA solution (GIBCO), subcultured, or used for functional assays and RNA purification [25].

2.2. ELISA. The contents of SOD, GSH, GPX, and MDA in the culture media were detected using ELISA kits following

the manufacturer's instructions (Shanghai Hengyuan Biological Technology, China) [26]. The culture media was added to a microdroplet plate that was coated with purified SOD, GSH, GPX, and MDA primary antibodies and incubated at 37°C for 2 hours [27]. After incubation, the plate was washed and HRP-labeled secondary antibodies were added. After incubation with the secondary antibodies, the plate was washed thoroughly, and a solution of 3,3',5,5'-tetramethylbenzidine substrate was added. A sulfuric acid solution was added to stop the reaction, and the color was analyzed using spectrophotometry at a wavelength of 450 nm [28]. The concentrations of SOD, GPX, GSH, and MDA in the culture media were then calculated according to the standard curve [29].

2.3. Immunofluorescence Analysis. The protocol for the immunofluorescent staining of the heart tissues was performed as described below. Samples were fixed using 4% paraformaldehyde and mounted on microscope slides [30]. The slides were subsequently treated with primary antibodies, and the relative immunofluorescence intensity was calculated as previously described [31].

2.4. Oxygen-Glucose Deprivation (OGD) Followed by Reoxygenation. Cells were incubated in 6-well plates (4×10^5 cell/well) for 24 h, cultured in glucose-free DMEM, and incubated in an anaerobic chamber containing 95% N₂ and 5% CO₂ at 37°C for 3 h to mimic ischemic-like conditions *in vitro* [32]. After incubation, the CECs were returned to the atmosphere with 95% air and 5% CO₂ and cultured in glucose-containing DMEM for 3 h for reoxygenation. The subsequent experiment was performed 24 h after reoxygenation [33].

2.5. RT-qPCR. Total RNA was extracted using TRIzol reagent kits (Invitrogen, CA, USA). After extraction, 1 µg of total RNA was reverse transcribed to cDNA using the PrimeScript RT reagent kits (Takara) [34]. RT-qPCR was performed using a SYBR Premix Ex Taq II (TaKaRa) and the ABI 7500 real-time PCR system (Applied Biosystems). Relative RNA expression was normalized to that of GAPDH and was determined using the $2^{-\Delta\Delta C_t}$ method [35].

2.6. CCK-8 Assay. Transfected cells were seeded into 96-well plates and cultured for 24 h. Next, 10 µL of the CCK-8 solution was added to each well, and the cells were incubated for 2 h. After incubation, absorbance was measured at 450 nm using a microplate reader (Bio-Rad, USA) [36].

2.7. Western Blot. Western blot was conducted as previously reported. The primary antibodies were purchased from Abcam (Cambridge, MA, USA), and HRP-conjugated secondary antibodies were obtained from Sangon (Shanghai, China) [37].

2.8. Mitochondrial Respiratory Chain Complex Activity Analysis. The activity of the mitochondrial respiratory chain was determined using the Mitochondrial Respiratory Chain Complex Activity Assay Kit (Solarbio, Beijing, China) according to the manufacturer's instructions [38]. Briefly,

the mitochondrial complex was extracted from the ovaries using the suitable reagents, and 10 μ L of the extract was added to each well of a 96-well plate. Then, the detection reagents were added to the wells, mixed gently, and incubated at 37°C for 2 min. The corresponding absorbance was evaluated before and after the reaction using a microplate reader (BioTek, Vermont, VT), and the difference in absorbance was calculated [39]. Finally, the enzymatic activity of the complex was calculated using the corresponding formula that was provided in the kit manual [40].

2.9. Measurement of ATP Levels. ATP production was detected using the luminometric ATP Assay Kit (AAT Bioquest, Sunnyvale, CA) according to the manufacturer's instructions [41]. Briefly, 50 oocytes were seeded into each well of a 96-well white plate, and 200 μ L of the ATP assay solution was added to the oocyte cultures. After gently mixing and incubating for 20 min at room temperature [42], the luminescence intensity was measured using the luminometer mode on a plate reader (Tecan, Zurich, Switzerland). The readings were normalized to the total protein content [43].

2.10. Measurement of ROS Production. Cells were cultured in clear bottom 6-well black plates (Corning, Corning, NY, USA), incubated in the presence or absence of compounds for 48 h at 37°C, washed with PBS (pH 7.4), and incubated with 2',7'-dichlorofluorescein diacetate (H2DCFDA) for 18 h [44]. Following incubation, the cells were washed twice with PBS (pH 7.4), and the fluorescence of 2',7'-dichlorofluorescein (DCF) was then measured at excitation/emission (Ex/Em) wavelengths of 485/530 nm [45].

2.11. Statistical Analysis. Data shown are mean \pm SEM of the number of independent experiments indicated (n) and represent experiments performed on at least three separate occasions with similar outcomes. Data were analyzed using one-way or two-way ANOVAs, and comparisons between groups were performed using a protected Tukey's test. Statistical significance was defined as $p < 0.05$.

3. Results

3.1. H/R Injury Mediates Endothelial Cell Oxidative Stress. In the present study, an H/R model was used in cardiac endothelial cells (CECs) to mimic coronary microvascular no-reflow injury *in vitro*. Cell viability was measured using the Cell Counting Kit-8 (CCK-8) assay. As shown in Figure 1(a), cell viability was significantly suppressed in H/R-treated CECs as compared with control CECs. Recent studies have reported that oxidative stress is the primary pathological factor that induces endothelial cell damage during coronary no-reflow injury. To confirm this finding, an enzyme-linked immunosorbent assay (ELISA) was used to analyze alterations in the activities of antioxidants in CECs following H/R injury. As shown in Figures 1(b)–1(d), the activities of glutathione (GSH), superoxide dismutase (SOD), and glutathione peroxidase (GPX) were significantly increased in the H/R-treated cells as compared with the

control group. This suggests that there was a decline in the antioxidative capacity of CECs following H/R injury. Additionally, the levels of malondialdehyde (MDA) were increased, and this may have been due to increased ROS production in the cytoplasm (Figure 1(e)). To further observe the oxidative stress in CECs, an ROS probe was used to stain the intracellular ROS. As shown in Figures 1(f) and 1(g), the levels of cytoplasmic ROS and mitochondrial ROS were significantly elevated in the H/R-treated CECs as compared with the control group. These results indicate that H/R is followed by oxidative stress in CECs under H/R injury.

3.2. Mitochondrial ROS Promotes Drp1 Phosphorylation and Mitochondrial Fission in Endothelial Cells following H/R Injury. Previous studies have identified that mitochondrial ROS induces endothelial cell dysfunction through the disruption of mitochondrial homeostasis. Further investigations demonstrated that mitochondrial performance (especially mitochondrial fission) in endothelial cells is drastically regulated by mitochondrial dynamics. Therefore, we investigated whether mitochondrial ROS affected mitochondrial dysfunction in endothelial cells under H/R injury via activating mitochondrial fission. Mitochondrial morphology was observed through immunofluorescence. The data shown in Figures 2(a) and 2(b) demonstrated that the morphology of mitochondria was converted into a fragmented shape after exposure to H/R injury. To determine if mitochondrial ROS play a causal role in inducing mitochondrial fission, Mito-Q, a mitochondria-specific antioxidant, was incubated with CECs before H/R injury, and mitochondrial morphology was observed again after H/R injury. As shown in Figures 2(a) and 2(b), the elongated mitochondrial morphology was sustained in CECs that underwent Mito-Q treatment before H/R injury as compared with CECs that underwent H/R injury but were not treated with Mito-Q. To further support the role of mitochondrial ROS-induced mitochondrial fission, RNA transcriptions of mitochondrial fission-related factors were conducted. The transcriptions of Drp1, Mff, and Fis1 were significantly elevated in CECs that underwent H/R injury as compared with those in control CECs (Figures 2(c)–2(e)). Conversely, treatment with Mito-Q prevented the increase of these pro-fission factors (Figures 2(c)–2(e)), suggesting that mitochondrial ROS plays a contributory role in initiating mitochondrial fission in endothelial cells.

3.3. Mitochondrial Dysfunction Is Induced by Mitochondrial ROS. Although we reported that mitochondrial fission could be activated by mitochondrial ROS in endothelial cells under H/R injury, it remains unclear whether mitochondrial function is disturbed by mitochondrial ROS in H/R-treated CECs. To address this question, mitochondrial function was assessed in response to Mito-Q treatment. As shown in Figure 3(a), cellular adenosine triphosphate (ATP) production, which is primarily generated by mitochondria, was downregulated in H/R-treated CECs as compared with control CECs. Additionally, ATP production was reversed to near-normal levels with Mito-Q administration. We also found that the activities of the mitochondrial respiration

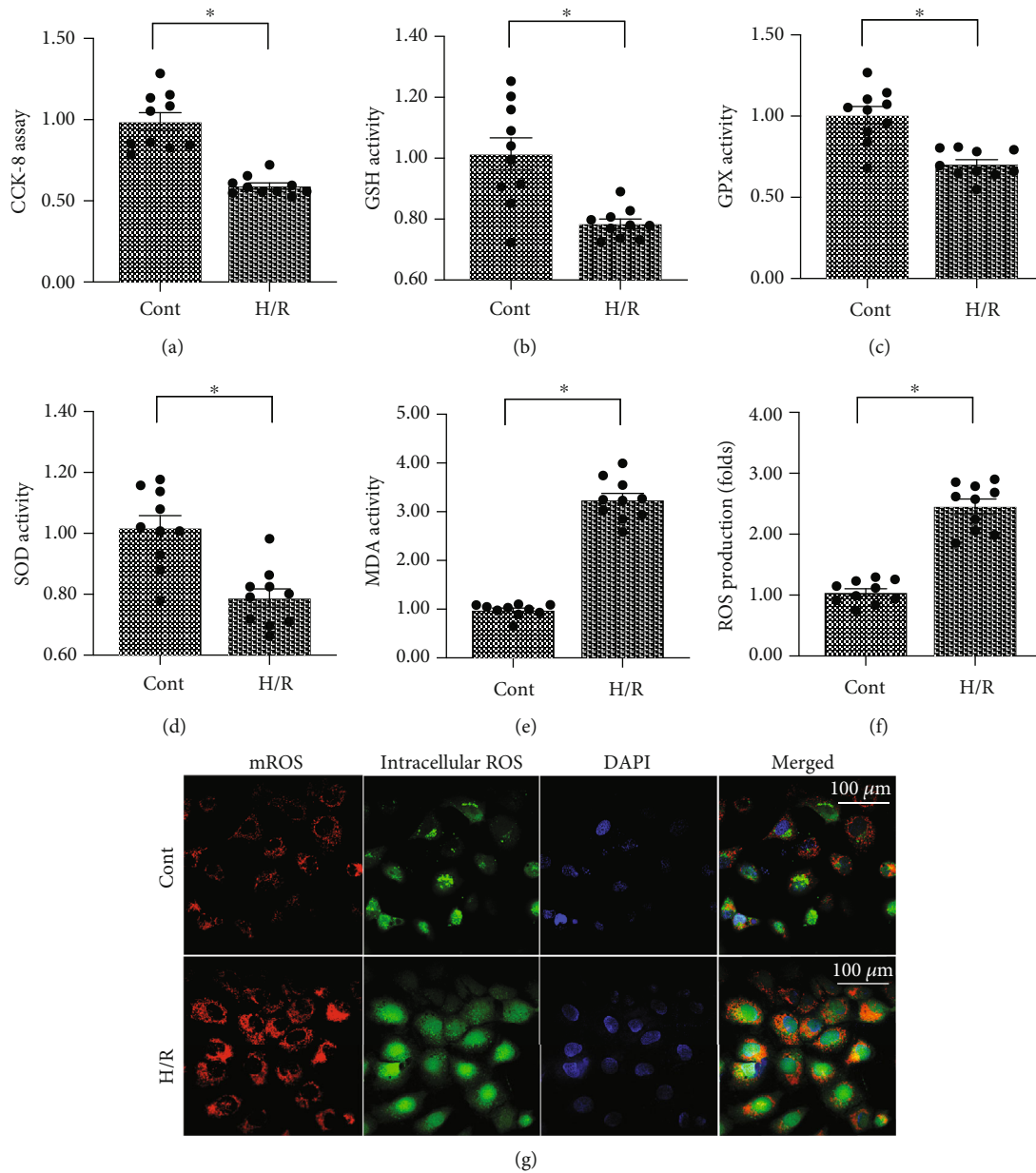


FIGURE 1: Hypoxia/reoxygenation injury mediates endothelial cell oxidative stress. (a) Cell viability was measured using the CCK-8 assay. Cardiac endothelial cells (CECs) underwent hypoxia/reoxygenation (H/R) injury. (b–e) The content of antioxidative factors was measured using an enzyme-linked immunosorbent assay (ELISA). (f, g) Intracellular ROS and mitochondrial ROS (mROS) were detected using DCFHDA and MitoSOX red mitochondrial superoxide indicator, respectively. * $p < 0.05$.

complex were reduced in H/R-treated CECs (Figures 3(b)–3(d)), and this alteration was improved by Mito-Q treatment. This finding suggests that mitochondrial ROS regulate mitochondria-mediated bioenergetics.

3.4. Inhibition of Mitochondrial Fission Also Sustains Mitochondrial Function in Endothelial Cells. To understand whether mitochondrial fission is also involved in the regulation of mitochondrial function in endothelial cells under H/R injury, Mdivi-1, an inhibitor of mitochondrial fission, was added to the endothelial cell culture media, and mitochondrial function was evaluated again [46]. As shown in

Figure 4(a), cellular ATP production was significantly reduced in H/R-treated endothelial cells as compared with control endothelial cells. Interestingly, administration of Mdivi-1 drastically improved ATP content in endothelial cells, and this was similar to the results obtained from the Mito-Q-treated endothelial cells. Our data also demonstrated that the activities of the mitochondrial respiration complex were inhibited in H/R-treated CECs (Figures 4(b)–4(d)). Interestingly, Mdivi-1 supplementation enhanced the activities of the mitochondrial respiration complex (Figures 4(b)–4(d)). These results suggest that mitochondria-related bioenergetics are normalized by mitochondrial fission inhibition.

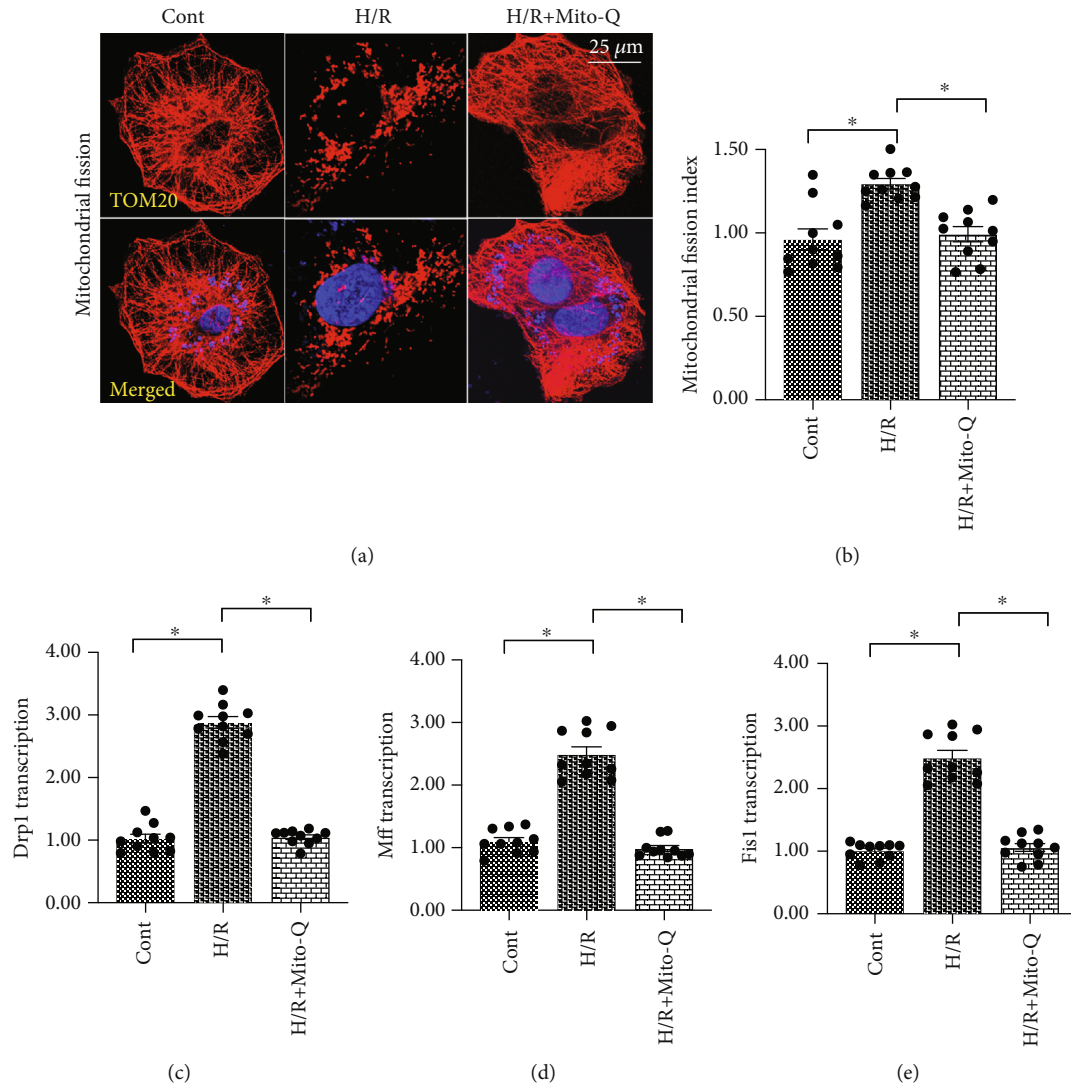


FIGURE 2: Mitochondrial ROS promotes Drp1 phosphorylation and mitochondrial fission in endothelial cells under hypoxia/reoxygenation injury. (a, b) Mitochondrial fission was measured using immunofluorescence. Cardiac endothelial cells (CECs) underwent hypoxia/reoxygenation (H/R) injury. Mito-Q, a mitochondrial antioxidant, was added to the CEC media to neutralize mROS. (c–e) qPCR was performed to analyze the transcription of Drp1, Mff, and Fis1 in CECs under H/R injury. * $p < 0.05$.

3.5. ROS Causes Drp1-Related Mitochondrial Fission through the JNK Pathway. Lastly, we evaluated the molecular mechanism underlying ROS-induced mitochondrial fission. Previous studies have demonstrated that mitochondrial fission is mainly regulated by Drp1 phosphorylation, and Drp1 posttranscriptional phosphorylation can be modified by the JNK pathway [47]. Thus, we investigated if ROS-mediated mitochondrial fission could be achieved through JNK-induced Drp1 phosphorylation. Results from western blotting demonstrated that the JNK pathway was significantly activated by H/R injury in CECs as evidenced by the presence of phosphorylated JNK (Figures 5(a)–5(c)). We also observed an increase in Drp1 phosphorylation after H/R injury. Interestingly, supplementation of Mito-Q repressed JNK phosphorylation and inhibited Drp1 phosphorylation (Figures 5(a)–5(c)), suggesting that mitochondrial ROS promote JNK and Drp1 phosphorylation (p-JNK and p-Drp1) in CECs. This finding was also supported by our immuno-

fluorescent findings. As shown in Figures 5(d)–5(f), the expressions of p-Drp1 and p-JNK were significantly increased in H/R-treated cells as compared with control cells. Interestingly, Mito-Q treatment repressed the increase in p-Drp1 and p-JNK following H/R injury (Figures 5(d)–5(f)). These findings suggest that mitochondrial fission in CECs is controlled by the ROS-Drp1-JNK signaling pathway.

4. Discussion

Coronary artery no-reflow is a complex problem in the area of reperfusion therapy [48]. Although there has been an advancement in drugs and interventional therapies in recent years, breakthrough progress has not been achieved in the prevention and treatment of coronary no-reflow injury following reperfusion therapy [2, 49]. Since infarction size, cardiac remodeling, myocardial function, and all-cause death are also determined by coronary no-reflow injury;

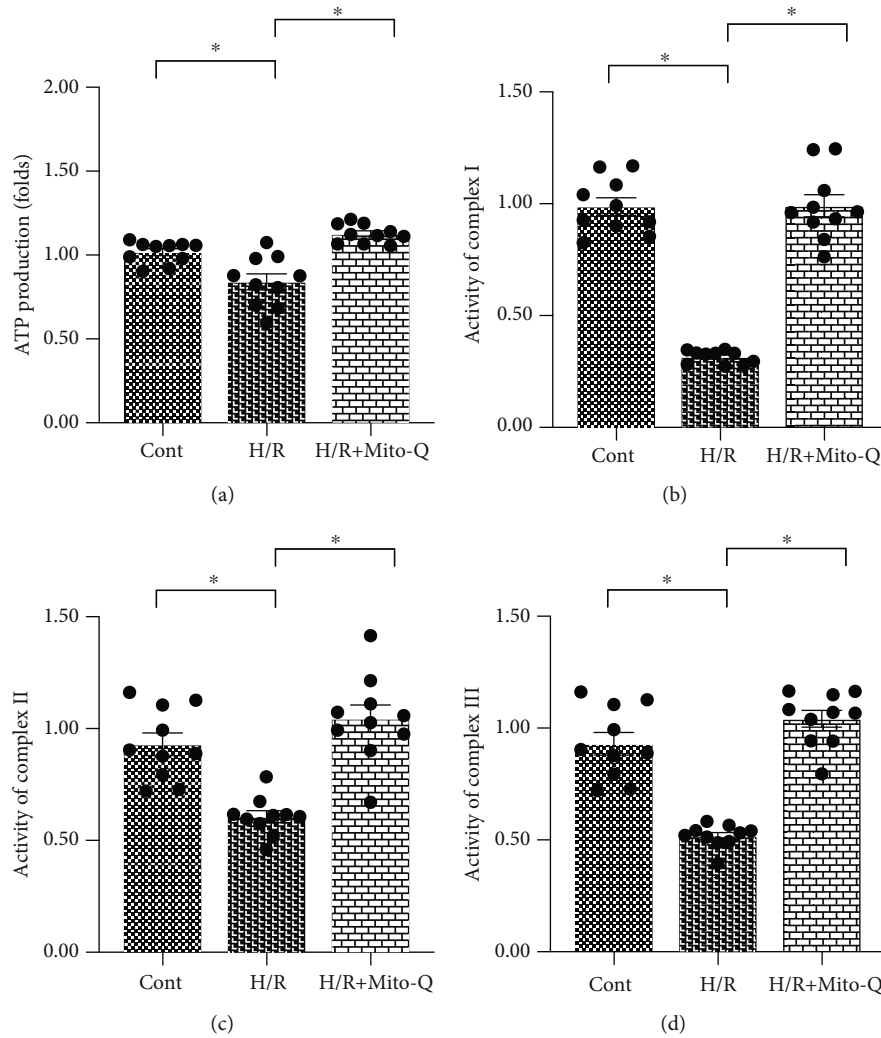


FIGURE 3: Mitochondrial dysfunction is induced by mitochondrial ROS. (a) Adenosine triphosphate (ATP) production was measured using an enzyme-linked immunosorbent assay (ELISA). Cardiac endothelial cells (CECs) underwent hypoxia/reoxygenation (H/R) injury. Mito-Q, a mitochondrial antioxidant, was added to the CEC media to neutralize mROS. (b–d) The activity of the mitochondrial respiration complex was determined using an ELISA. $*p < 0.05$.

understanding the molecular mechanisms underlying coronary no-reflow will promote specific diagnoses and therapies in clinical practice [11, 50]. In the present study, we used an H/R injury model to mimic coronary artery no-reflow injury *in vitro*. Our findings demonstrated that CEC damage was associated with mitochondrial dysfunction that was caused by increased mitochondrial fission. Further, we reported that oxidative stress was the primary inducer of mitochondrial fission via the activation of the JNK-Drp1 signaling pathway. ROS promoted JNK phosphorylation, which augmented Drp1 phosphorylation and resulted in mitochondrial fission in CECs. Excessive mitochondrial fission impaired mitochondrial bioenergetics, as evidenced by decreased ATP production and blunted mitochondrial respiration complex, which ultimately contributed to endothelial cell death. Overall, these findings demonstrate the molecular basis underlying ROS-induced endothelial cell damage and also identify the ROS-JNK-Drp1 pathway as the potential therapeutic target for the treatment of coronary no-reflow.

At the stage of myocardial ischemia, mitochondrial respiration is significantly impaired and glycolysis is augmented because of insufficient oxygen supply and interrupted blood flow, resulting in the accumulation of lactic acid [51, 52]. Since carbon dioxide in the blood stream cannot be quickly removed, the pH in endothelial cells significantly decreases [53]. As the pH decreases, massive hydrogen ions within endothelial cells promote the opening of Na^+/H^+ channels, which in turn promotes sodium translocation into the cytoplasm [54]. Subsequently, abnormal sodium stimulates sodium-calcium exchange channels that trigger intracellular calcium overload, which leads to coronary spasm and blunted coronary artery relaxation [55]. These alterations promote slow blood flow or terminal blood flow under hypoxic conditions. Although the recovery of blood flow will bring sufficient oxygen to the ischemic zone during the reperfusion stage [56], the damage to mitochondrial respiration that is induced by ischemic stress cannot be quickly restored in a short time, and this results in excessive ROS

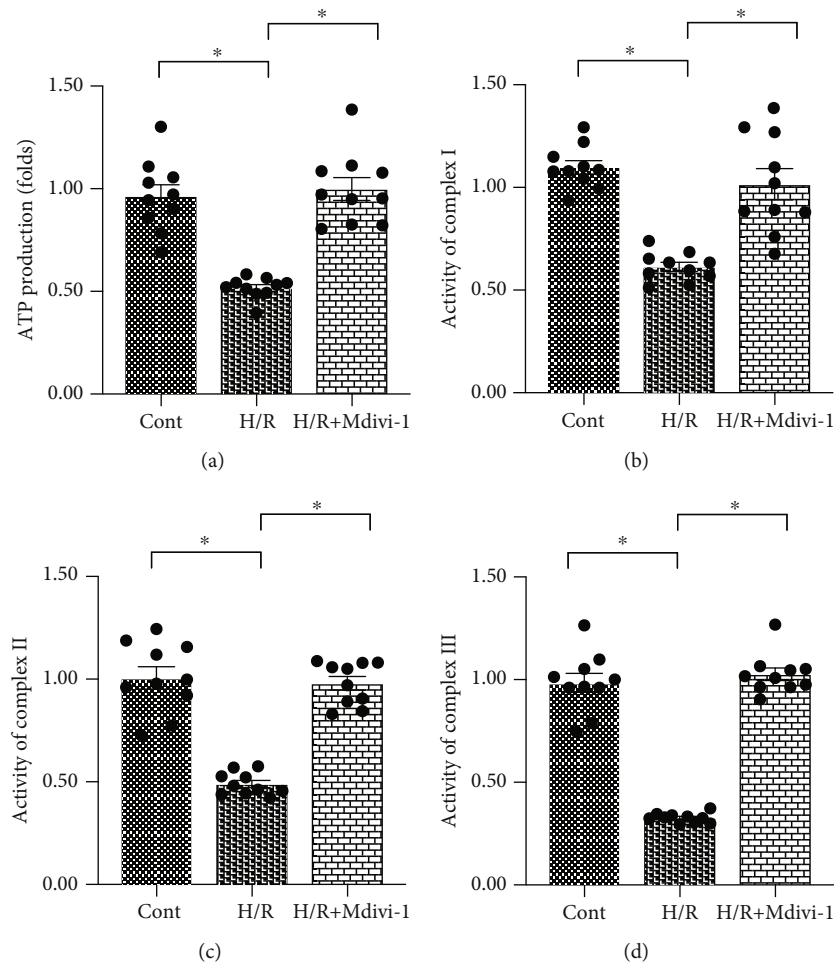


FIGURE 4: Inhibition of mitochondrial fission also sustains mitochondrial function in endothelial cells. (a) Adenosine triphosphate (ATP) production was measured using an enzyme-linked immunosorbent assay (ELISA). Cardiac endothelial cells (CECs) underwent hypoxia/reoxygenation (H/R) injury. Mdivi-1, a mitochondrial fission inhibitor, was added to the CEC culture media to repress mitochondrial fission. (b–d) The activity of the mitochondrial respiration complex was determined using an ELISA. * $p < 0.05$.

production in coronary endothelial cells [57]. In addition to oxidative stress, the inflammatory response is also initiated at the reperfusion stage. An uncontrolled inflammation response will aggravate myocardial edema [58] and ultimately compress the coronary artery and limit the diastolic function of the coronary artery. More importantly, inflammatory responses will also activate platelets to induce the formation of coronary thrombi [59, 60], leading to microcirculation embolism in the reperfusion phase. These alterations promote the development of coronary no-reflow injury even though the occluded epicardial arteries have been opened.

In the present study, we found that ROS are induced by H/R injury in CECs and correlate with the survival of CECs by mediating mitochondrial bioenergetics. Similarly, it was previously reported that ischemia/reperfusion-mediated senescence and vascular dysfunction of endothelial cells were attenuated by oxidants [61]. Endothelial cell necroptosis is also induced by ROS-mediated opening of the mitochondrial permeability transition pore (mPTP) [62]. Endothelial nitric oxide (NO) is a key regulator of vascular tone, and increased

NO is associated with coronary relaxation. However, excessive oxidative stress impairs the bioactivity of NO and ultimately represses NO-mediated vascular relaxation [63]. Mitochondrial fragmentation is induced by superoxide anion production in coronary endothelial cells in diabetic mice [64], suggesting a possible relationship between mitochondrial fission and oxidative stress. In a mouse model of cardiac ischemia/reperfusion injury, mitochondrial fission in coronary endothelial cells was regulated by the nicotinamide adenine dinucleotide phosphate (NADPH) oxidase 2 (Nox-2) signaling pathway and ROS production [65]. This finding confirms that oxidative stress plays a causal role in mediating mitochondrial fission in endothelial cells. Our data further identified that the JNK-Drp1 signaling pathway was the primary mechanism responsible for ROS-modified mitochondrial fission in coronary endothelial cells. This finding will help us to better understand the relationship between oxidative stress and mitochondrial dynamics in coronary endothelial cells during coronary no-reflow injury.

Mitochondrial dynamics are mitochondrial morphological mechanisms that include mitochondrial fission and

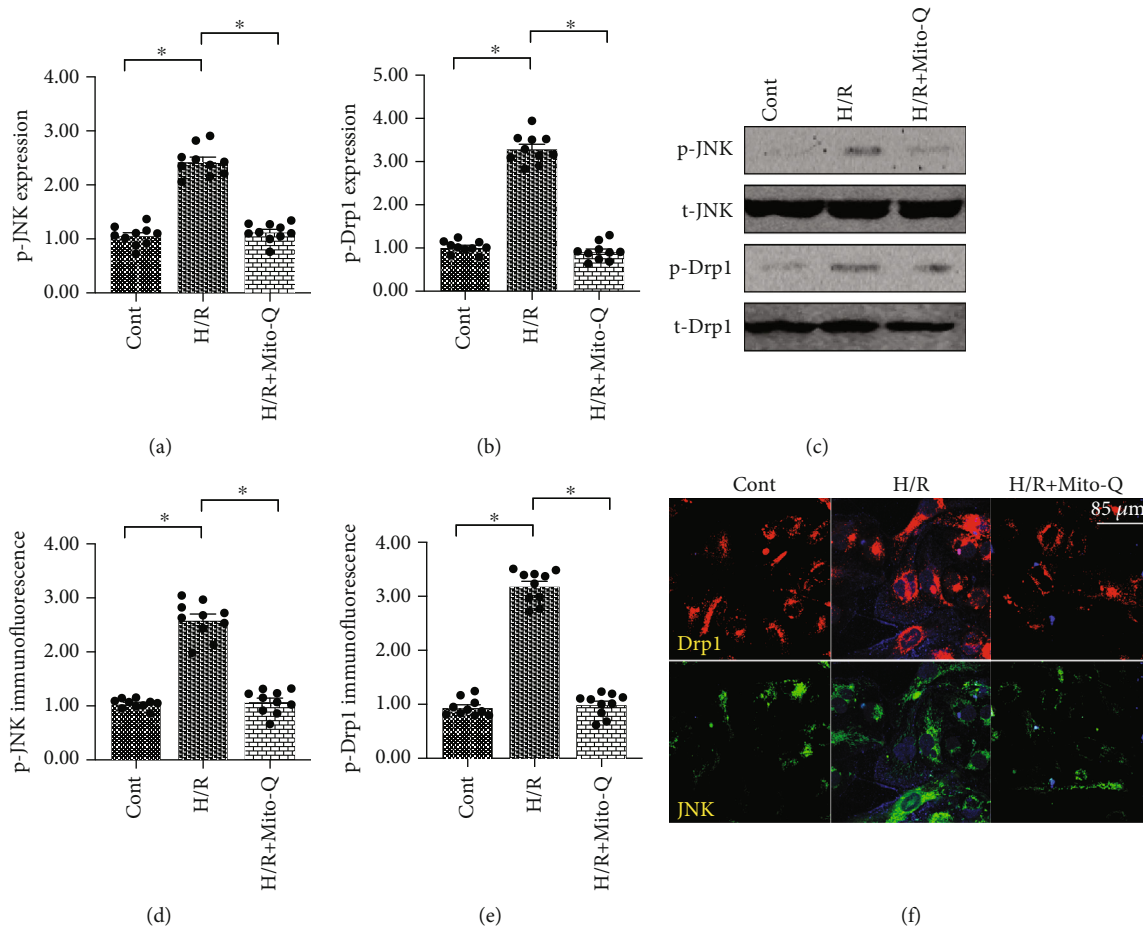


FIGURE 5: ROS causes Drp1-related mitochondrial fission through the JNK pathway. (a–c) Proteins were isolated from hypoxia/reoxygenation- (H/R-) treated CECs. Western blotting was performed to analyze the expression of JNK and Drp1. Mito-Q, a mitochondrial antioxidant, was added to the CEC culture media to neutralize mROS. (d–f) Immunofluorescence was performed to verify the expressions of JNK and Drp1. Mito-Q, a mitochondrial antioxidant, was added to the CEC culture media to neutralize mROS. * $p < 0.05$.

fusion. Mitochondrial fission is activated by hypoxia and/or reoxygenation, and multiple studies have confirmed that mitochondrial fission plays a pathological role in exacerbating myocardial damage during reperfusion therapy. For example, it was demonstrated that cardiac function was improved by the inhibition of mitochondrial fission at the reperfusion stage [66]. Another study revealed that reperfusion-mediated energetic crises were attenuated by mitochondrial fission suppression in a mouse model of cardiac ischemia/reperfusion injury [67]. It was also reported that intimal thickening after coronary damage was enhanced by mitochondrial fission due to dysregulated macrophage function [68, 69]. Further, it was demonstrated that inflammation and apoptosis of coronary endothelial cells were reduced via inhibition of mitochondrial fission or activation of mitophagy [70]. Decreased mitochondrial fission significantly promotes the production of NO in coronary endothelial cells, and this effect is followed by increased endothelium-dependent vasodilation [71]. Similarly, our data revealed that mitochondrial fission caused endothelial cell dysfunction as evidenced by decreased cell viability, impaired mitochondrial bioenergetics, and reduced ATP production. Based on these findings, mitochondrial fis-

sion may be a potential therapeutic target that sustains endothelial cell function and viability.

Overall, our results illustrate that coronary no-reflow injury is associated with endothelial cell damage that is caused by excessive oxidative stress. The ROS-JNK-Drp1 signaling pathway is activated at the stage of cardiac ischemia/reperfusion injury and contributes to mitochondrial fission, resulting in abnormal mitochondrial function and decreased endothelial cell viability. However, there are several limitations in the present study. First, our results are primarily based on cellular experiments, and animal studies are necessary to support our findings. Second, we used chemical inhibitors to determine the role of the ROS-JNK-Drp1 signaling pathway in regulating endothelial cell viability during coronary no-reflow. Additional studies using genetic ablation mice are required to confirm our findings.

Data Availability

The analyzed datasets that were generated during the study are available from the corresponding author upon reasonable request.

Conflicts of Interest

The authors declare that there is no conflict of interest regarding the publication of this paper.

Authors' Contributions

Y.C. contributed to the study concepts, study design, data acquisition, and manuscript preparation; Y.C. and C.L. contributed to the study concepts, study design, literature research, data acquisition, manuscript preparation, and editing; P.Z., J.L., X.Z., and Y.W. were the guarantors of integrity of the entire study and contributed to the definition of intellectual content, statistical analysis, and manuscript review; R.C. was the guarantor of integrity of the entire study and contributed to the data analysis and manuscript review; L.S. and H.Z. contributed to the clinical studies and data acquisition; and L.C. and H.Y. contributed to the experimental studies and data acquisition. The final version of the manuscript has been read and approved by all authors.

References

- [1] J. A. Reyes-Retana and L. C. Duque-Ossa, "Acute myocardial infarction biosensor: a review from bottom up," *Current Problems in Cardiology*, no. article 100739, 2020.
- [2] B. G. Schwartz and R. A. Kloner, "Coronary no reflow," *Journal of Molecular and Cellular Cardiology*, vol. 52, no. 4, pp. 873–882, 2012.
- [3] E. Eeckhout and M. J. Kern, "The coronary no-reflow phenomenon: a review of mechanisms and therapies," *European Heart Journal*, vol. 22, no. 9, pp. 729–739, 2001.
- [4] S. H. Rezkalla and R. A. Kloner, "Coronary no-reflow phenomenon: from the experimental laboratory to the cardiac catheterization laboratory," *Catheterization and Cardiovascular Interventions*, vol. 72, no. 7, pp. 950–957, 2008.
- [5] M. Scarpone, E. Cenko, and O. Manfrini, "Coronary no-reflow phenomenon in clinical practice," *Current Pharmaceutical Design*, vol. 24, no. 25, pp. 2927–2933, 2018.
- [6] H. Zhou and S. Toan, "Pathological roles of mitochondrial oxidative stress and mitochondrial dynamics in cardiac microvascular ischemia/reperfusion injury," *Biomolecules*, vol. 10, no. 1, p. 85, 2020.
- [7] I. Matsunari, "Microvascular function measurement in mice: From large to small," *Journal of Nuclear Cardiology*, 2020.
- [8] R. Altara and G. W. Booz, "Editorial: cardiac microvascular endothelium contribution to cardiac myocyte growth, structure, and contractile function," *Frontiers in Cardiovascular Medicine*, vol. 6, p. 130, 2019.
- [9] J. Zhong, H. Ouyang, M. Sun et al., "Tanshinone IIA attenuates cardiac microvascular ischemia-reperfusion injury via regulating the SIRT1-PGC1 α -mitochondrial apoptosis pathway," *Cell Stress & Chaperones*, vol. 24, no. 5, pp. 991–1003, 2019.
- [10] G. Heusch, "Coronary microvascular obstruction: the new frontier in cardioprotection," *Basic Research in Cardiology*, vol. 114, no. 6, p. ???, 2019.
- [11] I. Cuijpers, S. J. Simmonds, M. van Bilsen et al., "Microvascular and lymphatic dysfunction in HFpEF and its associated comorbidities," *Basic Research in Cardiology*, vol. 115, no. 4, p. 39, 2020.
- [12] X. M. Gao, Y. Su, S. Moore et al., "Relaxin mitigates microvascular damage and inflammation following cardiac ischemia-reperfusion," *Basic Research in Cardiology*, vol. 114, no. 4, p. 30, 2019.
- [13] J. Kumar, C. T. O'Connor, R. Kumar, S. K. Arnous, and T. J. Kiernan, "Coronary no-reflow in the modern era: a review of advances in diagnostic techniques and contemporary management," *Expert Review of Cardiovascular Therapy*, vol. 17, no. 8, pp. 605–623, 2019.
- [14] H. Zhu, S. Toan, D. Mui, and H. Zhou, "Mitochondrial quality surveillance as a therapeutic target in myocardial infarction," *Acta Physiologica*, no. article e13590, 2020.
- [15] H. Fan, Z. He, H. Huang et al., "Mitochondrial quality control in cardiomyocytes: a critical role in the progression of cardiovascular diseases," *Frontiers in Physiology*, vol. 11, p. 252, 2020.
- [16] C. Maneechote, S. Palee, S. Kerdphoo, T. Jaiwongkam, S. C. Chattipakorn, and N. Chattipakorn, "Pharmacological inhibition of mitochondrial fission attenuates cardiac ischemia-reperfusion injury in pre-diabetic rats," *Biochemical Pharmacology*, vol. 182, p. 114295, 2020.
- [17] H. Zhou, S. Toan, P. Zhu, J. Wang, J. Ren, and Y. Zhang, "DNA-PKcs promotes cardiac ischemia reperfusion injury through mitigating BI-1-governed mitochondrial homeostasis," *Basic Research in Cardiology*, vol. 115, no. 2, p. 11, 2020.
- [18] J. Wang and H. Zhou, "Mitochondrial quality control mechanisms as molecular targets in cardiac ischemia-reperfusion injury," *Acta Pharmaceutica Sinica B*, vol. 10, no. 10, pp. 1866–1879, 2020.
- [19] J. Zheng and C. Lu, "Oxidized LDL causes endothelial apoptosis by inhibiting mitochondrial fusion and mitochondria autophagy," *Frontiers in Cell and Development Biology*, vol. 8, p. 600950, 2020.
- [20] M. Huang, R. Wei, Y. Wang, T. Su, P. Li, and X. Chen, "The uremic toxin hippurate promotes endothelial dysfunction via the activation of Drp1-mediated mitochondrial fission," *Redox Biology*, vol. 16, pp. 303–313, 2018.
- [21] Q. Wang, M. Zhang, G. Torres et al., "Metformin suppresses diabetes-accelerated atherosclerosis via the inhibition of Drp1-mediated mitochondrial fission," *Diabetes*, vol. 66, no. 1, pp. 193–205, 2016.
- [22] M. Wallert, M. Ziegler, X. Wang et al., " α -Tocopherol preserves cardiac function by reducing oxidative stress and inflammation in ischemia/reperfusion injury," *Redox Biology*, vol. 26, article 101292, 2019.
- [23] R. Qin, D. Lin, L. Zhang, F. Xiao, and L. Guo, "Mst1 deletion reduces hyperglycemia-mediated vascular dysfunction via attenuating mitochondrial fission and modulating the JNK signaling pathway," *Journal of Cellular Physiology*, vol. 235, no. 1, pp. 294–303, 2019.
- [24] R. K. Adapala, A. K. Kanugula, S. Paruchuri, W. M. Chilian, and C. K. Thodeti, "TRPV4 deletion protects heart from myocardial infarction-induced adverse remodeling via modulation of cardiac fibroblast differentiation," *Basic Research in Cardiology*, vol. 115, no. 2, p. 14, 2020.
- [25] D. Bausch, S. Fritz, L. Bolm et al., "Hedgehog signaling promotes angiogenesis directly and indirectly in pancreatic cancer," *Angiogenesis*, vol. 23, no. 3, pp. 479–492, 2020.
- [26] E. Afşar, E. Kırmlıoğlu, T. Çeker, Ç. Yılmaz, N. Demir, and M. Aslan, "Effect of ER stress on sphingolipid levels and

- apoptotic pathways in retinal pigment epithelial cells,” *Redox Biology*, vol. 30, p. 101430, 2020.
- [27] Y. Feng, M. Zhong, Y. Tang et al., “The role and underlying mechanism of exosomal CA1 in chemotherapy resistance in diffuse large B cell lymphoma,” *Molecular Therapy - Nucleic Acids*, vol. 21, pp. 452–463, 2020.
- [28] L. Che, K. G. Alavattam, P. J. Stambrook, S. H. Namekawa, and C. Du, “BRUCE preserves genomic stability in the male germline of mice,” *Cell Death and Differentiation*, vol. 27, no. 8, pp. 2402–2416, 2020.
- [29] X. Fan, K. Li, L. Zhu et al., “Prolonged therapeutic effects of photoactivated adipose-derived stem cells following ischaemic injury,” *Acta Physiologica*, vol. 230, no. 1, article e13475, 2020.
- [30] D. J. Hausenloy, M. Ntsekhe, and D. M. Yellon, “A future for remote ischaemic conditioning in high-risk patients,” *Basic Research in Cardiology*, vol. 115, no. 3, pp. 1–4, 2020.
- [31] A. Domingues, C. Boisson-Vidal, P. Marquet de Rouge et al., “Targeting endothelial thioredoxin-interacting protein (TXNIP) protects from metabolic disorder-related impairment of vascular function and post-ischemic revascularisation,” *Angiogenesis*, vol. 23, no. 2, pp. 249–264, 2020.
- [32] J. Wang, P. Zhu, R. Li, J. Ren, Y. Zhang, and H. Zhou, “Bax inhibitor 1 preserves mitochondrial homeostasis in acute kidney injury through promoting mitochondrial retention of PHB2,” *Theranostics*, vol. 10, no. 1, pp. 384–397, 2020.
- [33] H. Zhou, P. Zhu, J. Wang, S. Toan, and J. Ren, “DNA-PKcs promotes alcohol-related liver disease by activating Drp1-related mitochondrial fission and repressing FUNDC1-required mitophagy,” *Signal Transduction and Targeted Therapy*, vol. 4, no. 1, p. 56, 2019.
- [34] G. Seano and R. K. Jain, “Vessel co-option in glioblastoma: emerging insights and opportunities,” *Angiogenesis*, vol. 23, no. 1, pp. 9–16, 2020.
- [35] E. Steffen, W. B. E. Mayer von Wittgenstein, M. Hennig et al., “Murine sca1/flk1-positive cells are not endothelial progenitor cells, but B2 lymphocytes,” *Basic Research in Cardiology*, vol. 115, no. 2, p. 18, 2020.
- [36] P. Janus, A. Toma-Jonik, N. Vydra et al., “Pro-death signaling of cytoprotective heat shock factor 1: upregulation of NOXA leading to apoptosis in heat-sensitive cells,” *Cell Death and Differentiation*, vol. 27, no. 7, pp. 2280–2292, 2020.
- [37] Y. Song, B. Wang, X. Zhu et al., “Human umbilical cord blood-derived MSCs exosome attenuate myocardial injury by inhibiting ferroptosis in acute myocardial infarction mice,” *Cell Biology Toxicology*, 2020.
- [38] K. Li, Y. Liu, Z. Xu et al., “Prevention of avian retrovirus infection in chickens using CRISPR-Cas9 delivered by Marek’s disease virus,” *Molecular Therapy - Nucleic Acids*, vol. 21, pp. 343–353, 2020.
- [39] E. Singh, R. E. Redgrave, H. M. Phillips, and H. M. Arthur, “Arterial endoglin does not protect against arteriovenous malformations,” *Angiogenesis*, vol. 23, no. 4, pp. 559–566, 2020.
- [40] R. Szulcek, G. Sanchez-Duffhues, N. Rol et al., “Exacerbated inflammatory signaling underlies aberrant response to BMP9 in pulmonary arterial hypertension lung endothelial cells,” *Angiogenesis*, vol. 23, no. 4, pp. 699–714, 2020.
- [41] S. A. Watson, A. Dendorfer, T. Thum, and F. Perbellini, “A practical guide for investigating cardiac physiology using living myocardial slices,” *Basic Research in Cardiology*, vol. 115, no. 6, p. 61, 2020.
- [42] M. I. Nawaz, S. Rezzola, C. Tobia et al., “D-Peptide analogues of Boc-Phe-Leu-Phe-Leu-Phe-COOH induce neovascularization via endothelial N-formyl peptide receptor 3,” *Angiogenesis*, vol. 23, no. 3, pp. 357–369, 2020.
- [43] M. Kammoun, J. Piquereau, L. Nadal-Desbarats et al., “Novel role of Tieg1in muscle metabolism and mitochondrial oxidative capacities,” *Acta Physiologica*, vol. 228, no. 3, article e13394, 2019.
- [44] J. Wang, P. Zhu, S. Toan, R. Li, J. Ren, and H. Zhou, “Pum2-Mff axis fine-tunes mitochondrial quality control in acute ischemic kidney injury,” *Cell Biology and Toxicology*, vol. 36, no. 4, pp. 365–378, 2020.
- [45] A. Vasseur, L. Cabel, O. Tredan et al., “Prognostic value of CEC count in HER2-negative metastatic breast cancer patients treated with bevacizumab and chemotherapy: a prospective validation study (UCBG COMET),” *Angiogenesis*, vol. 23, no. 2, pp. 193–202, 2020.
- [46] J. Wang, S. Toan, and H. Zhou, “New insights into the role of mitochondria in cardiac microvascular ischemia/reperfusion injury,” *Angiogenesis*, vol. 23, no. 3, pp. 299–314, 2020.
- [47] J. Wang, P. Zhu, R. Li, J. Ren, and H. Zhou, “Fundc1-dependent mitophagy is obligatory to ischemic preconditioning-conferred renoprotection in ischemic AKI via suppression of Drp1-mediated mitochondrial fission,” *Redox Biology*, vol. 30, p. 101415, 2020.
- [48] G. Caiazzo, R. L. Musci, L. Frediani et al., “State of the art: no-reflow phenomenon,” *Cardiology Clinics*, vol. 38, no. 4, pp. 563–573, 2020.
- [49] W. E. Hughes, A. M. Beyer, and D. D. Gutterman, “Vascular autophagy in health and disease,” *Basic Research in Cardiology*, vol. 115, no. 4, p. 41, 2020.
- [50] Y. Sawashita, N. Hirata, Y. Yoshikawa, H. Terada, Y. Tokinaga, and M. Yamakage, “Remote ischemic preconditioning reduces myocardial ischemia-reperfusion injury through unacylated ghrelin-induced activation of the JAK/STAT pathway,” *Basic Research in Cardiology*, vol. 115, no. 4, p. 50, 2020.
- [51] C. Maldonado, M. D. Nguyen, P. Bauer et al., “Rapid lipid modification of endothelial cell membranes in cardiac ischemia/reperfusion injury: a novel therapeutic strategy to reduce infarct size,” *Cardiovascular Drugs and Therapy*, vol. 35, no. 1, pp. 113–123, 2021.
- [52] Y. H. Zuo, Y. B. Liu, C. S. Cheng et al., “Isovaleroylbinankad-surin A ameliorates cardiac ischemia/reperfusion injury through activating GR dependent RISK signaling,” *Pharmacological Research*, vol. 158, p. 104897, 2020.
- [53] A. Daiber and T. Münzel, “Interplay of the red blood cell and vascular endothelial nitric oxide synthase system to combat cardiac complications of anemia,” *Basic Research in Cardiology*, vol. 115, no. 4, p. 44, 2020.
- [54] K. J. Haushalter, J. M. Schilling, Y. Song et al., “Cardiac ischemia-reperfusion injury induces ROS-dependent loss of PKA regulatory subunit RI α ,” *American Journal of Physiology. Heart and Circulatory Physiology*, vol. 317, no. 6, pp. H1231–h1242, 2019.
- [55] A. V. Kuznetsov, Javadov, Margreiter, Grimm, Hagenbuchner, and Ausserlechner, “The role of mitochondria in the mechanisms of cardiac ischemia-reperfusion injury,” *Antioxidants*, vol. 8, no. 10, p. 454, 2019.

- [56] X. Li, S. Luo, J. Zhang et al., "lncRNA H19 alleviated myocardial I/RI via suppressing miR-877-3p/Bcl-2-mediated mitochondrial apoptosis," *Molecular Therapy - Nucleic Acids*, vol. 17, pp. 297–309, 2019.
- [57] M. Sedighi, R. D. E. Sewell, A. Nazari et al., "A review on the most important medicinal plants effective in cardiac ischemia-reperfusion injury," *Current Pharmaceutical Design*, vol. 25, no. 3, pp. 352–358, 2019.
- [58] M. Kohlhauser, V. R. Pell, N. Burger et al., "Protection against cardiac ischemia-reperfusion injury by hypothermia and by inhibition of succinate accumulation and oxidation is additive," *Basic Research in Cardiology*, vol. 114, no. 3, p. 18, 2019.
- [59] J. Bradic, V. Zivkovic, I. Srejsovic et al., "Protective effects of Galium verum L. extract against cardiac ischemia/reperfusion injury in spontaneously hypertensive rats," *Oxidative Medicine and Cellular Longevity*, vol. 2019, Article ID 4235405, 11 pages, 2019.
- [60] N. Lubos, S. van der Gaag, M. Gerçek, S. Kant, R. E. Leube, and C. A. Krusche, "Inflammation shapes pathogenesis of murine arrhythmogenic cardiomyopathy," *Basic Research in Cardiology*, vol. 115, no. 4, p. 42, 2020.
- [61] G. Bidault, M. Garcia, J. Capeau, R. Morichon, C. Vigouroux, and V. Béréziat, "Progerin expression induces inflammation, oxidative stress and senescence in human coronary endothelial cells," *Cells*, vol. 9, no. 5, p. 1201, 2020.
- [62] P. Zhu, S. Hu, Q. Jin et al., "Ripk3 promotes ER stress-induced necroptosis in cardiac IR injury: a mechanism involving calcium overload/XO/ROS/mPTP pathway," *Redox Biology*, vol. 16, pp. 157–168, 2018.
- [63] E. Grossini, C. Gramaglia, S. Farruggio et al., "Asenapine increases nitric oxide release and protects porcine coronary artery endothelial cells against peroxidation," *Vascular Pharmacology*, vol. 60, no. 3, pp. 127–141, 2014.
- [64] A. Makino, B. T. Scott, and W. H. Dillmann, "Mitochondrial fragmentation and superoxide anion production in coronary endothelial cells from a mouse model of type 1 diabetes," *Diabetologia*, vol. 53, no. 8, pp. 1783–1794, 2010.
- [65] H. Zhou, C. Shi, S. Hu, H. Zhu, J. Ren, and Y. Chen, "BI1 is associated with microvascular protection in cardiac ischemia reperfusion injury via repressing Syk-Nox2-Drp1-mitochondrial fission pathways," *Angiogenesis*, vol. 21, no. 3, pp. 599–615, 2018.
- [66] Y. Zhao, R. Guo, L. Li et al., "Tongmai formula improves cardiac function via regulating mitochondrial quality control in the myocardium with ischemia/reperfusion injury," *Bio-medicine & Pharmacotherapy*, vol. 132, p. 110897, 2020.
- [67] L. Chen, X. Y. Chen, Q. L. Wang et al., "Astragaloside IV derivative (LS-102) alleviated myocardial ischemia reperfusion injury by inhibiting Drp1Ser616 phosphorylation-mediated mitochondrial fission," *Frontiers in Pharmacology*, vol. 11, p. 1083, 2020.
- [68] R. Umezū, J. I. Koga, T. Matoba et al., "Macrophage (Drp1) dynamin-related protein 1 accelerates intimal thickening after vascular injury," *Arteriosclerosis, Thrombosis, and Vascular Biology*, vol. 40, no. 7, pp. e214–e226, 2020.
- [69] K. Qiao, Y. Liu, Z. Xu et al., "RNA m6A methylation promotes the formation of vasculogenic mimicry in hepatocellular carcinoma via Hippo pathway," *Angiogenesis*, 2020.
- [70] H. Zhou, J. Wang, P. Zhu et al., "NR4A1 aggravates the cardiac microvascular ischemia reperfusion injury through suppressing FUNDC1-mediated mitophagy and promoting Mff-required mitochondrial fission by CK2 α ," *Basic Research in Cardiology*, vol. 113, no. 4, p. 23, 2018.
- [71] R. J. Giedt, C. Yang, J. L. Zweier, A. Matzavinos, and B. R. Alevriadou, "Mitochondrial fission in endothelial cells after simulated ischemia/reperfusion: role of nitric oxide and reactive oxygen species," *Free Radical Biology & Medicine*, vol. 52, no. 2, pp. 348–356, 2012.